

# **The Methanotrophic Interactome: Structure and Stress Response**

Von der Naturwissenschaftlichen Fakultät der  
Gottfried Wilhelm Leibniz Universität Hannover

zur Erlangung des Grades  
Doktor der Naturwissenschaften (Dr. rer. nat.)

genehmigte Dissertation  
von  
Thomas Kaupper, M. Sc.

2024

**Referent:** Prof. Dr. rer. nat. A. Marcus Horn

**Korreferent:** Prof. Dr. rer. nat. Thomas Brüser

**Korreferent:** Prof. Dr. sc. ETH Zürich Rainer Meckenstock

**Tag der Promotion:** 02.11.2023



---

*To my father*

*Thank you for everything you have done for me*

---

# Zusammenfassung

Methanotrophe Mikroorganismen sind in der Umwelt allgegenwärtig und fungieren in vielen Methan-emittierenden Umgebungen als Biofilter für das Treibhausgas Methan, da sie die einzige Gilde von Mikroorganismen sind, die Methan oxidieren können. Viele Studien haben die Methanotrophen in verschiedenen Habitaten untersucht, aber nur wenige haben das Interaktom der Methanotrophen, d. h. die mit den Methanotrophen assoziierten nicht-methanotrophen / heterotrophen Organismen, in Betracht gezogen. Methanotrophe leben nicht in Abgeschiedenheit, sondern werden sowohl positiv als auch negativ von nicht-methanotrophen Organismen beeinflusst. Daher kann das Interaktom zur Funktion der methanotrophen Gemeinschaft beitragen und die Stressantwort beeinflussen.

In dieser Arbeit wird eine neuartige Strategie angewandt, bei der die Analyse von 'Co-occurrence' Netzwerken verwendet wird, um auf trophische Interaktionsnetzwerke im Zusammenhang mit Methanotrophen zu schließen. Eine Vorauswahl der aktiven und replizierenden Gemeinschaft wird durch DNA-stabile Isotopenbeprobung erleichtert, um eine Überbewertung solcher Netzwerke zu vermeiden. Diese Arbeit gibt außerdem Aufschluss über die Standortspezifität methanotropher Netzwerke und über die Auswirkungen von Stressfaktoren auf die Gemeinschaft. Ersteres wird durch den Vergleich des methanotrophen Interaktoms von fünf verschiedenen Methan-emittierenden Umgebungen aufgedeckt, da die gleichen trophisch interagierenden Taxa selten in mehreren Umgebungen gefunden werden. Letzteres wird durch die Anwendung eines milden und eines starken Stressoren in Methan-emittierenden Umgebungen gezeigt und die Auswirkungen auf das Interaktom der Methanotrophen nachgewiesen. Während ein leichter Austrocknungsstress, der auf einen Reisfeldboden angewandt wurde, nur geringe Auswirkungen auf das Interaktom hat und möglicherweise die interagierende Gemeinschaft stärkt, hat ein schwerer Stressor, wie z.B. der Abbau und die Wiederherstellung eines Torf-Moores, erhebliche Auswirkungen auf das Interaktom, was wiederum die Stressreaktion des Systems auf künftige Stressoren beeinträchtigen kann. Allerdings spiegeln sich diese Veränderungen nicht im Interaktom wider. Schließlich wird der Einfluss abiotischer und biotischer Parameter auf die Wiederbesiedlung sterilisierter Böden anhand der methanotrophen Aktivität und der Entwicklung der Gemeinschaft analysiert. Die anfängliche Zusammensetzung der Gemeinschaft wirkt sich in gewissem Maße auf die Entwicklung der methanotrophen Gemeinschaft aus, während die edaphischen Eigenschaften hauptsächlich die Aktivität der methanotrophen Gemeinschaft beeinflussen.

Insgesamt ist das Interaktom der Methanotrophen standortspezifisch und der Einfluss von Stressoren auf das Interaktom kann von abiotischen und biotischen Parametern abhängen. Obwohl sich die Bodenfunktionen nach der Stresseinwirkung erholen, bleiben die Netzwerke beeinträchtigt.

**Keywords:** Methan-oxidation; Methanotrophe Mikroorganismen; Stressoren; 'Co-occurrence' Netzwerke; Interaktom; DNA-stabile Isotopenbeprobung

---

# Abstract

Methanotrophs are ubiquitous organisms in the environment, acting as a biofilter for the potent greenhouse gas methane in many methane emitting environments, being the only guild of organisms capable of methane oxidation. Many studies have investigated methanotrophs in various environments, but few have taken the methanotrophic interactome, i.e., the methanotroph-associated non-methanotrophic organisms, into account. Methanotrophs do not live in seclusion, being influenced, both positively and negatively, by non-methanotrophic organisms. Thus, the methanotrophic interactome may contribute to methanotrophic community functioning and promote stress response.

In this thesis, a novel strategy applies co-occurrence network analyses to infer methanotroph-related trophic interaction networks. A pre-selection of the active and metabolizing community was facilitated by DNA-stable isotope probing to avoid overestimation of such networks that can occur otherwise. This work further provides insights into the site-specificity of methanotrophic networks and community-related stressor impacts. The former was revealed by comparing the methanotrophic interactome of five different methane-emitting environments, as the same trophically interacting taxa were seldom found in multiple environments. The latter was demonstrated by applying a mild and severe stressor to methane-emitting environments, and the impact on the methanotrophic interactome was determined. While mild desiccation / re-wetting stress applied to paddy soil had a minor impact on the methanotrophic interactome and potentially strengthened the interacting community, a severe stressor, such as peatland mining and restoration, had a significant impact on the interactome, which in turn likely impairs the system's stress response to future stressors. Changes in the interactome were not reflected in the methanotrophic activity and abundance, which weakens these parameters as indicators of soil functional restoration. Lastly, the influence of abiotic and biotic parameters on the re-colonization of gamma-irradiated soil was analyzed, indicated by methanotrophic activity and community development. To an extent, the initial community composition affects methanotrophic community succession, while edaphic properties mainly influence methanotrophic activity.

Altogether, the methanotrophic interactome was site-specific, and the influence of stressors on the methanotrophic interactome may be dependent on abiotic and biotic parameters. Even though the soil functions recovered after disturbance, the co-occurrence networks remained impaired.

**Keywords:** Methane oxidation; Methanotrophs; Co-occurrence networks; Interactome; Stressors; DNA-stable isotope probing

---

# Acknowledgments

First and foremost, I would like to thank Prof. Dr. Marcus A. Horn, my supervisor who mentored me during my master's and PhD period. Thank you for all the nice and inspiring discussions, both on- or off-topic. For everything that I have learned from you. For the opportunities you offered me for scientific research and conference attendance. And also thank you for your support during difficult times during my PhD period. Even though my PhD period had its ups and downs, it was great fun working with you and I will never forget these times. Thank you so much.

To my second supervisor, Dr. Adrian Ho, who guided me through the last years during my master's and PhD period. Thank you for all that you have taught me, for the inspiring ideas and great discussions and for your support, whenever needed. You were always there with ideas or workarounds, if I encountered a problem or something didn't work out as planned. You have brought me where I am today. Thank you!

Thirdly, to Prof. Dr. Thomas Brüser, for the inspiring discussions during our institute seminars. For the questions that make you look beyond the box and from which I have learned a lot. As well, thank you for taking the time to support me, even if you didn't have any.

To all the great colleagues of the whole Institute of Microbiology. Here, throughout the six years during my master's and PhD period I have learned most of what I know today. Thank you for all the support and the great discussions in our institute seminars. Special thanks to all the Hörnchens, the best working group one could think of. You made work not feel like work. Thank you for enduring all my bad jokes and crazy ideas (that sometimes were even good ones), for all the inspiring discussions and to always lend a hand when help was needed. I will never forget all of our group events, the uncountable BBQs and games nights. I will really miss you guys.

Last, but not least, to my family for all they have done for me. There are no words to describe how thankful I am to have you. You are the best!

# Table of Contents

<b>Dedication</b>	<b>I</b>
<b>Zusammenfassung</b>	<b>II</b>
<b>Abstract</b>	<b>III</b>
<b>Acknowledgments</b>	<b>IV</b>
<b>Table of contents</b>	<b>V</b>
<b>List of Figures</b>	<b>IX</b>
<b>List of Tables</b>	<b>XI</b>
<b>List of Abbreviations</b>	<b>XII</b>
<b>Structural Note</b>	<b>XIV</b>
<b>1 General Introduction</b>	<b>1</b>
1.1 Background . . . . .	2
1.2 Methane - the Potent Greenhouse Gas . . . . .	2
1.3 The Anaerobic Food Chain and Methanogenesis . . . . .	5
1.4 Anaerobic Methanotrophy . . . . .	6
1.5 Aerobic Methanotrophy . . . . .	7
1.5.1 History, Physiology and Taxonomy of Methanotrophs . . . . .	8
1.5.2 Metabolism and Carbon Assimilation Pathways . . . . .	11
1.5.3 Habitat and Role of Aerobic Methanotrophs . . . . .	17
1.6 The Methanotrophic Interactome . . . . .	20
1.7 Hypothesis and Aim of the Project . . . . .	21
<b>2 Novel Experimental Strategy - SIP-coupled Co-occurrence Network Analysis</b>	<b>23</b>
2.1 Background . . . . .	24
2.2 Stable Isotope Probing . . . . .	24
2.3 Network Construction . . . . .	25
<b>3 The Methane-Driven Interaction Network in Terrestrial Methane Hotspots</b>	<b>28</b>
3.1 Abstract . . . . .	29
3.2 Background . . . . .	30
3.3 Results and Discussion . . . . .	32
3.3.1 Aerobic Methanotrophy, and Environmental Variables Influencing the Metabolically Active Bacterial Community Composition . . . . .	32
3.3.2 The Methanotrophic Interactome Over Space and Time . . . . .	36

3.3.3	Insights Into Intra-Methanotroph and Methanotroph/Non-Methanotroph Interaction Within the Methanotrophic Interactome	38
3.3.4	Comparison of the Interaction Networks Derived From the Total ( <sup>unlabelled</sup> C-DNA) and Metabolically Active ( <sup>13</sup> C-DNA) Microbial Communities	43
3.4	Conclusion	44
3.5	Materials and Methods	44
3.5.1	Chemicals and reagents	44
3.5.2	Soil microcosm incubation, and soil physico-chemical characterization	45
3.5.3	DNA-SIP with <sup>13</sup> C-CH <sub>4</sub>	46
3.5.4	Quantitative PCR (qPCR)	47
3.5.5	16S rRNA gene amplicon preparation and Illumina MiSeq sequencing	47
3.5.6	16S rRNA gene amplicon analyses	48
3.5.7	Co-occurrence network analysis	49
3.5.8	Statistical analysis	50
<b>4</b>	<b>When the Going Gets Tough: Emergence of a Complex Methane - Driven Interaction Network During Recovery from Desiccation - Rewetting</b>	<b>51</b>
4.1	Abstract	52
4.2	Introduction	52
4.3	Materials and Methods	54
4.3.1	Soil Sampling and Microcosm Set-Up	54
4.3.2	Methane and Inorganic N Measurements	55
4.3.3	DNA Extraction and Isopycnic Ultracentrifugation	55
4.3.4	Group-Specific qPCR Assays	56
4.3.5	Amplification for the <i>pmoA</i> and 16S rRNA Genes for Illumina MiSeq Sequencing	57
4.3.6	<i>pmoA</i> and 16S rRNA Gene Amplicon Analyses	58
4.3.7	Co-Occurrence Network Analysis	59
4.3.8	Statistical Analysis	60
4.4	Results	60
4.4.1	The Abiotic Environment	60
4.4.2	Response in Methanotroph Abundance	60
4.4.3	Effects of Desiccation - Rewetting on the Methanotrophic Community Composition, as Determined by DNA-based SIP	61
4.4.4	Effects of Desiccation - Rewetting on the Total Bacterial Community Composition, as Determined by DNA-based SIP	63
4.4.5	Response of the Co-Occurrence Network Structure to Desiccation - Rewetting	65
4.5	Discussion	67
4.5.1	Recovery and Resilience of the Methanotrophic Activity and Community Composition Following Desiccation - Rewetting	67
4.5.2	The Emergence of a More Complex and Connected Methane-Driven Interactome After Desiccation - Rewetting	69

4.6	Conclusion . . . . .	72
<b>5</b>	<b>Recovery of Methanotrophic Activity Is Not Reflected in the Methane-Driven Interaction Network after Peat Mining</b>	<b>73</b>
5.1	Abstract . . . . .	74
5.2	Importance . . . . .	74
5.3	Introduction . . . . .	75
5.4	Results . . . . .	78
5.4.1	Comparison of the Methanotrophic Activity and Abundance, and the Abiotic Environment in the Pristine and Restored Peatlands .	78
5.4.2	Response of the Metabolically Active Bacterial Community Composition to Peat Restoration, as Determined by DNA-based SIP .	78
5.4.3	Insights Into the Methane-Driven Co-Occurrence Interaction Network in the Pristine and Restored Peatlands . . . . .	81
5.5	Discussion . . . . .	83
5.5.1	Recovery of the Active Methanotrophs After Peat Restoration . .	83
5.5.2	Insights Into the Recovery of the Methanotrophic Interactome After Peat Restoration . . . . .	85
5.6	Conclusion . . . . .	87
5.7	Materials and Methods . . . . .	87
5.7.1	Peat sampling and incubation setup . . . . .	87
5.7.2	Methane and inorganic N measurements . . . . .	88
5.7.3	DNA extraction and quantitative PCR (qPCR) . . . . .	88
5.7.4	<sup>13</sup> C-CH <sub>4</sub> stable Isotope probing . . . . .	89
5.7.5	16S rRNA gene amplicon sequencing . . . . .	89
5.7.6	16S rRNA gene sequencing analysis . . . . .	90
5.7.7	Statistical analyses . . . . .	91
<b>6</b>	<b>Disentangling Abiotic and Biotic Controls of Aerobic Methane Oxidation During Re-Colonization</b>	<b>92</b>
6.1	Abstract . . . . .	93
6.2	Introduction . . . . .	93
6.3	Abiotic Parameters Exert a Stronger Effect on Aerobic Methane Oxidation than the Initial Methanotrophic Community Composition . . . . .	98
6.4	Methanotroph Population Dynamics; the Emergence of the Alphaproteobacterial Methanotrophs During Recolonization . . . . .	100
<b>7</b>	<b>General Discussion</b>	<b>104</b>
7.1	Recapitulation of Findings . . . . .	105
7.2	Importance of Selected Methane Emitting Environments . . . . .	106
7.3	Resistance and Resilience of the methane oxidizing bacteria (MOB) Interactome . . . . .	108
7.4	The MOB Core Interactome . . . . .	113
7.5	Limitations and Advantageous of SIP and Co-occurrence Networks . . .	114
7.6	Limited Information on Pure Culture Interactions . . . . .	118
7.7	Conclusion . . . . .	118

7.8	Summary . . . . .	120
7.9	Outlook . . . . .	121
<b>8</b>	<b>References</b>	<b>122</b>
	<b>Appendix</b>	<b>154</b>
A	Published version of presented articles . . . . .	154
A.1	The methane-driven interaction network in terrestrial methane hotspots . . . . .	155
A.2	Supplementary information - The methane-driven interaction network in terrestrial methane hotspots . . . . .	172
A.3	When the going gets tough: Emergence of a complex methane-driven interaction network during recovery from desiccation-rewetting . . . . .	181
A.4	Supplementary information - When the going gets tough: emergence of a complex methane-driven interaction network during recovery from desiccation-rewetting . . . . .	191
A.5	Recovery of Methanotrophic Activity Is Not Reflected in the Methane-Driven Interaction Network after Peat Mining . . . . .	199
A.6	Supplementary information - Recovery of Methanotrophic Activity Is Not Reflected in the Methane-Driven Interaction Network after Peat Mining . . . . .	212
A.7	Disentangling abiotic and biotic controls of aerobic methane oxidation during re-colonization . . . . .	216
A.8	Supplementary information - Disentangling abiotic and biotic controls of aerobic methane oxidation during re-colonization . . . . .	222
B	Further published articles in peer-reviewed journals . . . . .	229
<b>9</b>	<b>Curriculum Vitae</b>	<b>232</b>
<b>10</b>	<b>List of Publications</b>	<b>235</b>
A	Published articles in peer-reviewed journals . . . . .	235
B	Published abstracts at national and international conferences . . . . .	237



## List of Figures

1.1	Atmospheric CH <sub>4</sub> concentration from 1984 to 2022. . . . .	3
1.2	Anthropogenic and natural sources and sinks of CH <sub>4</sub> . . . . .	4
1.3	Processes involved in fermentation . . . . .	6
1.4	Oxidation pathway of CH <sub>4</sub> to CO <sub>2</sub> of Type I and Type II MOB. . . . .	9
1.5	Phylogenetic trees showing the phylogeny of MOB type strains based on 16S rRNA gene sequences and PmoA sequences . . . . .	10
1.6	Potential CH <sub>4</sub> oxidation pathway in cells cultured under high and low copper conditions . . . . .	12
2.1	Simplified network . . . . .	26
3.1	RDA showing compositional differences of the metabolically active bacterial community from widespread CH <sub>4</sub> hotspots . . . . .	33
3.2	Venn diagram showing shared co-occurring taxa in all environments. . .	39
3.3	Venn diagram showing shared co-occurring taxa over time in the pristine peatland. . . . .	42
4.1	CH <sub>4</sub> uptake rate in the un-disturbed and disturbed incubations . . . . .	61
4.2	Temporal changes in the <i>pmoA</i> gene abundance of Type Ia (a), Type Ib (b), and Type II (c) MOB, as determined from group-specific qPCR assays	62
4.3	Principal component analysis showing the response of the active MOB and bacterial community composition to desiccation-rewetting . . . . .	64
4.4	Active bacterial community composition in the un-disturbed and disturbed incubations . . . . .	65
4.5	Co-occurrence network analysis of the active bacterial community based on the 16S ribosomal ribonucleic acid (rRNA) gene during pre-incubation, and after desiccation-rewetting. . . . .	68
5.1	Relative <i>pmoA</i> gene abundance along the density gradient from the pristine and restored peatlands . . . . .	79
5.2	Principal-component analysis showing the clustering of the 16S rRNA gene sequences according to the different fractions and sites . . . . .	80
5.3	The bacterial and MOB community composition in the starting material and after incubation . . . . .	82
5.4	Co-occurrence network analysis in the pristine and restored peatlands.	84
6.1	Experimental setup showing reciprocal inoculation of native soils in gamma-irradiated fractions of the soils . . . . .	94
6.2	methane (CH <sub>4</sub> ) uptake rate and total CH <sub>4</sub> consumed during recolonization	96
6.3	PCA showing the response of the MOB community composition during recolonization . . . . .	99
6.4	Response of the <i>pmoA</i> gene abundance of Type Ia (A), Type Ib (B), and Type II (C) MOB during re-colonization . . . . .	101

7.1	Conceptual model summarizing the influence of a mild and severe disturbance on the co-occurrence network. . . . .	111
7.2	Conceptual model recapitulating the results combining SIP and co-occurrence network construction. . . . .	115
7.3	Graphical model of the microbial community and network complexity development after disturbance . . . . .	119
S1	The <i>pmoA</i> and 16S rRNA gene abundances in the starting material and after incubation in diverse environments . . . . .	174
S2	Relative <i>pmoA</i> gene abundance along the density gradient of the <sup>13</sup> C- and <sup>unlabelled</sup> C-CH <sub>4</sub> incubations in diverse environments . . . . .	175
S3	Relative <i>pmoA</i> gene abundance along the density gradient in the pristine peatland over time . . . . .	176
S4	Relative abundance of the methanotroph-affiliated OTUs in diverse environments . . . . .	177
S5	Relative abundance of the methanotroph-affiliated OTUs in the pristine peatland over time . . . . .	177
S6	Principal component analysis showing the clustering of the 16S rRNA gene sequences in the ‘light’ and ‘heavy’ fractions in diverse environments . . . . .	178
S7	Principal component analysis of the 16S rRNA gene sequences in the ‘light’ and ‘heavy’ fractions of the pristine peatland over time . . . . .	178
S8	Co-occurrence network analysis of methane hotspots derived from the <sup>13</sup> C- and <sup>unlabelled</sup> C-DNA. . . . .	179
S9	Co-occurrence network analysis over time in the pristine peat derived from the <sup>13</sup> C- and <sup>unlabelled</sup> C-DNA. . . . .	180
S10	Experimental setup . . . . .	193
S11	Representative relative abundance of the <i>pmoA</i> gene recovered from each density gradient . . . . .	194
S12	Changes in soluble ammonium and nitrate concentrations in the undisturbed and disturbed incubations . . . . .	195
S13	Correlation between the methane uptake rates and <i>pmoA</i> gene abundances of type Ia, Ib, and II methanotrophs . . . . .	196
S14	Principal component analysis showing the separation of the bacterial communities derived from the ‘heavy’ and ‘light’ fractions . . . . .	197
S15	Differential abundance of the bacterial taxa at the OTU level . . . . .	198
S16	Headspace methane concentration during incubation . . . . .	214
S17	Boxplot showing the distribution of significantly different phyla . . . . .	214
S18	Differential abundance of OTUs in the pristine and restored peatlands derived from the <sup>13</sup> C-enriched 16S rRNA gene sequences . . . . .	215
S19	Headspace methane in the gamma-irradiated rice paddy and upland soils . . . . .	226
S20	Changes in ammonium concentrations during incubation . . . . .	226
S21	Rarefaction curve for all samples and replicates . . . . .	227
S22	Mean relative abundance and affiliation of the <i>pmoA</i> gene in the PP, PU, UP, and UU incubations . . . . .	228

## List of Tables

1.1	Taxonomic classification of proteobacterial and verrucomicrobial MOB . . . . .	11
2.1	Description of network parameters . . . . .	27
3.1	Selected soil physico-chemical properties, and CH <sub>4</sub> uptake rates from CH <sub>4</sub> hotspots . . . . .	35
3.2	Correlations and topological properties of the co-occurrence network analysis derived from widespread CH <sub>4</sub> hotspots. . . . .	37
3.3	Correlations and topological properties of the co-occurrence network analysis from the pristine peatland over time. . . . .	38
4.1	Correlations and topological properties of the interaction networks during preincubation, and recovery from desiccation-rewetting at 1–7 and 27–71 days intervals. . . . .	66
5.1	Selected physicochemical properties, <i>pmoA</i> and 16S rRNA gene abundances, and CH <sub>4</sub> uptake rates in the pristine and restored peatlands . . . . .	77
5.2	Topological properties of the co-occurrence network analysis in the pristine and restored peatlands . . . . .	81
6.1	Physico-chemical parameters of the wetland and upland agricultural soils. . . . .	97
S1	Selected physico-chemical parameters and methane uptake rates of individual replicates in methane hotspots . . . . .	173
S2	Significantly positively and negatively co-occurring OTUs between environments . . . . .	173
S3	Significantly positively and negatively co-occurring OTUs in the pristine peatland over time . . . . .	173
S4	Sample names/treatment and corresponding accession numbers . . . . .	173
S5	qPCR primer concentrations and thermal profiles . . . . .	192
S6	Topological properties of the interaction networks . . . . .	192
S7	Top 5 OTUs with more betweenness centrality in the undisturbed and disturbed incubations . . . . .	192
S8	Top 10 OTUs with more betweenness centrality, representing the key nodes in the pristine and restored peatlands . . . . .	213

# List of Abbreviations

<b>ANME</b>	anaerobic methanotrophs
<b>AOB</b>	ammonia oxidizing bacteria
<b>AOM</b>	anaerobic oxidation of methane
<b>NH<sub>4</sub><sup>+</sup></b>	ammonium
<b>CBB</b>	Calvin–Benson–Bassham
<b>CO<sub>2</sub></b>	carbon dioxide
<b>CO</b>	carbon monoxide
<b>Cu</b>	copper
<b>DCA</b>	detrended correspondence analysis
<b>DNA</b>	deoxyribonucleic acid
<b>H<sub>2</sub></b>	di-hydrogen
<b>FaIDH</b>	formaldehyde dehydrogenase
<b>FDH</b>	formate dehydrogenase
<b>GC</b>	gas chromatograph
<b>GHG</b>	greenhouse gas
<b>GWP</b>	global warming potential
<b>MDH</b>	methanol dehydrogenase
<b>CH<sub>4</sub></b>	methane
<b>MMO</b>	methane monooxygenase
<b>MOB</b>	methane oxidizing bacteria
<b><i>mcrA</i></b>	methyl-co-enzyme M reductase subunit A gene
<b>mRNA</b>	messenger ribonucleic acid
<b>NADH</b>	nicotinamidadenindinukleotid
<b>NADPH</b>	nicotinamidadenindinukleotidphosphat
<b>N<sub>2</sub>O</b>	nitrous oxide
<b>PCR</b>	polymerase chain reaction
<b>O<sub>2</sub></b>	oxygen
<b>OTU</b>	operational taxonomic unit
<b>O(<sup>1</sup>D)</b>	excited atomic oxygen
<b>PCA</b>	principal component analysis
<b>PCR</b>	polymerase chain reaction
<b>PD-HID</b>	pulsed discharge helium ionization detector

<b>PHB</b>	poly- $\beta$ -hydroxybutyrate
<b>PLFA</b>	phospholipid fatty acid
<b>pMMO</b>	particulate methane monooxygenase
<b>qPCR</b>	real-time quantitative polymerase chain reaction
<b>RDA</b>	redundancy analysis
<b>RNA</b>	ribonucleic acid
<b>RPC</b>	Rice Paddy Cluster
<b>rRNA</b>	ribosomal ribonucleic acid
<b>RubisCO</b>	ribulose-1,5-bisphosphate carboxylase-oxygenase
<b>RuMP</b>	ribulose monophosphate pathway
<b>SIP</b>	stable-isotope probing
<b>sMMO</b>	soluble methane monooxygenase
<b>SOC</b>	soil organic carbon
<b>SRB</b>	sulfate-reducing bacteria
<b>TCA</b>	tricarboxylic acid

## Structural Note

In the following the topic is introduced and the articles with major contribution from myself (first authorship) are presented in the main text. Afterwards the results are discussed. In the end of the main part, the literature for all sections beforehand is given.

During my doctoral studies I have contributed to 7 publications that can be found in the list of publications (see Chapter 10), as well as in the appendix in the published version. The presented articles from this thesis are given in the published version in the appendix (see Subsection A.1, A.3, A.5 and A.7). Supplementary information for each manuscript presented in the main text is given directly after the corresponding article in the appendix. Additional articles published during the PhD period are given in the appendix section (see Section B). Here, the supplementary information can be found online.

### **Published articles presented in the main text**

#### **When the Going Gets Tough: Emergence of a Complex Methane-Driven Interaction Network During Recovery from Desiccation-Rewetting**

Kaupper, T., Mendes, L. W., Lee, H. J., Mo, Y., Poehlein, A., Jia, Z., Horn, M. A., Ho, A.  
published in: Soil Biology and Biochemistry

#### **Recovery of Methanotrophic Activity is Not Reflected in the Methane-Driven Interaction Network after Peat Mining**

Kaupper, T., Mendes, L. W., Harnisz, M., Krause, S. M. B., Horn, M. A., Ho, A.  
published in: Applied and Environmental Microbiology

#### **The Methane-Driven Interaction Network in Terrestrial Methane Hotspots.**

Kaupper, T., Mendes, L. W., Poehlein, A., Frohloff, D., Rohrbach, S., Horn, M. A., Ho, A.  
published in: Environmental Microbiome

#### **Disentangling abiotic and biotic controls of aerobic methane oxidation during re-colonization**

Kaupper, T., Luehrs, J., Lee, H. J., Mo, Y., Jia, Z., Horn, M. A., Ho, A.  
published in: Soil Biology and Biochemistry

# **Chapter 1**

## **General Introduction**

## 1.1 Background

Climate change or global warming is powered by greenhouse gas (GHG) emissions and affects all living organisms, e.g., microbes, animals, as well as humans, on planet Earth. With an increase in temperature and weather extremes (Song et al., 2022), new challenges arise in nature. Anthropogenic or naturally occurring droughts, (bio-)turbation, or habitat destruction are just a few examples of stressors that influence all organisms. Yet, researchers from all around the world have put focus on the impact of climate change and its consequences. Restoration or renaturation of destroyed ecosystems, optimization of land use, and further are introduced by governments to limit these consequences. In this thesis, an overview on microbial recovery after drought stress, microbial habitat (re-)colonization after restoration, and a comparative view on environment-dependent microbial community structures in terrestrial ecosystems is provided.

## 1.2 Methane - the Potent Greenhouse Gas

In 1776, the Italian physicist Alessandro Volta collected rising bubbles from the bottom of a pond, finding that this mixture of gases was flammable (Dalton, 2005; Reay et al., 2007). This was the first (known) discovery of methane ( $\text{CH}_4$ ), one of the most potent GHGs. Half a decade later, John Dalton termed the gas as 'carburetted hydrogen' and suggested that one carbon atom is combined with two hydrogen atoms (Dalton, 2005). To date,  $\text{CH}_4$  is the simplest known hydrocarbon, consisting of a single carbon atom with four hydrogen atoms bound to it.

$\text{CH}_4$  is highly flammable, and thus natural gas, which consists mainly of  $\text{CH}_4$ , is used as fuel worldwide; e.g., in 2005 in the EU  $\approx 25\%$  of the total energy was produced from natural gas (EEA, 2010). Although  $\text{CH}_4$  - in the form of natural gas - is an essential driver of industry and heating material in households, there are significant issues to its use. The industrial revolution  $\approx 260$  years ago was the start of massive anthropological GHG emissions (Cicerone and Oremland, 1988; IPCC, 2007). Apart from carbon dioxide ( $\text{CO}_2$ ) and nitrous oxide ( $\text{N}_2\text{O}$ ) as potent GHGs, atmospheric  $\text{CH}_4$  concentration has more than doubled (Mancinelli, 1995; Montzka et al., 2011; Saunio et al., 2020) and is continuously increasing (see Figure 1.1; Cicerone and Oremland, 1988; Fraser et al., 1987).

Main anthropogenic sources of  $\text{CH}_4$  are fossil fuel production and its use (see Figure 1.1), as well as the continual increase in agriculture and livestock (Ritchie and



Roser, 2013) to feed the growing human population. The latter is accompanied by increasing waste production worldwide, and hence, landfills are important sources of  $\text{CH}_4$  (see Section 1.3; Bogner et al., 1997, 1995).

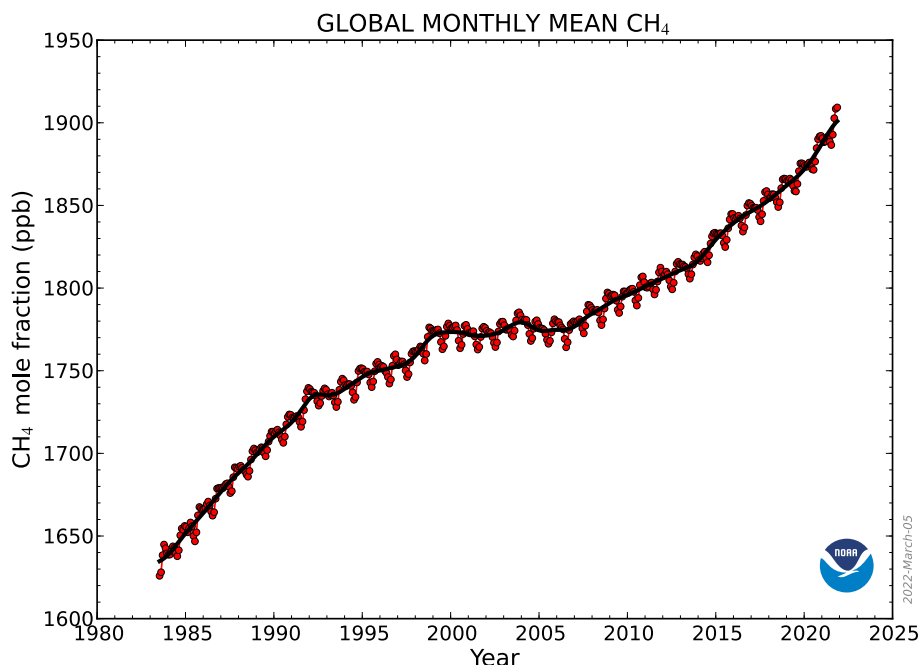


**Figure 1.1** Atmospheric  $\text{CH}_4$  concentration from 1984 to 2022. From Dlugokencky (2022).

Compared to  $\text{CO}_2$ ,  $\text{CH}_4$  has a 25 times higher global warming potential (GWP) (Boucher et al., 2009; Reay et al., 2007; Schiermeier, 2020), raising interest in its regulation or atmospheric depletion. Even though methane has a relatively short lifetime in the atmosphere ( $\sim 12$  years), it is then chemically degraded by OH radicals to  $\text{CO}_2$ , carbon monoxide (CO), water, and further by-products (Bergamaschi and Bousquet, 2008; Bodelier and Steenbergh, 2014; Cicerone and Oremland, 1988; Reay et al., 2007; Saunio et al., 2020; Schiermeier, 2020; Włodarczyk, 2011). The atmospheric  $\text{CH}_4$  degradation via OH radicals accounts for  $\approx 90\%$  of the total  $\text{CH}_4$  sink but further contributes to the greenhouse effect due to its consequent release of  $\text{CO}_2$  and water vapor (Ehhalt et al., 2001). The remaining  $\text{CH}_4$  sink capacity is the biological oxidation of  $\text{CH}_4$  to  $\text{CO}_2$ , which is presented later in this thesis, and the reaction of  $\text{CH}_4$  with chlorine radicals or excited atomic oxygen ( $\text{O}(^1\text{D})$ ) that is produced in the photolysis of ozone (Bergamaschi and Bousquet, 2008; Ehhalt et al., 2001; Platt et al., 2004). Besides water vapor,  $\text{CO}_2$ ,  $\text{N}_2\text{O}$ , and  $\text{CH}_4$ , other gases, like ozone-depleting substances, hydrofluorocarbons, sulfur hexafluoride, and perfluorocarbons (IPCC, 2007; Montzka et al., 2011), contribute to the greenhouse effect, where atmospheric transmission of outgoing thermal radiation from the earth is inhibited and reflected back to the planet

(Greenhouse Effect, 2011; Hatano, 2011). This additional reflected thermal radiation causes a continuous increase in global temperature greater than the critical rate of  $0.1^{\circ}\text{C}/\text{decade}$  (Lal, 2004), leading to global warming and, consequently, global climate change.

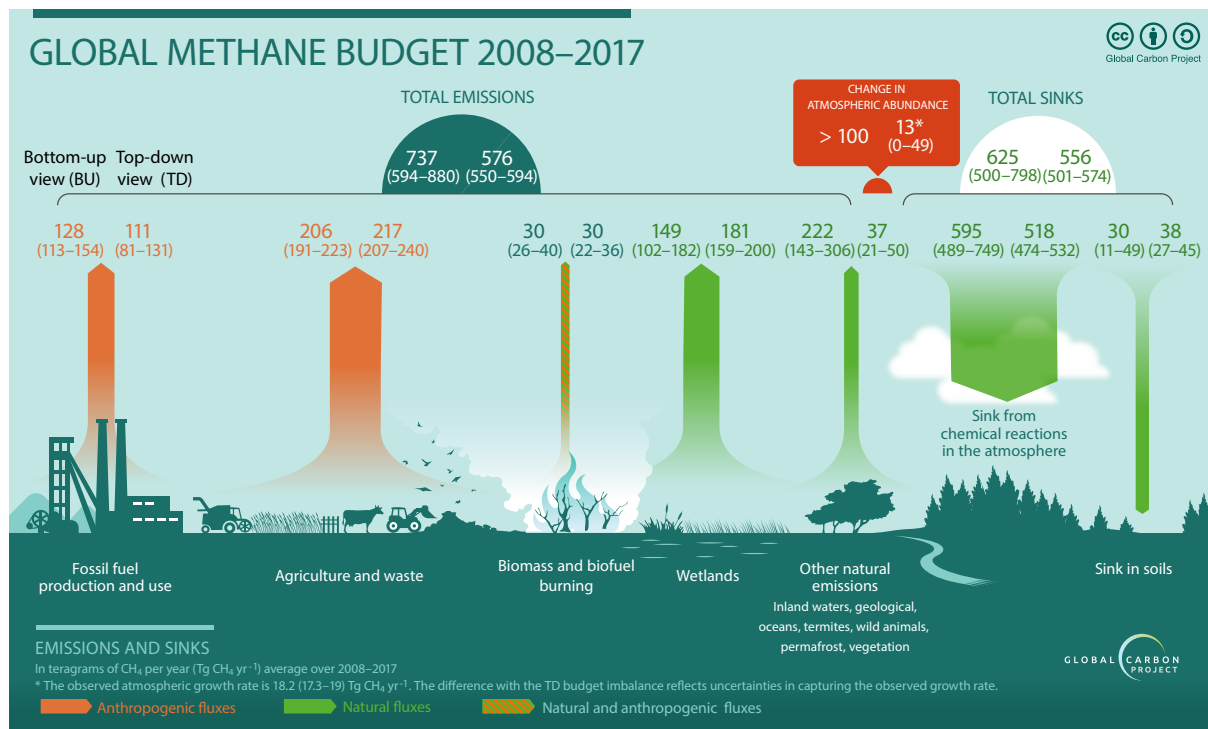


**Figure 1.2** Anthropogenic and natural sources and sinks of CH<sub>4</sub>. Global CH<sub>4</sub> budget between 2008 and 2017. Estimated individual as well as total emission/sink categories are given in Tg CH<sub>4</sub> yr<sup>-1</sup>. From Saunio et al. (2020).

Thus, the regulation or depletion of atmospheric CH<sub>4</sub> may be a first step towards reducing climate change consequences. Anthropocentric sources contribute approximately half of the CH<sub>4</sub> release (see Figure 1.2; Bodelier and Steenbergh, 2014; Ciaia et al., 2013). Production or burning of fossil fuels, landfills, as well as livestock, are the main drivers of anthropogenic emissions and GWP, as well as agriculture and land use change (Bodelier et al., 2000; Jackson et al., 2008; Kaupper et al., 2020a; Liu et al., 2017). Of equal importance in the global CH<sub>4</sub> sources are the remaining 50 % that is produced in soils and wetlands (Bodelier and Steenbergh, 2014). Whether an environment is a sink or a source for CH<sub>4</sub> depends on the dynamics in CH<sub>4</sub> production (methanogenesis; see Section 1.3) and CH<sub>4</sub> oxidation (methanotrophy; see Section 1.5). Soils and especially wetlands are massive carbon storage systems, so-called carbon sinks, that are natural (or artificial) pools of carbon-containing compounds (Włodarczyk, 2011), like dead plant material. Further carbon sinks are (deep) oceans, where CO<sub>2</sub> is solubilized, where (complex) carbon compounds are 'stored' (Lal, 2008).

This process is known as carbon sequestration, where carbon is temporarily deposited in the form of soil organic carbon (SOC), preventing its release as CO<sub>2</sub> into the atmosphere (Lal, 2004, 2008). Nevertheless, the CH<sub>4</sub> source potential of a system and, thus, CH<sub>4</sub> emission comes from methanogenesis in anaerobic layers.

### 1.3 The Anaerobic Food Chain and Methanogenesis

Besides anthropogenic sources for CH<sub>4</sub>, also natural/biological sources contribute to the global CH<sub>4</sub> emission budget. As mentioned, peatlands are a stockpile of carbon in the form of dead plant material decomposed slowly but continuously. And it is not just the carbon-rich peatlands where anaerobic degradation takes place. Independent of the environment, in the anoxic layers, carbon compounds are degraded, e.g., in landfills (Gurijala and Suflita, 1993), rice paddy soils (Watanabe and Kimura, 1995; Watanabe et al., 1999) and peatlands (Juottonen et al., 2012), converted to CH<sub>4</sub> and released into the atmosphere. In these environments, methanogenesis drives GHG emissions and global warming.

Generally, fermentation and, subsequently, methanogenesis occur in the deeper anaerobic soil layers, where little to no alternative electron acceptors e.g., nitrate, sulfate, iron or, manganese, are available (Gurijala and Suflita, 1993; Metje and Frenzel, 2007). Wherever fermentation occurs - and the metabolic capability in a consortium of microorganisms is present - complex carbon molecules, like cellulose, lignin, etc., are broken down into smaller, simpler, and more easily degradable carbon compounds by primary fermenters (Hydrolysis; see Figure 1.3; Chin et al., 1998; Conrad, 2002). Secondary fermenters, or 'syntrophs', feed on these various short-chain fatty acids (e.g., butyrate, propionate, lactate) producing, e.g., acetate, di-hydrogen (H<sub>2</sub>) and CO<sub>2</sub> (Drake et al., 2009; Liesack, 2000; Metje and Frenzel, 2007). The last step is catalyzed by strictly anaerobic methanogenic archaea (Woese et al., 1978) that either use acetate (acetoclastic methanogens) or CO<sub>2</sub> and di-hydrogen (hydrogenotrophic methanogens) to form CH<sub>4</sub> (see Figure 1.3). In the environment, acetoclastic methanogens majorly contribute (up to 60 %) to CH<sub>4</sub> production. The remaining is produced by hydrogenotrophic methanogens from CO<sub>2</sub> and H<sub>2</sub> (Conrad, 1999; Hatano, 2011; Le Mer and Roger, 2001). All methanogenic pathways use the methyl-co-enzyme M reductase in the last transformation step, forming CH<sub>4</sub> (Ellermann et al., 1988; McBride and Wolfe, 1971; Niu et al., 2018). Consequently, the methyl-co-enzyme M reductase subunit A gene (*mcrA*) encoding for the  $\alpha$  subunit of the methyl-co-enzyme M reductase has been used as a molecular marker for methanogens (Ho et al., 2015a; Juottonen et al., 2006, 2012). As CH<sub>4</sub> production plays a tremendous role in GHG emission and

global warming, even more important is the biological counterpart, the (aerobic)  $\text{CH}_4$  oxidation performed by methane oxidizing bacteria (MOB).

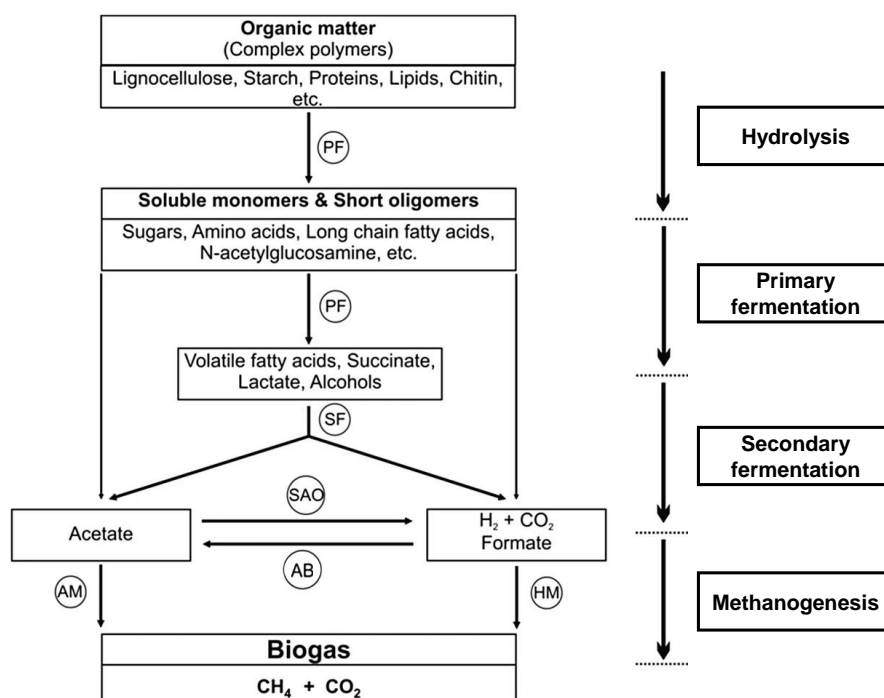


**Figure 1.3** Simplified scheme of the anaerobic degradation of complex organic matter to  $\text{CH}_4$  and  $\text{CO}_2$ . PF: Primary fermenters, SF: Secondary fermenters (Syntrophs), SAO: Syntrophic acetate fermenters, AB: Acetogenic bacteria, AM: Acetogenic methanogens, HM: Hydrogenotrophic methanogens. Modified from Liebetrau et al. (2019).

## 1.4 Anaerobic Methanotrophy

The produced  $\text{CH}_4$  from methanogenesis can be metabolized under anoxic conditions, i.e., in the anaerobic oxidation of methane (AOM) performed by anaerobic methanotrophs (ANME). Different electron acceptors besides oxygen ( $\text{O}_2$ ) are known by now to be used in AOM, e.g., sulfate, nitrate, and nitrite, as well as iron and manganese minerals (Beal et al., 2009; Bhattarai et al., 2019; Welte et al., 2016; Zhang et al., 2020). When AOM was first discovered, ANME were found to couple AOM to sulfate reduction in a potentially syntrophic consortium with sulfate-reducing bacteria (SRB) (Boetius et al., 2000; Orphan et al., 2001). It is hypothesized that the ANME and SRB share intermediates (i.e., acetate or formate) or electrons via direct electron transfer between cells (Bhattarai et al., 2019; McGlynn et al., 2015 and references therein). Later two groups of organisms were identified coupling nitrate or nitrite reduction to AOM: “*Candidatus Methanoperedens nitroreducens*” (archaea; nitrate reduction; Ha-

roon et al., 2013) and “*Candidatus Methyloirabilis oxyfera*” (bacteria; nitrite reduction; Ettwig et al., 2010). In “*Candidatus Methanoperedens nitroreducens*”, nitrate is used as an electron acceptor for reversed methanogenesis (Haroon et al., 2013), whereas in “*Candidatus Methyloirabilis oxyfera*”, it is hypothesized that O<sub>2</sub> is produced intracellularly by the conversion of NO to N<sub>2</sub> and O<sub>2</sub> (Ettwig et al., 2010). The produced O<sub>2</sub> is then used for CH<sub>4</sub> oxidation.

Organisms capable of AOM are found within the archaea and bacteria. Within the archaea, by now, three distinct groups were identified named as ANME-1 (related to Methanomicrobiales and Methanosarcinales), ANME-2 (related to Methanosarcinales), and ANME-3 (related to *Methanococoides* spp.) based on their 16S rRNA and *mcrA* gene phylogeny (Timmers et al., 2017 and Bhattarai et al., 2019 and references therein). Here, the reverse reaction of the methyl coenzyme M reductase may catalyze the oxidation of CH<sub>4</sub> with the addition of electron acceptors (Hallam et al., 2004; Haroon et al., 2013).

Bacteria within the *Methyloirabilis* genus of the novel NC10 phylum, e.g., “*Candidatus Methyloirabilis oxyfera*” are the only described organisms that potentially produce their O<sub>2</sub> intracellularly. Furthermore, they possess conventional particulate methane monooxygenase (pMMO) and methanol dehydrogenase (MDH) enzymes as known for aerobic CH<sub>4</sub> oxidizers (see Subsection 1.5.2, Ettwig et al., 2010).

Many metabolic pathways for AOM are under debate, and the lack of pure cultures within the NC10 phylum and within the ANME groups limit the knowledge on AOM. Thus, the focus of this thesis is set on the aerobic MOB (from here on termed as MOB), as they are ubiquitous and predominant active members in terrestrial bacterial communities. Furthermore, MOB were studied intensively throughout the last century in pure cultures, as well as simple or complex communities using MOB as a model system. Thus, their community composition/development, ecological traits, and stress response to disturbances are well documented (see Section 1.5 below).

## 1.5 Aerobic Methanotrophy

Even though wetlands, landfills and other environments are natural sources of CH<sub>4</sub>, the activity of the MOB counterbalances its emission. Being ubiquitously distributed in the environment, they are the main biological sink for CH<sub>4</sub> in nature. MOB, together with ANME, are a special guild of microorganisms, as it is the only group of organisms capable of metabolizing CH<sub>4</sub>. This particular feature made MOB a subject of countless experiments all around the world within the last decades.

### 1.5.1 History, Physiology and Taxonomy of Methanotrophs

**Discovery of the Methanotrophs** The MOB were first discovered in 1906 (Semrau et al., 2010), but it took quite a while until MOB could finally be isolated (Whittenbury et al., 1970b). These strains are characterized as obligatory dependent on CH<sub>4</sub> as their sole carbon and energy source (Semrau et al., 2011; Smith and Ribbons, 1970) and potentially evolved from methylotrophs (Kang et al., 2019), a group of organisms capable of metabolizing C<sub>1</sub> compounds. First electron-microscopic images revealed morphological peculiarities within the MOB, possessing intracellular membranes (Dalton, 2005; Davies and Whittenbury, 1970; Semrau et al., 2010; Smith and Ribbons, 1970). With further investigations and isolations, additional characteristics divide the MOB into two types depending on the carbon assimilation pathway, fatty-acid content, spore formation, and G+C content. Regardless of these distinct characteristics, organisms of all MOB were generally found to be gram-negative (Dedysh et al., 1998; Deutzmann et al., 2014; Eshinimaev et al., 2008; Hanson and Hanson, 1996; Heyer et al., 2005; Hoefman et al., 2014b; Islam et al., 2020; Mancinelli, 1995; Op den Camp et al., 2009; Vigliotta et al., 2007; Vorobev et al., 2011).

The initial conversion of CH<sub>4</sub> to methanol is catalyzed by enzymes within the group of monooxygenases, more specifically, methane monooxygenases (MMOs). The two known forms of the MMO are the particulate, membrane-bound form (pMMO) and the soluble, cytoplasmic form (sMMO). Most MOB possess the particulate form, some genera/species have both forms (e.g., *Methylococcus capsulatus*, and some *Methylocystis* sp., *Methylosinus trichosporium* and further; Semrau et al., 2018, 2010; Ward et al., 2004) and a few genera only have the soluble form of the MMO (*Methylocella*, *Methyloferula*; Chen et al., 2010; Dedysh et al., 2005; Semrau et al., 2018, 2010; Vorobev et al., 2011). These aforementioned findings corroborate the 'Type'-subdivision of the MOB.

**Type-dependent Classification of the Methanotrophs** At first, it was known that two main classes of bacteria harbored the MOB, the Gamma- and Alphaproteobacteria (see Table 1.1). Regarding their affiliation to these classes, as well as the above-mentioned characteristics, the MOB were grouped into Type I and Type II, respectively. Moreover, other characteristics, like internal membranes (see above), phospholipid fatty acid (PLFA) profiles, and the C-assimilation pathway separate Type I and Type II MOB. While the ribulose monophosphate pathway (RuMP)-cycle is used by the gammaproteobacterial MOB, the serin cycle is used for C-assimilation by alphaproteobacterial MOB (see Figure 1.4; Cai et al., 2016; Culpepper and Rosenzweig, 2012;

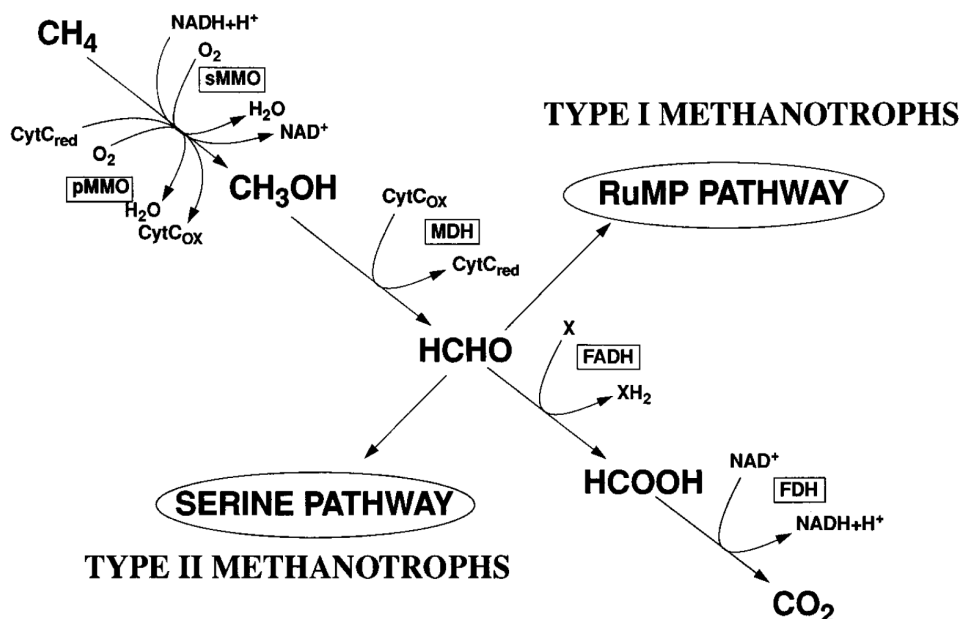


**Figure 1.4** Oxidation pathway of CH<sub>4</sub> to CO<sub>2</sub> of Type I and Type II MOB. Abbrev.: CytC, cytochrome c; FADH, formaldehyde dehydrogenase; FDH, formate dehydrogenase. From Hanson and Hanson (1996).

Eshinimaev et al., 2008; Hanson and Hanson, 1996; Knief, 2015; Zhu et al., 2016). PLFA chain length seemed to separate MOB well into the two types (Type I - 14C and 16C PLFAs; Type II - 18C PLFAs; Bodelier et al., 2009). However, there are specific MOB that do not fit this grouping - a Type II MOB containing 16C and 18C PLFAs (Dedysh et al., 2007) and a Type I MOB also containing 18C PLFAs (Heyer et al., 2005; Hirayama et al., 2014).

Independent of these inconsistencies in classification, Type I is further divided into subgroups, which are Ia (former Type I MOB), Ib (former Type X) MOB, and Ic, which can be distinguished by *pmoA* and 16S rRNA gene phylogeny, physiology, biochemistry, stress response, and morphology (see Figure 1.5, Culpepper and Rosenzweig, 2012; Ho et al., 2013a; Knief, 2015; Krause et al., 2010). Former Type X MOB, reclassified as Type Ib (Hoefman, 2013; Knief, 2015; Lüke, 2010), that also belong to the Gammaproteobacteria, use the RuMP pathway as well, but they also have low levels of ribulose-biphosphate carboxylase, an enzyme of the serine pathway (Culpepper and Rosenzweig, 2012; Semrau et al., 2010). Furthermore, Type Ic MOB use the RuMP pathway for carbon assimilation. These MOB were grouped dependent on their thermophilic and halophilic characteristics (Hirayama et al., 2014; Islam et al., 2020). MOB of Type Ib, Type II, and Verrucomicrobia (see below) were identified to possess the RubisCO, phosphoenolpyruvat carboxylase enzyme (serin cycle) or Calvin–Benson–Bassham (CBB) cycle, making these organisms capable of autotrophic CO<sub>2</sub>-fixation (Hanson and Hanson, 1996; Jahnke et al., 1999; Taylor, 1977; Taylor et al.,

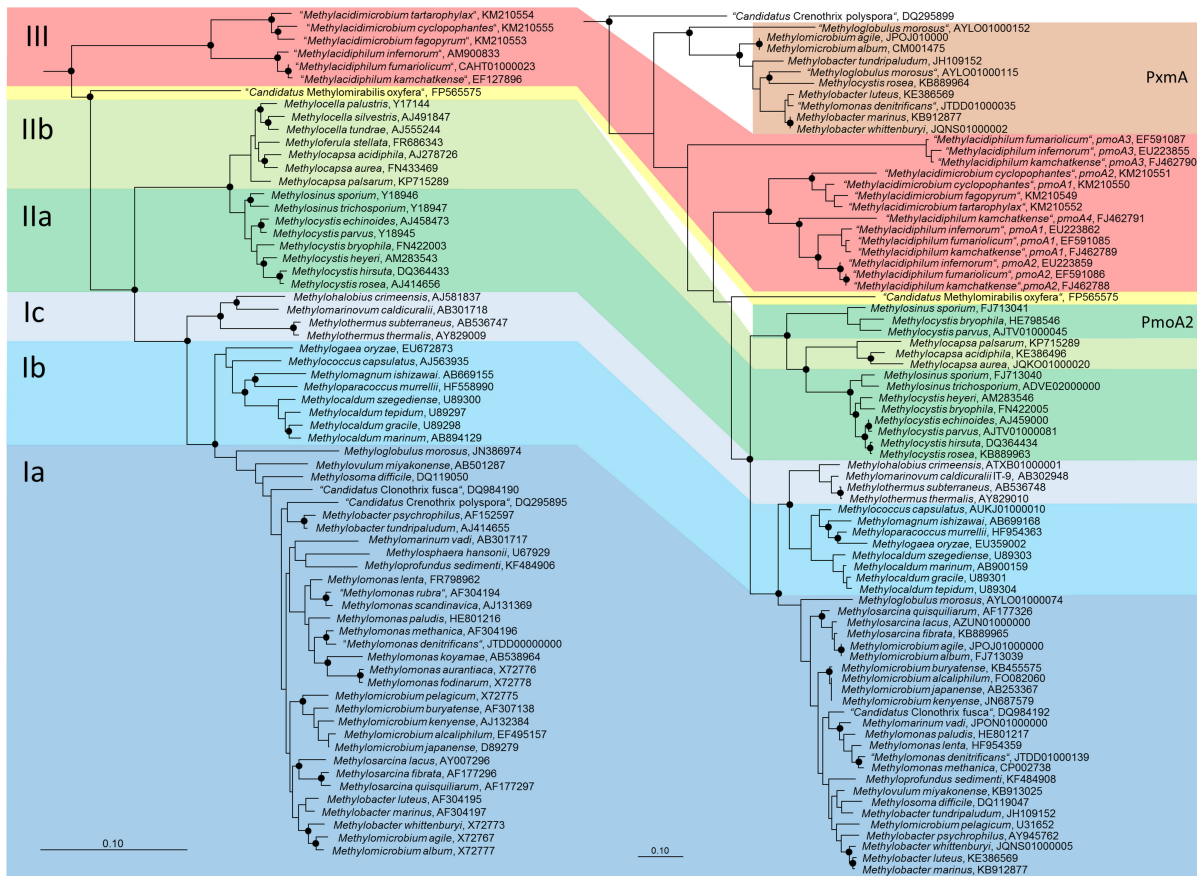


**Figure 1.5** Phylogenetic trees showing the phylogeny of MOB type strains based on 16S rRNA gene sequences (left tree) and PmoA sequences (right tree). From Knief (2015).

1981; Templeton et al., 2006; Vorobev et al., 2011).

First discovered 2007 by three research groups in parallel, verrucomicrobial MOB are extremely acidophilic (Mohammadi et al., 2017; Op den Camp et al., 2009; Sharp et al., 2014, 2012). The first verrucomicrobial MOB isolates were named '*Acidimethylosilex fumarolicum*' strain SolV (Pol et al., 2007), '*Methylokorus infernorum*' strain V4 (Dunfield et al., 2007), and '*Methyloacida kamchatkensis*' strain Kam1 (Islam et al., 2008) potentially all representing the same genus (Op den Camp et al., 2009) and were later renamed as *Methylacidiphilum infernorum* V4T, *Methylacidiphilum fumarolicum* SolV and *Methylacidiphilum kamchatkense* Kam1 of the family Methylacidiphilaceae (Op den Camp et al., 2009). Up to then, no MOB was found to be acid-tolerant below pH 4 (Dedysch et al., 1998), and only a few thermotolerant MOB grew beyond 60°C (Op den Camp et al., 2009; Tsubota et al., 2005). Within the phylum of Verrucomicrobia, there is the family of Methylacidiphilaceae that consists of the two genera *Methylacidiphilum* and *Methylacidimicrobium*, often referred to as Type III (see Table 1.1, Figure 1.5, Islam et al., 2020; Knief, 2015). These organisms do not use the RuMP pathway for carbon



**Table 1.1** Taxonomic classification of proteobacterial and verrucomicrobial MOB.

MOB type	Family	Genus
<b>Gammaproteobacteria</b>		
Ia	Methylomonadaceae	<i>Methylobacter</i> , <i>Methylomicrobium</i> , <i>Methylomonas</i> , <i>Methylosphaera</i> , <i>Methylosarcina</i> , <i>Methylosoma</i> , <i>Methylovulum</i> , <i>Methyloprofundus</i> , 'Candidatus Clonothrix'
Ib	Methylococcaceae	<i>Methylocaldum</i> , <i>Methylococcus</i> , <i>Methyloparacoccus</i> , <i>Methyloglobulus</i> , <i>Methylogaea</i>
Ic	Methylothermaceae	<i>Methylohalobius</i> , <i>Methylothermus</i> , <i>Methylomarinovum</i>
<b>Alphaproteobacteria</b>		
IIa	Methylocystaceae	<i>Methylosinus</i> , <i>Methylocystis</i>
IIb	Beijerinckiaceae	<i>Methylocella</i> , <i>Methyloferula</i> , <i>Methylocapsa</i>
<b>Verrucomicrobia</b>		
III	Methylacidiphilaceae	<i>Methylacidiphilum</i> , <i>Methylacidimicrobium</i>

References: Deng et al., 2013; Deutzmann et al., 2014; Geymonat et al., 2011; Gilbert et al., 2000; Heyer et al., 2005; Hirayama et al., 2014; Hoefman, 2013; Hoefman et al., 2014b; Islam et al., 2020; Knief, 2015; Liu et al., 2017; Op den Camp et al., 2009; Orata et al., 2018; Semrau et al., 2010; Tavormina et al., 2015; Theisen et al., 2005; Trotsenko and Murrell, 2008; Vigliotta et al., 2007; Whittenbury et al., 1970b

assimilation and internal membranes are missing, even though pMMO is expressed (Islam et al., 2008; Pol et al., 2007). As well, these organisms possess a full CBB cycle for CO<sub>2</sub> fixation (Dunfield et al., 2007; Op den Camp et al., 2009). The findings of such 'out-of-the-box' MOB weaken the established classification system.

As mentioned before, there are some characteristics that are no longer exclusively found in one of the groups. Thus the major carbon fixation pathway might be the only distinctive feature (Knief, 2015). To date, reclassification, e.g., on genome level (Orata et al., 2018), or abolition of this system is discussed, as more and more characteristics of the different types overlap and grouping may cause confusion (Op den Camp et al., 2009).

## 1.5.2 Metabolism and Carbon Assimilation Pathways

As the MMOs and the carbon assimilation pathway are decisive for MOB proliferation in the environment and, as just introduced, are of greater importance for MOB classification, the most prominent pathways are introduced in the following.

The two MMOs catalyze the first step in CH<sub>4</sub> metabolism, the energy-demanding transformation of CH<sub>4</sub> to methanol. As CH<sub>4</sub> is the most inert hydrocarbon, the chem-

ical reaction of  $\text{CH}_4$  to methanol is challenging (Arakawa et al., 2001; Lieberman and Rosenzweig, 2004; Periana et al., 2004), and MOB are of great interest for the chemical industry, as MOB perform this reaction at ambient temperatures. Most MOB only possess the pMMO, while some possess both the pMMO and soluble methane monooxygenase (sMMO), whereas few only use the sMMO for  $\text{CH}_4$  turnover.

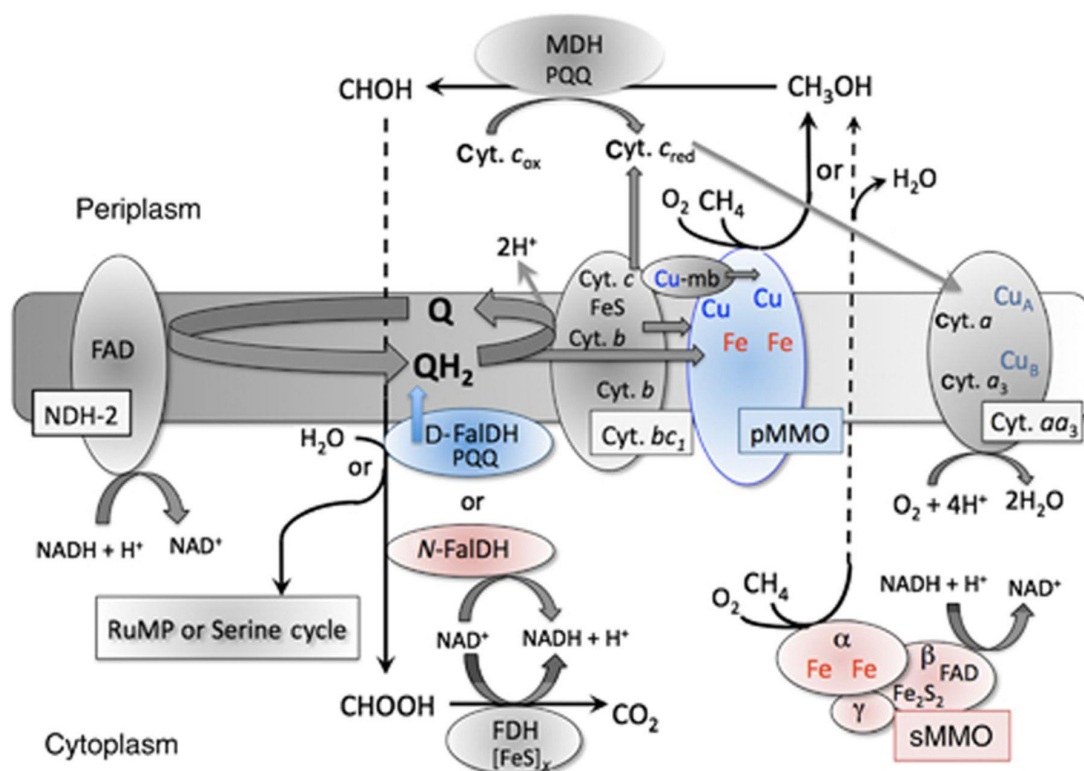


**Figure 1.6** Potential  $\text{CH}_4$  oxidation pathway in cells cultured under high and low Cu conditions. Proteins showing positive (shown in blue) or negative (shown in red) effect on increased Cu concentrations. Cu, copper; Cyt, cytochrome; D-FalDH, dye-linked/quinone-linked formaldehyde dehydrogenase (positive effect); FDH, formate dehydrogenase; N-FalDH, NAD(P)-linked formaldehyde dehydrogenase (negative effect); NDH-2, type 2 NADH dehydrogenase; pMMO, membrane-associated or particulate methane monooxygenase (positive effect); Q, ubiquinone; FAD, flavin adenine dinucleotide; MDH, methanol dehydrogenase; PQQ, pyrroloquinoline quinone (positive effect); sMMO, cytoplasmic or soluble methane monooxygenase (negative effect); RuMP, ribulose monophosphate. From Semrau et al. (2010)

**Particulate Methane Monooxygenase** The pMMO catalyzes the first reaction in MOB metabolism, which is  $\text{O}_2$  and nicotinamide adenine dinucleotide (NADH) or ubiquinone dependent (Hakemian and Rosenzweig, 2007; Kalyuzhnaya et al., 2015; Semrau et al., 2010). The pMMO is located in the cytoplasmic membrane of the MOB, as well as in the internal membrane stacks (Balasubramanian and Rosenzweig, 2007; Murrell, 2010; Semrau et al., 2010) and consists of three subunits ( $\alpha$ -subunit, PmoB, encoded

by *pmoB*;  $\beta$ -subunit, PmoA, encoded by *pmoA*; and  $\gamma$ -subunit, PmoC, encoded by *pmoC*) forming a trimer sub-unit structure ( $\alpha\beta\gamma$ )<sub>3</sub> (Balasubramanian and Rosenzweig, 2007; Culpepper and Rosenzweig, 2012; Semrau et al., 2010; Wang et al., 2017). While PmoB sub-unit partially consists of a soluble cytoplasmic domain, PmoA and PmoC sub-units are composed of transmembrane helices (Culpepper and Rosenzweig, 2012). The genes encoding the sub-units are located in the *pmoCAB* operon; usually, the MOB possess one to three copies of this operon (Gilbert et al., 2000; Miroshnikov et al., 2017; Op den Camp et al., 2009; Ward et al., 2004). The catalytic center in the active site in sub-unit PmoB is still unknown and highly discussed, but many researchers have agreed on a di-copper metal center (Balasubramanian and Rosenzweig, 2007; Balasubramanian et al., 2010; Culpepper and Rosenzweig, 2012). It was known before that copper plays an essential role in the expression of the pMMO, as experiments have shown no growth of only pMMO possessing MOB or no expression of pMMO in copper (Cu)-free media (Collins et al., 1991). The theory of the active site in PmoA or PmoB was corroborated by the finding that <sup>14</sup>C-labeled acetylene that fully inhibits CH<sub>4</sub> oxidation binds to either PmoA or PmoB (DiSpirito et al., 1992; Zahn and DiSpirito, 1996). Later, the *pmoB* sub-unit was found to contain the pMMO active site (Balasubramanian et al., 2010). Cu is not just a part of the active site in the pMMO; it is also a regulatory factor for the expression of either pMMO or sMMO (Murrell et al., 2000a; Murrell, 2010; Semrau et al., 2010; Stanley et al., 1983). Under Cu-limiting conditions, some MOB that possess both the pMMO and sMMO can express the sMMO-enzyme to retain CH<sub>4</sub> oxidation function. Additionally - and potentially to prevent methanol intoxication inside the cells - it is suggested that the MDH assembles with the pMMO complex (Balasubramanian and Rosenzweig, 2007; Culpepper and Rosenzweig, 2014).

In microbial ecology, the pMMO has become a molecular marker for MOB being present in almost all MOB (Kolb et al., 2003; McDonald and Murrell, 1997), besides *Methyloferula stellata* and *Methylocella silvestris* (Theisen et al., 2005; Vorobev et al., 2011), that is widely used to identify and quantify MOB. Corroborating the polyphyletic relation mentioned before, verrucomicrobial *pmoCAB* operons may stem from a different evolutionary origin (Op den Camp et al., 2009). Furthermore, it has been shown that some MOB possess an additional divergent *pmoCAB* operon, termed *pmoCAB2* or *pxmABC*, that encodes for a pMMO (pXMO/pMMO2) with different CH<sub>4</sub> oxidation kinetics compared to the pMMO (Baani and Liesack, 2008; Dunfield et al., 2002; Ricke et al., 2004; Tavormina et al., 2011; Tchawa Yimga et al., 2003). While both, pMMO1 and pMMO2 are active at CH<sub>4</sub> concentrations > 700 ppmv, only pMMO2 can oxidize CH<sub>4</sub> down at (circum-)atmospheric levels (Baani and Liesack, 2008). This is also re-

flected in the  $K_m$ -values of both enzymes being  $\sim 10$  times higher for pMMO1 compared to pMMO2 (Baani and Liesack, 2008; determined in pure cultures). Independent of their evolutionary origin or CH<sub>4</sub> affinity, pMMO genes are an important tool for analysis and identification of MOB.

**Copper and Copper Transport System - Methanobactin** Even before the identification of the Cu-containing active site of the pMMO, the importance of Cu for MOB was recognized (Burrows et al., 1984; Collins et al., 1991; Graham et al., 1993; Stanley et al., 1983). Cu was known to improve MOB activity in a certain concentration range but can also inhibit MOB activity outside this range (Graham et al., 1993). Some MOB possess a chalcophore that binds Cu-ions with high specificity, termed methanobactin. It is excreted by MOB for Cu uptake, potentially giving MOB an important advantage in nutrient/Cu-limited environments (Balasubramanian and Rosenzweig, 2008). Additionally, *Methylococcus capsulatus* expresses a Cu-binding MopE protein for highly specific Cu binding and uptake (Karlsen et al., 2003; Ve et al., 2012). Especially for MOB that possess both pMMO and sMMO, the Cu:biomass ratio is the decisive factor for MMO gene expression; when the Cu:biomass ratio exceeds a certain level, pMMO is expressed while under Cu-limitation (low Cu:biomass ratio), sMMO is expressed, potentially directly regulated by intracellular Cu-ions (Burrows et al., 1984; Nielsen et al., 1996, 1997; Stanley et al., 1983), or regulated by methanobactin acting as a signaling molecule (Balasubramanian and Rosenzweig, 2008; Farhan UI-Haque et al., 2015), a mechanism that is named 'copper switch'.

**Soluble Methane Monooxygenase** MOB that do not possess the genetic potential to express the pMMO use the sMMO for CH<sub>4</sub> oxidation. In MOB that possess both, sMMO expression is regulated by Cu availability. As for pMMO, the reaction here is also O<sub>2</sub> dependent but uses NADH as an electron carrier (See Figure 1.6). The sMMO is located in the cytoplasm and has a catalytic di-iron active center (Balasubramanian et al., 2010). The protein is expressed in the *mmoXYBZDC* operon with *mmoX* encoding the  $\alpha$ -, *mmoY* the  $\beta$ - and *mmoZ* the  $\gamma$ -sub-unit of the hydroxylase, arranged in a  $\alpha_2\beta_2\gamma_2$  configuration; *mmoB*, *mmoD*, and *mmoC* encode Protein B, and the nicotinamidadeninucleotidephosphat (NADPH)-dependent reductase unit, respectively (Murrell et al., 2000b; Semrau et al., 2010; Smith et al., 2010; Theisen et al., 2005; Wang et al., 2017). Besides small differences between the sMMO and the pMMO, like electron carrier, substrate specificity (Burrows et al., 1984), and CH<sub>4</sub> affinity (Lee et al., 2006), the two MMOs mainly perform the same transformation that is characteristic of the MOB. Independent of the MMO type, the dissimilatory carbon flow is similar in all MOB.

**Carbon Usage** In the dissimilarity pathway in MOB methanol is further oxidized by MDHs to formaldehyde via a cytochrome c-type electron acceptor (see Figure 1.6). Usually two types of MDHs are expressed in MOB; a calcium-dependent MDH and a lanthanide-dependent MDH (Gu et al., 2016; Krause et al., 2017). Both MDHs also play a role in MOB-heterotroph interactions (see Section 1.6). Next, formaldehyde is either assimilated (see below) or further oxidized to formic acid via a NAD<sup>+</sup>-linked formaldehyde dehydrogenase (FaLDH) (N-FaLDH; see Figure 1.6), a dye/cytochrome linked FaLDH (D-FaLDH; see Figure 1.6), or via a tetrahydromethanopterin/methanofuran pathway (DiSpirito et al., 2004). In the last step, formate is oxidized to CO<sub>2</sub>, which is then released into the atmosphere. This reaction is catalyzed by a NAD<sup>+</sup>-dependent formate dehydrogenase (FDH), an [FeS]<sub>x</sub>-cluster containing enzyme (See Figure 1.6; DiSpirito et al., 2004; Hanson and Hanson, 1996).

Carbon assimilation by MOB is performed via RuMP-pathway, Serin cycle, or CO<sub>2</sub>-fixation. Mainly Type I MOB, e.g., *Methylobacter sp.*, *Methyloglobulus sp.* and further (Deutzmann et al., 2014; Semrau et al., 2010), assimilate carbon via formaldehyde using the RuMP pathway being thermodynamically most favorable (Kalyuzhnaya et al., 2019). Here, formaldehyde is transformed to Hexulose 6-P and further to Glucose 6-P, which is then cleaved via Entner-Doudoroff or Embden-Meyerhof-Parnas pathway forming phosphotrioses (Trotsenko and Murrell, 2008). Pyruvate is then transformed to Acetyl-CoA and introduced into the tricarboxylic acid (TCA)-cycle for biomass formation (Cai et al., 2016; Fu et al., 2019). In the serin cycle, that is mainly used by Type II MOB, e.g., *Methylocella sp.* (Dedysh et al., 2000), *Methylosinus sp.* (Matsen et al., 2013) or *Methyloferula sp.* (Vorobev et al., 2011), carbon is assimilated from formic acid via the amino acid glycine that is then transformed to serin. With the cleavage of ammonia, trioses are formed that are modified to phosphotrioses which are then also channeled into the TCA-cycle via Acetyl-CoA as an intermediate (Cai et al., 2022; Trotsenko and Murrell, 2008). In some MOB - solely or additionally to the RuMP or serin pathway - the CBB cycle is used for carbon assimilation. These MOB express or have the genetic potential to express ribulose-1,5-bisphosphate carboxylase-oxygenase (RubisCO) that enables autotrophic growth via CO<sub>2</sub> fixation (Khadem et al., 2011; Taylor, 1977; Taylor et al., 1981; Vorobev et al., 2011). In Type I MOB, where CBB enzymes are less active, up to 15 % of cell carbon is derived from CO<sub>2</sub>, while in Type II up to 50 % of the cell biomass comes from CO<sub>2</sub> fixation (Trotsenko and Murrell, 2008). For longtime carbon storage alphaproteobacterial MOB form intracellular poly-β-hydroxybutyrate (PHB) granules (Hirayama et al., 2014; Hoefman et al., 2014b; Khmelenina et al., 2019; Vorobev et al., 2011). Besides carbon, nitrogen uptake is as well essential for the MOB with beneficial and detrimental effects.

**Nitrogen Uptake** Microorganisms have a demand for nitrogen e.g., for the synthesis of nucleic acids or proteins from amino acids. MOB have been shown to take up nitrogen in different forms, such as ammonium ( $\text{NH}_4^+$ ), nitrite, nitrate (Danilova et al., 2013; Geymonat et al., 2011), or di-nitrogen. Some MOB are diazotrophic, having the capability to fix gaseous di-nitrogen via nitrogenases (encoded by *nifH*; Danilova et al., 2013; Dedysch et al., 2000; Graham et al., 1993; Hirayama et al., 2014; Murrell and Dalton, 1983), covering MOB and potentially heterotrophic nitrogen demand in ombrotrophic environments, like peatlands (Ho and Bodelier, 2015; Larmola et al., 2014) or decaying wood (Mäkipää et al., 2018). Nevertheless, nitrogenases seem to be active in MOB only under N-limiting conditions, as N fixation has a high energy demand (Graham et al., 1993).

Far more ecologically important is the impact of  $\text{NH}_4^+$  salts on MOB. The addition (or presence) of nitrogen as  $\text{NH}_4^+$  salts reduces the  $\text{CH}_4$  uptake of the cells at certain concentrations (van Dijk et al., 2021), likely due to a concentration-dependent competition of  $\text{NH}_4^+$  and  $\text{CH}_4$  in the MMO active site (Nyerges and Stein, 2009; Semrau et al., 2010). It is still unclear if  $\text{NH}_4^+$  salts inhibit or enhance  $\text{CH}_4$  uptake, as no tipping point could be defined yet (van Dijk et al., 2021). Some studies show an increase in MOB population size and/or activity (Semrau et al., 2010). Other studies demonstrated the addition of  $\text{NH}_4^+$  salts or urea to rice paddy (Mohanty et al., 2006; Noll et al., 2008) and forest soils (Mohanty et al., 2006) favors the growth of Type I MOB over Type II, because these can be used primarily by Type I as a nitrogen source.

$\text{NH}_4^+$  is a concentration dependent competitive inhibitor for MMOs. When  $\text{NH}_4^+$  is metabolized by a MMO due to the structural similarity to  $\text{CH}_4$ , hydroxylamine, a highly toxic molecule, is formed. The capability of MOB to (1) further metabolize hydroxylamine to  $\text{NO}_x$  via hydroxylamine oxidoreductase, or (2) reduce hydroxylamine back to  $\text{NH}_4^+$ , are dependent on the genetic potential of certain MOB and are still up for debate (Stein et al., 2012). Recently, a study by Versantvoort and colleagues (2020) has shown that verrucomicrobial MOB express a hydroxylamine oxidoreductase converting hydroxylamine to  $\text{NO}$ ; which is then further oxidized to nitrite and finally nitrate (Mohammadi et al., 2017). With regard to a potential common ancestor of MOB and ammonia oxidizing bacteria (AOB), the metabolic potential necessary for the MOB to detoxify hydroxylamine strengthens this theory (Stein et al., 2012). But it is not just  $\text{NH}_4^+$  that can be metabolized besides  $\text{CH}_4$  as the finding of facultative MOB changed the dogma of  $\text{CH}_4$  being the only carbon and energy source.

**Facultative Methanotrophs** Although it has been assumed that MOB metabolize  $\text{CH}_4$  as their 'sole carbon and energy source' (Chen et al., 2007; Heyer et al., 2002;

Stanley et al., 1983; Vorobev et al., 2011), it was long proposed that MOB are capable to co-metabolize further carbon sources beside C<sub>1</sub> compounds and that MOB can even be facultative (Whittenbury et al., 1970b). With the identification of facultative MOB, this concept was proven (Dedysh et al., 2005).

Because of the large range of environments where MOB can be found (see Sub-section 1.5.3) and the wide variety of phylogenetic characteristics, some MOB can metabolize not just one-carbon compounds, like CH<sub>4</sub> and methanol, but can also metabolize, for example, short chain alkanes, like propane (Crombie and Murrell, 2014), or organic acids, like acetate, pyruvate or malate (Chen et al., 2010; Dedysh and Dunfield, 2010; Semrau et al., 2011, 2010). The unspecificity of the sMMO enables the MOB to break down and co-metabolize alkanes up to C-8, ethers, cyclic alkenes, or aromatic ring structures (Balasubramanian and Rosenzweig, 2007; Semrau et al., 2010), while pMMO can break down alkanes up to C-5 (Balasubramanian and Rosenzweig, 2007; Burrows et al., 1984; Dedysh and Dunfield, 2010). In cases of, e.g., acetate produced during fermentation of plant material in acidic peatlands, present facultative MOB may metabolize acetate preferentially, as it directly provides energy without the need for reductant supply, as required for CH<sub>4</sub> (Dedysh et al., 2005). Nevertheless, the MOB remain the only guild of microorganisms capable of metabolizing CH<sub>4</sub>, even though they may use other carbon sources additionally. Besides the discovered variety in carbon sources also different electron acceptors, apart from O<sub>2</sub> in MOB, were found to be used by ANME (see Section 1.4, Deutzmann and Schink, 2011; Knittel and Boetius, 2009, 2010; Timmers et al., 2017; Welte et al., 2016).

### 1.5.3 Habitat and Role of Aerobic Methanotrophs

**Ubiquity of Methanotrophs** MOB are ubiquitous microorganisms in the environment, occurring in terrestrial, marine and aquatic ecosystems, typically at oxic/anoxic interfaces (Hanson and Hanson, 1996; Knief, 2015; Reim et al., 2012). Here, the MOB, mainly living in the upper, oxic soil layers, metabolize up to 90 % of the CH<sub>4</sub> that is produced and released in the lower anaerobic soil layers from methanogenic archaea (Chen and Murrell, 2010; Conrad and Rothfuss, 1991; DiSpirito et al., 2016; Fechner and Hemond, 1992; Kalidass et al., 2015; Kallistova et al., 2005; Mancinelli, 1995).

To date, MOB communities in the environment are well studied. With the application of various methods (e.g., cultivation/isolation (Dedysh et al., 2005), CH<sub>4</sub> uptake (this thesis; Gupta et al., 2012; Ho et al., 2018, 2015b), gene specific (q)PCR (this thesis; Ho and Frenzel, 2012; Ho et al., 2018, 2015b, 2021; Kolb et al., 2003; Reim et al., 2012), DGGE (Chen et al., 2007; Horz et al., 2001; Rietl et al., 2017; Sherry et al.,

2016), stable-isotope probing (SIP) (this thesis; Cébron et al., 2007a,b; Gupta et al., 2012; He et al., 2012c, 2015; Sultana et al., 2019), (T)RFLP (Horz et al., 2001; Reim et al., 2012; Uz et al., 2003), PLFA profiling (Bodelier et al., 2009; He et al., 2015; Ho et al., 2019b), messenger ribonucleic acid (mRNA) based micro-arrays (Cébron et al., 2007a; Ho et al., 2013b; Kumaresan et al., 2011), genome and amplicon sequencing (this thesis; Ho et al., 2020; Sultana et al., 2019; Ward et al., 2004), co-occurrence networks (this thesis; Ho et al., 2020)) MOB or MOB communities could be identified - or isolated - from a plethora of environments. Being ubiquitous in the environment, MOB communities are found in e.g., peatlands (this thesis; Dedysh, 2009; Dedysh et al., 2007, 1998; Deng et al., 2013; Vorobev et al., 2011; Wieczorek et al., 2011), rice paddy soils (this thesis; Ho et al., 2011b, 2013b, 2016b, 2020, 2018; Noll et al., 2008; van Dijk et al., 2021; Zhu et al., 2020), flooded sediments / river sediment / marine sediment (this thesis; Deutzmann et al., 2014; Sherry et al., 2016; Tavormina et al., 2015), landfills (this thesis; Kallistova et al., 2005; Kumaresan et al., 2011; Mancinelli, 1995; Uz et al., 2003), soda lakes / alkaline thermal springs (Eshinimaev et al., 2008; Islam et al., 2020), upland soils (Ho et al., 2019b), slurry surface crusts (Duan et al., 2017), natural gas seeps (Ul-Haque et al., 2019), plant surfaces (Iguchi et al., 2012, 2013), masonry (Kussmaul et al., 1998) along with others. This huge variety of MOB harboring environments is characterized by diverse physico-chemical characteristics to which the MOB have adapted. Ranging from psychrophilic environments, where MOB were identified growing at 5 - 20°C (Berestovskaya et al., 2002; Dedysh et al., 2007; Sherry et al., 2016; Vorobev et al., 2011), mesophilic environments (this thesis; Dedysh et al., 2007; Deutzmann et al., 2014; Hoefman et al., 2014b; Zhu et al., 2020) up to thermophilic environments, where proteobacterial and verrucomicrobial MOB are found active and growing up to ~ 60°C (Islam et al., 2020; Sherry et al., 2016; Tsubota et al., 2005). Besides temperature, pH plays a major role in many environments, from highly acidic environments (pH < 5; Dunfield et al., 2007; Pol et al., 2007) to alkaline soda lakes (pH < 9.3; Eshinimaev et al., 2008; Islam et al., 2020) MOB are found to be active. The importance of MOB as biofilters in various CH<sub>4</sub> emitting environments, for example in rice paddy fields or wetlands is well known.

**Methanotroph Survival Strategies and Environmental Stressors** Many natural and anthropogenic stressors influence the MOB, their surrounding and their associated community. As methanotrophy is an essential factor in GHG reduction, the impact of such stressors is of tremendous importance for the climate and, thus, of high research interest. Various environments that harbor MOB have different physico-chemical characteristics but are also affected by different / specific (re-occurring) stressors. During



the last decades, many natural and anthropogenic stressors of ecosystem-related relevance have been investigated. Natural and anthropogenic stressors, e.g., salinity / pH (Deng et al., 2017; Ho et al., 2018; Sherry et al., 2016), starvation in terms of CH<sub>4</sub> and/or O<sub>2</sub> availability (Benstead and King, 1997; Tavormina et al., 2017; Walkiewicz et al., 2018), drought / water availability (this thesis; Ho et al., 2016b), heat stress (Ho and Frenzel, 2012; Ho et al., 2016b), artificial / natural fertilization (Ho et al., 2020), land use change, perturbation and habitat destruction (this thesis; Eusufzai et al., 2010; Kumaresan et al., 2011; Liu et al., 2017; Meyer et al., 2017; Pérez-Valera et al., 2017; Reumer et al., 2018), plant growth (Eller and Frenzel, 2001), predation / virulence (Lee et al., 2021; Murase and Frenzel, 2007, 2008) or animal grazing / perturbation (Héry et al., 2008; Li et al., 2020; Rietl et al., 2017; Wang et al., 2022) were found to influence the MOB, their associated community or the soil community in general. But it is not just the impact of the stressors on the community that is important and needs to be considered but also the recovery of the (MOB) community and the legacy of the exposure to stress that shapes the restoration (or loss) of the previous soil community and function (Jurburg et al., 2017; Krause et al., 2018). To overcome and survive these stressors, the MOB have developed certain life strategies.

Forming cysts or cyst-like structures is one of the mechanisms of MOB to overcome stressor impacts or to resist them (Whittenbury et al., 1970a,b), maintaining the system's original stable state (Loreau et al., 2002). Resistance is a key mechanism for MOB to withstand the perturbation caused. In ecology, a stable state of a system is hard to define, as continuous natural changes influence the system (Griffiths and Philippot, 2013). Recovery of activity of a system is thought to indicate if a (bacterial) community has recovered, indicating a system has returned to a stable state (Girvan et al., 2005; Gunderson, 2000; Ives and Carpenter, 2007) and soil functions have recovered, even though ecological parameters, e.g., bacterial community composition may have changed. Functional redundancy drives this recovery in activity as factors, e.g., bacteria of a certain function that may have been depleted during perturbation, are buffered by different properties, like other bacteria that can perform the same task (functionally redundant) but could not have competed for these ecological niches (Ho et al., 2011b). Besides resistance for organisms to stressors, the inactive or dormant seed bank community, which is formed by the soil legacy, is one of the main drivers of restoration of soil activity and function after stressor impact (Eller et al., 2005; Ho et al., 2016b). As well, the response of surviving organisms rapidly growing back to / beyond their starting abundance driven by the nutrient availability of e.g., dead organisms (Ho et al., 2016b), drives soil functional resilience. The MOB have developed different life strategies making them well adapted for various environments and the

consequent stressors. These traits make them perfect model organisms to study the effect of natural or anthropogenic stressors on the MOB and their interactome.

## 1.6 The Methanotrophic Interactome

Besides abiotic characteristics, like soil physicochemical parameters and nutrient concentrations influencing the MOB (van Grinsven et al., 2021a,b), they can also be influenced by their biotic surrounding. 'No methanotroph is an island' perfectly describes how MOB live and survive in the environment. To date, there are numerous studies describing interactions of MOB with non-MOB / heterotrophic organisms.

MOB, being a subgroup of methylotrophs, catalyze the reaction from  $\text{CH}_4$  to methanol. Methanol is a small  $\text{C}_1$  molecule that can easily penetrate cell walls, which makes MOB constantly, but passively, excreting methanol (Krause et al., 2017). Here, methylotrophs come into play, as these organisms are capable of methanol metabolism (Chistoserdova, 2011; Chistoserdova et al., 2009; Lidstrom, 2006). Thus MOB and methylotrophs or other organisms capable of methanol metabolism often co-occur in environmental niches, forming trophic interactions (Krause et al., 2017; Lueders et al., 2004b; van Grinsven et al., 2021b). It has been shown that heterotrophic organisms can also influence MOB activity (Ho et al., 2014; Iguchi et al., 2011; Jeong et al., 2014; Veraart et al., 2018) or even manipulate MOB to increase methanol excretion (Krause et al., 2017). But it is not just the MOB that passively feed other organisms. Heterotrophs may provide essential vitamins and co-factors for the MOB, increasing their activity (Iguchi et al., 2011; Rani et al., 2021). Ho and colleagues (2014) have shown that in pure cultures MOB activity increases with heterotrophic richness. As most MOB attach to soil particles (Priemé et al., 1996) and some of them are non-motile (Bowman, 2006; Dedysh et al., 2007; Dunfield et al., 2002), the interaction is often locally restricted. In short, MOB may cluster together with interacting organisms in general - not just methylotrophs - exchanging carbon and co-factors or manipulating their activity (Rani et al., 2021; van Grinsven et al., 2021b), corroborating the idea that heterotrophs play a significant role in MOB life. But there are not only positive interactions in the environment, as predators have been shown to 'hunt' for MOB (Lee et al., 2021; Murase and Frenzel, 2008). *Bdellovibrio sp.* and members of Myxococcales are known to graze on the MOB. In summary, these interacting MOB and non-MOB / heterotrophic organisms are defined as the MOB interactome, as organisms co-occurring more than by chance driven by the carbon derived from  $\text{CH}_4$  provided by the MOB (Ho et al., 2016a).

## 1.7 Hypothesis and Aim of the Project

MOB are found ubiquitously in the environment, being intensively studied throughout the last century. Nevertheless, few studies have taken the heterotrophic/non-methanotrophic organisms as drivers of MOB proliferation into account. This thesis investigates not just the importance of the MOB in different CH<sub>4</sub> emitting habitats but also considers interacting heterotrophs, more precisely, the MOB interactome, as a relevant determinant regulating community functioning. The focus of the following studies lies on the aerobic MOB used as a model system, as their community and stress response to physical and chemical disturbances, as well as ecological traits, are extensively documented (see Chapter 1).

**General hypothesis:** The MOB interactome is driven by biotic and abiotic parameters equally, forming similar trophic interactions dependent on the soil biological and physico-chemical properties. Disturbances may alter the composition of the MOB interactome while soil function (here, methanotrophy) remains.

**Identification of the MOB interactome in different habitats - Chapter 3** To map the MOB interactome over time and space in CH<sub>4</sub> emitting habitats, deoxyribonucleic acid (DNA)-SIP coupled co-occurrence network analysis was applied. Using this approach, MOB and non-MOB trophic interactions were identified from diverse habitats, enabling comparison of the CH<sub>4</sub>-driven interaction network across space and over time.

**Hypothesis:** The MOB interactome, including intra-MOB interaction, forms a (tight) network of specific interacting microorganisms in space and time.

**Response of the MOB interactome to a mild stressor - Chapter 4** To determine the relevance of the MOB interactome following a single disturbance event i.e., desiccation and CH<sub>4</sub> starvation, DNA-SIP coupled co-occurrence network analysis is applied. This strategy will allow the direct association of putative interacting microorganisms in the CH<sub>4</sub>-derived food web to how a close-knit community may confer resilience against stress.

**Hypothesis:** CH<sub>4</sub> oxidation is moderately affected by the structure of the MOB-associated heterotrophs in an MOB interactome rather than MOB abundance and composition following mild disturbances.

**Response of the MOB interactome to a severe stressor - Chapter 5** To determine how the MOB interactome may re-establish after restoration of an excavated peatland a pairwise comparison of a pristine and a restored peatland was conducted. Using DNA-SIP coupled to a co-occurrence network analysis, the complexity of the CH<sub>4</sub>-driven interaction networks were compared.

**Hypothesis:** CH<sub>4</sub> oxidation is strongly affected by the structure of the MOB-associated heterotrophs in an MOB interactome rather than MOB abundance and composition following severe disturbances.

**Identification of parameters affecting re-colonization - Chapter 6** MOB community development is dependent on abiotic and biotic parameters, driving CH<sub>4</sub> oxidation in various habitats. In a soil microcosm incubation a sterilized fraction of a paddy and upland soil are reciprocally inoculated with the corresponding unsterilized soil to analyze recolonization, MOB community development and CH<sub>4</sub> oxidation potential dependent on the soil physico-chemical parameters independent of the starting community.

**Hypothesis:** Soil CH<sub>4</sub> uptake potential is mainly regulated by abiotic than biotic determinants (e.g., community composition) in MOB communities independent on the starting community.

## **Chapter 2**

# **Novel Experimental Strategy - SIP-coupled Co-occurrence Network Analysis**

## 2.1 Background

Due to their ability to survive and proliferate in various habitats, introducing carbon into soil systems via cross-feeding, and their ability to reduce GHG emissions (see Chapter 1), MOB have been used as model organisms in innumerable experiments before. Throughout the last decades, researchers have more and more unraveled the importance of the non-MOB for the MOB (Ho et al., 2016a, 2014, 2020; Krause et al., 2017). Experiments in pure and mixed cultures were applied, confirming the significance of the MOB interaction partners for the MOB (Ho et al., 2014; Jeong et al., 2014; Veraart et al., 2018). In soil systems, it is anticipated that MOB interaction partners can support the MOB in terms of stress response to restore soil function (see Section 1.6). Co-occurrence networks are used to infer (trophic) interactions between organisms (this thesis; Barberán et al., 2012; Berry and Widder, 2014) or to identify the core community of a system (Murdock et al., 2021; Purkamo et al., 2016), but often these interactions were inferred directly from sampled soil (e.g., Barberán et al., 2012; Cheng et al., 2021; de Vries et al., 2018; Pérez-Valera et al., 2017; Zhang et al., 2019). In these studies, all organisms, independent of their activity/dormancy are probably introduced into the network, increasing the number of random/spurious interactions.

In the following studies, a novel approach has been applied, combining SIP with a co-occurrence network analysis to directly relate found correlations to the actively growing community, corroborating the meaningfulness of the potential trophic interactions identified in the following experiments. The experiments were conducted to investigate the impact of stressors on microbial communities and to analyze how trophic interactions in communities from different CH<sub>4</sub>-emitting environments are structured using methanotrophy as a model system. Below, the theoretical background to SIP and the co-occurrence networks is introduced.

## 2.2 Stable Isotope Probing

SIP is a well established method in microbiology that has been used for more than 20 years (e.g., Cébron et al., 2007a; Chen et al., 2008b; Hetz and Horn, 2021; Lueders et al., 2004b; Radajewski et al., 2000 and further). In SIP, using, e.g., <sup>13</sup>C-labeled carbon molecules, the assimilating organisms can be labeled and later identified. Various targets (i.e., cell components) for SIP have been tested and successfully used, like proteins, PLFAs, ribonucleic acid (RNA), and DNA (Boschker et al., 1998; Dörr et al., 2010; Jehmlich et al., 2016; Manefield et al., 2004; Neufeld et al., 2007a; Radajewski et al., 2003; Vogt et al., 2016). In DNA-SIP, <sup>13</sup>C-labeled substrate is fed to systems

to be metabolized by microorganisms that incorporate the  $^{13}\text{C}$  into their DNA during replication. In contrast to RNA-SIP, where it is sufficient for organisms to be active, producing ribosomal ribonucleic acids (rRNAs) or mRNAs, in DNA-SIP, the organisms have to be active and growing. Thus, incubation times for DNA-SIP have to be well-adjusted to have at least two replications of the target organisms. In short, DNA can be extracted from the incubations; then  $^{12}\text{C}$  and  $^{13}\text{C}$  DNA are separated in isopycnic density gradient centrifugation and afterwards fractionated. Heavy and light fractions can be determined via, e.g., DNA concentration determination or real-time quantitative polymerase chain reaction (qPCR) targeting 16S rRNA gene or functional genes, and fractions with the highest gene abundance can be sequenced to investigate the labeled community. A more detailed explanation of the proceeding is given in Neufeld et al. (2007b), Lueders (2010), and Dunford and Neufeld (2010) (see also chapters 3, 4, and 5 in the respective 'Methods and Materials' sections). SIP alone can already improve the information about the active community in soil systems, omitting the 'background' microbial organisms that are dead or dormant, or simply not active. The labeled community can be further analyzed using a co-occurrence network analysis to deduce microbial interaction.

## 2.3 Network Construction

Here, the focus is set on the MOB in various habitats investigating their interactome. The MOB interactome is a consortium of microorganisms that co-occur more than by chance, as indicated by a strong positive or negative correlation dependent on  $\text{CH}_4$ -derived carbon. DNA-SIP pre-selects for the actively growing organisms that can metabolize the labeled  $^{13}\text{C}$ - $\text{CH}_4$  and cross-feed to interaction partners at higher trophic levels. In SIP, unlabeled  $^{12}\text{C}$ -DNA is separated from heavier  $^{13}\text{C}$ -DNA that is enriched with  $^{13}\text{C}$  carbon derived from  $^{13}\text{C}$  metabolites in actively growing organisms. This procedure reduces the chance for spurious correlation due to the exclusion of dormant/inactive cells that may randomly form strong correlations. Often, co-occurrence networks are derived from extracted nucleic acids being directly applied to co-occurrence network construction after sequencing, as mentioned before. Only a few have taken the improvement of SIP before co-occurrence network construction into consideration (e.g., Li et al., 2018; Sun et al., 2018). In this thesis, experiments were conducted shedding light on how DNA-SIP coupled co-occurrence network construction improves the identification of potential trophic interactions in various  $\text{CH}_4$ -emitting habitats and how reformation or restoration of trophic interaction networks after stressor impact indicate changes in community stability.

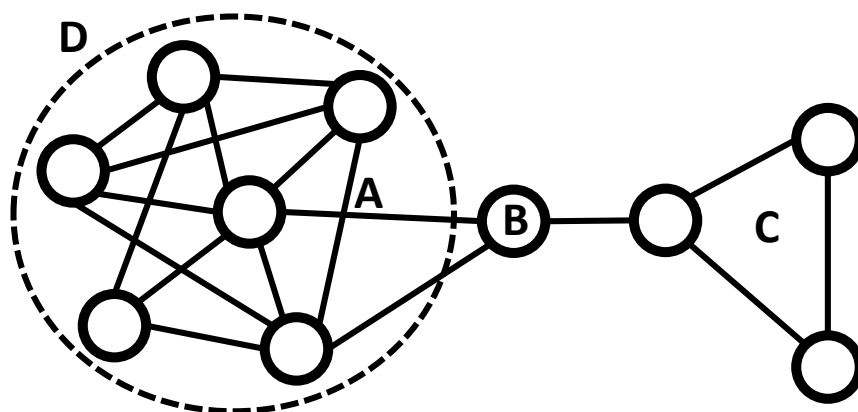


**Figure 2.1** Simplified network with edges (A), nodes (B), as well as nodes of high betweenness centrality (B), triangle node connections forming clusters (C) and highly connected modules (D). Parameters are described in Table 2.1.

In interaction networks, positive interactions are referred to as beneficial interactions, e.g., mutualism or syntrophy, sharing nutrients, co-factors, and carbon sources via cross-feeding, while negative correlations indicate competition between taxa or predation (see Section 1.6) depicted by edges between nodes (see 'A' and 'B' in Figure 2.1). Highly connected modules of nodes (Modularity; see Table 2.1) may have specific soil functions (Cao et al., 2022; Ravasz et al., 2002), potentially forming (sub-)communities (Newman, 2003). Important nodes inside the network, acting as a bridge between modules, are nodes of high betweenness centrality. If a single node is often crossed on a path within the network, the node might fulfill a specific function in the system that is not fulfilled by other taxa (Girvan and Newman, 2002; Newman, 2003; Poudel et al., 2016). A loss of such nodes might lead to a collapse of the network (Borgatti, 2005; Iyer et al., 2013). Nodes in the network tend to form triangle structures clustering together (Average clustering coefficient; see Table 2.1). This measure describes the local connectivity and can be associated with network robustness in terms of disturbances (Iyer et al., 2013; Li et al., 2017). Trophic interaction networks are the main focus of this thesis; as yet, little is known about how trophic interactions differ dependent on the environment (see Chapter 3) as well as on the influence of stressors on trophic interaction networks (see Chapter 4 and 5).



**Table 2.1** Description of network parameters

Parameter	Description	Depiction in Figure 2.1	Reference
<b>Edge</b>	The edges depict the nodes potential positive or negative interactions derived from the correlation.	A	
<b>Node</b>	The number of nodes describes the amount of operational taxonomic units (OTUs)/ amplicon sequence variants (ASVs) that form the network i.e., how many organisms are involved.	B	
<b>Degree / Average degree</b>	The degree and the average degree depict how many connections a node has in the network.		Newman, 2003
<b>Network diameter / Average path length</b>	How many nodes are connected forming the longest path in the network. The average path length depicts how many nodes are crossed on average between to random nodes in the network.		
<b>Modularity</b>	Modularity describes the tendency of nodes to form highly connected groups inside the network potentially providing a specific function.	D	Newman and Girvan, 2004, Newman, 2006, Ravasz et al., 2002
<b>Number of communities</b>	The number of communities then depicts the number of such highly connected modules in the network.		
<b>Betweenness centrality</b>	Betweenness centrality, similar to 'edge betweenness', depicts the count of how often a node is crossed on the path between random nodes in the network.		Freeman, 1977, Poudel et al., 2016
<b>Average clustering coefficient</b>	Nodes tend to form triangle structures in networks, clustering together. Newman (2003) describes this as 'the friend of my friend potentially is also my friend' forming a triangular node structure.	C	Newman, 2003, Poudel et al., 2016

## Chapter 3

# The Methane-Driven Interaction Network in Terrestrial Methane Hotspots

Thomas Kaupper<sup>1</sup>, Lucas W. Mendes<sup>2</sup>, Anja Poehlein<sup>3</sup>, Daria Frohloff<sup>1</sup>, Stephan Rohrbach<sup>1</sup>, Marcus A. Horn<sup>1\*</sup>, Adrian Ho<sup>1\*</sup>.

Published in *Environmental Microbiome* (2022) 17:15

---

<sup>1</sup>Institute for Microbiology, Leibniz Universität Hannover, Herrenhäuser Str. 2, 30419 Hannover, Germany.

<sup>2</sup>Center for Nuclear Energy in Agriculture, University of São Paulo CENA-USP, Brazil.

<sup>3</sup>Department of Genomic and Applied Microbiology and Göttingen Genomics Laboratory, Institute of Microbiology and Genetics, George-August University Göttingen, Grisebachstr. 8, D-37077 Göttingen, Germany.

The published version can be found online:  
<https://doi.org/10.1186/s40793-022-00409-1>

## 3.1 Abstract

### Background

Biological interaction affects diverse facets of microbial life by modulating the activity, diversity, abundance, and composition of microbial communities. Aerobic CH<sub>4</sub> oxidation is a community function, with emergent community traits arising from the interaction of the CH<sub>4</sub>-oxidizers (MOB) and non-MOB. Yet little is known of the spatial and temporal organization of these interaction networks in naturally-occurring complex communities. We hypothesized that the assembled bacterial community of the interaction network in CH<sub>4</sub> hotspots would converge, driven by high substrate availability that favors specific MOB, and in turn influences the recruitment of non-MOB. These environments would also share more co-occurring than site-specific taxa.

### Results

We applied SIP using <sup>13</sup>C-CH<sub>4</sub> coupled to a co-occurrence network analysis to probe trophic interactions in widespread CH<sub>4</sub>-emitting environments, and over time. Network analysis revealed predominantly unique co-occurring taxa from different environments, indicating distinctly co-evolved communities more strongly influenced by other parameters than high CH<sub>4</sub> availability. Also, results showed a narrower network topology range over time than between environments. Co-occurrence pattern points to Chthoniobacter as a relevant yet-unrecognized interacting partner particularly of the gammaproteobacterial MOB, deserving future attention. In almost all instances, the networks derived from the <sup>13</sup>C-CH<sub>4</sub> incubation exhibited a less connected and complex topology than the networks derived from the <sup>unlabelled</sup>C-CH<sub>4</sub> incubations, likely attributable to the exclusion of the inactive microbial population and spurious connections; DNA-based networks (without SIP) may thus overestimate the CH<sub>4</sub>-dependent network complexity.

### Conclusion

We demonstrated that site-specific environmental parameters more strongly shaped the co-occurrence of bacterial taxa than substrate availability. Given that members of the interactome without the capacity to oxidize CH<sub>4</sub> can exert interaction-induced effects on community function, understanding the co-occurrence pattern of the CH<sub>4</sub>-driven interaction network is key to elucidating community function, which goes beyond relating activity to community composition, abundances, and diversity. More generally, we provide a methodological strategy that substantiates the ecological linkages between potentially interacting microorganisms with broad applications to elucidate the role of microbial interaction in community function.

## 3.2 Background

Microbial interactions are widespread, leading to a plethora of interdependent relationships with stimulatory and inhibitory effects on community function (D'Souza et al., 2018; Ho et al., 2014; Johnson et al., 2020; Morris et al., 2013). It is becoming evident that aerobic CH<sub>4</sub> oxidation is a community function, whereby microorganisms lacking the enzymatic repertoire to oxidize CH<sub>4</sub> are also relevant. These microorganisms (non-MOB) play a significant role, stimulating MOB activity and growth, and increasing MOB-mediated micropollutant degradation (Benner et al., 2015; Ho et al., 2014; Veraart et al., 2018). Interestingly, the accompanying non-MOB have also been implicated in the resilience of MOB activity during recovery from disturbances (García-Contreras and Loarca, 2021; Kaupper et al., 2021a,b). Emergent properties may thus arise from the interaction of the MOB and non-MOB, both constituting the “MOB interactome” defined here as the consortium of co-occurring microorganisms that can be tracked via the flow of <sup>13</sup>C-CH<sub>4</sub> from the MOB (primary consumers) to other microorganisms in the soil food web (Ho et al., 2016a; Kaupper et al., 2021b).

Microbial interactions in complex communities, including the MOB interactome, have been explored using a co-occurrence network analysis based on specific genes (e.g., 16S rRNA, 18S rRNA genes) amplified from isolated nucleic acids (DNA, RNA) (Barberán et al., 2012; Ho et al., 2020; Li et al., 2021; Peura et al., 2015; Rossmann et al., 2020; Tripathi et al., 2016; Williams et al., 2014). Microbial taxa that are positively correlated in the network analysis can be interpreted as having complementary roles, sharing the same habitat niche, or are driven by cross-feeding (Barberán et al., 2012; D'Souza et al., 2018; Morris et al., 2013; Peura et al., 2015; Zelezniak et al., 2015), whereas negative correlations are attributable to competing taxa, predation, or niche partitioning (Chang et al., 2021; Dann et al., 2019; Ghoul and Mitri, 2016; Johnson et al., 2020). The aerobic MOB thrive in the presence of other organisms, forming (mutually) beneficial associations (e.g., receiving essential vitamins; Iguchi et al., 2011), as well as adverse relationships (e.g., selective predation by protists; Murase and Frenzel, 2008) with their biotic environment. These interactions can be species-specific (Iguchi et al., 2011; Stock et al., 2013; Veraart et al., 2018), underscoring the relevance of the physiology, and ecological traits inherent to diverse MOB in selecting for interacting partners, influencing the membership of the MOB interactome. Accordingly, the aerobic MOB belong to Gamma- / Alpha-proteobacteria and Verrucomicrobia, with the active verrucomicrobial MOB typically detected in acidic and geothermal environments (e.g., peatlands, volcanic and geothermal soils; Kaupper et al., 2021a; Schmitz et al., 2021; Sharp et al., 2014). These MOB can be distinguished based on their physiology,

including C-assimilation pathway and substrate utilization (e.g., facultative methanotrophy) and PLFA profile, among other distinct ecological characteristics (Dedysh and Dunfield, 2011; Guerrero-Cruz et al., 2021; Praeg et al., 2021; Trotsenko and Murrell, 2008; Ul-Haque et al., 2019). In terrestrial ecosystems, the aerobic MOB play a crucial role as a CH<sub>4</sub>-biofilter at oxic-anoxic interfaces where they consume a large portion of CH<sub>4</sub> produced before being emitted into the atmosphere (Reim et al., 2012), in addition to being a CH<sub>4</sub> sink in well-aerated soils (Ho et al., 2019b; Shrestha et al., 2012; Täumer et al., 2021). Besides the MOB and interaction with methylotrophs (Krause et al., 2017; van Grinsven et al., 2021a), very little is known of the organization (over space and time), and other constituents of the MOB interactome despite their relevance in modulating community function.

Here, we elaborate on the CH<sub>4</sub>-driven interaction network in naturally-occurring complex communities from widespread CH<sub>4</sub> hotspots (pristine/restored ombrotrophic peatlands, and paddy, riparian, and landfill cover soils). Considering that a high substrate (CH<sub>4</sub>) availability favors gammaproteobacterial MOB (e.g., *Methylobacter*, *Methylosarcina*; Ho et al., 2013a; Krause et al., 2012; Reim et al., 2012), in turn influence the recruitment of the non-MOB, we hypothesize that members of the MOB interactome from these environments would converge, having more shared than site-specific co-occurring taxa. To address our hypothesis, we applied SIP using <sup>13</sup>C-CH<sub>4</sub> coupled to a co-occurrence network analysis of the <sup>13</sup>C-enriched 16S rRNA gene, which not only enabled direct association of MOB activity to the network structure, but also provided a tangible link between the co-occurring taxa involved in the trophic interaction. This is in contrast to previous work deriving the networks from isolated nucleic acids (DNA and RNA), where relationships between taxa were inferred rather than demonstrated. Capitalizing on the SIP-network analysis, we determined different scales of organization, that is, consistency of co-occurring taxa that were nested among the metabolically active sub-population between environments (spatial scale), and over time (temporal scale) in the pristine peatland to assess the stability of the network structure during the incubation. Furthermore, comparing the <sup>unlabelled</sup>C- and <sup>13</sup>C-based networks, we postulate that the networks derived from the DNA isolated from the soils (i.e., <sup>unlabelled</sup>C-CH<sub>4</sub> incubation, without SIP) would be relatively more complex because of the inclusion of the metabolically inactive community members, non-trophic interactions, and weak or spurious correlations. Hence, we examined the applicability of our methodological approach, while shedding light on the spatial and temporal organization of the MOB interactome.

## 3.3 Results and Discussion

### 3.3.1 Aerobic Methanotrophy, and Environmental Variables Influencing the Metabolically Active Bacterial Community Composition

MOB activity was detected in all environments and was within the range expected for low-affinity CH<sub>4</sub> oxidation typical in CH<sub>4</sub> hotspots (Table 3.1; Conrad, 2009; Singh et al., 2010). In these environments, the MOB serve as a CH<sub>4</sub>-biofilter, consuming high concentrations of CH<sub>4</sub> generated in the anoxic soil layers before releasing into the atmosphere (Henneberger et al., 2012; Ho et al., 2013a; Reim et al., 2012). Although low-affinity MOB were detected, some of these MOB may also consume CH<sub>4</sub> at (circum-)atmospheric levels, doubling as a CH<sub>4</sub> sink under low CH<sub>4</sub> availability (Cai et al., 2016; Ho et al., 2019b; Tveit et al., 2019). The MOB activity was corroborated by the significant increase ( $p < 0.05$ ) in the *pmoA* gene abundance and/or the *pmoA*:16S rRNA gene abundance ratio (%) during the incubation (Tables 3.1 & S1, Figure S1), indicating MOB growth.

Importantly, assimilation of CH<sub>4</sub>-derived <sup>13</sup>C into the MOB was evidenced by the detection of the <sup>13</sup>C-DNA following density gradient fractionation in the SIP approach, which showed well-separated unlabelled C-("light") and <sup>13</sup>C-DNA ("heavy") fractions (Figures S2 & S3). The microorganisms derived from the <sup>13</sup>C-enriched 16S rRNA gene thus represent the metabolically active, <sup>13</sup>C-CH<sub>4</sub> derived consuming, and replicating community members. Despite the relatively low proportion of MOB (Figures S1, S4 & S5), the bacterial community composition, as determined from the amplicon sequence analysis of the 16S rRNA gene in the "light" and "heavy" fractions were discernible, clearly separated along the axes in the principal component analysis (PCA) (Figures S6 & S7), supporting the density gradient fractionation. However, with a relatively lower proportion of MOB in the riparian soil (Figure S1), differences in the "light" and "heavy" fractions were no longer reflected in the total bacterial population (i.e., at the 16S rRNA gene level; Figure S6). Generally, the SIP approach not only confirmed the assimilation of <sup>13</sup>C-CH<sub>4</sub> by the MOB, but also captured the subsequent dispersal of the <sup>13</sup>C into the CH<sub>4</sub>-driven soil food web.

Compositional changes during the incubation may reflect on the temporal dynamics of the bacterial, including the MOB community (e.g., Ho et al., 2011b, 2015b; Noll et al., 2005). Nevertheless, with the exception of the peat, the metabolically active, that is, <sup>13</sup>C assimilating and replicating bacterial community composition after the incubation was representative of the community in the starting material (Figure S4). The metabolically

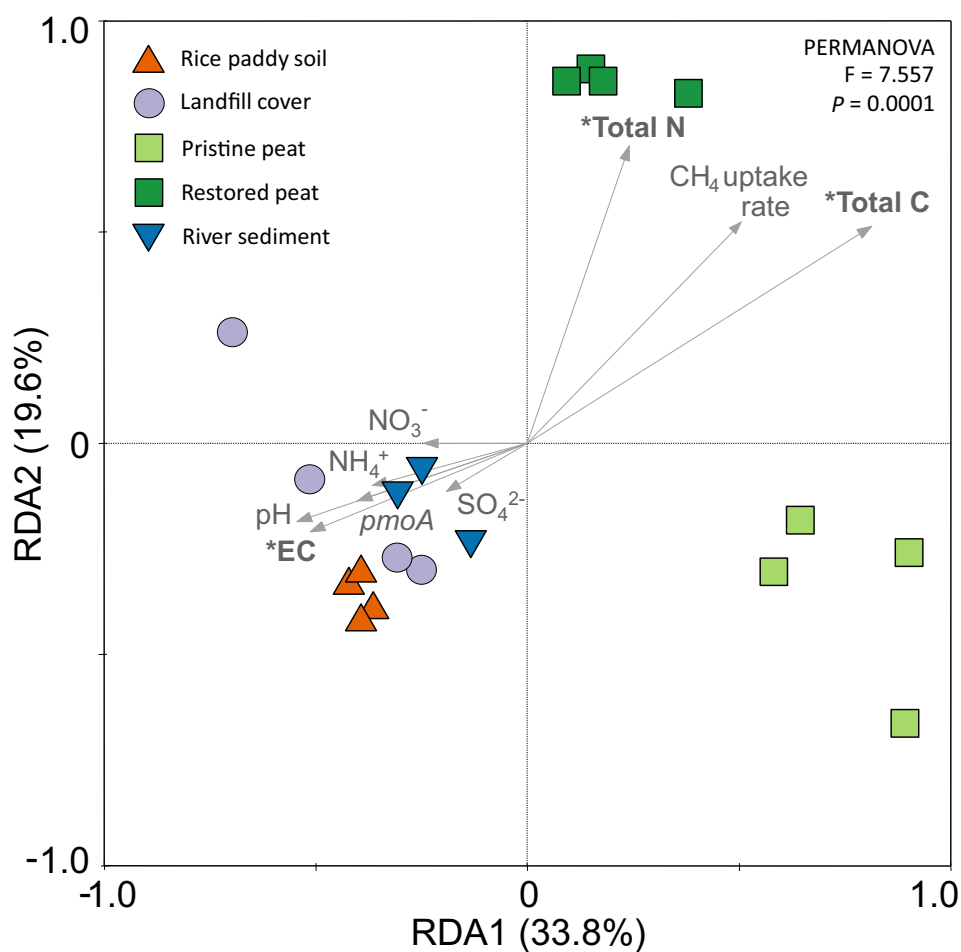


**Figure 3.1** RDA showing compositional differences of the metabolically active bacterial community ( $^{13}\text{C}$ -enriched 16S rRNA gene diversity) from widespread  $\text{CH}_4$  hotspots, and the variables (inorganic N, sulphate, pH, EC, total N and C,  $\text{CH}_4$  uptake rates, and *pmoA* gene abundance) affecting the community as constraints. Significant ( $p < 0.01$ ) variables affecting the community composition are emboldened (EC, total C and N). Abbreviations: EC, electrical conductivity; *pmoA*, *pmoA* gene abundance as proxy for MOB abundance

active bacterial community composition was distinct in the ombrotrophic peatlands, as revealed in a redundancy analysis (RDA; Figure 3.1). The redundancy analysis (RDA) integrates the abiotic parameters in Table 3.1 to the  $^{13}\text{C}$ -labelled bacterial community composition in all environments. The bacterial composition in the riparian, landfill cover, and paddy soils were more similar clustering closely together, and could be separated from the community in the ombrotrophic peatlands along RDA axis 1; > 53 % of the variation of the bacterial community composition could be explained by RDA 1 and RDA 2 (Figure 3.1). The bacterial community composition can be profoundly influenced by the soil physico-chemical parameters including substrate availability and land use, with the latter potentially having a stronger impact on the compositional dif-

ferences among the MOB (Drenovsky et al., 2010; Ho et al., 2017b; Kaupper et al., 2021b; Praeg et al., 2021). Among the environmental parameters, total C and N, and electrical conductivity (EC) indicative of soil salinity, significantly ( $p < 0.05$ ) affected the active bacterial community (Figure 3.1). While EC favours the community in the riparian, landfill cover, and paddy soils, total C and N strongly affected the community particularly in the restored ombrotrophic peatland. This is not entirely unexpected as ombrotrophic peatlands are nutrient-impooverished environments, where the peat-inhabiting microorganisms would more strongly respond to C and N than in the other relatively nutrient-rich environments (Table 3.1; Keller et al., 2006). In the other environments, it is noteworthy that despite the different ecosystems represented, that is, freshwater wetlands (paddy and riparian soil) and well-aerated landfill cover soil, the active bacterial community composition was more similar, possibly forming interaction networks comprising of shared community members.



**Table 3.1** Selected soil physico-chemical properties, and CH<sub>4</sub> uptake rates from CH<sub>4</sub> hotspots. The location, coordinates and sampling times are given in the original version of the publication (see section A.1)

Environment	pH	EC (mS cm <sup>-1</sup> )	Total C (mg g <sub>dw</sub> <sup>-1</sup> )	Total N (mg g <sub>dw</sub> <sup>-1</sup> )	NH <sub>4</sub> <sup>+</sup> (μmol g <sub>dw</sub> <sup>-1</sup> )	NO <sub>3</sub> <sup>-</sup> (μmol g <sub>dw</sub> <sup>-1</sup> )	SO <sub>4</sub> <sup>2-</sup> (μmol g <sub>dw</sub> <sup>-1</sup> )	CH <sub>4</sub> uptake rate (μmol g <sub>dw</sub> <sup>-1</sup> h <sup>-1</sup> )	References
<b>Paddy soil</b>	6.6±0.05a	BD	13.9±0.5a	1.3±0.04a	1±0.02ac	0.6±0.01abc	0.8±0.2a	0.44±0.19b	Kaupper et al. (2021b)
<b>Landfill cover</b>	8.81±0.11b	0.07±0.01a	136±12b	10.1±0.5bc	12.2±8.3c	1.9±1.2bc	28±32bd	0.67±0.24ab	This study
<b>Pristine peatland</b>	4.39±0.19c	BD	457±4.2c	6.9±1.2ab	0.2±0.08b	0.6±0.2bc	3.3±0.6bcd	1±0.26a	Kaupper et al. (2021a); this study
<b>Restored peatland</b>	4.68±0.12c	BD	492±6d	12.5±0.4c	0.7±0.3a	0.7±0.6abc	2.3±0.3c	1±0.16a	Kaupper et al. (2021a)
<b>Riparian soil</b>	8.22±0.18d	0.06±0.01a	32.2±8.4e	2.5±0.8ab	0.4±0.2a	0.07±0.07a	1.8±0.4a	0.15±0.05c	This study

### 3.3.2 The Methanotrophic Interactome Over Space and Time

The interaction among members of the CH<sub>4</sub>-driven food web was explored using a co-occurrence network analysis derived from the <sup>13</sup>C-enriched 16S rRNA genes. A comparison of the networks from the different environments revealed that the <sup>13</sup>C-labelled riparian soil community was relatively more connected and complex, as indicated by the higher number of interacting community members (nodes), number of connections (edges), and number of connections per node or node connectivity (average degree), but was less modular, having fewer compartmentalized groups of interaction within the network than the other environments (Table 3.2, Figure S8; Bissett et al., 2013; Peura et al., 2015; Zhou et al., 2010). In contrast, the restored peatland harboured the least connected and complex interaction network (Table 3.2). Presumably, increased co-occurrence is fueled by a higher metabolic exchange and/or competition among members of the MOB interactome in the riparian soil (van Elsas et al., 2012; Zelezniak et al., 2015).

Because temporal community patterns may lead to the elimination of highly connected taxa (Estrada, 2007) which affects the network complexity (Peura et al., 2015), the interaction network in the pristine peatland was additionally determined after 8, 13, and 19 days incubation to monitor the changes of the network topology over time (Table 3.3, Figure S9). Besides being a source of CH<sub>4</sub>-derived organic C, MOB also drive the N-cycle by fixing N<sub>2</sub> to assimilable N forms, and hence, are a key microbial group linking C and N cycling in ombrotrophic peatlands (Ho and Bodelier, 2015; Larmola et al., 2014). The connectedness and complexity of the <sup>13</sup>C-enriched 16S rRNA gene-derived interaction network, as deduced from the number of nodes, edges, and degree, fluctuated within a relatively narrow range over time when compared to the differences in the network topology between environments (Tables 3.2 & 3.3). However, modularity decreased from day 8 to 13, and remained relatively unchanged thereafter, indicating a reduced number of independently connected groups of nodes or compartments within the network over time (Zhou et al., 2010). Initially, compartments that are formed centered around the MOB before <sup>13</sup>C dispersal to other community members at higher trophic levels. With continuous CH<sub>4</sub> availability during the incubation, it is not unreasonable to assume that the CH<sub>4</sub>-derived <sup>13</sup>C would be more evenly and widely dispersed in the MOB interactome, becoming less modular over time (Kaupper et al., 2021b). Such temporal changes in the network topology are anticipated given that the soil is a dynamic environment. Nevertheless, it appears that some network topological features (e.g., degree, number of nodes and edges) were relatively more consistent than others (e.g., modularity) over time.

**Table 3.2** Correlations and topological properties of the co-occurrence network analysis derived from widespread CH<sub>4</sub> hotspots. The networks are given in Figure S8. The number of connections for "Positive edges", "Negative edges", "Met/Met", "Met/non-Met" and "Non-Met/non-Met" are given in the original version of the publication (see section A.1)

Network properties	Paddy soil		Landfill cover		Pristine peatland		Restored peatland		Riparian soil	
	13C	UnlabelledC	13C	UnlabelledC	13C	UnlabelledC	13C	UnlabelledC	13C	UnlabelledC
<b>Number of nodes<sup>a</sup></b>	299	536	329	655	344	622	258	681	737	667
<b>Number of edges<sup>b</sup></b>	980	2839	2078	8899	1684	4219	846	6918	10,003	6261
<b>Positive edges<sup>c</sup></b>	82%	76%	64%	59%	61%	65%	66%	62%	76%	76%
<b>Negative edges<sup>d</sup></b>	18%	24%	36%	41%	39%	35%	34%	38%	24%	24%
<b>Met/Met</b>	8%	0.3%	1%	0.5%	0.2%	0.5%	2.2%	0.1%	9.5%	0.1%
<b>Met/non-Met</b>	32%	2.7%	17%	2.5%	10.5%	5.5%	22.4%	6.9%	37%	4.9%
<b>Non-Met/non-Met</b>	60%	97%	82%	97%	89.3%	94%	75.4%	93%	53.5%	95%
<b>Modularity<sup>e</sup></b>	0.817	1.166	1.557	2.067	2.316	1.734	1.812	1.894	0.692	0.992
<b>Number of communities<sup>f</sup></b>	55	91	32	30	39	67	38	40	19	74
<b>Network diameter<sup>g</sup></b>	16	14	10	10	11	10	11	11	12	10
<b>Average path length<sup>h</sup></b>	5.913	5.803	3.969	3.607	4.402	4.372	5.01	4.228	4.201	4.433
<b>Average degree<sup>i</sup></b>	6.55	10.59	12.63	27.173	9.79	13.566	6.55	20.317	27.14	18.774
<b>Av. clustering coefficient<sup>j</sup></b>	0.365	0.416	0.409	0.418	0.413	0.397	0.397	0.413	0.319	0.345

Met/Met correlation within MOB, Met/non-Met correlation between MOB and non-MOB, Non-met/non-Met correlation between non-methanotrophs

<sup>a</sup> Microbial taxon (at genus level) with at least one significant ( $p < 0.01$ ) and strong (SparCC  $> 0.8$  or  $< -0.8$ ) correlation;

<sup>b</sup> Number of connections/correlations obtained by SparCC analysis;

<sup>c</sup> SparCC positive correlation ( $> 0.7$  with  $P < 0.01$ );

<sup>d</sup> SparCC negative correlation ( $< -0.7$  with  $P < 0.01$ );

<sup>e</sup> The capability of the nodes to form highly connected communities, that is, a structure with high density of between nodes connections (inferred by Gephi);

<sup>f</sup> A community is defined as a group of nodes densely connected internally (Gephi);

<sup>g</sup> The longest distance between nodes in the network, measured in number of edges (Gephi);

<sup>h</sup> Average network distance between all pair of nodes or the average length off all edges in the network (Gephi);

<sup>i</sup> The average number of connections per node in the network, that is, the node connectivity (Gephi);

<sup>j</sup> How nodes are embedded in their neighborhood and the degree to which they tend to cluster together (Gephi)

**Table 3.3** Correlations and topological properties of the co-occurrence network analysis from the pristine peatland over time. The networks are given in Figure S9. The number of connections for "Positive edges", "Negative edges", "Met/Met", "Met/non-Met" and "Non-Met/non-Met" are given in the original version of the publication (see section A.1)

Network properties	8 days		13 days		19 days	
	<sup>13</sup> C	Unlabelled C	<sup>13</sup> C	Unlabelled C	<sup>13</sup> C	Unlabelled C
<b>Number of nodes<sup>a</sup></b>	297	608	347	628	205	578
<b>Number of edges<sup>b</sup></b>	1265	4651	1758	3845	687	4117
<b>Positive edges<sup>c</sup></b>	57%	64%	60%	69%	61%	62%
<b>Negative edges<sup>d</sup></b>	43%	36%	40%	31%	39%	38%
<b>Met/Met</b>	0.3%	0.1%	0.3%	0.1%	1.2%	0.02%
<b>Met/non-Met</b>	10.2%	5%	10.5%	6%	19.6%	3.3%
<b>Non-Met/non-Met</b>	89.5%	94.9%	89.2%	93.9%	79.2%	96.6%
<b>Modularity<sup>e</sup></b>	3.317	1.752	2.440	1.445	2.478	2.150
<b>Number of communities<sup>f</sup></b>	34	66	37	79	35	44
<b>Network diameter<sup>g</sup></b>	14	14	11	10	17	12
<b>Average path length<sup>h</sup></b>	5.233	4.243	4.463	4.441	5.038	4.181
<b>Average degree<sup>i</sup></b>	8.519	15.29	10.13	12.24	6.702	14.24
<b>Av. clustering coefficient<sup>j</sup></b>	0.421	0.404	0.415	0.399	0.430	0.374

Description of the network properties are as given in Table 3.2

Met/Met correlation within MOB, Met/non-Met correlation between MOB and non-MOB, Non-met/non-Met correlation between non-methanotrophs

### 3.3.3 Insights Into Intra-Methanotroph and Methanotroph / Non-Methanotroph Interaction Within the Methanotrophic Interactome

The co-occurring MOB/MOB (intra-MOB) and MOB/non-MOB interactions were further explored to determine whether co-occurring taxa are conserved across different environments, and to identify non-MOB as interacting partners of the MOB. The non-MOB and MOB that co-occur are anticipated to form close associations, forming tight-knit clusters that are centered around the MOB (Ho et al., 2016a, 2020). On the other hand, linkages between non-MOB that occurred at higher proportion (Tables 3.2 & 3.3) represent heterotrophic microorganisms that assimilated the <sup>13</sup>C at higher trophic levels. The co-occurring MOB/MOB and MOB/non-MOB taxa exhibited site specificity, with the majority of the co-occurring microorganisms unique to an environment (Figure 3.2). Differing from our hypothesis, this suggests that microbial communities distinctly co-evolved in the different environments, and other factors besides high CH<sub>4</sub> availability drives

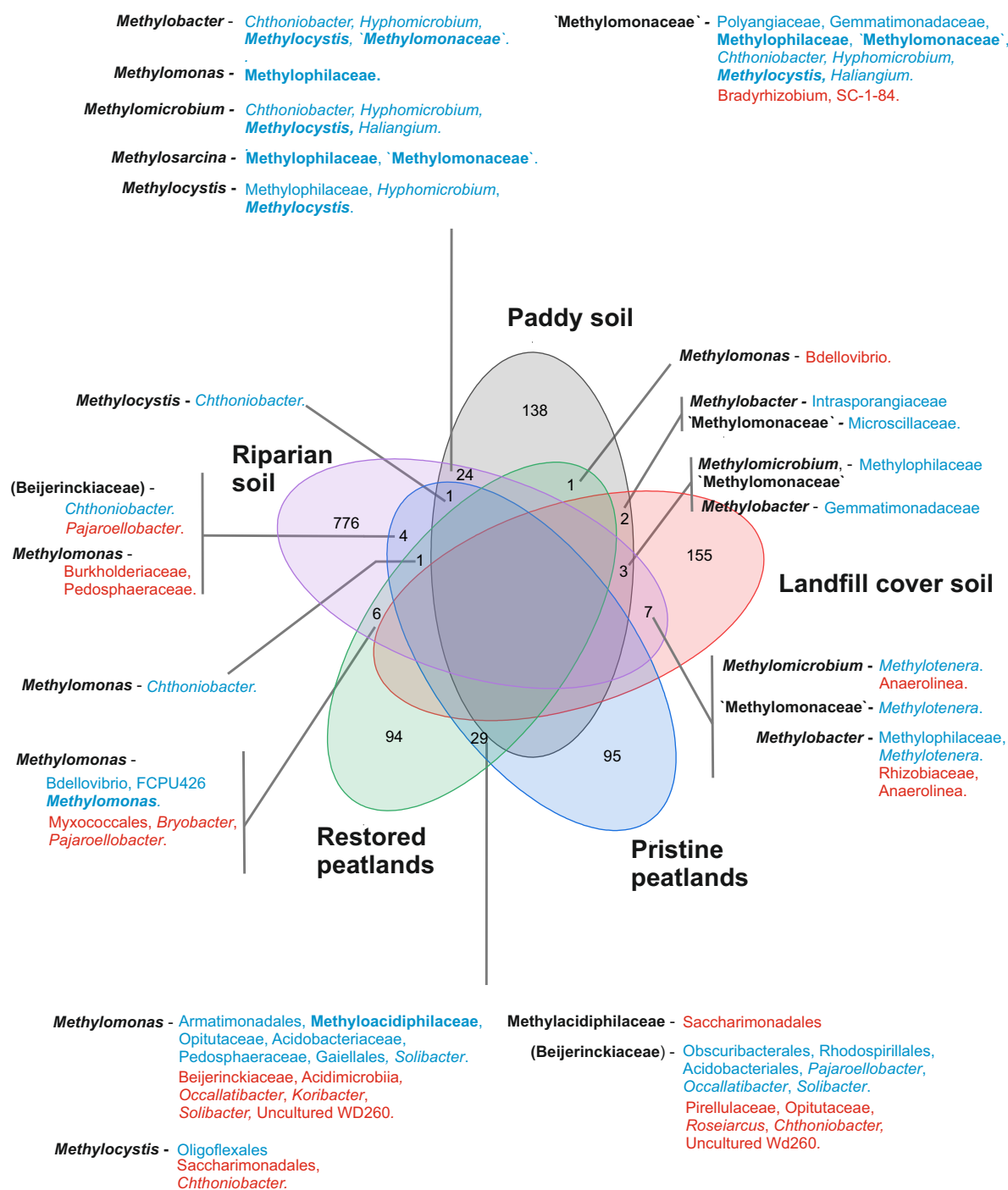


**Figure 3.2** Venn diagram showing shared co-occurring taxa in all environments. MOB are emboldened. Taxa in blue and red denote significant positive and negative correlations, respectively. Beijerinckiaceae is given in brackets as many MOB, along with other methylotrophs belong to this family, but remain ambiguous at the resolvable taxonomic affiliation; hence Beijerinckiaceae are potentially MOB. Bacterial affiliations are identified to the highest taxonomic resolution (genus/species) whenever possible. The unique co-occurring taxa specific to each environment and classified OTUs are given in the Table S2.

the co-occurrence of these microorganisms. Interestingly, more shared co-occurring taxa from the pristine and restored peatlands (acidic freshwater ecosystem), as well as in the riparian and paddy soil (circum-neutral freshwater ecosystems) were detected (Figure 3.2), suggesting some commonalities in the environmental selection of these co-occurring microorganisms.

Communal metabolism drives the interaction network of the  $^{13}\text{C}$ -enriched members of the MOB interactome (Ho et al., 2016a; Kaupper et al., 2021a,b; Krause et al., 2017; Taubert et al., 2019). Although the incorporation of  $^{13}\text{C}$  derived from dead microbial biomass can not be completely excluded, this would have been minimized with a metabolically active and growing  $\text{CH}_4$ -oxidizing population. Also,  $\text{CH}_4$ -derived  $^{13}\text{C}\text{-CO}_2$  may be incorporated by chemoautotrophs in the community, but the majority of the co-occurring genus/species were heterotrophs. Here, we focused on the shared taxa from the different environments which represent the more universal co-occurring members of the interaction network (Figure 3.2). Expectedly, many MOB (e.g., *Methylobacter*, *Methylomonas*, *Methylomicrobium*, *Methylosarcina*, *Methylocystis*, and members of Methyloacidiphilaceae) co-occur, sharing similar niche in diverse environments. Among other co-occurring taxa common to many environments, non-MOB methylotrophs (e.g., *Methylotenera*, *Hyphomicrobium*, and members of Methylophilaceae) were significantly co-enriched alongside MOB (Figure 3.2; Dumont et al., 2011; Kaupper et al., 2021a,b; Oshkin et al., 2015; Taubert et al., 2019). Indeed, cross-feeding drives their co-occurrence via passive release of methanol by the MOB. Also, the non-MOB methylotrophs have been demonstrated to induce the release of methanol as a C source for growth by modifying the expression of the methanol dehydrogenase in MOB (Krause et al., 2017), in addition to utilizing other  $\text{CH}_4$ -derived one C compounds (e.g., formaldehyde, formate). Considering that some members of Myxococcales (e.g., Haliangiaceae; Petters et al., 2021) are recognized microbial predators shown to exert a regulatory effect in bacterial communities (Lueders et al., 2006; Muñoz-Dorado et al., 2016; Ye et al., 2020), their significant positive and negative correlations in the restored peatland and riparian soil suggest selective predation on the MOB, as shown before in freshwater environments (Murae and Frenzel, 2007). The apparently contrasting correlations may be explained by the predator-prey relationship, where predator and prey alternately fluctuate over time. Thus, correlations of Myxococcales with the MOB may vary from positive (e.g., during nutrient availability derived from lysed cells after predation) to negative (e.g., during predation on MOB) through time. Overall, although co-occurrence patterns may differ across environments, few relationships were persistent reflecting on the biological interactions that were independent of the environmental conditions. Besides predation and methylotrophic interaction, other

interacting members of the MOB interactome remain elusive.

Of interest, *Chthoniobacter* appears to be closely associated with the MOB in diverse environments (peatlands, paddy, and riparian soils), and was overwhelmingly (the only exception occurred at days 8-13 interval in the pristine peatland; Figure 3.3) positively correlated to the gammaproteobacterial MOB (*Methylobacter*, *Methylomicrobium*, *Methylomonas*, and other “Methylomonaceae”); *Chthoniobacter* positively and negatively correlated to the alphaproteobacterial MOB *Methylocystis*, depending on the environment (Figure 3.2, Table S2). Unlike the methylotrophs, a cultured representative of *Chthoniobacter* (*C. flavus*) is a soil-inhabiting heterotroph that cannot utilize products of CH<sub>4</sub> oxidation (i.e., methanol, formate) nor other organic acids (except pyruvate) and amino acids for growth (Sangwan et al., 2004). This suggests that leaked pyruvate and/or sugars derived from the RuMP pathway during C-assimilation specifically in gammaproteobacterial MOB may shape the cross-feeding between *Chthoniobacter* and the MOB. Another co-enriched non-MOB taxon belonged to *Haliangium*, detected only in the paddy and riparian soils (Figure 3.2, Table S2). Cultured representatives of *Haliangium* (group Myxobacteria) seemingly inhabit and show a preference for mineral soils (Petters et al., 2021), corroborating with their absence in the pristine and restored peatlands (Figures 3.2 and 3.3). However, the co-occurrence network analysis revealed statistical relationships; the biological interdependencies or causative mechanisms driving the inferred interaction requires further investigation, facilitated by co-culture studies (Krause et al., 2017; Kwon et al., 2019a). Also noteworthy is that a taxon may simultaneously be positively and negatively correlated to the same MOB (e.g., *Ca. Solibacter*, *Pajaroellobacter*, *Occallatibacter*; Figure 3.2). Admittedly, our sequencing analysis suffers from the lack of finer taxonomic resolution. This could partly explain the seemingly contradictory correlations, which may also stem from the inherently different ecological traits possessed by members of the same genus or even strain and/or that the same microorganism may have evolved to play distinct roles in different environments (Ho et al., 2017a; Hoefman et al., 2014a). Hence, further exploration of the inherent microbial traits driving the co-occurrence of the MOB and specific non-MOB warrants attention.

Additionally, we monitored shifts in the co-occurring taxa over time (8, 13, and 19 days intervals) in the pristine peatland to determine the persistent non-MOB interacting partners (Figure 3.3, Table S3). Unique co-occurring taxa emerged at different time intervals, with some co-occurring microorganisms overlapping between time intervals. The 20 co-occurring taxa that were consistently present at all time intervals were regarded as the core community members. The core community was thus likely to comprise microorganisms that were in close and stable interaction with the MOB. Like-

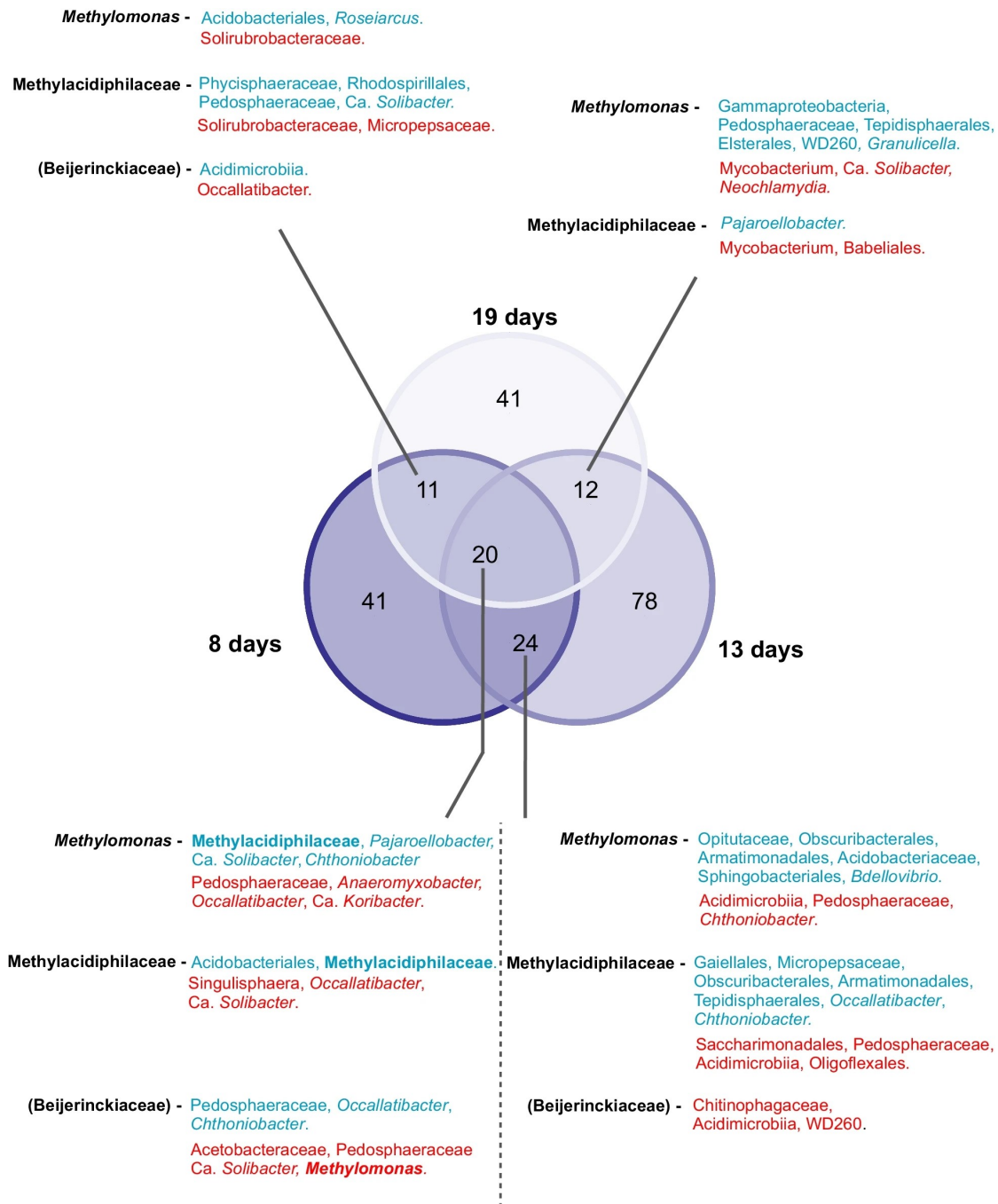


**Figure 3.3** Venn diagram showing shared co-occurring taxa over time in the pristine peatland. The taxa that co-occurred at all time intervals were regarded as the “core” community members. MOB are emboldened. Taxa in blue and red denote significant positive and negative correlation, respectively. Like Figure 3.2, Beijerinckiaceae is given in brackets. Bacterial affiliations are identified to the highest taxonomic resolution (genus/species) whenever possible. The unique co-occurring taxa at each time interval, and shared co-occurring taxa at two time intervals, along with the classified OTUs are given in Table S3.



wise, *Chthoniobacter* was consistently positively correlated to the gammaproteobacterial MOB in the core community. Generally, our analysis revealed some consistency in the co-occurring patterns of the interaction network over space and time, paving the way for future detailed studies to elucidate the underlying mechanisms and metabolites driving the co-occurrence of specific taxa.

### 3.3.4 Comparison of the Interaction Networks Derived From the Total (<sup>unlabelled</sup>C-DNA) and Metabolically Active (<sup>13</sup>C-DNA) Microbial Communities

Network analyses are commonly derived from nucleic acids isolated from the environment. Depending on the sampling strategy, the environmental samples are often collected apart and composited prior to nucleic acid extraction. Considering that microorganisms are largely restricted in their movements and particularly for the MOB, strongly adhere to soil particles (Priemé et al., 1996; Scheu et al., 2005), the interactions between microorganisms in these networks are thus inferred. Also, the complexity of these networks may have been overestimated given that the inferred interaction includes a large fraction of soil microorganisms that may not be metabolically active (Lennon and Jones, 2011; Schlöter et al., 2018). Here, we addressed these limitations by coupling <sup>13</sup>C-CH<sub>4</sub> SIP to a co-occurrence network analysis which provides a strong link, tracking trophic interactions of microorganisms involved in the flow of the <sup>13</sup>C in the CH<sub>4</sub>-based food web. Although a relatively more complex interaction topology is intuitively anticipated in networks derived from the total community (<sup>unlabelled</sup>C-DNA), this assumption has yet to be empirically validated. Indeed, the network structure derived from the 16S rRNA gene sequences, representing the total community exhibited higher connectivity and complexity, as indicated by the higher number of nodes, edges, and degree when compared to the network of the active community (i.e., <sup>13</sup>C-enriched 16S rRNA gene sequences; Tables 3.2 & 3.3). This was documented in all environments and over time in the pristine peat, except for the riparian soil where the network derived from the <sup>13</sup>C-enriched 16S rRNA gene sequences was comparably more connected and complex. Hence, results largely support our postulation that the coupling of SIP to network analysis can be applied to exclude or reduce spurious connections in the networks.

The unexpected trend in the riparian soil may have been caused by methodological artifacts, namely cross-contamination of the 'light' (<sup>unlabelled</sup>C-DNA) and 'heavy' (<sup>13</sup>C-DNA) fractions, but the densities of these fractions were well-separated (Figure S2). Notably, the riparian soil harboured a higher number of nodes derived from the <sup>13</sup>C-enriched

16S rRNA gene (Table 3.2) compared to the total community (<sup>unlabelled</sup>C-DNA), as well as in other environments. This is indicative of a higher number of interacting microorganisms within the MOB interactome in the riparian soil, which in turn, may foster higher metabolic exchange, contributing to the complexity of the CH<sub>4</sub>-driven interaction network (D'Souza et al., 2018; Ratzke et al., 2020; Zelezniak et al., 2015). Whether this is the rule for networks harbouring highly diverse nodes or an exception for the riparian soil, needs further confirmation. Regardless, we demonstrate that our approach (SIP-network analysis) is an effective tool to probe trophic interactions in complex communities approximating in-situ conditions.

### 3.4 Conclusion

Given that biological interactions modulate different aspects of microbial life in the environment, shaping the activity, biodiversity, community composition, abundance, and stability of microbial communities (Dal Co et al., 2020; Kaupper et al., 2021a,b; Peura et al., 2015; Ratzke et al., 2020), elucidating the interaction of assembled communities within the CH<sub>4</sub>-driven network is key to determining their response to environmental cues. While numerous studies utilized artificially assembled communities, we explored microbial interactions in naturally-occurring complex communities aided by SIP coupled to a co-occurrence network analysis to target the MOB interactome. Although co-occurring taxa were predominantly site-specific, it appears that some biological interactions (e.g., cross-feeding within methylophs) were independent of the environment. Results also indicate a relatively stable interaction network in the short-term, comparing networks between all environments and within the pristine peatland, with the emergence of a persistent core MOB interactome over time. More generally, we provide a methodological strategy to improve the network analysis derived from environmental samples by introducing SIP with labelled substrates to strengthen and substantiate the biological linkages between the potentially interacting microorganisms.

### 3.5 Materials and Methods

#### 3.5.1 Chemicals and reagents

Reagents (analytical and molecular biology grade) used were obtained from Carl Roth GmbH (Karlsruhe, Germany), VWR International (Hannover, Germany), and Merck (Bielefeld, Germany) unless explicitly stated otherwise. Gases (<sup>13</sup>C- and <sup>unlabelled</sup>C-

CH<sub>4</sub>) were ordered from Linde plc (Pullach, Germany). For ultracentrifugation, tubes, rotors, and ultra-centrifuge were sourced from Beckman Coulter (CA, USA). Further details on kits and reagents are given in the corresponding sections.

### 3.5.2 Soil microcosm incubation, and soil physico-chemical characterization

The soils were sampled from CH<sub>4</sub>-emitting environments, including a landfill cover, pristine ombrotrophic peatlands, and riparian soil (Table 3.1). Additionally, results from previous incubations with a rice paddy soil and ombrotrophic peatlands, were also re-analysed and included in this study (Kaupper et al., 2021a,b). These environments are anticipated to harbor aerobic low-affinity CH<sub>4</sub>-oxidizers. The soils were collected from the upper 10-15 cm using a corer. Three to four soil cores were collected and composited from each of four random plots spaced > 4 m apart, representing independent replicates. Samples from the peatlands (Poland; Table 3.1) were transported to the laboratory in ice with styrofoam containers, while the other samples (landfill cover and riparian soil; Lower Saxony, Germany) were immediately transported to the lab for incubation set-up. Because of the large amounts of waste debris, the landfill cover soil was further loosely sieved (< 5 mm) prior to incubation. Rice paddy soil was processed as described before (air-dried at room temperature and sieved to < 2 mm; Kaupper et al., 2021b). The site location, sampling time, and selected soil physico-chemical properties are provided in Table 3.1.

The landfill cover, pristine and restored ombrotrophic peatland, and riparian soils were incubated similarly; each microcosm consisted of 5-7 g fresh soil in a 120 ml bottle. After sealing the bottle with a butyl rubber stopper crimped with a metal cap, headspace CH<sub>4</sub> was adjusted to 1-2 % v/v (<sup>unlabelled</sup>C-CH<sub>4</sub> and <sup>13</sup>C-CH<sub>4</sub>, n=4 each) in air, reflecting on the anticipated in-situ CH<sub>4</sub> concentrations in the CH<sub>4</sub> hotspots. Incubation was performed at 27 °C, while shaking (110 rpm) in the dark. Upon CH<sub>4</sub> depletion, the microcosm was aerated for 30 mins before replenishing headspace CH<sub>4</sub> (1-2 % v/v), and incubation resumed as before. The incubation was terminated when approximately 30 μmol CH<sub>4</sub> per g fresh weight soil was consumed to ensure sufficient labelling. Furthermore, incubations were performed with samples from the pristine ombrotrophic peatland in this study to follow the temporal dynamics of the MOB interactome over a 19-day incubation after approximately 14 (day 8), 30 (day 13), and 60 (day 19) μmol CH<sub>4</sub> per g fresh weight peat were consumed. The incubation containing the rice paddy soil was performed differently. Here, each microcosm consisted of 10 g air-dried rice paddy soil saturated with 4.5 mL autoclaved deionized water in a Petri

dish. Incubation was performed statically at 25 °C in a flux chamber after adjusting headspace CH<sub>4</sub> to 1-2 % v/v (<sup>unlabelled</sup>C-CH<sub>4</sub>, n=2; <sup>13</sup>C-CH<sub>4</sub>, n=4) in air, as detailed in Kaupper et al. (2021b); incubation was terminated when approximately 30 μmol CH<sub>4</sub> per g soil was consumed. In all microcosms, the soil was homogenized, sampled, and stored in the -20 °C freezer till DNA extraction after the incubation.

CH<sub>4</sub> was measured daily during the incubation using a gas chromatograph (7890B GC System, Agilent Technologies, Santa Clara, USA) coupled to a pulsed discharge helium ionization detector (PD-HID), with helium as the carrier gas. Cumulative CH<sub>4</sub> uptake is reported. Inorganic nitrogen (ammonium and nitrate) concentrations were determined in autoclaved deionized water (1:1 or 1:2 w/v) after centrifugation and filtration (0.22 μm) with standard colorimetric methods (Horn et al., 2005; van Dijk et al., 2021), while total sulphate was determined using a modified colorimetric assay after Wolfson (1980); all colorimetric assays were performed using an Infinite M plate reader (TECAN, Meannedorf, Switzerland). Total C and N were determined from air-dried (50 °C) and milled soils using a Vario EL III elemental analyzer (Elementar Analysensysteme GmbH, Langenselbold, Germany).

### 3.5.3 DNA-SIP with <sup>13</sup>C-CH<sub>4</sub>

DNA was extracted using the DNeasy PowerSoil Kit (Qiagen, Hilden, Germany) according to the manufacturer's instructions. DNA was extracted in duplicate per sample to obtain sufficient amounts for the isopycnic ultracentrifugation.

The DNA-SIP with <sup>13</sup>C-CH<sub>4</sub> was performed as described before (Kaupper et al., 2021b; Neufeld et al., 2007b). Isopycnic ultracentrifugation was performed using an Optima L-80XP (Beckman Coulter Inc., USA) at 144000 g for 67 hours. Immediately after centrifugation, fractionation was performed using a peristaltic pump (Duelabo, Dusseldorf, Germany) at 2.8 rpm min<sup>-1</sup>. Nine or ten fractions were obtained per sample, after discarding the final fraction. Fractionation was unsuccessful for one out of the four replicates of the riparian soil. The density gradient of each fraction was determined using an AR200 digital refractometer (Reichert Technologies, Munich, Germany). Thereafter, the DNA from each fraction was precipitated and washed twice with ethanol, and the pellet was re-suspended in 30 μL ultrapure PCR water (INVITROGEN, Waltham, USA). The *pmoA* gene was quantified from the precipitated DNA for each fraction using qPCR (MTOT assay; Kolb et al., 2003) to distinguish the "heavy" (<sup>13</sup>C-enriched DNA) and "light" (<sup>unlabelled</sup>C-DNA) fractions after comparing the fractions derived from the <sup>13</sup>C- and <sup>unlabelled</sup>C-CH<sub>4</sub> incubations (Figure S2 & S3). The "heavy" and "light" DNA fractions were identified as defined in Neufeld et al. (2007b). The 16S rRNA

gene from these fractions was subsequently amplified for Illumina MiSeq sequencing and network construction.

### 3.5.4 Quantitative PCR (qPCR)

The qPCR assay was performed to enumerate the *pmoA* gene abundance after fractionation (DNA-SIP), and to follow the change in the *pmoA* relative to the 16S rRNA gene abundance during the incubation. The increase in the *pmoA*:16S rRNA gene abundance ratio is indicative of MOB growth (Kaupper et al., 2021a), complementing the DNA-SIP. The qPCR was performed using a BIORAD CFX Connect RT System (Biorad, Hercules, USA). Each qPCR reaction (total volume, 20  $\mu$ L) targeting the *pmoA* gene consisted of 10  $\mu$ L SYBR 2X Sensifast (BIOLINE, London, UK), 3.5  $\mu$ L of A189f/mb661r primer each (4  $\mu$ M), 1  $\mu$ L BSA (1 %), and 2  $\mu$ L template DNA. Each qPCR reaction (total volume, 20  $\mu$ L) targeting the 16S rRNA gene consisted of 10  $\mu$ L SYBR 2X Sensifast, 1.2  $\mu$ L MgCl<sub>2</sub> (50 mM), 2.0  $\mu$ L of 341F/907R primer each (10  $\mu$ M), 1.8  $\mu$ L of PCR-grade water, 1  $\mu$ L BSA (1 %), and 2  $\mu$ L template DNA. The polymerase chain reaction (PCR) thermal profiles are given elsewhere (Kaupper et al., 2021a; Kolb et al., 2003). Template DNA was undiluted when quantifying the *pmoA* gene after fractionation, and diluted 50 or 100-fold with RNase- and DNase-free water when enumerating the *pmoA* and 16S rRNA gene from the DNA isolated from the soil. These dilutions resulted in the optimal gene copy numbers. The calibration curve, ranging from 10<sup>1</sup> to 10<sup>7</sup> copy number of target genes, was derived from clones (*pmoA* gene) or plasmid DNA (16S rRNA gene) as described before (Ho et al., 2011b). The PCR efficiency was on average 90% - 95%, depending on the qPCR assay. Amplicon specificity was assessed from the melt curve, and further confirmed by 1 % agarose gel electrophoresis.

### 3.5.5 16S rRNA gene amplicon preparation and Illumina MiSeq sequencing

The 16S rRNA gene was amplified with the primer pair 341F/805R. Each PCR reaction (total volume, 40  $\mu$ L) consisted of 20  $\mu$ L KAPA HIFI (Roche, Basel, Switzerland), 2  $\mu$ L forward/reverse tagged-primer each (10  $\mu$ M), 2  $\mu$ L BSA (1 %), 4  $\mu$ L template DNA, and 10  $\mu$ L PCR-grade water. The template DNA was replaced with equivalent amounts of PCR-grade water and DNA derived from *Rhodanobacter denitrificans* in the negative and positive control, respectively. The positive control was confirmed after sequencing, resulting in the retrieval of sequences affiliated to *R. denitrificans*, as

expected; there was no amplification in the negative control. The PCR thermal profile consisted of an initial denaturation step at 95 °C for 3 min, followed by 30 cycles of denaturation at 98 °C for 20 s, annealing at 53 °C for 15 s, and elongation at 72 °C for 15 s. The final elongation step was at 72 °C for 1 min. Amplicon specificity was verified by 1 % agarose gel electrophoresis. Thereafter, the PCR product was purified using the GeneRead Size Selection Kit (Qiagen, Hilden, Germany) to be used as template (5 µL) for the second PCR. The second PCR was performed to attach the adapters to the amplicons using the Nextera XT index kit (Illumina, San Diego, USA). The reagents, reagent concentrations, and thermal profile for the second PCR are given elsewhere (Kaupper et al., 2021b). After the second PCR, the amplicons were purified using the MagSi-NGSPREP Plus Magnetic beads (Steinbrenner Laborsysteme GmbH, Wiesenbach, Germany) according to the manufacturer's instructions. Equimolar amounts (133 ng) of the amplicons from each sample were pooled for library preparation and sequencing using the Illumina MiSeq version 3 chemistry (paired-end, 600 cycles).

### 3.5.6 16S rRNA gene amplicon analyses

Firstly, the 16S rRNA gene paired-end reads were merged using PEAR (Zhang et al., 2014), and subsequently processed using QIIME 2 version 2019.10. The de-multiplex and quality control steps were performed with DADA2 (Callahan et al., 2016) using the consensus method to remove remaining chimeric and low-quality sequences. After filtering, approximately 5,650,000 high quality sequences were obtained, with an average of ~ 49,570 sequences per sample. Singletons and doubletons were removed, and the samples were rarefied to 11,600 sequences following the sample with the lowest number of sequences. Classification was performed at 97 % similarity based on the Silva database v. 132 (Quast et al., 2013). Because the aerobic MOB are restricted to < 30 genera from two phyla (Guerrero-Cruz et al., 2021), they were identified using the “search” function in the operational taxonomic unit (OTU) table. The composition of the active bacterial community from different environments was visualized as a RDA based on the relative abundance of the 16S rRNA gene diversity. The data matrix was initially analysed using the detrended correspondence analysis (DCA), indicating a linear data distribution and the best-fit mathematical model was the RDA. Also, plot clustering was performed using permutational multivariate analysis of variance (PERMANOVA; Anderson, 2001) to test whether the different environments harboured significantly different active bacterial communities and whether the communities in the “heavy” and “light” fractions were distinct. The PERMANOVA was calculated using PAST 4 software

(Hammer et al., 2001). The RDA analysis was implemented in Canoco 4.5 (Biometrics, Wageningen, The Netherlands). The 16S rRNA gene sequences (sample names/treatments and corresponding accession numbers are listed in Table S4) were deposited at the National Center for Biotechnology Information (NCBI) under the BioProject ID number PRJNA751592.

### 3.5.7 Co-occurrence network analysis

The complexity of the interaction was explored using a co-occurrence network analysis, based on the 16S rRNA gene (OTU level) derived from the  $^{13}\text{C}$ -enriched DNA (“heavy” fraction), representing the active community. Moreover, networks were also constructed from the unlabelled DNA from the  $^{12}\text{C}$ - $\text{CH}_4$  incubations to be compared to the networks derived from the  $^{13}\text{C}$ -enriched DNA. The networks were derived from at least 3 replicates. Previously, we showed that networks derived from an uneven number of replicates (e.g., 3-5) and a randomly chosen subset of replicates showed comparable results (Kaupper et al., 2021b). To remove weak and spurious correlations, only the OTUs with  $\geq 10$  sequences were included in the analysis, which represented  $> 90\%$  of the total amount of sequences. The co-occurrence analysis between absolute OTUs counts were calculated using the Python module “SparCC”, a tool designed to generate and assess the correlations of the compositional data (Friedman and Alm, 2012). True SparCC correlations with a magnitude of  $> 0.8$  (positive correlation) or  $< -0.8$  (negative correlation), and statistical significance of  $p < 0.01$  were selected for the network construction. The p-values were obtained by 99 permutations of random selections of the data tables. All networks were constructed in parallel using the same analytical pipeline, including re-analysis of networks from the rice paddy soil and peatland together with the current dataset. This enables direct comparison of the networks derived from the different environments and over time. Assessment of the networks was based on their topological properties, which includes the number of nodes and edges, modularity, number of communities, network diameter, average path length, degree, and clustering coefficient (interpretation of these network properties are provided in Table 3.2; Ho et al., 2021; Newman, 2003; Peura et al., 2015). Additionally, the correlations between the MOB, and MOB/non-MOB were identified to determine potential intra-MOB and non-MOB interacting partners. The network construction and topological properties were calculated with Gephi (Bastian et al., 2009).

### **3.5.8 Statistical analysis**

Statistical analysis was performed in PAST 4 software (Hammer et al., 2001). Normal distribution was tested using the Shapiro-Wilk test, and homogeneity of variance was tested using Levene's test. Where normality and homogeneity of data were met, an ANOVA with Tukey post-hoc test ( $p < 0.05$ ) was performed for comparisons between sites and over time in the pristine peatland. Otherwise, a Kruskal-Wallis ANOVA and Dunn's post-hoc test ( $p < 0.05$ ) were performed.



## Chapter 4

# When the Going Gets Tough: Emergence of a Complex Methane-Driven Interaction Network During Recovery from Desiccation-Rewetting

Thomas Kaupper<sup>1</sup>, Lucas W. Mendes<sup>2</sup>, Hyo Jung Lee<sup>3</sup>, Yongliang Mo<sup>4</sup>, Anja Poehlein<sup>5</sup>, Zhongjun Jia<sup>4</sup>, Marcus A. Horn<sup>1</sup>, Adrian Ho<sup>1</sup>.

Published in *Soil Biology and Biochemistry* (2021) 153:108109  
Copyright Elsevier

---

<sup>1</sup>Institute for Microbiology, Leibniz Universität Hannover, Herrenhäuser Str. 2, 30419 Hannover, Germany.

<sup>2</sup>Center for Nuclear Energy in Agriculture, University of São Paulo CENA-USP, Brazil.

<sup>3</sup>Department of Biology, Kunsan National University, Gunsan, Republic of Korea.

<sup>4</sup>Institute of Soil Science, Chinese Academy of Sciences, No.71 East Beijing Road, Xuan-Wu District, Nanjing City, 210008 PR China.

<sup>5</sup>Department of Genomic and Applied Microbiology and Göttingen Genomics Laboratory, Institute of Microbiology and Genetics, George-August University Göttingen, Grisebachstr. 8, D-37077 Göttingen, Germany.

The published version can be found online:  
<https://doi.org/10.1016/j.soilbio.2020.108109>

## 4.1 Abstract

Microorganisms interact in complex communities, affecting microbially-mediated processes in the environment. Particularly, aerobic MOB showed significantly stimulated growth and activity in the presence of accompanying microorganisms in an interaction network (interactome). Yet, little is known of how the interactome responds to disturbances, and how community functioning is affected by the disturbance-induced structuring of the interaction network. Here, we employed a time-series stable isotope probing (SIP) approach using  $^{13}\text{C}$ - $\text{CH}_4$  coupled to a co-occurrence network analysis after Illumina MiSeq sequencing of the  $^{13}\text{C}$ -enriched 16S rRNA gene to directly relate the response in MOB activity to the network structure of the interactome after desiccation-rewetting of a paddy soil.  $\text{CH}_4$  uptake rate decreased immediately ( $< 5$  days) after short-term desiccation-rewetting. Although the MOB subgroups differentially responded to desiccation-rewetting, the metabolically active bacterial community composition, including the MOB, recovered after the disturbance. However, the interaction network was profoundly altered, becoming more complex but, less modular after desiccation-rewetting, despite the recovery in the MOB activity and community composition/abundances. This suggests that the legacy of the disturbance persists in the interaction network. The change in the network structure may have consequences for community functioning with recurring desiccation-rewetting.

## 4.2 Introduction

Biological interactions are widespread in microbial communities. Microorganisms form a plethora of interdependent relationships with their biotic environment, with synergistic and/or antagonistic effects. Concerning methanotrophy, emergent properties enhancing community functioning may arise from such interactions. Indeed, aerobic MOB exhibit higher co-metabolic biodegradation rates of micropollutants and show significantly higher MOB activity in a multi-species consortium than as monocultures (Begonja and Hrsak, 2001; Benner et al., 2015; Ho et al., 2014; Krause et al., 2017; Veraart et al., 2018). Therefore, accompanying microorganisms that do not possess the metabolic potential and do not seemingly contribute to  $\text{CH}_4$  oxidation may also be relevant, exerting an indirect interaction-induced effect on community functioning. While changes in the MOB community composition and/or abundances have been correlated to the  $\text{CH}_4$  oxidation rate in response to environmental cues and disturbances (Christiansen et al., 2016; Danilova et al., 2015; Ho et al., 2011a; Reis et al., 2020; Reumer et al., 2018), interaction-induced effects that alter the structure of the interaction network (i.e.,

MOB interactome; Ho et al., 2016a) remains unclear. Here, we define the MOB interactome as a sub-population of the entire community, encompassing the MOB and accompanying non-MOB that is tracked via the flow of CH<sub>4</sub>-derived <sup>13</sup>C; the members of the interactome co-occur more than by chance, as determined in a co-occurrence network analysis (Ho et al., 2016a). The recovery in the community composition and abundance does not necessarily translate to the return of the network structure to the pre-disturbance state (Pérez-Valera et al., 2017). Therefore, the response of the interactome is a lesser known but important determinant, potentially imposing an effect on community functioning during recovery from disturbances (Ratzke et al., 2020).

Aerobic MOB belong to the Gammaproteobacteria (Type Ia and Ib subgroups), Alphaproteobacteria (Type II subgroup), and Verrucomicrobia, and may show habitat preference (Knief, 2015), with the verrucomicrobial MOB typically inhabiting acidic and thermophilic geothermal environments (Op den Camp et al., 2009; Sharp et al., 2014). The proteobacterial MOB are ubiquitous and thought to be relevant in terrestrial ecosystems, acting as a CH<sub>4</sub> sink in well-aerated upland soils and CH<sub>4</sub> biofilter at oxic-anoxic interfaces (Ho et al., 2019b; Kaupper et al., 2020a; Praeg et al., 2017; Reim et al., 2012; Shrestha et al., 2012). Accordingly, proteobacterial MOB can be distinguished based on their biochemistry and ecophysiology, which reflect on their ecological life strategies and response to disturbances (Ho et al., 2017a; Semrau et al., 2010; Trotsenko and Murrell, 2008). The *pmoA* gene (encoding for the pMMO) phylogeny corresponds with that of the 16S rRNA gene, and is commonly targeted to characterize the MOB in complex communities (e.g., Dumont et al., 2011; Karwautz et al., 2018; Knief, 2015; Kolb et al., 2003). Therefore, aerobic CH<sub>4</sub> oxidation is catalyzed by a defined microbial guild with relatively low diversity (mainly, proteobacteria in non-geothermal environments) when compared to other microbial groups catalyzing generalized processes (e.g., denitrification, respiration). This allows the MOB to be clearly distinguished from the non-MOB in complex communities, making the MOB interactome a suitable model system for our study.

Here, we elaborate the response of a CH<sub>4</sub>-driven interaction network to desiccation-rewetting to determine how MOB activity is affected by the disturbance-induced structuring of the interactome. A DNA-based SIP approach using <sup>13</sup>C-CH<sub>4</sub> was coupled to a co-occurrence network analysis after Illumina MiSeq sequencing of the 16S rRNA gene, allowing direct association of MOB activity to the structure of the interaction network (CH<sub>4</sub> food web). Although the network analysis is a useful tool to explore interactions in complex microbial communities (e.g., Barberán et al., 2012; Ho et al., 2016a, 2020; Mo et al., 2020; Morriën et al., 2017; Ratzke et al., 2020), biological interpretation of the analysis (e.g., causative mechanisms driving the interaction) re-

quires further probing. Given that the MOB are the only members of the interactome capable of using CH<sub>4</sub> as a carbon and energy source, it is not unreasonable to assume that <sup>13</sup>C-labeled non-MOB microorganisms depended on and interacted with the MOB (e.g., via cross-feeding and co-aggregation; Ho et al., 2016a; Pérez-Valera et al., 2017). Coupling SIP to the network analysis thus confirms the unidirectional flow of substrate from the metabolically active MOB to non-MOB. We hypothesized that a more complex interaction network will arise as a response to desiccation-rewetting, as documented in other single or sporadic disturbance events, given sufficient recovery time (Eldridge et al., 2015; Pérez-Valera et al., 2017). With the elimination of less desiccation-resistant/tolerant microorganisms, it is not unreasonable to postulate that the surviving community members were forced to interact more among themselves, increasing metabolic exchange which further drives their co-occurrence over time (Dal Co et al., 2020; Ratzke et al., 2020; Tripathi et al., 2016; Zelezniak et al., 2015).

## 4.3 Materials and Methods

### 4.3.1 Soil Sampling and Microcosm Set-Up

The paddy soil (upper 10-15 cm) was collected from a rice field belonging to the Italian Rice Research Institute, Vercelli, Italy (45°20' N, 8°25' W). The soil pH and electrical conductivity (EC) were 6.5 and 0.2 dS m<sup>-1</sup>, respectively. The C and N concentrations were 13.9 mg C g<sub>dw</sub><sup>-1</sup> and 1.3 mg N g<sub>dw</sub><sup>-1</sup>, respectively. The concentrations of nitrite and nitrate (NO<sub>x</sub><sup>-</sup>), sulphate, and phosphate were 34.4 µg N g<sub>dw</sub><sup>-1</sup>, 96 µg g<sub>dw</sub><sup>-1</sup>, and 0.6 µg g<sub>dw</sub><sup>-1</sup>, respectively. Agricultural practices in the rice field have been reported in detail elsewhere (Krueger et al., 2001). Generally, rice was cropped in the paddy soil twice a year (May/June to September/October and January/February to May/June), with each rice growing season spanning over 4-5 months; rice was not grown for approximately two months in winter (Krueger et al., 2001). The paddy field was drained prior to rice harvest and left fallow for 2-3 weeks before the commencement of the next rice growing season. Soil sampling was performed in May 2015 after drainage and rice harvest. After sampling, the soil was air-dried at ambient temperature and sieved (2 mm) to eliminate (fine) roots and debris, before being stored in a plastic container at room temperature till incubation set-up (November, 2017). Paddy soil prepared and stored under the same conditions < 5 years after sampling showed comparable potentially active MOB community composition (mRNA-based community analysis) over ~80 days incubation after re-wetting (Collet et al., 2015).

Each microcosm consisted of 10 g soil saturated with 4.5 mL autoclaved deionized

water in a Petri dish. The saturated soil was homogenized, and pre-incubated under  $\sim 10$  % v/v  $\text{CH}_4$  in air at  $25^\circ\text{C}$  in an air-tight jar. Following pre-incubation (7 days), desiccation was induced by placing the microcosms under a laminar flow cabinet overnight (15 hours) to achieve a gravimetric water loss of  $> 95$  % in the disturbed microcosm (Figure S10; Ho et al., 2016c). After desiccation, water loss was replenished by adding the corresponding amount of autoclaved deionized water, and incubation resumed under the same conditions as before. Microcosms not exposed to desiccation-rewetting (un-disturbed) served as reference. A total of 42 microcosms were constructed (Figure S10). At designated intervals (i.e., pre-incubation, as well as 1 – 7, 27 – 34, and 64 – 71 days after disturbance; Figure S10),  $^{13}\text{C}$ - $\text{CH}_4$  labelling incubation was performed; the microcosms ( $n=6$ ) were transferred into a flux chamber and incubated under 2 % v/v  $\text{CH}_4$  ( $^{13}\text{C}$ - $\text{CH}_4$ ,  $n=4$ ; unlabelled  $\text{C}$ - $\text{CH}_4$ ,  $n=2$ ) in air. Headspace  $\text{CH}_4$  was replenished when  $\text{CH}_4$  in the flux chamber was reduced to  $< 0.5$  % v/v. Incubation in the flux chamber was performed over 6 - 7 days or until at least  $500 \mu\text{mol CH}_4$  was consumed to ensure sufficient labelling (Neufeld et al., 2007b). After incubation, the soil was homogenized, shock-frozen, and stored in the  $-20^\circ\text{C}$  freezer until DNA extraction.

### 4.3.2 Methane and Inorganic N Measurements

Headspace  $\text{CH}_4$  was measured daily in all replicates (i.e., both unlabelled  $\text{C}$ - and  $^{13}\text{C}$ - $\text{CH}_4$  incubations) using a gas chromatograph (7890B GC System, Agilent Technologies, Santa Clara, USA) coupled to a pulsed discharge helium ionization detector (PD-HID), with helium as the carrier gas. The  $\text{CH}_4$  uptake rates were determined by linear regression from the slope of  $\text{CH}_4$  depletion with at least three time intervals (12-24 hours between intervals). Soluble ammonium and nitrate were determined in all replicates in autoclaved deionized water (1:2.5 w/v) after centrifugation and filtration ( $0.2 \mu\text{m}$ ) of the soil suspension. Soluble ammonium was determined colorimetrically (Horn et al., 2005) using an Infinite M plex plate reader (TECAN, Meannedorf, Switzerland), whereas nitrate was determined using a Sievers 208i NO analyzer system (GE Analytical Instruments, Boulder, CO, USA) with 50 mM  $\text{VCl}_3$  in 1 M sterile HCl as a reducing agent.

### 4.3.3 DNA Extraction and Isopycnic Ultracentrifugation

DNA was extracted using the DNeasy PowerSoil Kit (Qiagen, Hilden, Germany) according to the manufacturer's instruction. DNA was extracted in duplicate for each sample ( $n=6$ , per treatment and time) and pooled after elution to obtain sufficient amounts

for the isopycnic ultracentrifugation.

DNA stable isotope probing was performed according to Neufeld et al. (2007b). Isopycnic ultracentrifugation was performed at 144000 g for 67 hours using an Optima L-80XP (Beckman Coulter Inc., USA). Each ultracentrifugation run consisted of DNA extracted from incubations containing  $^{13}\text{C}$ - and  $^{\text{unlabelled}}\text{C}$ - $\text{CH}_4$  to distinguish the 'light' from the 'heavy' fractions (Figure S11). Fractionation was performed immediately after centrifugation using a hydraulic pump (Duelabo, Dusseldorf, Germany) at 3 rpm  $\text{min}^{-1}$ . Although 10 - 11 fractions were obtained, the last fraction was discarded, yielding 9 - 10 fractions per sample. Fractionation was unsuccessful for DNA sampled from two of the four replicate in the disturbed microcosm ( $^{13}\text{C}$ - $\text{CH}_4$  incubation, 64 - 71 days interval). Given that a minimum of three replicates is needed to construct each network, post-disturbance samples were grouped into days 1 - 7 (immediately after disturbance) and 27 - 71 (during recovery) for subsequent  $^{13}\text{C}$ -enriched 16S rRNA gene-derived network analysis (see Subsection 4.3.7). In the other time intervals, at least three replicates were obtained in the  $^{13}\text{C}$ - $\text{CH}_4$  incubation. The density gradient of each fraction was determined by weighing on a precision scale (technical replicate,  $n=10$ ). DNA precipitation was performed over night, as described in Neufeld et al. (2007b); nucleic acid was washed twice with ethanol, and the pellet was suspended in 30  $\mu\text{L}$  of ultrapure PCR water (INVITROGEN, Waltham, USA). The *pmoA* gene was enumerated from each fraction using a qPCR assay (MTOT; Table S5) to distinguish the 'heavy' from the 'light' fraction after comparing DNA from the  $^{13}\text{C}$ - and  $^{\text{unlabelled}}\text{C}$ - $\text{CH}_4$  incubations (Figure S11). The identified 'heavy' and 'light' DNA fractions as defined in Neufeld et al. (2007b) were amplified for Illumina MiSeq sequencing.

#### 4.3.4 Group-Specific qPCR Assays

The qPCR assays (MBAC, MCOC, and TYPEII targeting Type Ia, Ib, and II, respectively) were performed to follow the abundance of the MOB sub-groups over time (Table S5). Additionally, a qPCR assay targeting the total MOB population (MTOT) was applied to the DNA samples after fractionation to distinguish the 'heavy' from the 'light' fraction. The qPCR was performed using a BIORAD CFX Connect RT System (Biorad, Hercules, USA). Briefly, each reaction (total volume, 20  $\mu\text{L}$ ) consisted of 10  $\mu\text{L}$  SYBR 2X Sensifast (BIOLINE, London, UK), 3.5  $\mu\text{L}$  of forward/reverse primer each, 1  $\mu\text{L}$  0.04 % BSA, and 2  $\mu\text{L}$  template DNA. Template DNA was diluted 50-fold with RNase- and DNase-free water for the MBAC, MCOC, and TYPEII assays, and was undiluted for the MTOT assay. Diluting the template DNA 50-fold resulted in the optimal *pmoA* gene copy numbers. The primer combinations and concentrations, as well as the PCR

thermal profiles, are given elsewhere (see Table S5, Kaupper et al., 2020b; Kolb et al., 2003). The calibration curve ( $10^1$ - $10^8$  copy number of target genes) was derived from gene libraries as described before (Ho et al., 2011a). The qPCR amplification efficiency was 83 – 91%, with  $R^2$  ranging from 0.994 - 0.997. Amplicon specificity was determined from the melt curve, and confirmed by 1 % agarose gel electrophoresis yielding a band of the correct size in a preliminary qPCR run.

#### 4.3.5 Amplification for the *pmoA* and 16S rRNA Genes for Illumina MiSeq Sequencing

The *pmoA* gene was amplified using the primer pair A189f/mb661r, with the forward primer containing a fused 6 bp bar code. Each PCR reaction comprised of 25  $\mu$ L SYBR Premix Ex Taq<sup>TM</sup> (Tli RNaseH Plus, TaKaRa, Japan), 1  $\mu$ L forward/reverse primer each (10  $\mu$ M), 2  $\mu$ L template DNA (DNA concentration diluted to 2-8 ng  $\mu$ L<sup>-1</sup>), and 21  $\mu$ L sterilized distilled water, giving a total volume of 50  $\mu$ L. The PCR thermal profile consisted of an initial denaturation step at 94°C for 2 min, followed by 39 cycles of denaturation at 94°C for 30 s, annealing at 60°C for 30 s, and elongation at 72°C for 45 s. The final elongation step was at 72°C for 5 mins. The PCR products were verified on 1.2 % agarose gel electrophoresis showing a single band of the correct size, before purification using the E.Z.N.A. Cycle-Pure kit (Omega Bio-tek, USA). Subsequently, the purified amplicons were pooled at equimolar DNA amounts (200 ng) for sequencing using Illumina MiSeq version 3 chemistry (paired-end, 600 cycles). The *pmoA* sequence library was prepared using the TruSeq Nano DNA LT Sample Prep Kit set A (Illumina, Beijing, China).

The 16S rRNA gene was amplified using the primer pair 341F/805R. Each PCR reaction comprised of 4  $\mu$ L Buffers B and S each (CRYSTAL Taq-DNA-Polymerase, BiolabProducts, Germany), 4  $\mu$ L MgCl<sub>2</sub> (25 mM), 0.2  $\mu$ L Taq polymerase (5 U  $\mu$ L<sup>-1</sup>) (CRYSTAL Taq-DNA-Polymerase), 1.6  $\mu$ L dNTPs (10 mM), 2  $\mu$ L forward and reverse tagged-primers each (10  $\mu$ M), 4  $\mu$ L template DNA, and 18.2  $\mu$ L sterilized distilled water. The PCR thermal profile consisted of an initial denaturation step at 94°C for 7 min, followed by 30 cycles of denaturation at 94°C for 30 s, annealing at 53°C for 30 s, and elongation at 72°C for 30 s. The final elongation step was at 72°C for 5 mins. After the specificity of the amplicon was checked by 1 % agarose gel electrophoresis, the PCR product was purified using the GeneRead Size Selection Kit (Qiagen, Hilden, Germany). Subsequently, a second PCR was performed with adapters using the Nextera XT Index Kit (Illumina, San Diego, USA). The second PCR reaction consisted of 12.5  $\mu$ L 2X KAPA HiFi HotStart Ready Mix (Roche, Mannheim, Germany), 2.5  $\mu$ L of

each tagged primers (10  $\mu$  M), 2.5  $\mu$ L PCR grade water, and 5  $\mu$ L template from the first PCR. The amplicons were then purified using the MagSi-NGSPREP Plus Magnetic beads (Steinbrenner Laborsysteme GmbH, Wiesenbacj, Germany). Normalization of the amplicons before sequencing was performed using the Janus Automated Workstation (Perkin Elmer, Waltham Massachusetts, USA). Sequencing was performed using Illumina MiSeq version 3 chemistry (paired-end, 600 cycles).

### 4.3.6 *pmoA* and 16S rRNA Gene Amplicon Analyses

The *pmoA* gene amplicon was analyzed as described before (Reumer et al., 2018). Briefly, the paired-end reads were sorted based on the length and the quality of the primers ( $\leq 2$  errors) and barcodes ( $\leq 1$  error) after assembly in Mothur version 1.42.1 using the 'make.contigs' command (Schloss et al., 2009). Primers and barcodes which did not meet these requirements were removed. Similarly, chimeric reads were also removed in Mothur using the 'chimera.uchime' command with the 'self' option. After filtering, the initial  $\sim 1175000$  contigs generated from Illumina Miseq sequencing was reduced to  $\sim 628000$  high quality contigs, with approximately 15300 contigs per sample. The *pmoA* sequences were classified using BLAST by comparing to the GenBank nonredundant (nr) database and the lowest common ancestor algorithm in MEGAN version 5.11.3, based on curated *pmoA* gene database and MEGAN tree, respectively as detailed in Dumont et al. (2014). The high quality *pmoA* sequences could be affiliated (family, genus, or species level) to known cultured MOB. Based on the relative abundance of the *pmoA* gene sequences, a PCA was performed to determine the response of the MOB to desiccation-rewetting. To construct the PCA, the data matrix was initially analyzed using the DCA, which indicated linearly distributed data and revealed that the best-fit mathematical model was the PCA. To test whether the treatments harbored significantly different bacterial community composition and structure, plot clustering was tested using permutational multivariate analysis of variance (PERMANOVA; Anderson, 2001). The PCA was conducted in Canoco 4.5 (Biometrics, Wageningen, The Netherlands), and the PERMANOVA was calculated using PAST 4 software (Hammer et al., 2001). The *pmoA* gene sequences were deposited at the National Center for Biotechnology Information (NCBI), SRA database under the BioProject accession number PRJNA634611.

The 16S rRNA gene paired-end reads were firstly merged using PEAR (Zhang et al., 2014). Next, the merged sequences were processed using QIIME 2 version 2019.10, with de-multiplex and quality control performed with DADA2 (Callahan, 2017) using the consensus method to remove any remaining chimeric and low-quality sequences.



Approximately 1300000 high quality contigs were retained after filtering (on average, ~ 18000 contigs per sample). After the removal of singletons and doubletons, the samples were rarefied to 7560 sequences following the number of the lowest sample. The taxonomic affiliation was performed at 97 % similarity according to the Silva database v. 132 (Quast et al., 2013). The affiliations of the OTUs are given to the finest taxonomic resolution, whenever available. A PCA was performed to compare the bacterial community composition in the un-disturbed and disturbed incubations. The 16S rRNA-based PCA was constructed as described for the *pmoA*-based PCA using Canoco 4.5 (Biometrics, Wageningen, the Netherlands) after analysis of variance (PERMANOVA) in PAST 4 software. The 16S rRNA gene sequences were deposited at the NCBI, SRA database under the BioProject accession number PRJNA634611.

### 4.3.7 Co-Occurrence Network Analysis

To explore the complexity of the interaction between bacterial taxa (OTU-level) within the interactome, a co-occurrence network analysis was performed based on the 16S rRNA gene derived from the <sup>13</sup>C-enriched DNA ('heavy' fraction). For network construction, non-random co-occurrence analyses between bacterial OTUs were calculated using SparCC, a tool designed to assess correlations for compositional data (Friedman and Alm, 2012). For each network, P-values were obtained by 99 permutations of random selections of the data tables, applying the same analytical pipeline. The true SparCC correlations were selected based on statistical significance of  $p < 0.01$ , with a magnitude of  $> 0.7$  or  $< -0.7$ . The networks were assessed based on their topological features such as the number of nodes and edges (connectivity), modularity, number of communities, average path length, network diameter, average degree, and clustering coefficient (Table 4.1; Newman, 2003). The nodes in the networks represent OTUs, whereas the edges represent significantly positive or negative correlations between two nodes. Also, key nodes were identified based on the betweenness centrality, a measure of the frequency of a node acting as a bridge along the shortest path between two other nodes (Poudel et al., 2016). Hence, nodes with high betweenness centrality can be regarded to represent important key taxa within the interaction network (Borgatti, 2005). The co-occurrence network analysis was performed using the Python module 'SparCC', and the network construction and properties were calculated with Gephi (Bastian et al., 2009).

### 4.3.8 Statistical Analysis

Significant differences ( $p < 0.05$ ) in the CH<sub>4</sub> uptake rate and qPCR analyses per time between treatments (un-disturbed and disturbed incubations) were performed using IBM SPSS Statistics (IBM, Armonk, USA). The data were tested for normal distribution using the Kolmogorov-Smirnov test and the Shapiro-Wilk test. Where normal distribution was met, a two-sided paired t-test was performed. Otherwise, a non-parametric test (Wilcoxon signed rank test) was performed. Additionally, CH<sub>4</sub> uptake rates were correlated to the abundances of Type Ia, Ib, and II *pmoA* gene separately by linear regression in Origin (OriginLab Corporation, Northampton, MA, USA).

## 4.4 Results

### 4.4.1 The Abiotic Environment

The trend in CH<sub>4</sub> uptake was largely comparable in the un-disturbed and disturbed incubations, where activity peaked at 27 – 34 days before reaching similar rates after 71 days (Figure 4.1). However, CH<sub>4</sub> uptake was significantly lower ( $p < 0.05$ ) immediately after desiccation-rewetting when compared to the un-disturbed incubation (un-disturbed,  $0.64 \pm 0.06 \mu\text{mol h}^{-1} \text{g}_{\text{dw}}^{-1}$ ; desiccated-rewetted,  $0.5 \pm 0.05 \mu\text{mol h}^{-1} \text{g}_{\text{dw}}^{-1}$ ); the adverse effects of the disturbance on CH<sub>4</sub> uptake were transient (< 5 days).

Soluble ammonium and nitrate were rapidly consumed during pre-incubation (Figure S12). The inorganic N concentrations significantly increased ( $p < 0.05$ ) after desiccation-rewetting. However, the elevated inorganic N concentrations were not sustained. Soluble ammonium and nitrate concentrations decreased to values similar to those after pre-incubation at ~ 34 days. Particularly, ammonium concentration was significantly higher in the un-disturbed than in the disturbed microcosm after incubation (day 71).

### 4.4.2 Response in Methanotroph Abundance

Group-specific qPCR assays were performed to enumerate the *pmoA* genes belonging to Type Ia, Ib, and II MOB to be used as proxies for MOB abundances. Generally, the gammaproteobacterial MOB were less responsive to desiccation-rewetting than the alphaproteobacterial ones (Figure 4.2). Although values were within the same order of magnitude and the discrepancies documented were not appreciable, changes in the abundance of Type Ia and Ib MOB were statistically significant comparing the

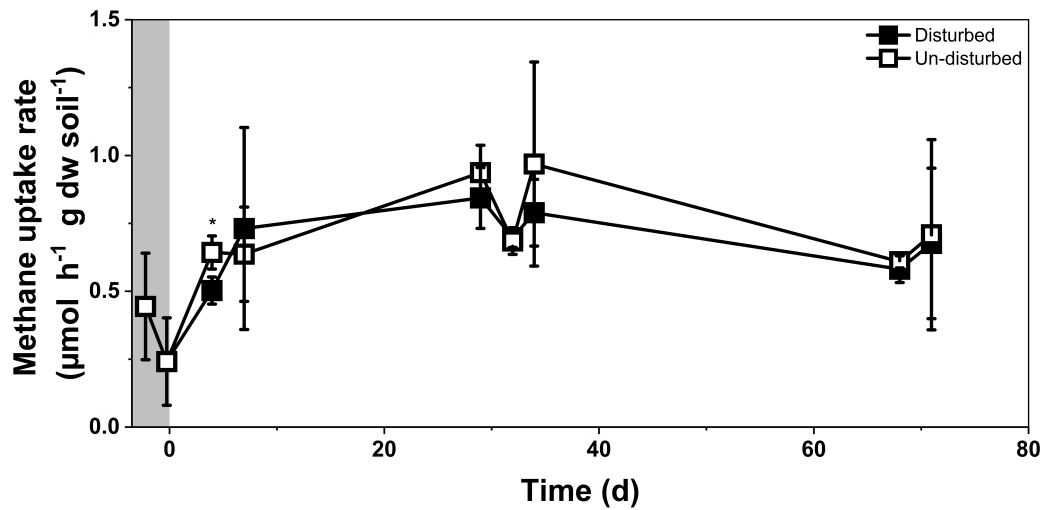


**Figure 4.1** CH<sub>4</sub> uptake rate in the un-disturbed and disturbed incubations determined during the pre-incubation, as well as 1–7, 27–34, and 64–71 days interval after desiccation-rewetting. Incubations with <sup>13</sup>C- and <sup>unlabeled</sup>C-CH<sub>4</sub> were combined (mean ± s.d., n = 6) for each treatment. Pre-incubation is denoted by the shaded area. Significant difference in the CH<sub>4</sub> uptake rate between treatments is indicated by an asterisk (t-test, p < 0.05).

un-disturbed to the desiccation-rewetted microcosms. Consistently, like for the Type II MOB, CH<sub>4</sub> uptake rates were significantly (p < 0.05) correlated to the abundances of Type Ib MOB (Figure S13). It is also noteworthy that Type I MOB were appreciably more abundant in the disturbed microcosm after the incubation despite showing an adverse effect on population numbers soon after desiccation-rewetting (Figure 4.2). Particularly, the Type II MOB abundance recovered well, appreciably increased by around two orders of magnitude after desiccation-rewetting (7 – 71 days). By comparison, Type I MOB abundance also increased but within a relatively narrow range (Type Ia MOB,  $2.1 \cdot 10^7 \pm 7.4 \cdot 10^6$  to  $3.4 \cdot 10^7 \pm 7.0 \cdot 10^6$ ; Type Ib MOB,  $2.5 \cdot 10^7 \pm 7.9 \cdot 10^6$  to  $1.9 \cdot 10^8 \pm 6.6 \cdot 10^7$  gene copy numbers g dw soil<sup>-1</sup>) during the same time frame (Figure 4.2). It appears that although Type II MOB constitute a minor overall fraction of the MOB population, they were more responsive and significantly increased in abundance after desiccation-rewetting.

#### 4.4.3 Effects of Desiccation - Rewetting on the Methanotrophic Community Composition, as Determined by DNA-based SIP

The bacterial communities, including the MOB in the 'heavy' and 'light' fractions were distinct, as revealed in a PCA for each time interval, showing a clear separation of the <sup>13</sup>C-enriched and <sup>unlabeled</sup>C-DNA (Figure S14). The 16S rRNA- and *pmoA* gene-derived

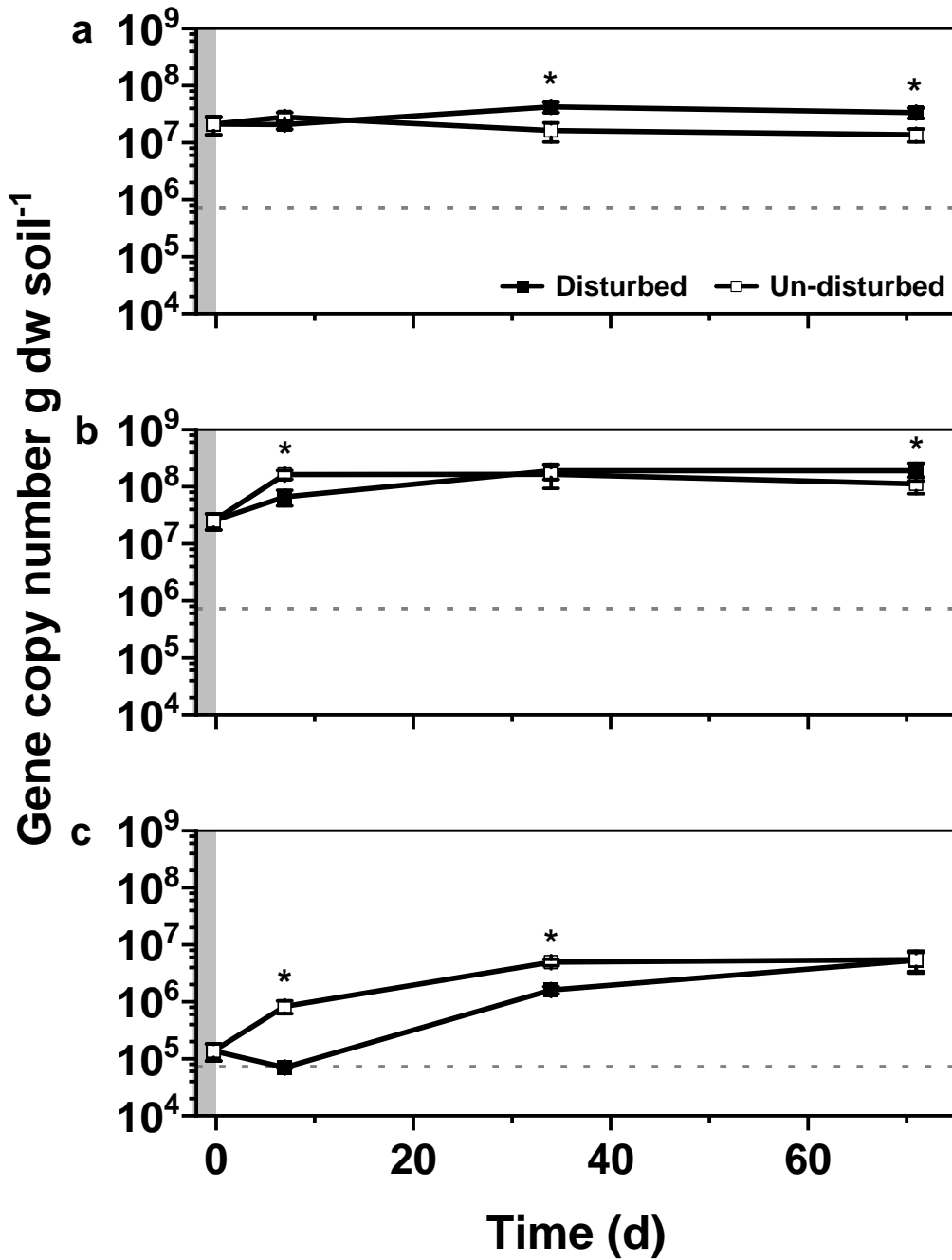


**Figure 4.2** Temporal changes in the *pmoA* gene abundance of Type Ia (a), Type Ib (b), and Type II (c) MOB, as determined from group-specific qPCR assays. Each qPCR reaction was performed in duplicate for each DNA extract ( $n = 6$ ), giving a total of 12 replicates per treatment, time, and assay. Pre-incubation is denoted by the shaded area, and dashed lines indicate the detection limit of the qPCR assays. Significant difference in the *pmoA* gene abundance between treatments is indicated by an asterisk (t-test,  $p < 0.05$ ).

sequencing analyses were then performed on the  $^{13}\text{C}$ -enriched DNA, representing the metabolically active and replicating community. The *pmoA* gene was sequenced before (after pre-incubation) and immediately after disturbance (1 – 7 days interval), as well as after incubation (64 – 71 days interval) to follow the recovery of the MOB community composition. The *pmoA* gene sequences, visualized as a PCA (Figure 4.3), revealed a distinct active MOB community prior to the disturbance (pre-incubation), and the community shifted soon after desiccation-rewetting, diverging from the community in the un-disturbed microcosm. Over 96 % of the variation in the MOB community composition could be explained by PC1 and PC2 (67.9 % and 28.5 % of the total variance, respectively). The active MOB which emerged soon after desiccation-rewetting (1 – 7 days interval) were predominantly comprised of members belonging to the putative Rice Paddy Cluster (RPC) closely affiliated to *Methylocaldum* (Type Ib; Lüke et al., 2014; Shiau et al., 2018b). 71 days post-desiccation-rewetting, the recovering community in the disturbed, as well as in the un-disturbed microcosms were more scattered, largely comprising of Type I MOB. The active MOB showed dynamic population shifts after desiccation-rewetting, with the recovered community becoming more varied after incubation.

#### **4.4.4 Effects of Desiccation - Rewetting on the Total Bacterial Community Composition, as Determined by DNA-based SIP**

The active bacterial community was largely comprised of members belonging to Gammaproteobacteria (families Methylomonaceae, Methylophilaceae, Burkholderiaceae, Rhodocyclaceae, and Nitrosomonadaceae), Bacteroidetes (family Chitinophagaceae and Microscillaceae), and Gemmatimonadetes (family Gemmatimonadaceae), collectively representing the majority of the population (> 75 %; Figure 4.4). Like the *pmoA* gene sequence analysis, the PCA derived from the 16S rRNA gene sequences revealed a compositional shift in the bacterial community after desiccation-rewetting, but the community recovered after 71 days, closely resembling the composition in the un-disturbed microcosm (Figure 4.3). Comparing the community in the un-disturbed and disturbed microcosms, *Methylocaldum* (Type Ib MOB), and *Methylobacter* (Type Ia) as well as members of Burkholderiaceae, were respectively detected at appreciably higher relative abundance soon after desiccation-rewetting (1-7 days interval) and during recovery (27-71 days interval), consistent with the *pmoA* gene sequence analysis (Figure S15). The active members of the bacterial community in the un-disturbed microcosm were generally more diverse; microorganisms present at differentially higher relative abundances belonged to Proteobacteria, Bacteroidetes,

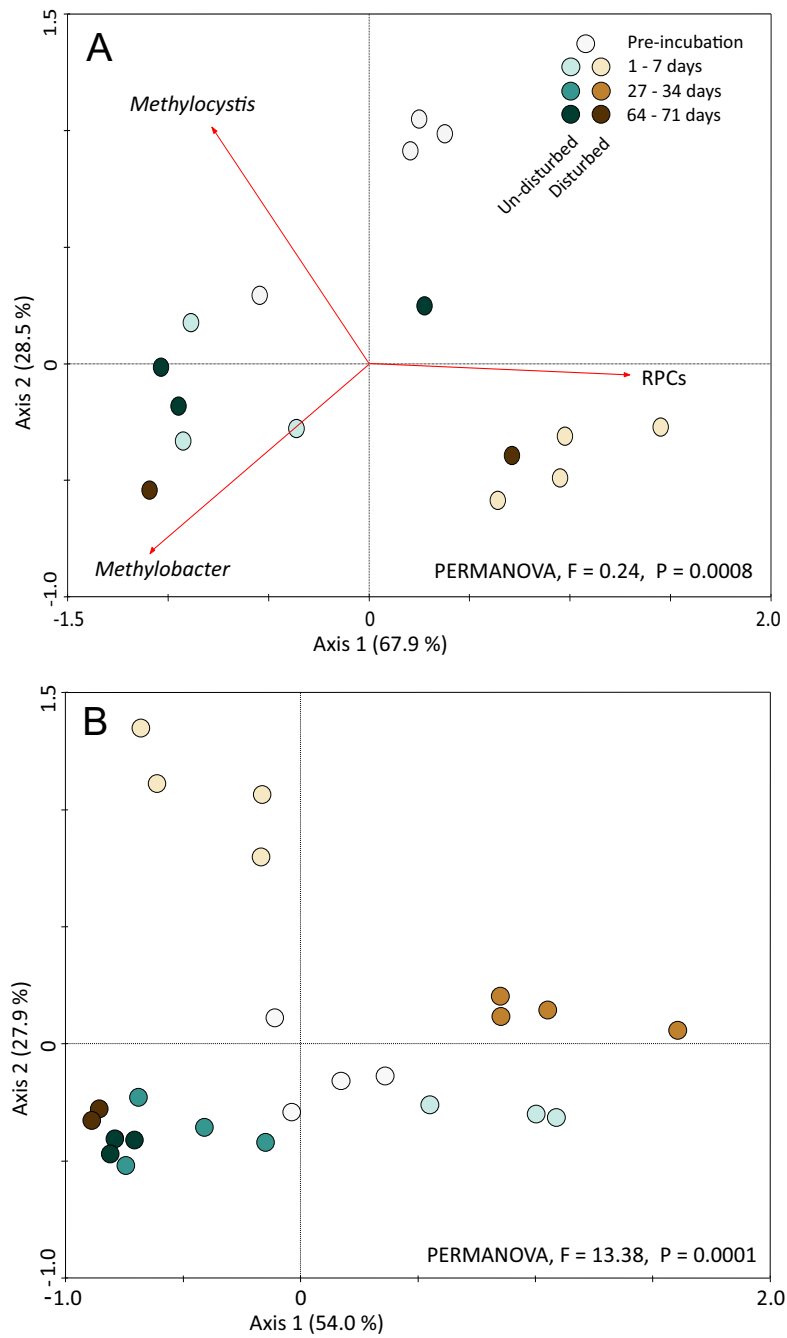


**Figure 4.3** Principal component analysis showing the response of the active MOB (A) and bacterial (B) community composition to desiccation-rewetting, as determined from the relative abundances of the *pmoA* and 16S rRNA gene sequences, respectively. Both the *pmoA* and 16S rRNA gene sequences were derived from the  $^{13}\text{C}$ -enriched DNA ('heavy' fraction). In (A), the vectors represent the predominant MOB belonging to Type Ia (*Methylobacter*), Type Ib (RPC, rice paddy cluster), and Type II (*Methylocystis*).

Verrucomicrobia, and Acidobacteria (family/genus level identification, Figures 4.4 and S15). Generally, the *pmoA* and 16S rRNA gene sequencing analyses were consistent, revealing the compositional shift and recovery of the active community.

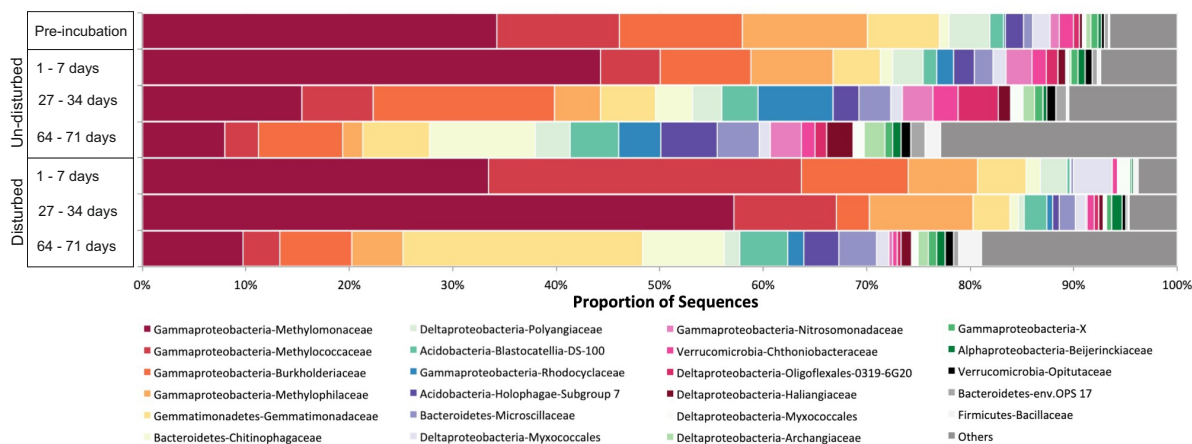


**Figure 4.4** The mean active bacterial community composition in the un-disturbed and disturbed incubations, based on the 16S rRNA gene sequence analysis. The 16S rRNA gene sequences were derived from the  $^{13}\text{C}$ -enriched DNA after incubation at 1–7, 27–34, and 64–71 days intervals.

#### 4.4.5 Response of the Co-Occurrence Network Structure to Desiccation - Rewetting

A 16S rRNA gene-based co-occurrence network analysis derived from the  $^{13}\text{C}$ -enriched 'heavy' fraction was performed to explore the complexity of the  $\text{CH}_4$ -driven interactome immediately after, and during the recovery from desiccation-rewetting (resilience; Figure 4.5). These networks were assessed by their topological properties comparing the un-disturbed and disturbed incubations (Table 4.1). Generally, both the microbial communities in the un-disturbed and after desiccation-rewetting increased in connectivity over time (i.e., higher no. of edges, degree, clustering coefficient; Table 4.1). However, a more connected network emerged after desiccation-rewetting (> 27 days), exhibiting a higher number of connections (edges), connections per node (degree), and clustering coefficient than in the un-disturbed community (Table 4.1). Accordingly, the desiccation-rewetted community was characterized by a shorter average path length (Table 4.1). Although modularity generally decreased in all microcosms after pre-incubation, the community showed a less modular structure after desiccation-rewetting when compared to the un-disturbed community during recovery. Additionally, to account for biases arising from the imbalance number of replicates used to construct the networks (i.e., grouping of 27-34 and 64-71 days intervals yielding a higher number

of replicates,  $n = 6$  or  $7$ ), the networks were re-constructed using 4 randomly selected replicates from all replicates for the 27-71 days interval. The results obtained were consistent and support the general trends documented in the networks using all replicates (Table S6). Overall, the network structure of the active bacterial community became more complex and connected after recovery from desiccation-rewetting, demonstrating that the disturbance fostered a closer association of community members within the interactome.

**Table 4.1** Correlations and topological properties of the interaction networks during preincubation, and recovery from desiccation-rewetting at 1–7 and 27–71 days intervals.

Network properties	Pre-incubation	Un-disturbed		Disturbed	
		1-7 d	27-71 d	1-7 d	27-71 d
<b>Number of nodes<sup>a</sup></b>	165	181	211	210	156
<b>Number of edges<sup>b</sup></b>	769	616	1547	888	1835
<b>Positive edges<sup>c</sup></b>	435 (56%)	368 (60%)	919 (59%)	493 (56%)	1235 (67%)
<b>Negative edges<sup>d</sup></b>	334 (43%)	248 (40%)	628 (41%)	395 (44%)	600 (33%)
<b>Modularity<sup>e</sup></b>	2.96	2.32	1.81	2.78	0.88
<b>Number of communities<sup>f</sup></b>	26	38	29	58	12
<b>Network diameter<sup>g</sup></b>	6	9	12	8	6
<b>Average path length<sup>h</sup></b>	2.95	3.35	3.09	2.99	2.49
<b>Average degree<sup>i</sup></b>	9.32	6.80	14.66	8.45	23.52
<b>Average clustering coefficient<sup>j</sup></b>	0.430	0.385	0.449	0.358	0.567

<sup>a</sup> Microbial taxon (at genus level) with at least one significant ( $P < 0.01$ ) and strong ( $\text{SparCC} > 0.7$  or  $< -0.7$ ) correlation.

<sup>b</sup> Number of connections/correlations obtained by SparCC analysis.

<sup>c</sup> SparCC positive correlation ( $> 0.7$  with  $P < 0.01$ ).

<sup>d</sup> SparCC negative correlation ( $< -0.7$  with  $P < 0.01$ ).

<sup>e</sup> The capability of the nodes to form highly connected communities, that is, a structure with high density of between nodes connections (inferred by Gephi).

<sup>f</sup> A community is defined as a group of nodes densely connected internally (Gephi).

<sup>g</sup> The longest distance between nodes in the network, measured in number of edges (Gephi).

<sup>h</sup> Average network distance between all pair of nodes or the average length off all edges in the network (Gephi).

<sup>i</sup> The average number of connections per node in the network, that is, the node connectivity (Gephi).

<sup>j</sup> How nodes are embedded in their neighborhood and the degree to which they tend to cluster together (Gephi).

The top five nodes with the highest betweenness centrality were identified in all treat-



ments (Figure 4.5 & Table S7). As anticipated, the key nodes comprised of MOB, as well as non-MOB methylophs; the MOB are a subset of the methylophs (Chistoserdova, 2015). Surprisingly, many other non-MOB bacterial taxa also formed the key nodes. These taxa were rather unique to each treatment (un-disturbed and disturbed) at 1-7 and 27-71 days intervals (Figure 4.5 & Table S7). It appears that non-MOB, albeit unable to assimilate CH<sub>4</sub> directly, were also relevant members of the interactome.

## 4.5 Discussion

### 4.5.1 Recovery and Resilience of the Methanotrophic Activity and Community Composition Following Desiccation - Rewetting

The MOB activity was resilient to desiccation-rewetting. Periodic exposure of the paddy soil to lower soil water content after drainage for rice harvest may have selected for a desiccation-tolerant MOB community. This may partly explain the transient (< 5 days) adverse effect on CH<sub>4</sub> uptake rates, which rapidly recovered. Nevertheless, the recovery in MOB activity to single disturbance events is not entirely unexpected, as has been shown before (e.g., soil structural disruption, Kumaresan et al., 2011; long-term drought spanning over decades, Collet et al., 2015; desiccation and heat stress, Ho et al., 2016b,c). Similarly, MOB activity recovered from multiple disturbances, with soils harboring low-affinity MOB showing resilience to repeated desiccation and ammonium stress (van Kruistum et al., 2018), and compounded disturbances associated to land transformation given sufficient recovery time (e.g., over 15 years after peat excavation; Reumer et al., 2018). However, the recovery in CH<sub>4</sub> oxidation may be accompanied by compositional shifts in the MOB community, affecting the trajectory of MOB succession after disturbance (Ho et al., 2016c).

In contrast to previous work (e.g., Collet et al., 2015; Ho et al., 2018, 2016c; Jurgburg et al., 2017; Krause et al., 2017; Kumaresan et al., 2011; Reumer et al., 2018), a time-series <sup>13</sup>C-CH<sub>4</sub> labeling approach was employed in this study to directly relate not only the MOB activity to the response of the metabolically active MOB, but also to the structure of the interaction network, to desiccation-rewetting. The active bacterial community composition, including the MOB, recovered well as indicated by the 16S rRNA gene sequence analysis, which showed that the disturbed community resembled that of the un-disturbed community, clustering closely together after incubation (PCA; Figure 4.3). Specifically, *Methylocaldum* was predominant soon after desiccation-rewetting, whereas *Methylobacter* and Burkholderiaceae were present at relatively higher abundances during recovery from the disturbance (Figures 4.4

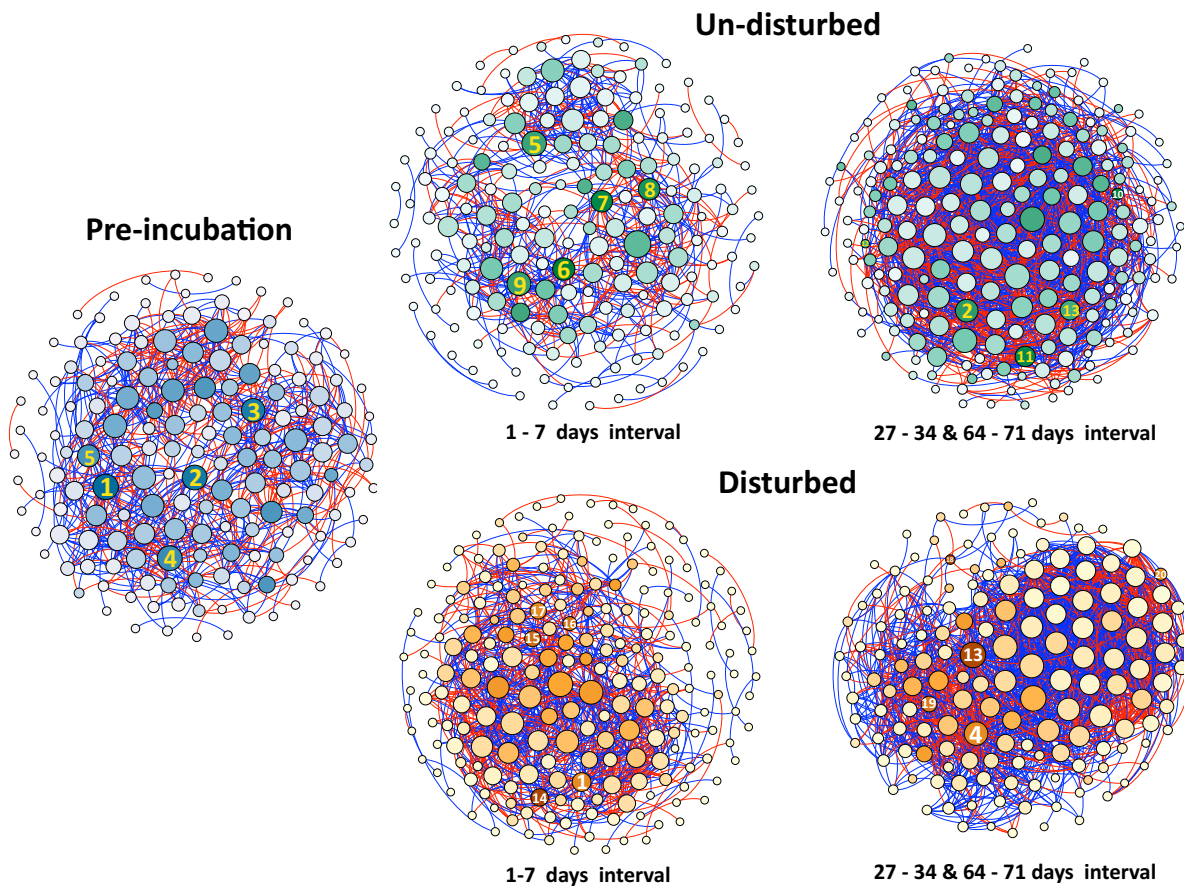


**Figure 4.5** Co-occurrence network analysis of the active bacterial community based on the 16S rRNA gene during pre-incubation, and after desiccation-rewetting. The 16S rRNA gene sequences were derived from the  $^{13}\text{C}$ -enriched DNA ('heavy' fraction). Samples from 27 to 34 and 64–71 days intervals were combined to have sufficient replicates for the network analysis; density gradient ultracentrifugation was unsuccessful in 2 of 4 replicated  $^{13}\text{C}$ – $\text{CH}_4$  incubations in the disturbed microcosm at 64–71 days interval. Significant ( $p < 0.01$ ) positive (magnitude  $> 0.7$ ) and negative (magnitude,  $< - 0.7$ ) SparCC correlations are respectively denoted by the blue and red edges. Each node represents a bacterial taxa at the OTU level, and the size of the node corresponds to the number of connections (degree). The colour intensity indicates the betweenness centrality (darker shades indicating higher values). The numbers in the key nodes (top five nodes with highest betweenness centrality) refer to (1) Methylophilaceae, (2) Rhodocyclaceae, (3) *Gemmatirosa*, (4) *Crenothrix* ( $\text{CH}_4$ -oxidizer), (5) Acidobacteria subgroup 6, (6) Gemmatimonadaceae, (7) *Methylomonas* (MOB), (8) *Noviherbaspirillum*, (9) Beijerinckiaceae, (10) *Paenibacillus*, (11) Acidobacteria subgroup 7, (12) Opiritaceae, (13) Unclassified Bacteria, (14) *Sphingomonas*, (15) Blastocatellia, (16) *Ideonella*, (17) *Chthoniobacter*, (18) Proteobacteria, (19) Chitinophagaceae (20) Microscillaceae. Detailed topological properties of the networks are provided in Table 4.1.

and S15). Gammaproteobacterial MOB, including *Methylocaldum* and *Methylobacter* species, are generally known to be rapid colonizers, proliferating under high nutrient and CH<sub>4</sub> availability (Ho et al., 2013a, 2016b), whereas the dominance and role of Burkholderiaceae during recovery from disturbances remain elusive. However, members of the family Burkholderiaceae exhibit metabolic versatility, with *Cupriavidus* reported to stimulate MOB growth (Stock et al., 2013). Furthermore, *Ralstonia*, another Burkholderiaceae, has been documented to co-occur with MOB in a <sup>13</sup>C-CH<sub>4</sub> labeling study, likely caused by cross-feeding, suggesting that there was a trophic interaction with MOB (Qiu et al., 2008). Like for the gammaproteobacterial Type Ib MOB, the significant correlation between CH<sub>4</sub> uptake rates and the alphaproteobacterial MOB, suggests a coupling of MOB activity and the growth of these sub-groups (Figure S13). The alphaproteobacterial MOB (*Methylocystis*; Type II) were seemingly more responsive to the disturbance, exhibiting a gradual increase in numerical abundance during the incubation (Figure 4.2). This reinforces previous studies documenting the emergence of this sub-group (*Methylocystis-Methylosinus*) after stress events (Ho et al., 2011a, 2016b,c; van Kruistum et al., 2018). It is thought that desiccation-rewetting may trigger the proliferation of alphaproteobacterial MOB either by awakening dormant members of the seedbank community and/or generating open niches for recolonization (Collet et al., 2015; Ho et al., 2016c; Kaupper et al., 2020b; Whittenbury et al., 1970a). Also, the gradual increase in alphaproteobacterial MOB abundance may be attributable to a relatively slower recovery after being adversely affected by desiccation-rewetting, having a lower initial abundance than gammaproteobacterial MOB. Admittedly, we cannot exclude experimental artifacts deriving from soil preparation which may affect the MOB, but the soil was mildly pre-processed (i.e., air-dried at ambient temperature and sieved), ensuring homogeneity for a standardized incubation. Overall, the differential response among MOB sub-groups was consistent with trends detected previously.

#### **4.5.2 The Emergence of a More Complex and Connected Methane-Driven Interactome After Desiccation - Rewetting**

MOB thrive in the presence of specific accompanying microorganisms, exhibiting higher activity and growth as cocultures than as monocultures (Benner et al., 2015; Ho et al., 2014; Iguchi et al., 2011; Jeong et al., 2014; Krause et al., 2017; Stock et al., 2013; Veraart et al., 2018). This emphasizes the relevance of interdependent relationships among members of a MOB interactome for community functioning. Although MOB activity and community composition may recover, disturbances may exert an impact on the structure of the microbial network, affecting the interaction among community

members which may have consequences in future disturbances (Berg and Ellers, 2010; Bissett et al., 2013; Ho et al., 2020; Ratzke et al., 2020; Sun et al., 2013).

Interestingly, the MOB interactome became more complex and increased in connectivity during recovery (> 27 days) from desiccation-rewetting (Table 4.1 & Figure 4.5). The disturbance-induced highly connected interactome suggests higher competition for specific niches (van Elsas et al., 2012), which likely became available after the disturbance event. This enables rapid re-colonization of the open niches, resulting in the recovery of MOB activity and abundance, particularly when CH<sub>4</sub> is not limiting (Ho et al., 2011a; Kaupper et al., 2020b; Pan et al., 2014). The emergence of a more complex network after disturbance also suggests that the loss of some microorganisms were compensated by other community members having similar roles; the community was thus sufficiently redundant to sustain MOB activity (Eldridge et al., 2015; Mendes et al., 2015; Tripathi et al., 2016). Similarly, when compared to an un-perturbed soil, the bacterial network after bio-perturbation (> 12 months) caused by the foraging activity of burrowing mammals increased in connectedness (Eldridge et al., 2015). In another form of disturbance, the microbial network was altered, increasing in the number of positively co-occurring bacteria during the recovery from a forest fire (12 months; Pérez-Valera et al., 2017). In line with these studies, the interaction networks increased in complexity, becoming more connected after deforestation for oil palm (Tripathi et al., 2016) and after abandonment of agriculture (Morriën et al., 2017).

Like these disturbances, desiccation-rewetting fostered closer associations among interacting members of the MOB interactome, supporting our hypothesis. The increase in network complexity, as indicated by a higher number of edges, degree, and clustering efficiency suggests a more connected network, concomitant to a shorter average path length which indicates a tighter and more efficient network, in response to desiccation-rewetting (Dal Co et al., 2020; Mendes et al., 2018; Zhou et al., 2010). Hence, desiccation-rewetting likely augmented or consolidated metabolic exchange to increase co-occurrence among community members within the interactome, giving rise to a more complex interaction network (Ratzke et al., 2020; Zelezniak et al., 2015). The increase in network complexity directly related to the recovery in MOB activity. Nevertheless, modularity decreased over time, possessing fewer independently connected groups (compartments) within the network (Zhou et al., 2010), more pronounced in the desiccation-rewetted community. A highly modular network is thought to restrict and localize the effects of a disturbance within compartments in the network (Ruiz-Moreno et al., 2006; Zhou et al., 2010). Therefore, the loss of modularity after contemporary disturbances suggests that future disturbances will more evenly affect community members. Hence, community composition and activity, when examined

alongside the network structure, provided a more comprehensive understanding of microbial responses to contemporary and future disturbances.

Expectedly, the nodes with high betweenness centrality were found to comprise of methylotrophs, including the MOB (Figure 4.5). These key nodes were not necessarily bacterial taxa that were present at significantly higher relative abundances (e.g., Burkholderiaceae; Figure 4.4) but rather, refer to nodes acting as a bridge between other nodes with significantly higher frequencies (Poudel et al., 2016). As such, the key nodes within the network are crucial members of the MOB interactome, potentially having a significant regulatory effect on the other members of the interactome; the loss of the key nodes is anticipated to unravel the interaction network (van der Heijden and Hartmann, 2016; Williams et al., 2014). Because the methylotrophs can oxidize methanol and other intermediary products of CH<sub>4</sub> oxidation (e.g., formaldehyde, formate), cross-feeding between the MOB and non-MOB methylotrophs (e.g., *Methylotenera*, *Methylophilus*) drives their co-occurrence, as has been established before (Krause et al., 2017). Interestingly, many non-MOB/methylotrophs also formed the key nodes. Given that the non-MOB cannot utilize CH<sub>4</sub> as a carbon and energy source, their identification as key nodes indicates their potential regulatory role, indirectly via interaction-induced effects, on the MOB activity (van der Heijden and Hartmann, 2016). Among the non-MOB key nodes, other members of Sphingomonadaceae (*Sphingopyxis*) but not specifically *Sphingomonas*, have been shown to significantly stimulate the expression of the *pmoA* gene when co-cultured with an alphaproteobacterial MOB (*Methylocystis*; Jeong et al., 2014). Members of Gemmatimonadaceae have been co-detected along with the MOB in <sup>13</sup>C-CH<sub>4</sub> labeling SIP studies, but their exact role within the interactome remains to be elucidated (Zheng et al., 2014). Similarly, the underlying mechanisms that drive the interaction between other co-occurring bacterial taxa and the MOB warrant further exploration through isolation and co-culture studies (Kwon et al., 2019a). However, it is likely that some members of the co-occurring taxa may reciprocally interact with the MOB, supporting MOB growth and activity (e.g., *Sphingomonas*), and contributed to the resilience of the MOB following desiccation-rewetting. Accordingly, the bacterial taxa representing key nodes were distinct in the un-disturbed microcosm and after desiccation-rewetting, despite compositional recovery among metabolically active members of the community (Figure 4.3). This indicates sufficient redundancy among active members of the MOB interactome; presumably, the different key taxa in the un-disturbed and disturbed community shared similar traits relevant for community functioning.

## 4.6 Conclusion

Our findings, based on the time-resolved  $^{13}\text{C}$ - $\text{CH}_4$  approach, reinforced previous DNA-based studies, showing the differential response among the MOB to disturbances, likely reflecting on their ecological life strategies (Ho et al., 2013a). Widening current understanding, we showed that although MOB activity recovered after desiccation-rewetting and the post-disturbance microbial community may resemble those in the undisturbed soil, the disturbance legacy manifests in the structure of the co-occurrence network, which became more complex but less modular. Therefore, community interaction profoundly changed after desiccation-rewetting, which may have consequences for community functioning with recurring and/or compounded disturbances. More generally, our findings move beyond biodiversity-functioning relationships to encompass interaction-induced responses in community functioning.

## Chapter 5

# Recovery of Methanotrophic Activity Is Not Reflected in the Methane-Driven Interaction Network after Peat Mining

Thomas Kaupper<sup>1</sup>, Lucas W. Mendes<sup>2</sup>, Monica Harnisz<sup>3</sup>, Sascha M.B. Krause<sup>4</sup>, Marcus A. Horn<sup>1</sup>, Adrian Ho<sup>1</sup>.

Published in *Applied Environmental Microbiology* (2021), 87(5):e02355-20

---

<sup>1</sup>Institute of Microbiology, Leibniz Universität Hannover, Herrenhäuser Str. 2, 30419 Hannover, Germany.

<sup>2</sup>Center for Nuclear Energy in Agriculture, University of São Paulo-USP, Brazil.

<sup>3</sup>Department of Environmental Microbiology, University of Warmia and Mazury in Olsztyn, Olsztyn, Poland.

<sup>4</sup>Zhejiang Tiantong Forest Ecosystem National Observation and Research Station, School of Ecological and Environmental Sciences, East China Normal University, Shanghai 200241, China.

The published version can be found online:  
<https://doi.org/10.1128/AEM.02355-20>

## 5.1 Abstract

Aerobic MOB are crucial in ombrotrophic peatlands, driving the CH<sub>4</sub> and nitrogen cycles. Peat mining adversely affects the MOB, but activity and community composition/abundances may recover after restoration. Considering that the MOB activity and growth are significantly stimulated in the presence of other microorganisms, the CH<sub>4</sub>-driven interaction network, encompassing MOB and non-MOB (i.e., MOB interactome), may also be relevant conferring community resilience. Yet, little is known of the response and recovery of the MOB interactome to disturbances. Here, we determined the recovery of the MOB interactome as inferred by a co-occurrence network analysis, comparing a pristine and restored peatland. We coupled a DNA-based SIP approach using <sup>13</sup>C-CH<sub>4</sub> to a co-occurrence network analysis derived from the <sup>13</sup>C-enriched 16S rRNA gene sequences to relate the response in MOB activity to the structuring of the interaction network. MOB activity and abundances recovered after peat restoration since 2000. '*Methylomonaceae*' was the predominantly active MOB in both peatlands, but differed in the relative abundance of *Methylacidiphilaceae* and *Methylocystis*. However, bacterial community composition was distinct in both peatlands. Likewise, the MOB interactome was profoundly altered in the restored peatland. Structuring of the interaction network after peat mining resulted in the loss of complexity and modularity, indicating a less connected and efficient network, which may have consequences in the event of recurring/future disturbances. Therefore, determining the response of the CH<sub>4</sub>-driven interaction network, in addition to relating MOB activity to community composition/abundances, provided a more comprehensive understanding of the resilience of the MOB.

## 5.2 Importance

The resilience and recovery of microorganisms from disturbances are often determined with regard to their activity and community composition/abundances. Rarely has the response of the network of interacting microorganisms been considered, despite accumulating evidence showing that microbial interaction modulates community functioning. Comparing the CH<sub>4</sub>-driven interaction network of a pristine and restored peatland, our findings revealed that the metabolically active microorganisms were less connected and formed less modular 'hubs' in the restored peatland, indicative of a less complex network which may have consequences with recurring disturbances and environmental changes. This also suggests that the resilience and full recovery in the MOB activity and abundances do not reflect on the interaction network. Therefore, it is relevant



to consider the interaction-induced response, in addition to documenting changes in activity and community composition/abundances, to provide a comprehensive understanding of the resilience of microorganisms to disturbances.

### 5.3 Introduction

Peat is harvested to meet global fuel and feed demands (e.g., renewable combustible fuel, soil additives; Cleary et al., 2005; Pryce, 1991). Mining profoundly alters the peat physico-chemical properties (e.g., increases pH and compaction, and reduces the availability of inorganic compounds; Andersen et al., 2006; Basiliko et al., 2007), exerting an effect on the indigenous microbial communities with consequences for microbially-mediated processes such as GHG emissions (Juottonen et al., 2012; Putkinen et al., 2018). Depending on the mining method (block-cut, vacuum-harvested peat), peat restoration to a pristine-like state can take decades, during which the rewetted peatlands may become a source of carbon, with altered CO<sub>2</sub> and CH<sub>4</sub> emissions (Basiliko et al., 2007; Holl et al., 2020). In particular, CH<sub>4</sub> emission in ombrotrophic peatlands is governed by the balance of CH<sub>4</sub> production in the anoxic peat layers, and aerobic CH<sub>4</sub> oxidation at niches where CH<sub>4</sub>-O<sub>2</sub> counter gradients occur (e.g., peat-overlying water layer). Hence, the aerobic MOB are key to mitigating CH<sub>4</sub> emission in peatlands, acting as a CH<sub>4</sub> bio-filter (Yavitt et al., 1988). Besides, diazotrophic MOB are a significant source of assimilable nitrogen, driving the N-cycle in ombrotrophic peatlands (Ho and Bodelier, 2015; Larmola et al., 2014; Vile et al., 2014). The MOB are thus highly relevant members of the peatland microbiome, participating in the C- and N-cycles. While changes in the abiotic environment following peat restoration have been the focus of earlier work (Andersen et al., 2006; Basiliko et al., 2007), the microbial community composition and abundances, specifically methanotrophy, in ombrotrophic peatlands have since gained attention (Esson et al., 2016; Kip et al., 2010; Liebner and Svenning, 2013; Reumer et al., 2018). Still, less is known about the response of the relevant and metabolically active community members to peat restoration, and it remains to be determined how well the CH<sub>4</sub>-driven network of interacting microorganisms recovers in the re-established peatland.

Ombrotrophic *Sphagnum*-dominated peatlands are relatively harsh environments, characterized by low pH and are nutrient-depauperated (Dedysh, 2011). These conditions, along with the antimicrobial properties of *Sphagnum*, may exert pressure to select for specific aerobic MOB (Kostka et al., 2016). Not surprisingly, the MOB being strongly influenced by their abiotic environment, showed habitat specificity (Kaupper et al., 2020b; Knief, 2015). Predominantly active MOB in ombrotrophic peatlands fall

into *Alphaproteobacteria* (Type II MOB), which include *Methylocystis* and *Methyloinus* (family *Methylocystaceae*), as well as members belonging to the family  *Beijerinckiaceae* (*Methylocella*, *Methyloferula*, and *Methylocapsa*); class *Gammaproteobacteri* MOB (Type I) belonging to *Methylomonas* and *Methylovulum* were more recently found to be active members of the community (Belova et al., 2011; Chen et al., 2008a; Danilova et al., 2013; Esson et al., 2016; Gupta et al., 2012; Liebner and Svenning, 2013). The MOB form a plethora of interdependent relationships with other organisms, at times supporting multi-trophic foodwebs in high CH<sub>4</sub>-emitting environments (Agasild et al., 2014; Ho et al., 2016a; Hutchens et al., 2004; Krause et al., 2017). Accordingly, CH<sub>4</sub> oxidation and growth rates, as well as the transcription of the *pmoA* gene (encoding for the pMMO) were significantly stimulated when the MOB were co-cultured together with other microorganisms compared to monocultures (Ho et al., 2014; Jeong et al., 2014; Stock et al., 2013; Veraart et al., 2018). As such, non-MOB that do not seemingly contribute to CH<sub>4</sub> oxidation are also relevant, indirectly affecting community functioning via interaction-induced effects. Therefore, considering the CH<sub>4</sub>-driven interaction network is important to elaborate community response during peat restoration but, has so far received little attention.

Here, we aimed to compare and contrast the CH<sub>4</sub>-driven interaction network in ombrotrophic peatlands to follow the recovery in the network structure during peat restoration. Although MOB activity and community composition/abundances may recover after *Sphagnum* re-growth upon peat rewetting (Putkinen et al., 2018; Reumer et al., 2018), the legacy of peat mining may persist in the structure of the interaction network (Pérez-Valera et al., 2017). Revisiting the sites of our previous work (pristine and restored peatlands; Reumer et al., 2018), we performed SIP using <sup>13</sup>C-CH<sub>4</sub> to track the unidirectional flow of CH<sub>4</sub> into the foodweb. Instead of deriving the co-occurrence network analysis from isolated DNA (e.g., Barberán et al., 2012; Mo et al., 2020), we performed a network analysis using the <sup>13</sup>C-enriched 16S rRNA gene from SIP to infer the CH<sub>4</sub>-driven interaction network (i.e., MOB interactome). We define the MOB interactome as a subset of the entire bacterial community comprising of both MOB and non-MOB that is tracked via the flow of CH<sub>4</sub>-derived <sup>13</sup>C. Coupling SIP to the co-occurrence network analysis not only provides direct ecological linkages of the metabolically active members of the interaction network thereby minimizing spurious and weak connections, but also unambiguously relate community functioning (CH<sub>4</sub> oxidation as the functional response variable) to the network structure.

**Table 5.1** Selected physicochemical properties, *pmoA* and 16S rRNA gene abundances, and CH<sub>4</sub> uptake rates in the pristine and restored peatlands<sup>a</sup>

Peatland status	pH	Ammonium ( $\mu\text{mol} \cdot \text{g}$ dry wt <sup>-1</sup> )	Nitrate ( $\mu\text{mol} \cdot \text{g}$ dry wt <sup>-1</sup> )	CH <sub>4</sub> uptake rate ( $\mu\text{mol} \cdot \text{g}$ dry wt <sup>-1</sup> · day <sup>-1</sup> ) <sup>b</sup>	<i>pmoA</i> gene abundance (copy no. · g dry wt <sup>-1</sup> )	16S rRNA gene abundance (copy no. · g dry wt <sup>-1</sup> )	Mean <i>pmoA</i> / 16S rRNA gene abundance (%)
<b>Pristine</b>	4.4 ± 0.19 C	0.2 ± 0.02 C	0.6 ± 0.07 C				
After incubation setup				24.7 ± 6.17 C	(6.0 ± 3.29) · 10 <sup>4</sup> C	(6.81 ± 3.41) · 10 <sup>7</sup> C	0.08
After replenishing headspace CH <sub>4</sub>				45.6 ± 8.61 A	(3.5 ± 2.47) · 10 <sup>5</sup> A	(9.31 ± 4.9) · 10 <sup>7</sup> A	0.53
<b>Restored</b>	4.7 ± 0.12 C	0.7 ± 0.08 D	0.7 ± 0.21 C				
After incubation setup				24.7 ± 3.82 C	(4.9 ± 4.02) · 10 <sup>5</sup> D	(2.48 ± 0.93) · 10 <sup>8</sup> D	0.21
After replenishing headspace CH <sub>4</sub>				31.2 ± 9.57 B	(2.8 ± 1.47) · 10 <sup>6</sup> B	(2.52 ± 1.48) · 10 <sup>8</sup> B	1.46

<sup>a</sup> Uppercase letters indicate a level of significance at  $P < 0.05$  between sites. C and D refer to data after incubation setup, and A and B refer to data after replenishing headspace CH<sub>4</sub>.

<sup>b</sup> CH<sub>4</sub> uptake rates were determined by linear regression after incubation setup (C and D,  $P < 0.05$ ; days 0 to 8) and after replenishing headspace CH<sub>4</sub> (A and B,  $P < 0.05$ ; days 8 to 13 or 14) (CH<sub>4</sub> depletion curve; see Figure S16 in the supplemental material).

## 5.4 Results

### 5.4.1 Comparison of the Methanotrophic Activity and Abundance, and the Abiotic Environment in the Pristine and Restored Peatlands

Headspace  $\text{CH}_4$  was immediately consumed upon incubation setup (initial and after  $\text{CH}_4$  replenishment; Figure S16) in both peatlands, indicating the presence of a thriving indigenous MOB population. The initial  $\text{CH}_4$  uptake rate reflecting the in-situ rate (Steenbergh et al., 2009), was comparable in both peatlands at  $\sim 24 \mu\text{mol g}_{\text{dw}}^{-1} \text{d}^{-1}$  (Table 5.1). This suggests the recovery in MOB activity in the restored peatland, consistent with a previous study of the same peatlands over two consecutive years (in 2015 and 2016; Reumer et al., 2018). The  $\text{CH}_4$  uptake rate increased in both peatlands after replenishing headspace  $\text{CH}_4$  achieving an ‘induced rate’ which was likely caused by population growth during incubation (Table 5.1; Steenbergh et al., 2009). This was corroborated by with the increased *pmoA* gene abundance by approximately an order of magnitude after the incubation, indicating MOB growth. Also, the proportion of MOB (i.e., *pmoA*/16S rRNA gene abundance ratio) increased during the incubation (Table 5.1). Similarly, the total bacteria, and specifically the MOB population size, recovered to even higher abundances following peat restoration, as was previously documented (Reumer et al., 2018).

The pH was comparable in both peatlands, within the range of 4.4 – 4.7 (Table 5.1). Soluble ammonium was significantly higher after peat restoration, while nitrate concentrations were comparable (Table 5.1), consistent with previous work (Reumer et al., 2018).

### 5.4.2 Response of the Metabolically Active Bacterial Community Composition to Peat Restoration, as Determined by DNA-based SIP

A SIP approach using  $[\text{}^{13}\text{C}]\text{CH}_4$  was performed to track the flow of  $^{13}\text{C}$  into the DNA of metabolically active and replicating microorganisms. Because the MOB are the only microorganisms capable of assimilating  $\text{CH}_4$ ,  $^{13}\text{C}$  incorporated into the DNA of non-MOB indicate the reliance of these microorganisms on the  $\text{CH}_4$ -derived carbon for growth. Each ultracentrifugation run was performed for DNA extracted from incubations with  $[\text{}^{13}\text{C}]\text{CH}_4$  and  $[\text{unlabelled}\text{C}]\text{CH}_4$  to distinguish the ‘heavy’ and ‘light’ fractions after amplification of the *pmoA* gene for each gradient fraction (Figure 5.1). Admittedly, we

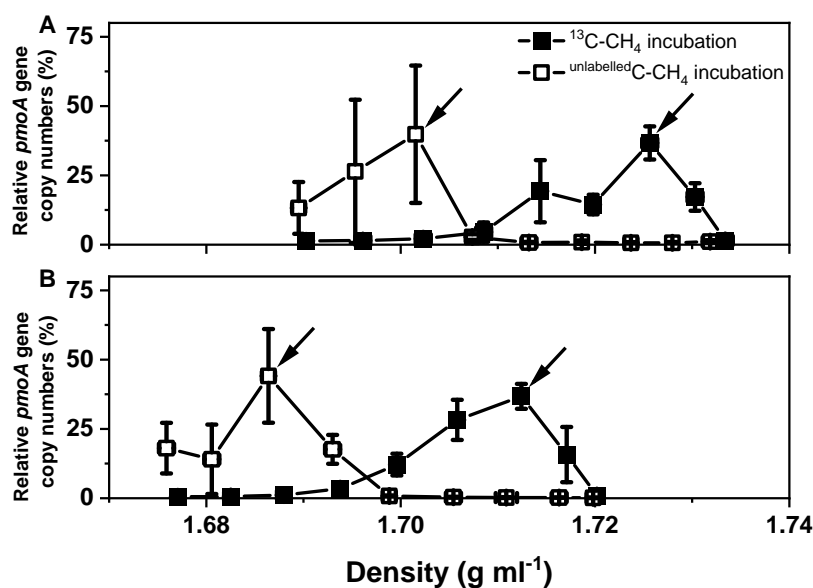


**Figure 5.1** Relative *pmoA* gene abundance along the density gradient of the [ $^{13}\text{C}$ ]CH $_4$  and [ $^{12}\text{C}$ ]CH $_4$  incubations from the pristine (A) and restored (B) peatlands (mean  $\pm$  standard deviation [SD];  $n = 4$ ). The relative abundance was calculated as the proportion of each fraction over the total sum of the gene abundance for each sample. DNA from the “light” and “heavy” fractions (denoted by arrows) in the [ $^{13}\text{C}$ ]CH $_4$  incubations was used for 16S rRNA gene amplicon sequencing.

cannot completely exclude the presence of unlabelled 16S rRNA gene with a high GC content in the ‘heavy’ fraction (Lueders et al., 2004a). The ‘heavy’ fraction could be clearly separated from the ‘light’ fraction in both peat incubations (Figure 5.1), and was further supported by the clustering of the distinct communities in both fractions, based on the 16S rRNA gene sequencing analysis (PCA; Figure 5.2). Subsequently, the co-occurrence network analysis was performed on the  $^{13}\text{C}$ -enriched 16S rRNA gene sequences, representing the active community members.

The  $^{13}\text{C}$ -enriched bacterial community composition was distinct in the pristine and restored peatlands, indicating that the total community in the restored peatland had not fully recovered to a pristine-like state (Figure 5.2). Among the  $^{13}\text{C}$ -labelled bacterial phyla, Proteobacteria was predominantly present in both peatlands ( $> 65\%$ ; Figure 5.3). However, the phylum was detected at a significantly higher relative abundance in the restored site (Figure S17). Within *Proteobacteria*, *Beijerinckiaceae*, *Oligoflexales*, *Polyangiaceae*, *Pajaroellobacter*, *Elsterales*, *Myxococcales*, and *Burkholderiaceae*, as well as the genera *Anaeromyxobacter*, *Occallatibacter*, and *Cavicella* were detected at significantly ( $p < 0.05$ ) differentially higher proportion (over-abundant) in the restored when compared to the pristine peatlands (Figure S18). However, a member of the *Beijerinckiaceae* (represented by OTU 1; Figure S18) was more abundant in the pristine peatland. Among other phyla, *Acidobacteria*, *Bacteroidetes*, and WPS-2 were

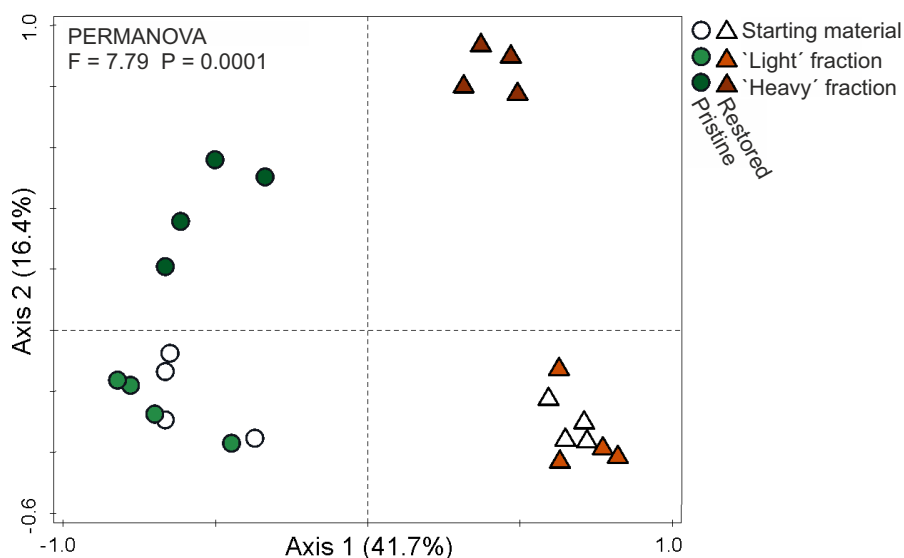


**Figure 5.2** Principal-component analysis showing the clustering of the 16S rRNA gene sequences according to the different fractions (light and heavy) and sites (pristine and restored peatlands) of the incubation with  $[^{13}\text{C}]\text{CH}_4$ . The circle and triangle indicate pristine and restored peatlands, respectively.

present at significantly higher relative abundances in the pristine peatland (Figure S17). Considering finer taxonomic resolution, differentially higher relative abundances of *Occallatibacter*, *Granulicella*, *Acidimicrobiaceae*, *Acidobacteriales*, *Candidatus Solibacter*, and *Candidatus Koribacter* belonging to *Acidobacteria*, and *Chitinophagales* within *Bacterioidetes* were detected in the pristine peatland (Figure S18). WPS-2 is a candidate division represented by an as yet uncultured bacterium. Generally, members of *Acidobacteria* and *Proteobacteria*, along with *Actinobacteria* are typical active inhabitants of ombrotrophic peatlands (Deng et al., 2014; Ivanova et al., 2016; Palmer and Horn, 2012).

The MOB consisted of < 2 % of the total bacterial population in both peatlands (starting material), based on the 16S rRNA gene sequencing analysis (Figure 5.2A). After incubation, the MOB population comprised of ~ 20 % and ~ 74 % of the total active community ('heavy' fraction) in the pristine and restored peatland, respectively. The predominantly active MOB, as retrieved from the 16S rRNA gene sequences, belonged to '*Methylomonaceae*' including the genus *Methylomonas* (> 72 % of the total MOB population) in both peatlands, whereas the genus *Methylocystis* was relatively more abundant in the restored than pristine peatland (Figure 5.3). Conversely, *Methylacidiphilaceae* was detected at a higher relative abundance in the pristine than restored peatland. Although constituting the majority of the MOB community compo-

sition in the starting material, members of *Methylacidiphilaceae* were not as actively assimilating CH<sub>4</sub> as '*Methylomonaceae*' under the incubation conditions; metabolically active *Methylacidiphilaceae* was detected at ~ 22 % and < 2 % in the 'heavy' fraction of the pristine and restored peatland, respectively, after incubation (Figure 5.3).

**Table 5.2** Topological properties of the co-occurrence network analysis in the pristine and restored peatlands

Network properties	Pristine peatland	Restored peatland
<b>No. of nodes<sup>a</sup></b>	600	464
<b>No. of edges<sup>b</sup></b>	5,397	3,476
<b>Positive edges (no. [%])<sup>c</sup></b>	2,871 (53.2)	2,234 (64.3)
<b>Negative edges (no. [%])<sup>d</sup></b>	2,526 (46.8)	1,242 (35.7)
<b>Modularity<sup>e</sup></b>	7.30	1.82
<b>No. of communities<sup>f</sup></b>	47	57
<b>Network diam<sup>g</sup></b>	10	11
<b>Avg path length<sup>h</sup></b>	4.27	4.30
<b>Avg degree<sup>i</sup></b>	17.99	14.98
<b>Avg clustering coefficient<sup>j</sup></b>	0.55	0.53

<sup>a</sup> Microbial taxon (at OTU level) with at least one significant ( $P < 0.01$ ) and strong (SparCC of more than 0.9 or less than -0.9) correlation.

<sup>b</sup> Number of connections/correlations obtained by SparCC analysis.

<sup>c</sup> SparCC positive correlation (more than 0.9 with  $P < 0.01$ ).

<sup>d</sup> SparCC negative correlation (less than -0.9 with  $P < 0.01$ ).

<sup>e</sup> Capability of the nodes to form highly connected communities, that is, a structure with a high density of between-node connections (inferred by Gephi).

<sup>f</sup> A community is defined as a group of nodes densely connected internally.

<sup>g</sup> The longest distance between nodes in the network, measured in number of edges.

<sup>h</sup> Average network distance for all pairs of nodes or the average length of all edges in the network.

<sup>i</sup> The average number of connections per node in the network, that is, the node connectivity.

<sup>j</sup> How nodes are embedded in their neighborhood and the degree to which they tend to cluster together.

### 5.4.3 Insights Into the Methane-Driven Co-Occurrence Interaction Network in the Pristine and Restored Peatlands

Subsequently, a co-occurrence network analysis was performed on the <sup>13</sup>C-enriched 16S rRNA gene sequences, targeting the community members of the MOB interactome in the pristine and restored peatlands (Figure 5.4). The network topological properties indicate that the pristine peatland harboured a more complex and connected community, exhibiting a higher number of edges (number of connections), degree (number of

connections per node or node connectivity), and clustering coefficient (the degree to which the nodes cluster together) than in the restored peatland (Table 5.2). Accordingly, the pristine peatland also possessed a more diverse metabolically active community (number of significant nodes, representing bacterial taxa at the OTU-level), and showed a more modular network structure than the restored peatland (Table 5.2). Higher modularity is indicative of a more compartmentalized network, having more independently connected groups within the interaction network (Williams et al., 2014; Zhou et al., 2010). The network diameter and average path length between co-occurring nodes, indicative of the network efficiency (Bissett et al., 2013; Zhou et al., 2010), were largely comparable in both peatlands (Table 5.2). Having a comparatively less complex and connected network structure thus indicate that the MOB interactome in the restored peatland since 2000 had not returned to a pristine-like state, despite the resilience in the MOB activity and abundance.

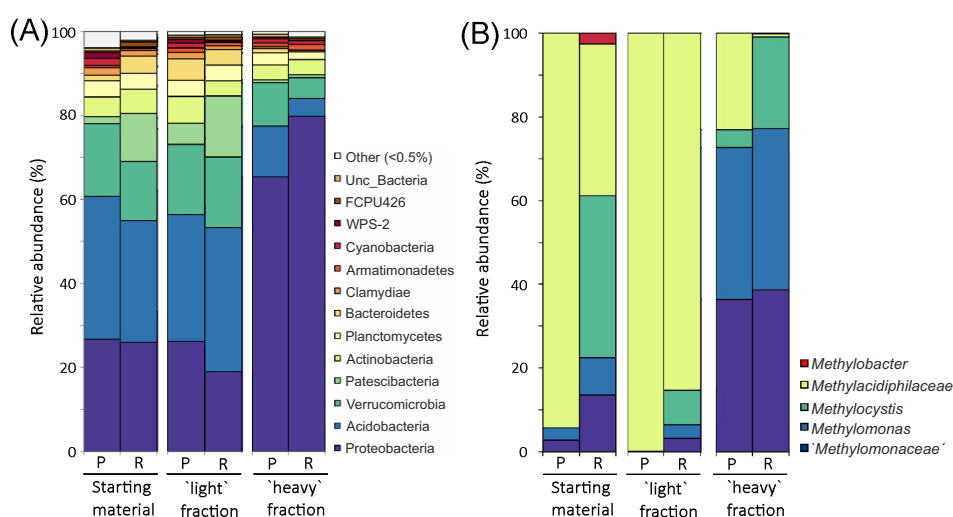


**Figure 5.3** The bacterial (A) and MOB (B) community composition in the starting material (prior to the incubation) and after  $[^{13}\text{C}]\text{CH}_4$  incubation (light and heavy fractions) (mean;  $n = 4$ ). The 16S rRNA gene sequences affiliated with MOB in panel B were retrieved from the total community in panel A. The 16S rRNA gene sequences affiliated with the MOB were present at  $< 2\%$  of the total community in the starting material, and at  $\sim 20\%$  and  $\sim 74\%$ , respectively, in the pristine and restored peatland after incubation (heavy fraction). P and R denote pristine and restored peatlands, respectively.

The nodes with high betweenness centrality were identified as the key nodes (Figure 5.4) (Poudel et al., 2016), which likely played a significant regulatory role within the interaction network, affecting MOB activity (Borgatti, 2005; van der Heijden and Hartmann, 2016). In particular, the key nodes are not necessarily the more abundant OTUs (Figure S18), but rather, refer to nodes acting as a bridge between other nodes at a relatively higher frequency (Poudel et al., 2016). The ten key nodes with



the highest betweenness centrality were identified in both the pristine and restored peatlands (Figure 5.4). Expectedly, these nodes were represented by proteobacterial MOB (*Methylomonas* and *Methylocystis*), as well as verrucomicrobial MOB belonging to *Methylacidiphilaceae* in the pristine peatland, whereas the MOB-related key nodes in the restored peatland were affiliated to *Methylomonas*. It is noteworthy that *Beijerinckiaceae* (phylum, *Proteobacteria*), a key node in the restored peatland (Figure 5.4), also constitutes MOB harboring the sMMO (*Methylocella*, *Methylocapsa*, and *Methyloferula*; Dedysh, 2011), as well as other methylotrophs, but these microorganisms may have been overlooked at the coarse taxonomic resolution. Unexpectedly, many non-MOB formed the key nodes and appeared to be site-specific (Figure 5.4). Although unable to assimilate CH<sub>4</sub> directly, the non-MOB also appear to be relevant members of the interaction network.

## 5.5 Discussion

### 5.5.1 Recovery of the Active Methanotrophs After Peat Restoration

MOB activity and population size recovered after peat restoration, comparing the pristine and restored sites (Table 5.1). Likewise, pH and nitrate concentrations returned to pristine-like levels but, ammonium concentrations remained significantly higher in the restored site. These trends were also documented in a previous study of the same sites sampled in 2015 and 2016, suggesting the presence of a relatively persistent MOB population possibly attributable to narrow fluctuations in environmental conditions (Reumer et al., 2018). It thus appears that the MOB recovered < 15 years after *Sphagnum* re-established during peat restoration.

The metabolically active bacterial community composition including the MOB were determined by targeting the <sup>13</sup>C-enriched 16S rRNA gene after <sup>13</sup>C-CH<sub>4</sub> SIP. Predominantly active MOB belonged to '*Methylomonaceae*' (> 72 % of the MOB community composition) in both peatlands, while *Methylacidiphilaceae* and *Methylocystis* formed the rest of the MOB community (Figure 5.3). In particular, *Methylocystis* is thought to possess ecological traits suitable for the relatively inhospitable and fluctuating environmental conditions in ombrotrophic peatlands, having the metabolic potential to fix N<sub>2</sub>, utilize other substrates besides CH<sub>4</sub> (e.g., acetate), and were favored by the lower pH (Belova et al., 2011; Han et al., 2018; Im et al., 2011; Zhao et al., 2020). Besides *Methylocystis*, members of '*Methylomonaceae*' (e.g., *Methylomonas* strains) and *Methylacidiphilaceae* (e.g., *Methyloacidiphilum fumariolicum* solV) which also formed

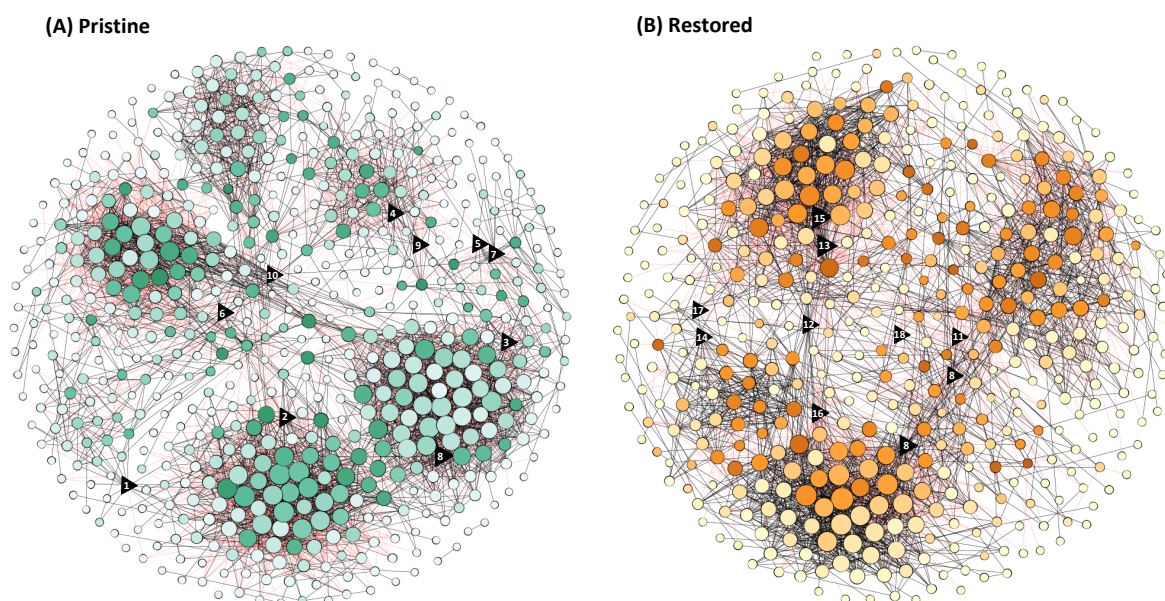


**Figure 5.4** Co-occurrence network analysis in the pristine (A) and restored (B) peatlands. The network analysis was derived from the  $^{13}\text{C}$ -enriched 16S rRNA gene sequences (heavy fraction), representing the metabolically active community of the interaction network. The topological properties of the networks are given in Table 5.2. Significant connection ( $p < 0.01$ ) with a SparCC correlation of a magnitude of more than 0.7 (positive correlation, blue edges) or less than -0.7 (negative correlation, red edges) are given. Each node represents a bacterial taxon at the OTU level, given to the lowest taxonomic rank (family, genus, or species) when available. The size of the node is proportional to the number of connections, and a darker shade of a color indicates higher betweenness centrality. The top 10 nodes with the highest betweenness centrality, representing the key nodes, are given as triangles, and the number inside the key nodes refers to their affiliation as follows: 1, *Rhodospirillales*; 2, uncultured bacteria; 3, *Burkholderiaceae*; 4, *Methylomonas* (MOB); 5, “*Candidatus Solibacter*”; 6, *Gammaproteobacteria*; 7, *Methylocystis* (MOB); 8, *Babeliales*; 9, *Pirellulaceae*; 10, *Methylacidiphilaceae* (MOB); 11, *Bdellovibrio*; 12, *Magnetospirillaceae*; 13, *Acidimicrobiia*; 14, *Sphingobacteriales*; 15, *Roseiarcus*; 16, *Beijerinckiaceae*; 17, *Myxococcales*; and 18, *Methylomonas paludis* (MOB). The OTUs representing the microorganisms and betweenness centrality values of each OTU are listed in Table S8 in the supplemental material.

the active community, are also potentially diazotrophic, as indicated by the presence of the *nifH* gene (encoding for the nitrogenase) (Auman et al., 2001; Khadem et al., 2011). Consistent with previous studies, active gammaproteobacterial MOB (namely, *Methylomonas* and *Methylovulum*) have also been found to co-dominate alongside *Methylocystis* in some peatlands (Chen et al., 2008a; Esson et al., 2016; Gupta et al., 2012). This suggests that traits to grow and survive in acidic peatlands are not confined to a particular MOB subgroup.

Previously, we characterized the MOB community composition in the pristine and restored sites (same sites as in this study), along with the community in an actively mined peatland, and abandoned peatlands since 2004 and 2009 (Reumer et al., 2018). The MOB community composition in the restored peatland resembled those in the pris-

tine peatland, clustering more closely together as shown in a correspondence analysis (Reumer et al., 2018). This indicates that the MOB community composition recovered following peat restoration. Here, although the relative abundance of *Methylacidiphilaceae* and *Methylocystis* differed in the pristine and restored peatlands, the predominantly active MOB comprised of the same family members (Figure 5.3). However, the active bacterial community composition in response to CH<sub>4</sub>, was distinct in both peatlands (Figure 5.2 and 5.3). Hence, specific microbial sub-populations may have shown relatively faster recovery than the total bacterial community composition after peat mining.

### 5.5.2 Insights Into the Recovery of the Methanotrophic Interactome After Peat Restoration

The recovery in the MOB activity and community composition/abundances was not reflected in the structure of the interaction network, even after approximately two decades of peat rewetting (Table 5.2 and Figure 5.4). The pristine peatland harboured a more complex MOB interactome, possessing a higher number of nodes with significant correlations, edges, degree, and clustering coefficient, as well as having higher modularity (Table 5.2). These topological features are indicative of a more connected and robust network (Bissett et al., 2013; Faust and Raes, 2012; Mendes et al., 2018), and suggest that the MOB interactome in the pristine peatland was characterized by relatively higher metabolic exchange and competition among community members that likely increased their co-occurrence (van Elsas et al., 2012; Zelezniak et al., 2015). Also, having relatively higher modularity in the pristine peatland is anticipated to constrain the effects of environmental stressors/disturbance on localized areas (compartments) within the network (Kitano, 2004). In contrast, the loss of modularity in the restored peatland suggests that stress effects would be more uniformly distributed among community members, which may become more vulnerable in the face of intensified or recurring disturbances (Faust and Raes, 2012; Ho et al., 2020). Hence, the CH<sub>4</sub>-driven community in the restored peatland may not be as resilient as the community in the pristine peatland in responding to future changes in environmental conditions. Indeed, a recent study showed the unraveling of the MOB interactome concomitant to significantly impaired MOB activity following NH<sub>4</sub>Cl-induced stressor intensification (Ho et al., 2020). Overall, considering the co-occurrence network analysis in addition to activity measurements and characterization of the community composition / abundances may provide a more comprehensive understanding, moving beyond diversity-ecosystem functioning relationship (e.g., Krause et al., 2018), to encompass potential interaction-induced ef-

fects.

Admittedly, we could not account for seasonal variations affecting the interaction networks. However, the consistent trends in MOB activity and community composition / abundances in the pristine and restored peatlands in previous (sampled in August 2015 and June 2016; Reumer et al., 2018) and current work (May 2019; Table 5.1), despite a three-year interval, suggest that a specific MOB population persists over time. Although we anticipate a relatively consistent MOB population, the seasonal dynamics of the interaction network warrants attention in future studies.

The MOB are the only microbial group capable of assimilating CH<sub>4</sub>, having the role of a 'primary' producer, whereby the CH<sub>4</sub>-derived carbon is anticipated to fuel the community. Nevertheless, the MOB may gain from other members of the interactome (e.g., stimulation of MOB growth by cobalamin excreted by other microorganisms; Iguchi et al., 2011), which may have been inadvertently excluded by the experimental design capturing the unidirectional flow of <sup>13</sup>C. Expectedly, the key nodes included the MOB (Figure 5.4). Surprisingly, the key nodes were overwhelmingly represented by the non-MOB and were distinct in the pristine and restored peatlands. This indicates sufficiently redundant community members sharing traits to fulfill similar roles ensuring community functioning within the MOB interactome (Barberán et al., 2012; Williams et al., 2014). It is not unreasonable to assume that selective predation on the MOB may have occurred (Murase and Frenzel, 2007). For instance, members of *Myxococcales*, a key taxon in the restored peat, have been widely recognized as predators, swarming their prey in a coordinated and cooperative manner during feeding (Muñoz-Dorado et al., 2016). *Beijerinckiaceae*, another key taxon, includes non-MOB methylotrophs which likely benefited from (intermediary) products of CH<sub>4</sub> oxidation (e.g., methanol, formaldehyde, formate). Hence, the cross-feeding between MOB and non-MOB methylotrophs (e.g., *Methylotenera*) drives their co-occurrence (Ho et al., 2020; Krause et al., 2017). It is noteworthy that *Beijerinckiaceae* also includes MOB, but the MOB and non-MOB methylotrophs could not be distinguished at the taxonomic resolution in this study. Also, *Burkholderiaceae* may comprise of microorganisms shown to have a stimulatory effect on MOB growth in co-cultures (i.e., *Cupriavidus*; Stock et al., 2013). Although some of the key taxa (e.g., *Burkholderiaceae*, *Sphingobacteriales*, *Beijerinckiaceae*, and *Bdellovibrio*) have been identified to co-occur alongside and interacted with the MOB (Ho et al., 2020; Qiu et al., 2008; Stock et al., 2013), the underlying mechanisms driving the biological interaction and organization (e.g., commensalism, mutualism; Johnson et al., 2020; Morris et al., 2013) warrant further probing by isolation and co-culture studies (Kwon et al., 2019b). Despite lacking the metabolic capability to assimilate CH<sub>4</sub>, the detection of the non-MOB as key nodes indicate their potentially significant role within

the interaction network. In particular, the key nodes in the restored peatlands may act to expedite the natural restoration process (Wubs et al., 2016).

## 5.6 Conclusion

We elaborated on the CH<sub>4</sub>-driven interaction network after peat mining by comparing a pristine and restored peatland. Our findings showed the structuring of the interaction network resulting in the loss of complexity, connectedness, and modularity in the restored peatland, which may have consequences in the face of future disturbances and environmental changes. This also suggests that the re-established peatlands had not yet fully recovered, despite showing resilience in the MOB activity. More generally, our study suggests the inclusion of interaction-induced responses, in addition to documenting shifts in community composition/abundances, as a step forward to understand the resilience of microbial communities to disturbances.

## 5.7 Materials and Methods

### 5.7.1 Peat sampling and incubation setup

The sampling sites are ombrotrophic peatlands located in Warmia and Mazury province, Poland. The upper ~ 10 cm of peat below the water surface was collected in May 2019 from a pristine peatland (Zielony Mechacz; 53°54'24'' N, 19°41'41'' E) and was regarded as the reference site for comparison to the restored peatland (Rucianka; 54°15'34'' N, 19°44'0.4'' E). These peatlands were selected based on a previous study, showing recovery in the MOB activity and abundances after peat mining (Reumer et al., 2018). The atmospheric temperature at the time of sampling was 21-25°C. Five cores (10 cm height x 3.5 cm diameter) were sampled from four randomly selected plots (spaced > 4 m apart) from each site and composited, giving four independent replicates per site. The pristine peatland was declared a nature reserve since 1962, while peatland in the restored site was dammed, rewetted, and remained water-logged since 2000 after peat excavation using the block peat method. In both sites, *Sphagnum spp.* (e.g., *S. fimbriatum*, *S. fluuosum*, *S. fallax*, and *S. capillifolium*) dominated the vegetation, interspersed with *Orthotrichum lyellii*. The pH in both peatlands was within a narrow range of 4.4 - 4.7. Detailed peat hydrology and selected physico-chemical parameters are given elsewhere (Table 5.1) (Reumer et al., 2018). The samples were transported to the laboratory with coolers in ice.

Each incubation containing 5 g fresh sample in a 120 ml bottle was performed in eight replicates for the pristine and restored peat. After sealing the bottle with a butyl rubber stopper and crimp cap, the headspace CH<sub>4</sub> concentration in the bottle was adjusted to ~2 % v/v unlabelled C- or <sup>13</sup>C-CH<sub>4</sub> (n=4 each) in air. Incubation was performed at 27°C while shaking (110 rpm) in the dark. Headspace CH<sub>4</sub> concentration was monitored during the incubation. Upon CH<sub>4</sub> depletion, headspace was replenished with 2 % v/v unlabelled C- or <sup>13</sup>C-CH<sub>4</sub> in air, and incubation was resumed under the same conditions as before. Incubation was terminated after approximately 30 μmol CH<sub>4</sub> g fresh sample<sup>-1</sup> was consumed (13 – 14 days; Figure S16) to ensure sufficient <sup>13</sup>C labelling (Neufeld et al., 2007b). The samples were immediately homogenized and collected after incubation to be stored in the -20°C freezer till DNA extraction.

### 5.7.2 Methane and inorganic N measurements

Headspace CH<sub>4</sub> was monitored daily using a gas chromatograph (7890B GC System, Agilent Technologies, Santa Clara, USA) coupled to a PD-HID. Helium was used as the carrier gas. The CH<sub>4</sub> uptake rate was determined by linear regression. The gravimetric water content (~ 93 % in both peat samples) was determined after drying the peat in the 70°C oven until the weight remained constant. Soluble ammonium and nitrate were determined in autoclaved deionized water (1:1 w/v) colorimetrically as described before (Gadkari, 1984; Horn et al., 2005) using an Infinite M plex reader (TECAN, Meannedorf, Switzerland).

### 5.7.3 DNA extraction and quantitative PCR (qPCR)

DNA was extracted using the DNeasy PowerSoil Kit (Qiagen, Hilden, Germany) according to the manufacturer's instructions. A *pmoA* gene-targeted qPCR assay (A189f/mb661r primer pair) was performed to enumerate the MOB abundance. Additionally, a qPCR targeting the 16S rRNA gene (341F/907R primer pair) was performed to determine the abundance of the total bacterial population. Both qPCR assays were performed using the BIORAD CFX Connect Real-time PCR System (Biorad, Hercules, USA). The *pmoA* gene-targeted qPCR was performed as described before (Kolb et al., 2003) with minor modifications (Ho et al., 2019b); the reagents and reagent concentrations, as well as the PCR thermal profile for the qPCR assay are given elsewhere (Ho et al., 2019b). Each reaction in the 16S rRNA gene-targeted qPCR (total volume, 20 μL) consisted of 10 μL SensiMix (2X), 1.2 μL MgCl<sub>2</sub> (50 mM), 1 μL BSA (1 %), 2 μL of each primer (10 μM), 1.8 μL of H<sub>2</sub>O and 2 μL of template DNA. The PCR thermal

profile consisted of an initial denaturation step at 95 °C for 8 min, followed by 45 cycles of denaturation at 95 °C for 15 s, annealing at 55.7 °C for 15 s, and elongation at 72 °C for 40 s, with an additional data acquisition step at 80 °C for 8 s. The template DNA from the peat (starting material and after incubation) was diluted 50-fold (mean total DNA, 13.5 - 46.5 ng DNA  $\mu\text{L}^{-1}$ ) for both qPCR assays to determine the *pmoA*/16S rRNA gene abundance ratio (Table 5.1), while template DNA to determine the relative *pmoA* gene abundance after fractionation for the SIP analysis was undiluted (see Sub-section 5.7.4 below). The calibration curve ( $10^1$  to  $10^8$  *pmoA* or 16S rRNA gene copy numbers) was derived from the gene library (Ho et al., 2011a, 2017b). The specificity of the amplicons was determined from the melt curve and further verified on 1 % agarose gel electrophoresis, showing a single band of the correct size. The qPCR efficiency was 94.3 %, with an  $R^2$  of 0.988.

#### 5.7.4 $^{13}\text{C}\text{-CH}_4$ stable Isotope probing

Isopycnic ultracentrifugation (144000 g for 67 hours) was performed using the Optima L-80XP ultracentrifuge (Beckman Coulter Inc., USA) as described before (Neufeld et al., 2007b). Briefly, fractionation was immediately performed after ultracentrifugation using a peristaltic pump (3 rpm  $\text{min}^{-1}$ ), yielding 10-11 fractions whereby the final fraction was discarded. The density of each fraction was determined using an AR200 digital refractometer (Reichert Technologies, Munich, Germany). DNA was precipitated by introducing two washing steps with ethanol, and the pellet was suspended in 30  $\mu\text{L}$  ultrapure PCR water (INVITROGEN, Waltham, USA). Thereafter, the *pmoA* gene was enumerated from each fraction using the qPCR assay described above to distinguish the 'light' from the 'heavy' fraction by comparing the DNA retrieved from the  $^{13}\text{C}$ - and  $^{12}\text{C}$ - $\text{CH}_4$  incubations (Figure 5.1). The 16S rRNA gene from the 'light' and 'heavy' fractions, as well as from the starting material were subsequently amplified for Illumina Miseq sequencing.

#### 5.7.5 16S rRNA gene amplicon sequencing

The 16S rRNA gene was amplified using the primer pair 341F / 805R, as detailed before (Ho et al., 2020). Briefly, each PCR reaction comprised of 20  $\mu\text{L}$  2X KAPA HiFi Hot-Start Ready Mix (Roche, Mannheim, Germany), 2  $\mu\text{L}$  forward/reverse tagged-primers each (10  $\mu\text{M}$ ), 2  $\mu\text{L}$  BSA (1 %), and 4  $\mu\text{L}$  DNA template. PCR grade water was added to achieve a total volume of 40  $\mu\text{L}$ . The PCR thermal profile consisted of an initial denaturation step at 94°C for 7 min, followed by 30 cycles of denaturation at 94°C for

30 s, annealing at 53°C for 30 s, and elongation at 72°C for 30 s. The final elongation step was at 72°C for 5 mins. The amplicons were purified using the GeneRead Size Selection Kit (Qiagen, Hilden, Germany) after verification on 1 % agarose gel electrophoresis. Thereafter, a second PCR was performed using 5 µL template from the first PCR to attach the adapters to the 16S rRNA gene amplicon using the Nextera XT Index Kit (Illumina, San Diego, USA). The PCR reagents, reagent concentrations, and thermal profile for the second PCR is given elsewhere (Ho et al., 2020). Following the second PCR, the 16S rRNA gene amplicon was purified using the MagSi-NGSPREP Plus Magnetic beads (Steinbrenner Laborsysteme GmbH, Wiesenbach, Germany) according to the manufacturer's instructions. After purification, equimolar amounts of 16S rRNA gene amplicons (133 ng) were pooled for library preparation and sequencing (Illumina MiSeq version 3 chemistry, paired-end 600 cycles).

### 5.7.6 16S rRNA gene sequencing analysis

The 16S rRNA gene sequences were processed using QIIME 2 version 2019.10, as described before (Ho et al., 2020). Briefly, after merging the paired-end reads using PEAR (Zhang et al., 2014), the sequences were de-multiplexed, and quality control was performed with DADA2 (Callahan, 2017) to remove remaining chimeric and low-quality sequences. Approximately 1 010 000 high-quality contigs (on average, 31 604 contigs per sample) were obtained. After removing singletons and doubletons, the samples were rarefied to 18 800 contigs following the number of the sample with the lowest contigs. The classification was performed at 97 % similarity against the Silva database v. 132 (Quast et al., 2013); the generated matrix based on the relative abundance of the OTUs was further used for statistical analyses. The affiliation of the OTUs is given to the lowest taxonomic rank (family, genus, or species), whenever possible. The 16S rRNA gene sequences were deposited at the National Center for Biotechnology Information (NCBI) under the accession numbers SRR15925518-SRR15925549 (project number PRJNA659768).

A PCA was performed to assess the separation of the <sup>13</sup>C-enriched (active) from the unlabelled <sup>12</sup>C (inactive) bacterial community composition, and to determine the recovery of the community composition following peat restoration. The PCA was constructed using Canoco 4.5 (Biometrics, Wageningen, the Netherlands). To test the significance of the PCA clustering, permutational multivariate analysis of variance (PERMANOVA) was performed with the software Past 4.01 (Hammer et al., 2001). Furthermore, the differential relative abundance (over-abundant) OTUs in the restored, when compared to the pristine peatlands were determined using the STAMP software (Parks et al., 2014).



The P-values were calculated based on the two-sided Welch's t-test and corrected using Benjamini-Hochberg False discovery rate.

Additionally, a co-occurrence network analysis was performed using the  $^{13}\text{C}$ -enriched 16S rRNA gene sequences to explore potential interaction among the active members of the MOB interactome. The network analysis was performed using the Python module 'SparCC' and the network properties were calculated with Gephi (Table 5.2) (Bastian et al., 2009). The same analytical pipeline was applied to each network (pristine and restored peatlands). The P-values were obtained by 99 permutations of random selections of the data table for each network. The true SparCC non-random correlations were selected based on a magnitude of  $> 0.7$  or  $< -0.7$ , with a statistical significance of  $p < 0.01$ . Comparison between the networks was assessed based on their topological properties namely, the number of nodes, edges, modularity, number of communities, average path length, network diameter, average degree, and clustering coefficient (Table 5.2) (Newman, 2003). Furthermore, the OTUs with high betweenness centrality i.e., the number of times a node acts as a bridge along the shortest path between two other nodes, were determined (Poudel et al., 2016). These nodes are regarded as key nodes, representing microorganisms that likely play a significant role within the MOB interactome (Borgatti, 2005).

### 5.7.7 Statistical analyses

Normal distribution was tested using the Kolmogorov-Smirnov test at  $p = 0.05$ . Equal distribution of variance was tested and one-sided t-tests ( $p = 0.05$ ) were then performed comparing the pristine and restored peatlands. Where normal distribution was not met, a Mann-Whitney-U-test was performed.

## **Chapter 6**

# **Disentangling Abiotic and Biotic Controls of Aerobic Methane Oxidation During Re-Colonization**

Thomas Kaupper<sup>1\*</sup>, Janita Luehrs<sup>1\*</sup>, Hyo Jung Lee<sup>2</sup>, Yongliang Mo<sup>3</sup>,  
Zhongjun Jia<sup>3</sup>, Marcus A. Horn<sup>1</sup>, Adrian Ho<sup>1</sup>

Published in *Soil Biology and Biochemistry* (2020), 142:107729  
Copyright Elsevier

---

<sup>1</sup>Institute of Microbiology, Leibniz Universität Hannover, Herrenhäuser Str. 2, 30419  
Hannover, Germany.

<sup>2</sup>Department of Biology, Kunsan National University, Gunsan, Republic of Korea

<sup>3</sup>Institute of Soil Science, Chinese Academy of Sciences, No. 71 East Beijing Road,  
Xuan-Wu District, Nanjing City, PR China

\* Equal contribution

The published version can be found online:  
<https://doi.org/10.1016/j.soilbio.2020.107729>

## 6.1 Abstract

Aerobic CH<sub>4</sub> oxidation is driven by both abiotic and biotic factors which are often confounded in the soil environment. Using a laboratory-scale reciprocal inoculation experiment with two native soils (paddy and upland agricultural soils) and the gamma-irradiated fraction of these soils, we aim to disentangle and determine the relative contribution of abiotic (i.e., soil edaphic properties) and biotic (i.e., initial MOB community composition) controls of CH<sub>4</sub> oxidation during re-colonization. CH<sub>4</sub> uptake was appreciably higher in incubations containing gamma-irradiated paddy soil after inoculation with both native soils despite of different initial MOB community composition, suggesting an overriding effect of the soil edaphic properties in positively regulating CH<sub>4</sub> oxidation. Population dynamics, monitored via culture-independent techniques targeting the *pmoA* gene showed comparable community composition in incubations with the same starting inoculum. Therefore, the initial community composition affects the trajectory of community succession to an extent, but not at the expense of the MOB activity under high CH<sub>4</sub> availability; edaphic properties override initial community composition in regulating CH<sub>4</sub> oxidation.

## 6.2 Introduction

MOB represent a specialized microbial guild characterized by their ability to use CH<sub>4</sub> as a carbon and energy source. Aerobic MOB belong to Verrucomicrobia and Proteobacteria, with members of the proteobacterial MOB fall within the classes Gammaproteobacteria (comprising of subgroups Type Ia and Ib) and Alphaproteobacteria (subgroup Type II). While the verrucomicrobial MOB were discovered in low pH (< 5) and high temperature (> 50°C) geothermal springs, the proteobacterial MOB are widespread, but show habitat specificity (Knief, 2015; Op den Camp et al., 2009). MOB possess the enzyme MMO which enable them to oxidize CH<sub>4</sub> to methanol, the initial step in CH<sub>4</sub> oxidation (Semrau et al., 2010). Typically, the structural genes encoding for the soluble and particulate form of the MMO enzyme (*mmoX* and *pmoA*, respectively) are targeted to survey the MOB diversity in complex microbial communities (Wen et al., 2016). In wetland ecosystems, MOB inhabit oxic-anoxic interfaces with O<sub>2</sub>-CH<sub>4</sub> counter-gradients (e.g., soil-overlying water, aquatic plant roots) where they act as a filter to consume CH<sub>4</sub> produced in the deeper anoxic sediment layers (Reim et al., 2012). On the other hand, MOB in well-aerated upland soils serve as a CH<sub>4</sub> sink, consuming atmospheric CH<sub>4</sub> (Ho et al., 2019b, 2015b; Kolb, 2009; Pratscher et al., 2018; Shrestha et al., 2012). In both these roles, abiotic (e.g., substrate concentra-

tions, micronutrients, and other soil physico-chemical properties; Bodelier, 2011a; Ho et al., 2013b, 2018; Hütsch et al., 1994; Semrau et al., 2018; Veraart et al., 2015) and biotic factors (e.g., MOB community composition/abundance and interaction-induced response in community functioning; Ho et al., 2016a; Malghani et al., 2016; Reumer et al., 2018; Schnyder et al., 2018; Veraart et al., 2018) are known to drive aerobic CH<sub>4</sub> oxidation. Collectively, we refer to the non-biological attributes inherent to the soil as abiotic parameters, whereas biotic determinant is exemplified by the initial MOB community composition.

Soil manipulation (e.g., amendment) studies, and experimental design capitalizing on soil chronosequence with natural environmental gradients are typically used to relate changes in (a)biotic factors to community functioning (e.g., Bissett et al., 2012; Ho et al., 2013b, 2018; Rousk et al., 2010; Shiau et al., 2018b). Often, the abiotic and biotic determinants are confounded, obscuring the contribution of either factors to the regulation of CH<sub>4</sub> oxidation. Rarely are there factors explicitly tested independently and simultaneously.

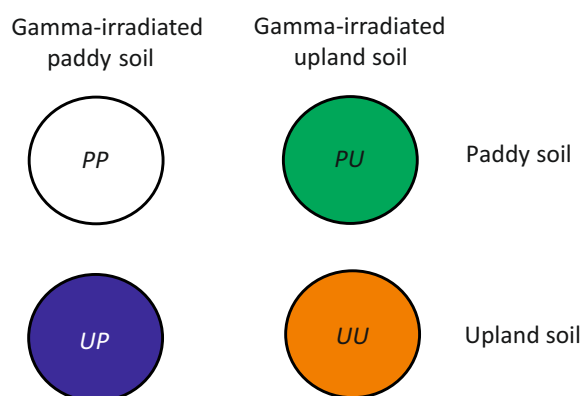


**Figure 6.1** Experimental setup showing reciprocal inoculation of native soils in gamma-irradiated fractions of the soils. Three microcosms per time and amendment were established. The microcosms consisted of paddy soil + gamma-irradiated paddy soil (designated as ‘PP’), paddy soil + gamma-irradiated upland soil (‘PU’), upland soil + gamma-irradiated paddy soil (‘UP’), and upland soil + gamma-irradiated upland soil (‘UU’). To confirm the sterility of the soil after gamma-irradiation, the soil (9.5 g) was saturated with autoclaved deionized water (0.45 ml g<sub>dw</sub> soil<sup>-1</sup>) in a 120 ml bottle with an adjusted headspace CH<sub>4</sub> concentration of 1 %<sub>v/v</sub>. The soil was considered free of viable MOB when headspace CH<sub>4</sub> remained unchanged over three weeks (Figure S19).

Here, we aim to disentangle abiotic and biotic controls of CH<sub>4</sub> oxidation by employing a reciprocal inoculation experimental design using two native soils and the gamma-irradiated (25 kGy; <sup>60</sup>Co) fractions of these soils (Figure 6.1), which enabled us to relate the (a)biotic determinants to CH<sub>4</sub> oxidation. We anticipate that if (i) abiotic determinants exert a stronger control than biotic determinants in regulating CH<sub>4</sub> oxidation, the same abiotic environment (i.e., gamma-irradiated soil) will consistently support high CH<sub>4</sub> up-

take regardless of the initial community composition, (ii) biotic determinants exert a stronger control than abiotic determinants, the same native soil harboring the initial MOB community will consistently exhibit high CH<sub>4</sub> uptake regardless of the edaphic properties, and (iii) there is no consistent effect, less predictive and/or stochastic factors (e.g., priority effect, site history) may have an overriding impact on the contemporary MOB activity. To address our suppositions, we incubated soil microcosms containing native and gamma-irradiated native soils in all combinations (Figure 6.1) for 35 days, and followed the potential CH<sub>4</sub> oxidation rate over time (Figure 6.2). Two soils (wetland paddy and upland agricultural soils) with distinct physico-chemical properties, and harbor different MOB communities with proven CH<sub>4</sub> uptake capacity under high CH<sub>4</sub> availability (> 2 % v/v) were used (Table 6.1; Ho et al., 2013b, 2015b). Soil processing, and soil microcosm setup and sampling are detailed in the Supplementary Materials.

The temporal succession of the MOB community composition was monitored during the incubation using group-specific qPCR assays (i.e., MBAC, MCOC, and TYPEII assays targeting the MOB subgroups Type Ia, Ib, and II, respectively; Ho et al., 2016c; Kolb et al., 2003; Supplementary Materials) and Illumina MiSeq sequencing of the *pmoA* gene. The *pmoA* gene, instead of the *mmoX* gene, was targeted because the *mmoX* gene transcript or the MOB harbouring only the *mmoX* gene were not detected or below the detection limit in these soils (Ho et al., 2015b; Reim et al., 2012). While the group-specific qPCR assays were performed to be used as proxies for MOB abundances, high throughput sequencing of the *pmoA* gene was performed to follow compositional shifts in the MOB community. The *pmoA* gene sequences were analysed as described before (Reumer et al., 2018; Supplementary Materials), and were deposited at the NCBI Sequence Read Archive under the accession number SRR9924748 (NCBI BioProject PRJNA559227).

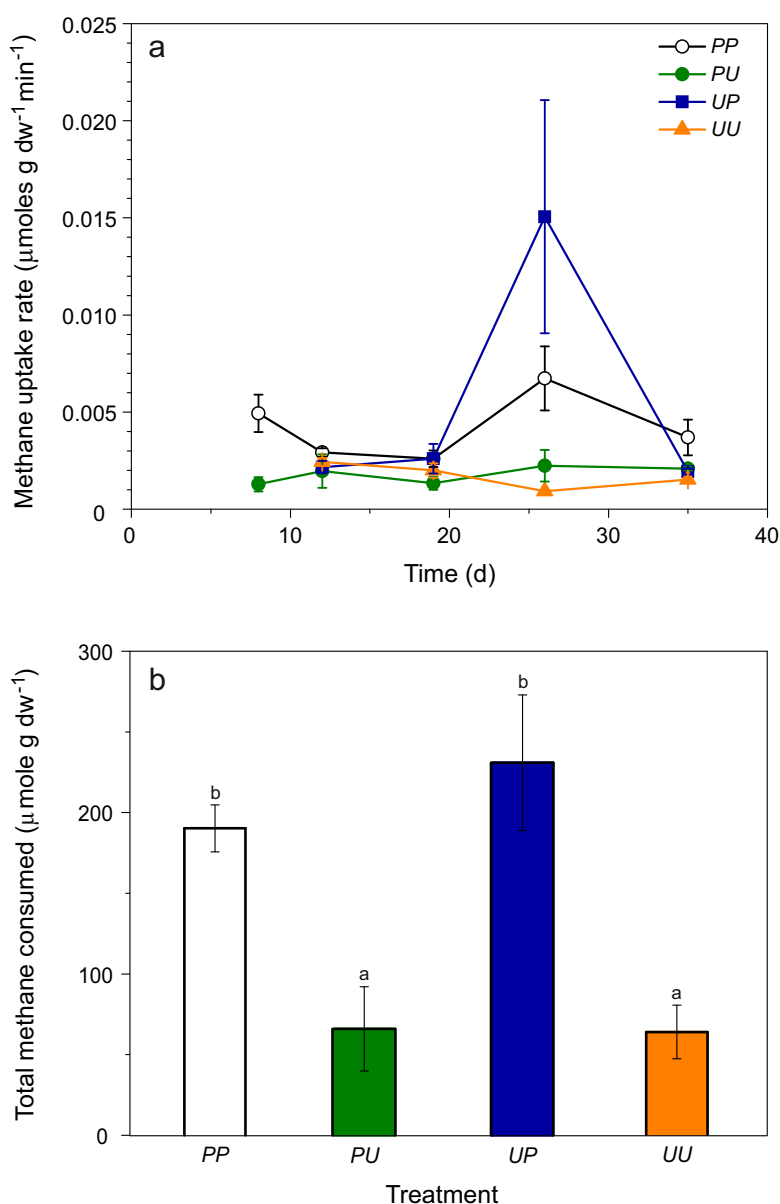


**Figure 6.2** CH<sub>4</sub> uptake rate (a) and total CH<sub>4</sub> consumed (b) during recolonization (mean ± s.d.; n = 3). Each soil microcosm consisted of 9.5 g gamma-irradiated soil and 0.5 g native soil in a Petri dish. The soil was saturated with autoclaved deionized water (0.45 ml g dw soil<sup>-1</sup>) and homogenized before being incubated in a gas tight jar under 10 %<sub>v/v</sub> CH<sub>4</sub> in air in the dark at 27°C. Headspace air in the jar was replenish every 2–3 days to ensure that CH<sub>4</sub> was not limiting. At designated intervals (days 8, 12, 19, 26, and 35), individual microcosm was removed from the jar, and placed in a flux chamber to determine the CH<sub>4</sub> uptake rate, measured over 5–6 h (minimum of three time points) by linear regression (a), as described before (Ho et al., 2011b). Negligible or no CH<sub>4</sub> uptake was detected < 8 days in the UP and UU incubation hence, the first sampling was performed at day 12, allowing direct comparisons between treatments per time. Additionally, total CH<sub>4</sub> consumed for each treatment during the incubation (over 35 days) was determined by integrating the area below the curve of CH<sub>4</sub> uptake rates (b). Headspace CH<sub>4</sub> was measured using gas chromatograph (GC) coupled to a thermal conductivity and pulsed discharge helium ionization detector (7890B, Agilent Technologies, JAS GC systems, Moers, Germany). In (a), letters indicate the level of significance (ANOVA; p < 0.01) in the total CH<sub>4</sub> consumed between treatments.

**Table 6.1** Selected physico-chemical parameters of the wetland and upland agricultural soils.

Soil (Coordinates)	Texture	pH <sup>a</sup>	Total C  μmoles C g <sub>dw</sub> soil <sup>-1</sup>	Total N  μmoles N g <sub>dw</sub> soil <sup>-1</sup>	Organic matter content  LOI %	Total nutrient contents (μmoles g <sub>dw</sub> soil <sup>-1</sup> )			Vegetation (during sampling)	Reference
						NH <sub>4</sub> <sup>+</sup>	NO <sub>x</sub> <sup>b</sup>	PO <sub>4</sub> <sup>3-</sup>		
<b>Paddy soil</b> (45° 20' N, 8° 25' E)	Calcareous clay	5.4	1158.3	92.9	4.0	1.0	0.3	6.3 · 10 <sup>-3</sup>	Rice (fallow)	Ho et al. (2015a)
<b>Upland soil</b> (51° 32' N, 05° 50' E)	Gley podzol (sandy loam)	5.4	1850.0	92.9	4.7	0.1	3.7 · 10 <sup>-2</sup>	9.5 · 10 <sup>-3</sup>	Potato (fallow)	Ho et al. (2015b)

Abbreviation: LOI, loss on ignition

<sup>a</sup> pH determined in 1 M KCl (1:5, vol:vol)

<sup>b</sup> Total of NO<sub>2</sub> and NO<sub>3</sub>

### 6.3 Abiotic Parameters Exert a Stronger Effect on Aerobic Methane Oxidation than the Initial Methanotrophic Community Composition

The potential for CH<sub>4</sub> oxidation (total CH<sub>4</sub> consumed) was consistently significantly higher in the microcosms containing the gamma-irradiated paddy soil (PP, 190 ± 15 μmoles g<sub>dw</sub><sup>-1</sup>; UP, 231 ± 42 μmoles g<sub>dw</sub><sup>-1</sup>), and was significantly lower and remained relatively constant during incubation in the microcosms containing the gamma-irradiated upland soil (PU, 66 ± 26 μmoles g<sub>dw</sub><sup>-1</sup>; and UU, 64 ± 17 μmoles g<sub>dw</sub><sup>-1</sup>), regardless of the initial community composition (Figure 6.2). This suggests that the abiotic, rather than the biotic determinants, more strongly regulated CH<sub>4</sub> oxidation, in line with our first supposition. Higher MOB activity in microcosms containing gamma-irradiated paddy soil coincided with the higher initial ammonium concentration (paddy soil, 3.4 – 4.2 μmoles g<sub>dw</sub> soil<sup>-1</sup>; upland soil, 2.0 – 2.7 μmoles g<sub>dw</sub> soil<sup>-1</sup>; Figure S20). Also, NH<sub>4</sub><sup>+</sup> and NO<sub>x</sub> concentrations in the inoculum was on average 8-10 folds higher in the paddy than upland soil, whereas PO<sub>4</sub><sup>3-</sup> was comparable in both soils (Table 6.1). Higher inorganic N concentrations likely alleviated N limitation when coupled to high CH<sub>4</sub> availability in the gamma-irradiated paddy soil, stimulating MOB growth and CH<sub>4</sub> uptake (< 12 days) when compared to the incubations containing the gamma-irradiated upland soil. Besides inorganic N, we cannot exclude the availability of other N compounds (e.g., organic N) given the high total N in these soils (Table 6.1). Besides macronutrients, MOB activity can be restricted by micronutrients (e.g., lanthanides, copper; Knapp et al., 2007; Semrau et al., 2018, 2010). Hence, we cannot completely exclude that differences in the micronutrient and trace element contents in the paddy and upland soils may have also affected CH<sub>4</sub> oxidation rates. Since pH was similar in both soils (pH 5.4; Table 6.1), discrepancy in CH<sub>4</sub> uptake was likely caused by factors other than pH in our incubations. Likewise, water content, which can restrict substrate (CH<sub>4</sub> and O<sub>2</sub>) diffusion into the soil was kept constant, and is unlikely to account for the discrepant trend in CH<sub>4</sub> uptake (Hiltbrunner et al., 2012; Shrestha et al., 2012). However, the water potential which may affect water availability for microbial activity, potentially contributing to shifts in the community composition, could be different in both soils (Harris, 1981). Admittedly, not all abiotic factors potentially contributing to the discrepancy in CH<sub>4</sub> uptake in both soils were determined. Nevertheless, it became evident that the soil abiotic parameters more strongly affected the MOB activity, resulting in significantly higher CH<sub>4</sub> uptake rates during the early stage (< 35 days) of recolonization under high CH<sub>4</sub> availability.



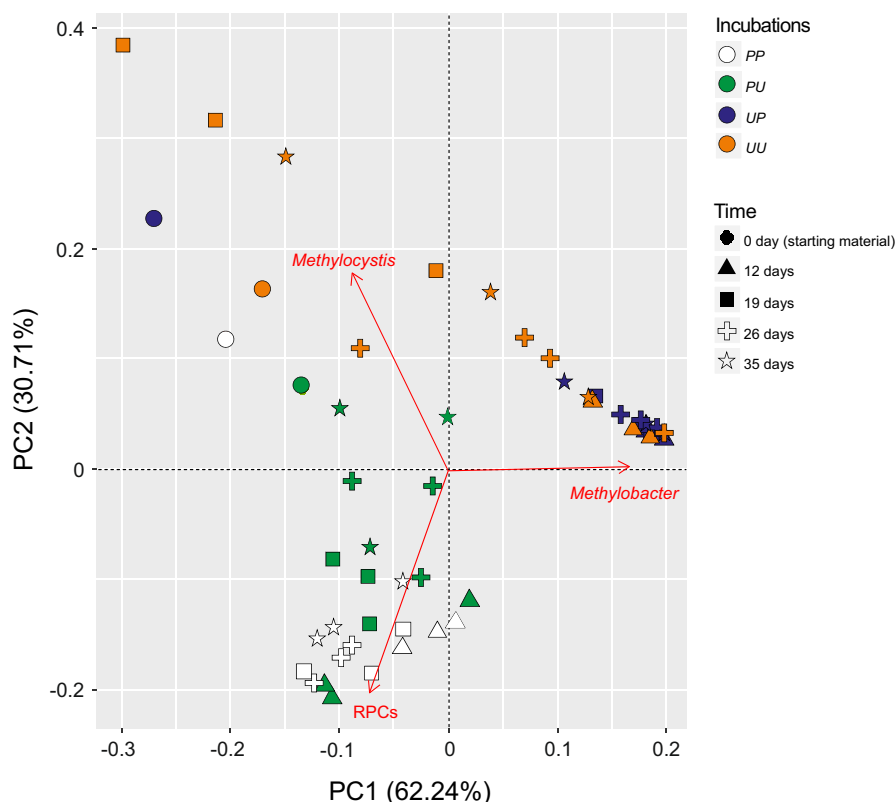


**Figure 6.3** PCA showing the response of the MOB community composition during recolonization. The composition of the MOB community was derived from sequencing of the *pmoA* gene performed for each DNA extract ( $n = 3$ ) per time and treatment. The PCA was performed in the R statistics software environment (R Core Team, 2014) using the function 'prcomp'. Visualization of the PCA was performed using the 'ggfortify' package. Rarefaction curves generated for each sample showed a good coverage of the *pmoA* gene diversity (see Figure S21). The affiliation and distribution of the *pmoA* gene sequences are given in Figure S22. The vectors indicate predominant MOB genera/group. Abbreviations: RPC, rice paddy cluster (Type Ib-related MOB).

Microorganisms compete for nutrients and space, occupying specific niches in the soil which fulfills their physiological requirements hence, shaping the microbial activity and community composition (Little et al., 2008; Pan et al., 2014). Here, the gamma-irradiated soils provide open niches, allowing rapid recolonization by the inoculum-borne MOB under high  $\text{CH}_4$  availability. The microcosms containing native soils and their gamma-irradiated fractions (PP and UU) thus represent the optimum native/gamma-irradiated soil combinations because the inoculum consists of MOB with established niche specialization (e.g., as a result of shared site history) for the specific soil. Interestingly, although PP exhibited significantly higher  $\text{CH}_4$  uptake than PU as anticipated,  $\text{CH}_4$  uptake in UU was significantly lower than UP, indicating that conditions in the upland soil was not optimal and constrained MOB activity; the paddy soil likely possessed more suitable conditions (e.g., high inorganic N), favoring the

survival of the MOB. This suggests that the MOB community composition, although indigenous to the upland soil, plays a relatively less important role in determining contemporary CH<sub>4</sub> uptake rates than abiotic controls (Ho et al., 2016b).

## 6.4 Methanotroph Population Dynamics; the Emergence of the Alphaproteobacterial Methanotrophs During Recolonization

The total MOB abundance appreciably increased after incubation in all microcosms by approximately three to four orders of magnitude during incubation (Figure 6.4), consistent with previous recolonization studies (Ho et al., 2011b; Pan et al., 2014). In particular, the significant increase ( $p < 0.01$ ) in all MOB sub-groups (Type Ia, four-fold; Type Ib, seven-fold; Type II, three-fold) corroborated with the higher CH<sub>4</sub> uptake in the UP incubation (Figure 6.2 and 6.4). On the other hand, PP microcosm which exhibits comparable total CH<sub>4</sub> uptake to UP, was accompanied by a significant increase ( $p < 0.01$ ) in Type II MOB abundance (Figure 6.4). Likewise, the abundance of Type II MOB significantly increased ( $p < 0.01$ ) in the other incubations (PU and UU). Before being succeeded by the Type II MOB, Type Ib MOB formed the majority in the paddy soil-inoculated microcosms (< 19 days; PP and PU), in agreement with their general predominance in rice paddy environments (Lüke et al., 2014). However, the high abundance of Type Ib MOB in PU is not consistent with the relatively low CH<sub>4</sub> uptake detected in this microcosm. This may be attributable to the relatively more oligotrophic condition (e.g., lower inorganic N, NH<sub>4</sub><sup>+</sup>, NO<sub>3</sub><sup>-</sup>) or faster transition to oligotrophic condition in the gamma-irradiated upland soil than in the gamma-irradiated paddy soil incubations, resulting in lower cell-specific activity (Ho et al., 2011b) not only in PU, but also in the UU microcosms. Although the MOB sub-groups were differentially affected during recolonization, the trajectory of the MOB succession was consistent across all microcosms, with the Type II MOB increasing in abundance and was generally more responsive than the Type I during recolonization (> 12 days; Figure 6.4). This may reflect on the ecological characteristics of the community members in the native soil (see discussion below; Ho et al., 2017a). Nevertheless, irrespective of the community members, it is likely that reduced competition coupled to high CH<sub>4</sub> availability spurred recolonization.

The *pmoA* gene sequences, visualized as a PCA (Figure 6.3) revealed a divergent community composition in the PP/PU and UP/UU incubations which could be largely

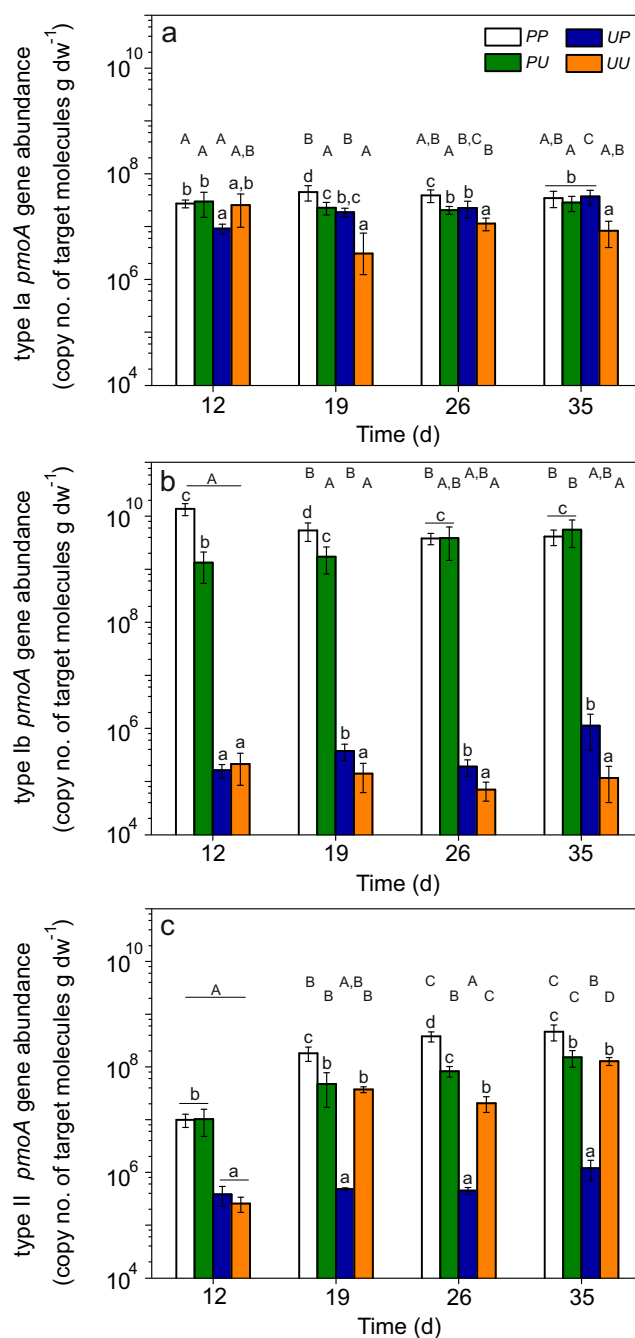


**Figure 6.4** Response of the *pmoA* gene abundance of Type Ia (A), Type Ib (B), and Type II (C) MOB during re-colonization. The qPCR was performed in duplicate for each DNA extract ( $n = 3$ ), giving a total of six replicates per time, treatment, and assay. The lower case letters indicate the level of significance (ANOVA;  $p < 0.01$ ) between treatments per time. The upper case letters indicate the level of significance (ANOVA;  $p < 0.01$ ) between sampling days per treatment. Values at the start of the incubation were at or below the detection limits of the qPCR assays used. The lower detection limit of the qPCR assays is indicated by the dashed line ( $1.8 - 8.5 \cdot 10^5$  copy no. of target molecules  $g_{dw} \text{ soil}^{-1}$ ).

separated along PC axis 2 (Figure 6.3). Over 90 % of the variation in the MOB community composition could be explained by PC1 and PC2 (62.24 % and 30.71 % of the total

variance, respectively). The predominant MOB were represented by members of Type Ia (*Methylobacter*), Type Ib (RPCs), and Type II (*Methylocystis*). The RPCs are putative MOB closely related to *Methylocaldum* (Lüke et al., 2014; Shiao et al., 2018a). Hence, the MiSeq sequencing enabled the identification of key MOB within each sub-group. The PCA revealed a RPCs-dominated population in microcosms inoculated with native paddy soils (PP and PU), and *Methylobacter* dominated the community inoculated with native upland soils (UP and UU), with the UU incubation having a broader inventory of dominant MOB comprising of *Methylocystis*, besides *Methylobacter*, reflecting on the dynamic shifts in the community composition. Hence, comparing the qPCR and *pmoA* gene sequencing analyses (Figure 6.4 and 6.3), the general trend in community dominance and succession was consistent in both analyses.

When the same community was inoculated in different gamma-irradiated soils, comparable predominant communities developed, indicating that the initial community composition plays a role in shaping the dynamics of the MOB population, but not to an extent that profoundly affects CH<sub>4</sub> uptake. In particular, gammaproteobacterial MOB affiliated to *Methylobacter* and RPCs were predominant in the microcosms inoculated with the upland and paddy soil, respectively, while Type II MOB related to *Methylocystis* increased in abundance, more pronounced in the UU incubation (Figure 6.3 and S22). Previously, the potentially active community members when incubated near in-situ CH<sub>4</sub> concentrations in the paddy (~ 1 % v/v) and upland (30-40 ppmv) soils were predominantly comprised of Type I and Type II MOB, respectively (Ho et al., 2019b, 2013b). Here, Type I MOB were initially dominant in the microcosms inoculated with both soils. Considering that the gammaproteobacterial MOB, particularly members of Type Ia (e.g., *Methylobacter*, *Methylosarcina*, *Methylomicrobium*, *Methylomonas*), are thought to be more competitive under high or excess CH<sub>4</sub> availability, these MOB may have been favored during incubation under high (10 % v/v) CH<sub>4</sub> concentrations (Ho et al., 2017a; Krause et al., 2012; Reim et al., 2012 and references therein). However, consistent in all incubations, Type II MOB presumably comprised of *Methylocystis* significantly increased over time, and even dominated the population after 19 days, despite of the prevalence of Type I MOB (Figure 6.4 and 6.3). The emergence of *Methylocystis* during recolonization is not entirely unexpected. Another alphaproteobacterial MOB (*Methylosinus*) showed colonization potential in a soil and sediment, increasing in numerical abundance over time (< 3.5 months incubation; Ho et al., 2011b; Pan et al., 2014). Likewise, in a synthetic community comprising of aerobic MOB, only alphaproteobacterial ones (*Methylosinus* or *Methylocystis*) became dominant over time (Schnyder et al., 2018). The successional trajectory indicates that Type II MOB may become important for community functioning during late succession when conditions turned

oligotrophic (e.g., after nutrient, including ammonium depletion; Ho et al., 2017a).

Overall, results support our first supposition, indicating that CH<sub>4</sub> oxidation is primarily governed by the soil physico-chemical properties, provided CH<sub>4</sub> is available. The initial community composition influences the population dynamics of the MOB without having pronounced effects on CH<sub>4</sub> oxidation. Considering accumulating evidence indicating the relevance of biotic determinants in modulating CH<sub>4</sub> oxidation (e.g., Chang et al., 2018; Ho et al., 2016a; Veraart et al., 2018), we further suggest that while soil edaphic properties modulate the MOB activity at the pioneering stages of recolonization, biotic determinants (e.g., MOB community structure, and interaction) may become relevant in established communities.

# **Chapter 7**

## **General Discussion**

## 7.1 Recapitulation of Findings

MOB provide an essential ecosystem function, oxidizing CH<sub>4</sub>, the prominent GHG, before its release into the atmosphere, being a primary producer in CH<sub>4</sub> emitting environments providing CH<sub>4</sub>-derived carbon. Literature has shown that MOB do not live in seclusion, being dependent on their interactome, a consortium of MOB and non-MOB organisms, promoting MOB survival and activity (Ho et al., 2014; Krause et al., 2017). To date, the MOB interactome remains understudied, yet providing such key factors for soil function. This work explores the MOB interactomes in various CH<sub>4</sub>-emitting habitats and the response of the interactome to disturbance using a novel strategy by combining DNA-SIP with a co-occurrence network analysis. Furthermore, biotic and abiotic parameters are investigated for their influence on the MOB interactome community composition.

**Summary of Chapter 3** The identification of the MOB interactomes over space and time revealed distinct MOB interaction partners dependent on the environment shaped dominantly by abiotic parameters. The time scale analysis provides information on a MOB 'core' interactome that is present throughout the incubation period indicating mutual dependencies, e.g., by continuous local proximity of interacting organisms. In the case of methylophs, which can metabolize methanol and further C<sub>1</sub> compounds excreted by MOB, it is shown that this guild of organisms tends to form clusters with MOB, creating physical contact and thus, constant local trophic interaction (Kalyuzhnaya et al., 2013; Krause et al., 2017). Many heterotrophs that are part of the MOB interactome identified in this study belong to the methylophs. Furthermore, predators and yet unidentified interaction partners were found to be part of the interactome.

**Summary of Chapter 4 and Chapter 5** The impact of a mild and severe stressor (Chapter 4 and Chapter 5, respectively) on the MOB interactome has revealed functional resilience in these systems, independent of the severity of the stressor given sufficient recovery time. Desiccation/re-wetting was applied to a rice paddy soil, a common stressor in such systems, as paddy soils get drained during rice harvesting; while a restored peatland was analyzed for functional and community resilience after peat mining and approximately 20 years of restoration process. In both systems, MOB activity has recovered, as well as MOB abundance, indicating the return of both systems to their undisturbed state. Nevertheless, dependent on the stressor, the structure of the co-occurrence network changed. While in the mild stressor approach (desiccation/re-wetting), the network increased in complexity, indicating a stronger association

of fewer organisms, in the severe stressor approach (peatland restoration after peat mining), the network became less connected and complex, indicating a loss in diversity buffered by functional redundancy. Even though in both systems MOB activity and abundance recovered, the structure of the interactome was profoundly altered.

**Summary of Chapter 6** MOB community development and CH<sub>4</sub> oxidation as a soil function is analyzed for its relation to abiotic and biotic soil parameters. Here, sterilized paddy and upland soil was reciprocally inoculated with the corresponding unsterilized soil to determine whether biotic or abiotic parameters shape the developing community composition and CH<sub>4</sub> oxidation. Dependent on the sterilized soil, CH<sub>4</sub> uptake rates developed similarly, while the MOB community composition remained similar to its initial composition. After the early succession of Type Ia MOB, being usually more competitive, the Type II MOB dominated the community, potentially driven by nutrient limitation in the later incubation stages. Nevertheless, these results indicate that CH<sub>4</sub> oxidation levels may be regulated by abiotic parameters independent of the initial community composition.

## 7.2 Importance of Selected Methane Emitting Environments

All selected habitats are known CH<sub>4</sub> emitting environments (see Subsection 1.5.3; **Table 3.1**; Kaupper et al., 2020a; van Dijk et al., 2021), where MOB act as CH<sub>4</sub> biofilters. Besides the reduction of GHG emissions, these environments provide food or capacities for future energy production. For example, in food production, the world's nutritional energy supply is mainly covered by rice, wheat, and coarse grains. Especially in Asia, rice primarily contributes to the total dietary energy (Khush, 2003; Rohman et al., 2014). During rice cultivation in water-saturated soils, aerenchyma inside the rice plants transport CH<sub>4</sub> from the roots upwards and release it into the atmosphere (Conrad, 2009; Holzapfel-Pschorn and Seiler, 1986; Watanabe and Kimura, 1995) while O<sub>2</sub> is transported and released into the soil by the roots (Frenzel et al., 1992; Schulze et al., 2005; van der Gon and Neue, 1996). Consequently, the dissolved O<sub>2</sub> can be used as an electron acceptor for aerobic microorganisms, e.g., MOB, in the rhizosphere (Frenzel, 2000; Khalifa et al., 2015; Kögel-Knabner et al., 2010). A maximum of 80 % of the CH<sub>4</sub> is oxidized by MOB in the upper soil layers in rice paddies in some phases during the rice growing season (Eller et al., 2005; Hanson and Hanson, 1996). In the whole season, approx. 30 % to 50 % of total CH<sub>4</sub> is directly oxidized (Bodelier, 2011a;



Eller et al., 2005; Krüger and Frenzel, 2003), underpinning the importance of MOB communities in rice cultivation.

Especially nutrient-rich environments, such as landfills, provide vast amounts of bioavailable carbon, making them significant sources of CH<sub>4</sub> / GHG emissions. The reduction or recycling of the emitted GHG increased the interest in environmental research, as well as research in bio-gas retrieval or biofilter functions (Ho et al., 2019a and references therein). In the upper layers of the landfill or in the landfill cover soil MOB oxidize minor amounts of the emitted CH<sub>4</sub> (~ 10 %; Bogner et al., 1997) before it is released into the atmosphere. With respect to the enormous amounts of carbon deposited / fermented in landfills, one may expect an enriched community of MOB that is partially driven by relatively high amounts of emitted CH<sub>4</sub>. However, MOB only made up a rather low proportion of the total bacterial community (< 5 %; see **Figure S1**, Rohrbach et al., 2022), nevertheless providing easily available carbon for their interactome, e.g., via cross-feeding.

In contrast, peatlands are often nutrient-impooverished environments, containing approx. a third of the total world soil carbon (Gorham, 1991). They are one of the major natural GHG sources and sinks in the environment, playing a crucial role in the global CH<sub>4</sub> and GHG budget. In peatlands, carbon is stored in the form of (dead) plant material in waterlogged, and thus mainly in anaerobic systems, forming peat material. Most peatlands, especially ombrotrophic peatlands, are characterized by relatively harsh conditions, e.g., low pH (~ 3) and limited amounts of nutrients (NH<sub>4</sub><sup>+</sup>, NO<sub>3</sub><sup>-</sup>, PO<sub>4</sub><sup>3-</sup>, etc.) (see **Table 5.1**, Andersen et al., 2006; Gorham, 1991; Reumer et al., 2018). Bacterial communities have developed life strategies to survive in such harsh conditions. Microbial interactions are crucial in such environments as diversity is expected to be low (Graef et al., 2011), and thus, specific functions may only be carried out by specific community members.

All habitats contained a natural enrichment of MOB, as indicated by the relatively high CH<sub>4</sub> oxidation capabilities (i.e., low-affinity CH<sub>4</sub> oxidation) and MOB abundance (see **Table 3.1** and **Figure S1**), although possessing various / contrasting soil physico-chemical properties and community compositions (**Table 3.1** and **Figure 3.1**). Given our incubation set-up with ~ 3 % CH<sub>4</sub> in the head-space, one may expect an enrichment of gammaproteobacterial MOB (Krause et al., 2012) that assemble new / more trophic interactions due to the sudden carbon availability. In consequence, MOB may form similar trophic interactions independent of the soil physico-chemical parameters, as well making (gammaproteobacterial) MOB a driver for disturbance induced community / interactome reconstruction.

### 7.3 Resistance and Resilience of the MOB Interactome

One of the most prominent (anthropogenic) disturbances is peat harvesting. When harvested and dried, peat material can be used as a combustible (IPCC, 2014), while the peatlands get partially or fully destroyed. During the last decades, peatland restoration was performed after harvesting, rebuilding these carbon storage systems, and allowing microbiomes to re-establish. Previous studies have shown that soil characteristics and community functions, e.g., methanogenesis or CH<sub>4</sub> oxidation, recovered to an extent during peatland restoration (see **Table 5.1**, Andersen et al., 2006; Basiliko et al., 2007; Reumer et al., 2018), but it is still unclear how the bacterial community develops; if recovery of soil function also reflects community recovery and how the bacterial community might react to further stressors. Here, the MOB activity and abundance may have recovered given sufficient time; nevertheless, the community composition changed during peatland restoration and the network became less complex (see **Chapter 5**). This indicates that the whole system has not yet fully recovered to its undisturbed state. The succession of MOB to withstand stressors or recolonize available niches after organism die-off (see **Chapter 4, 5, and 6**) is derived from specific traits of the MOB.

Such recovery in activity can be related to functional redundancy. Functional redundancy describes the ability of microbial taxa to carry out processes at similar rates compared to other taxa and under the same environmental conditions (Allison and Martiny, 2008). Thus, the microbial community can compensate for the loss of organisms with specific functions. Functional redundancy comes into play when organisms of the microbial community are neither resilient nor resistant to a disturbance. While resistance can be described as the capability of a community to withstand a disturbance and to remain unchanged, resilience is the return of a microbial community to its pre-disturbed composition after a disturbance (Allison and Martiny, 2008). To overcome disturbances, MOB have developed different strategies for survival (Ho et al., 2013a). While Type Ia MOB are rather resistant, competitive, driven by nutrient availability and form cysts to survive (e.g., *Methylobacter* sp., Whittenbury et al., 1970a), Type Ib can react fast to sudden nutrient availability, being highly resilient after stressor impacts (see **Figure 4.2**, Ho et al., 2013a). Additionally, some Type II MOB can also form resting stages, becoming active under nutrient-limited conditions (see **Chapter 4**, Ho et al., 2013a; Krause et al., 2012).

Even though MOB can withstand stressors or quickly re-colonize niches, heterotrophic/non-MOB organisms are known to influence MOB, both positively or negatively, as they provide essential nutrients, like vitamins (Iguchi et al., 2011), increase the MOB CH<sub>4</sub> oxidation activity (Ho et al., 2014), or manipulate their

metabolism to make the MOB excrete e.g., methanol for their metabolism (Krause et al., 2017). Nevertheless, the increase in complexity of the MOB-related heterotrophic community is shown to be beneficial for the MOB, increasing methane oxidation rates (Ho et al., 2014). Consequently, the MOB thrive better when accompanied by their interactome. In this thesis, it is shown that the MOB interactome may even support the recovery of the MOB after disturbances, contributing to soil function maintenance, e.g., CH<sub>4</sub> oxidation. Disturbances may influence CH<sub>4</sub> oxidation rates in the short term, recovering in the long term (see **Figure 4.1** and **5.1**, Ho et al., 2016c). Additionally, MOB abundance quickly recovered, reaching levels of pre-disturbance, driven by high substrate and niche availability, potentially even out-competing the undisturbed community (see **Figure 4.3** and **5.1**, Ho et al., 2011b, 2016b,c). Furthermore, highly connected interaction networks or modules inside the network consisting of functionally redundant nodes as well buffer the impact of a stressor on the system, as community function can be maintained to some extent even though some nodes get depleted (Hooper et al., 2012). A network consisting of fewer nodes and edges and lower modularity after disturbance due to, e.g., species loss may be more vulnerable to future disturbances, compared to highly connected networks consisting of functionally redundant organisms, as the stress would be more evenly distributed (as discussed before in **Sub-section 5.5.2**). One can only speculate on the impairment of the single disturbance on the MOB interactome in terms of future disturbances, as no re-occurring stressors have been applied, as done before (Ho et al., 2016b,c).

Resistance, resilience, and functional redundancy of microorganisms may depict the stability and recovery of microbial communities in soil systems after a disturbance (Bissett et al., 2013; Bodelier, 2011b). Here, we have shown that besides the recovery of the soil CH<sub>4</sub> oxidation potential and the MOB-associated microorganisms, the networks mainly portray the impact of the stressor (see **Figure 4.5** and **5.4** as well as **Table 4.1** and **5.2**). It is expected for the rice paddy soil to be less impaired by the rather mild disturbance of desiccation / re-wetting, as this system is frequently drained for rice harvesting; thus, the legacy of the system may have supported its resilience (see **Figure 4.3**, Ho et al., 2016b,c; Jurburg et al., 2017; Krause et al., 2018). Even though microorganisms and whole microbiomes may have protection mechanisms to buffer a stressor impact (Cyst/spore formation, Whittenbury et al., 1970a; cross-protection, Yurtsev et al., 2016; functional redundancy, Naeem, 1998), the effect on the whole (trophic) interaction network yet remains poorly studied.

Functional redundancy buffers the impact of a stressor on the trophic interaction network. Even though functional redundancy may not be necessary for a stable and continuous system (Loreau, 2004), it may be of importance under instable con-

ditions, e.g., sudden or continual change in soil biotic/abiotic parameters or species loss. Potentially, functional redundancy is driven by the importance of a functional group in the soil and its diversity, assuring the persistence of the community (Jurburg and Salles, 2015). For example, in Ho et al. (2020), a loss of CH<sub>4</sub> oxidation activity due to a continuously increasing ammonia stress and, consequently, inhibition of CH<sub>4</sub> oxidation may cause a collapse of the whole system as there would be a lack of carbon input into the food web via the MOB. Nevertheless, species loss has massively decreased the complexity of the MOB interactome, the function remained after a lag phase (Ho et al., 2020). In this thesis, functional redundancy was only investigated as the recovery of CH<sub>4</sub> oxidation activity in a rice paddy soil and peatlands after a mild and severe stressor impact, respectively, as well as the change / re-establishment of the community composition (short term in **Figure 4.1** and **Figure 4.3**; long term in **Table 5.1** and **Figure 5.2**). Species loss also makes niches available for dormant community members (the seed bank community, Ho et al., 2016b; Lennon and Jones, 2011) that become active, e.g., due to sudden nutrient availability, colonizing available niches forming new trophic interactions. Furthermore, one may also expect rare taxa to be important drivers of community dynamics providing multi-function (Chen et al., 2020; Jousset et al., 2017; Shade et al., 2014; Sogin et al., 2006) to be competitive, colonizing available niches, supporting the functional redundancy of the system. Besides trophic interactions, non-trophic interactions also enhance the persistence of the microbial food web (Hammill et al., 2015). In this thesis, the scope is limited to trophic interactions.

The interactome of an environmental system may maintain soil function up to a certain strength of the disturbance or loss of essential community members until the soil function no longer persists (e.g., MOB under NH<sub>4</sub><sup>+</sup> stress; Ho et al., 2020). In theory, a community can always recover from a disturbance until a 'tipping point' is passed, from which the community may reach a new alternative 'stable state' (Beisner et al., 2003; Griffiths and Philippot, 2013; Veraart et al., 2012). A stable state is a state in which a system remains and to which it returns after minor disturbance (see **Figure 7.1**, Beisner et al., 2003; Faust and Raes, 2012). Even though a stable state in an environmental system and the tipping point at which a system may change dramatically are theoretical models, they have been tested in experiments contributing to their applicability (Veraart et al., 2012). In this thesis, both potential outcomes were shown. In **Chapter 4**, the full recovery of the soil function (especially methanotrophy) and community structure reached its pre-disturbed state (see **Figure 4.1** and **4.3**), while a severe disturbance may have led the system to pass a tipping point, leading the peatland system to a new stable state, where soil function in terms of CH<sub>4</sub> oxidation activity has been restored

(see **Table 5.1**), even though the community composition may still be different (see **Figure 5.2**). This change may as well be reflected in the co-occurrence networks. In the mild disturbance, independent of the loss in nodes, the number of edges increased, compensating for the organism loss and restoring community function (**Figure 7.1**). In contrast, the severe disturbance led to a decrease in nodes, edges and modularity, that decreased connectivity, and sub-clustering of nodes. Here, the system may have turned to an alternative stable state, with different biotic and abiotic conditions, but still maintaining soil functions (**Figure 7.1**).

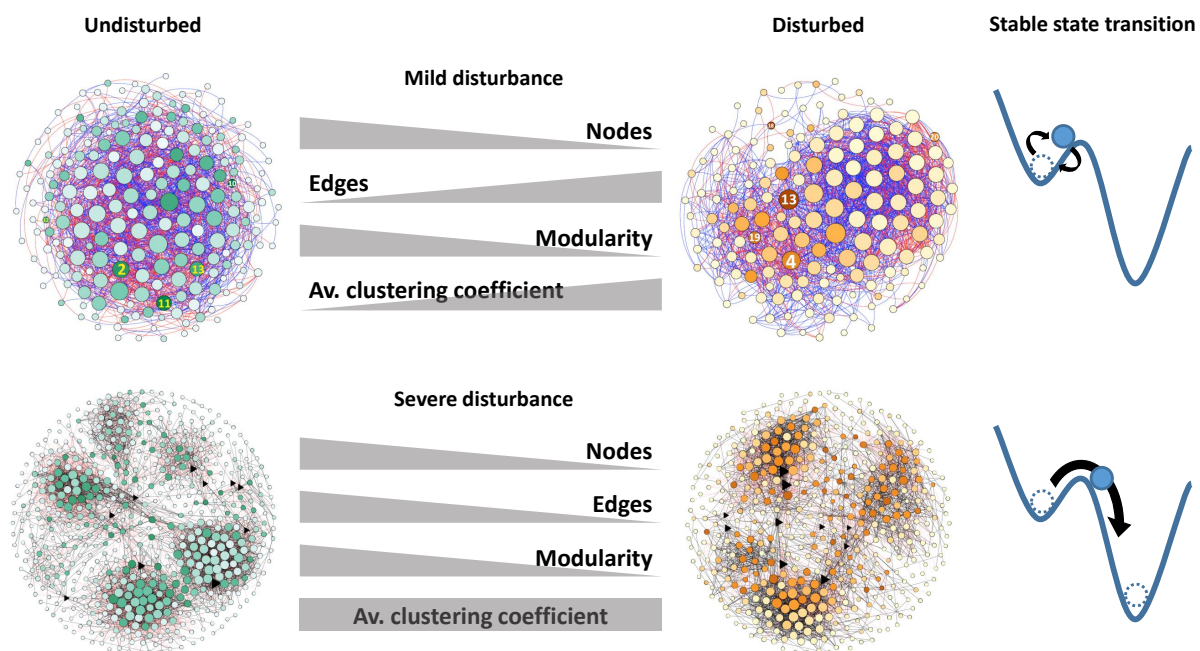


**Figure 7.1** Conceptual model summarizing the influence of a mild and severe disturbance on the co-occurrence network (see **Chapter 4** and **5**). Mild disturbance (top panel) reduced the number of nodes while the number of edges increased, leading to a total increase in connectivity as well as average clustering coefficient. Modularity was lower in the disturbed network. The increased connectivity may have buffered the influence of the disturbance on the community, even though the network remains impaired. Nevertheless, the community may have returned to its stable state, not passing a tipping point (right top panel). Compared to this, the severe disturbance (bottom panel) lead to a decrease in connectivity, depicted by a decrease in nodes and edges, as well as modularity, potentially weakening the system for future disturbances. Here, the system may have passed a tipping point that lead the system to an alternative stable state (right bottom panel) still maintaining soil function.

No general rule for the anticipation or reaction of a community to/after disturbance can be drawn as environmental systems are complex and driven by multiple factors. In **Figure 3.2** it is shown that no common interactome can be identified in the selected habitats, and **Chapters 4** and **5** illustrate the stress response of such systems, reacting differently based on the severity of the stress (summarized in **Figure 7.1**, Ho et al., 2016b) and also dependent on the legacy of the system (Krause et al., 2018;

van Kruistum et al., 2018). Here, a mild stressor led to an increase in complexity and connectivity, while modularity decreased; a severe stressor led to a decrease in complexity and connectivity, as well as modularity. Taken together, both interaction networks remained impaired after the disturbance, weakening their stability in terms of future disturbances. Besides biotic parameters that may shape the community in the long term (see **Chapter 6**), abiotic parameters were shown to play a major role in MOB community development during recolonization.

Edaphic parameters have the main influence on MOB activity and re-colonization potential shortly after disturbances (see **Chapter 6**). In a microcosm experiment, the re-colonization of MOB in sterilized soil highlighted the similar development of the MOB community dependent on the initially inoculated community with a limited extent to CH<sub>4</sub> oxidation (see **Figure 6.2** and **Figure 6.4**). CH<sub>4</sub> oxidation activities have developed independent of the inoculated community, supporting the hypothesis that abiotic, more than biotic parameters (e.g., initial community composition) shape the MOB activity.

Yet, it is already known that abiotic parameters can shape microbiomes (Fierer, 2017; Kaupper et al., 2020a; Lauber et al., 2008; Sun et al., 2013; Zheng et al., 2019), e.g., during a disturbance, when conditions suddenly change, or during a continuous shift. Comparing the investigated habitats, total C, total N, and ion concentration (analyzed via electrical conductivity (EC)) have mainly driven community development (see **Figure 3.1**). A release in nutrients, e.g., caused by a disturbance, as shown in **Figure S12**, may have contributed to fast MOB recovery due to sudden nutrient availability. Surprisingly, NH<sub>4</sub><sup>+</sup> concentration was not a significant variable shaping the microbial communities in various habitats (**Figure 3.1**), enhancing or inhibiting methane oxidation dependent on its concentration (Ho et al., 2020; van Dijk et al., 2021). Besides total C and N, EC had a significant impact on the community development underpinning the influence of abiotic parameters for community development, even though tested parameters (pH, NH<sub>4</sub><sup>+</sup>, NO<sub>3</sub><sup>-</sup>, and SO<sub>4</sub><sup>2-</sup>) did not influence the community remarkably (see **Figure 3.1**). Consequently, disturbances and consequent changes in abiotic parameters can cause beneficial / detrimental changes in the community composition, either in the short term (e.g., **Figure 4.3**, Ho et al., 2016c; van Kruistum et al., 2018) or long-term / permanently (e.g., **Figure 5.2**, Ho et al., 2016c; Reumer et al., 2018). As a change in abiotic parameters as well influences the development of the active community, future experiments may include the edaphic parameters in the co-occurrence network analysis, as done by Mandakovic et al. (2018), potentially identifying edaphic parameters that (re-)shape the microbiome / interactome in pristine habitats or after disturbance.

## 7.4 The MOB Core Interactome

The soil core microbiome is defined by organisms, present in all samples or over longer periods, potentially providing essential functions within their habitat and maintaining bacterial community structure during environmental change (Hernandez-Agreda et al., 2017; Mandakovic et al., 2018; Neu et al., 2021). Expanding this definition, consequently, the microbial 'core interactome' can be defined as trophic interactions between the same taxa either found in various environments or over time in the same environment, maintaining (fundamental) soil function even during / after stressor impact. Such interactions may be stronger compared to random or weak interactions; thus, organisms are interacting more than by chance, as it can be inferred from the co-occurrence analysis. Here, the identification was strengthened by the application of DNA-SIP, reducing spurious correlations in the co-occurrence network (see **Table 3.2** and **Table 3.3**). Members of the non-core interactome may hence contribute to soil function in loose interactions or provide subordinate functions. Together with the remaining active (non-core) organisms, as well as the seed bank community (Ho et al., 2016b; Lennon and Jones, 2011), the core organisms form a dynamic soil system. Trophic interaction partners that may get removed from the system, e.g., due to stressors, may be replaced by the seed bank community when inactive / dormant cells get active (Ho et al., 2016b; Krause et al., 2012). As core communities can be present throughout the year and depth independent (Degenhardt et al., 2020), one may speculate on the persistence of the trophic interactome of environmental systems. Here, we have shown that a part of the active community forms continuous trophic interactions over the course of 19 days (see **Figure 3.3**). This time frame is insufficient to indicate interactions over the course of a year. Still, one may expect a continuous core community to form persistent trophic interactions, e.g., in niche communities that are limited in motility.

Often, co-occurrence networks are used to identify the core microbiome, that is, the shared nodes between environments or treatments (e.g., Mandakovic et al., 2018). To date, there is only little literature comparing the edges, thus the shared and unique interactions between sites or over time (e.g., Mandakovic et al., 2018; Williams et al., 2014). Both approaches provide insights into the core network / interactome, giving valuable information on the most important organisms. Still, only the shared edges (trophic interactions) provide insight into how the trophic network is structured, as done in **Chapter 3**. Nevertheless, the identification of the direction of the positive or negative interactions and, consequently, the model of biological interaction remains challenging (Pinto et al., 2022). Here, one can only speculate on the mode of interaction (i.e., positive interactions: Mutualism or commensalism; negative: Competition, para-

sitism, predation or ammensalism) between interacting taxa. Methylootrophs that were co-enriched alongside the methanotrophs are assumed to interact positively with MOB as the MOB (involuntarily) share the methanol (see **Figure 3.2**; Dumont et al., 2011; Taubert et al., 2019) while potentially receiving essential nutrients forming a mutualistic or commensalistic interaction. Surprisingly, predatory organisms were found to positively and negatively correlate to MOB. Here, the negative mode of interaction is likely predation, while the positive interaction may be explained by nutrient availability after cell lysis, from which the MOB may have taken advantage.

In contrast to our hypothesis, the MOB interactomes were distinct in the different habitats, indicating that not just carbon source availability drives the MOB-dependent interactome (see **Figure 3.2**). Ecological niches, predation, and abiotic parameters may affect the MOB and their interaction partners more than just CH<sub>4</sub> availability. Supporting our hypothesis, it is shown in a pristine peatland that the identified interactome is continuous (see **Figure 3.3**). One may extrapolate this to all investigated environments and, thus, only a fraction of the identified interactome may persist over time, while others are only ephemeral. To determine the MOB core interactome, longer incubations may be of interest to reveal the constantly interacting organisms.

## 7.5 Limitations and Advantages of SIP and Co-occurrence Networks

Throughout the last years, co-occurrence network analysis has been discussed controversially for its use in identifying interactions in ecology (Blanchet et al., 2020; Faust, 2021; Goberna and Verdú, 2022; Guseva et al., 2022; Hirano and Takemoto, 2019; Pinto et al., 2022; Poudel et al., 2016). Correlations can only infer interactions '*post hoc ergo propter hoc*' ("After this, therefore because of it") and do not imply causation. Co-occurrence network analysis is one of the few tools ecologists have to infer trophic interactions, yet its meaningfulness may be limited. In this work, a novel strategy for the identification of interaction partners is applied and tested for the MOB interactome, combining DNA-SIP to co-occurrence network analysis. DNA-SIP increases the accuracy in identifying active members of the community via the assimilation and incorporation of the labeled substrate into the cell biomass. Consequent separation and sequencing of the labeled DNA from the total nucleic acids reveal the actively growing community members (Neufeld et al., 2007b). In combination with a co-occurrence network analysis, only active organisms are considered for the correlation, increasing the meaningfulness of the detected correlations by following a labeled substrate (e.g., <sup>13</sup>C-



CH<sub>4</sub>) through the food web via cross-feeding, here, identifying the MOB interactome (see **Chapter 3, 4 and 5**). Applying SIP before the co-occurrence network analysis and filtering for significant strong positive/negative correlations decreased the complexity of the network (see **Table 3.2**), excluding spurious/random correlations, e.g., from dormant organisms. Complexity decreased in the co-occurrence networks in almost all habitats when only considering the <sup>13</sup>C labeled fraction of the community (see **Table 3.2, Table 3.3, and Figure 7.2**). A decrease in complexity is depicted by a reduced number of nodes and edges. Thus, fewer organisms are part of the network forming fewer interactions, creating a less complex network. This strategy highlights the improvement of the network analysis by SIP-pre-filtering for the actively CH<sub>4</sub> and derived secondary metabolite assimilating community.

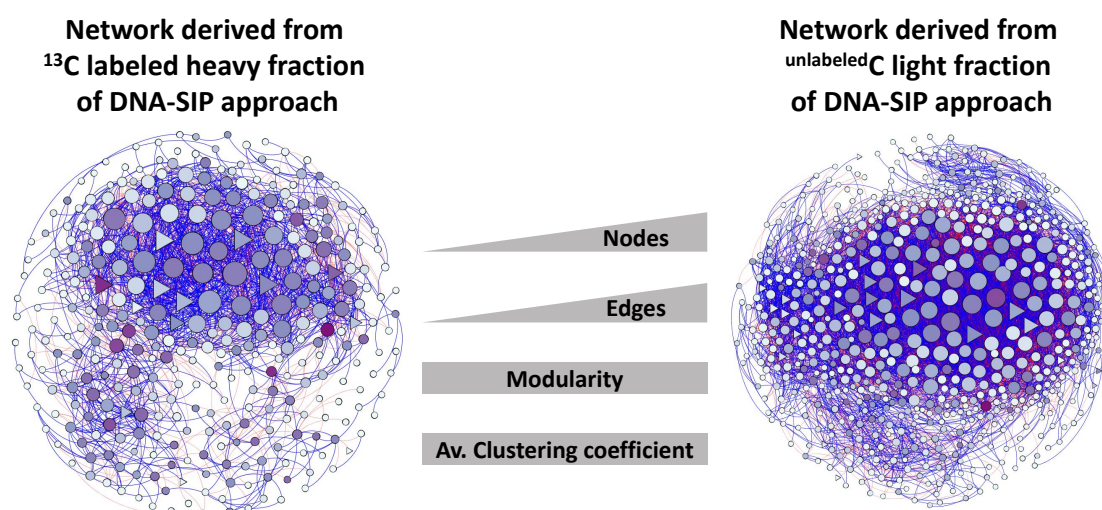


**Figure 7.2** Conceptual model recapitulating the results from the novel strategy applied in this thesis combining SIP and co-occurrence network construction (see **Chapter 3**). DNA-SIP reduced the number of nodes and edges (left network) compared to the unlabeled network (right network). Independent of this decrease in connectivity, modularity and average clustering coefficient remained similar comparing labeled and unlabeled networks. DNA-SIP coupled co-occurrence network analysis may have excluded dormant or inactive members of the community via labeling of the active and growing community, representing the over-interpretation of interactions in non-SIP co-occurrence networks.

SIP has shown to be a valid tool to screen environmental systems for active and growing organisms (e.g., Gupta et al., 2012; He et al., 2012a,b,c; Hetz and Horn, 2021; Lee et al., 2021; Lueders et al., 2004b) and for their trophic interactomes (**Chapter 3, 4 and 5**). Nevertheless, it is to mention that the addition of labeled substrate or nutrients in concentrations higher than in nature may select for specific organisms and reshapes the community due to sudden carbon availability (Cébron et al., 2007b; Neufeld et al., 2007a). Here, specifically the MOB, more precisely low-affinity MOB, were targeted using <sup>13</sup>C-labeled CH<sub>4</sub>, as the MOB are a small guild solely capable of CH<sub>4</sub>

metabolism. Consequently, the scope of this thesis is limited to the MOB interactome, not being able to directly relate the findings to the whole soil system. Nevertheless, this focus strengthens the validation of found interactions, as heterotrophic organisms that are labeled must have derived  $^{13}\text{C}$ -carbon via the MOB, being a strong indicator of trophic interaction. The finding of a potential trophic interaction still comes with the difficulty to identify the interaction mechanism (Pinto et al., 2022). Unfortunately, we can only speculate on some found trophic interactions and their interaction partners, i.e., a *Chthoniobacter* species or predators.

A yet unknown interaction mechanism of a *Chthoniobacter* sp. with various MOB interaction partners was identified. This interaction was found either continuous with a *Methylomonas* sp. in the core interactome or only transient with an organism of the *Methylacidiphilaceae* (**Figure 3.2** and **Figure 3.3**). To the knowledge of the author, no research group has identified the contribution of *Chthoniobacter* sp. to the MOB interactome, yet members of the *Chthoniobacteraceae* were identified in various habitats that are as well colonized by MOB (e.g., peatlands: Dedysh et al., 2021; Graham et al., 2017; rice fields: Hester et al., 2022; mineral spring caves: Karwautz et al., 2018). The finding is unexpected as no obvious MOB-associated carbon uptake mechanisms, either via metabolites or predation, could be predicted. Nevertheless, carbon transfer of MOB to *Chthoniobacter* sp. via digestion of biofilms containing  $^{13}\text{C}$ -labeled exopolysaccharides produced either by MOB (Wei et al., 2015) or heterotrophic organisms (e.g., Myxobacteria, Berleman and Kirby, 2009) could be possible.

Further trophic dependencies were shown, with microbial predators being part of the MOB interactome. Microbial predators (e.g., *Bdellovibrio* sp. and members of Myxococcales) were mainly identified in the spacial approach, as these organisms are less found in oligotrophic environments (see **Chapter 3**). Independent of their relevance for the microbial food web (Petters et al., 2021), it is unexpected for predatory organisms to be part of the core (MOB) interactome, as these organisms do not have a high nutritional dependency on specific metabolites (e.g.,  $\text{C}_1$  molecules in MOB and methylotrophs) or local proximity due to their mobility (Berleman and Kirby, 2009), even though they can 'hunt' for specific bacteria releasing nutrients into the system (e.g., Myxobacteria Berleman and Kirby, 2009; protists, Geisen et al., 2018). The identification and validation of such interactions still remain troublesome, but also methodological issues affect the finding of potential interactions.

In SIP studies, one should always consider the influence of the nucleic acid GC content, as it affects the banding within the density gradient (e.g., Lee et al., 2022; Neufeld et al., 2007a). The influence of DNA with high GC content banding in the region of the heavy  $^{13}\text{C}$ -labeled fraction is a known problem in SIP studies (Lueders et al., 2004a).

This is of great importance for network constructions, as it may increase the number of interactions due to the banding of high GC-content unlabeled DNA in the  $^{13}\text{C}$  heavy fraction, increasing the number of OTUs. Nevertheless, here (see **Chapter 3, 4, and 5**), the correlations have been filtered for very strong and significant correlations, decreasing the chance of random correlations between OTUs derived from labeled and heavy GC unlabeled DNA potentially present in the sequencing data. The consideration and subtraction of these unlabeled nucleic acids will remain a challenge for SIP, as well as SIP-coupled network studies.

In this thesis, 16S rRNA gene Illumina amplicon sequencing data was used for the correlation to infer interactions from the network (see **Chapter 3, 4, and 5**). This data cannot truly reflect the abundance of organisms in the soil due to commonly known biases produced, e.g., during nucleic acid extraction or amplification during PCR (Eisenstein, 2018; Suzuki and Giovannoni, 1996 and references therein). Additionally, the variability of the abundance and diversity of the 16S rRNA gene per organism (Acinas et al., 2004) plays a tremendous role in the co-occurrence network construction. Introducing the 16S rRNA gene abundance per organism into the data may change the abundance of several OTUs, leading to stronger or weaker correlations. In future work, researchers may include the prokaryotic / eukaryotic rRNA gene abundance and sequence variability (Kembel et al., 2012; Louca et al., 2018) into the network calculations, increasing the validity of inferred (trophic) interactions.

Trophic interactions not only occur on MOB-MOB or MOB-heterotrophic bacteria levels, but can be formed between bacteria, archaea, and eukaryotes on different trophic levels (e.g., Distel and Cavanaugh, 1994; Hernandez-Agreda et al., 2017; Ho and Bodelier, 2015; Lee et al., 2021; Lueders et al., 2004b; Raghoebarsing et al., 2005; Sanseverino et al., 2012; Schulz and Boyle, 2006; Yoshida et al., 2014) which were not taken into account in this thesis. Future experiments may reveal the methanotrophic interactome regarding the missing or overlooked organisms and unknown paths of carbon flow derived from MOB.

Even though we can not confirm our hypothesis that MOB form similar interactomes in different  $\text{CH}_4$  emitting habitats, a shown continuity in trophic interactions approved our hypothesis of persistent trophic interactions within a soil system, potentially forming the core interactome. DNA-SIP coupled co-occurrence network analysis is shown to provide interactions between taxa, supported by the pre-selection for actively growing organisms, increasing the credibility of the identified interacting taxa in stressed systems and when comparing habitats.

## 7.6 Limited Information on Pure Culture Interactions

Soil abiotic parameters shape the composition and activity of a microbiome (see **Chapter 3** and **6**, respectively). Nevertheless, the identification of microbial (trophic) interaction is often tested or validated in pure cultures, and efforts are made to identify / predict microbial interactions from such incubations (Kehe et al., 2021; Nestor et al., 2022). Edaphic properties shape the soil bacterial community, and biotic parameters, but it is challenging or impossible to mimic soil properties *in vitro*. Nevertheless, inferring interactions from a mixture of pure cultures remains one of the few tools to identify interacting organisms. It was shown that interactions in such mixed culture systems occur (Ho et al., 2014; Kehe et al., 2021) and may reflect potential interactions that can occur in nature (e.g., MOB-methylotroph, Krause et al., 2017, or MOB-predator, Murase and Frenzel, 2008), but still cannot mimic abiotic/biotic soil conditions. Interactions identified in soils may be more complex than just simple one-to-one interactions, potentially having dependencies on the presence/absence of further metabolites/organisms. Derived from our network analysis (see **Chapter 3, 4, and 5**), the clustering coefficient depicts the number of triangle structures in the network (see **Table 2.1**), referring to more complex interactions than simple one-to-one structures (see **Table 2.1**, Billick and Case, 1994; Faust, 2021). Such interactions, as well as necessary metabolites, co-factors, interaction partners, abiotic parameters, etc., are almost impossible to unravel and recreate. Even though DNA-SIP coupled network analysis or pure culture work to identify trophic interactions in soils may not be optimal tools, these methods are incredibly important to provide further insights into the almost unlimited trophic/non-trophic interactions in microbial food webs.

## 7.7 Conclusion

To unravel trophic interactions in environmental systems, MOB were used as a model system. The MOB interactome is known to influence MOB activity, as well as stress response. In this thesis, the interactome of various CH<sub>4</sub>-emitting habitats was investigated using a novel strategy by combining DNA-SIP with co-occurrence networks. This approach reduced the OTUs introduced into the network to the actively metabolizing and growing community. The investigated habitats had few overlapping interacting taxa, indicating site specificity of the MOB interactome. As stressors influence microbial communities regularly, a mild and severe stressor was applied to MOB-associated communities using the novel DNA-SIP co-occurrence network approach. In both systems, the soil function (here, methanotrophy) recovered. When a mild stressor was

applied, the community composition returned to its pre-disturbed state, while in the severe stressor application, the community composition changed. Nevertheless, after both stressors, the co-occurrence networks remained impaired, potentially being more vulnerable to future stressors. Lastly, the determining factors for community composition during recolonization were determined, highlighting that in the early stages, abiotic factors may have a greater influence on the developing community than biotic parameters, which changes during the later recolonization phase. Consequently, MOB interactomes are versatile, and community response may be greatly influenced first by abiotic parameters after a disturbance and later by biotic / community-dependent parameters. Concluding, we have shown that the development of the MOB community and interactome is dependent on abiotic and biotic parameters depicted by the varying interactomes found in contrasting habitats. Resistance and resilience of the interactome may be dependent on the severity of the stressor and on the legacy of the system. Consequently, the general hypothesis is disproved, as no general rule for MOB community and interactome composition and stress response dependent on the habitat can be drawn here. Future experiments may include further processes present in soil systems and generate models to predict community responses to disturbances from the given parameters (e.g., soil physico-chemical parameters, community composition, and co-occurrence networks).

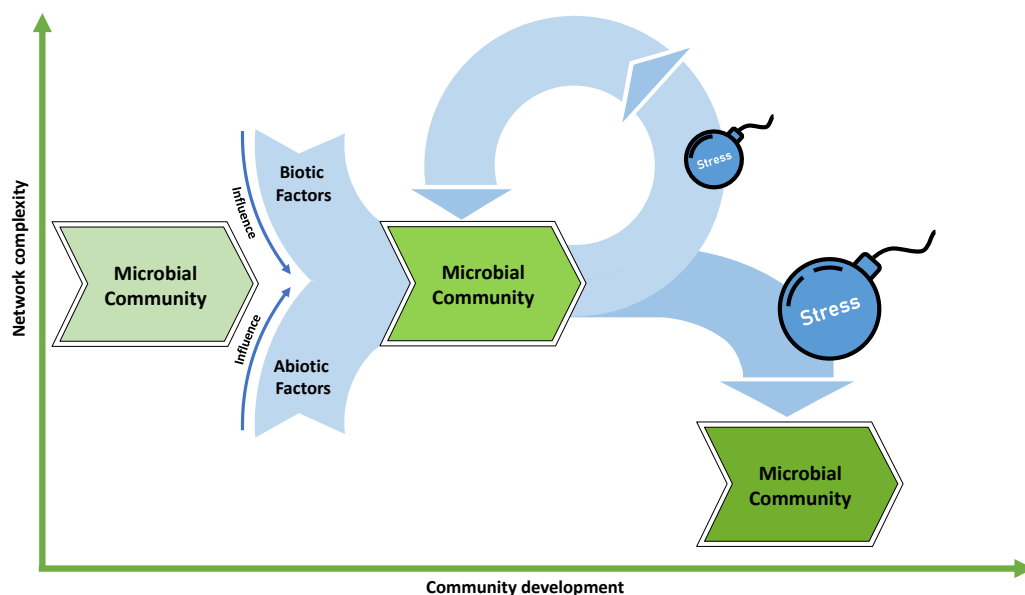


**Figure 7.3** Graphical model of the microbial community and network complexity development after disturbance. After a mild stressor (small wrecking ball), the microbial community may return to its undisturbed state, while transiently, the network gets more complex. Contrasting, after a severe stressor (big wrecking ball), the community composition changes and the co-occurrence network gets less complex.

## 7.8 Summary

MOB provide a fundamental soil function, being the only group of organisms capable of CH<sub>4</sub> oxidation, reducing soil GHG emissions in CH<sub>4</sub> emitting environments, or acting as a CH<sub>4</sub> sink. These functions make MOB subject to many investigations of how one can use MOB against CH<sub>4</sub> emissions. MOB do not live in seclusion in environmental systems, acting as primary producers introducing carbon into the soil food web. The MOB trophic interactome yet remained understudied even though non-methanotrophic organisms have significant influence on the MOB.

In this thesis, the MOB interactome is compared in five different CH<sub>4</sub>-emitting habitats, depicting the site specificity of the MOB interaction partners, potentially driven by soil physico-chemical parameters. In a temporal approach, a continuity of the trophic interactions was identified, potentially forming the MOB core interactome. The identification of the MOB interactome raised the question of how these interactomes behave under stress. Two experiments have been performed comparing a mild stressor (here: desiccation / re-wetting) in rice paddy soil and a severe stressor (here: peat mining and restoration) in a peatland. In both habitats, CH<sub>4</sub> oxidation potential returned to its undisturbed state, indicating a full recovery of the system. In contrast, the co-occurrence networks, and thus, the MOB interactome indicates a remaining impairment that may have tremendous consequences in terms of reoccurring stressors. Besides biotic soil parameters, abiotic parameters were identified to drive community development and composition. Comparing the re-colonization of sterilized soils, it is shown that abiotic parameters mainly shape the developing community independent of the inoculated community composition.

Taken together, MOB provide CH<sub>4</sub> oxidation as an important soil function, affected more by abiotic than biotic parameters. The methanotrophic interactome is distinct in CH<sub>4</sub>-emitting habitats and remains impaired after stressor application, even though soil function, e.g., the CH<sub>4</sub> oxidation potential, may recover. Even though various methods have been developed to infer microbial interactions, in the future, methods may validly identify (trophic) interactions directly in soil systems, shedding light on the microbial food web.

## 7.9 Outlook

The finding of the MMOs raise the industrial interest in MOB. As CH<sub>4</sub> is quite inert, the CH<sub>4</sub> molecule needs to be 'activated' first by the abstraction of the first hydrogen atom, which requires energy (104 kcal mol<sup>-1</sup>; Blanksby and Ellison, 2003; Dalton, 2005). Especially, this transformation makes MOB interesting for chemists, as the reaction of CH<sub>4</sub> to methanol is a high-energy and catalyst-demanding reaction (Yang et al., 2021). To date, MOB are still of great interest for industrial, chemical, or environmental applications with regard to their unique metabolism.

MOB provide versatile functions, that are, the oxidation of CH<sub>4</sub> at ambient temperatures for biofuel production (Gęsicka et al., 2021; Lee et al., 2016) or plastic precursor production (Gęsicka et al., 2021), metal detoxification in soils and bio-remediation (Pandey et al., 2014) as well as animal feed (Chen et al., 2022, 2021; Yu et al., 2022). MOB have shown to be robust against stressors in soil, interacting with their abiotic and biotic surrounding, being a primary carbon producer in CH<sub>4</sub> emitting environments. To understand the full potential that the MOB provide, the MOB have to be investigated further, e.g., in pure cultures, but especially in soil systems. MOB growth and activity is improved when co-cultured with non-MOB. Furthermore, this thesis highlighted the trophic interactions maintained by the MOB in complex communities in environmental systems. Unfortunately, the scope of this thesis is limited to trophic interactions between prokaryotes. To extend the findings of this thesis, one may consider including interactions of the MOB with eukaryotes or viruses.

Yet largely unexplored, viruses contribute massively to biomass cycling (e.g., in lakes and oceans, up to 50 % of the microbes are lysed each day; Peduzzi and Schiemer, 2004) in aquatic and terrestrial systems. Microbial cell debris after viral lysis provide a substantial amount of nutrients in the form of proteins, fatty acids, and nucleic acids to surrounding organisms. Such a release of nutrients may even have a greater effect in oligotrophic environments where nutrients are limited. Besides viral lysis, predation causes a similar effect. In this thesis, predatory prokaryotic organisms were identified (see Chapter 3, 4, and 5), known to graze on MOB. Additionally, eukaryotic predatory organisms (i.e., protozoa) are known to feed on MOB (Murase and Frenzel, 2007, 2008), which were not taken into account in this thesis. Future experiments may reveal how viral and predator-related cell lysis affect and restructure the MOB interactome and potentially provide information on the resistance or resilience of the MOB interactome also towards its soil function (CH<sub>4</sub> oxidation potential).

## Chapter 8 References

- Acinas, S. G., Marcelino, L. A., Klepac-Ceraj, V., and Polz, M. F. (2004). Divergence and redundancy of 16S rRNA sequences in genomes with multiple *rrn* operons. *Journal of bacteriology*, 186(9):2629–2635.
- Agasild, H., Zingel, P., Tuvikene, L., Tuvikene, A., Timm, H., Feldmann, T., Salujõe, J., Toming, K., Jones, R. I., and Nõges, T. (2014). Biogenic methane contributes to the food web of a large, shallow lake. *Freshwater Biology*, 59(2):272–285.
- Allison, S. D. and Martiny, J. B. H. (2008). Resistance, resilience, and redundancy in microbial communities. *Proceedings of the National Academy of Sciences*, 105:11512–11519.
- Andersen, R., Francez, A.-J., and Rochefort, L. (2006). The physicochemical and microbiological status of a restored bog in Québec: Identification of relevant criteria to monitor success. *Soil Biology and Biochemistry*, 38(6):1375–1387.
- Anderson, M. J. (2001). A new method for non-parametric multivariate analysis of variance. *Austral Ecology*, 26(1):32–46.
- Arakawa, H., Aresta, M., Armor, J. N., Barteau, M. A., Beckman, E. J., Bell, A. T., Bercaw, J. E., Creutz, C., Dinjus, E., Dixon, D. A., Domen, K., DuBois, D. L., Eckert, J., Fujita, E., Gibson, D. H., Goddard, W. A., Goodman, D. W., Keller, J., Kubas, G. J., Kung, H. H., Lyons, J. E., Manzer, L. E., Marks, T. J., Morokuma, K., Nicholas, K. M., Periana, R., Que, L., Rostrup-Nielson, J., Sachtler, W. M., Schmidt, L. D., Sen, A., Somorjai, G. A., Stair, P. C., Stults, B. R., and Tumas, W. (2001). Catalysis research of relevance to carbon management: progress, challenges, and opportunities. *Chemical reviews*, 101(4):953–996.
- Auman, A. J., Speake, C. C., and Lidstrom, M. E. (2001). *nifH* sequences and nitrogen fixation in type I and type II methanotrophs. *Applied and environmental microbiology*, 67(9):4009–4016.
- Baani, M. and Liesack, W. (2008). Two isozymes of particulate methane monooxygenase with different methane oxidation kinetics are found in *Methylocystis* sp. strain SC2. *Proceedings of the National Academy of Sciences*, 105(29):10203–10208.
- Balasubramanian, R. and Rosenzweig, A. C. (2007). Structural and mechanistic insights into methane oxidation by particulate methane monooxygenase. *Accounts of chemical research*, 40(7):573–580.
- Balasubramanian, R. and Rosenzweig, A. C. (2008). Copper methanobactin: a molecule whose time has come. *Current opinion in chemical biology*, 12(2):245–249.
- Balasubramanian, R., Smith, S. M., Rawat, S., Yatsunyk, L. A., Stemmler, T. L., and Rosenzweig, A. C. (2010). Oxidation of methane by a biological dicopper centre. *Nature*, 465(7294):115–119.
- Barberán, A., Bates, S. T., Casamayor, E. O., and Fierer, N. (2012). Using network analysis to explore co-occurrence patterns in soil microbial communities. *The ISME journal*, 6(2):343–351.
- Basiliko, N., Blodau, C., Roehm, C., Bengtson, P., and Moore, T. R. (2007). Regulation of Decomposition and Methane Dynamics across Natural, Commercially Mined, and Restored Northern Peatlands. *Ecosystems*, 10(7):1148–1165.
- Bastian, M., Heymann, S., and Jacomy, M. (2009). Gephi: An Open Source Software for Exploring and Manipulating Networks. *International AAAI Conference on Weblogs and Social Media*, 3(1):361–362.
- Beal, E. J., House, C. H., and Orphan, V. J. (2009). Manganese- and iron-dependent marine methane oxidation. *Science (New York, N.Y.)*, 325(5937):184–187.



- Begonja, A. and Hrsak, D. (2001). Effect of Growth Conditions on the Expression of Soluble Methane Monooxygenase. *Food technology and biotechnology*, 39(1):29–35.
- Beisner, B. E., Haydon, D. T., and Cuddington, K. (2003). Alternative stable states in ecology. *Frontiers in Ecology and the Environment*, 1(7):376–382.
- Belova, S. E., Baani, M., Suzina, N. E., Bodelier, P. L. E., Liesack, W., and Dedysh, S. N. (2011). Acetate utilization as a survival strategy of peat-inhabiting *Methylocystis* spp. *Environmental microbiology reports*, 3(1):36–46.
- Benner, J., de Smet, D., Ho, A., Kerckhof, F.-M., Vanhaecke, L., Heylen, K., and Boon, N. (2015). Exploring methane-oxidizing communities for the co-metabolic degradation of organic micropollutants. *Applied microbiology and biotechnology*, 99(8):3609–3618.
- Benstead, J. and King, G. M. (1997). Response of methanotrophic activity in forest soil to methane availability. *FEMS microbiology ecology*, 23(4):333–340.
- Berestovskaya, Y. Y., Vasil'eva, L. V., Chestnykh, O. V., and Zavarzin, G. A. (2002). Methanotrophs of the Psychrophilic Microbial Community of the Russian Arctic Tundra. *Microbiology*, 71(4):460–466.
- Berg, M. P. and Ellers, J. (2010). Trait plasticity in species interactions: a driving force of community dynamics. *Evolutionary Ecology*, 24(3):617–629.
- Bergamaschi, P. and Bousquet, P. (2008). Estimating Sources and Sinks of Methane: An Atmospheric View. In Caldwell, M. M., Heldmaier, G., Jackson, R. B., Lange, O. L., Mooney, H. A., Schulze, E.-D., Sommer, U., Dolman, A. J., Valentini, R., and Freibauer, A., editors, *The Continental-Scale Greenhouse Gas Balance of Europe*, volume 203, pages 113–133. Springer New York, New York, NY.
- Berleman, J. E. and Kirby, J. R. (2009). Deciphering the hunting strategy of a bacterial wolfpack. *FEMS Microbiology Reviews*, 33(5):942–957.
- Berry, D. and Widder, S. (2014). Deciphering microbial interactions and detecting keystone species with co-occurrence networks. *Frontiers in microbiology*, 5:219.
- Bhattarai, S., Cassarini, C., and Lens, P. N. L. (2019). Physiology and Distribution of Archaeal Methanotrophs That Couple Anaerobic Oxidation of Methane with Sulfate Reduction. *Microbiology and molecular biology reviews : MMBR*, 83(3).
- Billick, I. and Case, T. J. (1994). Higher Order Interactions in Ecological Communities: What Are They and How Can They be Detected? *Ecology*, 75(6):1529–1543.
- Bissett, A., Abell, G. C. J., Bodrossy, L., Richardson, A. E., and Thrall, P. H. (2012). Methanotrophic communities in Australian woodland soils of varying salinity. *FEMS microbiology ecology*, 80(3):685–695.
- Bissett, A., Brown, M. V., Siciliano, S. D., and Thrall, P. H. (2013). Microbial community responses to anthropogenically induced environmental change: towards a systems approach. *Ecology letters*, 16(S1):128–139.
- Blanchet, F. G., Cazelles, K., and Gravel, D. (2020). Co-occurrence is not evidence of ecological interactions. *Ecology letters*, 23(7):1050–1063.
- Blanksby, S. J. and Ellison, G. B. (2003). Bond dissociation energies of organic molecules. *Accounts of chemical research*, 36(4):255–263.
- Bodelier, P. L. E. (2011a). Interactions between nitrogenous fertilizers and methane cycling in wetland and upland soils. *Current Opinion in Environmental Sustainability*, 3(5):379–388.

- Bodelier, P. L. E. (2011b). Toward understanding, managing, and protecting microbial ecosystems. *Frontiers in microbiology*, 2:80.
- Bodelier, P. L. E., Gillisen, M.-J. B., Hordijk, K., Damsté, J. S. S., Rijpstra, W. I. C., Geenevasen, J. A. J., and Dunfield, P. F. (2009). A reanalysis of phospholipid fatty acids as ecological biomarkers for methanotrophic bacteria. *The ISME journal*, 3(5):606–617.
- Bodelier, P. L. E., Roslev, P., Henckel, T., and Frenzel, P. (2000). Stimulation by ammonium-based fertilizers of methane oxidation in soil around rice roots. *Nature*, 403(6768):421–424.
- Bodelier, P. L. E. and Steenbergh, A. K. (2014). Interactions between methane and the nitrogen cycle in light of climate change. *Current Opinion in Environmental Sustainability*, 9-10:26–36.
- Boetius, A., Ravensschlag, K., Schubert, C. J., Rickert, D., Widdel, F., Gieseke, A., Amann, R., Jørgensen, B. B., Witte, U., and Pfannkuche, O. (2000). A marine microbial consortium apparently mediating anaerobic oxidation of methane. *Nature*, 407(6804):623–626.
- Bogner, J., Meadows, M., and Czepiel, P. (1997). Fluxes of methane between landfills and the atmosphere: natural and engineered controls. *Soil Use and Management*, 13(s4):268–277.
- Bogner, J., Spokas, K., Burton, E., Sweeney, R., and Corona, V. (1995). Landfills as atmospheric methane sources and sinks. *Chemosphere*, 31(9):4119–4130.
- Borgatti, S. P. (2005). Centrality and network flow. *Social Networks*, 27(1):55–71.
- Boschker, H. T. S., Nold, S. C., Wellsbury, P., Bos, D., de Graaf, W., Pel, R., Parkes, R. J., and Capenberg, T. E. (1998). Direct linking of microbial populations to specific biogeochemical processes by <sup>13</sup>C-labelling of biomarkers. *Nature*, 392(6678):801–805.
- Boucher, O., Friedlingstein, P., Collins, B., and Shine, K. P. (2009). The indirect global warming potential and global temperature change potential due to methane oxidation. *Environmental Research Letters*, 4(4):044007.
- Bowman, J. (2006). The Methanotrophs — The Families Methylococcaceae and Methylocystaceae. In Dworkin, M., Falkow, S., Rosenberg, E., Schleifer, K.-H., and Stackebrandt, E., editors, *The Prokaryotes*, volume 56, pages 266–289. Springer New York, New York, NY.
- Burrows, K. J., Cornish, A., Scott, D., and Higgins, I. J. (1984). Substrate Specificities of the Soluble and Particulate Methane Mono-oxygenases of *Methylosinus trichosporium* OB3b. *Microbiology*, 130(12):3327–3333.
- Cai, Y., Yun, J., and Jia, Z. (2022). Phylogeny and Metabolic Potential of the Methanotrophic Lineage MO3 in Beijerinckiaceae from the Paddy Soil through Metagenome-Assembled Genome Reconstruction. *Microorganisms*, 10(5):955.
- Cai, Y., Zheng, Y., Bodelier, P. L. E., Conrad, R., and Jia, Z. (2016). Conventional methanotrophs are responsible for atmospheric methane oxidation in paddy soils. *Nature communications*, 7:11728.
- Callahan, B. (2017). Rdp Taxonomic Training Data Formatted For Dada2 (Rdp Trainset 16/Release 11.5). *Zenodo*.
- Callahan, B. J., McMurdie, P. J., Rosen, M. J., Han, A. W., Johnson, A. J. A., and Holmes, S. P. (2016). DADA2: High-resolution sample inference from Illumina amplicon data. *Nature methods*, 13(7):581–583.
- Cao, W., Cai, Y., Bao, Z., Wang, S., Yan, X., and Jia, Z. (2022). Methanotrophy Alleviates Nitrogen Constraint of Carbon Turnover by Rice Root-Associated Microbiomes. *Frontiers in Microbiology*, 13.

- Cébron, A., Bodrossy, L., Chen, Y., Singer, A. C., Thompson, I. P., Prosser, J. I., and Murrell, J. C. (2007a). Identity of active methanotrophs in landfill cover soil as revealed by DNA-stable isotope probing. *FEMS microbiology ecology*, 62(1):12–23.
- Cébron, A., Bodrossy, L., Stralis-Pavese, N., Singer, A. C., Thompson, I. P., Prosser, J. I., and Murrell, J. C. (2007b). Nutrient amendments in soil DNA stable isotope probing experiments reduce the observed methanotroph diversity. *Applied and environmental microbiology*, 73(3):798–807.
- Chang, J., Gu, W., Park, D., Semrau, J. D., DiSpirito, A. A., and Yoon, S. (2018). Methanobactin from *Methylosinus trichosporium* OB3b inhibits N<sub>2</sub>O reduction in denitrifiers. *The ISME journal*, 12(8):2086–2089.
- Chang, J., Kim, D. D., Semrau, J. D., Lee, J., Heo, H., Gu, W., and Yoon, S. (2021). Enhancement of nitrous oxide emissions in soil microbial consortia via copper competition between proteobacterial methanotrophs and denitrifiers. *Applied and environmental microbiology*, 87(5):e02301–20.
- Chen, Q.-L., Ding, J., Zhu, D., Hu, H.-W., Delgado-Baquerizo, M., Ma, Y.-B., He, J.-Z., and Zhu, Y.-G. (2020). Rare microbial taxa as the major drivers of ecosystem multifunctionality in long-term fertilized soils. *Soil Biology and Biochemistry*, 141:107686.
- Chen, X.-P., Zhu, Y.-G., Xia, Y., Shen, J.-P., and He, J.-Z. (2008a). Ammonia-oxidizing archaea: important players in paddy rhizosphere soil? *Environmental microbiology*, 10(8):1978–1987.
- Chen, Y., Chi, S., Zhang, S., Dong, X., Yang, Q., Liu, H., Tan, B., and Xie, S. (2022). Evaluation of Methanotroph (*Methylococcus capsulatus*, Bath) bacteria meal on body composition, lipid metabolism, protein synthesis and muscle metabolites of Pacific white shrimp (*Litopenaeus vannamei*). *Aquaculture*, 547:737517.
- Chen, Y., Chi, S., Zhang, S., Dong, X., Yang, Q., Liu, H., Zhang, W., Deng, J., Tan, B., and Xie, S. (2021). Replacement of fish meal with Methanotroph (*Methylococcus capsulatus*, Bath) bacteria meal in the diets of Pacific white shrimp (*Litopenaeus vannamei*). *Aquaculture*, 541:736801.
- Chen, Y., Crombie, A., Rahman, M. T., Dedysh, S. N., Liesack, W., Stott, M. B., Alam, M., Theisen, A. R., Murrell, J. C., and Dunfield, P. F. (2010). Complete genome sequence of the aerobic facultative methanotroph *Methylocella silvestris* BL2. *Journal of bacteriology*, 192(14):3840–3841.
- Chen, Y., Dumont, M. G., Cébron, A., and Murrell, J. C. (2007). Identification of active methanotrophs in a landfill cover soil through detection of expression of 16S rRNA and functional genes. *Environmental microbiology*, 9(11):2855–2869.
- Chen, Y., Dumont, M. G., Neufeld, J. D., Bodrossy, L., Stralis-Pavese, N., McNamara, N. P., Ostle, N., Briones, M. J. I., and Murrell, J. C. (2008b). Revealing the uncultivated majority: combining DNA stable-isotope probing, multiple displacement amplification and metagenomic analyses of uncultivated *Methylocystis* in acidic peatlands. *Environmental microbiology*, 10(10):2609–2622.
- Chen, Y. and Murrell, J. C. (2010). Ecology of Aerobic Methanotrophs and their Role in Methane Cycling. In Timmis, K. N., editor, *Handbook of Hydrocarbon and Lipid Microbiology*, pages 3067–3076. Springer Berlin Heidelberg, Berlin, Heidelberg.
- Cheng, X.-Y., Liu, X.-Y., Wang, H.-M., Su, C.-T., Zhao, R., Bodelier, P. L. E., Wang, W.-Q., Ma, L.-Y., and Lu, X.-L. (2021). USC $\gamma$  Dominated Community Composition and Cooccurrence Network of Methanotrophs and Bacteria in Subterranean Karst Caves. *Microbiology spectrum*, 9(1):e0082021.
- Chin, K.-J., Rainey, F. A., Janssen, P. H., and Conrad, R. (1998). Methanogenic Degradation of Polysaccharides and the Characterization of Polysaccharolytic Clostridia from Anoxic Rice Field Soil. *Systematic and applied microbiology*, 21(2):185–200.

- Chistoserdova, L. (2011). Modularity of methylotrophy, revisited. *Environmental microbiology*, 13(10):2603–2622.
- Chistoserdova, L. (2015). Methylotrophs in natural habitats: current insights through metagenomics. *Applied microbiology and biotechnology*, 99(14):5763–5779.
- Chistoserdova, L., Kalyuzhnaya, M. G., and Lidstrom, M. E. (2009). The expanding world of methylotrophic metabolism. *Annual Review of Microbiology*, 63:477–499.
- Christiansen, J. R., Levy-Booth, D., Prescott, C. E., and Grayston, S. J. (2016). Microbial and Environmental Controls of Methane Fluxes Along a Soil Moisture Gradient in a Pacific Coastal Temperate Rainforest. *Ecosystems*, 19(7):1255–1270.
- Ciais, P., Sabine, G. B., Bopp, V., Brovkin, J., Canadell, A., Chhabra, R., DeFries, J., Galloway, M., Heimann, C., Jones, C., Le Quéré, R.B., Myneni, and S. Piao and P. Thornton (2013). Carbon and Other Biogeochemical Cycles. In Stocker, T. F., D. Qin, G.-K. Plattner, M. Tignor, S.K. Allen, J. Boschung, A. Nauels: Y. Xia, V. Bex, and P.M. Midgley, editors, *Climate Change 2013: The Physical Science Basis. Contribution of Working Group I to the Fifth Assessment Report of the Intergovernmental Panel on Climate Change*. Cambridge University Press, Cambridge, United Kingdom and New York, NY, USA.
- Cicerone, R. J. and Oremland, R. S. (1988). Biogeochemical aspects of atmospheric methane. *Global Biogeochemical Cycles*, 2(4):299–327.
- Cleary, J., Roulet, N. T., and Moore, T. R. (2005). Greenhouse Gas Emissions from Canadian Peat Extraction, 1990–2000: A Life-cycle Analysis. *AMBIO: A Journal of the Human Environment*, 34(6):456–461.
- Collet, S., Reim, A., Ho, A., and Frenzel, P. (2015). Recovery of paddy soil methanotrophs from long term drought. *Soil Biology and Biochemistry*, 88:69–72.
- Collins, M. L., Buchholz, L. A., and Rensen, C. C. (1991). Effect of Copper on *Methylomonas albus* BG8. *Applied and environmental microbiology*, 57(4):1261–1264.
- Conrad, R. (1999). Contribution of hydrogen to methane production and control of hydrogen concentrations in methanogenic soils and sediments. *FEMS microbiology ecology*, 28(3):193–202.
- Conrad, R. (2002). Control of microbial methane production in wetland rice fields. *Nutrient Cycling in Agroecosystems*, 64(1/2):59–69.
- Conrad, R. (2009). The global methane cycle: recent advances in understanding the microbial processes involved. *Environmental microbiology reports*, 1(5):285–292.
- Conrad, R. and Rothfuss, F. (1991). Methane oxidation in the soil surface layer of a flooded rice field and the effect of ammonium. *Biology and Fertility of Soils*, 12(1):28–32.
- Crombie, A. T. and Murrell, J. C. (2014). Trace-gas metabolic versatility of the facultative methanotroph *Methylocella silvestris*. *Nature*, 510(7503):148–151.
- Culpepper, M. A. and Rosenzweig, A. C. (2012). Architecture and active site of particulate methane monooxygenase. *Critical reviews in biochemistry and molecular biology*, 47(6):483–492.
- Culpepper, M. A. and Rosenzweig, A. C. (2014). Structure and protein-protein interactions of methanol dehydrogenase from *Methylococcus capsulatus* (Bath). *Biochemistry*, 53(39):6211–6219.
- Dal Co, A., van Vliet, S., Kiviet, D. J., Schlegel, S., and Ackermann, M. (2020). Short-range interactions govern the dynamics and functions of microbial communities. *Nature ecology & evolution*, 4(3):366–375.

- Dalton, H. (2005). The Leeuwenhoek Lecture 2000 the natural and unnatural history of methane-oxidizing bacteria. *Philosophical transactions of the Royal Society of London. Series B, Biological sciences*, 360(1458):1207–1222.
- Danilova, O. V., Belova, S. E., Kulichevskaya, I. S., and Dedysh, S. N. (2015). Decline of activity and shifts in the methanotrophic community structure of an ombrotrophic peat bog after wildfire. *Microbiology*, 84(5):624–629.
- Danilova, O. V., Kulichevskaya, I. S., Rozova, O. N., Detkova, E. N., Bodelier, P. L. E., Trotsenko, Y. A., and Dedysh, S. N. (2013). *Methylomonas paludis* sp. nov., the first acid-tolerant member of the genus *Methylomonas*, from an acidic wetland. *International journal of systematic and evolutionary microbiology*, 63(Pt 6):2282–2289.
- Dann, L. M., Clanahan, M., Paterson, J. S., and Mitchell, J. G. (2019). Distinct niche partitioning of marine and freshwater microbes during colonisation. *FEMS microbiology ecology*, 95(8):fiz098.
- Davies, S. L. and Whittenbury, R. (1970). Fine structure of methane and other hydrocarbon-utilizing bacteria. *Journal of General Microbiology*, 61(2):227–232.
- de Vries, F. T., Griffiths, R. I., Bailey, M., Craig, H., Girlanda, M., Gweon, H. S., Hallin, S., Kaisermann, A., Keith, A. M., Kretzschmar, M., Lemanceau, P., Lumini, E., Mason, K. E., Oliver, A., Ostle, N., Prosser, J. I., Thion, C., Thomson, B., and Bardgett, R. D. (2018). Soil bacterial networks are less stable under drought than fungal networks. *Nature communications*, 9(1):3033.
- Dedysh, S. N. (2009). Exploring methanotroph diversity in acidic northern wetlands: Molecular and cultivation-based studies. *Microbiology*, 78(6):655–669.
- Dedysh, S. N. (2011). Cultivating uncultured bacteria from northern wetlands: knowledge gained and remaining gaps. *Frontiers in microbiology*, 2:184.
- Dedysh, S. N., Beletsky, A. V., Ivanova, A. A., Danilova, O. V., Begmatov, S., Kulichevskaya, I. S., Mardanov, A. V., and Ravin, N. V. (2021). Peat-Inhabiting Verrucomicrobia of the Order Methylacidiphilales Do Not Possess Methanotrophic Capabilities. *Microorganisms*, 9(12).
- Dedysh, S. N., Belova, S. E., Bodelier, P. L. E., Smirnova, K. V., Khmelenina, V. N., Chidthaisong, A., Trotsenko, Y. A., Liesack, W., and Dunfield, P. F. (2007). *Methylocystis heyeri* sp. nov., a novel type II methanotrophic bacterium possessing 'signature' fatty acids of type I methanotrophs. *International journal of systematic and evolutionary microbiology*, 57(Pt 3):472–479.
- Dedysh, S. N. and Dunfield, P. F. (2010). Facultative Methane Oxidizers. In Timmis, K. N., editor, *Handbook of Hydrocarbon and Lipid Microbiology*, pages 1967–1976. Springer Berlin Heidelberg, Berlin, Heidelberg.
- Dedysh, S. N. and Dunfield, P. F. (2011). Facultative and obligate methanotrophs how to identify and differentiate them. *Methods in enzymology*, 495:31–44.
- Dedysh, S. N., Knief, C., and Dunfield, P. F. (2005). *Methylocella* species are facultatively methanotrophic. *Journal of bacteriology*, 187(13):4665–4670.
- Dedysh, S. N., Liesack, W., Khmelenina, V. N., Suzina, N. E., Trotsenko, Y. A., Semrau, J. D., Bares, A. M., Panikov, N. S., and Tiedje, J. M. (2000). *Methylocella palustris* gen. nov., sp. nov., a new methane-oxidizing acidophilic bacterium from peat bogs, representing a novel subtype of serine-pathway methanotrophs. *International journal of systematic and evolutionary microbiology*, 50 Pt 3:955–969.
- Dedysh, S. N., Panikov, N. S., Liesack, W., Grosskopf, R., Zhou, J., and Tiedje, J. M. (1998). Isolation of acidophilic methane-oxidizing bacteria from northern peat wetlands. *Science (New York, N.Y.)*, 282(5387):281–284.

- Degenhardt, J., Dlugosch, L., Ahrens, J., Beck, M., Waska, H., and Engelen, B. (2020). Seasonal Dynamics of Microbial Diversity at a Sandy High Energy Beach Reveal a Resilient Core Community. *Frontiers in Marine Science*, 7.
- Deng, Y., Cui, X., Hernández, M., and Dumont, M. G. (2014). Microbial diversity in hummock and hollow soils of three wetlands on the Qinghai-Tibetan Plateau revealed by 16S rRNA pyrosequencing. *PLoS one*, 9(7):e103115.
- Deng, Y., Cui, X., Lüke, C., and Dumont, M. G. (2013). Aerobic methanotroph diversity in Riganqiao peatlands on the Qinghai-Tibetan Plateau. *Environmental microbiology reports*, 5(4):566–574.
- Deng, Y., Liu, Y., Dumont, M., and Conrad, R. (2017). Salinity Affects the Composition of the Aerobic Methanotroph Community in Alkaline Lake Sediments from the Tibetan Plateau. *Microbial ecology*, 73(1):101–110.
- Deutzmann, J. S., Hoppert, M., and Schink, B. (2014). Characterization and phylogeny of a novel methanotroph, *Methyloglobulus morosus* gen. nov., spec. nov. *Systematic and applied microbiology*, 37(3):165–169.
- Deutzmann, J. S. and Schink, B. (2011). Anaerobic oxidation of methane in sediments of Lake Constance, an oligotrophic freshwater lake. *Applied and environmental microbiology*, 77(13):4429–4436.
- DiSpirito, A. A., Gullede, J., Shiemke, A. K., Murrell, J. C., Lidstrom, M. E., and Krema, C. L. (1992). Trichloroethylene oxidation by the membrane-associated methane monooxygenase in type I, type II and type X methanotrophs. *Biodegradation*, 2(3):151–164.
- DiSpirito, A. A., Kunz, R. C., Choi, D.-W., and Zahn, J. A. (2004). Chapter 7: Respiration in Methanotrophs. In Zannoni, D., editor, *Respiration in archaea and bacteria*, volume 16 of *Advances in photosynthesis and respiration*, pages 149–168. Springer, Dordrecht.
- DiSpirito, A. A., Semrau, J. D., Murrell, J. C., Gallagher, W. H., Dennison, C., and Vuilleumier, S. (2016). Methanobactin and the Link between Copper and Bacterial Methane Oxidation. *Microbiology and molecular biology reviews : MMBR*, 80(2):387–409.
- Distel, D. L. and Cavanaugh, C. M. (1994). Independent phylogenetic origins of methanotrophic and chemoautotrophic bacterial endosymbioses in marine bivalves. *Journal of bacteriology*, 176(7):1932–1938.
- Dörr, N., Glaser, B., and Kolb, S. (2010). Methanotrophic communities in Brazilian ferralsols from naturally forested, afforested, and agricultural sites. *Applied and environmental microbiology*, 76(4):1307–1310.
- Drake, H. L., Horn, M. A., and Wüst, P. K. (2009). Intermediary ecosystem metabolism as a main driver of methanogenesis in acidic wetland soil. *Environmental microbiology reports*, 1(5):307–318.
- Drenovsky, R. E., Steenwerth, K. L., Jackson, L. E., and Scow, K. M. (2010). Land use and climatic factors structure regional patterns in soil microbial communities. *Global ecology and biogeography : a journal of macroecology*, 19(1):27–39.
- D'Souza, G., Shitut, S., Preussger, D., Yousif, G., Waschina, S., and Kost, C. (2018). Ecology and evolution of metabolic cross-feeding interactions in bacteria. *Natural product reports*, 35(5):455–488.
- Duan, Y.-F., Reinsch, S., Ambus, P., Elsgaard, L., and Petersen, S. O. (2017). Activity of Type I Methanotrophs Dominates under High Methane Concentration: Methanotrophic Activity in Slurry Surface Crusts as Influenced by Methane, Oxygen, and Inorganic Nitrogen. *Journal of environmental quality*, 46(4):767–775.

- Dumont, M. G., Lüke, C., Deng, Y., and Frenzel, P. (2014). Classification of *pmoA* amplicon pyrosequences using BLAST and the lowest common ancestor method in MEGAN. *Frontiers in microbiology*, 5:34.
- Dumont, M. G., Pommerenke, B., Casper, P., and Conrad, R. (2011). DNA-, rRNA- and mRNA-based stable isotope probing of aerobic methanotrophs in lake sediment. *Environmental microbiology*, 13(5):1153–1167.
- Dunfield, P. F., Yimga, M. T., Dedysh, S. N., Berger, U., Liesack, W., and Heyer, J. (2002). Isolation of a *Methylocystis* strain containing a novel *pmoA*-like gene. *FEMS microbiology ecology*, 41(1):17–26.
- Dunfield, P. F., Yuryev, A., Senin, P., Smirnova, A. V., Stott, M. B., Hou, S., Ly, B., Saw, J. H., Zhou, Z., Ren, Y., Wang, J., Mountain, B. W., Crowe, M. A., Weatherby, T. M., Bodelier, P. L. E., Liesack, W., Feng, L., Wang, L., and Alam, M. (2007). Methane oxidation by an extremely acidophilic bacterium of the phylum Verrucomicrobia. *Nature*, 450(7171):879–882.
- Dunford, E. A. and Neufeld, J. D. (2010). DNA stable-isotope probing (DNA-SIP). *Journal of visualized experiments : JoVE*, 42.
- Dlugokencky, E. (11.03.2022). NOAA/GML ([https://gml.noaa.gov/ccgg/trends\\_ch4/](https://gml.noaa.gov/ccgg/trends_ch4/)).
- EEA (2010). Share of Energy Consumption by Fuel Type in the EU-25 in 2004: ([https://www.eea.europa.eu/ds\\_resolveuid/72fb32701c8e8e619cfc3e18bc72d61c](https://www.eea.europa.eu/ds_resolveuid/72fb32701c8e8e619cfc3e18bc72d61c)).
- Ehhalt, D., Prather, M., Dentener, F., Derwent, R., Dlugokencky, E., Holland, E., Isaksen, I., Katima, J., Kirchhoff, V., Matson, P., Midgley, P., and Wang, M. (2001). Atmospheric Chemistry and Greenhouse Gases. In IPCC, editor, *Climate Change 2001: The Scientific Basis. Contribution of Working Group I to the Third Assessment Report of the Intergovernmental Panel on Climate Change*. Cambridge Univ. Press, Cambridge, United Kingdom and New York, NY, USA.
- Eisenstein, M. (2018). Microbiology: making the best of PCR bias. *Nature methods*, 15(5):317–320.
- Eldridge, D. J., Woodhouse, J. N., Curlevski, N. J. A., Hayward, M., Brown, M. V., and Neilan, B. A. (2015). Soil-foraging animals alter the composition and co-occurrence of microbial communities in a desert shrubland. *The ISME journal*, 9(12):2671–2681.
- Eller, G. and Frenzel, P. (2001). Changes in activity and community structure of methane-oxidizing bacteria over the growth period of rice. *Applied and environmental microbiology*, 67(6):2395–2403.
- Eller, G., Krüger, M., and Frenzel, P. (2005). Comparing field and microcosm experiments: a case study on methano- and methylo-trophic bacteria in paddy soil. *FEMS microbiology ecology*, 51(2):279–291.
- Ellermann, J., Hedderich, R., Böcher, R., and Thauer, R. K. (1988). The final step in methane formation. Investigations with highly purified methyl-CoM reductase (component C) from *Methanobacterium thermoautotrophicum* (strain Marburg). *European journal of biochemistry*, 172(3):669–677.
- Eshinimaev, B. T., Khmelenina, V. N., and Trotsenko, Y. A. (2008). First isolation of a type II methanotroph from a soda lake. *Microbiology*, 77(5):628–631.
- Esson, K. C., Lin, X., Kumaresan, D., Chanton, J. P., Murrell, J. C., and Kostka, J. E. (2016). Alpha- and Gammaproteobacterial Methanotrophs Codominate the Active Methane-Oxidizing Communities in an Acidic Boreal Peat Bog. *Applied and environmental microbiology*, 82(8):2363–2371.
- Estrada, E. (2007). Food webs robustness to biodiversity loss: the roles of connectance, expansibility and degree distribution. *Journal of theoretical biology*, 244(2):296–307.

- Ettwig, K. F., Butler, M. K., Le Paslier, D., Pelletier, E., Mangenot, S., Kuypers, M. M. M., Schreiber, F., Dutilh, B. E., Zedelius, J., de Beer, D., Gloerich, J., Wessels, H. J. C. T., van Alen, T., Luesken, F., Wu, M. L., van de Pas-Schoonen, K. T., Op den Camp, H. J. M., Janssen-Megens, E. M., Francoijs, K.-J., Stunnenberg, H., Weissenbach, J., Jetten, M. S. M., and Strous, M. (2010). Nitrite-driven anaerobic methane oxidation by oxygenic bacteria. *Nature*, 464(7288):543–548.
- Eusufzai, M. K., Tokida, T., Okada, M., Sugiyama, S.-i., Liu, G. C., Nakajima, M., and Sameshima, R. (2010). Methane emission from rice fields as affected by land use change. *Agriculture, Ecosystems & Environment*, 139(4):742–748.
- Farhan Ul-Haque, M., Kalidass, B., Vorobev, A., Baral, B. S., DiSpirito, A. A., and Semrau, J. D. (2015). Methanobactin from *Methylocystis* sp. strain SB2 affects gene expression and methane monooxygenase activity in *Methylosinus trichosporium* OB3b. *Applied and environmental microbiology*, 81(7):2466–2473.
- Faust, K. (2021). Open challenges for microbial network construction and analysis. *The ISME journal*, 15(11):3111–3118.
- Faust, K. and Raes, J. (2012). Microbial interactions: from networks to models. *Nature reviews. Microbiology*, 10(8):538–550.
- Fechner, E. J. and Hemond, H. F. (1992). Methane transport and oxidation in the unsaturated zone of a *Sphagnum* peatland. *Global Biogeochemical Cycles*, 6(1):33–44.
- Fierer, N. (2017). Embracing the unknown: disentangling the complexities of the soil microbiome. *Nature reviews. Microbiology*, 15(10):579–590.
- Fraser, P. J., Hyson, P., Rasmussen, R. A., Crawford, A. J., and Khalil, M. A. K. (1987). Methane, carbon monoxide and methylchloroform in the southern hemisphere. In Ehhalt, D., Pearman, G., and Galbally, I., editors, *Scientific Application of Baseline Observations of Atmospheric Composition (SABOAC)*, volume 4, pages 3–42. Springer Netherlands, Dordrecht.
- Freeman, L. C. (1977). A Set of Measures of Centrality Based on Betweenness. *Sociometry*, 40(1):35.
- Frenzel, P. (2000). Plant-Associated Methane Oxidation in Rice Fields and Wetlands. In Schink, B., editor, *Advances in Microbial Ecology*, volume 16, pages 85–114. Springer US, Boston, MA.
- Frenzel, P., Rothfuss, F., and Conrad, R. (1992). Oxygen profiles and methane turnover in a flooded rice microcosm. *Biology and Fertility of Soils*, 14(2):84–89.
- Friedman, J. and Alm, E. J. (2012). Inferring correlation networks from genomic survey data. *PLoS computational biology*, 8(9):e1002687.
- Fu, Y., He, L., Reeve, J., Beck, D. A. C., and Lidstrom, M. E. (2019). Core Metabolism Shifts during Growth on Methanol versus Methane in the Methanotroph *Methylomicrobium buryatense* 5GB1. *mBio*, 10(2).
- Gadkari, D. (1984). Influence of the herbicides goltix and sencor on nitrification. *Zentralblatt für Mikrobiologie*, 139(8):623–631.
- García-Contreras, R. and Loarca, D. (2021). The bright side of social cheaters: potential beneficial roles of "social cheaters" in microbial communities. *FEMS microbiology ecology*, 97(1):fiae239.
- Geisen, S., Mitchell, E. A. D., Adl, S., Bonkowski, M., Dunthorn, M., Ekelund, F., Fernández, L. D., Jousset, A., Krashevskaya, V., Singer, D., Spiegel, F. W., Walochnik, J., and Lara, E. (2018). Soil protists: a fertile frontier in soil biology research. *FEMS Microbiology Reviews*, 42(3):293–323.
- Geşicka, A., Oleskiewicz-Popiel, P., and Łężyk, M. (2021). Recent trends in methane to bioproduct conversion by methanotrophs. *Biotechnology advances*, 53:107861.



- Geymonat, E., Ferrando, L., and Tarlera, S. E. (2011). *Methylogaea oryzae* gen. nov., sp. nov., a mesophilic methanotroph isolated from a rice paddy field. *International journal of systematic and evolutionary microbiology*, 61(Pt 11):2568–2572.
- Ghoul, M. and Mitri, S. (2016). The Ecology and Evolution of Microbial Competition. *Trends in Microbiology*, 24(10):833–845.
- Gilbert, B., McDonald, I. R., Finch, R., Stafford, G. P., Nielsen, A. K., and Murrell, J. C. (2000). Molecular analysis of the *pmo* (particulate methane monooxygenase) operons from two type II methanotrophs. *Applied and environmental microbiology*, 66(3):966–975.
- Girvan, M. and Newman, M. E. J. (2002). Community structure in social and biological networks. *Proceedings of the National Academy of Sciences*, 99(12):7821–7826.
- Girvan, M. S., Campbell, C. D., Killham, K., Prosser, J. I., and Glover, L. A. (2005). Bacterial diversity promotes community stability and functional resilience after perturbation. *Environmental Microbiology*, 7(3):301–313.
- Goberna, M. and Verdú, M. (2022). Cautionary notes on the use of co-occurrence networks in soil ecology. *Soil Biology and Biochemistry*, 166:108534.
- Gorham, E. (1991). Northern Peatlands: Role in the Carbon Cycle and Probable Responses to Climatic Warming. *Ecological Applications*, 1(2):182–195.
- Graef, C., Hestnes, A. G., Svenning, M. M., and Frenzel, P. (2011). The active methanotrophic community in a wetland from the High Arctic. *Environmental microbiology reports*, 3(4):466–472.
- Graham, D. W., Chaudhary, J. A., Hanson, R. S., and Arnold, R. G. (1993). Factors affecting competition between type I and type II methanotrophs in two-organism, continuous-flow reactors. *Microbial ecology*, 25(1):1–17.
- Graham, L. E., Graham, J. M., Knack, J. J., Trest, M. T., Piotrowski, M. J., and Arancibia-Avila, P. (2017). A Sub-Antarctic Peat Moss Metagenome Indicates Microbiome Resilience to Stress and Biogeochemical Functions of Early Paleozoic Terrestrial Ecosystems. *International Journal of Plant Sciences*, 178(8):618–628.
- Greenhouse Effect (2011). In Gliński, J., Horabik, J., and Lipiec, J., editors, *Encyclopedia of Agrophysics*, page 339. Springer Netherlands, Dordrecht.
- Griffiths, B. S. and Philippot, L. (2013). Insights into the resistance and resilience of the soil microbial community. *FEMS Microbiology Reviews*, 37(2):112–129.
- Gu, W., Farhan Ul Haque, M., DiSpirito, A. A., and Semrau, J. D. (2016). Uptake and effect of rare earth elements on gene expression in *Methylosinus trichosporium* OB3b. *FEMS microbiology letters*, 363(13).
- Guerrero-Cruz, S., Vaksmaa, A., Horn, M. A., Niemann, H., Pijuan, M., and Ho, A. (2021). Methanotrophs: Discoveries, Environmental Relevance, and a Perspective on Current and Future Applications. *Frontiers in microbiology*, 12:678057.
- Gunderson, L. (2000). Ecological Resilience—In Theory and Application. *Annual Review of Ecology and Systematics*, 31:425–429.
- Gupta, V., Smemo, K. A., Yavitt, J. B., and Basiliko, N. (2012). Active methanotrophs in two contrasting North American peatland ecosystems revealed using DNA-SIP. *Microbial ecology*, 63(2):438–445.
- Gurijala, K. R. and Suflita, J. M. (1993). Environmental factors influencing methanogenesis from refuse in landfill samples. *Environmental Science & Technology*, 27(6):1176–1181.

- Guseva, K., Darcy, S., Simon, E., Alteio, L. V., Montesinos-Navarro, A., and Kaiser, C. (2022). From diversity to complexity: Microbial networks in soils. *Soil Biology and Biochemistry*, 169:108604.
- Hakemian, A. S. and Rosenzweig, A. C. (2007). The biochemistry of methane oxidation. *Annual review of biochemistry*, 76:223–241.
- Hallam, S. J., Putnam, N., Preston, C. M., Detter, J. C., Rokhsar, D., Richardson, P. M., and DeLong, E. F. (2004). Reverse methanogenesis: testing the hypothesis with environmental genomics. *Science (New York, N.Y.)*, 305(5689):1457–1462.
- Hammer, Ø., Harper, D., and Ryan, P. (2001). PAST: Paleontological statistics software package for education and data analysis. *Palaeontologia Electronica*, 4(1):9pp.
- Hammill, E., Kratina, P., Vos, M., Petchey, O. L., and Anholt, B. R. (2015). Food web persistence is enhanced by non-trophic interactions. *Oecologia*, 178(2):549–556.
- Han, D., Dedysh, S. N., and Liesack, W. (2018). Unusual Genomic Traits Suggest *Methylocystis bryophila* S285 to Be Well Adapted for Life in Peatlands. *Genome biology and evolution*, 10(2):623–628.
- Hanson, R. S. and Hanson, T. E. (1996). Methanotrophic bacteria. *Microbiological Reviews*, 60(2):439–471.
- Haron, M. F., Hu, S., Shi, Y., Imelfort, M., Keller, J., Hugenholtz, P., Yuan, Z., and Tyson, G. W. (2013). Anaerobic oxidation of methane coupled to nitrate reduction in a novel archaeal lineage. *Nature*, 500(7464):567–570.
- Harris, R. F. (1981). Effect of Water Potential on Microbial Growth and Activity. In Parr, J. F., Gardner, W. R., and Elliott, L. F., editors, *Water Potential Relations in Soil Microbiology*, pages 23–95. Soil Science Society of America, Madison, WI, USA.
- Hatano, R. (2011). Greenhouse Gas Fluxes: Effects of Physical Conditions. In Gliński, J., Horabik, J., and Lipiec, J., editors, *Encyclopedia of Agrophysics*, pages 339–351. Springer Netherlands, Dordrecht.
- He, R., Wooller, M. J., Pohlman, J. W., Catranis, C., Quensen, J., Tiedje, J. M., and Leigh, M. B. (2012a). Identification of functionally active aerobic methanotrophs in sediments from an arctic lake using stable isotope probing. *Environmental Microbiology*, 14(6):1403–1419.
- He, R., Wooller, M. J., Pohlman, J. W., Quensen, J., Tiedje, J. M., and Leigh, M. B. (2012b). Diversity of active aerobic methanotrophs along depth profiles of arctic and subarctic lake water column and sediments. *The ISME journal*, 6(10):1937–1948.
- He, R., Wooller, M. J., Pohlman, J. W., Quensen, J., Tiedje, J. M., and Leigh, M. B. (2012c). Shifts in identity and activity of methanotrophs in arctic lake sediments in response to temperature changes. *Applied and environmental microbiology*, 78(13):4715–4723.
- He, R., Wooller, M. J., Pohlman, J. W., Tiedje, J. M., and Leigh, M. B. (2015). Methane-derived carbon flow through microbial communities in arctic lake sediments. *Environmental microbiology*, 17(9):3233–3250.
- Henneberger, R., Lüke, C., Mosberger, L., and Schroth, M. H. (2012). Structure and function of methanotrophic communities in a landfill-cover soil. *FEMS microbiology ecology*, 81(1):52–65.
- Hernandez-Agreda, A., Gates, R. D., and Ainsworth, T. D. (2017). Defining the Core Microbiome in Corals' Microbial Soup. *Trends in Microbiology*, 25(2):125–140.

- Héry, M., Singer, A. C., Kumaresan, D., Bodrossy, L., Stralis-Pavese, N., Prosser, J. I., Thompson, I. P., and Murrell, J. C. (2008). Effect of earthworms on the community structure of active methanotrophic bacteria in a landfill cover soil. *The ISME journal*, 2(1):92–104.
- Hester, E. R., Vaksmaa, A., Valè, G., Monaco, S., Jetten, M. S. M., and Lüke, C. (2022). Effect of water management on microbial diversity and composition in an Italian rice field system. *FEMS microbiology ecology*, 98(3).
- Hetz, S. A. and Horn, M. A. (2021). Burkholderiaceae Are Key Acetate Assimilators During Complete Denitrification in Acidic Cryoturbated Peat Circles of the Arctic Tundra. *Frontiers in microbiology*, 12:628269.
- Heyer, J., Berger, U., Hardt, M., and Dunfield, P. F. (2005). *Methylohalobius crimeensis* gen. nov., sp. nov., a moderately halophilic, methanotrophic bacterium isolated from hypersaline lakes of Crimea. *International journal of systematic and evolutionary microbiology*, 55(Pt 5):1817–1826.
- Heyer, J., Galchenko, V. F., and Dunfield, P. F. (2002). Molecular phylogeny of type II methane-oxidizing bacteria isolated from various environments. *Microbiology (Reading, England)*, 148(Pt 9):2831–2846.
- Hiltbrunner, D., Zimmermann, S., Karbin, S., Hagedorn, F., and Niklaus, P. A. (2012). Increasing soil methane sink along a 120-year afforestation chronosequence is driven by soil moisture. *Global Change Biology*, 18(12):3664–3671.
- Hirano, H. and Takemoto, K. (2019). Difficulty in inferring microbial community structure based on co-occurrence network approaches. *BMC bioinformatics*, 20(1):329.
- Hirayama, H., Abe, M., Miyazaki, M., Nunoura, T., Furushima, Y., Yamamoto, H., and Takai, K. (2014). *Methylomarinovum caldicuralii* gen. nov., sp. nov., a moderately thermophilic methanotroph isolated from a shallow submarine hydrothermal system, and proposal of the family Methylothermaceae fam. nov. *International journal of systematic and evolutionary microbiology*, 64(Pt 3):989–999.
- Ho, A., Angel, R., Veraart, A. J., Daebeler, A., Jia, Z., Kim, S. Y., Kerckhof, F.-M., Boon, N., and Bodelier, P. L. E. (2016a). Biotic Interactions in Microbial Communities as Modulators of Biogeochemical Processes: Methanotrophy as a Model System. *Frontiers in microbiology*, 7:1285.
- Ho, A. and Bodelier, P. L. E. (2015). Diazotrophic methanotrophs in peatlands: the missing link? *Plant and Soil*, 389(1-2):419–423.
- Ho, A., de Roy, K., Thas, O., de Neve, J., Hoefman, S., Vandamme, P., Heylen, K., and Boon, N. (2014). The more, the merrier: heterotroph richness stimulates methanotrophic activity. *The ISME journal*, 8(9):1945–1948.
- Ho, A., Di Lonardo, D. P., and Bodelier, P. L. E. (2017a). Revisiting life strategy concepts in environmental microbial ecology. *FEMS microbiology ecology*, 93(3):fix006.
- Ho, A., El-Hawwary, A., Kim, S. Y., Meima-Franke, M., and Bodelier, P. (2015a). Manure-associated stimulation of soil-borne methanogenic activity in agricultural soils. *Biology and Fertility of Soils*, 51(4):511–516.
- Ho, A. and Frenzel, P. (2012). Heat stress and methane-oxidizing bacteria: Effects on activity and population dynamics. *Soil Biology and Biochemistry*, 50:22–25.
- Ho, A., Ijaz, U. Z., Janssens, T. K. S., Ruijs, R., Kim, S. Y., de Boer, W., Termorshuizen, A., van der Putten, W. H., and Bodelier, P. L. E. (2017b). Effects of bio-based residue amendments on greenhouse gas emission from agricultural soil are stronger than effects of soil type with different microbial community composition. *GCB Bioenergy*, 9(12):1707–1720.

- Ho, A., Kerckhof, F.-M., Luke, C., Reim, A., Krause, S., Boon, N., and Bodelier, P. L. E. (2013a). Conceptualizing functional traits and ecological characteristics of methane-oxidizing bacteria as life strategies. *Environmental microbiology reports*, 5(3):335–345.
- Ho, A., Kwon, M., Horn, M. A., and Yoon, S. (2019a). Environmental Applications of Methanotrophs. In Lee, E. Y., editor, *Methanotrophs*, volume 32 of *Microbiology Monographs*, pages 231–255. Springer International Publishing, Cham.
- Ho, A., Lee, H. J., Reumer, M., Meima-Franke, M., Raaijmakers, C., Zweers, H., de Boer, W., van der Putten, W. H., and Bodelier, P. L. (2019b). Unexpected role of canonical aerobic methanotrophs in upland agricultural soils. *Soil Biology and Biochemistry*, 131:1–8.
- Ho, A., Lüke, C., Cao, Z., and Frenzel, P. (2011a). Ageing well: methane oxidation and methane oxidizing bacteria along a chronosequence of 2000 years. *Environmental microbiology reports*, 3(6):738–743.
- Ho, A., Lüke, C., and Frenzel, P. (2011b). Recovery of methanotrophs from disturbance: population dynamics, evenness and functioning. *The ISME journal*, 5(4):750–758.
- Ho, A., Lüke, C., Reim, A., and Frenzel, P. (2013b). Selective stimulation in a natural community of methane oxidizing bacteria: Effects of copper on *pmoA* transcription and activity. *Soil Biology and Biochemistry*, 65:211–216.
- Ho, A., Lüke, C., Reim, A., and Frenzel, P. (2016b). Resilience of (seed bank) aerobic methanotrophs and methanotrophic activity to desiccation and heat stress. *Soil Biology and Biochemistry*, 101:130–138.
- Ho, A., Mendes, L. W., Lee, H. J., Kaupper, T., Mo, Y., Poehlein, A., Bodelier, P. L. E., Jia, Z., and Horn, M. A. (2020). Response of a methane-driven interaction network to stressor intensification. *FEMS microbiology ecology*, 96(10):180.
- Ho, A., Mo, Y., Lee, H. J., Sauheitl, L., Jia, Z., and Horn, M. A. (2018). Effect of salt stress on aerobic methane oxidation and associated methanotrophs; a microcosm study of a natural community from a non-saline environment. *Soil Biology and Biochemistry*, 125:210–214.
- Ho, A., Reim, A., Kim, S. Y., Meima-Franke, M., Termorshuizen, A., de Boer, W., van der Putten, W. H., and Bodelier, P. L. E. (2015b). Unexpected stimulation of soil methane uptake as emergent property of agricultural soils following bio-based residue application. *Global Change Biology*, 21(10):3864–3879.
- Ho, A., van den Brink, E., Reim, A., Krause, S. M. B., and Bodelier, P. L. E. (2016c). Recurrence and Frequency of Disturbance have Cumulative Effect on Methanotrophic Activity, Abundance, and Community Structure. *Frontiers in microbiology*, 6:1493.
- Ho, A., Zuan, A. T. K., Mendes, L. W., Lee, H. J., Zulkeflee, Z., van Dijk, H., Kim, P. J., and Horn, M. A. (2021). Aerobic Methanotrophy and Co-occurrence Networks of a Tropical Rainforest and Oil Palm Plantations in Malaysia. *Microbial ecology*.
- Hoefman, S. (2013). *From Nature to Nurture: Isolation, Physiology and Preservation of Methane-Oxidizing Bacteria*. Dissertation, Ghent University, Ghent, Belgium, Ghent, Belgium.
- Hoefman, S., van der Ha, D., Boon, N., Vandamme, P., de Vos, P., and Heylen, K. (2014a). Niche differentiation in nitrogen metabolism among methanotrophs within an operational taxonomic unit. *BMC microbiology*, 14:83.
- Hoefman, S., van der Ha, D., Iguchi, H., Yurimoto, H., Sakai, Y., Boon, N., Vandamme, P., Heylen, K., and de Vos, P. (2014b). *Methyloparacoccus murrellii* gen. nov., sp. nov., a methanotroph isolated from pond water. *International journal of systematic and evolutionary microbiology*, 64(Pt 6):2100–2107.

- Holl, D., Pfeiffer, E.-M., and Kutzbach, L. (2020). Comparison of eddy covariance CO<sub>2</sub> and CH<sub>4</sub> fluxes from mined and recently rewetted sections in a northwestern German cutover bog. *Biogeosciences*, 17(10):2853–2874.
- Holzappel-Pschorn, A. and Seiler, W. (1986). Methane emission during a cultivation period from an Italian rice paddy. *Journal of Geophysical Research*, 91(D11):11803.
- Hooper, D. U., Adair, E. C., Cardinale, B. J., Byrnes, J. E. K., Hungate, B. A., Matulich, K. L., Gonzalez, A., Duffy, J. E., Gamfeldt, L., and O'Connor, M. I. (2012). A global synthesis reveals biodiversity loss as a major driver of ecosystem change. *Nature*, 486(7401):105–108.
- Horn, M. A., Ihssen, J., Matthies, C., Schramm, A., Acker, G., and Drake, H. L. (2005). *Dechloromonas denitrificans* sp. nov., *Flavobacterium denitrificans* sp. nov., *Paenibacillus anaericanus* sp. nov. and *Paenibacillus terrae* strain MH72, N<sub>2</sub>O-producing bacteria isolated from the gut of the earthworm *Aporrectodea caliginosa*. *International journal of systematic and evolutionary microbiology*, 55(Pt 3):1255–1265.
- Horz, H. P., Yimga, M. T., and Liesack, W. (2001). Detection of methanotroph diversity on roots of submerged rice plants by molecular retrieval of *pmoA*, *mmoX*, *mxoF*, and 16S rRNA and ribosomal DNA, including *pmoA*-based terminal restriction fragment length polymorphism profiling. *Applied and environmental microbiology*, 67(9):4177–4185.
- Hutchens, E., Radajewski, S., Dumont, M. G., McDonald, I. R., and Murrell, J. C. (2004). Analysis of methanotrophic bacteria in Movile Cave by stable isotope probing. *Environmental microbiology*, 6(2):111–120.
- Hütsch, B. W., Webster, C. P., and Powlson, D. S. (1994). Methane oxidation in soil as affected by land use, soil pH and N fertilization. *Soil Biology and Biochemistry*, 26(12):1613–1622.
- Iguchi, H., Sato, I., Sakakibara, M., Yurimoto, H., and Sakai, Y. (2012). Distribution of Methanotrophs in the Phyllosphere. *Bioscience, Biotechnology, and Biochemistry*, 76(8):1580–1583.
- Iguchi, H., Sato, I., Yurimoto, H., and Sakai, Y. (2013). Stress resistance and C1 metabolism involved in plant colonization of a methanotroph *Methylosinus* sp. B4S. *Archives of microbiology*, 195(10-11):717–726.
- Iguchi, H., Yurimoto, H., and Sakai, Y. (2011). Stimulation of methanotrophic growth in cocultures by cobalamin excreted by rhizobia. *Applied and environmental microbiology*, 77(24):8509–8515.
- Im, J., Lee, S.-W., Yoon, S., DiSpirito, A. A., and Semrau, J. D. (2011). Characterization of a novel facultative *Methylocystis* species capable of growth on methane, acetate and ethanol. *Environmental microbiology reports*, 3(2):174–181.
- IPCC (2007). *Climate Change 2007: Synthesis Report. Contribution of Working Groups I, II and III to the Fourth Assessment Report of the Intergovernmental Panel on Climate Change: [Core Writing Team, Pachauri, R.K and Reisinger, A. (eds.)]*. IPCC, Geneva, Switzerland.
- IPCC (2014). *Climate change 2014: Mitigation of climate change; Working Group III contribution to the Fifth Assessment Report of the Intergovernmental Panel on Climate Change: [Edenhofer, O., R. Pichs-Madruga, Y. Sokona, E. Farahani, S. Kadner, K. Seyboth, A. Adler, I. Baum, S. Brunner, P. Eickemeier, B. Kriemann, J. Savolainen, S. Schlömer, C. von Stechow, T. Zwickel, J.C. Minx (eds.)]*, volume Working group 3 of *Climate change 2014*. Cambridge Univ. Press, Cambridge, United Kingdom and New York, NY, USA.
- Islam, T., Gessesse, A., Garcia-Moyano, A., Murrell, J. C., and Øvreås, L. (2020). A Novel Moderately Thermophilic Type Ib Methanotroph Isolated from an Alkaline Thermal Spring in the Ethiopian Rift Valley. *Microorganisms*, 8(2).

- Islam, T., Jensen, S., Reigstad, L. J., Larsen, O., and Birkeland, N.-K. (2008). Methane oxidation at 55 °C and pH 2 by a thermoacidophilic bacterium belonging to the Verrucomicrobia phylum. *Proceedings of the National Academy of Sciences of the United States of America*, 105(1):300–304.
- Ivanova, A. A., Wegner, C.-E., Kim, Y., Liesack, W., and Dedysh, S. N. (2016). Identification of microbial populations driving biopolymer degradation in acidic peatlands by metatranscriptomic analysis. *Molecular ecology*, 25(19):4818–4835.
- Ives, A. R. and Carpenter, S. R. (2007). Stability and diversity of ecosystems. *Science (New York, N. Y.)*, 317(5834):58–62.
- Iyer, S., Killingback, T., Sundaram, B., and Wang, Z. (2013). Attack robustness and centrality of complex networks. *PloS one*, 8(4):e59613.
- Jackson, R. B., Randerson, J. T., Canadell, J. G., Anderson, R. G., Avissar, R., Baldocchi, D. D., Bonan, G. B., Caldeira, K., Diffenbaugh, N. S., Field, C. B., Hungate, B. A., Jobbágy, E. G., Kueppers, L. M., Nosetto, M. D., and Pataki, D. E. (2008). Protecting climate with forests. *Environmental Research Letters*, 3(4):044006.
- Jahnke, L. L., Summons, R. E., Hope, J. M., and Des Marais, D. J. (1999). Carbon isotopic fractionation in lipids from methanotrophic bacteria II: the effects of physiology and environmental parameters on the biosynthesis and isotopic signatures of biomarkers. *Geochimica et Cosmochimica Acta*, 63(1):79–93.
- Jehmlich, N., Vogt, C., Lünsmann, V., Richnow, H. H., and von Bergen, M. (2016). Protein-SIP in environmental studies. *Current opinion in biotechnology*, 41:26–33.
- Jeong, S.-Y., Cho, K.-S., and Kim, T. G. (2014). Density-dependent enhancement of methane oxidation activity and growth of *Methylocystis* sp. by a non-methanotrophic bacterium *Sphingopyxis* sp. *Biotechnology reports (Amsterdam, Netherlands)*, 4:128–133.
- Johnson, W. M., Alexander, H., Bier, R. L., Miller, D. R., Muscarella, M. E., Pitz, K. J., and Smith, H. (2020). Auxotrophic interactions: A stabilizing attribute of aquatic microbial communities? *FEMS microbiology ecology*, 96(11):fiaa115.
- Jousset, A., Bienhold, C., Chatzinotas, A., Gallien, L., Gobet, A., Kurm, V., Küsel, K., Rillig, M. C., Rivett, D. W., Salles, J. F., van der Heijden, M. G. A., Youssef, N. H., Zhang, X., Wei, Z., and Hol, W. H. G. (2017). Where less may be more: how the rare biosphere pulls ecosystems strings. *The ISME journal*, 11(4):853–862.
- Juottonen, H., Galand, P. E., and Yrjälä, K. (2006). Detection of methanogenic Archaea in peat: comparison of PCR primers targeting the *mcrA* gene. *Research in Microbiology*, 157(10):914–921.
- Juottonen, H., Hynninen, A., Nieminen, M., Tuomivirta, T. T., Tuittila, E.-S., Nousiainen, H., Kell, D. K., Yrjälä, K., Tervahauta, A., and Fritze, H. (2012). Methane-cycling microbial communities and methane emission in natural and restored peatlands. *Applied and environmental microbiology*, 78(17):6386–6389.
- Jurburg, S. D., Nunes, I., Brejnrod, A., Jacquiod, S., Priemé, A., Sørensen, S. J., van Elsas, J. D., and Salles, J. F. (2017). Legacy Effects on the Recovery of Soil Bacterial Communities from Extreme Temperature Perturbation. *Frontiers in microbiology*, 8:1832.
- Jurburg, S. D. and Salles, J. F. (2015). Functional Redundancy and Ecosystem Function — The Soil Microbiota as a Case Study. In Lo, Y.-H., Blanco, J. A., and Roy, S., editors, *Biodiversity in Ecosystems - Linking Structure and Function*. InTech.
- Kalidass, B., Ul-Haque, M. F., Baral, B. S., DiSpirito, A. A., and Semrau, J. D. (2015). Competition between metals for binding to methanobactin enables expression of soluble methane monooxygenase in the presence of copper. *Applied and environmental microbiology*, 81(3):1024–1031.

- Kallistova, A. Y., Kevbrina, M. V., Nekrasova, V. K., Glagolev, M. V., Serebryanaya, M. I., and Nozhevnikova, A. N. (2005). Methane Oxidation in Landfill Cover Soil. *Microbiology*, 74(5):608–614.
- Kalyuzhnaya, M. G., Gomez, O. A., and Murrell, J. C. (2019). The Methane-Oxidizing Bacteria (Methanotrophs). In McGenity, T. J., editor, *Taxonomy, genomics and ecophysiology of hydrocarbon-degrading microbes*, Springer Nature eReference Biomedical and Life Sciences, pages 245–278. Springer, Cham.
- Kalyuzhnaya, M. G., Puri, A. W., and Lidstrom, M. E. (2015). Metabolic engineering in methanotrophic bacteria. *Metabolic engineering*, 29:142–152.
- Kalyuzhnaya, M. G., Yang, S., Rozova, O. N., Smalley, N. E., Clubb, J., Lamb, A., Gowda, G. A. N., Raftery, D., Fu, Y., Bringel, F., Vuilleumier, S., Beck, D. A. C., Trotsenko, Y. A., Khmelenina, V. N., and Lidstrom, M. E. (2013). Highly efficient methane biocatalysis revealed in a methanotrophic bacterium. *Nature communications*, 4:2785.
- Kang, C. S., Dunfield, P. F., and Semrau, J. D. (2019). The origin of aerobic methanotrophy within the Proteobacteria. *FEMS microbiology letters*, 366(9).
- Karlsen, O. A., Berven, F. S., Stafford, G. P., Larsen, Ø., Murrell, J. C., Jensen, H. B., and Fjellbirkeland, A. (2003). The surface-associated and secreted MopE protein of *Methylococcus capsulatus* (Bath) responds to changes in the concentration of copper in the growth medium. *Applied and environmental microbiology*, 69(4):2386–2388.
- Karwautz, C., Kus, G., Stöckl, M., Neu, T. R., and Lueders, T. (2018). Microbial megacities fueled by methane oxidation in a mineral spring cave. *The ISME journal*, 12(1):87–100.
- Kaupper, T., Hetz, S., Kolb, S., Yoon, S., Horn, M. A., and Ho, A. (2020a). Deforestation for oil palm: impact on microbially mediated methane and nitrous oxide emissions, and soil bacterial communities. *Biology and Fertility of Soils*, 56(3):287–298.
- Kaupper, T., Luehrs, J., Lee, H. J., Mo, Y., Jia, Z., Horn, M. A., and Ho, A. (2020b). Disentangling abiotic and biotic controls of aerobic methane oxidation during re-colonization. *Soil Biology and Biochemistry*, 142:107729.
- Kaupper, T., Mendes, L. W., Harnisz, M., Krause, S. M. B., Horn, M. A., and Ho, A. (2021a). Recovery in methanotrophic activity does not reflect on the methane-driven interaction network after peat mining. *Applied and environmental microbiology*, 87(5):e02355–20.
- Kaupper, T., Mendes, L. W., Lee, H. J., Mo, Y., Poehlein, A., Jia, Z., Horn, M. A., and Ho, A. (2021b). When the going gets tough: Emergence of a complex methane-driven interaction network during recovery from desiccation-rewetting. *Soil Biology and Biochemistry*, 153:108109.
- Kehe, J., Ortiz, A., Kulesa, A., Gore, J., Blainey, P. C., and Friedman, J. (2021). Positive interactions are common among culturable bacteria. *Science advances*, 7(45):eabi7159.
- Keller, J. K., Bauers, A. K., Bridgham, S. D., Kellogg, L. E., and Iversen, C. M. (2006). Nutrient control of microbial carbon cycling along an ombrotrophic-minerotrophic peatland gradient. *Journal of Geophysical Research*, 111(G3).
- Kembel, S. W., Wu, M., Eisen, J. A., and Green, J. L. (2012). Incorporating 16S gene copy number information improves estimates of microbial diversity and abundance. *PLoS computational biology*, 8(10):e1002743.
- Khadem, A. F., Pol, A., Wiczorek, A., Mohammadi, S. S., Francoijs, K.-J., Stunnenberg, H. G., Jetten, M. S. M., and Op den Camp, H. J. M. (2011). Autotrophic methanotrophy in verrucomicrobia: *Methylococcus thermophilus* SolV uses the Calvin-Benson-Bassham cycle for carbon dioxide fixation. *Journal of bacteriology*, 193(17):4438–4446.

- Khalifa, A., Lee, C. G., Ogiso, T., Ueno, C., Dianou, D., Demachi, T., Katayama, A., and Asakawa, S. (2015). *Methylomagnum ishizawai* gen. nov., sp. nov., a mesophilic type I methanotroph isolated from rice rhizosphere. *International journal of systematic and evolutionary microbiology*, 65(10):3527–3534.
- Khmelenina, V. N., But, S. Y., Rozova, O. N., and Trotsenko, Y. A. (2019). Metabolic Features of Aerobic Methanotrophs: News and Views. *Current issues in molecular biology*, 33:85–100.
- Khush, G. (2003). Productivity improvements in rice. *Nutrition reviews*, 61(6 Pt 2):S114–6.
- Kip, N., van Winden, J. F., Pan, Y., Bodrossy, L., Reichart, G.-J., Smolders, A. J. P., Jetten, M. S. M., Damsté, J. S. S., and Op den Camp, H. J. M. (2010). Global prevalence of methane oxidation by symbiotic bacteria in peat-moss ecosystems. *Nature Geoscience*, 3(9):617–621.
- Kitano, H. (2004). Biological robustness. *Nature reviews. Genetics*, 5(11):826–837.
- Knapp, C. W., Fowle, D. A., Kulczycki, E., Roberts, J. A., and Graham, D. W. (2007). Methane monooxygenase gene expression mediated by methanobactin in the presence of mineral copper sources. *Proceedings of the National Academy of Sciences*, 104(29):12040–12045.
- Knief, C. (2015). Diversity and Habitat Preferences of Cultivated and Uncultivated Aerobic Methanotrophic Bacteria Evaluated Based on *pmoA* as Molecular Marker. *Frontiers in microbiology*, 6:1346.
- Knittel, K. and Boetius, A. (2009). Anaerobic oxidation of methane: progress with an unknown process. *Annual Review of Microbiology*, 63:311–334.
- Knittel, K. and Boetius, A. (2010). Anaerobic Methane Oxidizers. In Timmis, K. N., editor, *Handbook of Hydrocarbon and Lipid Microbiology*, pages 2023–2032. Springer Berlin Heidelberg, Berlin, Heidelberg.
- Kögel-Knabner, I., Amelung, W., Cao, Z., Fiedler, S., Frenzel, P., Jahn, R., Kalbitz, K., Kölbl, A., and Schloter, M. (2010). Biogeochemistry of paddy soils. *Geoderma*, 157(1-2):1–14.
- Kolb, S. (2009). The quest for atmospheric methane oxidizers in forest soils. *Environmental microbiology reports*, 1(5):336–346.
- Kolb, S., Knief, C., Stubner, S., and Conrad, R. (2003). Quantitative Detection of Methanotrophs in Soil by Novel *pmoA*-Targeted Real-Time PCR Assays. *Applied and environmental microbiology*, 69(5):2423–2429.
- Kostka, J. E., Weston, D. J., Glass, J. B., Lilleskov, E. A., Shaw, A. J., and Turetsky, M. R. (2016). The *Sphagnum* microbiome: new insights from an ancient plant lineage. *The New phytologist*, 211(1):57–64.
- Krause, S., Lüke, C., and Frenzel, P. (2010). Succession of methanotrophs in oxygen-methane counter-gradients of flooded rice paddies. *The ISME journal*, 4(12):1603–1607.
- Krause, S., Lüke, C., and Frenzel, P. (2012). Methane source strength and energy flow shape methanotrophic communities in oxygen-methane counter-gradients. *Environmental microbiology reports*, 4(2):203–208.
- Krause, S. M. B., Johnson, T., Samadhi Karunaratne, Y., Fu, Y., Beck, D. A. C., Chistoserdova, L., and Lidstrom, M. E. (2017). Lanthanide-dependent cross-feeding of methane-derived carbon is linked by microbial community interactions. *Proceedings of the National Academy of Sciences of the United States of America*, 114(2):358–363.
- Krause, S. M. B., Meima-Franke, M., Veraart, A. J., Ren, G., Ho, A., and Bodelier, P. L. E. (2018). Environmental legacy contributes to the resilience of methane consumption in a laboratory microcosm system. *Scientific reports*, 8(1):8862.



- Krueger, M., Frenzel, P., and Conrad, R. (2001). Microbial processes influencing methane emission from rice fields. *Global Change Biology*, 7(1):49–63.
- Krüger, M. and Frenzel, P. (2003). Effects of N-fertilisation on CH<sub>4</sub> oxidation and production, and consequences for CH<sub>4</sub> emissions from microcosms and rice fields. *Global Change Biology*, 9(5):773–784.
- Kumaresan, D., Stralis-Pavese, N., Abell, G. C. J., Bodrossy, L., and Murrell, J. C. (2011). Physical disturbance to ecological niches created by soil structure alters community composition of methanotrophs. *Environmental microbiology reports*, 3(5):613–621.
- Kusmaul, Wilimzig, and Bock (1998). Methanotrophs and methanogens in masonry. *Applied and environmental microbiology*, 64(11):4530–4532.
- Kwon, G., Kim, H., Song, C., and Jahng, D. (2019a). Co-culture of microalgae and enriched nitrifying bacteria for energy-efficient nitrification. *Biochemical Engineering Journal*, 152:107385.
- Kwon, M., Ho, A., and Yoon, S. (2019b). Novel approaches and reasons to isolate methanotrophic bacteria with biotechnological potentials: recent achievements and perspectives. *Applied Microbiology and Biotechnology*, 103(1):1–8.
- Lal, R. (2004). Soil carbon sequestration to mitigate climate change. *Geoderma*, 123(1-2):1–22.
- Lal, R. (2008). Carbon sequestration. *Philosophical transactions of the Royal Society of London. Series B, Biological sciences*, 363(1492):815–830.
- Larmola, T., Leppänen, S. M., Tuittila, E.-S., Aarva, M., Merilä, P., Fritze, H., and Tirola, M. (2014). Methanotrophy induces nitrogen fixation during peatland development. *Proceedings of the National Academy of Sciences of the United States of America*, 111(2):734–739.
- Lauber, C. L., Strickland, M. S., Bradford, M. A., and Fierer, N. (2008). The influence of soil properties on the structure of bacterial and fungal communities across land-use types. *Soil Biology and Biochemistry*, 40(9):2407–2415.
- Le Mer, J. and Roger, P. (2001). Production, oxidation, emission and consumption of methane by soils: A review. *European Journal of Soil Biology*, 37(1):25–50.
- Lee, O. K., Hur, D. H., Nguyen, D. T. N., and Lee, E. Y. (2016). Metabolic engineering of methanotrophs and its application to production of chemicals and biofuels from methane. *Biofuels, Bioproducts and Biorefining*, 10(6):848–863.
- Lee, S., Sieradzki, E. T., Nicol, G. W., and Hazard, C. (2022). Propagation of viral genomes by replicating ammonia-oxidising archaea during soil nitrification. *The ISME Journal*.
- Lee, S., Sieradzki, E. T., Nicolas, A. M., Walker, R. L., Firestone, M. K., Hazard, C., and Nicol, G. W. (2021). Methane-derived carbon flows into host-virus networks at different trophic levels in soil. *Proceedings of the National Academy of Sciences of the United States of America*, 118(32).
- Lee, S.-W., Keeney, D. R., Lim, D.-H., DiSpirito, A. A., and Semrau, J. D. (2006). Mixed pollutant degradation by *Methylosinus trichosporium* OB3b expressing either soluble or particulate methane monooxygenase: can the tortoise beat the hare? *Applied and environmental microbiology*, 72(12):7503–7509.
- Lennon, J. T. and Jones, S. E. (2011). Microbial seed banks: the ecological and evolutionary implications of dormancy. *Nature reviews. Microbiology*, 9(2):119–130.
- Li, B., Li, Z., Sun, X., Wang, Q., Xiao, E., and Sun, W. (2018). DNA-SIP Reveals the Diversity of Chemolithoautotrophic Bacteria Inhabiting Three Different Soil Types in Typical Karst Rocky Desertification Ecosystems in Southwest China. *Microbial ecology*, 76(4):976–990.

- Li, C., Hambright, K. D., Bowen, H. G., Trammell, M. A., Grossart, H.-P., Burford, M. A., Hamilton, D. P., Jiang, H., Latour, D., Meyer, E. I., Padisák, J., Zamor, R. M., and Krumholz, L. R. (2021). Global co-occurrence of methanogenic archaea and methanotrophic bacteria in *Microcystis* aggregates. *Environmental microbiology*, 23(11):6503–6519.
- Li, Y., Liu, Y., Pan, H., Hernández, M., Guan, X., Wang, W., Zhang, Q., Luo, Y., Di, H., and Xu, J. (2020). Impact of grazing on shaping abundance and composition of active methanotrophs and methane oxidation activity in a grassland soil. *Biology and Fertility of Soils*, 1:457.
- Li, Y., Shang, Y., and Yang, Y. (2017). Clustering coefficients of large networks. *Information Sciences*, 382-383:350–358.
- Lidstrom, M. E. (2006). Aerobic Methylophilic Prokaryotes. In Dworkin, M., Falkow, S., Rosenberg, E., Schleifer, K.-H., and Stackebrandt, E., editors, *The Prokaryotes*, pages 618–634. Springer New York, New York, NY.
- Lieberman, R. L. and Rosenzweig, A. C. (2004). Biological methane oxidation: regulation, biochemistry, and active site structure of particulate methane monooxygenase. *Critical reviews in biochemistry and molecular biology*, 39(3):147–164.
- Liebetrau, J., Sträuber, H., Kretzschmar, J., Denysenko, V., and Nelles, M. (2019). Anaerobic Digestion. In Wagemann, K. and Tippkötter, N., editors, *Biorefineries*, volume 166 of *Advances in Biochemical Engineering/Biotechnology*, pages 281–299. Springer International Publishing, Cham.
- Liebner, S. and Svenning, M. M. (2013). Environmental transcription of *mmoX* by methane-oxidizing Proteobacteria in a subarctic Palsa Peatland. *Applied and environmental microbiology*, 79(2):701–706.
- Liesack, W. (2000). Microbiology of flooded rice paddies. *FEMS Microbiology Reviews*, 24(5):625–645.
- Little, A. E. F., Robinson, C. J., Peterson, S. B., Raffa, K. F., and Handelsman, J. (2008). Rules of engagement: interspecies interactions that regulate microbial communities. *Annual Review of Microbiology*, 62:375–401.
- Liu, H., Wu, X., Li, Z., Wang, Q., Liu, D., and Liu, G. (2017). Responses of soil methanogens, methanotrophs, and methane fluxes to land-use conversion and fertilization in a hilly red soil region of southern China. *Environmental science and pollution research international*, 24(9):8731–8743.
- Loreau, M. (2004). Does functional redundancy exist? *Oikos*, 104(3):606–611.
- Loreau, M., Downing, A., Emmerson, M., Gonzalez, A., Hughes, J., Inchausti, P., Joshi, J., Norberg, J., and Sala, O. (2002). A new look at the relationship between diversity and stability. In Loreau, M., Naeem, S., and Inchausti, P., editors, *Biodiversity and ecosystem functioning*, pages 79–91. Oxford Univ. Press, Oxford.
- Louca, S., Doebeli, M., and Parfrey, L. W. (2018). Correcting for 16S rRNA gene copy numbers in microbiome surveys remains an unsolved problem. *Microbiome*, 6(1):41.
- Lueders, T. (2010). Stable Isotope Probing of Hydrocarbon-Degraders. In Timmis, K. N., editor, *Handbook of Hydrocarbon and Lipid Microbiology*, pages 4011–4026. Springer Berlin Heidelberg, Berlin, Heidelberg.
- Lueders, T., Kindler, R., Miltner, A., Friedrich, M. W., and Kaestner, M. (2006). Identification of bacterial micropredators distinctively active in a soil microbial food web. *Applied and environmental microbiology*, 72(8):5342–5348.
- Lueders, T., Manefield, M., and Friedrich, M. W. (2004a). Enhanced sensitivity of DNA- and rRNA-based stable isotope probing by fractionation and quantitative analysis of isopycnic centrifugation gradients. *Environmental microbiology*, 6(1):73–78.

- Lueders, T., Wagner, B., Claus, P., and Friedrich, M. W. (2004b). Stable isotope probing of rRNA and DNA reveals a dynamic methyloph community and trophic interactions with fungi and protozoa in oxic rice field soil. *Environmental Microbiology*, 6(1):60–72.
- Lüke, C. (2010). *Molecular ecology and biogeography of methanotrophic bacteria in wetland rice fields*. Dissertation, Philipps-Universität Marburg/Lahn, Marburg an der Lahn.
- Lüke, C., Frenzel, P., Ho, A., Fiantis, D., Schad, P., Schneider, B., Schwark, L., and Utami, S. R. (2014). Macroecology of methane-oxidizing bacteria: the  $\beta$ -diversity of *pmoA* genotypes in tropical and subtropical rice paddies. *Environmental microbiology*, 16(1):72–83.
- Mäkipää, R., Leppänen, S. M., Sanz Munoz, S., Smolander, A., Tirola, M., Tuomivirta, T., and Fritze, H. (2018). Methanotrophs are core members of the diazotroph community in decaying Norway spruce logs. *Soil Biology and Biochemistry*, 120:230–232.
- Malghani, S., Reim, A., von Fischer, J., Conrad, R., Kuebler, K., and Trumbore, S. E. (2016). Soil methanotroph abundance and community composition are not influenced by substrate availability in laboratory incubations. *Soil Biology and Biochemistry*, 101:184–194.
- Mancinelli, R. L. (1995). The regulation of methane oxidation in soil. *Annual Review of Microbiology*, 49:581–605.
- Mandakovic, D., Rojas, C., Maldonado, J., Latorre, M., Travisany, D., Delage, E., Bihouée, A., Jean, G., Díaz, F. P., Fernández-Gómez, B., Cabrera, P., Gaete, A., Latorre, C., Gutiérrez, R. A., Maass, A., Cambiazo, V., Navarrete, S. A., Eveillard, D., and González, M. (2018). Structure and co-occurrence patterns in microbial communities under acute environmental stress reveal ecological factors fostering resilience. *Scientific reports*, 8(1):5875.
- Manefield, M., Whiteley, A. S., and Bailey, M. J. (2004). What can stable isotope probing do for bioremediation? *International Biodeterioration & Biodegradation*, 54(2-3):163–166.
- Matsen, J. B., Yang, S., Stein, L. Y., Beck, D., and Kalyuzhnaya, M. G. (2013). Global Molecular Analyses of Methane Metabolism in Methanotrophic Alphaproteobacterium, *Methylosinus trichosporium* OB3b. Part I: Transcriptomic Study. *Frontiers in microbiology*, 4:40.
- McBride, B. C. and Wolfe, R. S. (1971). A new coenzyme of methyl transfer, coenzyme M. *Biochemistry*, 10(12):2317–2324.
- McDonald, I. R. and Murrell, J. C. (1997). The particulate methane monooxygenase gene *pmoA* and its use as a functional gene probe for methanotrophs. *FEMS microbiology letters*, 156(2):205–210.
- McGlynn, S. E., Chadwick, G. L., Kempes, C. P., and Orphan, V. J. (2015). Single cell activity reveals direct electron transfer in methanotrophic consortia. *Nature*, 526(7574):531–535.
- McNamara, N. P., Black, H., Beresford, N. A., and Parekh, N. R. (2003). Effects of acute gamma irradiation on chemical, physical and biological properties of soils. *Applied Soil Ecology*, 24(2):117–132.
- Mendes, L. W., Raaijmakers, J. M., de Hollander, M., Mendes, R., and Tsai, S. M. (2018). Influence of resistance breeding in common bean on rhizosphere microbiome composition and function. *The ISME journal*, 12(1):212–224.
- Mendes, L. W., Tsai, S. M., Navarrete, A. A., de Hollander, M., van Veen, J. A., and Kuramae, E. E. (2015). Soil-borne microbiome: linking diversity to function. *Microbial ecology*, 70(1):255–265.
- Metje, M. and Frenzel, P. (2007). Methanogenesis and methanogenic pathways in a peat from subarctic permafrost. *Environmental microbiology*, 9(4):954–964.

- Meyer, K. M., Klein, A. M., Rodrigues, J. L. M., Nüsslein, K., Tringe, S. G., Mirza, B. S., Tiedje, J. M., and Bohannan, B. J. M. (2017). Conversion of Amazon rainforest to agriculture alters community traits of methane-cycling organisms. *Molecular ecology*, 26(6):1547–1556.
- Miroshnikov, K. K., Didriksen, A., Naumoff, D. G., Huntemann, M., Clum, A., Pillay, M., Palaniappan, K., Varghese, N., Mikhailova, N., Mukherjee, S., Reddy, T. B. K., Daum, C., Shapiro, N., Ivanova, N., Kyrpides, N., Woyke, T., Dedysh, S. N., and Svenning, M. M. (2017). Draft Genome Sequence of *Methylocapsa palsarum* NE2T, an Obligate Methanotroph from Subarctic Soil. *Genome announcements*, 5(24).
- Mo, Y., Jin, F., Zheng, Y., Baoyin, T., Ho, A., and Jia, Z. (2020). Succession of bacterial community and methanotrophy during lake shrinkage. *Journal of Soils and Sediments*, 20(3):1545–1557.
- Mohammadi, S. S., Pol, A., van Alen, T., Jetten, M. S. M., and Op den Camp, H. J. M. (2017). Ammonia Oxidation and Nitrite Reduction in the Verrucomicrobial Methanotroph *Methylacidiphilum fumariolicum* SolV. *Frontiers in microbiology*, 8:1901.
- Mohanty, S. R., Bodelier, P. L. E., Floris, V., and Conrad, R. (2006). Differential effects of nitrogenous fertilizers on methane-consuming microbes in rice field and forest soils. *Applied and environmental microbiology*, 72(2):1346–1354.
- Montzka, S. A., Dlugokencky, E. J., and Butler, J. H. (2011). Non-CO<sub>2</sub> greenhouse gases and climate change. *Nature*, 476(7358):43–50.
- Morriën, E., Hannula, S. E., Snoek, L. B., Helmsing, N. R., Zweers, H., de Hollander, M., Soto, R. L., Bouffaud, M.-L., Buée, M., Dimmers, W., Duyts, H., Geisen, S., Girlanda, M., Griffiths, R. I., Jørgensen, H.-B., Jensen, J., Plassart, P., Redecker, D., Schmelz, R. M., Schmidt, O., Thomson, B. C., Tisserant, E., Uroz, S., Winding, A., Bailey, M. J., Bonkowski, M., Faber, J. H., Martin, F., Lemanceau, P., de Boer, W., van Veen, J. A., and van der Putten, W. H. (2017). Soil networks become more connected and take up more carbon as nature restoration progresses. *Nature communications*, 8:14349.
- Morris, B. E. L., Henneberger, R., Huber, H., and Moissl-Eichinger, C. (2013). Microbial syntrophy: interaction for the common good. *FEMS Microbiology Reviews*, 37(3):384–406.
- Muñoz-Dorado, J., Marcos-Torres, F. J., García-Bravo, E., Moraleda-Muñoz, A., and Pérez, J. (2016). Myxobacteria: Moving, Killing, Feeding, and Surviving Together. *Frontiers in microbiology*, 7:781.
- Murase, J. and Frenzel, P. (2007). A methane-driven microbial food web in a wetland rice soil. *Environmental Microbiology*, 9(12):3025–3034.
- Murase, J. and Frenzel, P. (2008). Selective grazing of methanotrophs by protozoa in a rice field soil. *FEMS microbiology ecology*, 65(3):408–414.
- Murdock, S. A., Tunnicliffe, V., Boschen-Rose, R. E., and Juniper, S. K. (2021). Emergent 'core communities' of microbes, meiofauna and macrofauna at hydrothermal vents. *ISME Communications*, 1(1).
- Murrell, J., McDonald, I. R., and Gilbert, B. (2000a). Regulation of expression of methane monooxygenases by copper ions. *Trends in Microbiology*, 8(5):221–225.
- Murrell, J. C. (2010). The Aerobic Methane Oxidizing Bacteria (Methanotrophs). In Timmis, K. N., editor, *Handbook of Hydrocarbon and Lipid Microbiology*, pages 1953–1966. Springer Berlin Heidelberg, Berlin, Heidelberg.
- Murrell, J. C. and Dalton, H. (1983). Nitrogen Fixation in Obligate Methanotrophs. *Microbiology*, 129(11):3481–3486.
- Murrell, J. C., Gilbert, B., and McDonald, I. R. (2000b). Molecular biology and regulation of methane monooxygenase. *Archives of Microbiology*, 173(5-6):325–332.

- Naeem, S. (1998). Species Redundancy and Ecosystem Reliability. *Conservation Biology*, 12(1):39–45.
- Nestor, E., Toledano, G., and Friedman, J. (2022). Interactions between culturable bacteria are predicted by individual species' growth. *bioRxiv*, page 502471.
- Neu, A. T., Allen, E. E., and Roy, K. (2021). Defining and quantifying the core microbiome: Challenges and prospects. *Proceedings of the National Academy of Sciences of the United States of America*, 118(51).
- Neufeld, J. D., Dumont, M. G., Vohra, J., and Murrell, J. C. (2007a). Methodological considerations for the use of stable isotope probing in microbial ecology. *Microbial ecology*, 53(3):435–442.
- Neufeld, J. D., Vohra, J., Dumont, M. G., Lueders, T., Manefield, M., Friedrich, M. W., and Murrell, J. C. (2007b). DNA stable-isotope probing. *Nature Protocols*, 2(4):860–866.
- Newman, M. E. J. (2003). The Structure and Function of Complex Networks. *SIAM Review*, 45(2):167–256.
- Newman, M. E. J. (2006). Modularity and community structure in networks. *Proceedings of the National Academy of Sciences*, 103(23):8577–8582.
- Newman, M. E. J. and Girvan, M. (2004). Finding and evaluating community structure in networks. *Physical review. E, Statistical, nonlinear, and soft matter physics*, 69(2 Pt 2):026113.
- Nielsen, A. K., Gerdes, K., Degn, H., and Colin, M. J. (1996). Regulation of bacterial methane oxidation: transcription of the soluble methane mono-oxygenase operon of *Methylococcus capsulatus* (Bath) is repressed by copper ions. *Microbiology (Reading, England)*, 142 ( Pt 5):1289–1296.
- Nielsen, A. K., Gerdes, K., and Murrell, J. C. (1997). Copper-dependent reciprocal transcriptional regulation of methane monooxygenase genes in *Methylococcus capsulatus* and *Methylosinus trichosporium*. *Molecular microbiology*, 25(2):399–409.
- Niu, M., Liang, W., and Wang, F. (2018). Methane biotransformation in the ocean and its effects on climate change: A review. *Science China Earth Sciences*, 61(12):1697–1713.
- Noll, M., Frenzel, P., and Conrad, R. (2008). Selective stimulation of type I methanotrophs in a rice paddy soil by urea fertilization revealed by RNA-based stable isotope probing. *FEMS microbiology ecology*, 65(1):125–132.
- Noll, M., Matthies, D., Frenzel, P., Derakshani, M., and Liesack, W. (2005). Succession of bacterial community structure and diversity in a paddy soil oxygen gradient. *Environmental Microbiology*, 7(3):382–395.
- Nyerges, G. and Stein, L. Y. (2009). Ammonia cometabolism and product inhibition vary considerably among species of methanotrophic bacteria. *FEMS microbiology letters*, 297(1):131–136.
- Op den Camp, H. J. M., Islam, T., Stott, M. B., Harhangi, H. R., Hynes, A., Schouten, S., Jetten, M. S. M., Birkeland, N.-K., Pol, A., and Dunfield, P. F. (2009). Environmental, genomic and taxonomic perspectives on methanotrophic Verrucomicrobia. *Environmental microbiology reports*, 1(5):293–306.
- Orata, F. D., Meier-Kolthoff, J. P., Sauvageau, D., and Stein, L. Y. (2018). Phylogenomic Analysis of the Gammaproteobacterial Methanotrophs (Order Methylococcales) Calls for the Reclassification of Members at the Genus and Species Levels. *Frontiers in microbiology*, 9:3162.
- Orphan, V. J., House, C. H., Hinrichs, K. U., McKeegan, K. D., and DeLong, E. F. (2001). Methane-consuming archaea revealed by directly coupled isotopic and phylogenetic analysis. *Science (New York, N.Y.)*, 293(5529):484–487.

- Oshkin, I. Y., Beck, D. A. C., Lamb, A. E., Tchesnokova, V., Benuska, G., McTaggart, T. L., Kalyuzhnaya, M. G., Dedysh, S. N., Lidstrom, M. E., and Chistoserdova, L. (2015). Methane-fed microbial microcosms show differential community dynamics and pinpoint taxa involved in communal response. *The ISME Journal*, 9(5):1119–1129.
- Palmer, K. and Horn, M. A. (2012). Actinobacterial nitrate reducers and proteobacterial denitrifiers are abundant in N<sub>2</sub>O-metabolizing peat. *Applied and environmental microbiology*, 78(16):5584–5596.
- Pan, Y., Abell, G. C. J., Bodelier, P. L. E., Meima-Franke, M., Sessitsch, A., and Bodrossy, L. (2014). Remarkable recovery and colonization behaviour of methane oxidizing bacteria in soil after disturbance is controlled by methane source only. *Microbial ecology*, 68(2):259–270.
- Pandey, V. C., Singh, J. S., Singh, D. P., and Singh, R. P. (2014). Methanotrophs: promising bacteria for environmental remediation. *International Journal of Environmental Science and Technology*, 11(1):241–250.
- Parks, D. H., Tyson, G. W., Hugenholtz, P., and Beiko, R. G. (2014). STAMP: statistical analysis of taxonomic and functional profiles. *Bioinformatics (Oxford, England)*, 30(21):3123–3124.
- Peduzzi, P. and Schiemer, F. (2004). Bacteria and viruses in the water column of tropical freshwater reservoirs. *Environmental Microbiology*, 6(7):707–715.
- Pérez-Valera, E., Goberna, M., Faust, K., Raes, J., García, C., and Verdú, M. (2017). Fire modifies the phylogenetic structure of soil bacterial co-occurrence networks. *Environmental microbiology*, 19(1):317–327.
- Periana, R. A., Bhalla, G., Tenn, W. J., Young, K. J., Liu, X. Y., Mironov, O., Jones, C. J., and Ziatdinov, V. R. (2004). Perspectives on some challenges and approaches for developing the next generation of selective, low temperature, oxidation catalysts for alkane hydroxylation based on the CH activation reaction. *Journal of Molecular Catalysis A: Chemical*, 220(1):7–25.
- Petters, S., Groß, V., Söllinger, A., Pichler, M., Reinhard, A., Bengtsson, M. M., and Urich, T. (2021). The soil microbial food web revisited: Predatory myxobacteria as keystone taxa? *The ISME journal*.
- Peura, S., Bertilsson, S., Jones, R. I., and Eiler, A. (2015). Resistant microbial cooccurrence patterns inferred by network topology. *Applied and environmental microbiology*, 81(6):2090–2097.
- Pinto, S., Benincà, E., van Nes, E. H., Scheffer, M., and Bogaards, J. A. (2022). Species abundance correlations carry limited information about microbial network interactions. *PLoS computational biology*, 18(9):e1010491.
- Platt, U., Allan, W., and Lowe, D. (2004). Hemispheric average Cl atom concentration from <sup>13</sup>C/<sup>12</sup>C ratios in atmospheric methane. *Atmospheric Chemistry and Physics*, 4(9/10):2393–2399.
- Pol, A., Heijmans, K., Harhangi, H. R., Tedesco, D., Jetten, M. S. M., and Op den Camp, H. J. M. (2007). Methanotrophy below pH 1 by a new Verrucomicrobia species. *Nature*, 450(7171):874–878.
- Poudel, R., Jumpponen, A., Schlatter, D. C., Paulitz, T. C., Gardener, B. B. M., Kinkel, L. L., and Garrett, K. A. (2016). Microbiome Networks: A Systems Framework for Identifying Candidate Microbial Assemblages for Disease Management. *Phytopathology*, 106(10):1083–1096.
- Praeg, N., Schachner, I., Schuster, L., and Illmer, P. (2021). Carbon-dependent growth, community structure and methane oxidation performance of a soil-derived methanotrophic mixed culture. *FEMS microbiology letters*, 368(2):fnaa212.
- Praeg, N., Wagner, A. O., and Illmer, P. (2017). Plant species, temperature, and bedrock affect net methane flux out of grassland and forest soils. *Plant and Soil*, 410(1-2):193–206.

- Pratscher, J., Vollmers, J., Wiegand, S., Dumont, M. G., and Kaster, A.-K. (2018). Unravelling the Identity, Metabolic Potential and Global Biogeography of the Atmospheric Methane-Oxidizing Upland Soil Cluster  $\alpha$ . *Environmental microbiology*, 20(3):1016–1029.
- Priemé, A., Bonilla Sitaula, J., Klemetsson, Å. S. K., and Bakken, L. R. (1996). Extraction of methane-oxidizing bacteria from soil particles. *FEMS microbiology ecology*, 21(1):59–68.
- Pryce, S. (1991). Alternatives to peat. *Professional Horticulture*, 5(3):101–106.
- Purkamo, L., Bomberg, M., Kietäväinen, R., Salavirta, H., Nyssönen, M., Nuppenen-Puputti, M., Aho-nen, L., Kukkonen, I., and Itävaara, M. (2016). Microbial co-occurrence patterns in deep Precambrian bedrock fracture fluids. *Biogeosciences*, 13(10):3091–3108.
- Putkinen, A., Tuittila, E.-S., Siljanen, H. M., Bodrossy, L., and Fritze, H. (2018). Recovery of methane turnover and the associated microbial communities in restored cutover peatlands is strongly linked with increasing *Sphagnum* abundance. *Soil Biology and Biochemistry*, 116:110–119.
- Qiu, Q., Noll, M., Abraham, W.-R., Lu, Y., and Conrad, R. (2008). Applying stable isotope probing of phospholipid fatty acids and rRNA in a Chinese rice field to study activity and composition of the methanotrophic bacterial communities in situ. *The ISME journal*, 2(6):602–614.
- Quast, C., Pruesse, E., Yilmaz, P., Gerken, J., Schweer, T., Yarza, P., Peplies, J., and Glöckner, F. O. (2013). The SILVA ribosomal RNA gene database project: improved data processing and web-based tools. *Nucleic acids research*, 41(Database issue):D590–6.
- R Core Team (2014). R: A language and environment for statistical computing.
- Radajewski, S., Ineson, P., Parekh, N. R., and Murrell, J. C. (2000). Stable-isotope probing as a tool in microbial ecology. *Nature*, 403(6770):646–649.
- Radajewski, S., McDonald, I. R., and Murrell, J. C. (2003). Stable-isotope probing of nucleic acids: a window to the function of uncultured microorganisms. *Current opinion in biotechnology*, 14(3):296–302.
- Raghoebarsing, A. A., Smolders, A. J. P., Schmid, M. C., Rijpstra, W. I. C., Wolters-Arts, M., Derksen, J., Jetten, M. S. M., Schouten, S., Sinninghe Damsté, J. S., Lamers, L. P. M., Roelofs, J. G. M., Op den Camp, H. J. M., and Strous, M. (2005). Methanotrophic symbionts provide carbon for photosynthesis in peat bogs. *Nature*, 436(7054):1153–1156.
- Rani, V., Kaushik, R., Majumder, S., Rani, A. T., Devi, A. A., Divekar, P., Khatri, P., Pandey, K. K., and Singh, J. (2021). Synergistic Interaction of Methanotrophs and Methylo-trophs in Regulating Methane Emission. In Bhatt, P., Gangola, S., Udayanga, D., and Kumar, G., editors, *Microbial Technology for Sustainable Environment*, volume 112, pages 419–437. Springer Singapore, Singapore.
- Ratzke, C., Barrere, J., and Gore, J. (2020). Strength of species interactions determines biodiversity and stability in microbial communities. *Nature ecology & evolution*, 4(3):376–383.
- Ravasz, E., Somera, A. L., Mongru, D. A., Oltvai, Z. N., and Barabási, A. L. (2002). Hierarchical organization of modularity in metabolic networks. *Science (New York, N.Y.)*, 297(5586):1551–1555.
- Reay, D. S., Smith, K. A., and Hewitt, C. N. (2007). Methane: importance, sources and sinks. In Reay, D., Hewitt, C. N., and Smith, K., Grace, J., editors, *Greenhouse gas sinks*, pages 143–151. CABI, Wallingford, Oxfordshire, UK.
- Reim, A., Lüke, C., Krause, S., Pratscher, J., and Frenzel, P. (2012). One millimetre makes the difference: high-resolution analysis of methane-oxidizing bacteria and their specific activity at the oxic-anoxic interface in a flooded paddy soil. *The ISME journal*, 6(11):2128–2139.

- Reis, P. C. J., Thottathil, S. D., Ruiz-González, C., and Prairie, Y. T. (2020). Niche separation within aerobic methanotrophic bacteria across lakes and its link to methane oxidation rates. *Environmental microbiology*, 22(2):738–751.
- Reumer, M., Harnisz, M., Lee, H. J., Reim, A., Grunert, O., Putkinen, A., Fritze, H., Bodelier, P. L. E., and Ho, A. (2018). Impact of Peat Mining and Restoration on Methane Turnover Potential and Methane-Cycling Microorganisms in a Northern Bog. *Applied and environmental microbiology*, 84(3):e02218–17.
- Ricke, P., Erkel, C., Kube, M., Reinhardt, R., and Liesack, W. (2004). Comparative analysis of the conventional and novel *pmo* (particulate methane monooxygenase) operons from *Methylocystis* strain SC2. *Applied and environmental microbiology*, 70(5):3055–3063.
- Rietl, A. J., Nyman, J. A., Lindau, C. W., and Jackson, C. R. (2017). Wetland methane emissions altered by vegetation disturbance: An interaction between stem clipping and nutrient enrichment. *Aquatic Botany*, 136:205–211.
- Ritchie, H. and Roser, M. (2013). Land Use: <https://ourworldindata.org/land-use>.
- Rohman, A., Helmiyati, S., Hapsari, M., and Larasati Setyaningrum D. (2014). Rice in health and nutrition. *International Food Research Journal*, 21(1):13–24.
- Rohrbach, S., Gkoutselis, G., Hink, L., Weig, A. R., Obst, M., Diekmann, A., Ho, A., Rambold, G., and Horn, M. A. (2022). Microplastic polymer properties as deterministic factors driving terrestrial plastisphere microbiome assembly and succession in the field. *Environmental Microbiology*.
- Rossmann, M., Pérez-Jaramillo, J. E., Kavamura, V. N., Chiaramonte, J. B., Dumack, K., Fiore-Donno, A. M., Mendes, L. W., Ferreira, M. M. C., Bonkowski, M., Raaijmakers, J. M., Mauchline, T. H., and Mendes, R. (2020). Multitrophic interactions in the rhizosphere microbiome of wheat: from bacteria and fungi to protists. *FEMS microbiology ecology*, 96(4):fiaa032.
- Rousk, J., Bååth, E., Brookes, P. C., Lauber, C. L., Lozupone, C., Caporaso, J. G., Knight, R., and Fierer, N. (2010). Soil bacterial and fungal communities across a pH gradient in an arable soil. *The ISME journal*, 4(10):1340–1351.
- Ruiz-Moreno, D., Pascual, M., and Riolo, R. (2006). Exploring network space with genetic algorithms: modularity, resilience and reactivity. In Pascua, I. and Dunne, J. A., editors, *Ecological Networks: Linking Structure to Dynamics In Food Webs*, pages 187–208. Oxford University Press, New York, NY.
- Sangwan, P., Chen, X., Hugenholtz, P., and Janssen, P. H. (2004). *Chthoniobacter flavus* gen. nov., sp. nov., the first pure-culture representative of subdivision two, *Spartobacteria classis* nov., of the phylum Verrucomicrobia. *Applied and environmental microbiology*, 70(10):5875–5881.
- Sanseverino, A. M., Bastviken, D., Sundh, I., Pickova, J., and Enrich-Prast, A. (2012). Methane carbon supports aquatic food webs to the fish level. *PloS one*, 7(8):e42723.
- Saunois, M., Stavert, A. R., Poulter, B., Bousquet, P., Canadell, J. G., Jackson, R. B., Raymond, P. A., Dlugokencky, E. J., Houweling, S., Patra, P. K., Ciais, P., Arora, V. K., Bastviken, D., Bergamaschi, P., Blake, D. R., Brailsford, G., Bruhwiler, L., Carlson, K. M., Carrol, M., Castaldi, S., Chandra, N., Crevoisier, C., Crill, P. M., Covey, K., Curry, C. L., Etiope, G., Frankenberg, C., Gedney, N., Hegglin, M. I., Höglund-Isaksson, L., Hugelius, G., Ishizawa, M., Ito, A., Janssens-Maenhout, G., Jensen, K. M., Joos, F., Kleinen, T., Krummel, P. B., Langenfelds, R. L., Laruelle, G. G., Liu, L., Machida, T., Maksyutov, S., McDonald, K. C., McNorton, J., Miller, P. A., Melton, J. R., Morino, I., Müller, J., Murguía-Flores, F., Naik, V., Niwa, Y., Noce, S., O'Doherty, S., Parker, R. J., Peng, C., Peng, S., Peters, G. P., Prigent, C., Prinn, R., Ramonet, M., Regnier, P., Riley, W. J., Rosentreter, J. A., Segers, A., Simpson, I. J., Shi, H., Smith, S. J., Steele, L. P., Thornton, B. F., Tian, H., Tohjima, Y., Tubiello, F. N., Tsuruta, A., Viovy, N., Voulgarakis, A., Weber, T. S., van Weele, M., van der Werf, G. R., Weiss,



- R. F., Worthy, D., Wunch, D., Yin, Y., Yoshida, Y., Zhang, W., Zhang, Z., Zhao, Y., Zheng, B., Zhu, Q., Zhu, Q., and Zhuang, Q. (2020). The Global Methane Budget 2000–2017. *Earth System Science Data*, 12(3):1561–1623.
- Scheu, S., Ruess, L., and Bonkowski, M. (2005). Interactions Between Microorganisms and Soil Micro- and Mesofauna. In Buscot, F., editor, *Microorganisms in soils*, Soil biology, pages 253–275. Springer, Berlin.
- Schiermeier, Q. (2020). Global methane levels soar to record high. *Nature*.
- Schloss, P. D., Westcott, S. L., Ryabin, T., Hall, J. R., Hartmann, M., Hollister, E. B., Lesniewski, R. A., Oakley, B. B., Parks, D. H., Robinson, C. J., Sahl, J. W., Stres, B., Thallinger, G. G., van Horn, D. J., and Weber, C. F. (2009). Introducing mothur: open-source, platform-independent, community-supported software for describing and comparing microbial communities. *Applied and environmental microbiology*, 75(23):7537–7541.
- Schlöter, M., Nannipieri, P., Sørensen, S. J., and van Elsas, J. D. (2018). Microbial indicators for soil quality. *Biology and Fertility of Soils*, 54(1):1–10.
- Schmitz, R. A., Peeters, S. H., Versantvoort, W., Picone, N., Pol, A., Jetten, M. S. M., and Op den Camp, H. J. M. (2021). Verrucomicrobial methanotrophs: ecophysiology of metabolically versatile acidophiles. *FEMS Microbiology Reviews*, page fuab007.
- Schnyder, E., Bodelier, P. L. E., Hartmann, M., Henneberger, R., and Niklaus, P. A. (2018). Positive diversity-functioning relationships in model communities of methanotrophic bacteria. *Ecology*, 99(3):714–723.
- Schulz, B. and Boyle, C. (2006). What are Endophytes? In Schulz, B. J. E., Boyle, C. J. C., and Sieber, T. N., editors, *Microbial Root Endophytes*, volume 9 of *Soil biology*, pages 1–13. Springer-Verlag Berlin Heidelberg, Berlin, Heidelberg.
- Schulze, E. D., Beck, E., and Müller-Hohenstein, K. (2005). *Plant Ecology*. Springer Berlin Heidelberg.
- Semrau, J. D., DiSpirito, A. A., Gu, W., and Yoon, S. (2018). Metals and Methanotrophy. *Applied and environmental microbiology*, 84(6).
- Semrau, J. D., DiSpirito, A. A., and Vuilleumier, S. (2011). Facultative methanotrophy: false leads, true results, and suggestions for future research. *FEMS microbiology letters*, 323(1):1–12.
- Semrau, J. D., DiSpirito, A. A., and Yoon, S. (2010). Methanotrophs and copper. *FEMS Microbiology Reviews*, 34(4):496–531.
- Shade, A., Jones, S. E., Caporaso, J. G., Handelsman, J., Knight, R., Fierer, N., and Gilbert, J. A. (2014). Conditionally rare taxa disproportionately contribute to temporal changes in microbial diversity. *mBio*, 5(4):e01371–14.
- Sharp, C. E., Smirnova, A. V., Graham, J. M., Stott, M. B., Khadka, R., Moore, T. R., Grasby, S. E., Strack, M., and Dunfield, P. F. (2014). Distribution and diversity of Verrucomicrobia methanotrophs in geothermal and acidic environments. *Environmental microbiology*, 16(6):1867–1878.
- Sharp, C. E., Stott, M. B., and Dunfield, P. F. (2012). Detection of autotrophic verrucomicrobial methanotrophs in a geothermal environment using stable isotope probing. *Frontiers in microbiology*, 3:303.
- Sherry, A., Osborne, K. A., Sidgwick, F. R., Gray, N. D., and Talbot, H. M. (2016). A temperate river estuary is a sink for methanotrophs adapted to extremes of pH, temperature and salinity. *Environmental microbiology reports*, 8(1):122–131.

- Shiau, Y.-J., Cai, Y., Jia, Z., Chen, C.-L., and Chiu, C.-Y. (2018a). Phylogenetically distinct methanotrophs modulate methane oxidation in rice paddies across Taiwan. *Soil Biology and Biochemistry*, 124:59–69.
- Shiau, Y.-J., Cai, Y., Lin, Y.-T., Jia, Z., and Chiu, C.-Y. (2018b). Community Structure of Active Aerobic Methanotrophs in Red Mangrove (*Kandelia obovata*) Soils Under Different Frequency of Tides. *Microbial ecology*, 75(3):761–770.
- Shrestha, P. M., Kammann, C., Lenhart, K., Dam, B., and Liesack, W. (2012). Linking activity, composition and seasonal dynamics of atmospheric methane oxidizers in a meadow soil. *The ISME journal*, 6(6):1115–1126.
- Singh, B. K., Bardgett, R. D., Smith, P., and Reay, D. S. (2010). Microorganisms and climate change: terrestrial feedbacks and mitigation options. *Nature reviews. Microbiology*, 8(11):779–790.
- Smith, T. J., Trotsenko, Y. A., and Murrell, J. C. (2010). Physiology and Biochemistry of the Aerobic Methane Oxidizing Bacteria. In Timmis, K. N., editor, *Handbook of Hydrocarbon and Lipid Microbiology*, pages 765–779. Springer Berlin Heidelberg, Berlin, Heidelberg.
- Smith, U. and Ribbons, D. W. (1970). Fine structure of *Methanomonas methanooxidans*. *Archiv. Mikrobiol. (Archiv für Mikrobiologie)*, 74(2):116–122.
- Sogin, M. L., Morrison, H. G., Huber, J. A., Mark Welch, D., Huse, S. M., Neal, P. R., Arrieta, J. M., and Herndl, G. J. (2006). Microbial diversity in the deep sea and the underexplored "rare biosphere". *Proceedings of the National Academy of Sciences*, 103(32):12115–12120.
- Song, F., Zhang, G. J., Ramanathan, V., and Leung, L. R. (2022). Trends in surface equivalent potential temperature: A more comprehensive metric for global warming and weather extremes. *Proceedings of the National Academy of Sciences of the United States of America*, 119(6).
- Stanley, S. H., Prior, S. D., Leak, D. J., and Dalton, H. (1983). Copper stress underlies the fundamental change in intracellular location of methane mono-oxygenase in methane-oxidizing organisms: Studies in batch and continuous cultures. *Biotechnology Letters*, 5(7):487–492.
- Steenbergh, A. K., Meima, M. M., Kamst, M., and Bodelier, P. L. E. (2009). Biphasic kinetics of a methanotrophic community is a combination of growth and increased activity per cell. *FEMS microbiology ecology*, 71(1):12–22.
- Stein, L. Y., Roy, R., and Dunfield, P. F. (2012). Aerobic Methanotrophy and Nitrification: Processes and Connections. *eLS*, 103:15.
- Stock, M., Hoefman, S., Kerckhof, F.-M., Boon, N., de Vos, P., de Baets, B., Heylen, K., and Waegeman, W. (2013). Exploration and prediction of interactions between methanotrophs and heterotrophs. *Research in Microbiology*, 164(10):1045–1054.
- Sultana, N., Zhao, J., Zheng, Y., Cai, Y., Faheem, M., Peng, X., Wang, W., and Jia, Z. (2019). Stable isotope probing of active methane oxidizers in rice field soils from cold regions. *Biology and Fertility of Soils*, 55(3):243–250.
- Sun, M. Y., Dafforn, K. A., Johnston, E. L., and Brown, M. V. (2013). Core sediment bacteria drive community response to anthropogenic contamination over multiple environmental gradients. *Environmental microbiology*, 15(9):2517–2531.
- Sun, W., Krumins, V., Dong, Y., Gao, P., Ma, C., Hu, M., Li, B., Xia, B., He, Z., and Xiong, S. (2018). A Combination of Stable Isotope Probing, Illumina Sequencing, and Co-occurrence Network to Investigate Thermophilic Acetate- and Lactate-Utilizing Bacteria. *Microbial ecology*, 75(1):113–122.
- Suzuki, M. T. and Giovannoni, S. J. (1996). Bias caused by template annealing in the amplification of mixtures of 16S rRNA genes by PCR. *Applied and environmental microbiology*, 62(2):625–630.

- Taubert, M., Grob, C., Crombie, A., Howat, A. M., Burns, O. J., Weber, M., Lott, C., Kaster, A.-K., Vollmers, J., Jehmlich, N., von Bergen, M., Chen, Y., and Murrell, J. C. (2019). Communal metabolism by Methylococcaceae and Methylophilaceae is driving rapid aerobic methane oxidation in sediments of a shallow seep near Elba, Italy. *Environmental microbiology*, 21(10):3780–3795.
- Täumer, J., Kolb, S., Boeddinghaus, R. S., Wang, H., Schöning, I., Schruppf, M., Urich, T., and Marhan, S. (2021). Divergent drivers of the microbial methane sink in temperate forest and grassland soils. *Global Change Biology*, 27(4):929–940.
- Tavormina, P. L., Hatzenpichler, R., McGlynn, S., Chadwick, G., Dawson, K. S., Connon, S. A., and Orphan, V. J. (2015). *Methyloprofundus sedimenti* gen. nov., sp. nov., an obligate methanotroph from ocean sediment belonging to the 'deep sea-1' clade of marine methanotrophs. *International journal of systematic and evolutionary microbiology*, 65(Pt 1):251–259.
- Tavormina, P. L., Kellermann, M. Y., Antony, C. P., Tocheva, E. I., Dalleska, N. F., Jensen, A. J., Valentine, D. L., Hinrichs, K.-U., Jensen, G. J., Dubilier, N., and Orphan, V. J. (2017). Starvation and recovery in the deep-sea methanotroph *Methyloprofundus sedimenti*. *Molecular microbiology*, 103(2):242–252.
- Tavormina, P. L., Orphan, V. J., Kalyuzhnaya, M. G., Jetten, M. S. M., and Klotz, M. G. (2011). A novel family of functional operons encoding methane/ammonia monooxygenase-related proteins in gammaproteobacterial methanotrophs. *Environmental microbiology reports*, 3(1):91–100.
- Taylor, S. (1977). Evidence for the presence of ribulose 1,5-bisphosphate carboxylase and phosphoribonuclease in *Methylococcus capsulatus* (bath). *FEMS microbiology letters*, 2(6):305–307.
- Taylor, S. C., Dalton, H., and Dow, C. S. (1981). Ribulose-1,5-bisphosphate Carboxylase/Oxygenase and Carbon Assimilation in *Methylococcus capsulatus* (Bath). *Microbiology (Reading, England)*, 122(1):89–94.
- Tchawa Yimga, M., Dunfield, P. F., Ricke, P., Heyer, J., and Liesack, W. (2003). Wide distribution of a novel *pmoA*-like gene copy among type II methanotrophs, and its expression in *Methylocystis* strain SC2. *Applied and environmental microbiology*, 69(9):5593–5602.
- Templeton, A. S., Chu, K.-H., Alvarez-Cohen, L., and Conrad, M. E. (2006). Variable carbon isotope fractionation expressed by aerobic CH<sub>4</sub>-oxidizing bacteria. *Geochimica et Cosmochimica Acta*, 70(7):1739–1752.
- Theisen, A. R., Ali, M. H., Radajewski, S., Dumont, M. G., Dunfield, P. F., McDonald, I. R., Dedysh, S. N., Miguez, C. B., and Murrell, J. C. (2005). Regulation of methane oxidation in the facultative methanotroph *Methylocella silvestris* BL2. *Molecular microbiology*, 58(3):682–692.
- Timmers, P. H. A., Welte, C. U., Koehorst, J. J., Plugge, C. M., Jetten, M. S. M., and Stams, A. J. M. (2017). Reverse Methanogenesis and Respiration in Methanotrophic Archaea. *Archaea (Vancouver, B.C.)*, 2017:1654237.
- Tripathi, B. M., Edwards, D. P., Mendes, L. W., Kim, M., Dong, K., Kim, H., and Adams, J. M. (2016). The impact of tropical forest logging and oil palm agriculture on the soil microbiome. *Molecular ecology*, 25(10):2244–2257.
- Trotsenko, Y. A. and Murrell, J. C. (2008). Metabolic Aspects of Aerobic Obligate Methanotrophy. In Laskin, A. I., Gadd, G. M., and Sariaslani, S., editors, *Advances in applied microbiology*, volume 63 of *Advances in applied microbiology*, pages 183–229. Academic Press, Amsterdam.
- Tsubota, J., Eshinimaev, B. T., Khmelenina, V. N., and Trotsenko, Y. A. (2005). *Methylothermus thermalis* gen. nov., sp. nov., a novel moderately thermophilic obligate methanotroph from a hot spring in Japan. *International journal of systematic and evolutionary microbiology*, 55(Pt 5):1877–1884.

- Tveit, A. T., Hestnes, A. G., Robinson, S. L., Schintlmeister, A., Dedysh, S. N., Jehmlich, N., von Bergen, M., Herbold, C., Wagner, M., Richter, A., and Svenning, M. M. (2019). Widespread soil bacterium that oxidizes atmospheric methane. *Proceedings of the National Academy of Sciences of the United States of America*, 116(17):8515–8524.
- Ul-Haque, M. F., Crombie, A. T., and Murrell, J. C. (2019). Novel facultative *Methylocella* strains are active methane consumers at terrestrial natural gas seeps. *Microbiome*, 7(1):134.
- Uz, I., Rasche, M. E., Townsend, T., Ogram, A. V., and Lindner, A. S. (2003). Characterization of methanogenic and methanotrophic assemblages in landfill samples. *Proceedings. Biological sciences*, 270 Suppl 2:S202–5.
- van der Gon, H. A. C. D. and Neue, H.-U. (1996). Oxidation of methane in the rhizosphere of rice plants. *Biology and Fertility of Soils*, 22(4):359–366.
- van der Heijden, M. G. A. and Hartmann, M. (2016). Networking in the Plant Microbiome. *PLoS biology*, 14(2):e1002378.
- van Dijk, H., Kaupper, T., Bothe, C., Lee, H. J., Bodelier, P. L. E., Horn, M. A., and Ho, A. (2021). Discrepancy in exchangeable and soluble ammonium-induced effects on aerobic methane oxidation: a microcosm study of a paddy soil. *Biology and Fertility of Soils*, 57(6):873–880.
- van Elsas, J. D., Chiurazzi, M., Mallon, C. A., Elhottova, D., Kristufek, V., and Salles, J. F. (2012). Microbial diversity determines the invasion of soil by a bacterial pathogen. *Proceedings of the National Academy of Sciences of the United States of America*, 109(4):1159–1164.
- van Grinsven, S., Oswald, K., Wehrli, B., Jegge, C., Zopfi, J., Lehmann, M. F., and Schubert, C. J. (2021a). Methane oxidation in the waters of a humic-rich boreal lake stimulated by photosynthesis, nitrite, Fe(III) and humics. *Biogeosciences*, 18(10):3087–3101.
- van Grinsven, S., Sinninghe Damsté, J. S., Harrison, J., Polerecky, L., and Villanueva, L. (2021b). Nitrate promotes the transfer of methane-derived carbon from the methanotroph *Methylobacter* sp. to the methylotroph *Methylotenera* sp. in eutrophic lake water. *Limnology and Oceanography*, 66(3):878–891.
- van Kruistum, H., Bodelier, P. L. E., Ho, A., Meima-Franke, M., and Veraart, A. J. (2018). Resistance and Recovery of Methane-Oxidizing Communities Depends on Stress Regime and History; A Microcosm Study. *Frontiers in microbiology*, 9:1714.
- Ve, T., Mathisen, K., Helland, R., Karlsen, O. A., Fjellbirkeland, A., Røhr, Å. K., Andersson, K. K., Pedersen, R.-B., Lillehaug, J. R., and Jensen, H. B. (2012). The *Methylococcus capsulatus* (Bath) secreted protein, MopE\*, binds both reduced and oxidized copper. *PloS one*, 7(8):e43146.
- Veraart, A. J., Faassen, E. J., Dakos, V., van Nes, E. H., Lürling, M., and Scheffer, M. (2012). Recovery rates reflect distance to a tipping point in a living system. *Nature*, 481(7381):357–359.
- Veraart, A. J., Garbeva, P., van Beersum, F., Ho, A., Hordijk, C. A., Meima-Franke, M., Zweers, A. J., and Bodelier, P. L. E. (2018). Living apart together-bacterial volatiles influence methanotrophic growth and activity. *The ISME journal*, 12(4):1163–1166.
- Veraart, A. J., Steenbergh, A. K., Ho, A., Kim, S. Y., and Bodelier, P. L. (2015). Beyond nitrogen: The importance of phosphorus for CH<sub>4</sub> oxidation in soils and sediments. *Geoderma*, 259-260:337–346.
- Versantvoort, W., Pol, A., Jetten, M. S. M., van Niftrik, L., Reimann, J., Kartal, B., and Op den Camp, H. J. M. (2020). Multiheme hydroxylamine oxidoreductases produce NO during ammonia oxidation in methanotrophs. *Proceedings of the National Academy of Sciences of the United States of America*, 117(39):24459–24463.

- Vigliotta, G., Nutricati, E., Carata, E., Tredici, S. M., de Stefano, M., Pontieri, P., Massardo, D. R., Prati, M. V., de Bellis, L., and Alifano, P. (2007). *Clostridium fusca* Roze 1896, a filamentous, sheathed, methanotrophic  $\gamma$ -proteobacterium. *Applied and environmental microbiology*, 73(11):3556–3565.
- Vile, M. A., Kelman Wieder, R., Živković, T., Scott, K. D., Vitt, D. H., Hartsock, J. A., Iosue, C. L., Quinn, J. C., Petix, M., Fillingim, H. M., Popma, J. M. A., Dynarski, K. A., Jackman, T. R., Albright, C. M., and Wyckoff, D. D. (2014). N<sub>2</sub>-fixation by methanotrophs sustains carbon and nitrogen accumulation in pristine peatlands. *Biogeochemistry*, 121(2):317–328.
- Vogt, C., Lueders, T., Richnow, H. H., Krüger, M., von Bergen, M., and Seifert, J. (2016). Stable Isotope Probing Approaches to Study Anaerobic Hydrocarbon Degradation and Degraders. *Journal of molecular microbiology and biotechnology*, 26(1-3):195–210.
- Vorobev, A. V., Baani, M., Doronina, N. V., Brady, A. L., Liesack, W., Dunfield, P. F., and Dedysh, S. N. (2011). *Methyloferula stellata* gen. nov., sp. nov., an acidophilic, obligately methanotrophic bacterium that possesses only a soluble methane monooxygenase. *International journal of systematic and evolutionary microbiology*, 61(Pt 10):2456–2463.
- Walkiewicz, A., Brzezińska, M., and Bieganowski, A. (2018). Methanotrophs are favored under hypoxia in ammonium-fertilized soils. *Biology and Fertility of Soils*, 54(7):861–870.
- Wang, V. C.-C., Maji, S., Chen, P. P.-Y., Lee, H. K., Yu, S. S.-F., and Chan, S. I. (2017). Alkane Oxidation: Methane Monooxygenases, Related Enzymes, and Their Biomimetics. *Chemical reviews*, 117(13):8574–8621.
- Wang, Y., Cai, Y., Hou, F., Jia, Z., and Bowatte, S. (2022). Sheep grazing impacts on soil methanotrophs and their activity in typical steppe in the Loess Plateau China. *Applied Soil Ecology*, 175:104440.
- Ward, N., Larsen, Ø., Sakwa, J., Bruseth, L., Khouri, H., Durkin, A. S., Dimitrov, G., Jiang, L., Scanlan, D., Kang, K. H., Lewis, M., Nelson, K. E., Methé, B., Wu, M., Heidelberg, J. F., Paulsen, I. T., Fouts, D., Ravel, J., Tettelin, H., Ren, Q., Read, T., DeBoy, R. T., Seshadri, R., Salzberg, S. L., Jensen, H. B., Birkeland, N. K., Nelson, W. C., Dodson, R. J., Grindhaug, S. H., Holt, I., Eidhammer, I., Jonassen, I., Vanaken, S., Utterback, T., Feldblyum, T. V., Fraser, C. M., Lillehaug, J. R., and Eisen, J. A. (2004). Genomic insights into methanotrophy: the complete genome sequence of *Methylococcus capsulatus* (Bath). *PLoS biology*, 2(10):e303.
- Watanabe, A. and Kimura, M. (1995). Methane production and its fate in paddy fields. *Soil Science and Plant Nutrition*, 41(2):225–233.
- Watanabe, A., Takeda, T., and Kimura, M. (1999). Evaluation of origins of CH<sub>4</sub> carbon emitted from rice paddies. *Journal of Geophysical Research: Atmospheres*, 104(D19):23623–23629.
- Wei, X.-M., Su, Y., Zhang, H.-T., Chen, M., and He, R. (2015). Responses of methanotrophic activity, community and EPS production to CH<sub>4</sub> and O<sub>2</sub> concentrations in waste biocover soils. *Waste management (New York, N.Y.)*, 42:118–127.
- Welte, C. U., Rasigraf, O., Vaksmaa, A., Versantvoort, W., Arshad, A., Op den Camp, H. J. M., Jetten, M. S. M., Lüke, C., and Reimann, J. (2016). Nitrate- and nitrite-dependent anaerobic oxidation of methane. *Environmental microbiology reports*, 8(6):941–955.
- Wen, X., Yang, S., and Liebner, S. (2016). Evaluation and update of cutoff values for methanotrophic *pmoA* gene sequences. *Archives of microbiology*, 198(7):629–636.
- Whittenbury, R., Davies, S. L., and Davey, J. F. (1970a). Exospores and cysts formed by methane-utilizing bacteria. *Journal of General Microbiology*, 61(2):219–226.
- Whittenbury, R., Phillips, K. C., and Wilkinson, J. F. (1970b). Enrichment, isolation and some properties of methane-utilizing bacteria. *Journal of General Microbiology*, 61(2):205–218.

- Wieczorek, A. S., Drake, H. L., and Kolb, S. (2011). Organic acids and ethanol inhibit the oxidation of methane by mire methanotrophs. *FEMS microbiology ecology*, 77(1):28–39.
- Williams, R. J., Howe, A., and Hofmockel, K. S. (2014). Demonstrating microbial co-occurrence pattern analyses within and between ecosystems. *Frontiers in microbiology*, 5:358.
- Włodarczyk, T. (2011). Greenhouse Gases Sink in Soils. In Gliński, J., Horabik, J., and Lipiec, J., editors, *Encyclopedia of Agrophysics*, pages 351–354. Springer Netherlands, Dordrecht.
- Woese, C. R., Magrum, L. J., and Fox, G. E. (1978). Archaeobacteria. *Journal of molecular evolution*, 11(3):245–251.
- Wolfson, J. M. (1980). Determination of Microgram Quantities of Inorganic Sulfate in Atmospheric Particulates. *Journal of the Air Pollution Control Association*, 30(6):688–690.
- Wubs, E. R. J., van der Putten, W. H., Bosch, M., and Bezemer, T. M. (2016). Soil inoculation steers restoration of terrestrial ecosystems. *Nature plants*, 2:16107.
- Yang, J., Du, X., and Qiao, B. (2021). Methane oxidation to methanol over copper-containing zeolite. *Chem*, 7(9):2270–2272.
- Yavitt, J. B., Lang, G. E., and Downey, D. M. (1988). Potential methane production and methane oxidation rates in peatland ecosystems of the Appalachian Mountains, United States. *Global Biogeochemical Cycles*, 2(3):253–268.
- Ye, X., Li, Z., Luo, X., Wang, W., Li, Y., Li, R., Zhang, B., Qiao, Y., Zhou, J., Fan, J., Wang, H., Huang, Y., Cao, H., Cui, Z., and Zhang, R. (2020). A predatory myxobacterium controls cucumber Fusarium wilt by regulating the soil microbial community. *Microbiome*, 8(1):49.
- Yoshida, N., Iguchi, H., Yurimoto, H., Murakami, A., and Sakai, Y. (2014). Aquatic plant surface as a niche for methanotrophs. *Frontiers in microbiology*, 5:30.
- Yu, H., Liang, H., Longshaw, M., Wang, J., Ge, X., Ren, M., and Zhang, L. (2022). Methanotroph (*Methylococcus capsulatus*, Bath) bacteria meal (FeedKind®) could effectively improve the growth, apparent digestibility coefficient, blood biochemical parameters, antioxidant indices of juvenile Jian carp (*Cyprinus carpio* var. Jian). *Animal Feed Science and Technology*, 288:115293.
- Yun, J., Yu, Z., Li, K., and Zhang, H. (2013). Diversity, abundance and vertical distribution of methane-oxidizing bacteria (methanotrophs) in the sediments of the Xianghai wetland, Songnen Plain, north-east China. *Journal of Soils and Sediments*, 13(1):242–252.
- Yurtsev, E. A., Conwill, A., and Gore, J. (2016). Oscillatory dynamics in a bacterial cross-protection mutualism. *Proceedings of the National Academy of Sciences of the United States of America*, 113(22):6236–6241.
- Zahn, J. A. and DiSpirito, A. A. (1996). Membrane-associated methane monooxygenase from *Methylococcus capsulatus* (Bath). *Journal of bacteriology*, 178(4):1018–1029.
- Zelezniak, A., Andrejev, S., Ponomarova, O., Mende, D. R., Bork, P., and Patil, K. R. (2015). Metabolic dependencies drive species co-occurrence in diverse microbial communities. *Proceedings of the National Academy of Sciences of the United States of America*, 112(20):6449–6454.
- Zhang, J., Kobert, K., Flouri, T., and Stamatakis, A. (2014). PEAR: a fast and accurate Illumina Paired-End reAd mergeR. *Bioinformatics (Oxford, England)*, 30(5):614–620.
- Zhang, L., Adams, J. M., Dumont, M. G., Li, Y., Shi, Y., He, D., He, J.-S., and Chu, H. (2019). Distinct methanotrophic communities exist in habitats with different soil water contents. *Soil Biology and Biochemistry*, 132:143–152.

- Zhang, Y., Zhang, X., Wang, F., Xia, W., and Jia, Z. (2020). Exogenous nitrogen addition inhibits sulfate-mediated anaerobic oxidation of methane in estuarine coastal sediments. *Ecological Engineering*, 158:106021.
- Zhao, J., Cai, Y., and Jia, Z. (2020). The pH-based ecological coherence of active canonical methanotrophs in paddy soils. *Biogeosciences*, 17(6):1451–1462.
- Zheng, Q., Hu, Y., Zhang, S., Noll, L., Böckle, T., Dietrich, M., Herbold, C. W., Eichorst, S. A., Wobken, D., Richter, A., and Wanek, W. (2019). Soil multifunctionality is affected by the soil environment and by microbial community composition and diversity. *Soil biology & biochemistry*, 136:107521.
- Zheng, Y., Huang, R., Wang, B. Z., Bodelier, P. L. E., and Jia, Z. J. (2014). Competitive interactions between methane- and ammonia-oxidizing bacteria modulate carbon and nitrogen cycling in paddy soil. *Biogeosciences*, 11(12):3353–3368.
- Zhou, J., Deng, Y., Luo, F., He, Z., Tu, Q., and Zhi, X. (2010). Functional molecular ecological networks. *mBio*, 1(4):1–10.
- Zhu, J., Wang, Q., Yuan, M., Tan, G.-Y. A., Sun, F., Wang, C., Wu, W., and Lee, P.-H. (2016). Microbiology and potential applications of aerobic methane oxidation coupled to denitrification (AME-D) process: A review. *Water research*, 90:203–215.
- Zhu, P., Cheng, M., Pei, D., Liu, Y., and Yan, X. (2020). *Methylomonas rhizoryzae* sp. nov., a type I methanotroph isolated from the rhizosphere soil of rice. *Antonie van Leeuwenhoek*, 113(12):2167–2176.

# **Appendix**

## **A Published version of presented articles**



## RESEARCH ARTICLE

## Open Access

# The methane-driven interaction network in terrestrial methane hotspots



Thomas Kaupper<sup>1</sup>, Lucas W. Mendes<sup>2</sup>, Anja Poehlein<sup>3</sup>, Daria Frohloff<sup>1</sup>, Stephan Rohrbach<sup>1</sup>, Marcus A. Horn<sup>1\*</sup> and Adrian Ho<sup>1\*</sup> 

## Abstract

**Background:** Biological interaction affects diverse facets of microbial life by modulating the activity, diversity, abundance, and composition of microbial communities. Aerobic methane oxidation is a community function, with emergent community traits arising from the interaction of the methane-oxidizers (methanotrophs) and non-methanotrophs. Yet little is known of the spatial and temporal organization of these interaction networks in naturally-occurring complex communities. We hypothesized that the assembled bacterial community of the interaction network in methane hotspots would converge, driven by high substrate availability that favors specific methanotrophs, and in turn influences the recruitment of non-methanotrophs. These environments would also share more co-occurring than site-specific taxa.

**Results:** We applied stable isotope probing (SIP) using  $^{13}\text{C}\text{-CH}_4$  coupled to a co-occurrence network analysis to probe trophic interactions in widespread methane-emitting environments, and over time. Network analysis revealed predominantly unique co-occurring taxa from different environments, indicating distinctly co-evolved communities more strongly influenced by other parameters than high methane availability. Also, results showed a narrower network topology range over time than between environments. Co-occurrence pattern points to *Chthoniobacter* as a relevant yet-unrecognized interacting partner particularly of the gammaproteobacterial methanotrophs, deserving future attention. In almost all instances, the networks derived from the  $^{13}\text{C}\text{-CH}_4$  incubation exhibited a less connected and complex topology than the networks derived from the  $^{12}\text{C}\text{-CH}_4$  incubations, likely attributable to the exclusion of the inactive microbial population and spurious connections; DNA-based networks (without SIP) may thus overestimate the methane-dependent network complexity.

**Conclusion:** We demonstrated that site-specific environmental parameters more strongly shaped the co-occurrence of bacterial taxa than substrate availability. Given that members of the interactome without the capacity to oxidize methane can exert interaction-induced effects on community function, understanding the co-occurrence pattern of the methane-driven interaction network is key to elucidating community function, which goes beyond relating activity to community composition, abundances, and diversity. More generally, we provide a methodological strategy that substantiates the ecological linkages between potentially interacting microorganisms with broad applications to elucidate the role of microbial interaction in community function.

**Keywords:** Stable-isotope probing, Microbial interaction, Aerobic methanotrophs, Freshwater methanotrophs, Methane bio-filter

\*Correspondence: [horn@ifmb.uni-hannover.de](mailto:horn@ifmb.uni-hannover.de); [adrian.ho@ifmb.uni-hannover.de](mailto:adrian.ho@ifmb.uni-hannover.de)

<sup>1</sup> Institute for Microbiology, Leibniz Universität Hannover, Herrenhäuser Str. 2, 30419 Hannover, Germany

Full list of author information is available at the end of the article

## Background

Microbial interactions are widespread, leading to a plethora of interdependent relationships with stimulatory and inhibitory effects on community function [1–4].



© The Author(s) 2022. **Open Access** This article is licensed under a Creative Commons Attribution 4.0 International License, which permits use, sharing, adaptation, distribution and reproduction in any medium or format, as long as you give appropriate credit to the original author(s) and the source, provide a link to the Creative Commons licence, and indicate if changes were made. The images or other third party material in this article are included in the article's Creative Commons licence, unless indicated otherwise in a credit line to the material. If material is not included in the article's Creative Commons licence and your intended use is not permitted by statutory regulation or exceeds the permitted use, you will need to obtain permission directly from the copyright holder. To view a copy of this licence, visit <http://creativecommons.org/licenses/by/4.0/>. The Creative Commons Public Domain Dedication waiver (<http://creativecommons.org/publicdomain/zero/1.0/>) applies to the data made available in this article, unless otherwise stated in a credit line to the data.

It is becoming evident that aerobic methane oxidation is a community function, whereby microorganisms lacking the enzymatic repertoire to oxidize methane are also relevant. These microorganisms (non-methanotrophs) play a significant role, stimulating methanotrophic activity and growth, and increasing methanotroph-mediated micropollutant degradation [2, 5, 6]. Interestingly, the accompanying non-methanotrophs have also been implicated in the resilience of methanotrophic activity during recovery from disturbances [7–9]. Emergent properties may thus arise from the interaction of the methanotrophs and non-methanotrophs, both constituting the “methanotroph interactome” defined here as the consortium of co-occurring microorganisms that can be tracked via the flow of  $^{13}\text{C}\text{-CH}_4$  from the methanotrophs (primary consumers) to other microorganisms in the soil food web [9, 10].

Microbial interactions in complex communities, including the methanotroph interactome, have been explored using a co-occurrence network analysis based on specific genes (e.g., 16S rRNA, 18S rRNA genes) amplified from isolated nucleic acids (DNA, RNA) [11–17]. Microbial taxa that are positively correlated in the network analysis can be interpreted as having complementary roles, sharing the same habitat niche, or are driven by cross-feeding [1, 3, 11, 13, 18], whereas negative correlations are attributable to competing taxa, predation, or niche partitioning [4, 19–21]. The aerobic methanotrophs thrive in the presence of other organisms, forming (mutually) beneficial associations (e.g., receiving essential vitamins; [22]), as well as adverse relationships (e.g., selective predation by protists; [23]) with their biotic environment. These interactions can be species-specific [5, 22, 24], underscoring the relevance of the physiology, and ecological traits inherent to diverse methanotrophs in selecting for interacting partners, influencing the membership of the methanotroph interactome. Accordingly, the aerobic methanotrophs belong to Gamma- / Alpha-proteobacteria and Verrucomicrobia, with the active verrucomicrobial methanotrophs typically detected in acidic and geothermal environments (e.g., peatlands, volcanic and geothermal soils; [8, 25, 26]). These methanotrophs can be distinguished based on their physiology, including C-assimilation pathway and substrate utilization (e.g., facultative methanotrophy) and PLFA profile, among other distinct ecological characteristics [27–31]. In terrestrial ecosystems, the aerobic methanotrophs play a crucial role as a methane-biofilter at oxic-anoxic interfaces where they consume a large portion of methane produced before being emitted into the atmosphere [32], in addition to being a methane sink in well-aerated soils [33–35]. Besides the methanotrophs and interaction with methylotrophs [36, 37],

very little is known of the organization (over space and time), and other constituents of the methanotroph interactome despite their relevance in modulating community function.

Here, we elaborate on the methane-driven interaction network in naturally-occurring complex communities from widespread methane hotspots (pristine/restored ombrotrophic peatlands, and paddy, riparian, and landfill cover soils). Considering that a high substrate (methane) availability favors gammaproteobacterial methanotrophs (e.g., *Methylobacter*, *Methylosarcina*; [32, 38, 39]), in turn influence the recruitment of the non-methanotrophs, we hypothesize that members of the methanotroph interactome from these environments would converge, having more shared than site-specific co-occurring taxa. To address our hypothesis, we applied stable isotope probing (SIP) using  $^{13}\text{C}\text{-CH}_4$  coupled to a co-occurrence network analysis of the  $^{13}\text{C}$ -enriched 16S rRNA gene, which not only enabled direct association of methanotrophic activity to the network structure, but also provided a tangible link between the co-occurring taxa involved in the trophic interaction. This is in contrast to previous work deriving the networks from isolated nucleic acids (DNA and RNA), where relationships between taxa were inferred rather than demonstrated. Capitalizing on the SIP-network analysis, we determined different scales of organization, that is, consistency of co-occurring taxa that were nested among the metabolically active sub-population between environments (spatial scale), and over time (temporal scale) in the pristine peatland to assess the stability of the network structure during the incubation. Furthermore, comparing the  $^{13}\text{C}$ - and  $^{12}\text{C}$ -based networks, we postulate that the networks derived from the DNA isolated from the soils (i.e.,  $^{12}\text{C}\text{-CH}_4$  incubation, without SIP) would be relatively more complex because of the inclusion of the metabolically inactive community members, non-trophic interactions, and weak or spurious correlations. Hence, we examined the applicability of our methodological approach, while shedding light on the spatial and temporal organization of the methanotroph interactome.

## Results and discussion

### Aerobic methanotrophy, and environmental variables influencing the metabolically active bacterial community composition

Methanotrophic activity was detected in all environments and was within the range expected for low-affinity methane oxidation typical in methane hotspots (Table 1; [40, 41]). In these environments, the methanotrophs serve as a methane-biofilter, consuming high concentrations of methane generated in the anoxic soil layers before releasing into the atmosphere [32, 39, 42].

**Table 1** Selected soil physico-chemical properties, and methane uptake rates from methane hotspots

Environment	Location (coordinates)	Sampling time	pH	EC (mS cm <sup>-1</sup> )	Total C (mg g <sub>dw</sub> <sup>-1</sup> )	Total N (μmol g <sub>dw</sub> <sup>-1</sup> )	NH <sub>4</sub> <sup>+</sup> (μmol g <sub>dw</sub> <sup>-1</sup> )	NO <sub>3</sub> <sup>-</sup> (μmol g <sub>dw</sub> <sup>-1</sup> )	SO <sub>4</sub> <sup>2-</sup>	CH <sub>4</sub> uptake rate (μmol g <sub>dw</sub> <sup>-1</sup> h <sup>-1</sup> )	References
Paddy soil	Italian Rice Research Institute, Verucelli, Italy (45° 20'N, 8° 25'E)	May 2015	6.6 ± 0.05a	BD	13.9 ± 0.5a	1.3 ± 0.04a	1 ± 0.02ac	0.6 ± 0.01abc	0.8 ± 0.2a	0.44 ± 0.19b	[9]
Landfill cover	AHA Landfill, Kohlenfeld, Germany (52°22'N 9°26'E)	Jan 2020	8.81 ± 0.11b	0.07 ± 0.01a	136 ± 12b	10.1 ± 0.5bc	12.2 ± 8.3c	1.9 ± 1.2bc	28 ± 32bd	0.67 ± 0.24ab	This study
Pristine peatland	Zielony Mechacz, Poland (53°54'24''N, 19°41'41''E)	May 2019	4.39 ± 0.19c	BD	457 ± 4.2c	6.9 ± 1.2ab	0.2 ± 0.08b	0.6 ± 0.2bc	3.3 ± 0.6bcd	1 ± 0.26a	[8], this study
Restored peatland	Rucianka, Poland (54°15'34''N, 19°44'0.4''E)	May 2019	4.68 ± 0.12c	BD	492 ± 6d	12.5 ± 0.4c	0.7 ± 0.3a	0.7 ± 0.6abc	2.3 ± 0.3c	1 ± 0.16a	[8]
Riparian soil	River Leine, Hannover, Germany (52°22'43.7''N 9°42'11.4''E)	May 2020	8.22 ± 0.18d	0.06 ± 0.01a	32.2 ± 8.4e	2.5 ± 0.8ab	0.4 ± 0.2a	0.07 ± 0.07a	1.8 ± 0.4a	0.15 ± 0.05c	This study

Although low-affinity methanotrophs were detected, some of these methanotrophs may also consume methane at (circum-)atmospheric levels, doubling as a methane sink under low methane availability [34, 43, 44]. The methanotrophic activity was corroborated by the significant increase ( $p < 0.05$ ) in the *pmoA* gene abundance and/or the *pmoA*:16S rRNA gene abundance ratio (%) during the incubation (Table 1, Additional file 11: Table S1, Additional file 2: Figure S1), indicating methanotrophic growth.

Importantly, assimilation of methane-derived  $^{13}\text{C}$  into the methanotrophs was evidenced by the detection of the  $^{13}\text{C}$ -DNA following density gradient fractionation in the SIP approach, which showed well-separated unlabelled  $^{12}\text{C}$ - (“light”) and  $^{13}\text{C}$ -DNA (“heavy”) fractions (Additional file 3: Figures S2 & Additional file 4: Figure S3). The microorganisms derived from the  $^{13}\text{C}$ -enriched 16S rRNA gene thus represent the metabolically active,  $^{13}\text{C}$ -methane derived consuming, and replicating community members. Despite the relatively low proportion of methanotrophs (Additional file 2: Figures S1, Additional file 5: Figure S4 & Additional file 6: Figure S5), the bacterial community composition, as determined from the amplicon sequence analysis of the 16S rRNA gene in the “light” and “heavy” fractions were discernible, clearly separated along the axes in the Principal Component Analysis (PCA, Additional file 7: Figure S6 & Additional file 8: Figure S7), supporting the density gradient fractionation. However, with a relatively lower proportion of methanotrophs in the riparian soil (Additional file 2: Figure S1), differences in the “light” and “heavy” fractions were no longer reflected in the total bacterial population (i.e., at the 16S rRNA gene level; Additional file 7: Figure S6). Generally, the SIP approach not only confirmed the assimilation of  $^{13}\text{C}$ -methane by the methanotrophs, but also captured the subsequent dispersal of the  $^{13}\text{C}$  into the methane-driven soil food web.

Compositional changes during the incubation may reflect on the temporal dynamics of the bacterial, including the methanotrophic community (e.g., [45–47]). Nevertheless, with the exception of the peat, the metabolically active, that is,  $^{13}\text{C}$  assimilating and replicating bacterial community composition after the incubation was representative of the community in the starting material (Additional file 5: Figure S4). The metabolically active bacterial community composition was distinct in the ombrotrophic peatlands, as revealed in a redundancy analysis (RDA; Fig. 1). The RDA integrates the abiotic parameters in Table 1 to the  $^{13}\text{C}$ -labelled bacterial community composition in all environments. The bacterial composition in the riparian, landfill cover, and paddy soils were more similar clustering closely together, and could be separated from the community in the

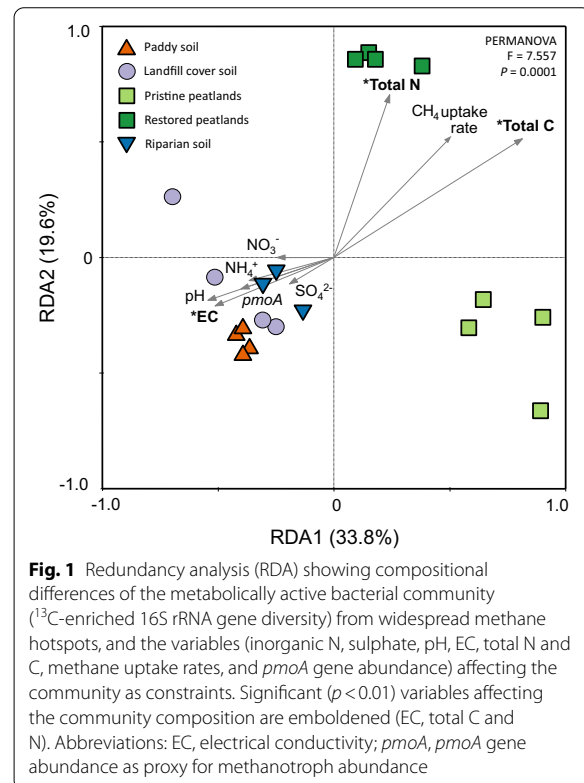


**Fig. 1** Redundancy analysis (RDA) showing compositional differences of the metabolically active bacterial community ( $^{13}\text{C}$ -enriched 16S rRNA gene diversity) from widespread methane hotspots, and the variables (inorganic N, sulphate, pH, EC, total N and C, methane uptake rates, and *pmoA* gene abundance) affecting the community as constraints. Significant ( $p < 0.01$ ) variables affecting the community composition are emboldened (EC, total C and N). Abbreviations: EC, electrical conductivity; *pmoA*, *pmoA* gene abundance as proxy for methanotroph abundance

ombrotrophic peatlands along RDA axis 1; >53% of the variation of the bacterial community composition could be explained by RDA 1 and RDA 2 (Fig. 1). The bacterial community composition can be profoundly influenced by the soil physico-chemical parameters including substrate availability and land use, with the latter potentially having a stronger impact on the compositional differences among the methanotrophs [9, 31, 48, 49]. Among the environmental parameters, total C and N, and electrical conductivity (EC) indicative of soil salinity, significantly ( $p < 0.05$ ) affected the active bacterial community (Fig. 1). While EC favours the community in the riparian, landfill cover, and paddy soils, total C and N strongly affected the community particularly in the restored ombrotrophic peatland. This is not entirely unexpected as ombrotrophic peatlands are nutrient-impoverted environments, where the peat-inhabiting microorganisms would more strongly respond to C and N than in the other relatively nutrient-rich environments (Table 1; [50]). In the other environments, it is noteworthy that despite the different ecosystems represented, that is, freshwater wetlands (paddy and riparian soil) and well-aerated landfill cover soil, the active bacterial community composition was more similar, possibly forming interaction networks comprising of shared community members.

### The methanotrophic interactome over space and time

The interaction among members of the methane-driven food web was explored using a co-occurrence network analysis derived from the  $^{13}\text{C}$ -enriched 16S rRNA genes. A comparison of the networks from the different environments revealed that the  $^{13}\text{C}$ -labelled riparian soil community was relatively more connected and complex, as indicated by the higher number of interacting community members (nodes), number of connections (edges), and number of connections per node or node connectivity (average degree), but was less modular, having fewer compartmentalized groups of interaction within the network than the other environments (Table 2, Additional file 9: Figure S8; [13, 51, 52]). In contrast, the restored peatland harboured the least connected and complex interaction network (Table 2). Presumably, increased co-occurrence is fueled by a higher metabolic exchange and/or competition among members of the methanotrophic interactome in the riparian soil [18, 53].

Because temporal community patterns may lead to the elimination of highly connected taxa [54] which affects the network complexity [13], the interaction network in the pristine peatland was additionally determined after 8, 13, and 19 days incubation to monitor the changes of the network topology over time (Table 3, Additional file 10: Figure S9). Besides being a source of methane-derived organic C, methanotrophs also drive the N-cycle by fixing  $\text{N}_2$  to assimilable N forms, and hence, are a key microbial group linking C and N cycling in ombrotrophic peatlands [55, 56]. The connectedness and complexity of the  $^{13}\text{C}$ -enriched 16S rRNA gene-derived interaction network, as deduced from the number of nodes, edges, and degree, fluctuated within a relatively narrow range over time when compared to the differences in the network topology between environments (Tables 2, 3). However, modularity decreased from day 8 to 13, and remained relatively unchanged thereafter, indicating a reduced number of independently connected groups of nodes or compartments within the network over time [51]. Initially, compartments that are formed centered around the methanotrophs before  $^{13}\text{C}$  dispersal to other community members at higher trophic levels. With continuous methane availability during the incubation, it is not unreasonable to assume that the methane-derived  $^{13}\text{C}$  would be more evenly and widely dispersed in the methanotrophic interactome, becoming less modular over time [9]. Such temporal changes in the network topology are anticipated given that the soil is a dynamic environment. Nevertheless, it appears that some network topological features (e.g., degree, number of nodes and edges) were relatively more consistent than others (e.g., modularity) over time.

### Insights into intra-methanotroph and methanotroph/non-methanotroph interaction within the methanotrophic interactome

The co-occurring methanotroph/methanotroph (intra-methanotroph) and methanotroph/non-methanotroph interactions were further explored to determine whether co-occurring taxa are conserved across different environments, and to identify non-methanotrophs as interacting partners of the methanotrophs. The non-methanotrophs and methanotrophs that co-occur are anticipated to form close associations, forming tight-knit clusters that are centered around the methanotrophs [10, 15]. On the other hand, linkages between non-methanotrophs that occurred at higher proportion (Tables 2, 3) represent heterotrophic microorganisms that assimilated the  $^{13}\text{C}$  at higher trophic levels. The co-occurring methanotroph/methanotroph and methanotroph/non-methanotroph taxa exhibited site specificity, with the majority of the co-occurring microorganisms unique to an environment (Fig. 2). Differing from our hypothesis, this suggests that microbial communities distinctly co-evolved in the different environments, and other factors besides high methane availability drives the co-occurrence of these microorganisms. Interestingly, more shared co-occurring taxa from the pristine and restored peatlands (acidic freshwater ecosystem), as well as in the riparian and paddy soil (circum-neutral freshwater ecosystems) were detected (Fig. 2), suggesting some commonalities in the environmental selection of these co-occurring microorganisms.

Communal metabolism drives the interaction network of the  $^{13}\text{C}$ -enriched members of the methanotrophic interactome [8–10, 36, 57]. Although the incorporation of  $^{13}\text{C}$  derived from dead microbial biomass can not be completely excluded, this would have been minimized with a metabolically active and growing methane-oxidizing population. Also, methane-derived  $^{13}\text{C}$ - $\text{CO}_2$  may be incorporated by chemoautotrophs in the community, but the majority of the co-occurring genus/species were heterotrophs. Here, we focused on the shared taxa from the different environments which represent the more universal co-occurring members of the interaction network (Fig. 2). Expectedly, many methanotrophs (e.g., *Methylobacter*, *Methylomonas*, *Methylomicrobium*, *Methylosarcina*, *Methylocystis*, and members of *Methyloacidiphilaceae*) co-occur, sharing similar niche in diverse environments. Among other co-occurring taxa common to many environments, non-methanotrophic methylotrophs (e.g., *Methylotenera*, *Hyphomicrobium*, and members of *Methylophilaceae*) were significantly co-enriched alongside methanotrophs (Fig. 2; [8, 9, 57–59]). Indeed, cross-feeding drives their co-occurrence via passive release of methanol by the methanotrophs. Also, the

**Table 2** Correlations and topological properties of the co-occurrence network analysis derived from widespread methane hotspots. The networks are given in the Additional file 9: Figure S8

Network properties	Paddy soil		Landfill cover		Pristine peatland		Restored peatland		Riparian soil	
	<sup>13</sup> C	Unlabelled <sup>c</sup>	<sup>13</sup> C	Unlabelled <sup>c</sup>	<sup>13</sup> C	Unlabelled <sup>c</sup>	<sup>13</sup> C	Unlabelled <sup>c</sup>	<sup>13</sup> C	Unlabelled <sup>c</sup>
Number of nodes <sup>a</sup>	299	536	329	655	344	622	258	681	737	667
Number of edges <sup>b</sup>	980	2839	2078	8899	1684	4219	846	6918	10,003	6261
Positive edges <sup>c</sup>	805 (82%)	2149 (76%)	1341 (64%)	5242 (59%)	1026 (61%)	2740 (65%)	558 (66%)	4269 (62%)	7631 (76%)	4785 (76%)
Negative edges <sup>d</sup>	175 (18%)	690 (24%)	737 (36%)	3657 (41%)	658 (39%)	1479 (35%)	288 (34%)	2649 (38%)	2372 (24%)	1476 (24%)
Met/Met	78 (8%)	1 (0.3%)	18 (1%)	49 (0.5%)	3 (0.2%)	8 (0.5%)	19 (2.2%)	8 (0.1%)	970 (9.5%)	6 (0.1%)
Met/non-Met	318 (32%)	78 (2.7%)	365 (17%)	188 (2.5%)	177 (10.5%)	250 (5.5%)	189 (22.4%)	441 (6.9%)	3707 (37%)	331 (4.9%)
Non-Met/non-Met	584 (60%)	2760 (97%)	1695 (82%)	8662 (97%)	1504 (89.3%)	3961 (94%)	638 (75.4%)	6469 (93%)	5326 (53.5%)	5924 (95%)
Modularity <sup>e</sup>	0.817	1.166	1.557	2.067	2.316	1.734	1.812	1.894	0.692	0.992
Number of communities <sup>f</sup>	55	91	32	30	39	67	38	40	19	74
Network diameter <sup>g</sup>	16	14	10	10	11	10	11	11	12	10
Average path length <sup>h</sup>	5.913	5.803	3.969	3.607	4.402	4.372	5.01	4.228	4.201	4.433
Average degree <sup>i</sup>	6.55	10.59	12.63	27.173	9.79	13.566	6.55	20.317	27.14	18.774
Av. clustering coefficient <sup>j</sup>	0.365	0.416	0.409	0.418	0.413	0.397	0.397	0.413	0.319	0.345

Met/Met correlation within methanotrophs, Met/non-Met correlation between methanotrophs and non-methanotrophs, Non-met/non-Met correlation between non-methanotrophs

<sup>a</sup> Microbial taxon (at genus level) with at least one significant ( $p < 0.01$ ) and strong (SparCC  $> 0.8$  or  $< -0.8$ ) correlation;

<sup>b</sup> Number of connections/correlations obtained by SparCC analysis;

<sup>c</sup> SparCC positive correlation ( $> 0.7$  with  $P < 0.01$ );

<sup>d</sup> SparCC negative correlation ( $< -0.7$  with  $P < 0.01$ );

<sup>e</sup> The capability of the nodes to form highly connected communities, that is, a structure with high density of between nodes connections (inferred by Gephi);

<sup>f</sup> A community is defined as a group of nodes densely connected internally (Gephi);

<sup>g</sup> The longest distance between nodes in the network, measured in number of edges (Gephi);

<sup>h</sup> Average network distance between all pair of nodes or the average length off all edges in the network (Gephi);

<sup>i</sup> The average number of connections per node in the network, that is, the node connectivity (Gephi);

<sup>j</sup> How nodes are embedded in their neighborhood and the degree to which they tend to cluster together (Gephi)



**Table 3** Correlations and topological properties of the co-occurrence network analysis from the pristine peatland over time. The networks are given in the Additional file 10: Figure S9

Network properties	8 days		13 days		19 days	
	<sup>13</sup> C	Unlabelled <sup>13</sup> C	<sup>13</sup> C	Unlabelled <sup>13</sup> C	<sup>13</sup> C	Unlabelled <sup>13</sup> C
Number of nodes <sup>a</sup>	297	608	347	628	205	578
Number of edges <sup>b</sup>	1265	4651	1758	3845	687	4117
Positive edges <sup>c</sup>	724 (57%)	2970 (64%)	1056 (60%)	2646 (69%)	418 (61%)	2561 (62%)
Negative edges <sup>d</sup>	541 (43%)	1681 (36%)	702 (40%)	1199 (31%)	269 (39%)	1556 (38%)
Met/Met	4 (0.3%)	4 (0.1%)	5 (0.3%)	3 (0.1%)	8 (1.2%)	1 (0.02%)
Met/non-Met	130 (10.2%)	231 (5%)	185 (10.5%)	230 (6%)	135 (19.6%)	138 (3.3%)
Non-Met/non-Met	1131 (89.5%)	4416 (94.9%)	1568 (89.2%)	3612 (93.9%)	544 (79.2%)	3978 (96.6%)
Modularity <sup>e</sup>	3.317	1.752	2.440	1.445	2.478	2.150
Number of communities <sup>f</sup>	34	66	37	79	35	44
Network diameter <sup>g</sup>	14	14	11	10	17	12
Average path length <sup>h</sup>	5.233	4.243	4.463	4.441	5.038	4.181
Average degree <sup>i</sup>	8.519	15.29	10.13	12.24	6.702	14.24
Av. clustering coefficient <sup>j</sup>	0.421	0.404	0.415	0.399	0.430	0.374

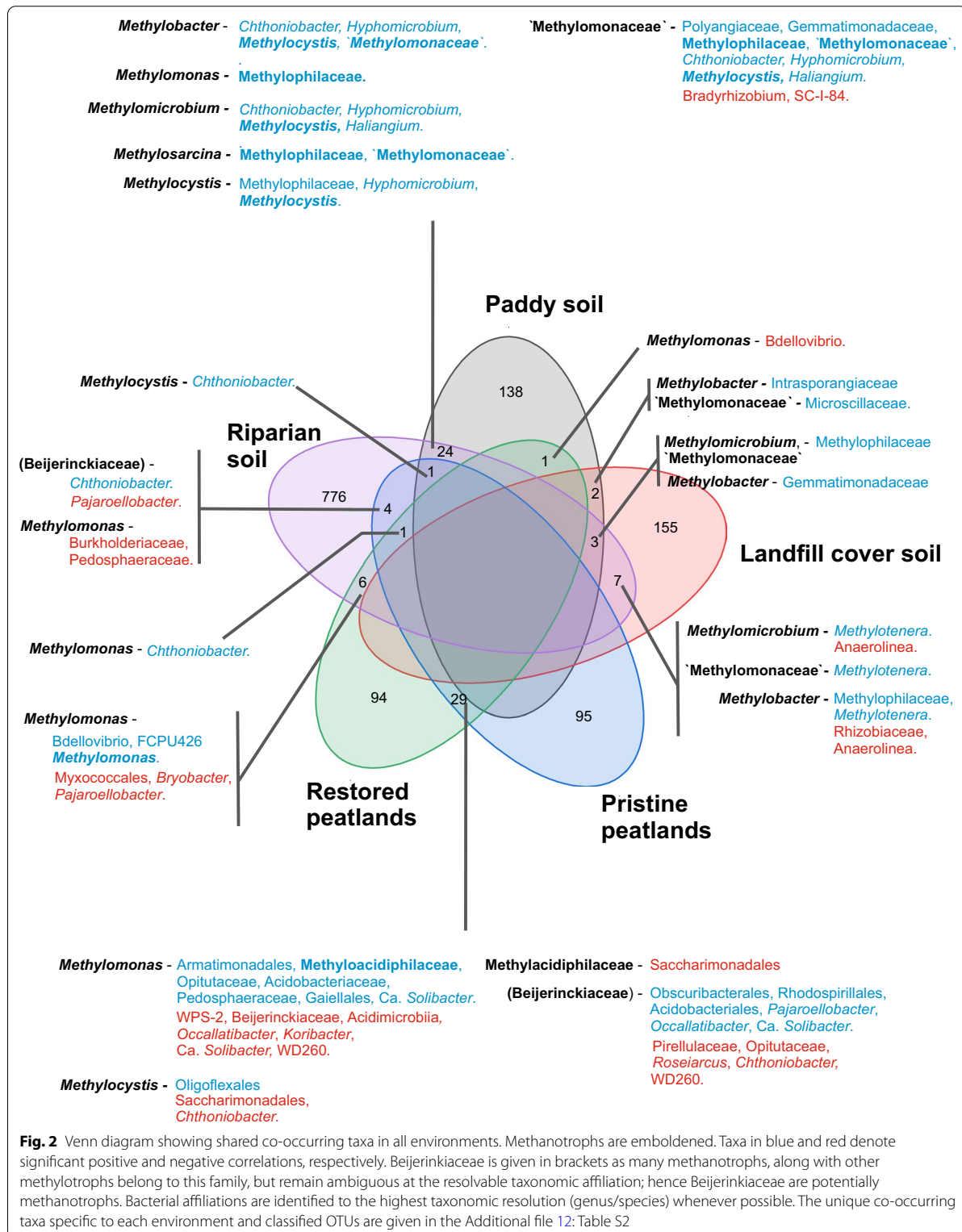
Description of the network properties are as given in Table 2

*Met/Met* correlation within methanotrophs, *Met/non-Met* correlation between methanotrophs and non-methanotrophs, *Non-met/non-Met* correlation between non-methanotrophs

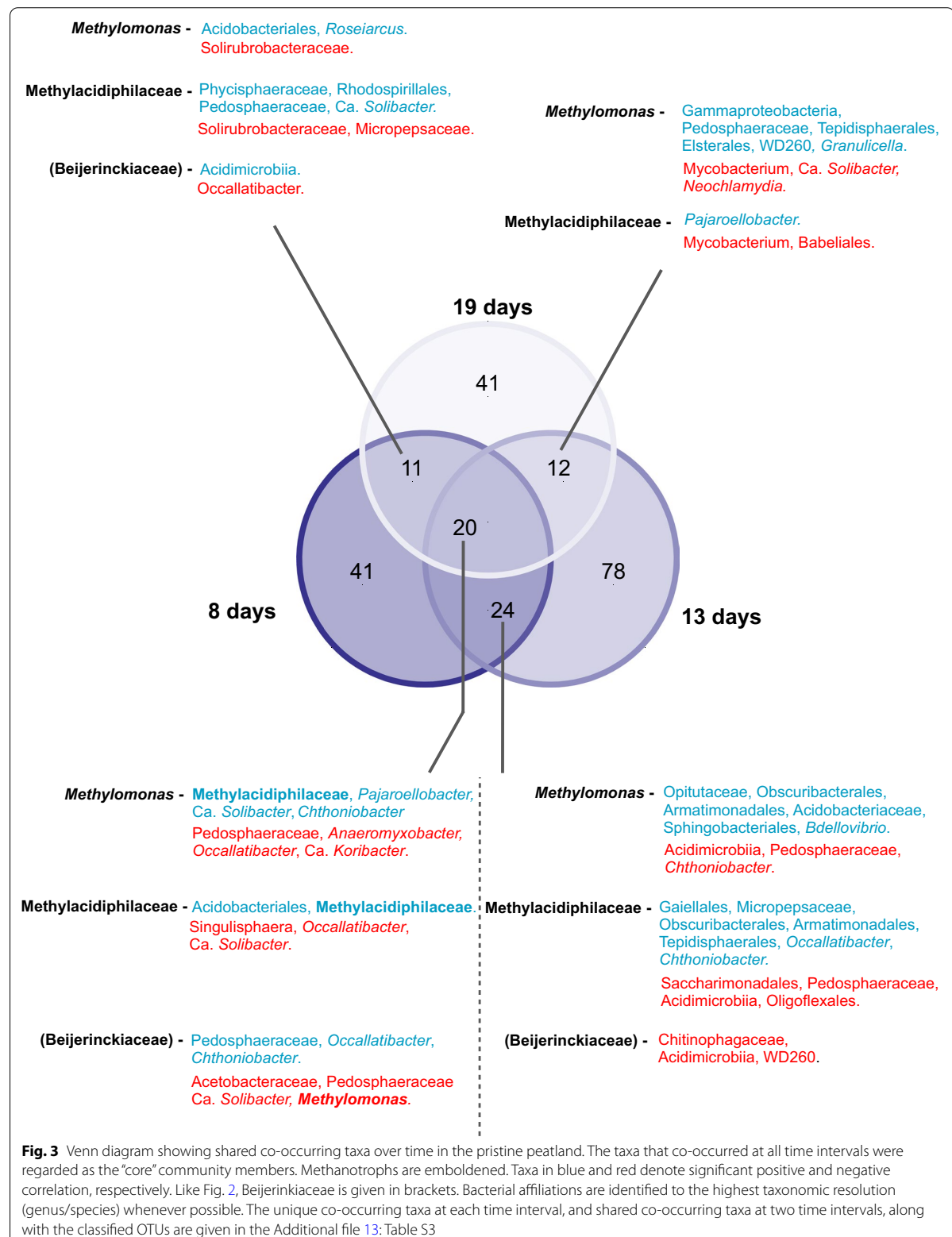
non-methanotrophic methylotrophs have been demonstrated to induce the release of methanol as a C source for growth by modifying the expression of the methanol dehydrogenase in methanotrophs [36], in addition to utilizing other methane-derived one C compounds (e.g., formaldehyde, formate). Considering that some members of Myxococcales (e.g., Haliangiaceae; [60]) are recognized microbial predators shown to exert a regulatory effect in bacterial communities [61–63], their significant positive and negative correlations in the restored peatland and riparian soil suggest selective predation on the methanotrophs, as shown before in freshwater environments [64]. The apparently contrasting correlations may be explained by the predator–prey relationship, where predator and prey alternately fluctuate over time. Thus, correlations of Myxococcales with the methanotrophs may vary from positive (e.g., during nutrient availability derived from lysed cells after predation) to negative (e.g., during predation on methanotrophs) through time. Overall, although co-occurrence patterns may differ across environments, few relationships were persistent reflecting on the biological interactions that were independent of the environmental conditions. Besides predation and methylotrophic interaction, other interacting members of the methanotroph interactome remain elusive.

Of interest, *Chthoniobacter* appears to be closely associated with the methanotrophs in diverse environments (peatlands, paddy, and riparian soils), and was overwhelmingly (the only exception occurred at days 8–13 interval in the pristine peatland; Fig. 3) positively

correlated to the gammaproteobacterial methanotrophs (*Methylobacter*, *Methylomicrobium*, *Methylomonas*, and other “Methylomonaceae”); *Chthoniobacter* positively and negatively correlated to the alphaproteobacterial methanotroph *Methylocystis*, depending on the environment (Fig. 2, Additional file 12: Table S2). Unlike the methylotrophs, a cultured representative of *Chthoniobacter* (*C. flavus*) is a soil-inhabiting heterotroph that cannot utilize products of methane oxidation (i.e., methanol, formate) nor other organic acids (except pyruvate) and amino acids for growth [65]. This suggests that leaked pyruvate and/or sugars derived from the ribulose monophosphate (RuMP) pathway during C-assimilation specifically in gammaproteobacterial methanotrophs may shape the cross-feeding between *Chthoniobacter* and the methanotrophs. Another co-enriched non-methanotroph taxon belonged to *Haliangium*, detected only in the paddy and riparian soils (Fig. 2, Additional file 12: Table S2). Cultured representatives of *Haliangium* (group Myxobacteria) seemingly inhabit and show a preference for mineral soils [60], corroborating with their absence in the pristine and restored peatlands (Figs. 2 and 3). However, the co-occurrence network analysis revealed statistical relationships; the biological interdependencies or causative mechanisms driving the inferred interaction requires further investigation, facilitated by co-culture studies [36, 66]. Also noteworthy is that a taxon may simultaneously be positively and negatively correlated to the same methanotroph (e.g., *Ca. Solibacter*, *Pajaroellobacter*, *Occallatibacter*; Fig. 2).







Admittedly, our sequencing analysis suffers from the lack of finer taxonomic resolution. This could partly explain the seemingly contradictory correlations, which may also stem from the inherently different ecological traits possessed by members of the same genus or even strain and/or that the same microorganism may have evolved to play distinct roles in different environments [67, 68]. Hence, further exploration of the inherent microbial traits driving the co-occurrence of the methanotrophs and specific non-methanotrophs warrants attention.

Additionally, we monitored shifts in the co-occurring taxa over time (8, 13, and 19 days intervals) in the pristine peatland to determine the persistent non-methanotrophic interacting partners (Fig. 3, Additional file 13: Table S3). Unique co-occurring taxa emerged at different time intervals, with some co-occurring microorganisms overlapping between time intervals. The 20 co-occurring taxa that were consistently present at all time intervals were regarded as the core community members. The core community was thus likely to comprise microorganisms that were in close and stable interaction with the methanotrophs. Likewise, *Chthoniobacter* was consistently positively correlated to the gammaproteobacterial methanotrophs in the core community. Generally, our analysis revealed some consistency in the co-occurring patterns of the interaction network over space and time, paving the way for future detailed studies to elucidate the underlying mechanisms and metabolites driving the co-occurrence of specific taxa.

#### Comparison of the interaction networks derived from the total (<sup>unlabelled</sup>C-DNA) and metabolically active (<sup>13</sup>C-DNA) microbial communities

Network analyses are commonly derived from nucleic acids isolated from the environment. Depending on the sampling strategy, the environmental samples are often collected apart and composited prior to nucleic acid extraction. Considering that microorganisms are largely restricted in their movements and particularly for the methanotrophs, strongly adhere to soil particles [69, 70], the interactions between microorganisms in these networks are thus inferred. Also, the complexity of these networks may have been overestimated given that the inferred interaction includes a large fraction of soil microorganisms that may not be metabolically active [71, 72]. Here, we addressed these limitations by coupling <sup>13</sup>C-CH<sub>4</sub> SIP to a co-occurrence network analysis which provides a strong link, tracking trophic interactions of microorganisms involved in the flow of the <sup>13</sup>C in the methane-based food web. Although a relatively more complex interaction topology is intuitively anticipated in networks derived from the total community

(<sup>unlabelled</sup>C-DNA), this assumption has yet to be empirically validated. Indeed, the network structure derived from the 16S rRNA gene sequences, representing the total community exhibited higher connectivity and complexity, as indicated by the higher number of nodes, edges, and degree when compared to the network of the active community (i.e., <sup>13</sup>C-enriched 16S rRNA gene sequences; Tables 2, 3). This was documented in all environments and over time in the pristine peat, except for the riparian soil where the network derived from the <sup>13</sup>C-enriched 16S rRNA gene sequences was comparably more connected and complex. Hence, results largely support our postulation that the coupling of SIP to network analysis can be applied to exclude or reduce spurious connections in the networks.

The unexpected trend in the riparian soil may have been caused by methodological artifacts, namely cross-contamination of the 'light' (<sup>unlabelled</sup>C-DNA) and 'heavy' (<sup>13</sup>C-DNA) fractions, but the densities of these fractions were well-separated (Additional file 3: Figure S2). Notably, the riparian soil harboured a higher number of nodes derived from the <sup>13</sup>C-enriched 16S rRNA gene (Table 2) compared to the total community (<sup>unlabelled</sup>C-DNA), as well as in other environments. This is indicative of a higher number of interacting microorganisms within the methanotrophic interactome in the riparian soil, which in turn, may foster higher metabolic exchange, contributing to the complexity of the methane-driven interaction network [3, 18, 73]. Whether this is the rule for networks harbouring highly diverse nodes or an exception for the riparian soil, needs further confirmation. Regardless, we demonstrate that our approach (SIP-network analysis) is an effective tool to probe trophic interactions in complex communities approximating *in-situ* conditions.

#### Conclusion

Given that biological interactions modulate different aspects of microbial life in the environment, shaping the activity, biodiversity, community composition, abundance, and stability of microbial communities [8, 9, 13, 73, 74], elucidating the interaction of assembled communities within the methane-driven network is key to determining their response to environmental cues. While numerous studies utilized artificially assembled communities, we explored microbial interactions in naturally-occurring complex communities aided by SIP coupled to a co-occurrence network analysis to target the methanotroph interactome. Although co-occurring taxa were predominantly site-specific, it appears that some biological interactions (e.g., cross-feeding within methylotrophs) were independent of the environment. Results also indicate a relatively stable interaction network in the short-term, comparing networks between all environments

and within the pristine peatland, with the emergence of a persistent core methanotroph interactome over time. More generally, we provide a methodological strategy to improve the network analysis derived from environmental samples by introducing SIP with labelled substrates to strengthen and substantiate the biological linkages between the potentially interacting microorganisms.

## Materials and methods

### Chemicals and reagents

Reagents (analytical and molecular biology grade) used were obtained from Carl Roth GmbH (Karlsruhe, Germany), VWR International (Hannover, Germany), and Merck (Bielefeld, Germany) unless explicitly stated otherwise. Gases ( $^{13}\text{C}$ - and  $^{\text{unlabelled}}\text{C-CH}_4$ ) were ordered from Linde plc (Pullach, Germany). For ultracentrifugation, tubes, rotors, and ultra-centrifuge were sourced from Beckman Coulter (CA, USA). Further details on kits and reagents are given in the corresponding sections.

### Soil microcosm incubation, and soil physico-chemical characterization

The soils were sampled from methane-emitting environments, including a landfill cover, pristine ombrotrophic peatlands, and riparian soil (Table 1). Additionally, results from previous incubations with a rice paddy soil and ombrotrophic peatlands, were also re-analysed and included in this study [8, 9]. These environments are anticipated to harbor aerobic low-affinity methane-oxidizers. The soils were collected from the upper 10–15 cm using a corer. Three to four soil cores were collected and composited from each of four random plots spaced > 4 m apart, representing independent replicates. Samples from the peatlands (Poland; Table 1) were transported to the laboratory in ice with styrofoam containers, while the other samples (landfill cover and riparian soil; Lower Saxony, Germany) were immediately transported to the lab for incubation set-up. Because of the large amounts of waste debris, the landfill cover soil was further loosely sieved (< 5 mm) prior to incubation. Rice paddy soil was processed as described before (air-dried at room temperature and sieved to < 2 mm; [9]). The site location, sampling time, and selected soil physico-chemical properties are provided in Table 1.

The landfill cover, pristine and restored ombrotrophic peatland, and riparian soils were incubated similarly; each microcosm consisted of 5–7 g fresh soil in a 120 ml bottle. After sealing the bottle with a butyl rubber stopper crimped with a metal cap, headspace methane was adjusted to 1–2%  $^{\text{unlabelled}}\text{C-CH}_4$  and  $^{13}\text{C-CH}_4$ ,  $n=4$  each) in air, reflecting on the anticipated *in-situ* methane concentrations in the methane hotspots. Incubation was performed at 27 °C, while shaking (110 rpm) in the

dark. Upon methane depletion, the microcosm was aerated for 30 min before replenishing headspace methane (1–2%  $^{\text{unlabelled}}\text{C-CH}_4$ ), and incubation resumed as before. The incubation was terminated when approximately 30  $\mu\text{mol CH}_4$  per g fresh weight soil was consumed to ensure sufficient labelling. Furthermore, incubations were performed with samples from the pristine ombrotrophic peatland in this study to follow the temporal dynamics of the methanotrophic interactome over a 19-day incubation after approximately 14 (day 8), 30 (day 13), and 60 (day 19)  $\mu\text{mol CH}_4$  per g fresh weight peat were consumed. The incubation containing the rice paddy soil was performed differently. Here, each microcosm consisted of 10 g air-dried rice paddy soil saturated with 4.5 mL autoclaved deionized water in a Petri dish. Incubation was performed statically at 25 °C in a flux chamber after adjusting headspace methane to 1–2%  $^{\text{unlabelled}}\text{C-CH}_4$ ,  $n=2$ ;  $^{13}\text{C-CH}_4$ ,  $n=4$ ) in air, as detailed in [9]; incubation was terminated when approximately 30  $\mu\text{mol CH}_4$  per g soil was consumed. In all microcosms, the soil was homogenized, sampled, and stored in the -20 °C freezer till DNA extraction after the incubation.

Methane was measured daily during the incubation using a gas chromatograph (7890B GC System, Agilent Technologies, Santa Clara, USA) coupled to a pulsed discharge helium ionization detector (PD-HID), with helium as the carrier gas. Cumulative methane uptake is reported. Inorganic nitrogen (ammonium and nitrate) concentrations were determined in autoclaved deionized water (1:1 or 1:2  $^{\text{unlabelled}}\text{C-CH}_4$ ) after centrifugation and filtration (0.22  $\mu\text{m}$ ) with standard colorimetric methods [75, 76], while total sulphate was determined using a modified colorimetric assay after Wolfson [77]; all colorimetric assays were performed using an Infinite M plex plate reader (TECAN, Meannedorf, Switzerland). Total C and N were determined from air-dried (50 °C) and milled soils using a Vario EL III elemental analyzer (Elementar Analysensysteme GmbH, Langensfeld, Germany).

### DNA-SIP with $^{13}\text{C-CH}_4$

DNA was extracted using the DNeasy PowerSoil Kit (Qiagen, Hilden, Germany) according to the manufacturer's instructions. DNA was extracted in duplicate per sample to obtain sufficient amounts for the isopycnic ultracentrifugation.

The DNA-SIP with  $^{13}\text{C-CH}_4$  was performed as described before [9, 78]. Isopycnic ultracentrifugation was performed using an Optima L-80XP (Beckman Coulter Inc., USA) at 144,000 g for 67 h. Immediately after centrifugation, fractionation was performed using a peristaltic pump (Duelabo, Dusseldorf, Germany) at 2.8 rpm  $\text{min}^{-1}$ . Nine or ten fractions were obtained per sample, after discarding the final fraction.

Fractionation was unsuccessful for one out of the four replicates of the riparian soil. The density gradient of each fraction was determined using an AR200 digital refractometer (Reichert Technologies, Munich, Germany). Thereafter, the DNA from each fraction was precipitated and washed twice with ethanol, and the pellet was re-suspended in 30  $\mu\text{L}$  ultrapure PCR water (INVITROGEN, Waltham, USA). The *pmoA* gene was quantified from the precipitated DNA for each fraction using quantitative PCR, qPCR (MTOT assay; [79]) to distinguish the “heavy” ( $^{13}\text{C}$ -enriched DNA) and “light” (unlabelled C-DNA) fractions after comparing the fractions derived from the  $^{13}\text{C}$ - and unlabelled C- $\text{CH}_4$  incubations (Additional file 3: Figure S2 & Additional file 4: Figure S3). The “heavy” and “light” DNA fractions were identified as defined in Neufeld et al. [78]. The 16S rRNA gene from these fractions was subsequently amplified for Illumina MiSeq sequencing and network construction.

#### Quantitative PCR (qPCR)

The qPCR assay was performed to enumerate the *pmoA* gene abundance after fractionation (DNA-SIP), and to follow the change in the *pmoA* relative to the 16S rRNA gene abundance during the incubation. The increase in the *pmoA*:16S rRNA gene abundance ratio is indicative of methanotrophic growth [8], complementing the DNA-SIP. The qPCR was performed using a BIORAD CFX Connect RT System (Biorad, Hercules, USA). Each qPCR reaction (total volume, 20  $\mu\text{L}$ ) targeting the *pmoA* gene consisted of 10  $\mu\text{L}$  SYBR 2X Sensifast (BIOLINE, London, UK), 3.5  $\mu\text{L}$  of A189f/mb661r primer each (4  $\mu\text{M}$ ), 1  $\mu\text{L}$  BSA (1%), and 2  $\mu\text{L}$  template DNA. Each qPCR reaction (total volume, 20  $\mu\text{L}$ ) targeting the 16S rRNA gene consisted of 10  $\mu\text{L}$  SYBR 2X Sensifast, 1.2  $\mu\text{L}$   $\text{MgCl}_2$  (50 mM), 2.0  $\mu\text{L}$  of 341F/907R primer each (10  $\mu\text{M}$ ), 1.8  $\mu\text{L}$  of PCR-grade water, 1  $\mu\text{L}$  BSA (1%), and 2  $\mu\text{L}$  template DNA. The PCR thermal profiles are given elsewhere [8, 79]. Template DNA was undiluted when quantifying the *pmoA* gene after fractionation, and diluted 50 or 100-fold with RNase- and DNase-free water when enumerating the *pmoA* and 16S rRNA gene from the DNA isolated from the soil. These dilutions resulted in the optimal gene copy numbers. The calibration curve, ranging from  $10^1$  to  $10^7$  copy number of target genes, was derived from clones (*pmoA* gene) or plasmid DNA (16S rRNA gene) as described before [47]. The PCR efficiency was on average 90–95%, depending on the qPCR assay. Amplicon specificity was assessed from the melt curve, and further confirmed by 1% agarose gel electrophoresis.

#### 16S rRNA gene amplicon preparation and Illumina MiSeq sequencing

The 16S rRNA gene was amplified with the primer pair 341F/805R. Each PCR reaction (total volume, 40  $\mu\text{L}$ ) consisted of 20  $\mu\text{L}$  KAPA HIFI (Roche, Basel, Switzerland), 2  $\mu\text{L}$  forward/reverse tagged-primer each (10  $\mu\text{M}$ ), 2  $\mu\text{L}$  BSA (1%), 4  $\mu\text{L}$  template DNA, and 10  $\mu\text{L}$  PCR-grade water. The template DNA was replaced with equivalent amounts of PCR-grade water and DNA derived from *Rhodanobacter denitrificans* in the negative and positive control, respectively. The positive control was confirmed after sequencing, resulting in the retrieval of sequences affiliated to *R. denitrificans*, as expected; there was no amplification in the negative control. The PCR thermal profile consisted of an initial denaturation step at 95  $^\circ\text{C}$  for 3 min, followed by 30 cycles of denaturation at 98  $^\circ\text{C}$  for 20 s, annealing at 53  $^\circ\text{C}$  for 15 s, and elongation at 72  $^\circ\text{C}$  for 15 s. The final elongation step was at 72  $^\circ\text{C}$  for 1 min. Amplicon specificity was verified by 1% agarose gel electrophoresis. Thereafter, the PCR product was purified using the GeneRead Size Selection Kit (Qiagen, Hilden, Germany) to be used as template (5  $\mu\text{L}$ ) for the second PCR. The second PCR was performed to attach the adapters to the amplicons using the Nextera XT index kit (Illumina, San Diego, USA). The reagents, reagent concentrations, and thermal profile for the second PCR are given elsewhere [9]. After the second PCR, the amplicons were purified using the MagSi-NGS<sup>PREP</sup> Plus Magnetic beads (Steinbrenner Laborsysteme GmbH, Wiesenbach, Germany) according to the manufacturer’s instructions. Equimolar amounts (133 ng) of the amplicons from each sample were pooled for library preparation and sequencing using the Illumina MiSeq version 3 chemistry (paired-end, 600 cycles).

#### 16S rRNA gene amplicon analyses

Firstly, the 16S rRNA gene paired-end reads were merged using PEAR [80], and subsequently processed using QIIME 2 version 2019.10. The de-multiplex and quality control steps were performed with DADA2 [81] using the consensus method to remove remaining chimeric and low-quality sequences. After filtering, approximately 5,650,000 high quality sequences were obtained, with an average of  $\sim 49,570$  sequences per sample. Singletons and doubletons were removed, and the samples were rarefied to 11,600 sequences following the sample with the lowest number of sequences. Classification was performed at 97% similarity based on the Silva database v. 132 [82]. Because the aerobic methanotrophs are restricted to <30 genera from two phyla [30], they were identified using the “search” function in the OTU table. The composition of the active bacterial community from different

environments was visualized as a RDA based on the relative abundance of the 16S rRNA gene diversity. The data matrix was initially analysed using the detrended correspondence analysis (DCA), indicating a linear data distribution and the best-fit mathematical model was the RDA. Also, plot clustering was performed using permutational multivariate analysis of variance (PERMANOVA; [83]) to test whether the different environments harboured significantly different active bacterial communities and whether the communities in the “heavy” and “light” fractions were distinct. The PERMANOVA was calculated using PAST 4 software [84]. The RDA analysis was implemented in Canoco 4.5 (Biometrics, Wageningen, The Netherlands). The 16S rRNA gene sequences (sample names/treatments and corresponding accession numbers are listed in Additional file 14: Table S4) were deposited at the National Center for Biotechnology Information (NCBI) under the BioProject ID number PRJNA751592.

#### Co-occurrence network analysis

The complexity of the interaction was explored using a co-occurrence network analysis, based on the 16S rRNA gene (OTU level) derived from the  $^{13}\text{C}$ -enriched DNA (“heavy” fraction), representing the active community. Moreover, networks were also constructed from the unlabelled DNA from the  $^{12}\text{C}$ - $\text{CH}_4$  incubations to be compared to the networks derived from the  $^{13}\text{C}$ -enriched DNA. The networks were derived from at least 3 replicates. Previously, we showed that networks derived from an uneven number of replicates (e.g., 3–5) and a randomly chosen subset of replicates showed comparable results [9]. To remove weak and spurious correlations, only the OTUs with  $\geq 10$  sequences were included in the analysis, which represented  $>90\%$  of the total amount of sequences. The co-occurrence analysis between absolute OTUs counts were calculated using the Python module “SparCC”, a tool designed to generate and assess the correlations of the compositional data [85]. True SparCC correlations with a magnitude of  $>0.8$  (positive correlation) or  $<-0.8$  (negative correlation), and statistical significance of  $p < 0.01$  were selected for the network construction. The  $p$ -values were obtained by 99 permutations of random selections of the data tables. All networks were constructed in parallel using the same analytical pipeline, including re-analysis of networks from the rice paddy soil and peatland together with the current dataset. This enables direct comparison of the networks derived from the different environments and over time. Assessment of the networks was based on their topological properties, which includes the number of nodes and edges, modularity, number of communities, network diameter, average path length, degree,

and clustering coefficient (interpretation of these network properties are provided in Table 2; [13, 86, 87]). Additionally, the correlations between the methanotrophs, and methanotrophs/non-methanotrophs were identified to determine potential intra-methanotroph and non-methanotroph interacting partners. The network construction and topological properties were calculated with Gephi [88].

#### Statistical analysis

Statistical analysis was performed in PAST 4 software [84]. Normal distribution was tested using the Shapiro–Wilk test, and homogeneity of variance was tested using Levene’s test. Where normality and homogeneity of data were met, an ANOVA with Tukey post-hoc test ( $p < 0.05$ ) was performed for comparisons between sites and over time in the pristine peatland. Otherwise, a Kruskal–Wallis ANOVA and Dunn’s post-hoc test ( $p < 0.05$ ) were performed.

#### Abbreviations

ANOVA: Analysis of variance; BSA: Bovine serum albumin; DNA: Deoxyribonucleic acid; OTU: Operational taxonomic unit; PCA: Principal component analysis; PCR: Polymerase chain reaction; PD-HID: Pulsed discharge helium ionization detector; PERMANOVA: Permutational multivariate analysis of variance; PLFA: Phospholipid fatty acids; pmoA: Particulate methane monooxygenase Subunit A; qPCR: Quantitative polymerase chain reaction; RDA: Redundancy analysis; RNA: Ribonucleic acid; SIP: Stable isotope probing.

#### Supplementary Information

The online version contains supplementary material available at <https://doi.org/10.1186/s40793-022-00409-1>.

**Additional file 1. Text file.** Supplementary table and figure legends.

**Additional file 2. Figure S1.** The *pmoA* and 16S rRNA gene abundances in the starting material and after incubation in diverse environments (mean  $\pm$  s.d.;  $n \geq 4$ ). The qPCR assay was performed in duplicate for each DNA extraction. The 16S rRNA and *pmoA* gene abundances for all samples were at least an order of magnitude higher than the lower detection limit of the qPCR assays. The upper and lower case letters indicate the level of significance ( $p < 0.05$ ) of the 16S rRNA gene and *pmoA* gene abundance between environments in the starting material. The asterisk indicates significant difference ( $p < 0.05$ ) in the starting *pmoA* gene abundance and after incubation. The numbers at the top of each bar refer to the *pmoA*:16S rRNA gene abundance ratio in percentage (%), which increased after incubation.

**Additional file 3. Figure S2.** Relative *pmoA* gene abundance along the density gradient of the  $^{13}\text{C}$ - and  $^{12}\text{C}$ - $\text{CH}_4$  incubations with the (a) paddy soil, (b) landfill cover soil, (c) restored peatland, (d) pristine peatland, and (e) riparian soil (mean  $\pm$  s.d.;  $n=4$  each). The results of the paddy soil (a; [2]) and the peatlands (c,d; [1]) were re-analysed for the present study. The *pmoA* gene relative abundance was calculated as the proportion of each fraction over the total sum of all fractions per sample. The density gradients of the  $^{13}\text{C}$ - and  $^{12}\text{C}$ - $\text{CH}_4$  incubations were compared to distinguish the “light” from the “heavy” fraction in the  $^{13}\text{C}$ - $\text{CH}_4$  incubation. The arrows denote the “light” and “heavy” fractions where the 16S rRNA gene was amplified for Illumina MiSeq sequencing in the  $^{13}\text{C}$ - $\text{CH}_4$  incubations.



**Additional file 4. Figure S3.** Relative *pmoA* gene abundance along the density gradient of the  $^{13}\text{C}$ - and  $^{12}\text{C}$ - $\text{CH}_4$  incubations in the pristine peat at days 8, 13, and 19 (mean  $\pm$  s.d.;  $n=4$  each). The *pmoA* gene relative abundance was calculated as the proportion of each fraction over the total sum of all fractions per sample. The arrows denote the "light" and "heavy" fractions where the 16S rRNA gene was amplified for Illumina MiSeq sequencing in the  $^{13}\text{C}$ - $\text{CH}_4$  incubations.

**Additional file 5. Figure S4.** Mean relative abundance of the methanotroph-affiliated OTUs in the paddy soil, landfill cover soil, pristine/restored peatlands, and riparian soil based on the 16S rRNA gene sequences in the starting material and after the incubation with  $^{13}\text{C}$ -methane ("light" and "heavy" fractions). The numbers at the bottom of the bars denote the mean proportion (%) of the methanotroph-affiliated OTUs among the total 16S rRNA gene sequences. Abbreviations; S.M, starting material; L, "light" fraction; H, "heavy" fraction.

**Additional file 6. Figure S5.** Mean relative abundance of the methanotroph-affiliated OTUs in the pristine peatland after 8, 13, and 19 days incubation with  $^{13}\text{C}$ -methane ("light" and "heavy" fractions), based on the 16S rRNA gene sequences. The numbers at the bottom of the bars denote the mean proportion (%) of the methanotroph-affiliated OTUs among the total 16S rRNA gene sequences.

**Additional file 7. Figure S6.** Principal component analysis showing the clustering of the 16S rRNA gene sequences in the "light" and "heavy" fractions of the (a) paddy soil (orange, triangle), (b) landfill cover soil (purple, circle), (c) pristine peatland (light green, square), (d) restored peatland (dark green, square), and (e) riparian soil (blue, inverted triangle). All replicates ( $n=4$ ) are given; in the incubation with the riparian soil, fractionation was unsuccessful for one replicate. Full colored and striped symbols represent the "light" and "heavy" fraction, respectively.

**Additional file 8. Figure S7.** Principal component analysis showing the clustering of the 16S rRNA gene sequences in the "light" and "heavy" fractions of the pristine peatland over time (days 8, 13, and 19). All replicates ( $n=4$ ) are given. Full colored and striped symbols represent the "heavy" and "light" fraction, respectively.

**Additional file 9. Figure S8.** Co-occurrence network analysis of methane hotspots derived from the  $^{13}\text{C}$ - and  $^{12}\text{C}$ -DNA. The corresponding topological parameters of the networks are provided in Table 2. Each node represents a bacterial taxon at the OTU level, while the size and shade of the node corresponds to the number of connections per node and the number of connections passing through the node (i.e., darker shade for nodes acting as a bridge between other nodes at higher frequencies), respectively. A connection denotes significant SparCC correlation ( $p < 0.01$ ) with a magnitude of  $> 0.8$  (positive correlation, blue edges) or  $< -0.8$  (negative correlations, red edges).

**Additional file 10. Figure S9.** Co-occurrence network analysis after 8, 13, and 19 days incubation of the pristine peat derived from the  $^{13}\text{C}$ - and  $^{12}\text{C}$ -DNA. The corresponding topological parameters of the networks are provided in Table 3. Each node represents a bacterial taxon at the OTU level, while the size and shade of the node corresponds to the number of connections per node and the number of connections passing through the node (i.e., darker shade for nodes acting as a bridge between other nodes at higher frequencies), respectively. A connection denotes significant SparCC correlation ( $p < 0.01$ ) with a magnitude of  $> 0.8$  (positive correlation, blue edges) or  $< -0.8$  (negative correlations, red edges).

**Additional file 11. Table S1.** Selected physico-chemical parameters and methane uptake rates of individual replicates in methane hotspots (rice paddy soil, landfill cover soil, pristine peatland, restored peatland, and riparian soil). Summarized data given in Table 1.

**Additional file 12. Table S2.** Significantly positively and negatively co-occurring ( $p < 0.01$ ) OTUs between environments, as determined by the co-occurrence network analysis. The first panel shows site-specific co-occurring OTUs, while the other panels show shared co-occurring OTUs between environments. The OTUs were given to the finest resolvable taxonomic affiliation based on the Silva database v. 132, whenever available. The number in brackets refer to the OTU numbers. Abbreviations: pos, positive correlations; neg, negative correlations; RP, rice paddy; LC,

landfill cover soil; PP, pristine peatland; RP, restored peatland; RS, riparian soil; MIP, methanotroph interacting partner (including other co-occurring methanotrophs).

**Additional file 13. Table S3.** Significantly positively and negatively co-occurring ( $p < 0.01$ ) OTUs in the pristine peatland over time (days 8, 13, and 19, respectively denoted by T1, T2, and T3), as determined by the co-occurrence network analysis. The first panel shows co-occurring OTUs at each time interval while the other panels show shared co-occurring OTUs between time intervals. The OTUs were given to the finest resolvable taxonomic affiliation based on the Silva database v. 132, whenever available. The number in brackets refer to the OTU numbers. Abbreviations: pos, positive correlations; neg, negative correlations; T1, after 8 days incubation; T2, after 13 days incubation; T3, after 19 days incubation; MIP, methanotroph interacting partner (including other co-occurring methanotrophs).

**Additional file 14. Table S4.** Sample names/treatment and corresponding accession numbers (BioProject PRJNA751592). Sample name is labelled in the following order: site, sampling time, 12C or 13C (i.e.,  $^{12}\text{C}$  or  $^{13}\text{C}$ - $\text{CH}_4$  incubations), H or L (i.e., "heavy" or "light" fractions). Note that for the pristine peatland, T1 and T3 correspond to days 8 and 19, respectively; samples from day 13 are published (Table 1; [1]).

#### Acknowledgements

We thank Stefanie Hetz for technical assistance with the stable isotope probing, and Hester van Dijk and Natalie Röder for assistance with sample collection and preparation. We also thank AHA (Germany) for permission to collect samples from the landfill cover.

#### Authors' contributions

MH and AH conceived the experiment. TK, LM, and AH planned the experiment. TK and SR collected the samples. TK and DF performed the experiments. AP performed the sequencing. TK, LM and AH analysed the data. TK and AH wrote the manuscript with contributions from all authors. All authors read and approved the final manuscript.

#### Funding

Open Access funding enabled and organized by Projekt DEAL. This study is financially supported by the Deutsche Forschungsgemeinschaft (grant no. HO6234/1-1) to TK and AH, and the Leibniz Universität Hannover, Germany to MH and AH. SR is financially supported by the DFG (Project no. 391977956, SFB 1357, subproject C04).

#### Availability of data and materials

The sequencing data generated in this study were deposited to the National Center for Biotechnology Information (NCBI) under the BioProject ID number PRJNA751592. The sequencing data can be accessed using the following web link: <https://www.ncbi.nlm.nih.gov/bioproject/PRJNA751592>. All other data generated or analysed during this study were included in this article and its Additional files.

#### Declarations

##### Ethics approval and consent to participate

Not applicable.

##### Consent for publication

Not applicable.

##### Competing interests

The authors declare that they have no competing interests.

##### Author details

<sup>1</sup>Institute for Microbiology, Leibniz Universität Hannover, Herrenhäuser Str. 2, 30419 Hannover, Germany. <sup>2</sup>Center for Nuclear Energy in Agriculture, University of São Paulo CENA-USP, Piracicaba, SP, Brazil. <sup>3</sup>Department of Genomic and Applied Microbiology and Göttingen Genomics Laboratory, Institute of Microbiology and Genetics, George-August University Göttingen, Grisebachstr. 8, 37077 Göttingen, Germany.

Received: 30 August 2021 Accepted: 15 March 2022  
Published online: 05 April 2022

## References

- Morris BEL, Henneberger R, Huber H, Moissl-Eichinger C. Microbial syntrophy: interaction for the common good. *FEMS Microbiol Rev.* 2013;37:384–406. <https://doi.org/10.1111/1574-6976.12019>.
- Ho A, de Roy K, Thas O, de Neve J, Hoefman S, Vandamme P, et al. The more, the merrier: heterotroph richness stimulates methanotrophic activity. *ISME J.* 2014;8:1945–8. <https://doi.org/10.1038/ismej.2014.74>.
- D'Souza G, Shitut S, Preussger D, Yousif G, Waschina S, Kost C. Ecology and evolution of metabolic cross-feeding interactions in bacteria. *Nat Prod Rep.* 2018;35:455–88. <https://doi.org/10.1039/c8np00009c>.
- Johnson WM, Alexander H, Bier RL, Miller DR, Muscarella ME, Pitz KJ, Smith H. Auxotrophic interactions: a stabilizing attribute of aquatic microbial communities? *FEMS Microbiol Ecol.* 2020;96:faa115. doi:<https://doi.org/10.1093/femsec/faa115>.
- Veraart AJ, Garbeva P, van Beersum F, Ho A, Hordijk CA, Meima-Franke M, et al. Living apart together-bacterial volatiles influence methanotrophic growth and activity. *ISME J.* 2018;12:1163–6. <https://doi.org/10.1038/s41396-018-0055-7>.
- Benner J, de Smet D, Ho A, Kerckhof F-M, Vanhaecke L, Heylen K, Boon N. Exploring methane-oxidizing communities for the co-metabolic degradation of organic micropollutants. *Appl Microbiol Biotechnol.* 2015;99:3609–18. <https://doi.org/10.1007/s00253-014-6226-1>.
- García-Contreras R, Loarca D. The bright side of social cheaters: potential beneficial roles of "social cheaters" in microbial communities. *FEMS Microbiol Ecol.* 2021;97:faa239. doi:<https://doi.org/10.1093/femsec/faa239>.
- Kaupper T, Mendes LW, Harnisz M, Krause SMB, Horn MA, Ho A. Recovery in methanotrophic activity does not reflect on the methane-driven interaction network after peat mining. *Appl Environ Microbiol.* 2021;87:e02355–e2420. <https://doi.org/10.1128/AEM.02355-20>.
- Kaupper T, Mendes LW, Lee HJ, Mo Y, Poehlein A, Jia Z, et al. When the going gets tough: emergence of a complex methane-driven interaction network during recovery from desiccation-rewetting. *Soil Biol Biochem.* 2021;153: 108109. <https://doi.org/10.1016/j.soilbio.2020.108109>.
- Ho A, Angel R, Veraart AJ, Daebeler A, Jia Z, Kim SY, et al. Biotic Interactions in microbial communities as modulators of biogeochemical processes: methanotrophy as a model system. *Front Microbiol.* 2016;7:1285. <https://doi.org/10.3389/fmicb.2016.01285>.
- Barberán A, Bates ST, Casamayor EO, Fierer N. Using network analysis to explore co-occurrence patterns in soil microbial communities. *ISME J.* 2012;6:343–51. <https://doi.org/10.1038/ismej.2011.119>.
- Williams RJ, Howe A, Hofmøckel KS. Demonstrating microbial co-occurrence pattern analyses within and between ecosystems. *Front Microbiol.* 2014;5:358. <https://doi.org/10.3389/fmicb.2014.00358>.
- Peura S, Bertilsson S, Jones RI, Eiler A. Resistant microbial co-occurrence patterns inferred by network topology. *Appl Environ Microbiol.* 2015;81:2090–7. <https://doi.org/10.1128/AEM.03660-14>.
- Tripathi BM, Edwards DP, Mendes LW, Kim M, Dong K, Kim H, Adams JM. The impact of tropical forest logging and oil palm agriculture on the soil microbiome. *Mol Ecol.* 2016;25:2244–57. <https://doi.org/10.1111/mec.13620>.
- Ho A, Mendes LW, Lee HJ, Kaupper T, Mo Y, Poehlein A, et al. Response of a methane-driven interaction network to stressor intensification. *FEMS Microbiol Ecol.* 2020;96:180. <https://doi.org/10.1093/femsec/faa180>.
- Rossmann M, Pérez-Jaramillo JE, Kavamura VN, Chiaramonte JB, Dumack K, Fiore-Donno AM, et al. Multitrophic interactions in the rhizosphere microbiome of wheat: from bacteria and fungi to protists. *FEMS Microbiol Ecol.* 2020;96:faa032. doi:<https://doi.org/10.1093/femsec/faa032>.
- Li D, Ni H, Jiao S, Lu Y, Zhou J, Sun B, Liang Y. Coexistence patterns of soil methanogens are closely tied to methane generation and community assembly in rice paddies. *Microbiome.* 2021;9:20. <https://doi.org/10.1186/s40168-020-00978-8>.
- Zelezniak A, Andrejev S, Ponomarova O, Mende DR, Bork P, Patil KR. Metabolic dependencies drive species co-occurrence in diverse microbial communities. *Proc Natl Acad Sci U S A.* 2015;112:6449–54. <https://doi.org/10.1073/pnas.1421834112>.
- Ghoul M, Mitri S. The ecology and evolution of microbial competition. *Trends Microbiol.* 2016;24:833–45. <https://doi.org/10.1016/j.tim.2016.06.011>.
- Dann LM, Clanahan M, Paterson JS, Mitchell JG. Distinct niche partitioning of marine and freshwater microbes during colonisation. *FEMS Microbiol Ecol.* 2019;95:fiz098. doi:<https://doi.org/10.1093/femsec/fiz098>.
- Chang J, Kim DD, Semrau JD, Lee J, Heo H, Gu W, Yoon S. Enhancement of nitrous oxide emissions in soil microbial consortia via copper competition between proteobacterial methanotrophs and denitrifiers. *Appl Environ Microbiol.* 2021;87:e02301–e2320. <https://doi.org/10.1128/AEM.02301-20>.
- Iguchi H, Yurimoto H, Sakai Y. Stimulation of methanotrophic growth in cocultures by cobalamin excreted by rhizobia. *Appl Environ Microbiol.* 2011;77:8509–15. <https://doi.org/10.1128/AEM.05834-11>.
- Murase J, Frenzel P. Selective grazing of methanotrophs by protozoa in a rice field soil. *FEMS Microbiol Ecol.* 2008;65:408–14. <https://doi.org/10.1111/j.1574-6941.2008.00511.x>.
- Stock M, Hoefman S, Kerckhof F-M, Boon N, de Vos P, de Baets B, et al. Exploration and prediction of interactions between methanotrophs and heterotrophs. *Res Microbiol.* 2013;164:1045–54. <https://doi.org/10.1016/j.resmic.2013.08.006>.
- Sharp CE, Smirnova AV, Graham JM, Stott MB, Khadka R, Moore TR, et al. Distribution and diversity of Verrucomicrobia methanotrophs in geothermal and acidic environments. *Environ Microbiol.* 2014;16:1867–78. <https://doi.org/10.1111/1462-2920.12454>.
- Schmitz RA, Peeters SH, Versantvoort W, Picone N, Pol A, Jetten MSM, Op den Camp HJM. Verrucomicrobial methanotrophs: ecophysiology of metabolically versatile acidophiles. *FEMS Microbiol Rev.* 2021:fuab007. doi:<https://doi.org/10.1093/femsre/fuab007>.
- Dedysh SN, Dunfield PF. Facultative and obligate methanotrophs how to identify and differentiate them. *Methods Enzymol.* 2011;495:31–44. <https://doi.org/10.1016/B978-0-12-386905-0.00003-6>.
- Trotsenko YA, Murrell JC. Metabolic Aspects of Aerobic Obligate Methanotrophy. In: Laskin AI, Gadd GM, Sariaslani S, editors. *Advances in applied microbiology*: Vol. 63. 1st ed. Amsterdam: Academic Press; 2008. p. 183–229. doi:[https://doi.org/10.1016/S0065-2164\(07\)00005-6](https://doi.org/10.1016/S0065-2164(07)00005-6).
- Farhan UI Haque M, Crombie AT, Murrell JC. Novel facultative Methylocella strains are active methane consumers at terrestrial natural gas seeps. *Microbiome.* 2019;7:134. doi:<https://doi.org/10.1186/s40168-019-0741-3>.
- Guerrero-Cruz S, Vaksmaa A, Horn MA, Niemann H, Pijuan M, Ho A. Methanotrophs: discoveries, environmental relevance, and a perspective on current and future applications. *Front Microbiol.* 2021;12: 678057. <https://doi.org/10.3389/fmicb.2021.678057>.
- Praeg N, Schachner I, Schuster L, Illmer P. Carbon-dependent growth, community structure and methane oxidation performance of a soil-derived methanotrophic mixed culture. *FEMS Microbiol Lett.* 2021;368:fnaa212. doi:<https://doi.org/10.1093/femsle/fnaa212>.
- Reim A, Lücke C, Krause S, Pratscher J, Frenzel P. One millimetre makes the difference: high-resolution analysis of methane-oxidizing bacteria and their specific activity at the oxic-anoxic interface in a flooded paddy soil. *ISME J.* 2012;6:2128–39. <https://doi.org/10.1038/ismej.2012.57>.
- Shrestha PM, Kammann C, Lenhart K, Dam B, Liesack W. Linking activity, composition and seasonal dynamics of atmospheric methane oxidizers in a meadow soil. *ISME J.* 2012;6:1115–26. <https://doi.org/10.1038/ismej.2011.179>.
- Ho A, Lee HJ, Reumer M, Meima-Franke M, Raaijmakers C, Zweers H, et al. Unexpected role of canonical aerobic methanotrophs in upland agricultural soils. *Soil Biol Biochem.* 2019;131:1–8. <https://doi.org/10.1016/j.soilbio.2018.12.020>.
- Täumer J, Kolb S, Boeddinghaus RS, Wang H, Schöning I, Schrupp M, et al. Divergent drivers of the microbial methane sink in temperate forest and grassland soils. *Glob Change Biol.* 2021;27:929–40. <https://doi.org/10.1111/gcb.15430>.
- Krause SMB, Johnson T, Samadhi Karunaratne Y, Fu Y, Beck DAC, Chistoserdova L, Lidstrom ME. Lanthanide-dependent cross-feeding of methane-derived carbon is linked by microbial community interactions. *Proc Natl Acad Sci U S A.* 2017;114:358–63. <https://doi.org/10.1073/pnas.1619871114>.
- van Grinsven S, Oswald K, Wehrli B, Jegge C, Zopfi J, Lehmann MF, Schubert CJ. Methane oxidation in the waters of a humic-rich boreal lake

- stimulated by photosynthesis, nitrite, Fe(III) and humics. *Biogeosciences*. 2021;18:3087–101. <https://doi.org/10.5194/bg-18-3087-2021>.
38. Krause S, Lüke C, Frenzel P. Methane source strength and energy flow shape methanotrophic communities in oxygen-methane counter-gradients. *Environ Microbiol Rep*. 2012;4:203–8. <https://doi.org/10.1111/j.1758-2229.2011.00322.x>.
  39. Ho A, Kerckhof F-M, Luke C, Reim A, Krause S, Boon N, Bodelier PLE. Conceptualizing functional traits and ecological characteristics of methane-oxidizing bacteria as life strategies. *Environ Microbiol Rep*. 2013;5:335–45. <https://doi.org/10.1111/j.1758-2229.2012.00370.x>.
  40. Conrad R. The global methane cycle: recent advances in understanding the microbial processes involved. *Environ Microbiol Rep*. 2009;1:285–92. <https://doi.org/10.1111/j.1758-2229.2009.00038.x>.
  41. Singh BK, Bardgett RD, Smith P, Reay DS. Microorganisms and climate change: terrestrial feedbacks and mitigation options. *Nat Rev Microbiol*. 2010;8:779–90. <https://doi.org/10.1038/nrmicro2439>.
  42. Henneberger R, Lüke C, Mosberger L, Schroth MH. Structure and function of methanotrophic communities in a landfill-cover soil. *FEMS Microbiol Ecol*. 2012;81:52–65. <https://doi.org/10.1111/j.1574-6941.2011.01278.x>.
  43. Tveit AT, Hestnes AG, Robinson SL, Schintlmeister A, Dedys SN, Jehmlich N, et al. Widespread soil bacterium that oxidizes atmospheric methane. *Proc Natl Acad Sci U S A*. 2019;116:8515–24. <https://doi.org/10.1073/pnas.1817812116>.
  44. Cai Y, Zheng Y, Bodelier PLE, Conrad R, Jia Z. Conventional methanotrophs are responsible for atmospheric methane oxidation in paddy soils. *Nat Commun*. 2016;7:11728. <https://doi.org/10.1038/ncomms11728>.
  45. Ho A, Reim A, Kim SY, Meima-Franke M, Termorshuizen A, de Boer W, et al. Unexpected stimulation of soil methane uptake as emergent property of agricultural soils following bio-based residue application. *Glob Change Biol*. 2015;21:3864–79. <https://doi.org/10.1111/gcb.12974>.
  46. Noll M, Matthies D, Frenzel P, Derakshani M, Liesack W. Succession of bacterial community structure and diversity in a paddy soil oxygen gradient. *Environ Microbiol*. 2005;7:382–95. <https://doi.org/10.1111/j.1462-2920.2005.00700.x>.
  47. Ho A, Lüke C, Frenzel P. Recovery of methanotrophs from disturbance: population dynamics, evenness and functioning. *ISME J*. 2011;5:750–8. <https://doi.org/10.1038/ismej.2010.163>.
  48. Drenovsky RE, Steenwerth KL, Jackson LE, Scow KM. Land use and climatic factors structure regional patterns in soil microbial communities. *Glob Ecol Biogeogr*. 2010;19:27–39. <https://doi.org/10.1111/j.1466-8238.2009.00486.x>.
  49. Ho A, Ijaz UZ, Janssens TKS, Ruijs R, Kim SY, de Boer W, et al. Effects of bio-based residue amendments on greenhouse gas emission from agricultural soil are stronger than effects of soil type with different microbial community composition. *GCB Bioenergy*. 2017;9:1707–20. <https://doi.org/10.1111/gcbb.12457>.
  50. Keller JK, Bauers AK, Bridgman SD, Kellogg LE, Iversen CM. Nutrient control of microbial carbon cycling along an ombrotrophic-minerotrophic peatland gradient. *J Geophys Res*. 2006. <https://doi.org/10.1029/2005JG000152>.
  51. Zhou J, Deng Y, Luo F, He Z, Tu Q, Zhi X. Functional molecular ecological networks. *MBio*. 2010;1:1–10. <https://doi.org/10.1128/mBio.00169-10>.
  52. Bissett A, Brown MV, Siciliano SD, Thrall PH. Microbial community responses to anthropogenically induced environmental change: towards a systems approach. *Ecol Lett*. 2013;16:128–39. <https://doi.org/10.1111/ele.12109>.
  53. van Elsas JD, Chiurazzi M, Mallon CA, Elhottova D, Kristufek V, Salles JF. Microbial diversity determines the invasion of soil by a bacterial pathogen. *Proc Natl Acad Sci U S A*. 2012;109:1159–64. <https://doi.org/10.1073/pnas.1109326109>.
  54. Estrada E. Food webs robustness to biodiversity loss: the roles of connectance, expansibility and degree distribution. *J Theor Biol*. 2007;244:296–307. <https://doi.org/10.1016/j.jtbi.2006.08.002>.
  55. Larmola T, Leppänen SM, Tuittila E-S, Aarva M, Merilä P, Fritze H, Tirola M. Methanotrophy induces nitrogen fixation during peatland development. *Proc Natl Acad Sci U S A*. 2014;111:734–9. <https://doi.org/10.1073/pnas.1314284111>.
  56. Ho A, Bodelier PLE. Diazotrophic methanotrophs in peatlands: the missing link? *Plant Soil*. 2015;389:419–23. <https://doi.org/10.1007/s11104-015-2393-9>.
  57. Taubert M, Grob C, Crombie A, Howat AM, Burns OJ, Weber M, et al. Communal metabolism by Methylococcaceae and Methylophilaceae is driving rapid aerobic methane oxidation in sediments of a shallow seep near Elba, Italy. *Environ Microbiol*. 2019;21:3780–95. <https://doi.org/10.1111/1462-2920.14728>.
  58. Oshkin IY, Beck DAC, Lamb AE, Tchesnokova V, Benuska G, McTaggart TL, et al. Methane-fed microbial microcosms show differential community dynamics and pinpoint taxa involved in communal response. *ISME J*. 2015;9:1119–29. <https://doi.org/10.1038/ismej.2014.203>.
  59. Dumont MG, Pommerenke B, Casper P, Conrad R. DNA-, rRNA- and mRNA-based stable isotope probing of aerobic methanotrophs in lake sediment. *Environ Microbiol*. 2011;13:1153–67. <https://doi.org/10.1111/j.1462-2920.2010.02415.x>.
  60. Petters S, Groß V, Söllinger A, Pichler R, Reinhard A, Bengtsson MM, Urich T. The soil microbial food web revisited: predatory myxobacteria as keystone taxa? *ISME J*. 2021. <https://doi.org/10.1038/s41396-021-00958-2>.
  61. Muñoz-Dorado J, Marcos-Torres FJ, García-Bravo E, Moraleda-Muñoz A, Pérez J. Myxobacteria: moving, killing, feeding, and surviving together. *Front Microbiol*. 2016;7:781. <https://doi.org/10.3389/fmicb.2016.00781>.
  62. Lueders T, Kindler R, Miltner A, Friedrich MW, Kaestner M. Identification of bacterial micropredators distinctively active in a soil microbial food web. *Appl Environ Microbiol*. 2006;72:5342–8. <https://doi.org/10.1128/AEM.00400-06>.
  63. Ye X, Li Z, Luo X, Wang W, Li Y, Li R, et al. A predatory myxobacterium controls cucumber Fusarium wilt by regulating the soil microbial community. *Microbiome*. 2020;8:49. <https://doi.org/10.1186/s40168-020-00824-x>.
  64. Murase J, Frenzel P. A methane-driven microbial food web in a wetland rice soil. *Environ Microbiol*. 2007;9:3025–34. <https://doi.org/10.1111/j.1462-2920.2007.01414.x>.
  65. Sangwan P, Chen X, Hugenholtz P, Janssen PH. *Chthoniobacter flavus* gen. nov., sp. nov., the first pure-culture representative of subdivision two, *Spartobacteria* classis nov., of the phylum *Verrucomicrobia*. *Appl Environ Microbiol*. 2004;70:5875–81. doi:<https://doi.org/10.1128/AEM.70.10.5875-5881.2004>.
  66. Kwon M, Ho A, Yoon S. Novel approaches and reasons to isolate methanotrophic bacteria with biotechnological potentials: recent achievements and perspectives. *Appl Microbiol Biotechnol*. 2019;103:1–8. <https://doi.org/10.1007/s00253-018-9435-1>.
  67. Hoefman S, van der Ha D, Boon N, Vandamme P, de Vos P, Heylen K. Niche differentiation in nitrogen metabolism among methanotrophs within an operational taxonomic unit. *BMC Microbiol*. 2014;14:83. <https://doi.org/10.1186/1471-2180-14-83>.
  68. Ho A, Di Lonardo DP, Bodelier PLE. Revisiting life strategy concepts in environmental microbial ecology. *FEMS Microbiol Ecol*. 2017;93:fx006. doi:<https://doi.org/10.1093/femsec/fix006>.
  69. Priemé A, Bonilla Sitaula J, Klemmedtsen ÅSK, Bakken LR. Extraction of methane-oxidizing bacteria from soil particles. *FEMS Microbiol Ecol*. 1996;21:59–68. <https://doi.org/10.1111/j.1574-6941.1996.tb00333.x>.
  70. Scheu S, Ruess L, Bonkowski M. Interactions Between Microorganisms and Soil Micro- and Mesofauna. In: Buscot F, editor. *Microorganisms in soils: Roles in genesis and functions*. Berlin: Springer; 2005. p. 253–75.
  71. Lennon JT, Jones SE. Microbial seed banks: the ecological and evolutionary implications of dormancy. *Nat Rev Microbiol*. 2011;9:119–30. <https://doi.org/10.1038/nrmicro2504>.
  72. Schloter M, Nannipieri P, Sørensen SJ, van Elsas JD. Microbial indicators for soil quality. *Biol Fertil Soils*. 2018;54:1–10. <https://doi.org/10.1007/s00374-017-1248-3>.
  73. Ratzke C, Barrere J, Gore J. Strength of species interactions determines biodiversity and stability in microbial communities. *Nat Ecol Evol*. 2020;4:376–83. <https://doi.org/10.1038/s41559-020-1099-4>.
  74. Dal Co A, van Vliet S, Kiviet DJ, Schlegel S, Ackermann M. Short-range interactions govern the dynamics and functions of microbial communities. *Nat Ecol Evol*. 2020;4:366–75. <https://doi.org/10.1038/s41559-019-1080-2>.
  75. Horn MA, Ihssen J, Matthies C, Schramm A, Acker G, Drake HL. *Dechloromonas denitrificans* sp. nov., *Flavobacterium denitrificans* sp. nov., *Paenibacillus anaericanus* sp. nov. and *Paenibacillus terrae* strain MH72, N<sub>2</sub>O-producing bacteria isolated from the gut of the earthworm *Aporrectodea caliginosa*. *Int J Syst Evol Microbiol*. 2005;55:1255–65. doi:<https://doi.org/10.1099/ijs.0.63484-0>.



76. van Dijk H, Kaupper T, Bothe C, Lee HJ, Bodelier PLE, Horn MA, Ho A. Discrepancy in exchangeable and soluble ammonium-induced effects on aerobic methane oxidation: a microcosm study of a paddy soil. *Biol Fertil Soils*. 2021;57:873–80. <https://doi.org/10.1007/s00374-021-01579-9>.
77. Wolfson JM. Determination of microgram quantities of inorganic sulfate in atmospheric particulates. *J Air Pollut Control Assoc*. 1980;30:688–90. <https://doi.org/10.1080/00022470.1980.10465998>.
78. Neufeld JD, Vohra J, Dumont MG, Lueders T, Manefield M, Friedrich MW, Murrell JC. DNA stable-isotope probing. *Nat Protoc*. 2007;2:860–6. <https://doi.org/10.1038/nprot.2007.109>.
79. Kolb S, Knief C, Stubner S, Conrad R. Quantitative detection of methanotrophs in soil by novel pmoA-targeted real-time PCR assays. *Appl Environ Microbiol*. 2003;69:2423–9. <https://doi.org/10.1128/AEM.69.5.2423-2429.2003>.
80. Zhang J, Kobert K, Flouri T, Stamatakis A. PEAR: a fast and accurate Illumina Paired-End reAd mergeR. *Bioinformatics*. 2014;30:614–20. <https://doi.org/10.1093/bioinformatics/btt593>.
81. Callahan BJ, McMurdie PJ, Rosen MJ, Han AW, Johnson AJA, Holmes SP. DADA2: High-resolution sample inference from Illumina amplicon data. *Nat Methods*. 2016;13:581–3. <https://doi.org/10.1038/nmeth.3869>.
82. Quast C, Pruesse E, Yilmaz P, Gerken J, Schweer T, Yarza P, et al. The SILVA ribosomal RNA gene database project: improved data processing and web-based tools. *Nucleic Acids Res*. 2013;41:D590–6. <https://doi.org/10.1093/nar/gks1219>.
83. Anderson MJ. A new method for non-parametric multivariate analysis of variance. *Austral Ecol*. 2001;26:32–46. <https://doi.org/10.1111/j.1442-9993.2001.01070.ppx>.
84. Hammer Ø, Harper D, Ryan P. PAST: Paleontological statistics software package for education and data analysis. *Palaeontologia Electron*. 2001;9pp.
85. Friedman J, Alm EJ. Inferring correlation networks from genomic survey data. *PLoS Comput Biol*. 2012;8: e1002687. <https://doi.org/10.1371/journal.pcbi.1002687>.
86. Newman MEJ. The structure and function of complex networks. *SIAM Rev*. 2003;45:167–256. <https://doi.org/10.1137/S003614450342480>.
87. Ho A, Zuan ATK, Mendes LW, Lee HJ, Zulkeflee Z, van Dijk H, et al. Aerobic methanotrophy and co-occurrence networks of a tropical rainforest and oil palm plantations in Malaysia. *Microb Ecol*. 2021. <https://doi.org/10.1007/s00248-021-01908-3>.
88. Bastian M, Heymann S, Jacomy M. Gephi: an open source software for exploring and manipulating networks. *International AAAI Conference on Weblogs and Social Media*. 2009:361–2.

### Publisher's Note

Springer Nature remains neutral with regard to jurisdictional claims in published maps and institutional affiliations.

#### Ready to submit your research? Choose BMC and benefit from:

- fast, convenient online submission
- thorough peer review by experienced researchers in your field
- rapid publication on acceptance
- support for research data, including large and complex data types
- gold Open Access which fosters wider collaboration and increased citations
- maximum visibility for your research: over 100M website views per year

At BMC, research is always in progress.

Learn more [biomedcentral.com/submissions](https://biomedcentral.com/submissions)



## **A.2 Supplementary information - The methane-driven interaction network in terrestrial methane hotspots**

Thomas Kaupper<sup>1</sup>, Lucas W. Mendes<sup>2</sup>, Anja Poehlein<sup>3</sup>, Daria Frohloff<sup>1</sup>, Stephan Rohrbach<sup>1</sup>, Marcus A. Horn<sup>1</sup>, Adrian Ho<sup>1</sup>.

<sup>1</sup> Institute for Microbiology, Leibniz Universität Hannover, Herrenhäuser Str. 2, 30419 Hannover, Germany.

<sup>2</sup> Center for Nuclear Energy in Agriculture, University of São Paulo CENA-USP, Brazil.

<sup>3</sup> Department of Genomic and Applied Microbiology and Göttingen Genomics Laboratory, Institute of Microbiology and Genetics, George-August University Göttingen, Grisebachstr. 8, D-37077 Göttingen, Germany.

Included:

- Supplementary table captions. The tables can be found online.
- Supplementary figures and figure captions

---

**Following tables are not included in the supplementary an can be accessed on the journal web page: Supplementary Information**

**Table S1** Selected physico-chemical parameters and methane uptake rates of individual replicates in methane hotspots (rice paddy soil, landfill cover soil, pristine peatland, restored peatland, and riparian soil). Summarized data given in Table 3.1.

**Table S2** Significantly positively and negatively co-occurring ( $p < 0.01$ ) OTUs between environments, as determined by the co-occurrence network analysis. The first panel shows site-specific co-occurring OTUs, while the other panels show shared co-occurring OTUs between environments. The OTUs were given to the finest resolveable taxonomic affiliation based on the Silva database v. 132, whenever available. The number in brackets refer to the OTU numbers. Abbreviations: pos, positive correlations; neg, negative correlations; RP, rice paddy; LC, landfill cover soil; PP, pristine peatland; RP, restored peatland; RS, riparian soil; MIP, methanotroph interacting partner (including other co-occurring methanotrophs).

**Table S3** Significantly positively and negatively co-occurring ( $p < 0.01$ ) OTUs in the pristine peatland over time (days 8, 13, and 19, respectively denoted by T1, T2, and T3), as determined by the co-occurrence network analysis. The first panel shows co-occurring OTUs at each time interval while the other panels show shared co-occurring OTUs between time intervals. The OTUs were given to the finest resolveable taxonomic affiliation based on the Silva database v. 132, whenever available. The number in brackets refer to the OTU numbers. Abbreviations: pos, positive correlations; neg, negative correlations; T1, after 8 days incubation; T2, after 13 days incubation; T3, after 19 days incubation; MIP, methanotroph interacting partner (including other co-occurring methanotrophs).

**Table S4** Sample names/treatment and corresponding accession numbers (BioProject PRJNA751592). Sample name is labelled in the following order: site, sampling time,  $^{12}\text{C}$  or  $^{13}\text{C}$  (i.e.,  $^{12}\text{C}$  or  $^{13}\text{C}$ -CH<sub>4</sub> incubations), H or L (i.e., “heavy” or “light” fractions).

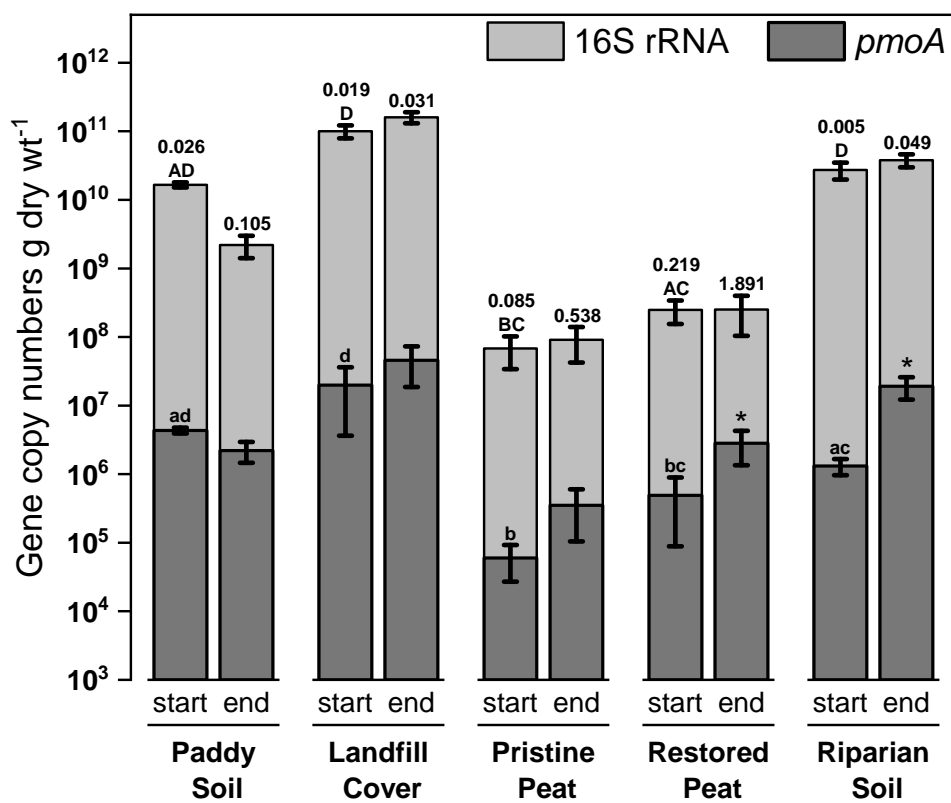


**Figure S1** The *pmoA* and 16S rRNA gene abundances in the starting material and after incubation in diverse environments (mean  $\pm$  s.d.;  $n \geq 4$ ). The qPCR assay was performed in duplicate for each DNA extraction. The 16S rRNA and *pmoA* gene abundances for all samples were at least an order of magnitude higher than the lower detection limit of the qPCR assays. The upper and lower case letters indicate the level of significance ( $p < 0.05$ ) of the 16S rRNA gene and *pmoA* gene abundance between environments in the starting material. The asterisk indicates significant difference ( $p < 0.05$ ) in the starting *pmoA* gene abundance and after incubation. The numbers at the top of each bar refer to the *pmoA*:16S rRNA gene abundance ratio in percentage (%), which increased after incubation.

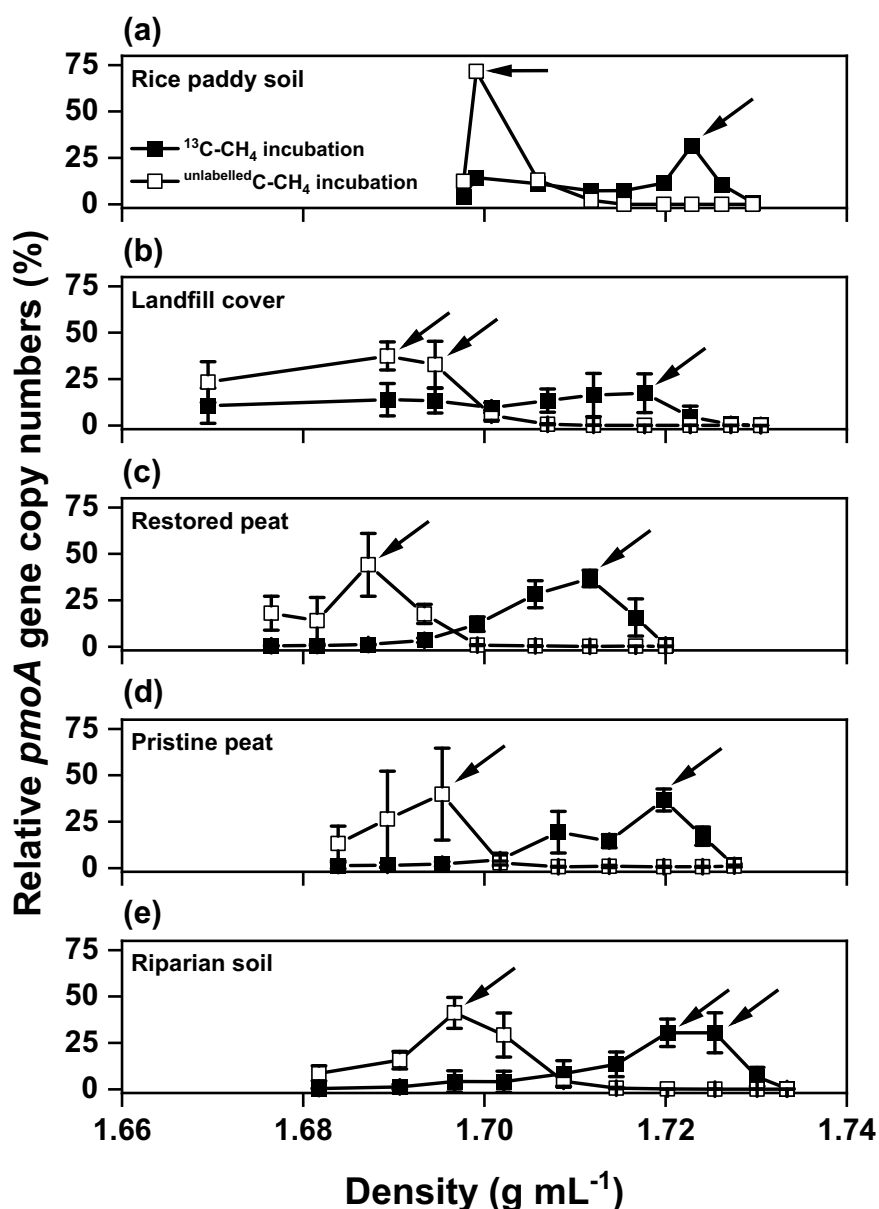


**Figure S2** Relative *pmoA* gene abundance along the density gradient of the <sup>13</sup>C- and unlabelled C-CH<sub>4</sub> incubations with the (a) paddy soil, (b) landfill cover soil, (c) restored peatland, (d) pristine peatland, and (e) riparian soil (mean ± s.d.; n=4 each). The results of the paddy soil (a; [1]) and the peatlands (c,d; [2]) were re-analysed for the present study. The *pmoA* gene relative abundance was calculated as the proportion of each fraction over the total sum of all fractions per sample. The density gradients of the <sup>13</sup>C- and unlabelled C-CH<sub>4</sub> incubations were compared to distinguish the “light” from the “heavy” fraction in the <sup>13</sup>C-CH<sub>4</sub> incubation. The arrows denote the “light” and “heavy” fractions where the 16S rRNA gene was amplified for Illumina MiSeq sequencing in the <sup>13</sup>C-CH<sub>4</sub> incubations.

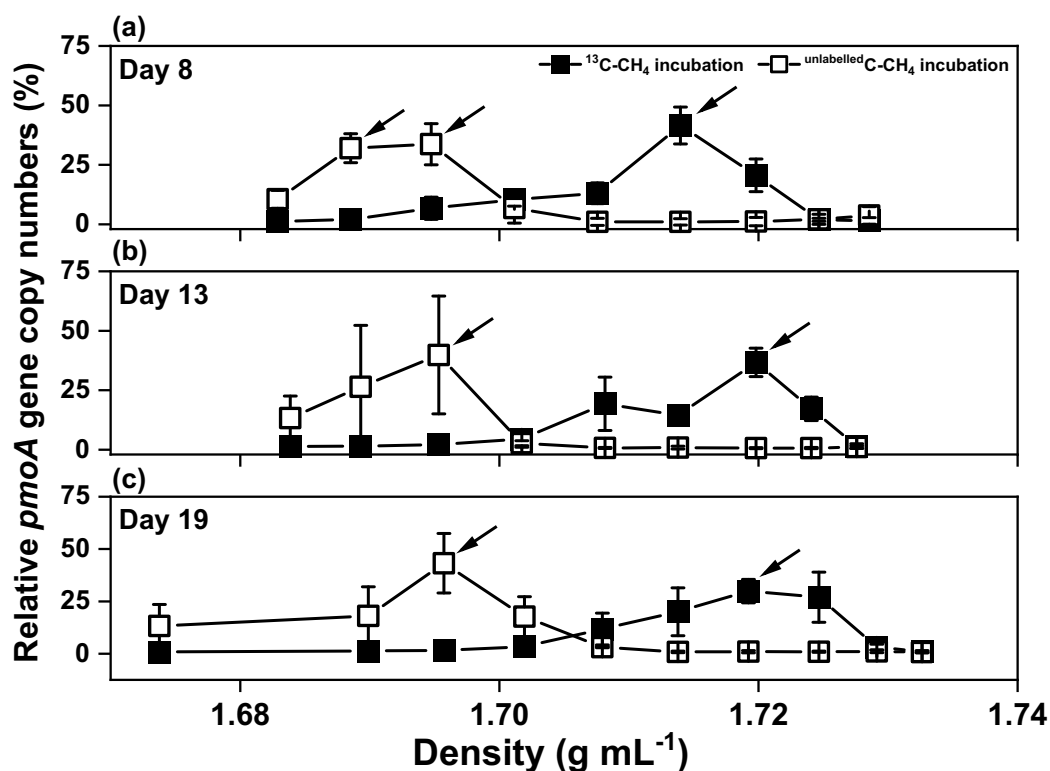


**Figure S3** Relative *pmoA* gene abundance along the density gradient of the <sup>13</sup>C- and unlabelled C-CH<sub>4</sub> incubations in the pristine peat at days 8, 13, and 19 (mean ± s.d.; n=4 each). The *pmoA* gene relative abundance was calculated as the proportion of each fraction over the total sum of all fractions per sample. The arrows denote the “light” and “heavy” fractions where the 16S rRNA gene was amplified for Illumina MiSeq sequencing in the <sup>13</sup>C-CH<sub>4</sub> incubations.

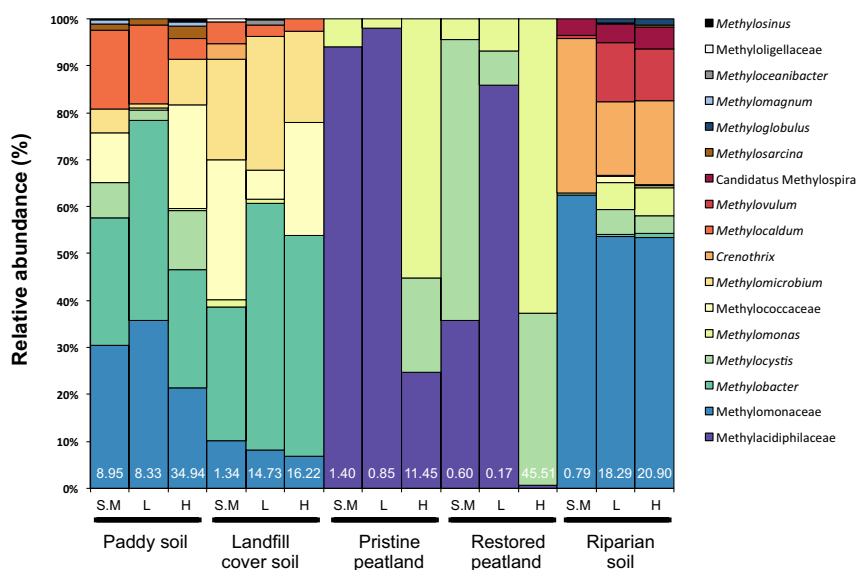


**Figure S4** Relative abundance of the methanotroph-affiliated OTUs in the paddy soil, landfill cover soil, pristine/restored peatlands, and riparian soil based on the 16S rRNA gene sequences in the starting material and after the incubation with  $^{13}\text{C}$ -methane (“light” and “heavy” fractions). The numbers at the bottom of the bars denote the mean proportion (%) of the methanotroph-affiliated OTUs among the total 16S rRNA gene sequences. Abbreviations; S.M, starting material; L, “light” fraction; H, “heavy” fraction.

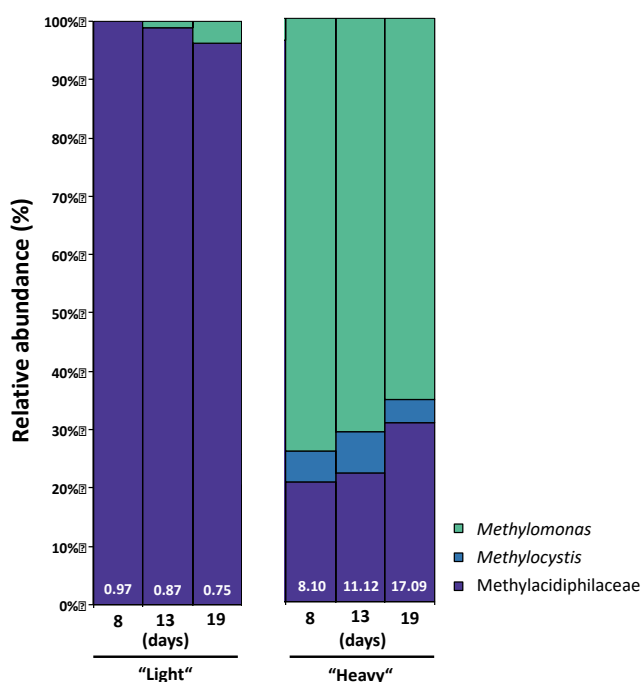


**Figure S5** Relative abundance of the methanotroph-affiliated OTUs in the starting material of the pristine peatland and after 8, 13, and 19 days incubation with  $^{13}\text{C}$ -methane (“light” and “heavy” fractions), based on the 16S rRNA gene sequences. The numbers above the bars denote the mean proportion (%) of the methanotroph-affiliated OTUs among the total 16S rRNA gene sequences. Abbreviations; S.M, starting material; L, “light” fraction; H, “heavy” fraction.

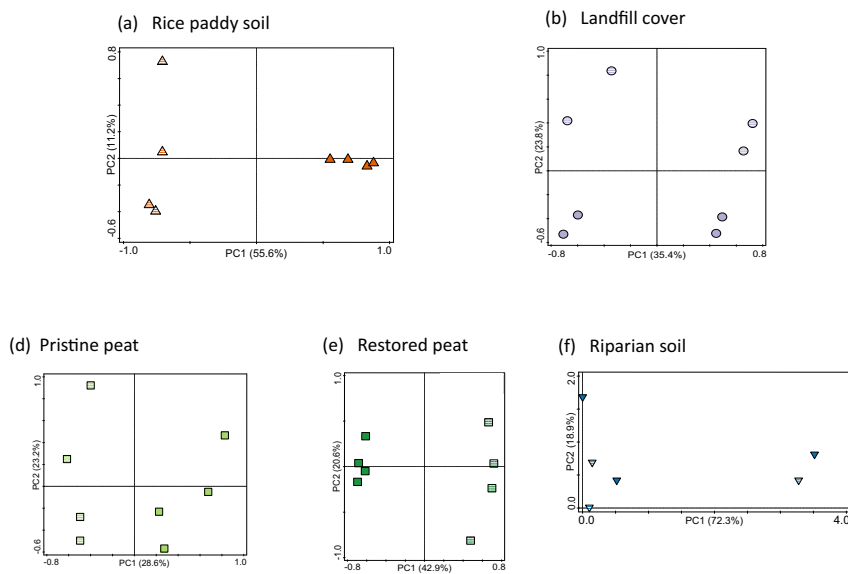


**Figure S6** Principal component analysis showing the clustering of the 16S rRNA gene sequences in the “light” and “heavy” fractions of the (a) paddy soil (orange, triangle), (b) landfill cover soil (purple, circle), (c) pristine peatland (light green, square), (d) restored peatland (dark green, square), and (e) riparian soil (blue, inverted triangle). All replicates ( $n=4$ ) are given; in the incubation with the riparian soil, fractionation was unsuccessful for one replicate. Full colored and striped symbols represent the “light” and “heavy” fraction, respectively.

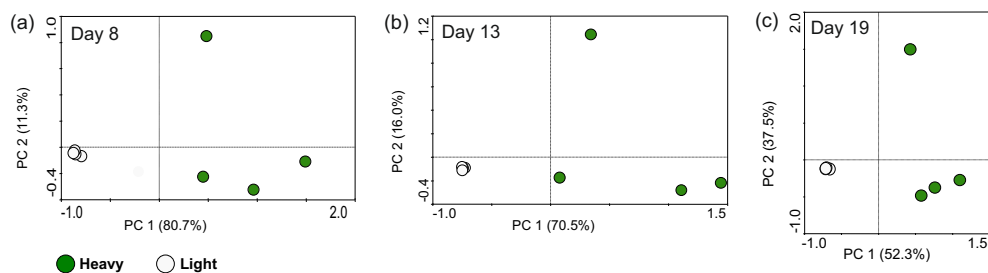


**Figure S7** Principal component analysis showing the clustering of the 16S rRNA gene sequences in the ‘light’ and ‘heavy’ fractions of the pristine peatland over time (days 8, 13, and 19). All replicates ( $n=4$ ) are given. Full colored and striped symbols represent the ‘heavy’ and ‘light’ fraction, respectively.



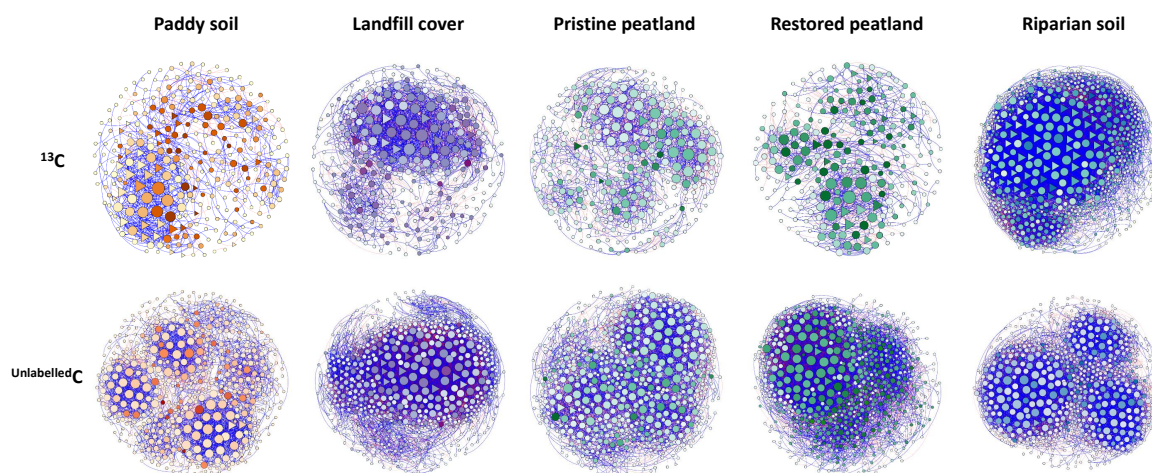


**Figure S8** Co-occurrence network analysis of methane hotspots derived from the  $^{13}\text{C}$ - and  $^{\text{unlabelled}}\text{C}$ -DNA. The corresponding topological parameters of the networks are provided in Table 3.2. Each node represents a bacterial taxon at the OTU level, while the size and shade of the node corresponds to the number of connections per node and the number of connections passing through the node (i.e., darker shade for nodes acting as a bridge between other nodes at higher frequencies), respectively. A connection denotes significant SparCC correlation ( $p < 0.01$ ) with a magnitude of  $> 0.8$  (positive correlation, blue edges) or  $< -0.8$  (negative correlations, red edges).

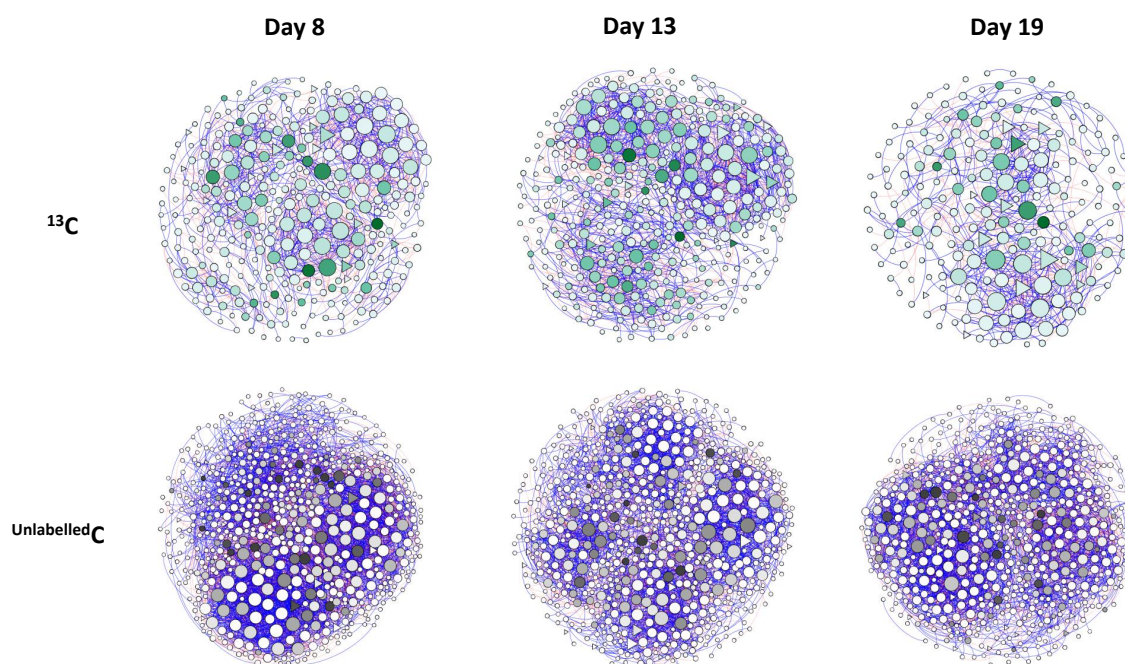


**Figure S9** Co-occurrence network analysis after 8, 13, and 19 days incubation of the pristine peat derived from the  $^{13}\text{C}$ - and  $^{\text{unlabelled}}\text{C}$ -DNA. The corresponding topological parameters of the networks are provided in Table 3.3. Each node represents a bacterial taxon at the OTU level, while the size and shade of the node corresponds to the number of connections per node and the number of connections passing through the node (i.e., darker shade for nodes acting as a bridge between other nodes at higher frequencies), respectively. A connection denotes significant SparCC correlation ( $p < 0.01$ ) with a magnitude of  $> 0.8$  (positive correlations, blue edges) or  $< -0.8$  (negative correlations, red edges).

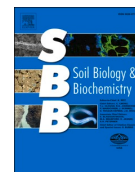
## References

- [1] Kaupper T, Mendes LW, Lee HJ, Mo Y, Poehlein A, Jia Z, Horn MA, Ho A. When the going gets tough: Emergence of a complex methane-driven interaction network during recovery from desiccation-rewetting. *Soil Biol Biochem.* 2021a; doi.org/10.1016/j.soilbio.2020.108109.
- [2] Kaupper T, Mendes LW, Harnisz M, Krause SMB, Horn MA, Ho A. Recovery of methanotrophic activity is not reflected in the methane-driven interaction network after peat mining. *App Environ Microbiol.* 2021b; doi.org/10.1128/AEM.02355-20.



Contents lists available at ScienceDirect

## Soil Biology and Biochemistry

journal homepage: <http://www.elsevier.com/locate/soilbio>

## When the going gets tough: Emergence of a complex methane-driven interaction network during recovery from desiccation-rewetting

Thomas Kaupper<sup>a</sup>, Lucas W. Mendes<sup>b</sup>, Hyo Jung Lee<sup>c</sup>, Yongliang Mo<sup>d</sup>, Anja Poehlein<sup>e</sup>, Zhongjun Jia<sup>d</sup>, Marcus A. Horn<sup>a,\*,\*\*</sup>, Adrian Ho<sup>a,\*</sup>

<sup>a</sup> Institute for Microbiology, Leibniz Universität Hannover, Herrenhäuser Str. 2, 30419, Hannover, Germany

<sup>b</sup> Center for Nuclear Energy in Agriculture, University of São Paulo CENA-USP, Brazil

<sup>c</sup> Department of Biology, Kunsan National University, Gunsan, Republic of Korea

<sup>d</sup> Institute of Soil Science, Chinese Academy of Sciences, No.71 East Beijing Road, Xuan-Wu District, Nanjing City, 210008, PR China

<sup>e</sup> Department of Genomic and Applied Microbiology and Göttingen Genomics Laboratory, Institute of Microbiology and Genetics, George-August University Göttingen, Grisebachstr. 8, D-37077, Göttingen, Germany

## ARTICLE INFO

## Keywords:

Stable-isotope probing  
Methane-based foodweb  
Community ecology  
Methanotrophs  
*pmoA*

## ABSTRACT

Microorganisms interact in complex communities, affecting microbially-mediated processes in the environment. Particularly, aerobic methanotrophs showed significantly stimulated growth and activity in the presence of accompanying microorganisms in an interaction network (interactome). Yet, little is known of how the interactome responds to disturbances, and how community functioning is affected by the disturbance-induced structuring of the interaction network. Here, we employed a time-series stable isotope probing (SIP) approach using <sup>13</sup>C-CH<sub>4</sub> coupled to a co-occurrence network analysis after Illumina MiSeq sequencing of the <sup>13</sup>C-enriched 16S rRNA gene to directly relate the response in methanotrophic activity to the network structure of the interactome after desiccation-rewetting of a paddy soil. Methane uptake rate decreased immediately (<5 days) after short-term desiccation-rewetting. Although the methanotroph subgroups differentially responded to desiccation-rewetting, the metabolically active bacterial community composition, including the methanotrophs, recovered after the disturbance. However, the interaction network was profoundly altered, becoming more complex but, less modular after desiccation-rewetting, despite the recovery in the methanotrophic activity and community composition/abundances. This suggests that the legacy of the disturbance persists in the interaction network. The change in the network structure may have consequences for community functioning with recurring desiccation-rewetting.

### 1. Introduction

Biological interactions are widespread in microbial communities. Microorganisms form a plethora of interdependent relationships with their biotic environment, with synergistic and/or antagonistic effects. Concerning methanotrophy, emergent properties enhancing community functioning may arise from such interactions. Indeed, aerobic methanotrophs exhibit higher co-metabolic biodegradation rates of micro-pollutants and show significantly higher methanotrophic activity in a multi-species consortium than as monocultures (Begonja and Hrsak, 2001; Ho et al., 2014; Benner et al., 2015; Krause et al., 2017; Veraart et al., 2018). Therefore, accompanying microorganisms that do not

possess the metabolic potential and do not seemingly contribute to methane oxidation may also be relevant, exerting an indirect interaction-induced effect on community functioning. While changes in the methanotrophic community composition and/or abundances have been correlated to the methane oxidation rate in response to environmental cues and disturbances (Ho et al., 2011; Danilova et al., 2015; Christiansen et al., 2016; Reumer et al., 2018; Reis et al., 2020), interaction-induced effects that alter the structure of the interaction network (i.e., methanotrophic interactome; Ho et al., 2016a) remains unclear. Here, we define the methanotrophic interactome as a sub-population of the entire community, encompassing the methanotrophs and accompanying non-methanotrophs that is tracked via the

\* Corresponding author.

\*\* Corresponding author.

E-mail addresses: [horn@ifmb.uni-hannover.de](mailto:horn@ifmb.uni-hannover.de) (M.A. Horn), [adrian.ho@ifmb.uni-hannover.de](mailto:adrian.ho@ifmb.uni-hannover.de) (A. Ho).

<https://doi.org/10.1016/j.soilbio.2020.108109>

Received 23 July 2020; Received in revised form 7 December 2020; Accepted 7 December 2020

Available online 11 December 2020

0038-0717/© 2020 Elsevier Ltd. All rights reserved.

flow of methane-derived  $^{13}\text{C}$ ; the members of the interactome co-occur more than by chance, as determined in a co-occurrence network analysis (Ho et al., 2016a). The recovery in the community composition and abundance does not necessarily translate to the return of the network structure to the pre-disturbance state (Pérez-Valera et al., 2017). Therefore, the response of the interactome is a lesser known but important determinant, potentially imposing an effect on community functioning during recovery from disturbances (Ratzke et al., 2020).

Aerobic methanotrophs belong to the Gammaproteobacteria (Type Ia and Ib subgroups), Alphaproteobacteria (Type II subgroup), and Verrucomicrobia, and may show habitat preference (Knief, 2015), with the verrucomicrobial methanotrophs typically inhabiting acidic and thermophilic geothermal environments (Op den Camp et al., 2009; Sharp et al., 2014). The proteobacterial methanotrophs are ubiquitous and thought to be relevant in terrestrial ecosystems, acting as a methane sink in well-aerated upland soils and methane biofilter at oxic-anoxic interfaces (Reim et al., 2012; Shrestha et al., 2012; Praeg et al., 2017; Ho et al., 2019; Kaupper et al., 2020a). Accordingly, proteobacterial methanotrophs can be distinguished based on their biochemistry and ecophysiology, which reflect on their ecological life strategies and response to disturbances (Trotsenko and Murrell, 2008; Semrau et al., 2010; Ho et al., 2017). The *pmoA* gene (encoding for the particulate methane monooxygenase) phylogeny corresponds with that of the 16S rRNA gene, and is commonly targeted to characterize the methanotrophs in complex communities (e.g., Kolb et al., 2003; Dumont et al., 2011; Knief, 2015; Karwautz et al., 2018). Therefore, aerobic methane oxidation is catalyzed by a defined microbial guild with relatively low diversity (mainly, proteobacteria in non-geothermal environments) when compared to other microbial groups catalyzing generalized processes (e.g., denitrification, respiration). This allows the methanotrophs to be clearly distinguished from the non-methanotrophs in complex communities, making the methanotrophic interactome a suitable model system for our study.

Here, we elaborate the response of a methane-driven interaction network to desiccation-rewetting to determine how methanotrophic activity is affected by the disturbance-induced structuring of the interactome. A DNA-based stable isotope probing (SIP) approach using  $^{13}\text{C}\text{-CH}_4$  was coupled to a co-occurrence network analysis after Illumina MiSeq sequencing of the 16S rRNA gene, allowing direct association of methanotrophic activity to the structure of the interaction network (methane food web). Although the network analysis is a useful tool to explore interactions in complex microbial communities (e.g., Barberán et al., 2012; Ho et al., 2016a; Morriën et al., 2017; Ho et al., 2020; Mo et al., 2020; Ratzke et al., 2020), biological interpretation of the analysis (e.g., causative mechanisms driving the interaction) requires further probing. Given that the methanotrophs are the only members of the interactome capable of using methane as a carbon and energy source, it is not unreasonable to assume that  $^{13}\text{C}$ -labeled non-methanotrophic microorganisms depended on and interacted with the methanotrophs (e.g., via cross-feeding and co-aggregation; Ho et al., 2016a; Pérez-Valera et al., 2017). Coupling SIP to the network analysis thus confirms the unidirectional flow of substrate from the metabolically active methanotrophs to non-methanotrophs. We hypothesized that a more complex interaction network will arise as a response to desiccation-rewetting, as documented in other single or sporadic disturbance events, given sufficient recovery time (Eldridge et al., 2015; Pérez-Valera et al., 2017). With the elimination of less desiccation-resistant/tolerant microorganisms, it is not unreasonable to postulate that the surviving community members were forced to interact more among themselves, increasing metabolic exchange which further drives their co-occurrence over time (Zelezniak et al., 2015; Tripathi et al., 2016; Dal Co et al., 2020; Ratzke et al., 2020).

## 2. Materials and methods

### 2.1. Soil sampling and microcosm set-up

The paddy soil (upper 10–15 cm) was collected from a rice field belonging to the Italian Rice Research Institute, Vercelli, Italy (45° 20'N, 8° 25'W). The soil pH and electrical conductivity (EC) were 6.5 and 0.2 dS  $\text{m}^{-1}$ , respectively. The C and N concentrations were 13.9 mg C g  $\text{dw}^{-1}$  and 1.3 mg N g  $\text{dw}^{-1}$ , respectively. The concentrations of nitrite and nitrate ( $\text{NO}_3^-$ ), sulphate, and phosphate were 34.4  $\mu\text{g N g dw}^{-1}$ , 96  $\mu\text{g g dw}^{-1}$ , and 0.6  $\mu\text{g g dw}^{-1}$ , respectively. Agricultural practices in the rice field have been reported in detail elsewhere (Krueger et al., 2001). Generally, rice was cropped in the paddy soil twice a year (May/June to September/October and January/February to May/June), with each rice growing season spanning over 4–5 months; rice was not grown for approximately two months in winter (Krueger et al., 2001). The paddy field was drained prior to rice harvest and left fallow for 2–3 weeks before the commencement of the next rice growing season. Soil sampling was performed in May 2015 after drainage and rice harvest. After sampling, the soil was air-dried at ambient temperature and sieved (2 mm) to eliminate (fine) roots and debris, before being stored in a plastic container at room temperature till incubation set-up (November 2017). Paddy soil prepared and stored under the same conditions <5 years after sampling showed comparable potentially active methanotrophic community composition (mRNA-based community analysis) over ~80 days incubation after re-wetting (Collet et al., 2015).

Each microcosm consisted of 10 g soil saturated with 4.5 mL autoclaved deionized water in a Petri dish. The saturated soil was homogenized, and pre-incubated under ~10 % $_{\text{v/v}}$  methane in air at 25 °C in an air-tight jar. Following pre-incubation (7 days), desiccation was induced by placing the microcosms under a laminar flow cabinet overnight (15 h) to achieve a gravimetric water loss of >95% in the disturbed microcosm (Fig. S1; Ho et al., 2016b). After desiccation, water loss was replenished by adding the corresponding amount of autoclaved deionized water, and incubation resumed under the same conditions as before. Microcosms not exposed to desiccation-rewetting (un-disturbed) served as reference. A total of 42 microcosms were constructed (Fig. S1). At designated intervals (i.e., pre-incubation, as well as 1–7, 27–34, and 64–71 days after disturbance; Fig. S1),  $^{13}\text{C}\text{-CH}_4$  labelling incubation was performed; the microcosms (n = 6) were transferred into a flux chamber and incubated under 2 % $_{\text{v/v}}$  methane ( $^{13}\text{C}\text{-CH}_4$ , n = 4;  $^{\text{unlabelled}}\text{C}\text{-CH}_4$ , n = 2) in air. Headspace methane was replenished when methane in the flux chamber was reduced to <0.5 % $_{\text{v/v}}$ . Incubation in the flux chamber was performed over 6–7 days or until at least 500  $\mu\text{mole}$  methane was consumed to ensure sufficient labelling (Neufeld et al., 2007). After incubation, the soil was homogenized, shock-frozen, and stored in the –20 °C freezer until DNA extraction.

### 2.2. Methane and inorganic N measurements

Headspace methane was measured daily in all replicates (i.e., both  $^{\text{unlabelled}}\text{C}$ - and  $^{13}\text{C}\text{-CH}_4$  incubations) using a gas chromatograph (7890B GC System, Agilent Technologies, Santa Clara, USA) coupled to a pulsed discharge helium ionization detector (PD-HID), with helium as the carrier gas. The methane uptake rates were determined by linear regression from the slope of methane depletion with at least three time intervals (12–24 h between intervals). Soluble ammonium and nitrate were determined in all replicates in autoclaved deionized water (1:2.5 $_{\text{w/v}}$ ) after centrifugation and filtration (0.2  $\mu\text{m}$ ) of the soil suspension. Soluble ammonium was determined colorimetrically (Horn et al., 2005) using an Infinite M plex plate reader (TECAN, Meandorf, Switzerland), whereas nitrate was determined using a Sievers 208i NO analyzer system (GE Analytical Instruments, Boulder, CO, USA) with 50 mM  $\text{VCl}_3$  in 1 M sterile HCl as a reducing agent.



### 2.3. DNA extraction and isopycnic ultracentrifugation

DNA was extracted using the DNeasy PowerSoil Kit (Qiagen, Hilden, Germany) according to the manufacturer's instruction. DNA was extracted in duplicate for each sample ( $n = 6$ , per treatment and time) and pooled after elution to obtain sufficient amounts for the isopycnic ultracentrifugation.

DNA stable isotope probing was performed according to Neufeld et al. (2007). Isopycnic ultracentrifugation was performed at 144000 g for 67 h using an Optima L-80XP (Beckman Coulter Inc., USA). Each ultracentrifugation run consisted of DNA extracted from incubations containing  $^{13}\text{C}$ - and  $^{12}\text{C}$ -methane to distinguish the 'light' from the 'heavy' fractions (Fig. S2). Fractionation was performed immediately after centrifugation using a hydraulic pump (Duelabo, Dusseldorf, Germany) at  $3 \text{ rpm min}^{-1}$ . Although 10–11 fractions were obtained, the last fraction was discarded, yielding 9–10 fractions per sample. Fractionation was unsuccessful for DNA sampled from two of the four replicate in the disturbed microcosm ( $^{13}\text{C}$ - $\text{CH}_4$  incubation, 64–71 days interval). Given that a minimum of three replicates is needed to construct each network, post-disturbance samples were grouped into days 1–7 (immediately after disturbance) and 27–71 (during recovery) for subsequent  $^{13}\text{C}$ -enriched 16S rRNA gene-derived network analysis (see Section 2.7). In the other time intervals, at least three replicates were obtained in the  $^{13}\text{C}$ - $\text{CH}_4$  incubation. The density gradient of each fraction was determined by weighing on a precision scale (technical replicate,  $n = 10$ ). DNA precipitation was performed over night, as described in Neufeld et al. (2007); nucleic acid was washed twice with ethanol, and the pellet was suspended in  $30 \mu\text{L}$  of ultrapure PCR water (INVITROGEN, Waltham, USA). The *pmoA* gene was enumerated from each fraction using a qPCR assay (MTOT; Table S1) to distinguish the 'heavy' from the 'light' fraction after comparing DNA from the  $^{13}\text{C}$ - and  $^{12}\text{C}$ - $\text{CH}_4$  incubations (Fig. S2). The identified 'heavy' and 'light' DNA fractions as defined in Neufeld et al. (2007) were amplified for Illumina MiSeq sequencing.

### 2.4. Group-specific qPCR assays

The qPCR assays (MBAC, MCOC, and TYPEII targeting type Ia, Ib, and II, respectively) were performed to follow the abundance of the methanotroph sub-groups over time (Table S1). Additionally, a qPCR assay targeting the total methanotrophic population (MTOT) was applied to the DNA samples after fractionation to distinguish the 'heavy' from the 'light' fraction. The qPCR was performed using a BIORAD CFX Connect RT System (Biorad, Hercules, USA). Briefly, each reaction (total volume,  $20 \mu\text{L}$ ) consisted of  $10 \mu\text{L}$  SYBR 2X Sensifast (BIOLINE, London, UK),  $3.5 \mu\text{L}$  of forward/reverse primer each,  $1 \mu\text{L}$   $0.04\%$  BSA, and  $2 \mu\text{L}$  template DNA. Template DNA was diluted 50-fold with RNase- and DNase-free water for the MBAC, MCOC, and TYPEII assays, and was undiluted for the MTOT assay. Diluting the template DNA 50-fold resulted in the optimal *pmoA* gene copy numbers. The primer combinations and concentrations, as well as the PCR thermal profiles, are given elsewhere (see Table S1, Kolb et al., 2003 and Kaupper et al., 2020b). The calibration curve ( $10^1$ – $10^8$  copy number of target genes) was derived from gene libraries as described before (Ho et al., 2011). The qPCR amplification efficiency was 83–91%, with  $R^2$  ranging from 0.994 to 0.997. Amplicon specificity was determined from the melt curve, and confirmed by 1% agarose gel electrophoresis yielding a band of the correct size in a preliminary qPCR run.

### 2.5. Amplification for the *pmoA* and 16S rRNA genes for Illumina MiSeq sequencing

The *pmoA* gene was amplified using the primer pair A189f/mb661r, with the forward primer containing a fused 6 bp bar code. Each PCR reaction comprised of  $25 \mu\text{L}$  SYBR Premix Ex Taq™ (Tli RNaseH Plus, TaKaRa, Japan),  $1 \mu\text{L}$  forward/reverse primer each ( $10 \mu\text{M}$ ),  $2 \mu\text{L}$

template DNA (DNA concentration diluted to  $2$ – $8 \text{ ng } \mu\text{L}^{-1}$ ), and  $21 \mu\text{L}$  sterilized distilled water, giving a total volume of  $50 \mu\text{L}$ . The PCR thermal profile consisted of an initial denaturation step at  $94 \text{ }^\circ\text{C}$  for 2 min, followed by 39 cycles of denaturation at  $94 \text{ }^\circ\text{C}$  for 30 s, annealing at  $60 \text{ }^\circ\text{C}$  for 30 s, and elongation at  $72 \text{ }^\circ\text{C}$  for 45 s. The final elongation step was at  $72 \text{ }^\circ\text{C}$  for 5 min. The PCR products were verified on 1.2% agarose gel electrophoresis showing a single band of the correct size, before purification using the E.Z.N.A. Cycle-Pure kit (Omega Bio-tek, USA). Subsequently, the purified amplicons were pooled at equimolar DNA amounts ( $200 \text{ ng}$ ) for sequencing using Illumina MiSeq version 3 chemistry (paired-end, 600 cycles). The *pmoA* sequence library was prepared using the TruSeq Nano DNA LT Sample Prep Kit set A (Illumina, Beijing, China).

The 16S rRNA gene was amplified using the primer pair 341F/805R. Each PCR reaction comprised of  $4 \mu\text{L}$  Buffers B and S each (CRYSTAL Taq-DNA-Polymerase, BiolabProducts, Germany),  $4 \mu\text{L}$   $\text{MgCl}_2$  ( $25 \text{ mM}$ ),  $0.2 \mu\text{L}$  Taq polymerase ( $5 \text{ U } \mu\text{L}^{-1}$ ) (CRYSTAL Taq-DNA-Polymerase),  $1.6 \mu\text{L}$  dNTPs ( $10 \text{ mM}$ ),  $2 \mu\text{L}$  forward and reverse tagged-primers each ( $10 \mu\text{M}$ ),  $4 \mu\text{L}$  template DNA, and  $18.2 \mu\text{L}$  sterilized distilled water. The PCR thermal profile consisted of an initial denaturation step at  $94 \text{ }^\circ\text{C}$  for 7 min, followed by 30 cycles of denaturation at  $94 \text{ }^\circ\text{C}$  for 30 s, annealing at  $53 \text{ }^\circ\text{C}$  for 30 s, and elongation at  $72 \text{ }^\circ\text{C}$  for 30 s. The final elongation step was at  $72 \text{ }^\circ\text{C}$  for 5 min. After the specificity of the amplicon was checked by 1% agarose gel electrophoresis, the PCR product was purified using the GeneRead Size Selection Kit (Qiagen, Hilden, Germany). Subsequently, a second PCR was performed with adapters using the Nextera XT Index Kit (Illumina, San Diego, USA). The second PCR reaction consisted of  $12.5 \mu\text{L}$  2X KAPA HiFi HotStart Ready Mix (Roche, Mannheim, Germany),  $2.5 \mu\text{L}$  of each tagged primers ( $10 \mu\text{M}$ ),  $2.5 \mu\text{L}$  PCR grade water, and  $5 \mu\text{L}$  template from the first PCR. The amplicons were then purified using the MagSi-NGS<sup>PREP</sup> Plus Magnetic beads (Steinbrenner Laborsysteme GmbH, Wiesenbach, Germany). Normalization of the amplicons before sequencing was performed using the Janus Automated Workstation (PerkinElmer, Waltham Massachusetts, USA). Sequencing was performed using Illumina MiSeq version 3 chemistry (paired-end, 600 cycles).

### 2.6. *pmoA* and 16S rRNA gene amplicon analyses

The *pmoA* gene amplicon was analyzed as described before (Reumer et al., 2018). Briefly, the paired-end reads were sorted based on the length and the quality of the primers ( $\leq 2$  errors) and barcodes ( $\leq 1$  error) after assembly in Mothur version 1.42.1 using the 'make.contigs' command (Schloss et al., 2009). Primers and barcodes which did not meet these requirements were removed. Similarly, chimeric reads were also removed in Mothur using the 'chimeras.uchime' command with the 'self' option. After filtering, the initial  $\sim 1\,175\,000$  contigs generated from Illumina MiSeq sequencing was reduced to  $\sim 628\,000$  high quality contigs, with approximately 15 300 contigs per sample. The *pmoA* sequences were classified using BLAST by comparing to the GenBank nonredundant (nr) database and the lowest common ancestor algorithm in MEGAN version 5.11.3, based on curated *pmoA* gene database and MEGAN tree, respectively as detailed in Dumont et al. (2014). The high quality *pmoA* sequences could be affiliated (family, genus, or species level) to known cultured methanotrophs. Based on the relative abundance of the *pmoA* gene sequences, a principal component analysis (PCA) was performed to determine the response of the methanotrophs to desiccation-rewetting. To construct the PCA, the data matrix was initially analyzed using the detrended correspondence analysis (DCA), which indicated linearly distributed data and revealed that the best-fit mathematical model was the PCA. To test whether the treatments harbored significantly different bacterial community composition and structure, plot clustering was tested using permutational multivariate analysis of variance (PERMANOVA; Anderson, 2001). The PCA was conducted in Canoco 4.5 (Biometrics, Wageningen, The Netherlands), and the PERMANOVA was calculated using PAST 4 software (Hammer

et al., 2001). The *pmoA* gene sequences were deposited at the National Center for Biotechnology Information (NCBI), SRA database under the BioProject accession number PRJNA634611.

The 16S rRNA gene paired-end reads were firstly merged using PEAR (Zhang et al., 2014). Next, the merged sequences were processed using QIIME 2 version 2019.10, with de-multiplex and quality control performed with DADA2 (Callahan, 2017) using the consensus method to remove any remaining chimeric and low-quality sequences. Approximately 1 300 000 high quality contigs were retained after filtering (on average, ~18 000 contigs per sample). After the removal of singletons and doubletons, the samples were rarefied to 7,560 sequences following the number of the lowest sample. The taxonomic affiliation was performed at 97% similarity according to the Silva database v. 132 (Quast et al., 2013). The affiliations of the OTUs are given to the finest taxonomic resolution, whenever available. A PCA was performed to compare the bacterial community composition in the un-disturbed and disturbed incubations. The 16S rRNA-based PCA was constructed as described for the *pmoA*-based PCA using Canoco 4.5 (Biometrics, Wageningen, the Netherlands) after analysis of variance (PERMANOVA) in the PAST 4 software. The 16S rRNA gene sequences were deposited at the NCBI, SRA database under the BioProject accession number PRJNA634611.

### 2.7. Co-occurrence network analysis

To explore the complexity of the interaction between bacterial taxa (OTU-level) within the interactome, a co-occurrence network analysis was performed based on the 16S rRNA gene derived from the <sup>13</sup>C-enriched DNA ('heavy' fraction). For network construction, non-random co-occurrence analyses between bacterial OTUs were calculated using SparCC, a tool designed to assess correlations for compositional data (Friedman and Alm, 2012). For each network, *P*-values were obtained by 99 permutations of random selections of the data tables, applying the same analytical pipeline. The true SparCC correlations were selected based on statistical significance of  $p < 0.01$ , with a magnitude of  $>0.7$  or  $< -0.7$ . The networks were assessed based on their topological features such as the number of nodes and edges (connectivity), modularity, number of communities, average path length, network diameter, average degree, and clustering coefficient (Table 1; Newman, 2003). The nodes in the networks represent OTUs, whereas the edges represent significantly positive or negative correlations between two nodes. Also, key nodes were identified based on the betweenness centrality, a measure of the frequency of a node acting as a bridge along the shortest path between two other nodes (Poudel et al., 2016). Hence, nodes with high betweenness centrality can be regarded to represent important key taxa within the interaction network (Borgatti, 2005). The co-occurrence network analysis was performed using the Python module 'SparCC', and the network construction and properties were calculated with Gephi (Bastian et al., 2009).

### 2.8. Statistical analysis

Significant differences ( $p < 0.05$ ) in the methane uptake rate and qPCR analyses per time between treatments (un-disturbed and disturbed incubations) were performed using IBM SPSS Statistics (IBM, Armonk, USA). The data were tested for normal distribution using the Kolmogorov-Smirnov test and the Shapiro-Wilk test. Where normal distribution was met, a two-sided paired *t*-test was performed. Otherwise, a non-parametric test (Wilcoxon signed rank test) was performed. Additionally, methane uptake rates were correlated to the abundances of type Ia, Ib, and II *pmoA* gene separately by linear regression in Origin (OriginLab Corporation, Northampton, MA, USA).

**Table 1**

Correlations and topological properties of the interaction networks during pre-incubation, and recovery from desiccation-rewetting at 1–7 and 27–71 days intervals.

Network properties	Pre-incubation	Un-disturbed		Disturbed	
		1–7 d	27–71d	1–7 d	27–71d
Number of nodes <sup>a</sup>	165	181	211	210	156
Number of edges <sup>b</sup>	769	616	1547	888	1835
Positive edges <sup>c</sup>	435 (56%)	368 (60%)	919 (59%)	493 (56%)	1235 (67%)
Negative edges <sup>d</sup>	334 (43%)	248 (40%)	628 (41%)	395 (44%)	600 (33%)
Modularity <sup>e</sup>	2.96	2.32	1.81	2.78	0.88
Number of communities <sup>f</sup>	26	38	29	58	12
Network diameter <sup>g</sup>	6	9	12	8	6
Average path length <sup>h</sup>	2.95	3.35	3.09	2.99	2.49
Average degree <sup>i</sup>	9.32	6.80	14.66	8.45	23.52
Average clustering coefficient <sup>j</sup>	0.430	0.385	0.449	0.358	0.567

<sup>a</sup> Microbial taxon (at genus level) with at least one significant ( $P < 0.01$ ) and strong (SparCC  $> 0.7$  or  $< -0.7$ ) correlation.

<sup>b</sup> Number of connections/correlations obtained by SparCC analysis.

<sup>c</sup> SparCC positive correlation ( $>0.7$  with  $P < 0.01$ ).

<sup>d</sup> SparCC negative correlation ( $<-0.7$  with  $P < 0.01$ ).

<sup>e</sup> The capability of the nodes to form highly connected communities, that is, a structure with high density of between nodes connections (inferred by Gephi).

<sup>f</sup> A community is defined as a group of nodes densely connected internally (Gephi).

<sup>g</sup> The longest distance between nodes in the network, measured in number of edges (Gephi).

<sup>h</sup> Average network distance between all pair of nodes or the average length off all edges in the network (Gephi).

<sup>i</sup> The average number of connections per node in the network, that is, the node connectivity (Gephi).

<sup>j</sup> How nodes are embedded in their neighborhood and the degree to which they tend to cluster together (Gephi).

## 3. Results

### 3.1. The abiotic environment

The trend in methane uptake was largely comparable in the un-disturbed and disturbed incubations, where activity peaked at 27–34 days before reaching similar rates after 71 days (Fig. 1). However, methane uptake was significantly lower ( $p < 0.05$ ) immediately after desiccation-rewetting when compared to the un-disturbed incubation (un-disturbed,  $0.64 \pm 0.06 \mu\text{mol h}^{-1} \text{g dw}^{-1}$ ; desiccated-rewetted,  $0.5 \pm 0.05 \mu\text{mol h}^{-1} \text{g dw}^{-1}$ ); the adverse effects of the disturbance on

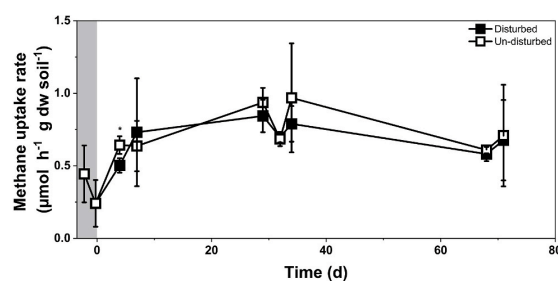


**Fig. 1.** Methane uptake rate in the un-disturbed and disturbed incubations determined during the pre-incubation, as well as 1–7, 27–34, and 64–71 days interval after desiccation-rewetting. Incubations with <sup>13</sup>C- and <sup>12</sup>C-CH<sub>4</sub> were combined (mean  $\pm$  s.d.,  $n = 6$ ) for each treatment. Pre-incubation is denoted by the shaded area. Significant difference in the methane uptake rate between treatments is indicated by an asterisk (*t*-test,  $p < 0.05$ ).

methane uptake were transient (<5 days).

Soluble ammonium and nitrate were rapidly consumed during pre-incubation (Fig. S3). The inorganic N concentrations significantly increased ( $p < 0.05$ ) after desiccation-rewetting. However, the elevated inorganic N concentrations were not sustained. Soluble ammonium and nitrate concentrations decreased to values similar to those after pre-incubation at ~34 days. Particularly, ammonium concentration was significantly higher in the un-disturbed than in the disturbed microcosm after incubation (day 71).

### 3.2. Response in methanotroph abundance

Group-specific qPCR assays were performed to enumerate the *pmoA* genes belonging to type Ia, Ib, and II methanotrophs to be used as proxies for methanotrophic abundances. Generally, the gammaproteobacterial methanotrophs were less responsive to desiccation-rewetting than the alphaproteobacterial ones (Fig. 2). Although values were within the same order of magnitude and the discrepancies documented were not appreciable, changes in the abundance of type Ia and Ib methanotrophs were statistically significant comparing the un-disturbed to the desiccation-rewetted microcosms. Consistently, like for the type II methanotrophs, methane uptake rates were significantly ( $p < 0.05$ ) correlated to the abundances of type Ib methanotrophs (Fig. S4). It is also noteworthy that type I methanotrophs were appreciably more abundant in the disturbed microcosm after the incubation despite showing an adverse effect on population numbers soon after desiccation-rewetting

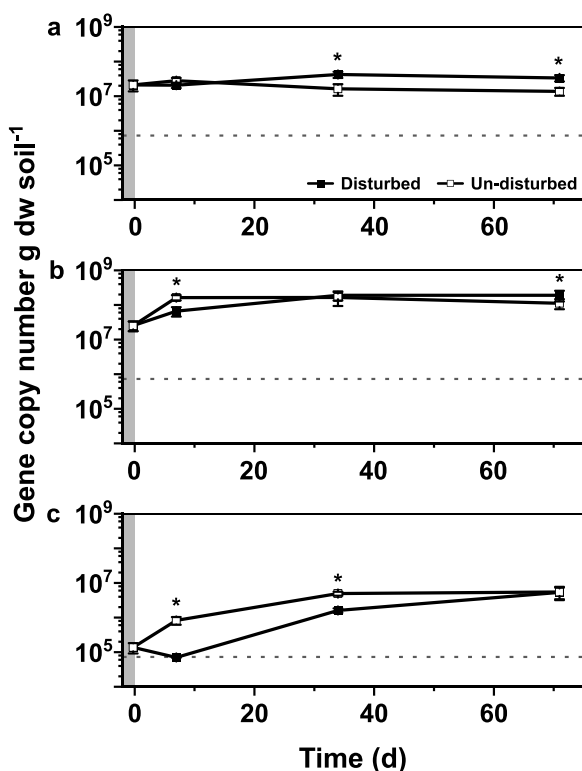


Fig. 2. Temporal changes in the *pmoA* gene abundance of type Ia (a), type Ib (b), and type II (c) methanotrophs, as determined from group-specific qPCR assays. Each qPCR reaction was performed in duplicate for each DNA extract ( $n = 6$ ), giving a total of 12 replicates per treatment, time, and assay. Pre-incubation is denoted by the shaded area, and dashed lines indicate the detection limit of the qPCR assays. Significant difference in the *pmoA* gene abundance between treatments is indicated by an asterisk ( $t$ -test,  $p < 0.05$ ).

(Fig. 2). Particularly, the type II methanotroph abundance recovered well, appreciably increased by around two orders of magnitude after desiccation-rewetting (7–71 days). By comparison, type I methanotroph abundance also increased but within a relatively narrow range (type Ia methanotrophs,  $2.1 \times 10^7 \pm 7.4 \times 10^6$  to  $3.4 \times 10^7 \pm 7.0 \times 10^6$ ; type Ib methanotrophs,  $2.5 \times 10^7 \pm 7.9 \times 10^6$  to  $1.9 \times 10^8 \pm 6.6 \times 10^7$  gene copy numbers  $g\ dw\ soil^{-1}$ ) during the same time frame (Fig. 2). It appears that although type II methanotrophs constitute a minor overall fraction of the methanotrophic population, they were more responsive and significantly increased in abundance after desiccation-rewetting.

### 3.3. Effects of desiccation-rewetting on the methanotrophic community composition, as determined by DNA-based SIP

The bacterial communities, including the methanotrophs in the 'heavy' and 'light' fractions were distinct, as revealed in a PCA for each time interval, showing a clear separation of the  $^{13}C$ -enriched and  $^{12}C$ -enriched DNA (Fig. S5). The 16S rRNA- and *pmoA* gene-derived sequencing analyses were then performed on the  $^{13}C$ -enriched DNA, representing the metabolically active and replicating community. The *pmoA* gene was sequenced before (after pre-incubation) and immediately after disturbance (1–7 days interval), as well as after incubation (64–71 days interval) to follow the recovery of the methanotrophic community composition. The *pmoA* gene sequences, visualized as a PCA (Fig. 3), revealed a distinct active methanotrophic community prior to the disturbance (pre-incubation), and the community shifted soon after desiccation-rewetting, diverging from the community in the un-disturbed microcosm. Over 96% of the variation in the methanotrophic community composition could be explained by PC1 and PC2 (67.9% and 28.5% of the total variance, respectively). The active methanotrophs which emerged soon after desiccation-rewetting (1–7 days interval) were predominantly comprised of members belonging to the putative Rice Paddy Cluster (RPC) closely affiliated to *Methylocaldum* (type Ib; Lüke et al., 2014; Shiao et al., 2018). 71 days post-desiccation-rewetting, the recovering community in the disturbed, as well as in the un-disturbed microcosms were more scattered, largely comprising of type I methanotrophs. The active methanotrophs showed dynamic population shifts after desiccation-rewetting, with the recovered community becoming more varied after incubation.

### 3.4. Effects of desiccation-rewetting on the total bacterial community composition, as determined by DNA-based SIP

The active bacterial community was largely comprised of members belonging to Gammaproteobacteria (families Methylomonadaceae, Methylophilaceae, Burkholderiaceae, Rhodocyclaceae, and Nitrosomonadaceae), Bacteroidetes (family Chitinophagaceae and Microscillaceae), and Gemmatimonadetes (family Gemmatimonadaceae), collectively representing the majority of the population (>75%; Fig. 4). Like the *pmoA* gene sequence analysis, the PCA derived from the 16S rRNA gene sequences revealed a compositional shift in the bacterial community after desiccation-rewetting, but the community recovered after 71 days, closely resembling the composition in the un-disturbed microcosm (Fig. 3). Comparing the community in the un-disturbed and disturbed microcosms, *Methylocaldum* (type Ib methanotroph), and *Methylobacter* (type Ia) as well as members of Burkholderiaceae, were respectively detected at appreciably higher relative abundance soon after desiccation-rewetting (1–7 days interval) and during recovery (27–71 days interval), consistent with the *pmoA* gene sequence analysis (Fig. S6). The active members of the bacterial community in the un-disturbed microcosm were generally more diverse; microorganisms present at differentially higher relative abundances belonged to Proteobacteria, Bacteroidetes, Verrucomicrobia, and Acidobacteria (family/genus level identification, Fig. 4 and S6). Generally, the *pmoA* and 16S rRNA gene sequencing analyses were consistent, revealing the compositional shift and recovery of the active community.

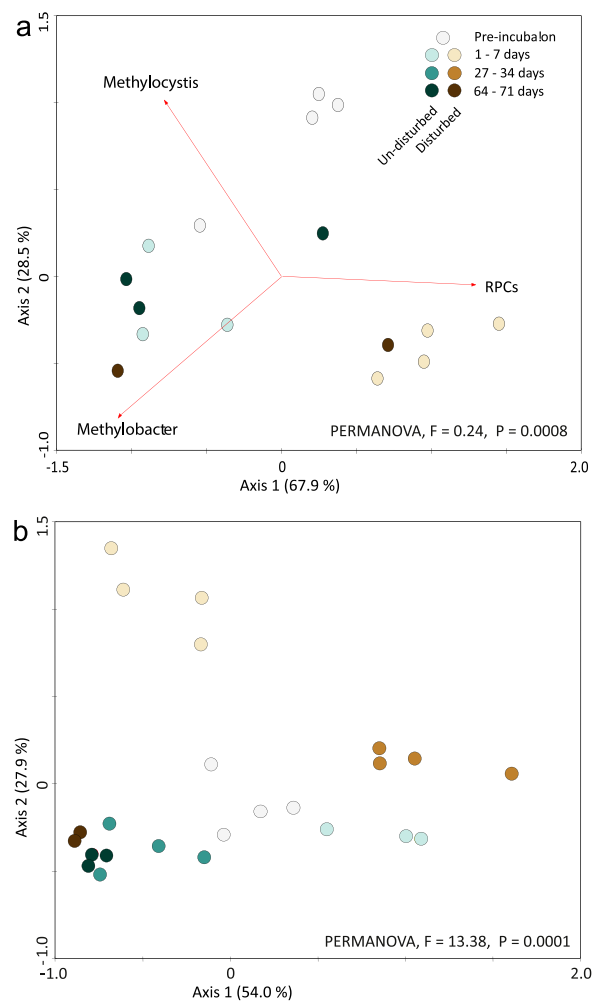


**Fig. 3.** Principal component analysis showing the response of the active methanotrophic (a) and bacterial (b) community composition to desiccation-rewetting, as determined from the relative abundances of the *pmoA* and 16S rRNA gene sequences, respectively. Both the *pmoA* and 16S rRNA gene sequences were derived from the  $^{13}\text{C}$ -enriched DNA ('heavy' fraction). In (A), the vectors represent the predominant methanotrophs belonging to type Ia (*Methylobacter*), type Ib (RPC, rice paddy cluster), and type II (*Methylocystis*).

### 3.5. Response of the co-occurrence network structure to desiccation-rewetting

A 16S rRNA gene-based co-occurrence network analysis derived from the  $^{13}\text{C}$ -enriched 'heavy' fraction was performed to explore the complexity of the methane-driven interactome immediately after, and during the recovery from desiccation-rewetting (resilience; Fig. 5). These networks were assessed by their topological properties comparing the un-disturbed and disturbed incubations (Table 1). Generally, both the microbial communities in the un-disturbed and after desiccation-rewetting increased in connectivity over time (i.e., higher no. of edges, degree, clustering coefficient; Table 1). However, a more connected network emerged after desiccation-rewetting (>27 days), exhibiting a higher number of connections (edges), connections per node (degree), and clustering coefficient than in the un-disturbed community (Table 1). Accordingly, the desiccation-rewetted community was characterized by a shorter average path length (Table 1).

Although modularity generally decreased in all microcosms after pre-incubation, the community showed a less modular structure after desiccation-rewetting when compared to the un-disturbed community during recovery. Additionally, to account for biases arising from the imbalance number of replicates used to construct the networks (i.e., grouping of 27–34 and 64–71 days intervals yielding a higher number of replicates,  $n = 6$  or  $7$ ), the networks were re-constructed using 4 randomly selected replicates from all replicates for the 27–71 days interval. The results obtained were consistent and support the general trends documented in the networks using all replicates (Table S2). Overall, the network structure of the active bacterial community became more complex and connected after recovery from desiccation-rewetting, demonstrating that the disturbance fostered a closer association of community members within the interactome.

The top five nodes with the highest betweenness centrality were identified in all treatments (Fig. 5 & Table S3). As anticipated, the key nodes comprised of methanotrophs, as well as non-methanotrophic methylotrophs; the methanotrophs are a subset of the methylotrophs (Chistoserdova, 2015). Surprisingly, many other non-methanotrophic bacterial taxa also formed the key nodes. These taxa were rather unique to each treatment (un-disturbed and disturbed) at 1–7 and 27–71 days intervals (Fig. 5 & Table S3). It appears that non-methanotrophs, albeit unable to assimilate methane directly, were also relevant members of the interactome.

## 4. Discussion

### 4.1. Recovery and resilience of the methanotrophic activity and community composition following desiccation-rewetting

The methanotrophic activity was resilient to desiccation-rewetting. Periodic exposure of the paddy soil to lower soil water content after drainage for rice harvest may have selected for a desiccation-tolerant methanotrophic community. This may partly explain the transient (<5 days) adverse effect on methane uptake rates, which rapidly recovered. Nevertheless, the recovery in methanotrophic activity to single disturbance events is not entirely unexpected, as has been shown before (e.g., soil structural disruption, (Kumaresan et al., 2011); long-term drought spanning over decades, (Collet et al., 2015); desiccation and heat stress, (Ho et al., 2016b, 2016c). Similarly, methanotrophic activity recovered from multiple disturbances, with soils harboring low-affinity methanotrophs showing resilience to repeated desiccation and ammonium stress (van Kruijstum et al., 2018), and compounded disturbances associated to land transformation given sufficient recovery time (e.g., over 15 years after peat excavation; Reumer et al., 2018). However, the recovery in methane oxidation may be accompanied by compositional shifts in the methanotrophic community, affecting the trajectory of methanotroph succession after disturbance (Ho et al., 2016b).

In contrast to previous work (e.g., Kumaresan et al., 2011; Collet et al., 2015; Ho et al., 2016b; Jurburg et al., 2017; Krause et al., 2017; Ho et al., 2018; Reumer et al., 2018), a time-series  $^{13}\text{C}$ -CH<sub>4</sub> labeling approach was employed in this study to directly relate not only the methanotrophic activity to the response of the metabolically active methanotrophs, but also to the structure of the interaction network, to desiccation-rewetting. The active bacterial community composition, including the methanotrophs, recovered well as indicated by the 16S rRNA gene sequence analysis, which showed that the disturbed community resembled that of the un-disturbed community, clustering closely together after incubation (PCA; Fig. 3). Specifically, *Methylocaldum* was predominant soon after desiccation-rewetting, whereas *Methylobacter* and Burkholderiaceae were present at relatively higher abundances during recovery from the disturbance (Fig. 4 and S6). Gammaproteobacterial methanotrophs, including *Methylocaldum* and *Methylobacter* species, are generally known to be rapid colonizers, proliferating under high nutrient and methane availability (Ho et al., 2013, 2016c), whereas the dominance and role of Burkholderiaceae



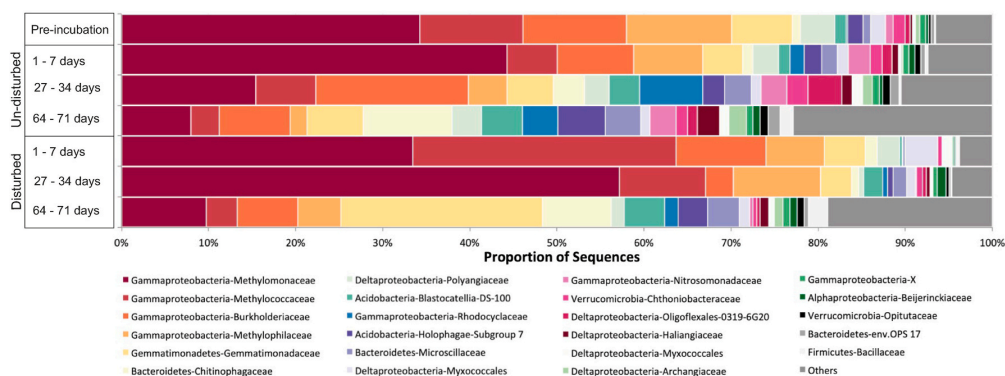


Fig. 4. The mean active bacterial community composition in the un-disturbed and disturbed incubations, based on the 16S rRNA gene sequence analysis. The 16S rRNA gene sequences were derived from the  $^{13}\text{C}$ -enriched DNA after incubation at 1–7, 27–34, and 64–71 days intervals.

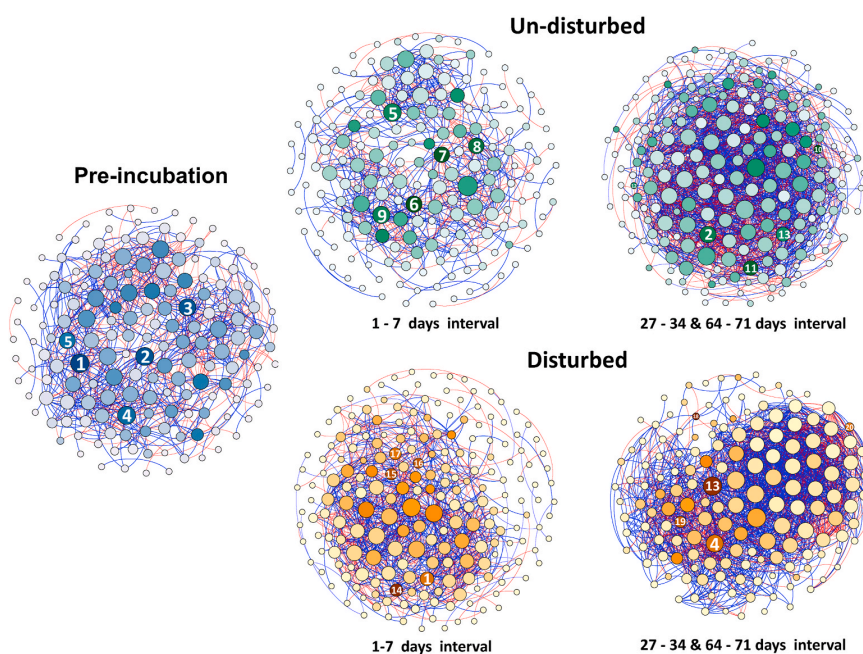


Fig. 5. Co-occurrence network analysis of the active bacterial community based on the 16S rRNA gene during pre-incubation, and after desiccation-rewetting. The 16S rRNA gene sequences were derived from the  $^{13}\text{C}$ -enriched DNA ('heavy' fraction). Samples from 27 to 34 and 64–71 days intervals were combined to have sufficient replicates for the network analysis; density gradient ultracentrifugation was unsuccessful in 2 of 4 replicated  $^{13}\text{C}$ - $\text{CH}_4$  incubations in the disturbed microcosm at 64–71 days interval. Significant ( $p < 0.01$ ) positive (magnitude  $> 0.7$ ) and negative (magnitude,  $< -0.7$ ) SparCC correlations are respectively denoted by the blue and red edges. Each node represents a bacterial taxa at the OTU level, and the size of the node corresponds to the number of connections (degree). The colour intensity indicates the betweenness centrality (darker shades indicating higher values). The numbers in the key nodes (top five nodes with highest betweenness centrality) refer to (1) Methylophilaceae, (2) Rhodocyclaceae, (3) *Gemmatirosa*, (4) *Crenothrix* (methane-oxidizer), (5) Acidobacteria subgroup 6, (6) Gemmatimonadaceae, (7) *Methylomonas* (methanotroph), (8) *Noviherbaspirillum*, (9) Beijerinckiaceae, (10) *Paenibacillus*, (11) Acidobacteria subgroup 7, (12) Opiritaceae, (13) Unclassified Bacteria, (14) *Sphingomonas*, (15) Blastocatellia, (16) *Ideonella*, (17) *Chthoniobacter*, (18) Proteobacteria, (19) Chitinophagaceae (20) Microscillaceae. Detailed topological properties of the networks are provided in Table 1. (For interpretation of the references to colour in this figure legend, the reader is referred to the Web version of this article.)

during recovery from disturbances remain elusive. However, members of the family Burkholderiaceae exhibit metabolic versatility, with *Cupriavidus* reported to stimulate methanotrophic growth (Stock et al., 2013). Furthermore, *Ralstonia*, another Burkholderiaceae, has been documented to co-occur with methanotrophs in a  $^{13}\text{C}$ - $\text{CH}_4$  labeling study, likely caused by cross-feeding, suggesting that there was a trophic interaction with methanotrophs (Qiu et al., 2008). Like for the gammaproteobacterial type Ib methanotrophs, the significant correlation between methane uptake rates and the alphaproteobacterial

methanotrophs suggests a coupling of methanotrophic activity and the growth of these methanotrophic sub-groups (Fig S4). The alphaproteobacterial methanotrophs (*Methylocystis*; type II) were seemingly more responsive to the disturbance, exhibiting a gradual increase in numerical abundance during the incubation (Fig. 2). This reinforces previous studies documenting the emergence of this sub-group (*Methylocystis-Methylotinus*) after stress events (Ho et al., 2011, 2016b, 2016c; van Kruistum et al., 2018). It is thought that desiccation-rewetting may trigger the proliferation of alphaproteobacterial methanotrophs either

by awakening dormant members of the seedbank community and/or generating open niches for recolonization (Whittenbury et al., 1970; Collet et al., 2015; Ho et al., 2016c; Kaupper et al., 2020b). Also, the gradual increase in alphaproteobacterial methanotroph abundance may be attributable to a relatively slower recovery after being adversely affected by desiccation-rewetting, having a lower initial abundance than gammaproteobacterial methanotrophs. Admittedly, we cannot exclude experimental artifacts deriving from soil preparation which may affect the methanotrophs, but the soil was mildly pre-processed (i.e., air-dried at ambient temperature and sieved), ensuring homogeneity for a standardized incubation. Overall, the differential response among methanotroph sub-groups was consistent with trends detected previously.

#### 4.2. The emergence of a more complex and connected methane-driven interactome after desiccation-rewetting

Methanotrophs thrive in the presence of specific accompanying microorganisms, exhibiting higher activity and growth as cocultures than as monocultures (Iguchi et al., 2011; Stock et al., 2013; Ho et al., 2014; Jeong et al., 2014; Benner et al., 2015; Krause et al., 2017; Veraart et al., 2018). This emphasizes the relevance of interdependent relationships among members of a methanotrophic interactome for community functioning. Although methanotrophic activity and community composition may recover, disturbances may exert an impact on the structure of the microbial network, affecting the interaction among community members which may have consequences in future disturbances (Berg and Ellers, 2010; Bissett et al., 2013; Sun et al., 2013; Ho et al., 2020; Ratzke et al., 2020).

Interestingly, the methanotrophic interactome became more complex and increased in connectivity during recovery (>27 days) from desiccation-rewetting (Table 1 & Fig. 5). The disturbance-induced highly connected interactome suggests higher competition for specific niches (van Elsas et al., 2012), which likely became available after the disturbance event. This enables rapid re-colonization of the open niches, resulting in the recovery of methanotrophic activity and abundance, particularly when methane is not limiting (Ho et al., 2011; Pan et al., 2014; Kaupper et al., 2020b). The emergence of a more complex network after disturbance also suggests that the loss of some microorganisms were compensated by other community members having similar roles; the community was thus sufficiently redundant to sustain methanotrophic activity (Eldridge et al., 2015; Mendes et al., 2015; Tripathi et al., 2016). Similarly, when compared to an un-perturbed soil, the bacterial network after bio-perturbation (>12 months) caused by the foraging activity of burrowing mammals increased in connectedness (Eldridge et al., 2015). In another form of disturbance, the microbial network was altered, increasing in the number of positively co-occurring bacteria during the recovery from a forest fire (12 months; Pérez-Valera et al., 2017). In line with these studies, the interaction networks increased in complexity, becoming more connected after deforestation for oil palm (Tripathi et al., 2016) and after abandonment of agriculture (Morriën et al., 2017).

Like these disturbances, desiccation-rewetting fostered closer associations among interacting members of the methanotrophic interactome, supporting our hypothesis. The increase in network complexity, as indicated by a higher number of edges, degree, and clustering efficiency suggests a more connected network, concomitant to a shorter average path length which indicates a tighter and more efficient network, in response to desiccation-rewetting (Zhou et al., 2010; Mendes et al., 2018; Dal Co et al., 2020). Hence, desiccation-rewetting likely augmented or consolidated metabolic exchange to increase co-occurrence among community members within the interactome, giving rise to a more complex interaction network (Zelezniak et al., 2015; Ratzke et al., 2020). The increase in network complexity directly related to the recovery in methanotrophic activity. Nevertheless, modularity decreased over time, possessing fewer independently connected groups (compartments) within the network (Zhou et al., 2010),

more pronounced in the desiccation-rewetted community. A highly modular network is thought to restrict and localize the effects of a disturbance within compartments in the network (Ruiz-Moreno et al., 2006; Zhou et al., 2010). Therefore, the loss of modularity after contemporary disturbances suggests that future disturbances will more evenly affect community members. Hence, community composition and activity, when examined alongside the network structure, provided a more comprehensive understanding of microbial responses to contemporary and future disturbances.

Expectedly, the nodes with high betweenness centrality were found to comprise of methylotrophs, including the methanotrophs (Fig. 5). These key nodes were not necessarily bacterial taxa that were present at significantly higher relative abundances (e.g., Burkholderiaceae; Fig. 4) but rather, refer to nodes acting as a bridge between other nodes with significantly higher frequencies (Poudel et al., 2016). As such, the key nodes within the network are crucial members of the methanotrophic interactome, potentially having a significant regulatory effect on the other members of the interactome; the loss of the key nodes is anticipated to unravel the interaction network (Williams et al., 2014; van der Heijden and Hartmann, 2016). Because the methylotrophs can oxidize methanol and other intermediary products of methane oxidation (e.g., formaldehyde, formate), cross-feeding between the methanotrophs and non-methanotrophic methylotrophs (e.g., *Methylotenera*, *Methylophilus*) drives their co-occurrence, as has been established before (Krause et al., 2017). Interestingly, many non-methanotrophs/methylotrophs also formed the key nodes. Given that the non-methanotrophs cannot utilize methane as a carbon and energy source, their identification as key nodes indicates their potential regulatory role, indirectly via interaction-induced effects, on the methanotrophic activity (van der Heijden and Hartmann, 2016). Among the non-methanotrophic key nodes, other members of Sphingomonadaceae (*Sphingopyxis*) but not specifically *Sphingomonas*, have been shown to significantly stimulate the expression of the *pmoA* gene when co-cultured with an alphaproteobacterial methanotroph (*Methylocystis*; Jeong et al., 2014). Members of Gemmatimonadaceae have been co-detected along with the methanotrophs in  $^{13}\text{C}$ -CH<sub>4</sub> labelling SIP studies, but their exact role within the interactome remains to be elucidated (Zheng et al., 2014). Similarly, the underlying mechanisms that drive the interaction between other co-occurring bacterial taxa and the methanotrophs warrant further exploration through isolation and co-culture studies (Kwon et al., 2018). However, it is likely that some members of the co-occurring taxa may reciprocally interact with the methanotrophs, supporting methanotrophic growth and activity (e.g., *Sphingomonas*), and contributed to the resilience of the methanotrophs following desiccation-rewetting. Accordingly, the bacterial taxa representing key nodes were distinct in the un-disturbed microcosm and after desiccation-rewetting, despite compositional recovery among metabolically active members of the community (Fig. 3). This indicates sufficient redundancy among active members of the methanotrophic interactome; presumably, the different key taxa in the un-disturbed and disturbed community shared similar traits relevant for community functioning.

## 5. Conclusion

Our findings, based on the time-resolved  $^{13}\text{C}$ -CH<sub>4</sub> SIP approach, reinforced previous DNA-based studies, showing the differential response among the methanotrophs to disturbances, likely reflecting on their ecological life strategies (Ho et al., 2013). Widening current understanding, we showed that although methanotrophic activity recovered after desiccation-rewetting and the post-disturbance microbial community may resemble those in the un-disturbed soil, the disturbance legacy manifests in the structure of the co-occurrence network, which became more complex but less modular. Therefore, community interaction profoundly changed after desiccation-rewetting, which may have consequences for community functioning with recurring and/or compounded disturbances. More generally, our findings move beyond

biodiversity-ecosystem functioning relationships to encompass interaction-induced responses in community functioning.

#### Declaration of competing interest

The authors declare that they have no known competing financial interests or personal relationships that could have appeared to influence the work reported in this paper.

#### Acknowledgements

We are grateful to Stefanie Hetz and Daria Frohloff for excellent research assistance. TK and AH are financially supported by the Deutsche Forschungsgemeinschaft (grant no. HO6234/1-1). AH and MAH are also financially supported by the Leibniz Universität Hannover, Germany.

#### Appendix A. Supplementary data

Supplementary data to this article can be found online at <https://doi.org/10.1016/j.soilbio.2020.108109>.

#### References

- Anderson, M.J., 2001. A new method for non-parametric multivariate analysis of variance. *Austral Ecology* 26, 32–46.
- Barberán, A., Bates, S.T., Casamayor, E.O., Fierer, N., 2012. Using network analysis to explore co-occurrence patterns in soil microbial communities. *The ISME Journal* 6, 343–351.
- Bastian, M., Heymann, S., Jacomy, M., 2009. Gephi: an open source software for exploring and manipulating networks. In: *International AAAI Conference on Weblogs and Social Media*, pp. 361–362.
- Begonja, A., Hrsak, D., 2001. Effect of growth conditions on the expression of soluble methane monooxygenase. *Food Technology and Biotechnology* 29–35.
- Benner, J., Smet, D. de, Ho, A., Kerckhof, F.-M., Vanhaecke, L., Heylen, K., Boon, N., 2015. Exploring methane-oxidizing communities for the co-metabolic degradation of organic micropollutants. *Applied Microbiology and Biotechnology* 99, 3609–3618.
- Berg, M.P., Eilers, J., 2010. Trait plasticity in species interactions: a driving force of community dynamics. *Evolutionary Ecology* 24, 617–629.
- Bissett, A., Brown, M.V., Siciliano, S.D., Thrall, P.H., 2013. Microbial community responses to anthropogenically induced environmental change: towards a systems approach. *Ecology Letters* 16 (Suppl. 1), 128–139.
- Borgatti, S.P., 2005. Centrality and network flow. *Social Networks* 27, 55–71.
- Callahan, B., 2017. Rdp Taxonomic Training Data Formatted for Dada2 (Rdp Trainset 16/Release 11.5). Zenodo.
- Chistoserdova, L., 2015. Methylophilic in natural habitats: current insights through metagenomics. *Applied Microbiology and Biotechnology* 99, 5763–5779.
- Christiansen, J.R., Levy-Booth, D., Prescott, C.E., Grayston, S.J., 2016. Microbial and environmental controls of methane fluxes along a soil moisture gradient in a Pacific coastal temperate rainforest. *Ecosystems* 19, 1255–1270.
- Collet, S., Reim, A., Ho, A., Frenzel, P., 2015. Recovery of paddy soil methanotrophs from long term drought. *Soil Biology and Biochemistry* 88, 69–72.
- Dal Co, A., van Vliet, S., Kiviet, D.J., Schlegel, S., Ackermann, M., 2020. Short-range interactions govern the dynamics and functions of microbial communities. *Nature ecology & evolution* 4, 366–375.
- Danilova, O.V., Belova, S.E., Kulichevskaya, L.S., Dedysh, S.N., 2015. Decline of activity and shifts in the methanotrophic community structure of an ombrotrophic peat bog after wildfire. *Microbiology* 84, 624–629.
- Dumont, M.G., Pommerenke, B., Casper, P., Conrad, R., 2011. DNA-, rRNA- and mRNA-based stable isotope probing of aerobic methanotrophs in lake sediment. *Environmental Microbiology* 13, 1153–1167.
- Dumont, M.G., Lüke, C., Deng, Y., Frenzel, P., 2014. Classification of pmoA amplicon pyrosequences using BLAST and the lowest common ancestor method in MEGAN. *Frontiers in Microbiology* 5.
- Eldridge, D.J., Woodhouse, J.N., Curlevski, N.J.A., Hayward, M., Brown, M.V., Neilan, B.A., 2015. Soil-foraging animals alter the composition and co-occurrence of microbial communities in a desert shrubland. *The ISME Journal* 9, 2671–2681.
- Friedman, J., Alm, E.J., 2012. Inferring correlation networks from genomic survey data. *PLoS Computational Biology* 8, e1002687.
- Hammer, Ø., Harper, D.A.T., Ryan, P.D., 2001. PAST: Paleontological Statistics Software Package for Education and Data Analysis. *Palaeontologia Electronica*, p. 9.
- Ho, A., Lüke, C., Cao, Z., Frenzel, P., 2011. Ageing well: methane oxidation and methane oxidizing bacteria along a chronosequence of 2000 years. *Environmental microbiology reports* 3, 738–743.
- Ho, A., Kerckhof, F.-M., Luke, C., Reim, A., Krause, S., Boon, N., Bodelier, P.L.E., 2013. Conceptualizing functional traits and ecological characteristics of methane-oxidizing bacteria as life strategies. *Environmental microbiology reports* 5, 335–345.
- Ho, A., Roy, K. de, Thas, O., Neve, J. de, Hoefman, S., Vandamme, P., Heylen, K., Boon, N., 2014. The more, the merrier: heterotroph richness stimulates methanotrophic activity. *The ISME Journal* 8, 1945–1948.
- Ho, A., Angel, R., Veraart, A.J., Daebeler, A., Jia, Z., Kim, S.Y., Kerckhof, F.-M., Boon, N., Bodelier, P.L.E., 2016a. Biotic interactions in microbial communities as modulators of biogeochemical processes: methanotrophy as a model system. *Frontiers in Microbiology* 7, 1285.
- Ho, A., van den Brink, E., Reim, A., Krause, S.M.B., Bodelier, P.L.E., 2016b. Recurrence and frequency of disturbance have cumulative effect on methanotrophic activity, abundance, and community structure. *Frontiers in Microbiology* 6, 1493.
- Ho, A., Lüke, C., Reim, A., Frenzel, P., 2016c. Resilience of (seed bank) aerobic methanotrophs and methanotrophic activity to desiccation and heat stress. *Soil Biology and Biochemistry* 101, 130–138.
- Ho, A., Di Lonardo, D.P., Bodelier, P.L.E., 2017. Revisiting life strategy concepts in environmental microbial ecology. *FEMS Microbiology Ecology* 93.
- Ho, A., Mo, Y., Lee, H.J., Sauheitl, L., Jia, Z., Horn, M.A., 2018. Effect of salt stress on aerobic methane oxidation and associated methanotrophs; a microcosm study of a natural community from a non-saline environment. *Soil Biology and Biochemistry* 125, 210–214.
- Ho, A., Lee, H.J., Reumer, M., Meima-Franke, M., Raaijmakers, C., Zweepers, H., Boer, W., van der Putten, W.H.de, Bodelier, P.L.E., 2019. Unexpected role of canonical aerobic methanotrophs in upland agricultural soils. *Soil Biology and Biochemistry* 131, 1–8.
- Ho, A., Mendes, L.W., Lee, H.J., Kaupper, T., Mo, Y., Poehlein, A., Bodelier, P.L.E., Jia, Z., Horn, M.A., 2020. Response of a methane-driven interaction network to stressor intensification. *FEMS Microbiology Ecology* 96.
- Horn, M.A., Ihssen, J., Matthies, C., Schramm, A., Acker, G., Drake, H.L., 2005. *Dechloromonas denitrificans* sp. nov., *Flavobacterium denitrificans* sp. nov., *Paenibacillus anaericanus* sp. nov. and *Paenibacillus terrae* strain MH72, N2O-producing bacteria isolated from the gut of the earthworm *Aporrectodea caliginosa*. *International Journal of Systematic and Evolutionary Microbiology* 55, 1255–1265.
- Iguchi, H., Yurimoto, H., Sakai, Y., 2011. Stimulation of methanotrophic growth in cocultures by cobalamin excreted by rhizobia. *Applied and Environmental Microbiology* 77, 8509–8515.
- Jeong, S.-Y., Cho, K.-S., Kim, T.G., 2014. Density-dependent enhancement of methane oxidation activity and growth of *Methylocystis* sp. by a non-methanotrophic bacterium *Sphingopyxis* sp. *Biotechnology reports (Amsterdam, Netherlands)* 4, 128–133.
- Jurburg, S.D., Nunes, I., Bregjrod, A., Jacquiod, S., Priemé, A., Sørensen, S.J., van Elsas, J.D., Salles, J.F., 2017. Legacy effects on the recovery of soil bacterial communities from extreme temperature perturbation. *Frontiers in Microbiology* 8, 1832.
- Karwautz, C., Kus, G., Stöckl, M., Neu, T.R., Lueders, T., 2018. Microbial megacities fueled by methane oxidation in a mineral spring cave. *The ISME Journal* 12, 87–100.
- Kaupper, T., Hetz, S., Kolb, S., Yoon, S., Horn, M.A., Ho, A., 2020a. Deforestation for oil palm: impact on microbially mediated methane and nitrous oxide emissions, and soil bacterial communities. *Biology and Fertility of Soils* 56, 287–298.
- Kaupper, T., Luehrs, J., Lee, H.J., Mo, Y., Jia, Z., Horn, M.A., Ho, A., 2020b. Disentangling abiotic and biotic controls of aerobic methane oxidation during recolonization. *Soil Biology and Biochemistry* 142, 107729.
- Knief, C., 2015. Diversity and habitat preferences of cultivated and uncultivated aerobic methanotrophic bacteria evaluated based on *pmoA* as molecular marker. *Frontiers in Microbiology* 6, 1346.
- Kolb, S., Knief, C., Stubner, S., Conrad, R., 2003. Quantitative detection of methanotrophs in soil by novel *pmoA*-targeted real-time PCR assays. *Applied and Environmental Microbiology* 69, 2423–2429.
- Krause, S.M.B., Johnson, T., Samadhi Karunaratne, Y., Fu, Y., Beck, D.A.C., Chistoserdova, L., Lidstrom, M.E., 2017. Lanthanide-dependent cross-feeding of methane-derived carbon is linked by microbial community interactions. *Proceedings of the National Academy of Sciences of the United States of America* 114, 358–363.
- Krueger, M., Frenzel, P., Conrad, R., 2001. Microbial processes influencing methane emission from rice fields. *Global Change Biology* 7, 49–63.
- Kumaresan, D., Stralis-Pavese, N., Abell, G.C.J., Bodrossy, L., Murrell, J.C., 2011. Physical disturbance to ecological niches created by soil structure alters community composition of methanotrophs. *Environmental microbiology reports* 3, 613–621.
- Kwon, M., Ho, A., Yoon, S., 2018. Novel approaches and reasons to isolate methanotrophic bacteria with biotechnological potentials: recent achievements and perspectives. *Applied Microbiology and Biotechnology* 103, 1–8.
- Lüke, C., Frenzel, P., Ho, A., Fiantis, D., Schad, P., Schneider, B., Schwark, L., Utami, S.R., 2014. Macroecology of methane-oxidizing bacteria: the  $\beta$ -diversity of *pmoA* genotypes in tropical and subtropical rice paddies. *Environmental Microbiology* 16, 72–83.
- Mendes, L.W., Tsai, S.M., Navarrete, A.A., Hollander, M., van Veen, J.A.de, Kuramae, E.E., 2015. Soil-borne microbiome: linking diversity to function. *Microbial Ecology* 70, 255–265.
- Mendes, L.W., Raaijmakers, J.M., Hollander, M. de, Mendes, R., Tsai, S.M., 2018. Influence of resistance breeding in common bean on rhizosphere microbiome composition and function. *The ISME Journal* 12, 212–224.
- Morrién, E., Hannula, S.E., Snoek, L.B., Helmsing, N.R., Zweepers, H., Hollander, M. de, Soto, R.L., Bouffaud, M.-L., Buée, M., Dimmers, W., Duyts, H., Geisen, S., Girlanda, M., Griffiths, R.I., Jørgensen, H.-B., Jensen, J., Plassart, P., Redecker, D., Schmelz, R.M., Schmidt, O., Thomson, B.C., Tisserant, E., Uroz, S., Winding, A., Bailey, M.J., Bonkowski, M., Faber, J.H., Martin, F., Lemanceau, P., Boer, W., van Veen, J.A.de, van der Putten, W.H., 2017. Soil networks become more connected and take up more carbon as nature restoration progresses. *Nature Communications* 8, 14349.

- Mo, Y., Jin, F., Zheng, Y., Baoyin, T., Ho, A., Jia, Z., 2020. Succession of bacterial community and methanotrophy during lake shrinkage. *Journal of Soils and Sediments* 20, 1545–1557.
- Neufeld, J.D., Vohra, J., Dumont, M.G., Lueders, T., Manefield, M., Friedrich, M.W., Murrell, J.C., 2007. DNA stable-isotope probing. *Nature Protocols* 2, 860–866.
- Newman, M.E.J., 2003. The structure and function of complex networks. *SIAM Review* 45, 167–256.
- Op den Camp, H.J.M., Islam, T., Stott, M.B., Harhangi, H.R., Hynes, A., Schouten, S., Jetten, M.S.M., Birkeland, N.-K., Pol, A., Dunfield, P.F., 2009. Environmental, genomic and taxonomic perspectives on methanotrophic Verrucomicrobia. *Environmental microbiology reports* 1, 293–306.
- Pan, Y., Abell, G.C.J., Bodelier, P.L.E., Meima-Franke, M., Sessitsch, A., Bodrossy, L., 2014. Remarkable recovery and colonization behaviour of methane oxidizing bacteria in soil after disturbance is controlled by methane source only. *Microbial Ecology* 68, 259–270.
- Pérez-Valera, E., Goberna, M., Faust, K., Raes, J., García, C., Verdú, M., 2017. Fire modifies the phylogenetic structure of soil bacterial co-occurrence networks. *Environmental Microbiology* 19, 317–327.
- Poude, R., Jumpponen, A., Schlatter, D.C., Paulitz, T.C., Gardener, B.B.M., Kinkel, L.L., Garrett, K.A., 2016. Microbiome networks: a systems framework for identifying candidate microbial assemblages for disease management. *Phytopathology* 106, 1083–1096.
- Praeg, N., Wagner, A.O., Illmer, P., 2017. Plant species, temperature, and bedrock affect net methane flux out of grassland and forest soils. *Plant and Soil* 410, 193–206.
- Qiu, Q., Noll, M., Abraham, W.-R., Lu, Y., Conrad, R., 2008. Applying stable isotope probing of phospholipid fatty acids and rRNA in a Chinese rice field to study activity and composition of the methanotrophic bacterial communities in situ. *The ISME Journal* 2, 602–614.
- Quast, C., Pruesse, E., Yilmaz, P., Gerken, J., Schweer, T., Yarza, P., Peplies, J., Glöckner, F.O., 2013. The SILVA ribosomal RNA gene database project: improved data processing and web-based tools. *Nucleic Acids Research* 41, D590–D596.
- Ratzke, C., Barrere, J., Gore, J., 2020. Strength of species interactions determines biodiversity and stability in microbial communities. *Nature ecology & evolution* 4, 376–383.
- Reim, A., Lüke, C., Krause, S., Pratscher, J., Frenzel, P., 2012. One millimetre makes the difference: high-resolution analysis of methane-oxidizing bacteria and their specific activity at the oxic-anoxic interface in a flooded paddy soil. *The ISME Journal* 6, 2128–2139.
- Reis, P.C.J., Thottathil, S.D., Ruiz-González, C., Prairie, Y.T., 2020. Niche separation within aerobic methanotrophic bacteria across lakes and its link to methane oxidation rates. *Environmental Microbiology* 22, 738–751.
- Reumer, M., Harnisz, M., Lee, H.J., Reim, A., Grunert, O., Putkinen, A., Fritze, H., Bodelier, P.L.E., Ho, A., 2018. Impact of peat mining and restoration on methane turnover potential and methane-cycling microorganisms in a northern bog. *Applied and Environmental Microbiology* 84.
- Ruiz-Moreno, D., Pascual, M., Riolo, R., 2006. Exploring network space with genetic algorithms: modularity, resilience and reactivity. In: Pascua, I.M., Dunne, J.A. (Eds.), *Ecological Networks: Linking Structure to Dynamics in Food Webs*. Oxford University Press, New York, NY, pp. 187–208.
- Schloss, P.D., Westcott, S.L., Ryabin, T., Hall, J.R., Hartmann, M., Hollister, E.B., Lesniewski, R.A., Oakley, B.B., Parks, D.H., Robinson, C.J., Sahl, J.W., Stres, B., Thallinger, G.G., van Horn, D.J., Weber, C.F., 2009. Introducing mothur: open-source, platform-independent, community-supported software for describing and comparing microbial communities. *Applied and Environmental Microbiology* 75, 7537–7541.
- Semrau, J.D., DiSpirito, A.A., Yoon, S., 2010. Methanotrophs and copper. *FEMS Microbiology Reviews* 34, 496–531.
- Sharp, C.E., Smirnova, A.V., Graham, J.M., Stott, M.B., Khadka, R., Moore, T.R., Grasby, S.E., Strack, M., Dunfield, P.F., 2014. Distribution and diversity of Verrucomicrobia methanotrophs in geothermal and acidic environments. *Environmental Microbiology* 16, 1867–1878.
- Shiau, Y.-J., Cai, Y., Jia, Z., Chen, C.-L., Chiu, C.-Y., 2018. Phylogenetically distinct methanotrophs modulate methane oxidation in rice paddies across Taiwan. *Soil Biology and Biochemistry* 124, 59–69.
- Shrestha, P.M., Kamman, C., Lenhart, K., Dam, B., Liesack, W., 2012. Linking activity, composition and seasonal dynamics of atmospheric methane oxidizers in a meadow soil. *The ISME Journal* 6, 1115–1126.
- Stock, M., Hoefman, S., Kerckhof, F.-M., Boon, N., Vos, P. de, Baets, B. de, Heylen, K., Waegeman, W., 2013. Exploration and prediction of interactions between methanotrophs and heterotrophs. *Research in Microbiology* 164, 1045–1054.
- Sun, M.Y., Dafforn, K.A., Johnston, E.L., Brown, M.V., 2013. Core sediment bacteria drive community response to anthropogenic contamination over multiple environmental gradients. *Environmental Microbiology* 15, 2517–2531.
- Tripathi, B.M., Edwards, D.P., Mendes, L.W., Kim, M., Dong, K., Kim, H., Adams, J.M., 2016. The impact of tropical forest logging and oil palm agriculture on the soil microbiome. *Molecular Ecology* 25, 2244–2257.
- Trotsenko, Y.A., Murrell, J.C., 2008. Metabolic aspects of aerobic obligate methanotrophy. In: Laskin, A.L., Gadd, G.M., Sariaslani, S. (Eds.), *Advances in Applied Microbiology*, first ed., vol. 63. Academic Press, Amsterdam, pp. 183–229.
- van der Heijden, M.G.A., Hartmann, M., 2016. Networking in the plant microbiome. *PLoS Biology* 14, e1002378.
- van Elsas, J.D., Chiurazzi, M., Mallon, C.A., Elhottova, D., Kristufek, V., Salles, J.F., 2012. Microbial diversity determines the invasion of soil by a bacterial pathogen. *Proceedings of the National Academy of Sciences of the United States of America* 109, 1159–1164.
- van Kruistum, H., Bodelier, P.L.E., Ho, A., Meima-Franke, M., Veraart, A.J., 2018. Resistance and recovery of methane-oxidizing communities depends on stress regime and history; A microcosm study. *Frontiers in Microbiology* 9, 1714.
- Veraart, A.J., Garbeva, P., van Beersum, F., Ho, A., Hordijk, C.A., Meima-Franke, M., Zweers, A.J., Bodelier, P.L.E., 2018. Living apart together-bacterial volatiles influence methanotrophic growth and activity. *The ISME Journal* 12, 1163–1166.
- Whittenbury, R., Davies, S.L., Davey, J.F., 1970. Exospores and cysts formed by methane-utilizing bacteria. *Journal of General Microbiology* 61, 219–226.
- Williams, R.J., Howe, A., Hofmockel, K.S., 2014. Demonstrating microbial co-occurrence pattern analyses within and between ecosystems. *Frontiers in Microbiology* 5, 358.
- Zelezniak, A., Andrejev, S., Ponomarova, O., Mende, D.R., Bork, P., Patil, K.R., 2015. Metabolic dependencies drive species co-occurrence in diverse microbial communities. *Proceedings of the National Academy of Sciences of the United States of America* 112, 6449–6454.
- Zhang, J., Kobert, K., Flouri, T., Stamatakis, A., 2014. PEAR: a fast and accurate Illumina Paired-End reAd mergeR. *Bioinformatics (Oxford, England)* 30, 614–620.
- Zheng, Y., Huang, R., Wang, B.Z., Bodelier, P.L.E., Jia, Z.J., 2014. Competitive interactions between methane- and ammonia-oxidizing bacteria modulate carbon and nitrogen cycling in paddy soil. *Biogeosciences* 11, 3353–3368.
- Zhou, J., Deng, Y., Luo, F., He, Z., Tu, Q., Zhi, X., 2010. Functional molecular ecological networks. *mBio* 1, 1–10.



#### **A.4 Supplementary information - When the going gets tough: emergence of a complex methane-driven interaction network during recovery from desiccation-rewetting**

Thomas Kaupper<sup>1</sup>, Lucas W. Mendes<sup>2</sup>, Hyo Jung Lee<sup>3</sup>, Yongliang Mo<sup>4</sup>, Anja Poehlein<sup>5</sup>, Zhongjun Jia<sup>4</sup>, Marcus A. Horn<sup>1</sup>, Adrian Ho<sup>1</sup>.

<sup>1</sup> Institute for Microbiology, Leibniz Universität Hannover, Herrenhäuser Str. 2, 30419 Hannover, Germany.

<sup>2</sup> Center of Nuclear Energy in Agriculture, University of São Paulo CENA-USP, Brazil.

<sup>3</sup> Department of Biology, Kunsan National University, Gunsan, Republic of Korea.

<sup>4</sup> Institute of Soil Science, Chinese Academy of Sciences, No.71 East Beijing Road, Xuan-Wu District, Nanjing City, 210008 PR China.

<sup>5</sup> Department of Genomic and Applied Microbiology and Göttingen Genomics Laboratory, Institute of Microbiology and Genetics, George-August University Göttingen, Grisebachstr. 8, D-37077 Göttingen, Germany.

Included:

- Supplementary table captions. The tables can be found online.
- Supplementary figures and figure captions.

**Following tables are not included in the supplementary an can be accessed on the journal web page: Supplementary Information**

**Table S5** qPCR primer concentrations and thermal profiles

**Table S6** Topological properties of the interaction networks at 27-71 days incubations derived from all replicates (n=6 or 7) and from 4 randomly selected combinations from all replicates (3 subsets).

**Table S7** Top 5 OTUs with more betweenness centrality in the undisturbed and disturbed incubations at 1-7 and 27-71 days interval. The representative sequences for the classified OTUs, based on the SILVA database v. 132, is provided. Methanotrophs are given in bold.

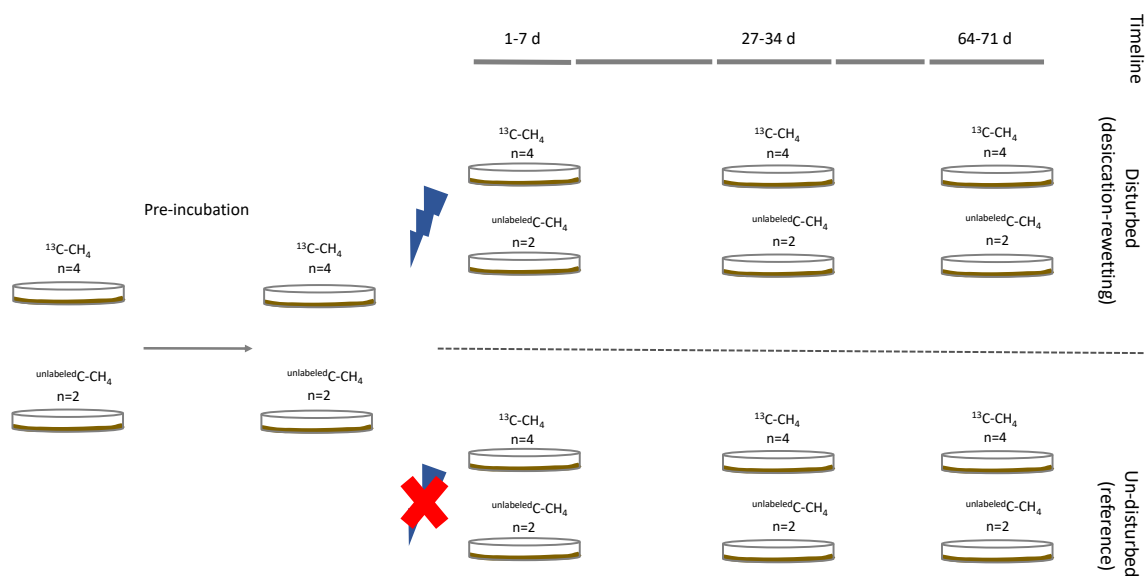


**Figure S10** Experimental setup showing  $^{13}\text{C}$ - and unlabelled  $\text{C-CH}_4$  incubations. Desiccation was induced overnight (15 h) after pre-incubation. Immediately after rewetting, the disturbed as well as un-disturbed (reference) microcosms were individually incubated under 2% v/v  $^{13}\text{C-}$  and unlabelled  $\text{C-CH}_4$  (1-7 days) in flux chambers (inset figure). Likewise, disturbed and un-disturbed microcosms were individually incubated under 2% v/v  $^{13}\text{C-}$  and unlabelled  $\text{C-CH}_4$  at 27-34 and 64-71 days interval after desiccation-rewetting to follow the recovery of the methanotrophic activity. In between the 1-7, 27-34, and 64-71 days intervals, the microcosms were incubated in a gas tight jar under 10% v/v unlabelled  $\text{C-CH}_4$ .

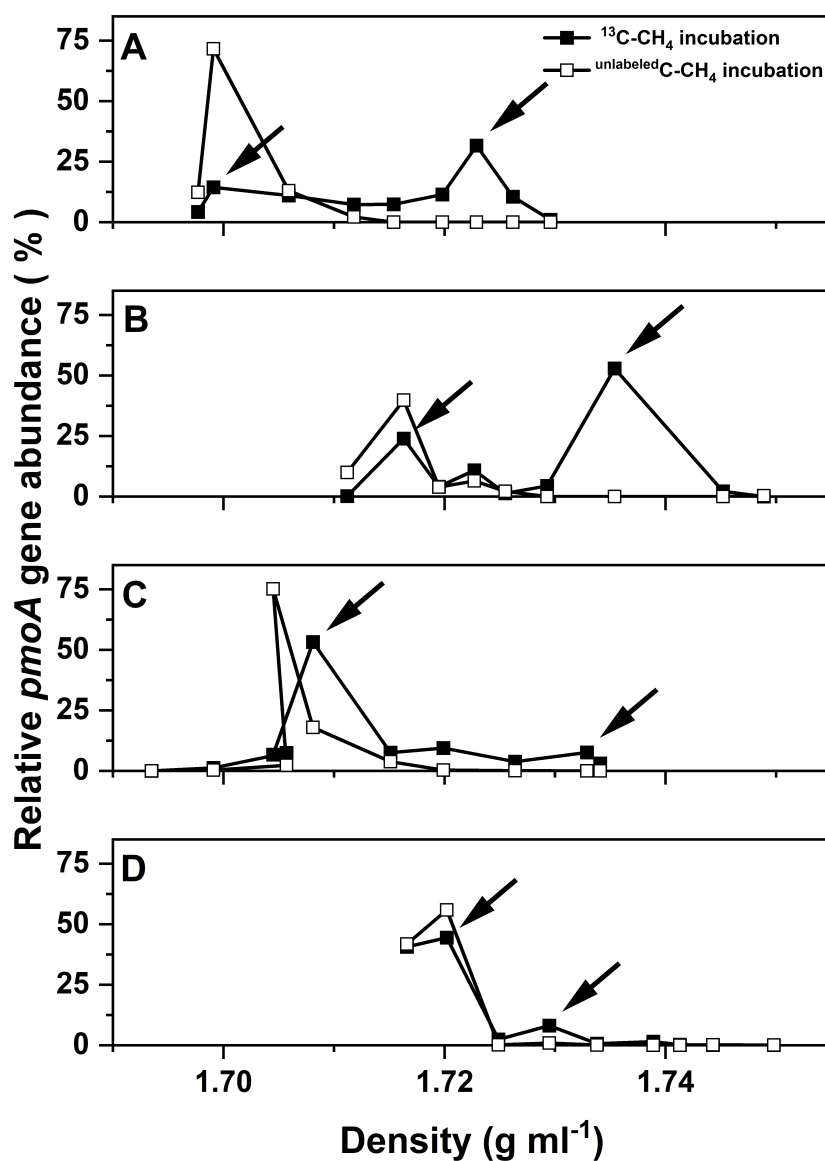


**Figure S11** Representative relative abundance of the *pmoA* gene recovered from each density gradient in the <sup>13</sup>C- and unlabeled C-CH<sub>4</sub> incubations after pre-incubation (a), 1-7 (b), 27-34 (c), and 64-71 (d) days incubation. The 'light' fractions of the <sup>13</sup>C- and unlabeled C-CH<sub>4</sub> incubations were compared to determine the 'heavy' fraction of the <sup>13</sup>C-CH<sub>4</sub> incubation. The arrow denotes the fraction used for sequencing the 16S rRNA and *pmoA* genes.



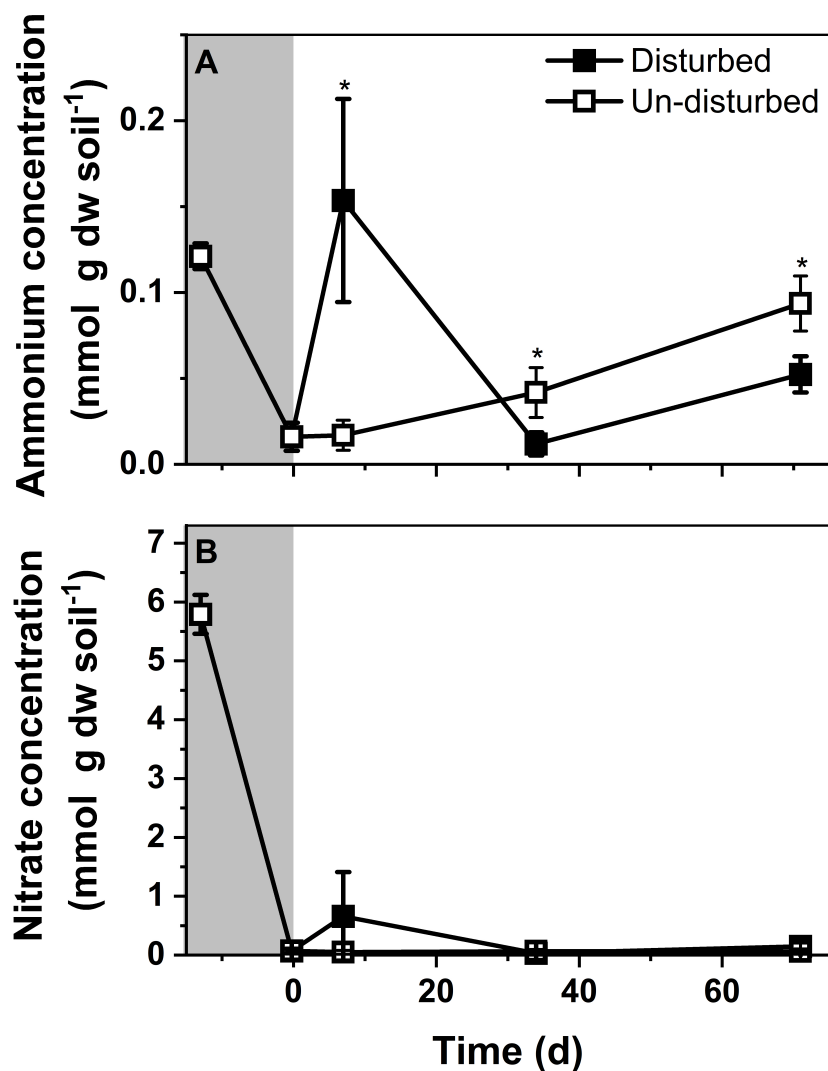


**Figure S12** Changes in soluble ammonium (a) and nitrate (b) concentrations in the un-disturbed and disturbed incubations (mean  $\pm$  s.d.,  $n=12$ ). Ammonium and nitrate assays were performed in duplicate for each sample. Incubations with  $^{13}\text{C}$ - and  $^{\text{unlabelled}}\text{C}$ - $\text{CH}_4$  were combined (mean  $\pm$  s.d.,  $n=6$ ) for each treatment, giving a total of 12 replicate per time. Shaded area denotes pre-incubation. Significant difference in the ammonium and nitrate concentrations comparing the un-disturbed and disturbed incubations is indicated by an asterisk (t-test,  $p < 0.05$ ).

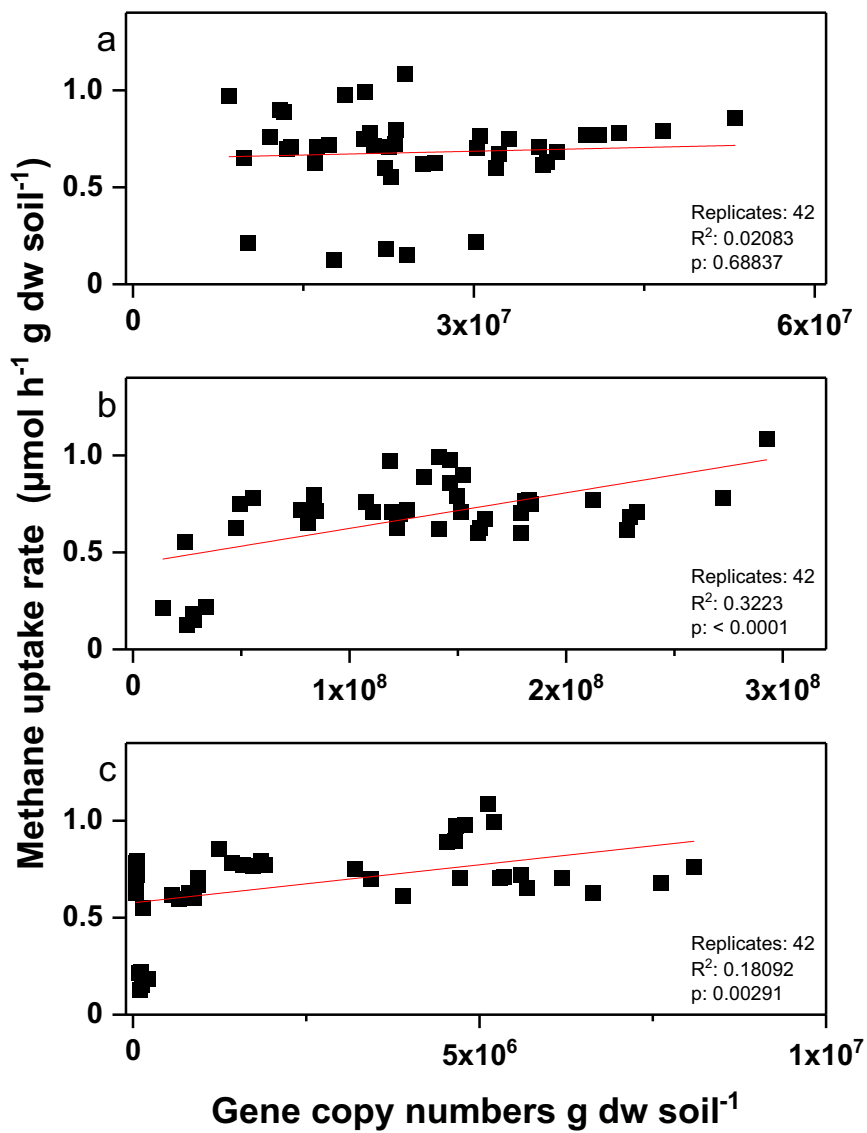


**Figure S13** Correlation between the methane uptake rates and *pmoA* gene abundances of type Ia (a), Ib (b), and II (c) methanotrophs. Replicates from all time points and treatments (un-disturbed and disturbed) were integrated into the linear correlation.

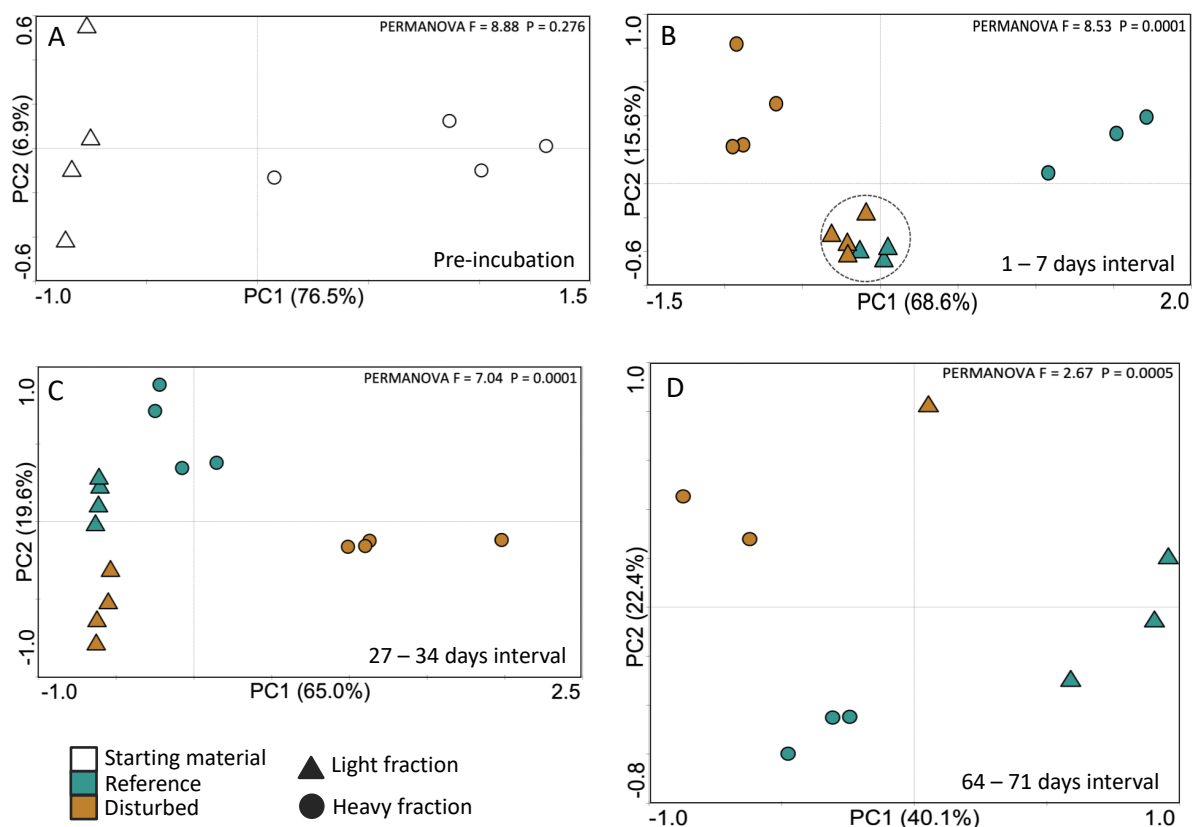



**Figure S14** Principal component analysis showing the separation of the bacterial communities (16S rRNA-based) derived from the 'heavy' ( $^{13}\text{C}$ -enriched DNA) and 'light' (unlabelled DNA) fractions during pre-incubation (a), and 1-7 (b), 27 – 34 (c) and 64 – 71 (d) days interval after desiccation-rewetting. The 'heavy' and 'light' fractions were determined after comparing the  $^{13}\text{C}$ - and unlabelled  $\text{C-CH}_4$  incubations (Figure S11).

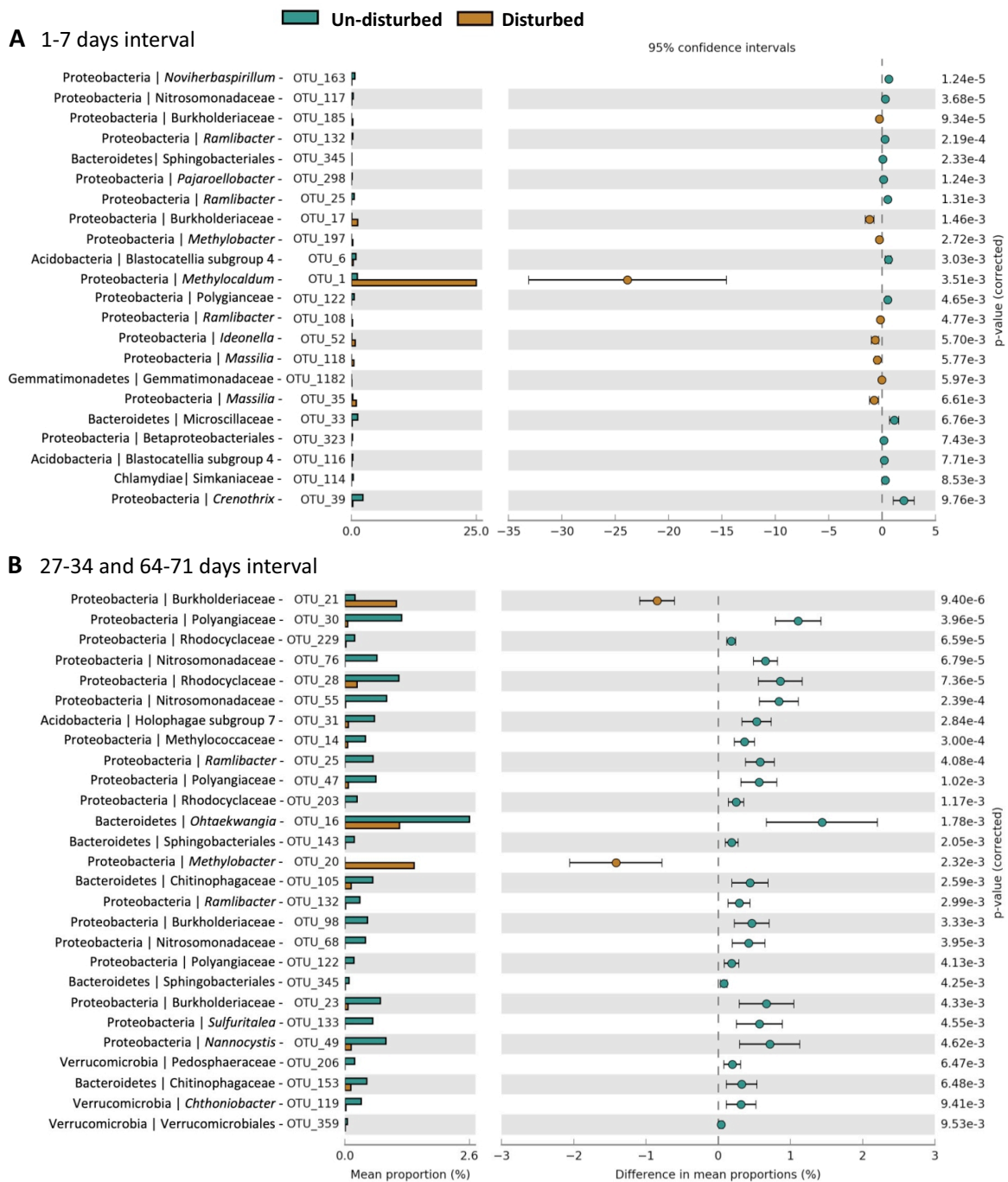


**Figure S15** Differential abundance of the bacterial taxa at the OTU level, based on the 16S rRNA gene sequences derived from the  $^{13}\text{C}$ -enriched DNA in the un-disturbed and disturbed incubations at 1-7 (a), and combined 27-34 and 64-71 (b) days interval. Affiliations of the OTUs at the finest taxonomic resolution (genus level) are given, whenever available. Only significantly different OTUs ( $p < 0.01$ ) between treatments are given.



## Recovery of Methanotrophic Activity Is Not Reflected in the Methane-Driven Interaction Network after Peat Mining

Thomas Kaupper,<sup>a</sup> Lucas W. Mendes,<sup>b</sup> Monica Harnisz,<sup>c</sup> Sascha M. B. Krause,<sup>d</sup> Marcus A. Horn,<sup>a</sup>  Adrian Ho<sup>a</sup>

<sup>a</sup>Institute of Microbiology, Leibniz Universität Hannover, Hannover, Germany

<sup>b</sup>Center for Nuclear Energy in Agriculture, University of São Paulo-USP, São Paulo, Brazil

<sup>c</sup>Department of Environmental Microbiology, University of Warmia and Mazury in Olsztyn, Olsztyn, Poland

<sup>d</sup>Zhejiang Tiantong Forest Ecosystem National Observation and Research Station, School of Ecological and Environmental Sciences, East China Normal University, Shanghai, China

**ABSTRACT** Aerobic methanotrophs are crucial in ombrotrophic peatlands, driving the methane and nitrogen cycles. Peat mining adversely affects methanotrophs, but activity and community composition/abundances may recover after restoration. Considering that the methanotrophic activity and growth are significantly stimulated in the presence of other microorganisms, the methane-driven interaction network, which encompasses methanotrophs and nonmethanotrophs (i.e., the methanotrophic interactome), may also be relevant in conferring community resilience. Yet, little is known of the methanotrophic interactome's response to and recovery from disturbances. Here, we determined the recovery of the methanotrophic interactome as inferred by a co-occurrence network analysis comparing pristine and restored peatlands. We coupled a DNA-based stable isotope probing (SIP) approach using [<sup>13</sup>C]CH<sub>4</sub> to a co-occurrence network analysis derived from the <sup>13</sup>C-enriched 16S rRNA gene sequences to relate the response in methanotrophic activity to the structuring of the interaction network. Methanotrophic activity and abundances recovered after peat restoration since 2000. “*Methylomonaceae*” taxa were the predominantly active methanotrophs in both peatlands, but the peatlands differed in the relative abundances of *Methylacidiphilaceae* and *Methylocystis*. However, bacterial community compositions were distinct in both peatlands. Likewise, the methanotrophic interactome was profoundly altered in the restored peatland. Structuring of the interaction network after peat mining resulted in the loss of complexity and modularity, indicating a less connected and efficient network, which may have consequences in the event of recurring/future disturbances. Therefore, determining the response of the methane-driven interaction network, in addition to relating methanotrophic activity to community composition/abundances, provided a more comprehensive understanding of the resilience of the methanotrophs.

**IMPORTANCE** Microbial resilience against and recovery from disturbances are often determined with regard to microorganisms' activity and community composition/abundances. Rarely has the response of the network of interacting microorganisms been considered, despite accumulating evidence showing that microbial interaction modulates community functioning. Comparing the methane-driven interaction networks of a pristine peatland and a restored peatland, our findings revealed that the metabolically active microorganisms were less connected and formed less-modular “hubs” in the restored peatland, which is indicative of a less complex network that may have consequences with recurring disturbances and environmental changes. This also suggests that the resilience and full recovery in the methanotrophic activity and abundances do not reflect on the interaction network. Therefore, it is relevant to consider the interaction-induced response, in addition to documenting changes in activity and community composition/abundances, to provide a comprehensive understanding of the resilience of microorganisms to disturbances.

**Citation** Kaupper T, Mendes LW, Harnisz M, Krause SMB, Horn MA, Ho A. 2021. Recovery of methanotrophic activity is not reflected in the methane-driven interaction network after peat mining. *Appl Environ Microbiol* 87:e02355-20. <https://doi.org/10.1128/AEM.02355-20>.

**Editor** Jeremy D. Semrau, University of Michigan-Ann Arbor

**Copyright** © 2021 American Society for Microbiology. All Rights Reserved.

Address correspondence to Marcus A. Horn, [horn@ifmb.uni-hannover.de](mailto:horn@ifmb.uni-hannover.de), or Adrian Ho, [Adrian.ho@ifmb.uni-hannover.de](mailto:Adrian.ho@ifmb.uni-hannover.de).

**Received** 23 September 2020

**Accepted** 7 December 2020

**Accepted manuscript posted online** 18 December 2020

**Published** 12 February 2021

**KEYWORDS** peatland restoration, methane oxidation, methane-based food web, methanotrophs, stable isotope probing

Peat is harvested to meet global fuel and feed demands (e.g., renewable combustible fuel and soil additives [1, 2]). Mining profoundly alters the peat physicochemical properties (e.g., increases pH and compaction and reduces the availability of inorganic compounds [3, 4]), exerting an effect on the indigenous microbial communities with consequences for microbially mediated processes such as greenhouse gas emissions (5, 6). Depending on the mining method (block-cut or vacuum-harvested peat), peat restoration to a pristine-like state can take decades, during which the rewetted peatlands may become a source of carbon, with altered carbon dioxide and methane emissions (3, 7). In particular, methane emission in ombrotrophic peatlands is governed by the balance of methane production in the anoxic peat layers, and aerobic methane oxidation in niches where methane-oxygen counter gradients occur (e.g., the peat-overlying water layer). Hence, aerobic methanotrophs are key to mitigating methane emission in peatlands, acting as a methane biofilter (8). Besides, diazotrophic methanotrophs are a significant source of assimilable nitrogen, driving the N cycle in ombrotrophic peatlands (9–11). Methanotrophs are thus highly relevant members of the peatland microbiome, participating in the C and N cycles. While changes in the abiotic environment following peat restoration have been the focus of earlier work (3, 4), the microbial community composition and abundances, specifically those of methanotrophs, in ombrotrophic peatlands have since gained attention (12–15). Still, less is known about the response of the relevant and metabolically active community members to peat restoration, and it remains to be determined how well the methane-driven network of interacting microorganisms recovers in the reestablished peatland.

Ombrotrophic *Sphagnum*-dominated peatlands are relatively harsh environments that are characterized by low pH and are nutrient depauperate (16). These conditions, along with the antimicrobial properties of *Sphagnum*, may exert pressure to select for specific aerobic methanotrophs (17). Not surprisingly, the methanotrophs, being strongly influenced by their abiotic environment, showed habitat specificity (18, 19). Predominantly active methanotrophs in ombrotrophic peatlands fall into the class *Alphaproteobacteria* (type II methanotrophs), which includes *Methylocystis* and *Methylosinus* (family *Methylocystaceae*), as well as members of the family *Beijerinckiaceae* (*Methylocella*, *Methyloferula*, and *Methylocapsa*); class *Gammaproteobacteri* methanotrophs (type I) belonging to *Methylomonas* and *Methylovulum* were more recently found to be active members of the community (14, 15, 20–23). The methanotrophs form a plethora of interdependent relationships with other organisms, at times supporting multitrophic food webs in high-methane-emission environments (24–27). Accordingly, methane oxidation and growth rates, as well as the transcription of the *pmoA* gene (encoding methane monooxygenase) were significantly stimulated when the methanotrophs were cocultured together with other microorganisms compared to monoculture (28–31). As such, nonmethanotrophs that do not seemingly contribute to methane oxidation are also relevant, indirectly affecting community functioning via interaction-induced effects. Therefore, considering the methane-driven interaction network is important to elaborate community response during peat restoration, but this has so far received little attention.

Here, we aimed to compare and contrast the methane-driven interaction network in ombrotrophic peatlands to follow the recovery in the network structure during peat restoration. Although methanotrophic activity and community composition/abundances may recover after *Sphagnum* regrowth upon peat rewetting (6, 13), the legacy of peat mining may persist in the structure of the interaction network (32, 80). Revisiting the sites of our previous work (pristine and restored peatlands [13]), we performed stable isotope probing (SIP) using [ $^{13}\text{C}$ ]CH<sub>4</sub> to track the unidirectional flow of methane into the food web. Instead of deriving the co-occurrence network analysis from isolated DNA (e.g., references 33 and 34), we performed a network analysis using the  $^{13}\text{C}$ -enriched 16S rRNA gene from SIP to infer the methane-driven interaction network (i.e.,

**TABLE 1** Selected physicochemical properties, *pmoA* and 16S rRNA gene abundances, and methane uptake rates in the pristine and restored peatlands<sup>a</sup>

Peatland status	pH	Ammonium (mmol · g dry wt <sup>-1</sup> )	Nitrate (μmol · g dry wt <sup>-1</sup> )	Methane uptake rate (μmol · g dry wt <sup>-1</sup> · day <sup>-1</sup> ) <sup>b</sup>	<i>pmoA</i> gene abundance (copy no. · g dry wt <sup>-1</sup> )	16S rRNA gene abundance (copy no. · g dry wt <sup>-1</sup> )	Mean <i>pmoA</i> / 16S rRNA gene abundance (%)
Pristine	4.4 ± 0.19 C	0.2 ± 0.02 C	0.6 ± 0.07 C				
After incubation setup				24.7 ± 6.17 C	(6.0 ± 3.29) × 10 <sup>4</sup> C	(6.81 ± 3.41) × 10 <sup>7</sup> C	0.08
After replenishing headspace methane				45.6 ± 8.61 A	(3.5 ± 2.47) × 10 <sup>5</sup> A	(9.13 ± 4.9) × 10 <sup>7</sup> A	0.53
Restored	4.7 ± 0.12 C	0.7 ± 0.08 D	0.7 ± 0.21 C				
After incubation setup				24.7 ± 3.82 C	(4.9 ± 4.02) × 10 <sup>5</sup> D	(2.48 ± 0.93) × 10 <sup>8</sup> D	0.21
After replenishing headspace methane				31.2 ± 9.57 B	(2.8 ± 1.47) × 10 <sup>6</sup> B	(2.52 ± 1.48) × 10 <sup>8</sup> B	1.46

<sup>a</sup>Uppercase letters indicate a level of significance at  $P < 0.05$  between sites. C and D refer to data after incubation setup, and A and B refer to data after replenishing headspace methane.

<sup>b</sup>Methane uptake rates were determined by linear regression after incubation setup (C and D,  $P < 0.05$ ; days 0 to 8) and after replenishing headspace methane (A and B,  $P < 0.05$ ; days 8 to 13 or 14) (methane depletion curve; see Fig. S1 in the supplemental material).

methanotrophic interactome). We define the methanotrophic interactome as a subset of the entire bacterial community comprising of both methanotrophs and nonmethanotrophs that is tracked via the flow of methane-derived <sup>13</sup>C. Coupling SIP to the co-occurrence network analysis not only provides direct ecological linkages of the metabolically active members of the interaction network, thereby minimizing spurious and weak connections, but also unambiguously relates community functioning (methane oxidation as the functional response variable) to the network structure.

## RESULTS

**Comparison of methanotrophic activity and abundance and the abiotic environment in the pristine and restored peatlands.** Headspace methane was immediately consumed upon incubation setup (initial and after methane replenishment; see Fig. S1 in the supplemental material) in both peatlands, indicating the presence of a thriving indigenous methanotrophic population. The initial methane uptake rate, reflecting the *in-situ* rate (35), was comparable in both peatlands at ~24 μmol · g dry weight<sup>-1</sup> · day<sup>-1</sup> (Table 1). This suggests recovery in methanotrophic activity in the restored peatland, consistent with a previous study of the same peatlands over two consecutive years (in 2015 and 2016 [13]). The methane uptake rate increased in both peatlands after replenishing headspace methane, achieving an “induced rate” that was likely caused by population growth during incubation (Table 1) (35). This was corroborated by the increased *pmoA* gene abundance by approximately an order of magnitude after the incubation, indicating methanotrophic growth. Also, the proportion of methanotrophs (i.e., the *pmoA*/16S rRNA gene abundance ratio) increased during the incubation (Table 1). Similarly, the total bacteria, and specifically the methanotrophic population size, recovered to even higher abundances following peat restoration, as was previously documented (13).

The pHs in the two peatlands were comparable, within the range of 4.4 to 4.7 (Table 1). Soluble ammonium was significantly higher after peat restoration, while nitrate concentrations were comparable (Table 1), consistent with previous work (13).

**Response of the metabolically active bacterial community composition to peat restoration, as determined by DNA-based SIP.** An SIP approach using [<sup>13</sup>C]CH<sub>4</sub> was performed to track the flow of <sup>13</sup>C into the DNA of metabolically active and replicating microorganisms. Because the methanotrophs are the only microorganisms capable of assimilating methane, <sup>13</sup>C incorporated into the DNA of nonmethanotrophs indicates the reliance of these microorganisms on methane-derived carbon for growth. Each ultracentrifugation run was performed for DNA extracted from incubations with [<sup>13</sup>C]CH<sub>4</sub> and [unlabelledC]CH<sub>4</sub> to distinguish the “heavy” and “light” fractions after amplification of the *pmoA* gene for each gradient fraction (Fig. 1). Admittedly, we cannot completely exclude the presence of unlabeled 16S rRNA gene with a high GC content in

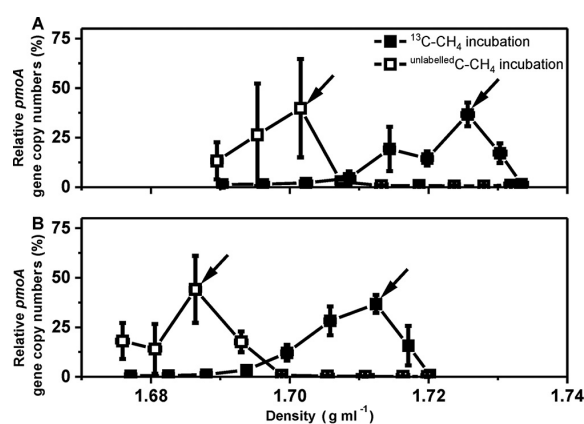


**FIG 1** Relative *pmoA* gene abundance along the density gradient of the [ $^{13}\text{C}$ ]CH $_4$  and [ $^{12}\text{C}$ ]CH $_4$  incubations from the pristine (A) and restored (B) peatlands (mean  $\pm$  standard deviation [SD];  $n=4$ ). The relative abundance was calculated as the proportion of each fraction over the total sum of the gene abundance for each sample. DNA from the “light” and “heavy” fractions (denoted by arrows) in the [ $^{13}\text{C}$ ]CH $_4$  incubations was used for 16S rRNA gene amplicon sequencing.

the heavy fraction (36). The heavy fraction could be clearly separated from the light fraction in both peat incubations (Fig. 1), and this was further supported by the clustering of the distinct communities in both fractions, based on the 16S rRNA gene sequencing analysis (principal-component analysis [PCA]; Fig. 2). Subsequently, co-occurrence network analysis was performed on the  $^{13}\text{C}$ -enriched 16S rRNA gene sequences, representing the active community members.

The  $^{13}\text{C}$ -enriched bacterial community composition was distinct in the pristine and restored peatlands, indicating that the total community in the restored peatland had not fully recovered to a pristine-like state (Fig. 2). Among the  $^{13}\text{C}$ -labeled bacterial phyla, *Proteobacteria* members were predominantly present in both peatlands (>65%; Fig. 3). However, members of the phylum were detected at a significantly higher relative abundance in the restored site (see Fig. S2 in the supplemental material). Within *Proteobacteria*, *Beijerinckiaceae*, *Oligoflexales*, *Polyangiaceae*, *Pajaroellobacter*, *Elsterales*, *Myxococcales*, and *Burkholderiaceae*, as well as the genera *Anaeromyxobacter*, *Occallatibacter*, and *Cavicella* were detected at significantly ( $P < 0.05$ ) differentially higher proportion (overabundant) in the restored compared to that in the pristine peatlands (see Fig. S3 in the supplemental material). However, a member of the *Beijerinckiaceae* (represented by operational taxonomic unit [OTU] 1; Fig. S3) was more abundant in the pristine peatland. Among other phyla, *Acidobacteria*, *Bacteroidetes*, and WPS-2 were present at significantly higher relative abundances in the pristine peatland (Fig. S2). Considering finer taxonomic resolution, differentially higher relative abundances of *Occallatibacter*, *Granulicella*, *Acidimicrobiaceae*, *Acidobacteriales*, “*Candidatus Solibacter*,” and “*Candidatus Koribacter*” belonging to *Acidobacteria*, and *Chitinophagales* within *Bacteroidetes* were detected in the pristine peatland (Fig. S3). WPS-2 is a candidate division represented by an as yet uncultured bacterium. Generally, members of *Acidobacteria* and *Proteobacteria*, along with *Actinobacteria*, are typical active inhabitants of ombrotrophic peatlands (37–39).

The methanotrophs consisted of <2% of the total bacterial population in both peatlands (starting material), based on 16S rRNA gene sequencing analysis (Fig. 3A). After incubation, the methanotrophic population comprised ~20% and ~74% of the total active community (heavy fraction) in the pristine and restored peatland, respectively. The predominantly active methanotrophs, as retrieved from the 16S rRNA gene sequences, belonged to “*Methylomonaceae*” and included the genus *Methylomonas* (>72% of the total methanotrophic population) in both peatlands, whereas the genus



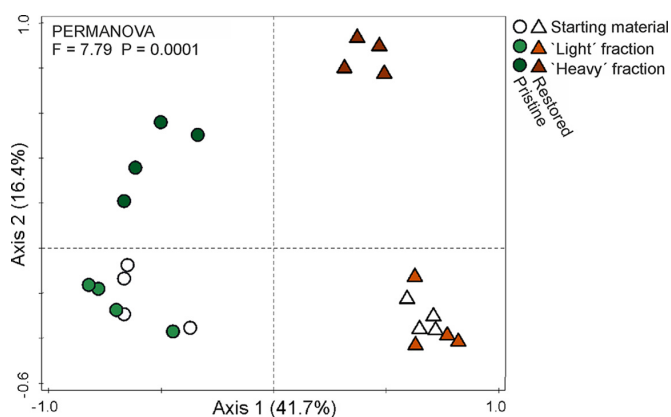


**FIG 2** Principal-component analysis showing the clustering of the 16S rRNA gene sequences according to the different fractions (light and heavy) and sites (pristine and restored peatlands) of the incubation with  $^{13}\text{C}$ CH<sub>4</sub>. The circle and triangle indicate pristine and restored peatlands, respectively.

*Methylocystis* was relatively more abundant in the restored than the pristine peatland (Fig. 3B). Conversely, *Methylacidiphilaceae* taxa were detected at a higher relative abundance in the pristine than the restored peatland. Although they constituted the majority of the methanotrophic community composition in the starting material, members of *Methylacidiphilaceae* did not assimilate methane as actively as "*Methylomonaceae*" under the incubation conditions; metabolically active *Methylacidiphilaceae* was detected at ~22% and <2% in the heavy fraction of the pristine and restored peatland, respectively, after incubation (Fig. 3).

**Insights into the methane-driven co-occurrence interaction network in the pristine and restored peatlands.** Subsequently, a co-occurrence network analysis was performed on the  $^{13}\text{C}$ -enriched 16S rRNA gene sequences, targeting the community members of the methanotrophic interactome in the pristine and restored peatlands

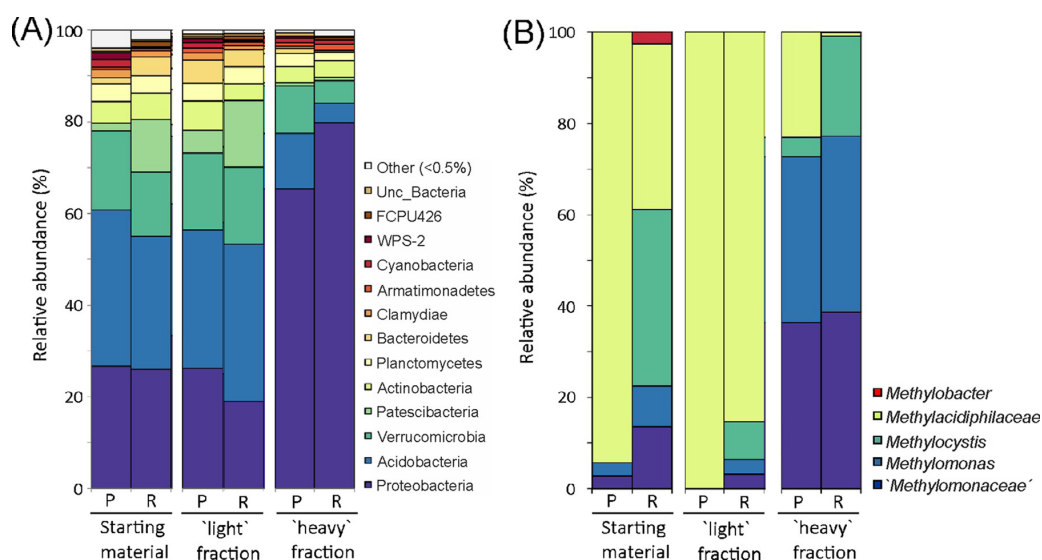


**FIG 3** The bacterial (A) and methanotrophic (B) community composition in the starting material (prior to the incubation) and after  $^{13}\text{C}$ CH<sub>4</sub> incubation (light and heavy fractions) (mean;  $n=4$ ). The 16S rRNA gene sequences affiliated with methanotrophs in panel B were retrieved from the total community in panel A. The 16S rRNA gene sequences affiliated with the methanotrophs were present at <2% of the total community in the starting material, and at ~20% and ~74%, respectively, in the pristine and restored peatland after incubation (heavy fraction). P and R denote pristine and restored peatlands, respectively.

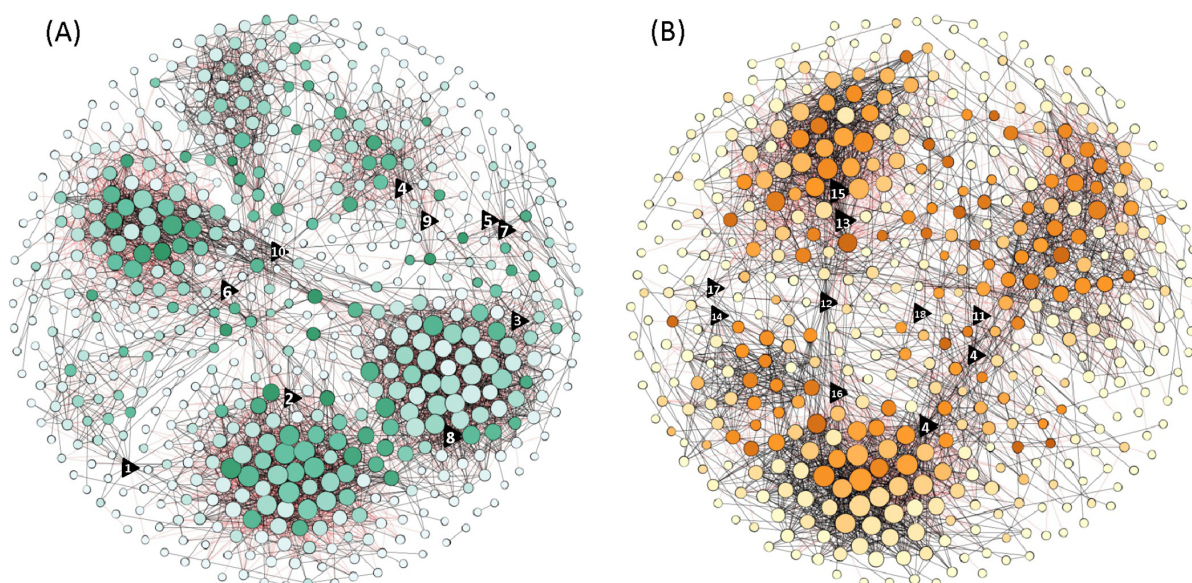


**FIG 4** Co-occurrence network analysis in the pristine (A) and restored (B) peatlands. The network analysis was derived from the  $^{13}\text{C}$ -enriched 16S rRNA gene sequences (heavy fraction), representing the metabolically active community of the interaction network. The topological properties of the networks are given in Table 2. Significant connection ( $P < 0.01$ ) with a SparCC correlation of a magnitude of more than 0.7 (positive correlation, blue edges) or less than  $-0.7$  (negative correlation, red edges) are given. Each node represents a bacterial taxon at the operational taxonomic unit (OTU) level, given to the lowest taxonomic rank (family, genus, or species) when available. The size of the node is proportional to the number of connections, and a darker shade of a color indicates higher betweenness centrality. The top 10 nodes with the highest betweenness centrality, representing the key nodes, are given as triangles, and the number inside the key nodes refers to their affiliation as follows: 1, *Rhodospirillales*; 2, uncultured bacteria; 3, *Burkholderiaceae*; 4, *Methylomonas* (methanotroph); 5, "*Candidatus Solibacter*"; 6, *Gammaproteobacteria*; 7, *Methylocystis* (methanotroph); 8, *Babeliales*; 9, *Pirellulaceae*; 10, *Methylacidiphilaceae* (methanotroph); 11, *Bdellovibrio*; 12, *Magnetospirillaceae*; 13, *Acidimicrobiia*; 14, *Sphingobacteriales*; 15, *Roseiarcus*; 16, *Beijerinckiaceae*; 17, *Myxococcales*; and 18, *Methylomonas paludis* (methanotroph). The OTUs representing the microorganisms and betweenness centrality values of each OTU are listed in Table S1 in the supplemental material.

(Fig. 4). The network topological properties indicate that the pristine peatland harbored a more complex and connected community, exhibiting a higher number of edges (number of connections), degree (number of connections per node or node connectivity), and clustering coefficient (the degree to which the nodes cluster together) than in the restored peatland (Table 2). Accordingly, the pristine peatland also possessed a more diverse metabolically active community (number of significant nodes, representing bacterial taxa at the OTU level), and showed a more modular network structure than the restored peatland (Table 2). Higher modularity is indicative of a more compartmentalized network, having more independently connected groups within the interaction network (40, 41). The network diameter and average path length between co-occurring nodes, indicative of the network efficiency (40, 42), were largely comparable in both peatlands (Table 2). Having a comparatively less complex and connected network structure thus indicates that the methanotrophic interactome in the restored peatland since 2000 had not returned to a pristine-like state, despite the resilience in the methanotrophic activity and abundance.

The nodes with high betweenness centrality were identified as the key nodes (Fig. 4) (43), which likely played a significant regulatory role within the interaction network, affecting methanotrophic activity (44, 45). In particular, the key nodes are not necessarily the more abundant OTUs (Fig. S3), but rather refer to nodes acting as a bridge between other nodes at a relatively higher frequency (43). The 10 key nodes with the highest betweenness centrality were identified in both the pristine and restored peatlands (Fig. 4). Expectedly, these nodes were represented by proteobacterial methanotrophs (*Methylomonas* and *Methylocystis*), as well as by verrucomicrobial methanotrophs belonging to *Methylacidiphilaceae* in the pristine peatland, whereas the methanotroph-related key nodes in the restored peatland were affiliated with *Methylomonas*. It is

**TABLE 2** Topological properties of the co-occurrence network analysis in the pristine and restored peatlands

Network properties	Pristine peatland	Restored peatland
No. of nodes <sup>a</sup>	600	464
No. of edges <sup>b</sup>	5,397	3,476
Positive edges (no. [%]) <sup>c</sup>	2,871 (53.2)	2,234 (64.3)
Negative edges (no. [%]) <sup>d</sup>	2,526 (46.8)	1,242 (35.7)
Modularity <sup>e</sup>	7.30	1.82
No. of communities <sup>f</sup>	47	57
Network diam <sup>g</sup>	10	11
Avg path length <sup>h</sup>	4.27	4.30
Avg degree <sup>i</sup>	17.99	14.98
Avg clustering coefficient <sup>j</sup>	0.55	0.53

<sup>a</sup>Microbial taxon (at operational taxonomic unit [OTU] level) with at least one significant ( $P < 0.01$ ) and strong (SparCC of more than 0.9 or less than  $-0.9$ ) correlation.

<sup>b</sup>Number of connections/correlations obtained by SparCC analysis.

<sup>c</sup>SparCC positive correlation (more than 0.9 with  $P < 0.01$ ).

<sup>d</sup>SparCC negative correlation (less than  $-0.9$  with  $P < 0.01$ ).

<sup>e</sup>Capability of the nodes to form highly connected communities, that is, a structure with a high density of between-node connections (inferred by Gephi).

<sup>f</sup>A community is defined as a group of nodes densely connected internally.

<sup>g</sup>The longest distance between nodes in the network, measured in number of edges.

<sup>h</sup>Average network distance for all pairs of nodes or the average length of all edges in the network.

<sup>i</sup>The average number of connections per node in the network, that is, the node connectivity.

<sup>j</sup>How nodes are embedded in their neighborhood and the degree to which they tend to cluster together.

noteworthy that *Beijerinckiaceae* (phylum *Proteobacteria*), a key node in the restored peatland (Fig. 4), also constitutes methanotrophs harboring soluble methane monooxygenase (sMMO) (*Methylocella*, *Methylocapsa*, and *Methyloferula* [16]), as well as other methylotrophs, but these microorganisms may have been overlooked at the coarse taxonomic resolution. Unexpectedly, many nonmethanotrophs formed the key nodes and appeared to be site specific (Fig. 4). Although they are unable to assimilate methane directly, the nonmethanotrophs also appear to be relevant members of the interaction network.

## DISCUSSION

**Recovery of the active methanotrophs after peat restoration.** Methanotrophic activity and population size recovered after peat restoration when pristine and restored sites were compared (Table 1). Likewise, pH and nitrate concentrations returned to pristine-like levels, but ammonium concentrations remained significantly higher in the restored site. These trends were also documented in a previous study of the same sites sampled in 2015 and 2016, suggesting the presence of a relatively persistent methanotrophic population, possibly attributable to narrow fluctuations in environmental conditions (13). It thus appears that the methanotrophs recovered  $<15$  years after *Sphagnum* reestablished during peat restoration.

The metabolically active bacterial community composition, including the methanotrophs, was determined by targeting the  $^{13}\text{C}$ -enriched 16S rRNA gene after [ $^{13}\text{C}$ ]CH<sub>4</sub> SIP. Predominantly active methanotrophs belonged to "*Methylomonaceae*" ( $>72\%$  of the methanotrophic community composition) in both peatlands, while *Methylacidiphilaceae* and *Methylocystis* formed the rest of the methanotrophic community (Fig. 3). In particular, *Methylocystis* is thought to possess ecological traits suitable for the relatively inhospitable and fluctuating environmental conditions in ombrotrophic peatlands, having the metabolic potential to fix N<sub>2</sub>, utilize other substrates besides methane (e.g., acetate), and being favored by the lower pH (23, 46–48). Besides *Methylocystis*, members of "*Methylomonaceae*" (e.g., *Methylomonas* strains) and *Methylacidiphilaceae* (e.g., *Methyloacidiphilum fumariolicum* SolV), which also formed the active community, are also potentially diazotrophic, as indicated by the presence of the *nifH* gene (encoding nitrogenase) (49, 50). Consistent with previous studies, active gammaproteobacterial methanotrophs (namely, *Methylomonas* and

*Methylovulum*) have also been found to codominate alongside *Methylocystis* in some peatlands (14, 20, 21). This suggests that traits to grow and survive in acidic peatlands are not confined to a particular methanotroph subgroup.

Previously, we characterized the methanotrophic community composition in the pristine and restored sites (same sites as in this study), along with the community in an actively mined peatland and those in abandoned peatlands since 2004 and 2009 (13). The methanotrophic community composition in the restored peatland resembled those in the pristine peatland, clustering more closely together as shown in a correspondence analysis (13). This indicates that the methanotrophic community composition recovered following peat restoration. Here, although the relative abundances of *Methylacidiphilaceae* and *Methylocystis* species differed in the pristine and restored peatlands, the predominantly active methanotrophs comprised the same family members (Fig. 3). However, the active bacterial community composition in response to methane was distinct in both peatlands (Fig. 2 and 3). Hence, specific microbial subpopulations may have shown relatively faster recovery than the total bacterial community composition after peat mining.

**Insights into the recovery of the methanotrophic interactome after peat restoration.** The recovery in the methanotrophic activity and community composition/abundances was not reflected in the structure of the interaction network, even after approximately 2 decades of peat rewetting (Table 2 and Fig. 4). The pristine peatland harbored a more complex methanotrophic interactome, possessing a higher number of nodes with significant correlations, edges, degree, and clustering coefficient, as well as having higher modularity (Table 2). These topological features are indicative of a more connected and robust network (42, 51, 52) and suggest that the methanotrophic interactome in the pristine peatland was characterized by relatively higher metabolic exchange and competition among community members that likely increased their co-occurrence (53, 54). Also, having relatively higher modularity in the pristine peatland is anticipated to constrain the effects of environmental stressors/disturbance on localized areas (compartments) within the network (55). In contrast, the loss of modularity in the restored peatland suggests that stress effects would be more uniformly distributed among community members, which may become more vulnerable in the face of intensified or recurring disturbances (51, 56). Hence, the methane-driven community in the restored peatland may not be as resilient as the community in the pristine peatland in responding to future changes in environmental conditions. Indeed, a recent study showed the unraveling of the methanotrophic interactome concomitant to significantly impair methanotrophic activity following  $\text{NH}_4\text{Cl}$ -induced stressor intensification (56). Overall, considering the co-occurrence network analysis in addition to activity measurements and characterization of the community composition/abundances may provide a more comprehensive understanding, moving beyond the diversity-ecosystem functioning relationship (e.g., reference 57), to encompass potential interaction-induced effects.

Admittedly, we could not account for seasonal variations affecting the interaction networks. However, the consistent trends in methanotrophic activity and community composition/abundances in the pristine and restored peatlands in previous (sampled in August 2015 and June 2016 [13]) and current work (May 2019; Table 1), despite a 3-year interval, suggest that a specific methanotrophic population persists over time. Although we anticipate a relatively consistent methanotrophic population, the seasonal dynamics of the interaction network warrant attention in future studies.

The methanotrophs are the only microbial group capable of assimilating methane, having the role of a "primary" producer, whereby the methane-derived carbon is anticipated to fuel the community. Nevertheless, the methanotrophs may gain from other members of the interactome (e.g., stimulation of methanotrophic growth by cobalamin excreted by other microorganisms [58]), which may have been inadvertently excluded by the experimental design capturing the unidirectional flow of  $^{13}\text{C}$ . Expectedly, the key nodes included the methanotrophs (Fig. 4). Surprisingly, the key nodes were overwhelmingly represented by the nonmethanotrophs and were distinct in the pristine

and restored peatlands. This indicates sufficiently redundant community members sharing traits to fulfill similar roles ensuring community functioning within the methanotrophic interactome (33, 41). It is not unreasonable to assume that selective predation on the methanotrophs may have occurred (59). For instance, members of *Myxococcales*, a key taxon in the restored peat, have been widely recognized as predators, swarming their prey in a coordinated and cooperative manner during feeding (60). *Beijerinckiaceae*, another key taxon, includes nonmethanotrophic methylotrophs which likely benefited from (intermediary) products of methane oxidation (e.g., methanol, formaldehyde, and formate). Hence, the cross-feeding between methanotrophs and nonmethanotrophic methylotrophs (e.g., *Methylotenera*) drives their co-occurrence (26, 56). It is noteworthy that *Beijerinckiaceae* also includes methanotrophs, but the methanotrophs and nonmethanotrophic methylotrophs could not be distinguished at the taxonomic resolution in this study. Also, *Burkholderiaceae* may comprise microorganisms shown to have a stimulatory effect on methanotrophic growth in cocultures (i.e., *Cupriavidus* [29]). Although some of the key taxa (e.g., *Burkholderiaceae*, *Sphingobacteriales*, *Beijerinckiaceae*, and *Bdellovibrio*) have been identified to co-occur alongside and interact with the methanotrophs (29, 56, 61), the underlying mechanisms driving the biological interaction and organization (e.g., commensalism and mutualism [62, 63]) warrant further probing by isolation and coculture studies (64). Despite lacking the metabolic capability to assimilate methane, the detection of the nonmethanotrophs as key nodes indicate their potentially significant role within the interaction network. In particular, the key nodes in the restored peatlands may act to expedite the natural restoration process (65).

**Conclusion.** We elaborated on the methane-driven interaction network after peat mining by comparing a pristine and restored peatland. Our findings showed the structuring of the interaction network resulting in the loss of complexity, connectedness, and modularity in the restored peatland, which may have consequences in the face of future disturbances and environmental changes. They also suggest that the reestablished peatlands had not yet fully recovered, despite showing resilience in methanotrophic activity. More generally, our study suggests the inclusion of interaction-induced responses, in addition to documenting shifts in community composition/abundances, as a step forward to understand the resilience of microbial communities to disturbances.

## MATERIALS AND METHODS

**Peat sampling and incubation setup.** The sampling sites are ombrotrophic peatlands located in Warmia and Mazury Province, Poland. The upper ~10 cm of peat below the water surface was collected in May 2019 from a pristine peatland (Zielony Mechacz; 53°54'24"N, 19°41'41"E) and was regarded as the reference site for comparison to the restored peatland (Rucianka; 54°15'34"N, 19°44'0.4"E). These peatlands were selected based on a previous study showing recovery in the methanotrophic activity and abundances after peat mining (13). The atmospheric temperature at the time of sampling was 21 to 25°C. Five cores (10-cm height × 3.5-cm diameter) were sampled from four randomly selected plots (spaced >4 m apart) from each site and composited, giving four independent replicates per site. The pristine peatland was declared a nature reserve since 1962, while peatland in the restored site was dammed, rewetted, and remained waterlogged since 2000 after peat excavation using the block peat method. In both sites, *Sphagnum* spp. (e.g., *Sphagnum fimbriatum*, *Sphagnum fluxuosum*, *Sphagnum fallax*, and *Sphagnum capillifolium*) dominated the vegetation, interspersed with *Orthotrichum lyellii*. The pH in both peatlands was within a narrow range of 4.4 to 4.7. Detailed peat hydrology and selected physicochemical parameters are given elsewhere (Table 1) (13). The samples were transported to the laboratory with coolers in ice.

Each incubation containing 5 g fresh sample in a 120-ml bottle was performed in eight replicates for the pristine and restored peat. After sealing the bottle with a butyl rubber stopper and crimp cap, the headspace methane concentration in the bottle was adjusted to ~2% (vol/vol) [<sup>12</sup>C]CH<sub>4</sub> or [<sup>13</sup>C]CH<sub>4</sub> (*n* = 4 each) in air. Incubation was performed at 27°C while shaking (110 rpm) in the dark. Headspace methane concentration was monitored during the incubation. Upon methane depletion, headspace was replenished with 2% (vol/vol) [<sup>12</sup>C]CH<sub>4</sub> or [<sup>13</sup>C]CH<sub>4</sub> in air, and incubation was resumed under the same conditions as before. Incubation was terminated after approximately 30 μmol CH<sub>4</sub> · g fresh sample<sup>-1</sup> was consumed (13 to 14 days; see Fig. S1 in the supplemental material) to ensure sufficient <sup>13</sup>C labeling (66). The samples were immediately homogenized and collected after incubation to be stored in the -20°C freezer until DNA extraction.

**Methane and inorganic N measurements.** Headspace methane was monitored daily using a gas chromatograph (7890B GC system; Agilent Technologies, Santa Clara, CA) coupled to a pulsed discharge



helium ionization detector (PD-HID). Helium was used as the carrier gas. The methane uptake rate was determined by linear regression. The gravimetric water content (~93% in both peat samples) was determined after drying the peat in the 70°C oven until the weight remained constant. Soluble ammonium and nitrate were determined colorimetrically in autoclaved deionized water (1:1 wt/vol) as described before (67, 68) using an Infinite M Plex reader (Tecan, Männedorf, Switzerland).

**DNA extraction and quantitative PCR.** DNA was extracted using the DNeasy PowerSoil kit (Qiagen, Hilden, Germany) according to the manufacturer's instructions. A *pmoA* gene-targeted quantitative PCR (qPCR) assay (A189f/mb661r primer pair) was performed to enumerate methanotroph abundance. Additionally, a qPCR targeting the 16S rRNA gene (341F/907R primer pair) was performed to determine the abundance of the total bacterial population. Both qPCR assays were performed using the CFX Connect real-time PCR system (Bio-Rad, Hercules, CA). The *pmoA* gene-targeted qPCR was performed as described before (69) with minor modifications (70); the reagents and reagent concentrations, as well as the PCR thermal profile for the qPCR assay, are given elsewhere (70). Each reaction in the 16S rRNA gene-targeted qPCR (total volume, 20  $\mu$ l) consisted of 10  $\mu$ l SensiMix (2 $\times$ ), 1.2  $\mu$ l MgCl<sub>2</sub> (50 mM), 1  $\mu$ l bovine serum albumin (BSA; 1%), 2  $\mu$ l of each primer (10  $\mu$ M), 1.8  $\mu$ l of H<sub>2</sub>O, and 2  $\mu$ l of template DNA. The PCR thermal profile consisted of an initial denaturation step at 95°C for 8 min, followed by 45 cycles of denaturation at 95°C for 15 s, annealing at 55.7°C for 15 s, and elongation at 72°C for 40 s, with an additional data acquisition step at 80°C for 8 s. The template DNA from the peat (starting material and after incubation) was diluted 50-fold (mean total DNA, 13.5 to 46.5 ng DNA  $\cdot$   $\mu$ l<sup>-1</sup>) for both qPCR assays to determine the *pmoA*/16S rRNA gene abundance ratio (Table 1), while template DNA to determine the relative *pmoA* gene abundance after fractionation for the SIP analysis was undiluted (see "<sup>13</sup>CCH<sub>4</sub> stable isotope probing," below). The calibration curve (10<sup>1</sup> to 10<sup>8</sup> *pmoA* or 16S rRNA gene copy numbers) was derived from the gene library (71, 72). The specificity of the amplicons was determined from the melt curve and further verified on 1% agarose gel electrophoresis, showing a single band of the correct size. The qPCR efficiency was 94.3%, with an *R*<sup>2</sup> of 0.988.

**[<sup>13</sup>C]CH<sub>4</sub> stable isotope probing.** Isopycnic ultracentrifugation (144,000  $\times$  *g* for 67 h) was performed using the Optima L-80XP ultracentrifuge (Beckman Coulter, Inc., USA) as described before (66). Briefly, fractionation was immediately performed after ultracentrifugation using a peristaltic pump (3 rpm  $\cdot$  min<sup>-1</sup>), yielding 10 or 11 fractions, from which the final fraction was discarded. The density of each fraction was determined using an AR200 digital refractometer (Reichert Technologies, Munich, Germany). DNA was precipitated by introducing two washing steps with ethanol, and the pellet was suspended in 30  $\mu$ l ultrapure PCR water (Invitrogen, Waltham, MA). Thereafter, the *pmoA* gene was enumerated from each fraction using the qPCR assay described above to distinguish the light from the heavy fraction by comparing the DNA retrieved from the [<sup>13</sup>C]CH<sub>4</sub> and [unlabelled]CH<sub>4</sub> incubations (Fig. 1). The 16S rRNA genes from the light and heavy fractions, as well as that from the starting material, were subsequently amplified for Illumina MiSeq sequencing.

**16S rRNA gene amplicon sequencing.** The 16S rRNA gene was amplified using the primer pair 341F/805R, as detailed before (56). Briefly, each PCR comprised 20  $\mu$ l 2 $\times$  Kapa HiFi HotStart ready mix (Roche, Mannheim, Germany), 2  $\mu$ l each forward/reverse tagged-primers (10  $\mu$ M), 2  $\mu$ l BSA (1%), and 4  $\mu$ l DNA template. PCR-grade water was added to achieve a total volume of 40  $\mu$ l. The PCR thermal profile consisted of an initial denaturation step at 94°C for 7 min, followed by 30 cycles of denaturation at 94°C for 30 s, annealing at 53°C for 30 s, and elongation at 72°C for 30 s. The final elongation step was at 72°C for 5 min. The amplicons were purified using the GeneRead size selection kit (Qiagen, Hilden, Germany) after verification on 1% agarose gel electrophoresis. Thereafter, a second PCR was performed using 5  $\mu$ l of template from the first PCR to attach the adapters to the 16S rRNA gene amplicon using the Nextera XT index kit (Illumina, San Diego, CA). The PCR reagents, reagent concentrations, and thermal profile for the second PCR are given elsewhere (56). Following the second PCR, the 16S rRNA gene amplicon was purified using the MagSi-NGS<sup>PREP</sup> Plus magnetic beads (Steinbrenner Laborsysteme GmbH, Wiesenbach, Germany) according to the manufacturer's instructions. After purification, equimolar amounts of 16S rRNA gene amplicons (133 ng) were pooled for library preparation and sequencing (Illumina MiSeq version 3 chemistry, paired-end, and 600 cycles).

**16S rRNA gene sequencing analysis.** The 16S rRNA gene sequences were processed using QIIME 2 version 2019.10, as described before (56). Briefly, after merging the paired-end reads using PEAR (73), the sequences were demultiplexed, and quality control was performed with DADA2 (74) to remove remaining chimeric and low-quality sequences. Approximately 1,010,000 high-quality contigs (on average, 31,604 contigs per sample) were obtained. After removing singletons and doubletons, the samples were rarefied to 18,800 contigs, following the number of the sample with the lowest contigs. The classification was performed at 97% similarity against the Silva database version 132 (75); the generated matrix based on the relative abundance of the OTUs was further used for statistical analyses. The affiliations of the OTUs are given to the lowest taxonomic rank (family, genus, or species), whenever possible.

A principal-component analysis (PCA) was performed to assess the separation of the <sup>13</sup>C-enriched (active) from the [unlabelled]C (inactive) bacterial community composition and to determine the recovery of the community composition following peat restoration. The PCA was constructed using Canoco version 4.5 (Biometrics, Wageningen, the Netherlands). To test the significance of the PCA clustering, permutational multivariate analysis of variance (PERMANOVA) was performed with the software PAST version 4.01 (76). Furthermore, the differential relative abundances of (overabundant) OTUs in the restored versus the pristine peatlands were determined using STAMP software (77). The *P* values were calculated based on the two-sided Welch's *t* test and corrected using the Benjamini-Hochberg false-discovery rate.

Additionally, a co-occurrence network analysis was performed using the <sup>13</sup>C-enriched 16S rRNA gene sequences to explore potential interaction among the active members of the methanotrophic

interactome. The network analysis was performed using the Python module SparCC, and the network properties were calculated with Gephi (Table 2) (78). The same analytical pipeline was applied to each network (pristine and restored peatlands). The *P* values were obtained by 99 permutations of random selections of the data table for each network. The true SparCC nonrandom correlations were selected based on a magnitude of more than 0.7 or less than  $-0.7$ , with a statistical significance of  $P < 0.01$ . Comparison between the networks was assessed based on their topological properties namely, the number of nodes, edges, modularity, number of communities, average path length, network diameter, average degree, and clustering coefficient (Table 2) (79). Furthermore, the OTUs with high betweenness centrality, i.e., the number of times a node acts as a bridge along the shortest path between two other nodes, were determined (43). These nodes are regarded as key nodes, representing microorganisms that likely play a significant role within the methanotrophic interactome (44).

**Statistical analyses.** Normal distribution was tested using the Kolmogorov-Smirnov test at  $P = 0.05$ . Equal distribution of variance was tested and one-sided *t* tests ( $P = 0.05$ ) were then performed comparing the pristine and restored peatlands. Where normal distribution was not met, a Mann-Whitney U test was performed.

**Data availability.** 16S rRNA gene sequences were deposited at the National Center for Biotechnology Information (NCBI) under the accession numbers SRR12542333 to SRR12542364 (project number PRJNA659768).

### SUPPLEMENTAL MATERIAL

Supplemental material is available online only.

**SUPPLEMENTAL FILE 1**, PDF file, 4.9 MB.

### ACKNOWLEDGMENTS

T.K. and A.H. are financially supported by the Deutsche Forschungsgemeinschaft (grant HO6234/1-1). A.H. and M.A.H. are also financially supported by the Leibniz Universität Hannover, Germany.

We declare no conflict of interest.

### REFERENCES

- Cleary J, Roulet NT, Moore TR. 2005. Greenhouse gas emissions from Canadian peat extraction, 1990–2000: a life-cycle analysis. *AMBIO* 34:456–461. <https://doi.org/10.1579/0044-7447-34.6.456>.
- Pryce S. 1991. Alternatives to peat. *Prof Hort* 5:101–106.
- Basilikko N, Blodau C, Roehm C, Bengtson P, Moore TR. 2007. Regulation of decomposition and methane dynamics across natural, commercially mined, and restored northern peatlands. *Ecosystems* 10:1148–1165. <https://doi.org/10.1007/s10021-007-9083-2>.
- Andersen R, Francez A-J, Rochefort L. 2006. The physicochemical and microbiological status of a restored bog in Québec: identification of relevant criteria to monitor success. *Soil Biol Biochem* 38:1375–1387. <https://doi.org/10.1016/j.soilbio.2005.10.012>.
- Juottonen H, Hynninen A, Nieminen M, Tuomivirta TT, Tuittila E-S, Nousiainen H, Kell DK, Yrjälä K, Tervahauta A, Fritze H. 2012. Methane-cycling microbial communities and methane emission in natural and restored peatlands. *Appl Environ Microbiol* 78:6386–6389. <https://doi.org/10.1128/AEM.00261-12>.
- Putkinen A, Tuittila E-S, Siljanen HMP, Bodrossy L, Fritze H. 2018. Recovery of methane turnover and the associated microbial communities in restored cutover peatlands is strongly linked with increasing *Sphagnum* abundance. *Soil Biol Biochem* 116:110–119. <https://doi.org/10.1016/j.soilbio.2017.10.005>.
- Holl D, Pfeiffer E-M, Kutzbach L. 2020. Comparison of eddy covariance CO<sub>2</sub> and CH<sub>4</sub> fluxes from mined and recently rewetted sections in a north-western German cutover bog. *Biogeosciences* 17:2853–2874. <https://doi.org/10.5194/bg-17-2853-2020>.
- Yavitt JB, Lang GE, Downey DM. 1988. Potential methane production and methane oxidation rates in peatland ecosystems of the Appalachian Mountains, United States. *Global Biogeochem Cycles* 2:253–268. <https://doi.org/10.1029/GB002i003p00253>.
- Ho A, Le Bodelier P. 2015. Diazotrophic methanotrophs in peatlands: the missing link? *Plant Soil* 389:419–423. <https://doi.org/10.1007/s11104-015-2393-9>.
- Larmola T, Leppänen SM, Tuittila E-S, Aarva M, Merilä P, Fritze H, Tirola M. 2014. Methanotrophy induces nitrogen fixation during peatland development. *Proc Natl Acad Sci U S A* 111:734–739. <https://doi.org/10.1073/pnas.1314284111>.
- Vile MA, Kelman Wieder R, Živković T, Scott KD, Vitt DH, Hartssock JA, Iosue CL, Quinn JC, Petix M, Fillingim HM, Popma JMA, Dynarski KA, Jackman TR, Albright CM, Wykoff DD. 2014. N<sub>2</sub>-fixation by methanotrophs sustains carbon and nitrogen accumulation in pristine peatlands. *Biogeochemistry* 121:317–328. <https://doi.org/10.1007/s10533-014-0019-6>.
- Kip N, van Winden JF, Pan Y, Bodrossy L, Reichart G-J, Smolders AJP, Jetten MSM, Damsté JSS, Op den Camp HJM. 2010. Global prevalence of methane oxidation by symbiotic bacteria in peat-moss ecosystems. *Nature Geosci* 3:617–621. <https://doi.org/10.1038/ngeo939>.
- Reumer M, Harnisz M, Lee HJ, Reim A, Grunert O, Putkinen A, Fritze H, Bodelier PLE, Ho A. 2017. Impact of peat mining and restoration on methane turnover potential and methane-cycling microorganisms in a northern bog. *Appl Environ Microbiol* 84:e02218-17. <https://doi.org/10.1128/AEM.02218-17>.
- Esson KC, Lin X, Kumaresan D, Chanton JP, Murrell JC, Kostka JE. 2016. Alpha- and gammaproteobacterial methanotrophs codominate the active methane-oxidizing communities in an acidic boreal peat bog. *Appl Environ Microbiol* 82:2363–2371. <https://doi.org/10.1128/AEM.03640-15>.
- Liebner S, Svenning MM. 2013. Environmental transcription of *mmoX* by methane-oxidizing proteobacteria in a subarctic peatland. *Appl Environ Microbiol* 79:701–706. <https://doi.org/10.1128/AEM.02292-12>.
- Dedysh SN. 2011. Cultivating uncultured bacteria from northern wetlands: knowledge gained and remaining gaps. *Front Microbiol* 2:184. <https://doi.org/10.3389/fmicb.2011.00184>.
- Kostka JE, Weston DJ, Glass JB, Lilleskov EA, Shaw AJ, Turetsky MR. 2016. The *Sphagnum* microbiome: new insights from an ancient plant lineage. *New Phytol* 211:57–64. <https://doi.org/10.1111/nph.13993>.
- Kaupper T, Luehrs J, Lee HJ, Mo Y, Jia Z, Horn MA, Ho A. 2020. Disentangling abiotic and biotic controls of aerobic methane oxidation during re-colonization. *Soil Biol Biochem* 142:107729. <https://doi.org/10.1016/j.soilbio.2020.107729>.
- Knief C. 2015. Diversity and habitat preferences of cultivated and uncultivated aerobic methanotrophic bacteria evaluated based on *pmoA* as molecular marker. *Front Microbiol* 6:1346. <https://doi.org/10.3389/fmicb.2015.01346>.
- Chen Y, Dumont MG, Neufeld JD, Bodrossy L, Stralis-Pavese N, McNamara NP, Ostle N, Briones MJJ, Murrell JC. 2008. Revealing the uncultivated majority: combining DNA stable-isotope probing, multiple displacement amplification and metagenomic analyses of uncultivated *Methylocystis* in acidic

- peatlands. *Environ Microbiol* 10:2609–2622. <https://doi.org/10.1111/j.1462-2920.2008.01683.x>.
21. Gupta V, Smemo KA, Yavitt JB, Basiliko N. 2012. Active methanotrophs in two contrasting North American peatland ecosystems revealed using DNA-SIP. *Microb Ecol* 63:438–445. <https://doi.org/10.1007/s00248-011-9902-z>.
  22. Danilova OV, Kulichevskaya IS, Rozova ON, Detkova EN, Bodelier PLE, Trotsenko YA, Dedysh SN. 2013. *Methylomonas paludis* sp. nov., the first acid-tolerant member of the genus *Methylomonas*, from an acidic wetland. *Int J Syst Evol Microbiol* 63:2282–2289. <https://doi.org/10.1099/ijs.0.045658-0>.
  23. Belova SE, Baani M, Suzina NE, Bodelier PLE, Liesack W, Dedysh SN. 2011. Acetate utilization as a survival strategy of peat-inhabiting *Methylocystis* spp. *Environ Microbiol Rep* 3:36–46. <https://doi.org/10.1111/j.1758-2229.2010.00180.x>.
  24. Hutchens E, Radajewski S, Dumont MG, McDonald IR, Murrell JC. 2004. Analysis of methanotrophic bacteria in Movile Cave by stable isotope probing. *Environ Microbiol* 6:111–120. <https://doi.org/10.1046/j.1462-2920.2003.00543.x>.
  25. Ho A, Angel R, Veraart AJ, Daebeler A, Jia Z, Kim SY, Kerckhof F-M, Boon N, Bodelier PLE. 2016. Biotic interactions in microbial communities as modulators of biogeochemical processes: methanotrophy as a model system. *Front Microbiol* 7:1285. <https://doi.org/10.3389/fmicb.2016.01285>.
  26. Krause SMB, Johnson T, Samadhi Karunaratne Y, Fu Y, Beck DAC, Chistoserdova L, Lidstrom ME. 2017. Lanthanide-dependent cross-feeding of methane-derived carbon is linked by microbial community interactions. *Proc Natl Acad Sci U S A* 114:358–363. <https://doi.org/10.1073/pnas.1619871114>.
  27. Agasild H, Zingel P, Tuvikene L, Tuvikene A, Timm H, Feldmann T, Salujõe J, Toming K, Jones RI, Nõges T. 2014. Biogenic methane contributes to the food web of a large, shallow lake. *Freshw Biol* 59:272–285. <https://doi.org/10.1111/fwb.12263>.
  28. Ho A, Roy K, de Thas O, de Neve J, Hoefman S, Vandamme P, Heylen K, Boon N. 2014. The more, the merrier: heterotroph richness stimulates methanotrophic activity. *ISME J* 8:1945–1948. <https://doi.org/10.1038/ismej.2014.74>.
  29. Stock M, Hoefman S, Kerckhof F-M, Boon N, de Vos P, de Baets B, Heylen K, Waegeman W. 2013. Exploration and prediction of interactions between methanotrophs and heterotrophs. *Res Microbiol* 164:1045–1054. <https://doi.org/10.1016/j.resmic.2013.08.006>.
  30. Jeong S-Y, Cho K-S, Kim TG. 2014. Density-dependent enhancement of methane oxidation activity and growth of *Methylocystis* sp. by a non-methanotrophic bacterium *Sphingopyxis* sp. *Biotechnol Rep (Amst)* 4:128–133. <https://doi.org/10.1016/j.btre.2014.09.007>.
  31. Veraart AJ, Garbeva P, van Beersum F, Ho A, Hordijk CA, Meima-Franke M, Zweers AJ, Bodelier PLE. 2018. Living apart together-bacterial volatiles influence methanotrophic growth and activity. *ISME J* 12:1163–1166. <https://doi.org/10.1038/s41396-018-0055-7>.
  32. Pérez-Valera E, Goberna M, Faust K, Raes J, García C, Verdú M. 2017. Fire modifies the phylogenetic structure of soil bacterial co-occurrence networks. *Environ Microbiol* 19:317–327. <https://doi.org/10.1111/1462-2920.13609>.
  33. Barberán A, Bates ST, Casamayor EO, Fierer N. 2012. Using network analysis to explore co-occurrence patterns in soil microbial communities. *ISME J* 6:343–351. <https://doi.org/10.1038/ismej.2011.119>.
  34. Mo Y, Jin F, Zheng Y, Baoyin T, Ho A, Jia Z. 2020. Succession of bacterial community and methanotrophy during lake shrinkage. *J Soils Sediments* 20:1545–1557. <https://doi.org/10.1007/s11368-019-02465-6>.
  35. Steenbergh AK, Meima MM, Kamst M, Bodelier PLE. 2010. Biphasic kinetics of a methanotrophic community is a combination of growth and increased activity per cell. *FEMS Microbiol Ecol* 71:12–22. <https://doi.org/10.1111/j.1574-6941.2009.00782.x>.
  36. Lueders T, Manefield M, Friedrich MW. 2004. Enhanced sensitivity of DNA- and rRNA-based stable isotope probing by fractionation and quantitative analysis of isopycnic centrifugation gradients. *Environ Microbiol* 6:73–78. <https://doi.org/10.1046/j.1462-2920.2003.00536.x>.
  37. Palmer K, Horn MA. 2012. Actinobacterial nitrate reducers and proteobacterial denitrifiers are abundant in N<sub>2</sub>O-metabolizing peat. *Appl Environ Microbiol* 78:5584–5596. <https://doi.org/10.1128/AEM.00810-12>.
  38. Deng Y, Cui X, Hernández M, Dumont MG. 2014. Microbial diversity in hummock and hollow soils of three wetlands on the Qinghai-Tibetan Plateau revealed by 16S rRNA pyrosequencing. *PLoS One* 9:e103115. <https://doi.org/10.1371/journal.pone.0103115>.
  39. Ivanova AA, Wegner C-E, Kim Y, Liesack W, Dedysh SN. 2016. Identification of microbial populations driving biopolymer degradation in acidic peatlands by metatranscriptomic analysis. *Mol Ecol* 25:4818–4835. <https://doi.org/10.1111/mec.13806>.
  40. Zhou J, Deng Y, Luo F, He Z, Tu Q, Zhi X. 2010. Functional molecular ecological networks. *mBio* 1:e00169-10. <https://doi.org/10.1128/mBio.00169-10>.
  41. Williams RJ, Howe A, Hofmockel KS. 2014. Demonstrating microbial co-occurrence pattern analyses within and between ecosystems. *Front Microbiol* 5:358. <https://doi.org/10.3389/fmicb.2014.00358>.
  42. Bissett A, Brown MV, Siciliano SD, Thrall PH. 2013. Microbial community responses to anthropogenically induced environmental change: towards a systems approach. *Ecol Lett* 16(Suppl 1):128–139. <https://doi.org/10.1111/ele.12109>.
  43. Poudel R, Jumpponen A, Schlatter DC, Paulitz TC, Gardener BBM, Kinkel LL, Garrett KA. 2016. Microbiome networks: a systems framework for identifying candidate microbial assemblages for disease management. *Phytopathology* 106:1083–1096. <https://doi.org/10.1094/PHYTO-02-16-0058-FI>.
  44. Borgatti SP. 2005. Centrality and network flow. *Social Networks* 27:55–71. <https://doi.org/10.1016/j.socnet.2004.11.008>.
  45. van der Heijden MGA, Hartmann M. 2016. Networking in the plant microbiome. *PLoS Biol* 14:e1002378. <https://doi.org/10.1371/journal.pbio.1002378>.
  46. Im J, Lee S-W, Yoon S, DiSpirito AA, Semrau JD. 2011. Characterization of a novel facultative *Methylocystis* species capable of growth on methane, acetate and ethanol. *Environ Microbiol Rep* 3:174–181. <https://doi.org/10.1111/j.1758-2229.2010.0204.x>.
  47. Han D, Dedysh SN, Liesack W. 2018. Unusual genomic traits suggest *Methylocystis bryophila* S285 to be well adapted for life in peatlands. *Genome Biol Evol* 10:623–628. <https://doi.org/10.1093/gbe/evy025>.
  48. Zhao J, Cai Y, Jia Z. 2020. The pH-based ecological coherence of active canonical methanotrophs in paddy soils. *Biogeosciences* 17:1451–1462. <https://doi.org/10.5194/bg-17-1451-2020>.
  49. Khadem AF, Pol A, Wiczorek A, Mohammadi SS, Francois K-J, Stunnenberg HG, Jetten MSM, Op den Camp HJM. 2011. Autotrophic methanotrophy in verrucosic bacteria: *Methyloacidiphilum fumarolicum* SolV uses the Calvin-Benson-Bassham cycle for carbon dioxide fixation. *J Bacteriol* 193:4438–4446. <https://doi.org/10.1128/JB.00407-11>.
  50. Auman AJ, Speake CC, Lidstrom ME. 2001. *nifH* sequences and nitrogen fixation in type I and type II methanotrophs. *Appl Environ Microbiol* 67:4009–4016. <https://doi.org/10.1128/aem.67.9.4009-4016.2001>.
  51. Faust K, Raes J. 2012. Microbial interactions: from networks to models. *Nat Rev Microbiol* 10:538–550. <https://doi.org/10.1038/nrmicro2832>.
  52. Mendes LW, Raaijmakers JM, de Hollander M, Mendes R, Tsai SM. 2018. Influence of resistance breeding in common bean on rhizosphere microbiome composition and function. *ISME J* 12:212–224. <https://doi.org/10.1038/ismej.2017.158>.
  53. van Elsas JD, Chiurazzi M, Mallon CA, Elhottova D, Kristufek V, Salles JF. 2012. Microbial diversity determines the invasion of soil by a bacterial pathogen. *Proc Natl Acad Sci U S A* 109:1159–1164. <https://doi.org/10.1073/pnas.1109326109>.
  54. Zelezniak A, Andrejev S, Ponomarova O, Mende DR, Bork P, Patil KR. 2015. Metabolic dependencies drive species co-occurrence in diverse microbial communities. *Proc Natl Acad Sci U S A* 112:6449–6454. <https://doi.org/10.1073/pnas.1421834112>.
  55. Kitano H. 2004. Biological robustness. *Nat Rev Genet* 5:826–837. <https://doi.org/10.1038/nrg1471>.
  56. Ho A, Mendes LW, Lee HJ, Kaupper T, Mo Y, Poehlein A, Bodelier PLE, Jia Z, Horn MA. 2020. Response of a methane-driven interaction network to stressor intensification. *FEMS Microbiol Ecol* 96:faa180. <https://doi.org/10.1093/femsec/faa180>.
  57. Krause SMB, Meima-Franke M, Veraart AJ, Ren G, Ho A, Bodelier PLE. 2018. Environmental legacy contributes to the resilience of methane consumption in a laboratory microcosm system. *Sci Rep* 8:8862. <https://doi.org/10.1038/s41598-018-27168-9>.
  58. Iguchi H, Yurimoto H, Sakai Y. 2011. Stimulation of methanotrophic growth in cocultures by cobalamin excreted by rhizobia. *Appl Environ Microbiol* 77:8509–8515. <https://doi.org/10.1128/AEM.05834-11>.
  59. Murase J, Frenzel P. 2007. A methane-driven microbial food web in a wetland rice soil. *Environ Microbiol* 9:3025–3034. <https://doi.org/10.1111/j.1462-2920.2007.01414.x>.
  60. Muñoz-Dorado J, Marcos-Torres FJ, García-Bravo E, Moraleda-Muñoz A, Pérez J. 2016. Myxobacteria: moving, killing, feeding, and surviving together. *Front Microbiol* 7:781. <https://doi.org/10.3389/fmicb.2016.00781>.
  61. Qiu Q, Noll M, Abraham W-R, Lu Y, Conrad R. 2008. Applying stable isotope probing of phospholipid fatty acids and rRNA in a Chinese rice field



- to study activity and composition of the methanotrophic bacterial communities *in situ*. ISME J 2:602–614. <https://doi.org/10.1038/ismej.2008.34>.
62. Morris BEL, Henneberger R, Huber H, Moissl-Eichinger C. 2013. Microbial syntrophy: interaction for the common good. FEMS Microbiol Rev 37:384–406. <https://doi.org/10.1111/1574-6976.12019>.
  63. Johnson WM, Alexander H, Bier RL, Miller DR, Muscarella ME, Pitz KJ, Smith H. 2020. Auxotrophic interactions: a stabilizing attribute of aquatic microbial communities? FEMS Microbiol Ecol 96:faa115. <https://doi.org/10.1093/femsec/faa115>.
  64. Kwon G, Kim H, Song C, Jahng D. 2019. Co-culture of microalgae and enriched nitrifying bacteria for energy-efficient nitrification. Biochemical Engineering J 152:107385. <https://doi.org/10.1016/j.bej.2019.107385>.
  65. Wubs ERJ, van der Putten WH, Bosch M, Bezemer TM. 2016. Soil inoculation steers restoration of terrestrial ecosystems. Nat Plants 2:16107. <https://doi.org/10.1038/nplants.2016.107>.
  66. Neufeld JD, Vohra J, Dumont MG, Lueders T, Manefield M, Friedrich MW, Murrell JC. 2007. DNA stable-isotope probing. Nat Protoc 2:860–866. <https://doi.org/10.1038/nprot.2007.109>.
  67. Gadkari D. 1984. Influence of the herbicides goltix and sencer on nitrification. Zentralblatt für Mikrobiologie 139:623–631. [https://doi.org/10.1016/S0232-4393\(84\)80056-6](https://doi.org/10.1016/S0232-4393(84)80056-6).
  68. Horn MA, Ihssen J, Matthies C, Schramm A, Acker G, Drake HL. 2005. *Dechloromonas denitrificans* sp. nov., *Flavobacterium denitrificans* sp. nov., *Paenibacillus anaericanus* sp. nov. and *Paenibacillus terrae* strain MH72, N<sub>2</sub>O-producing bacteria isolated from the gut of the earthworm *Aporrectodea caliginosa*. Int J Syst Evol Microbiol 55:1255–1265. <https://doi.org/10.1099/ijs.0.63484-0>.
  69. Kolb S, Knief C, Stubner S, Conrad R. 2003. Quantitative detection of methanotrophs in soil by novel *pmoA*-targeted real-time PCR assays. Appl Environ Microbiol 69:2423–2429. <https://doi.org/10.1128/aem.69.5.2423-2429.2003>.
  70. Ho A, Lee HJ, Reumer M, Meima-Franke M, Raaijmakers C, Zweers H, de Boer W, van der Putten WH, Bodelier PLE. 2019. Unexpected role of canonical aerobic methanotrophs in upland agricultural soils. Soil Biol Biochem 131:1–8. <https://doi.org/10.1016/j.soilbio.2018.12.020>.
  71. Ho A, Lüke C, Cao Z, Frenzel P. 2011. Ageing well: methane oxidation and methane oxidizing bacteria along a chronosequence of 2000 years. Environ Microbiol Rep 3:738–743. <https://doi.org/10.1111/j.1758-2229.2011.00292.x>.
  72. Ho A, Ijaz UZ, Janssens TKS, Ruijs R, Kim SY, de Boer W, Termorshuizen A, van der Putten WH, Bodelier PLE. 2017. Effects of bio-based residue amendments on greenhouse gas emission from agricultural soil are stronger than effects of soil type with different microbial community composition. GCB Bioenergy 9:1707–1720. <https://doi.org/10.1111/gcbb.12457>.
  73. Zhang J, Kobert K, Flouri T, Stamatakis A. 2014. PEAR: a fast and accurate Illumina Paired-End reAd mergeR. Bioinformatics 30:614–620. <https://doi.org/10.1093/bioinformatics/btt593>.
  74. Callahan B. 2017. Rdp taxonomic training data formatted for Dada2 (Rdp trainset 16/Release 11.5).
  75. Quast C, Pruesse E, Yilmaz P, Gerken J, Schweer T, Yarza P, Peplies J, Glöckner FO. 2013. The SILVA ribosomal RNA gene database project: improved data processing and web-based tools. Nucleic Acids Res 41: D590–D596. <https://doi.org/10.1093/nar/gks1219>.
  76. Hammer Ø, Harper DAT, Ryan PD. 2001. PAST: Paleontological statistics software package for education and data analysis. Palaeontologia Electronica 4(1):4.
  77. Parks DH, Tyson GW, Hugenholtz P, Beiko RG. 2014. STAMP: statistical analysis of taxonomic and functional profiles. Bioinformatics 30:3123–3124. <https://doi.org/10.1093/bioinformatics/btu494>.
  78. Bastian M, Heymann S, Jacomy M. 2009. Gephi: an open source software for exploring and manipulating networks, p. 361–362. In Third International AAAI Conference on Weblogs and Social Media.
  79. Newman MEJ. 2003. The structure and function of complex networks. SIAM Rev 45:167–256. <https://doi.org/10.1137/S003614450342480>.
  80. Kupper T, Mendes LW, Lee HJ, Mo Y, Poehlein A, Jia Z, Horn MA, Ho A. 2021. When the going gets tough: emergence of a complex methane-driven interaction network during recovery from desiccation-rewetting. Soil Biol Biochem 153:108109. <https://doi.org/10.1016/j.soilbio.2020.108109>.

## **A.6 Supplementary information - Recovery of Methanotrophic Activity Is Not Reflected in the Methane-Driven Interaction Network after Peat Mining**

Thomas Kaupper<sup>1</sup>, Lucas W. Mendes<sup>2</sup>, Monica Harnisz<sup>3</sup>, Sascha M.B. Krause<sup>4</sup>, Marcus A. Horn<sup>1</sup>, Adrian Ho<sup>1</sup>.

<sup>1</sup>Institute of Microbiology, Leibniz Universität Hannover, Herrenhäuser Str. 2, 30419 Hannover, Germany.

<sup>2</sup>Center for Nuclear Energy in Agriculture, University of São Paulo-USP, Brazil.

<sup>3</sup>Department of Environmental Microbiology, University of Warmia and Mazury in Olsztyn, Olsztyn, Poland.

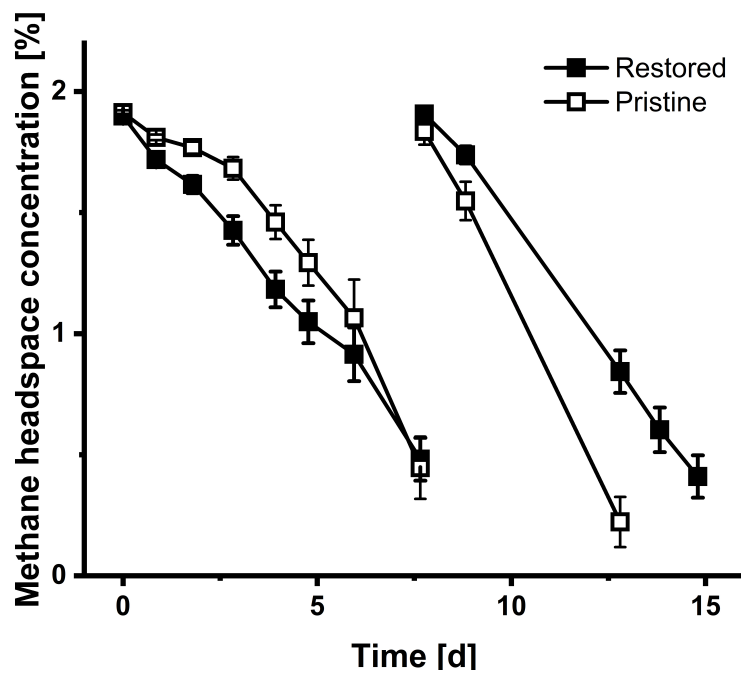
<sup>4</sup>Zhejiang Tiantong Forest Ecosystem National Observation and Research Station, School of Ecological and Environmental Sciences, East China Normal University, Shanghai 200241, China.

Included:

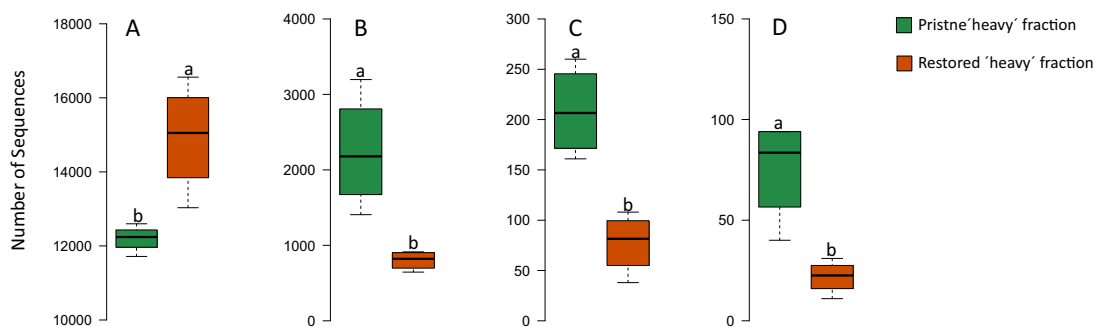
- Supplementary table.
- Supplementary figures and figure legends

**Table S8** Top 10 OTUs with more betweenness centrality, representing the key nodes in the pristine and restored peatlands derived from the  $^{13}\text{C}$ -enriched 16S rRNA gene (metabolically active microorganisms). The OTUs were classified to and given at the lowest taxonomic affiliation. Methanotrophs are highlighted in bold.

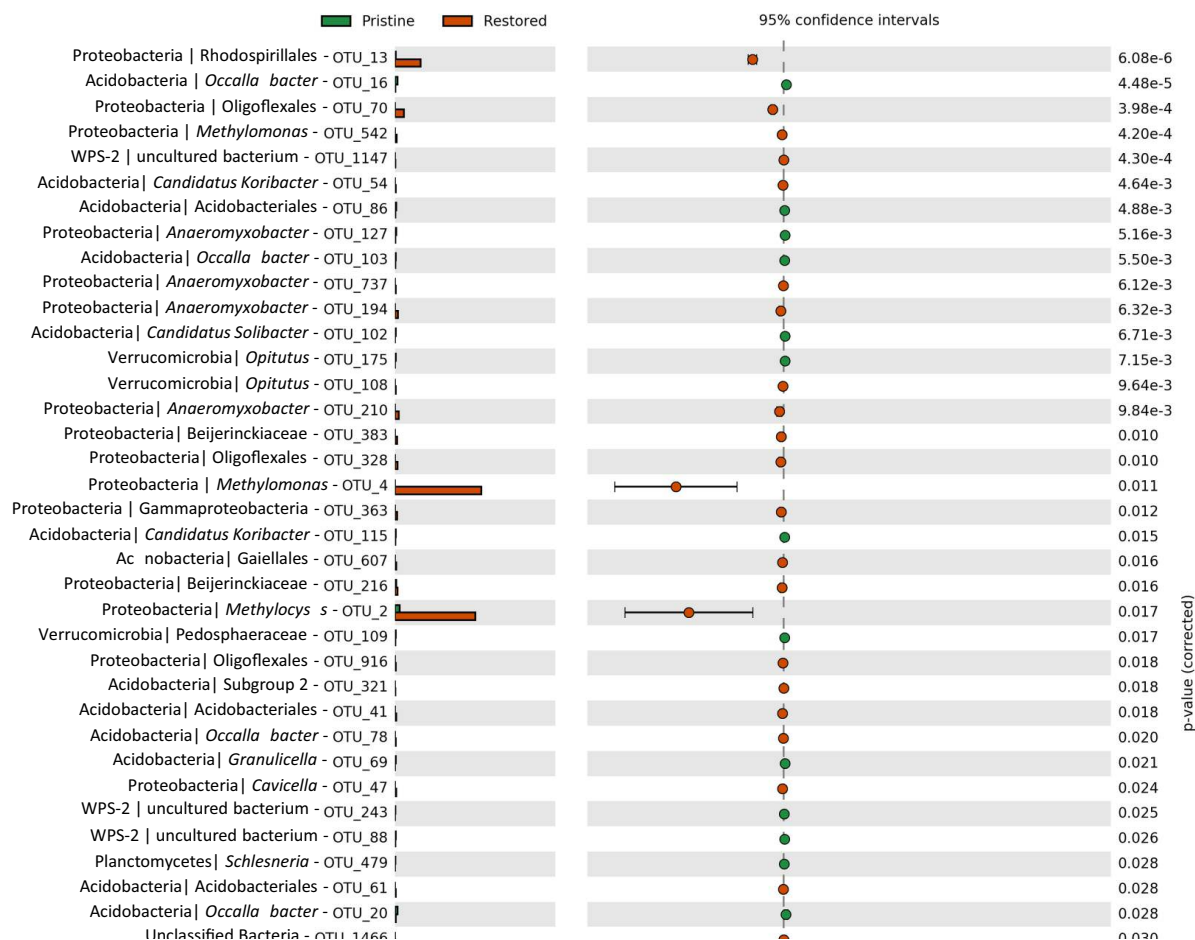
	<b>OTU</b>	<b>Classification</b>	<b>Betweenness centrality</b>
Pristine	OTU_24	Rhodospirillales	10656.9
	OTU_979	Uncultured Bacteria	9894.4
	OTU_123	Burkholderiaceae	9755.8
	OTU_8	<b>Methylomonas</b>	8653.7
	OTU_51	Candidatus Solibacter	8011.1
	OTU_26	Gammaproteobacteria	7406.9
	OTU_2	<b>Methylocystis</b>	6985.9
	OTU_160	Babeliales	6854.6
	OTU_944	Pirellulaceae	6601.7
	OTU_144	<b>Methylacidiphilaceae</b>	6484.9
Restored	OTU_146	<b>Methylomonas</b>	6872.3
	OTU_19	Bdellovibrio	6312.0
	OTU_192	Magnetospirillaceae	5617.5
	OTU_9	<b>Methylomonas</b>	5426.7
	OTU_205	Acidimicrobiia	5061.8
	OTU_158	Sphingobacteriales	5021.8
	OTU_395	Roseiarcus	4988.4
	OTU_1	Beijerinckiaceae	4900.8
	OTU_376	Myxococcales	4615.9
	OTU_15	<b>Methylomonas paludis</b>	4473.8



**Figure S16** Headspace methane concentration during incubation (mean $\pm$ s.d.; n = 8) in the pristine and restored peat. Arrow indicates methane replenishment.



**Figure S17** Boxplot showing the distribution of significantly different phyla i.e., Proteobacteria (a), Acidobacteria (b), Bacteroidetes (c), and WPS-2 (d) in the pristine and restored peatlands, derived from the  $^{13}\text{C}$ -enriched 16S rRNA gene sequences. WPS-2 is a candidate division represented by as yet uncultured bacterium.

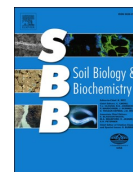


**Figure S18** Differential abundance of OTUs in the pristine and restored peatlands derived from the  $^{13}\text{C}$ -enriched 16S rRNA gene sequences. The post-hoc plot indicates the mean over-abundant OTUs in each peatland, and the difference in mean proportions between sites at 95% confidence intervals. Only significantly different OTUs ( $p > 0.05$ ) between sites are provided. The numbers represent different OTUs. The affiliations of the OTUs are given at the lowest taxonomic level (genus), whenever available. Microorganisms belonging to *Beijerinckiaceae* include non-methanotrophs, which could not be distinguished from the methanotrophs at the coarse taxonomic resolution.



Contents lists available at ScienceDirect

## Soil Biology and Biochemistry

journal homepage: <http://www.elsevier.com/locate/soilbio>

## Short Communication

## Disentangling abiotic and biotic controls of aerobic methane oxidation during re-colonization

Thomas Kaupper<sup>a,1</sup>, Janita Luehrs<sup>a,1</sup>, Hyo Jung Lee<sup>b</sup>, Yongliang Mo<sup>c</sup>, Zhongjun Jia<sup>c</sup>, Marcus A. Horn<sup>a,\*\*</sup>, Adrian Ho<sup>a,\*</sup><sup>a</sup> Institute for Microbiology, Leibniz Universität Hannover, Herrenhäuser Str. 2, 30419, Hannover, Germany<sup>b</sup> Department of Biology, Kunsan National University, Gunsan, Republic of Korea<sup>c</sup> Institute of Soil Science, Chinese Academy of Sciences, No. 71 East Beijing Road, Xuan-Wu District, Nanjing City, PR China

## ARTICLE INFO

## Keywords:

*pmoA*  
Rice paddy  
Upland soil  
*Methylocystis*  
*Methylobacter*  
Rice paddy clusters

## ABSTRACT

Aerobic methane oxidation is driven by both abiotic and biotic factors, which are often confounded in the soil environment. Using a laboratory-scale reciprocal inoculation experiment with two native soils (paddy and upland agricultural soils) and the gamma-irradiated fraction of these soils, we aim to disentangle and determine the relative contribution of abiotic (i.e., soil edaphic properties) and biotic (i.e., initial methanotrophic community composition) controls of methane oxidation during re-colonization. Methane uptake was appreciably higher in incubations containing gamma-irradiated paddy than upland soil despite the initial difference in the methanotrophic community composition. This suggested an overriding effect of the soil edaphic properties, which positively regulated methane oxidation. Community composition was similar in incubations with the same starting inoculum, based on quantitative and qualitative *pmoA* gene analyses. Thus, results suggested that the initial community composition affects the trajectory of community succession to an extent, but not at the expense of the methanotrophic activity under high methane availability. Still, methane oxidation was affected more by soil edaphic properties than by the initial composition of the methanotrophic community.

## 1. Introduction

Aerobic methane-oxidizing bacteria (methanotrophs) represent a specialized microbial guild characterized by their ability to use methane as a carbon and energy source. Aerobic methanotrophs belong to *Verrucomicrobia* and *Proteobacteria*, with members of the proteobacterial methanotrophs falling within the classes *Gammaproteobacteria* (comprising of subgroups type Ia and Ib) and *Alphaproteobacteria* (subgroup type II). While the verrucomicrobial methanotrophs were discovered in low pH (<5) and high temperature (>50 °C) geothermal environments, the proteobacterial methanotrophs are widespread, but show habitat specificity (Op den Camp et al., 2009; Knief, 2015). Methanotrophs possess the enzyme methane monooxygenase that enables them to oxidize methane to methanol, the initial step in methane oxidation (Semrau et al., 2010). Typically, the structural genes encoding for the soluble and particulate form of the methane monooxygenase enzyme (*mmoX* and *pmoA*, respectively) are targeted to survey the

methanotrophic diversity in complex microbial communities (Wen et al., 2016). In wetland ecosystems, methanotrophs inhabit oxic-anoxic interfaces with oxygen-methane counter-gradients (e.g., soil-overlying water, aquatic plant roots) where they act as a filter to consume methane produced in the deeper anoxic sediment layers (Reim et al., 2012). On the other hand, methanotrophs in well-aerated upland soils serve as a methane sink, consuming atmospheric methane (Kolb, 2009; Shrestha et al., 2012; Ho et al., 2015a, 2019; Pratscher et al., 2018). In both these roles, abiotic (e.g., substrate concentrations, micronutrients, and other soil physico-chemical properties; Hütsch et al., 1994; Bodelier, 2011; Veraart et al., 2015; Ho et al., 2013, 2018; Semrau et al., 2018) and biotic factors (e.g., methanotrophic community composition/abundance and interaction-induced response in community functioning; Ho et al., 2016a; Malghani et al., 2016; Chang et al., 2018; Reumer et al., 2018; Schnyder et al., 2018; Veraart et al., 2018) are known to drive aerobic methane oxidation. Collectively, we refer to the non-biological attributes inherent to the soil as abiotic parameters, whereas biotic

\* Corresponding author.

\*\* Corresponding author.

E-mail addresses: [horn@ifmb.uni-hannover.de](mailto:horn@ifmb.uni-hannover.de) (M.A. Horn), [Adrian.ho@ifmb.uni-hannover.de](mailto:Adrian.ho@ifmb.uni-hannover.de) (A. Ho).<sup>1</sup> Equal contribution.<https://doi.org/10.1016/j.soilbio.2020.107729>

Received 21 October 2019; Received in revised form 20 January 2020; Accepted 20 January 2020

Available online 23 January 2020

0038-0717/© 2020 Elsevier Ltd. All rights reserved.

determinants are exemplified by the initial methanotrophic community composition.

Soil manipulation (e.g., amendment) studies, and experimental design capitalizing on soil chronosequence with natural environmental gradients are typically used to relate changes in (a)biotic factors to community functioning (e.g., Rousk et al., 2010; Bissett et al., 2012; Ho et al., 2013, 2018; Palmer and Horn, 2015; Shiau et al., 2018). Often, the abiotic and biotic determinants are confounded, obscuring the contribution of either factors to the regulation of methane oxidation. Rarely are there factors explicitly tested independently and simultaneously.

Here, we aim to disentangle abiotic and biotic controls of methane oxidation by employing a reciprocal inoculation experimental design using two native soils and the gamma-irradiated (25 kGy;  $^{60}\text{Co}$ ) fractions of these soils (Fig. 1), which enabled us to relate the (a)biotic determinants to methane oxidation. We anticipate that if (i) abiotic determinants exert a stronger control than biotic determinants in regulating methane oxidation, the same abiotic environment (i.e., gamma-irradiated soil) will consistently support high methane uptake regardless of the initial community composition, (ii) biotic determinants exert a stronger control than abiotic determinants, the same native soil harboring the initial methanotrophic community will consistently exhibit high methane uptake regardless of the edaphic properties, and (iii) there is no consistent effect, less predictive and/or stochastic factors (e.g., priority effect, site history) may have an overriding impact on the contemporary methanotrophic activity. To address our suppositions, we incubated oxic soil microcosms containing native and gamma-irradiated native soils in all combinations (Fig. 1) for 35 days, and followed the potential methane oxidation rate over time (Fig. 2). Two soils (wetland paddy and upland agricultural soils) with distinct physico-chemical properties and different methanotrophic communities with proven methane uptake capacity under high methane availability ( $>2\%_{\text{v/v}}$ ) were used (Table 1; Ho et al., 2013, 2015a). Soil processing, and soil microcosm setup and sampling are detailed in the Supplementary Materials.

The temporal succession of the methanotrophic community composition was monitored during the incubation using group-specific qPCR assays (i.e., MBAC, MCOC, and TYPEII assays targeting the

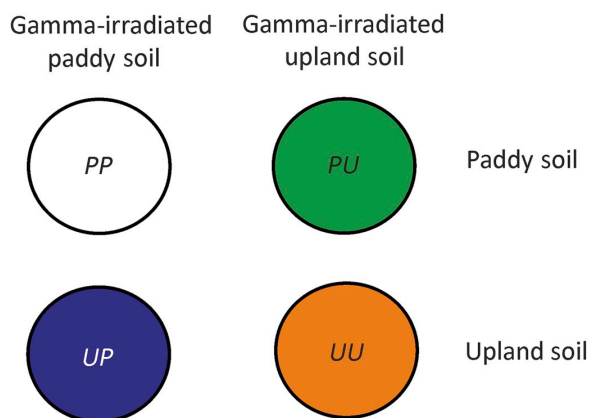


**Fig. 1.** Experimental setup showing reciprocal inoculation of native soils in gamma-irradiated fractions of the soils. Three microcosms per time and amendment were established. The microcosms consisted of paddy soil + gamma-irradiated paddy soil (designated as 'PP'), paddy soil + gamma-irradiated upland soil ('PU'), upland soil + gamma-irradiated paddy soil ('UP'), and upland soil + gamma-irradiated upland soil ('UU'). To confirm the sterility of the soil after gamma-irradiation, the soil (9.5 g) was saturated with autoclaved deionized water ( $0.45\text{ ml g dw soil}^{-1}$ ) in a 120 ml bottle with an adjusted headspace methane concentration of  $1\%_{\text{v/v}}$ . The soil was considered free of viable methanotrophs when headspace methane remained unchanged over three weeks (Fig. S1).

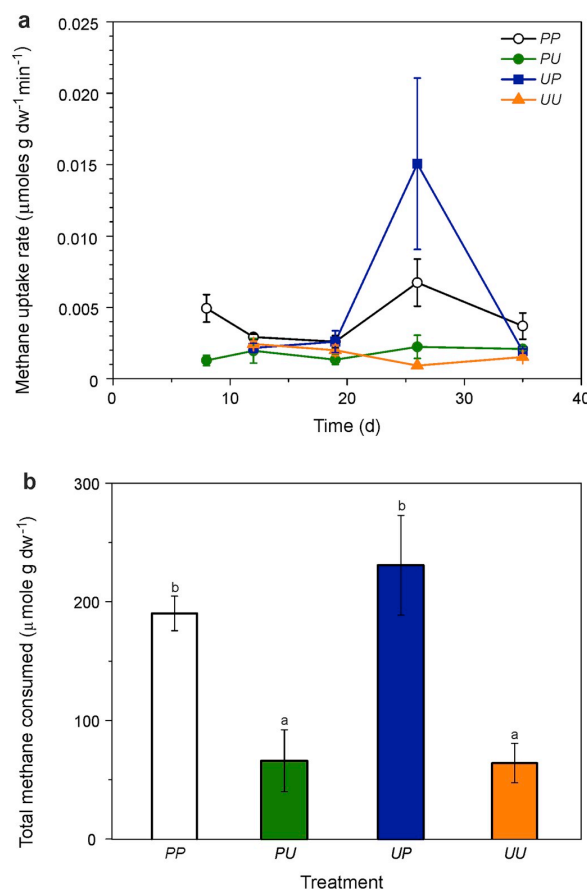


**Fig. 2.** Methane uptake rate (A) and total methane consumed (B) during recolonization (mean  $\pm$  s.d.;  $n = 3$ ). Each soil microcosm consisted of 9.5 g gamma-irradiated soil and 0.5 g native soil in a Petri dish. The soil was saturated with autoclaved deionized water ( $0.45\text{ ml g dw soil}^{-1}$ ) and homogenized before being incubated in a gas tight jar under  $10\%_{\text{v/v}}$  methane in air in the dark at  $27\text{ }^{\circ}\text{C}$ . Headspace air in the jar was replenish every 2–3 days to ensure that methane was not limiting. At designated intervals (days 8, 12, 19, 26, and 35), individual microcosm was removed from the jar, and placed in a flux chamber to determine the methane uptake rate, measured over 5–6 h (minimum of three time points) by linear regression (A), as described before (Ho et al., 2011). Negligible or no methane uptake was detected  $<8$  days in the UP and UU incubation hence, the first sampling was performed at day 12, allowing direct comparisons between treatments per time. Additionally, total methane consumed for each treatment during the incubation (over 35 days) was determined by integrating the area below the curve of methane uptake rates (B). Headspace methane was measured using gas chromatography (GC) coupled to a thermal conductivity and pulsed discharge helium ionization detector (7890B, Agilent Technologies, JAS GC systems, Moers, Germany). In (B), letters indicate the level of significance (ANOVA;  $p < 0.01$ ) in the total methane consumed between treatments.

methanotroph subgroups type Ia, Ib, and II, respectively; Kolb et al., 2003; Ho et al., 2016b; Supplementary Materials) and Illumina MiSeq sequencing of *pmoA* gene amplicons. The *pmoA* gene, instead of the *mmoX* gene, was targeted because the *mmoX* gene transcript or the methanotrophs harbouring only the *mmoX* gene were not detected or below the detection limit in these soils (Reim et al., 2012; Ho et al., 2015a). While the group-specific qPCR assays were performed to be used as proxies for methanotroph abundances, high throughput sequencing of the *pmoA* gene was performed to follow compositional changes in the

**Table 1**  
Selected physico-chemical parameters of the wetland and upland agricultural soils.

Soil(Coordinates)	Texture	pH <sup>a</sup>	Total C (μmoles C g dw soil <sup>-1</sup> )	Total N (μmoles N g dw soil <sup>-1</sup> )	Organic matter content (LOI %)	Total nutrient contents (μmoles g dw soil <sup>-1</sup> )			Vegetation (during sampling)	Reference
						NH <sub>4</sub> <sup>+</sup>	NO <sub>x</sub> <sup>b</sup>	PO <sub>4</sub> <sup>3-</sup>		
Paddy soil (45° 20' N, 8° 25' E)	Calcareous clay	5.4	1158.3	92.9	4.0	1.0	0.3	6.3 × 10 <sup>-3</sup>	Rice (fallow)	Ho et al. (2015b)
Upland soil (51° 32' N, 05° 50' E)	Gley podzol (sandy loam)	5.4	1850.0	92.9	4.7	0.1	3.7 × 10 <sup>-2</sup>	9.5 × 10 <sup>-3</sup>	Potato (fallow)	Ho et al. (2015a)

Abbreviation: LOI, loss on ignition.

<sup>a</sup> pH determined in 1 M KCl (1:5, vol:vol).

<sup>b</sup> Total of NO<sub>2</sub> and NO<sub>3</sub>.

methanotrophic community. The *pmoA* gene sequences were analysed as described before (Reumer et al., 2018; Supplementary Materials), and were deposited at the NCBI Sequence Read Archive under the accession number SRR9924748 (NCBI BioProject PRJNA559227).

## 2. Abiotic parameters exert a stronger effect on aerobic methane oxidation than the initial methanotrophic community composition

The potential for methane oxidation (total methane consumed) was consistently and significantly higher in the microcosms containing the gamma-irradiated paddy soil (*PP*, 190 ± 15 μmol g dw<sup>-1</sup>; *UP*, 231 ± 42 μmol g dw<sup>-1</sup>) than those containing the gamma-irradiated upland soil (*PU*, 66 ± 26 μmol g dw<sup>-1</sup>; and *UU*, 64 ± 17 μmol g dw<sup>-1</sup>), regardless of the initial community composition (Fig. 2). This suggests that the abiotic rather than the biotic determinants, more strongly regulated methane oxidation, which is in line with our first supposition. Higher methanotrophic activity in microcosms containing gamma-irradiated paddy than upland soil coincided with the higher initial ammonium concentration (paddy soil, 3.4–4.2 μmol g dw soil<sup>-1</sup>; upland soil, 2.0–2.7 μmol g dw soil<sup>-1</sup>; Fig. S2). Also, NH<sub>4</sub><sup>+</sup> and NO<sub>x</sub> concentrations in the inoculum was on average 8–10 folds higher in the paddy than upland soil, whereas PO<sub>4</sub><sup>3-</sup> was comparable in both soils (Table 1). Higher inorganic N concentrations likely alleviated N limitation when coupled to high methane availability in the gamma-irradiated paddy soil, stimulating methanotrophic growth and methane uptake (<12 days) when compared to the incubations containing the gamma-irradiated upland soil. However, we cannot exclude the availability of other N compounds (e.g., organic N) given the high total N in these soils (Table 1). Besides macronutrients, methanotrophic activity can be restricted by micronutrients (e.g., lanthanides, copper; Knapp et al., 2007; Semrau et al., 2010, 2018). Hence, we cannot completely exclude that differences in the micronutrient and trace element contents in the paddy and upland soils may have also affected methane oxidation rates. pH, and water content that may restrict methane and oxygen diffusion into the soil were similar during the incubation of both soils (Table 1; Supplementary Materials); therefore, difference in methane uptake between the soils were likely caused by factors other than these (Hiltbrunner et al., 2012; Shrestha et al., 2012). However, the water potential which may affect water availability for microbial activity, potentially contributing to shifts in the community composition, could be different in both soils (Harris, 1981). Admittedly, not all abiotic factors potentially contributing to the difference in methane uptake in both soils were determined. Nevertheless, it became evident that the soil abiotic parameters more strongly affected the methanotrophic activity, resulting in significantly higher methane uptake rates during the early stage (<35 days) of recolonization under high methane availability.

Microorganisms compete for nutrients as well as space, and occupy specific niches in the soil according to their physiological requirements. These are examples for mechanisms shaping the microbial activity and community composition (Little et al., 2008; Pan et al., 2014). Here, the gamma-irradiated soils provide open niches, allowing rapid

recolonization by the inoculum-borne methanotrophs under high methane availability. The microcosms containing native soils and their gamma-irradiated fractions (*PP* and *UU*) thus represent the optimum native/gamma-irradiated soil combinations because the inoculum consists of methanotrophs with established niche specialization (e.g., as a result of shared site history) for the specific soil. Interestingly, although *PP* exhibited significantly higher methane uptake than *PU* as anticipated, methane uptake in *UU* was significantly lower than *UP*, indicating that conditions in the upland soil were not optimal and constrained methanotrophic activity; the paddy soil likely possessed more suitable conditions (e.g., high inorganic N), favoring the survival of methanotrophs. This suggests that the methanotrophic community composition, although indigenous to the upland soil, plays a relatively less important role in determining contemporary methane uptake rates than abiotic controls (Ho et al., 2016c).

## 3. Methanotroph population dynamics; the emergence of the alphaproteobacterial methanotrophs during recolonization

The total methanotroph abundance was at or below the detection limit of the qPCR assays (1.8–8.5 × 10<sup>5</sup> copy no. of target molecules g dw soil<sup>-1</sup>) at the beginning of the incubations and appreciably increased in all microcosms by approximately three to four orders of magnitude during incubation (Fig. 3), consistent with previous recolonization studies (Ho et al., 2011; Pan et al., 2014). In particular, the significant increase ( $p < 0.01$ ) in all methanotroph sub-groups (days 12–35; type Ia, four-fold; type Ib, seven-fold; type II, three-fold) corroborated the higher total methane uptake in the *UP* incubations (Figs. 2 and 3). On the other hand, *PP* microcosms which exhibited similar total methane uptake to *UP*, showed a significant increase ( $p < 0.01$ ) in type II methanotroph abundance during the same time (Fig. 3). Likewise, the abundance of type II methanotrophs significantly increased ( $p < 0.01$ ) in the other incubations (from days 12–35 and days 12–19 in *PU* and *UU*, respectively). Before being succeeded by the type II methanotrophs, type Ib methanotrophs formed the majority in the paddy soil-inoculated microcosms (<19 days; *PP* and *PU*), in agreement with their general predominance in rice paddy environments (Lüke et al., 2013). However, the high abundance of type Ib methanotrophs in *PU* is not consistent with the relatively low methane uptake detected in this microcosm. This may be attributable to the relatively more oligotrophic condition (e.g., lower inorganic N, NH<sub>4</sub><sup>+</sup>, NO<sub>3</sub><sup>-</sup>) or faster transition to oligotrophic condition in the gamma-irradiated upland soil than in the gamma-irradiated paddy soil incubations, resulting in lower cell-specific activity (Ho et al., 2011) not only in *PU*, but also in the *UU* microcosms. Although the methanotroph sub-groups were differentially affected during recolonization, the trajectory of the methanotroph succession was consistent across all microcosms, with the type II methanotrophs increasing in abundance and being generally more responsive than the type I during recolonization (>12 days; Fig. 3). This may reflect on the ecological characteristics of the community members in the native soil (see discussion below; Ho et al., 2017). Nevertheless, irrespective of the community members, it is likely that reduced competition coupled to high methane



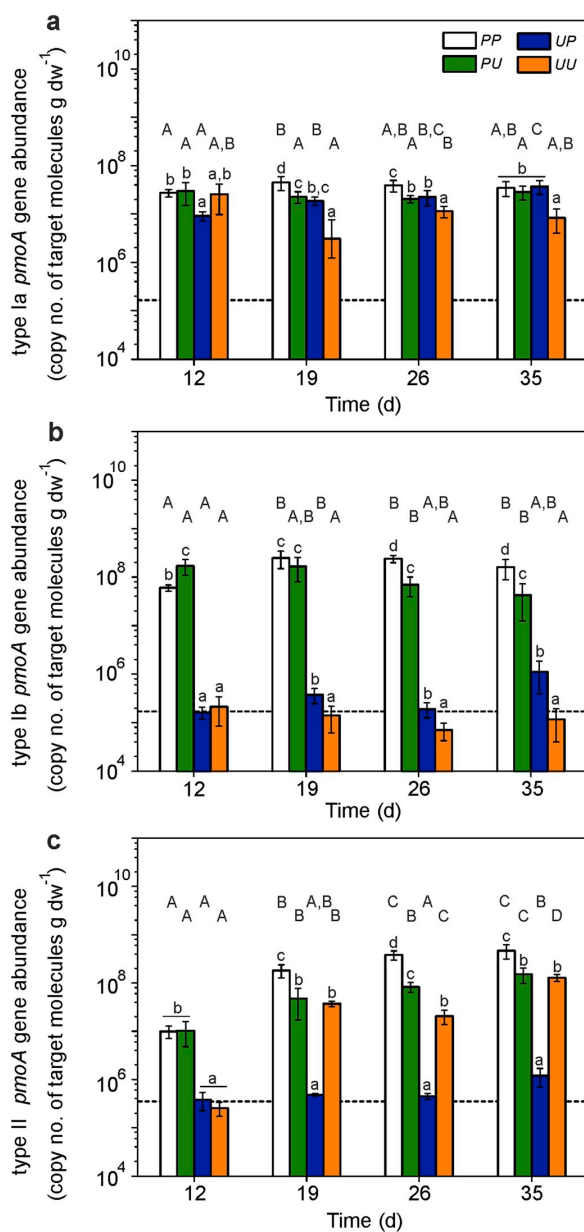


**Fig. 3.** Response of the *pmoA* gene abundance of type Ia (A), type Ib (B), and type II (C) methanotrophs during re-colonization. The qPCR was performed in duplicate for each DNA extract ( $n = 3$ ), giving a total of six replicates per time, treatment, and assay. The lower case letters indicate the level of significance (ANOVA;  $p < 0.01$ ) between treatments per time. The upper case letters indicate the level of significance (ANOVA;  $p < 0.01$ ) between sampling days per treatment. Values at the start of the incubation were at or below the detection limits of the qPCR assays used. The lower detection limit of the qPCR assay is indicated by the dashed line ( $1.8\text{--}8.5 \times 10^5$  copy no. of target molecules  $g\ dw\ soil^{-1}$ ).

availability spurred recolonization.

The *pmoA* gene sequences, visualized as a principal component analysis (PCA; Fig. 4) revealed a divergent community composition in the PP/PU and UP/UU incubations which could be largely separated

along PC axis 2 (Fig. 4). Over 90% of the variation in the methanotrophic community composition could be explained by PC1 and PC2 (62.24% and 30.71% of the total variance, respectively). The predominant methanotrophs were represented by members of type Ia (*Methylobacter*), type Ib (Rice Paddy Clusters, RPCs), and type II (*Methylocystis*). The RPCs are putative methanotrophs closely related to *Methylocaldum* (Lüke et al., 2013; Shiau et al., 2019). Hence, the MiSeq sequencing enabled the identification of key methanotrophs within each sub-group. The PCA revealed a RPCs-dominated population in microcosms inoculated with native paddy soils (PP and PU), and *Methylobacter* dominated the community inoculated with native upland soils (UP and UU), with the UU incubation having a broader inventory of dominant methanotrophs comprising of *Methylocystis*, besides *Methylobacter*, reflecting on the dynamic shifts in the community composition. Hence, comparing the qPCR and *pmoA* gene sequencing analyses (Figs. 3 and 4), the general trend in community dominance and succession was consistent in both analyses.

When the same community was inoculated in different gamma-irradiated soils, similar predominant communities developed, indicating that the initial community composition plays a role in shaping the dynamics of the methanotrophic population, but not to an extent that profoundly affects methane uptake. In particular, gammaproteobacterial methanotrophs affiliated to *Methylobacter* and RPCs were predominant in the microcosms inoculated with the upland and paddy soil, respectively, while type II methanotrophs related to *Methylocystis* increased in abundance, more pronounced in the UU incubation (Fig. 4 and Fig. S4). Previously, the potentially active community members when incubated near *in-situ* methane concentrations in the paddy ( $\sim 1\%$  v/v) and upland (30–40 ppm<sub>v</sub>) soils were predominantly comprised of type I and type II methanotrophs, respectively (Ho et al., 2013, 2019). Here, type I methanotrophs were initially dominant in the microcosms inoculated with both soils. Considering that the

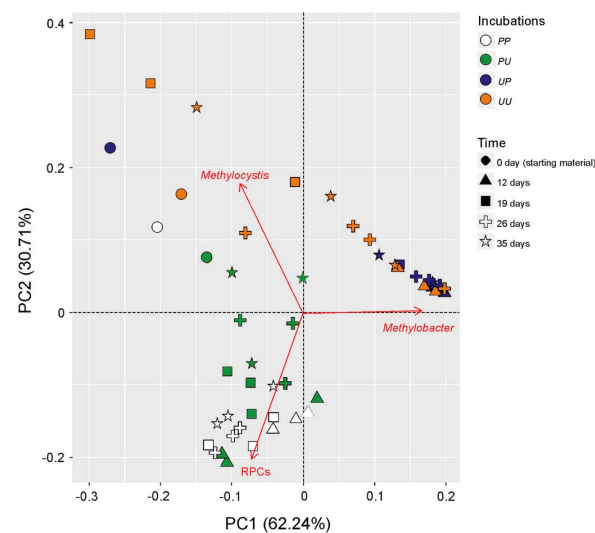


**Fig. 4.** Principal component analysis (PCA) showing the response of the methanotrophic community composition during recolonization. The composition of the methanotrophic community was derived from sequencing of the *pmoA* gene performed for each DNA extract ( $n = 3$ ) per time and treatment. The PCA was performed in the R statistics software environment (R Core Team, 2014) using the function 'prcomp'. Visualization of the PCA was performed using the 'ggfortify' package. Rarefaction curves generated for each sample showed a good coverage of the *pmoA* gene diversity (Fig. S3). The affiliation and distribution of the *pmoA* gene sequences are given in Fig. S4. The vectors indicate predominant methanotrophic genera/group. Abbreviations: RPC, rice paddy cluster (type Ib-related methanotroph).

gammaproteobacterial methanotrophs, particularly members of type Ia (e.g., *Methylobacter*, *Methylosarcina*, *Methylomicrobium*, *Methylomonas*), are thought to be more competitive under high or excess methane availability, these methanotrophs may have been favored during incubation under high (10%<sub>v/v</sub>) methane concentrations (Krause et al., 2012; Reim et al., 2012; Ho et al., 2017 and references therein). However, consistent in all incubations, type II methanotrophs presumably comprised of *Methylocystis* significantly increased over time, and even dominated the population after 19 days, despite of the prevalence of type I methanotrophs (Figs. 3 and 4). The emergence of *Methylocystis* during recolonization is not entirely unexpected. Another alphaproteobacterial methanotroph (*Methylosinus*) showed colonization potential in a soil and sediment, increasing in numerical abundance over time (<3.5 months incubation; Ho et al., 2011; Pan et al., 2014). Likewise, in a synthetic community comprising of aerobic methanotrophs, only alphaproteobacterial ones (*Methylosinus* or *Methylocystis*) became dominant over time (Schnyder et al., 2018). The successional trajectory indicates that type II methanotrophs may become important for community functioning during late succession when conditions turned oligotrophic (e.g., after nutrient, including ammonium depletion; Ho et al., 2017).

Overall, results support our first supposition, indicating that methane oxidation is primarily governed by the soil physico-chemical properties, provided methane is available. The initial community composition influences the population dynamics of the methanotrophs without having pronounced effects on methane oxidation. Considering accumulating evidence indicating the relevance of biotic determinants in modulating methane oxidation (e.g., Ho et al., 2016a; Chang et al., 2018; Veraart et al., 2018), we further suggest that while soil edaphic properties modulate the methanotrophic activity at the pioneering stages of recolonization, biotic determinants (e.g., methanotrophic community structure, and interaction) may become relevant in established communities.

#### Declaration of competing interest

None.

#### Acknowledgements

We are grateful to Natalie Röder for excellent technical assistance. Daria Frohloff and Stefanie Hetz are acknowledged for their help with the ammonium assay. Funding was provided by the German Research Association (DFG grant HO4020/3-1) and the Leibniz Universität Hannover (Hannover, Germany).

All authors have seen and approved the final version of the manuscript.

#### Appendix A. Supplementary data

Supplementary data to this article can be found online at <https://doi.org/10.1016/j.soilbio.2020.107729>.

#### References

- Bissett, A., Abell, G.C.J., Bodrossy, L., Richardson, A.E., Thrall, P.H., 2012. Methanotrophic communities in Australian woodland soils of varying salinity. *FEMS Microbiology Ecology* 80, 685–695.
- Bodelier, P.L.E., 2011. Interactions between nitrogenous fertilizers and methane cycling in wetland and upland soils. *Current Opinion in Environmental Sustainability* 3, 379–388.
- Chang, J., Gu, W., Park, D., Semrau, J.D., DiSpirito, A.A., Yoon, S., 2018. Methanobacterium from *Methylosinus trichosporium* OB3b inhibits N<sub>2</sub>O reduction in denitrifiers. *The ISME Journal* 12, 2086–2089.
- Harris, R., 1981. Effect of water potential on microbial growth and activity. In: Parr, J., Gardner, W., Elliot, L. (Eds.), *Water Potential Relations in Soil Microbiology*. Soil Science Society of America, Madison, pp. 23–95.
- Hiltbrunner, D., Zimmermann, S., Karbin, S., Hagedorn, F., Niklaus, P.A., 2012. Increasing soil methane sink along a 120-year afforestation chronosequence is driven by soil moisture. *Global Change Biology Bioenergy* 18, 3664–3571.
- Ho, A., Lee, H.Y., Reumer, M., Meima-Franke, M., Raaijmakers, C., Zweers, H., de Boer, W., van der Putten, W.H., Bodelier, P.L.E., 2019. Unexpected role of canonical aerobic methanotrophs in upland agricultural soils. *Soil Biology and Biochemistry* 131, 1–8.
- Ho, A., Mo, Y., Lee, H.J., Sauheitl, L., Jia, Z., Horn, M.A., 2018. Effects of salt stress on aerobic methane oxidation and associated methanotrophs; a microcosm study of a natural community from a non-saline environment. *Soil Biology and Biochemistry* 125, 210–214.
- Ho, A., Di Lonardo, D.P., Bodelier, P.L.E., 2017. Revisiting life strategy concepts in environmental microbial ecology. *FEMS Microbiology Ecology* 93, fix006.
- Ho, A., Angel, A., Veraart, A.J., Daebeler, A., Jia, Z., Kim, S.Y., Kerckhof, F.-M., Boon, N., Bodelier, P.L.E., 2016a. Biotic interactions in microbial communities as modulators of biogeochemical processes: methanotrophy as a model system. *Frontiers in Microbiology* 7, 1285.
- Ho, A., van den Brink, E., Reim, A., Krause, S.M.B., Bodelier, P.L.E., 2016b. Recurrence and frequency of disturbance have cumulative effect on methanotrophic activity, abundance, and community structure. *Frontiers in Microbiology* 6, 1493.
- Ho, A., Lüke, C., Reim, A., Frenzel, P., 2016c. Resilience of (seed bank) aerobic methanotrophs and methanotrophic activity to desiccation and heat stress. *Soil Biology and Biochemistry* 101, 130–138.
- Ho, A., Reim, A., Kim, S.Y., Meima-Franke, M., Termorshuizen, A., de Boer, W., van der Putten, W.H., Bodelier, P.L.E., 2015a. Unexpected stimulation of soil methane uptake as emergent property of agricultural soils following bio-based residue application. *Global Change Biology* 21, 3864–3879.
- Ho, A., El-Hawwary, A., Kim, S.Y., Meima-Franke, M., Bodelier, P.L.E., 2015b. Manure-associated stimulation of soil-borne methanogenic activity in agricultural soils. *Biology and Fertility of Soils* 51, 511–516.
- Ho, A., Lüke, C., Reim, A., Frenzel, P., 2013. Selective stimulation in a natural community of methane oxidizing bacteria: effects of copper on *pmoA* transcription and activity. *Soil Biology and Biochemistry* 65, 211–216.
- Ho, A., Lüke, C., Frenzel, P., 2011. Recovery of methanotrophs from disturbance: population dynamics, evenness and functioning. *The ISME Journal* 5, 750–758.
- Hütsch, B.W., Webster, C.P., Powlson, D.S., 1994. Methane oxidation in soil as affected by land use, soil pH and N fertilization. *Soil Biology and Biochemistry* 26, 1613–1622.
- Knapp, C.W., Fowle, D.A., Kulczycki, E., Roberts, J.A., Graham, D.W., 2007. Methane monooxygenase gene expression mediated by methanobacterium in the presence of mineral copper sources. *Proceedings of the National Academy of Sciences of the USA* 104, 12040–12045.
- Knief, C., 2015. Diversity and habitat preferences of cultivated and uncultivated aerobic methanotrophic bacteria evaluated based on *pmoA* as molecular marker. *Frontiers in Microbiology* 6, 1346.
- Kolb, S., 2009. The quest for atmospheric methane oxidizers in forest soils. *Environmental Microbiology Reports* 1, 336–346.
- Kolb, S., Knief, C., Stubner, S., Conrad, R., 2003. Quantitative detection of methanotrophs in soil by novel *pmoA*-targeted real-time PCR assays. *Applied and Environmental Microbiology* 69, 2423–2429.
- Krause, S.M.B., Lüke, C., Frenzel, P., 2012. Methane source strength and energy flow shape methanotrophic communities in oxygen-methane counter-gradients. *Environmental Microbiology Reports* 4, 203–208.
- Little, A.E.F., Robinson, C.J., Peterson, S.B., Raffa, K.F., Handelsman, J., 2008. Rules of engagement: interspecies interactions that regulate microbial communities. *Annual Review of Microbiology* 62, 375–401.
- Lüke, C., Frenzel, P., Ho, A., Fiantis, D., Schad, P., Schneider, B., Schwark, L., Utami, S.R., 2013. Macroecology of methane-oxidizing bacteria: the  $\beta$ -diversity of *pmoA* genotypes in tropical and subtropical rice paddies. *Environmental Microbiology* 16, 72–83.
- Malghani, S., Reim, A., von Fischer, J., Conrad, R., Kuebler, K., Trumbore, S.E., 2016. Soil methanotroph abundance and community composition are not influenced by substrate availability in laboratory incubations. *Soil Biology and Biochemistry* 101, 184–194.
- Op den Camp, H.J.M., Islam, T., Stott, M.B., Harhangi, H.R., Hynes, A., Schouten, S., Jetten, M.S.M., Birkeland, N.-K., Pol, A., Dunfield, P.F., 2009. Environmental, genomic and taxonomic perspectives on methanotrophic *Verrucomicrobia*. *Environmental Microbiology Reports* 1, 293–306.
- Palmer, K., Horn, M.A., 2015. Denitrification activity of a remarkably diverse fen denitrifier community in Finnish Lapland is N-oxide limited. *PLoS One* 10 e0123123.
- Pan, Y., Abell, G.C.J., Bodelier, P.L.E., Meima-Franke, M., Sessitsch, A., Bodrossy, L., 2014. Remarkable recovery and colonization behavior of methane oxidizing bacteria in soil after disturbance is controlled by methane source only. *Microbial Ecology* 68, 259–270.
- Pratscher, J., Vollmers, J., Wiegand, S., Dumont, M.G., Kaster, A.-K., 2018. Unravelling the identity, metabolic potential and global biogeography of the atmospheric methane-oxidizing upland soil cluster  $\alpha$ . *Environmental Microbiology* 20, 1016–1029.
- R Core Team, 2014. *R: a Language and Environment for Statistical Computing*. R Foundation for statistical computing, Vienna, Austria.
- Reim, A., Lüke, C., Krause, S., Pratscher, J., Frenzel, P., 2012. One millimeter makes the difference: high-resolution analysis of methane-oxidizing bacteria and their specific activity at the oxic-anoxic interface in a flooded paddy soil. *The ISME Journal* 6, 2128–2139.
- Reumer, M., Harnisz, M., Lee, H.J., Reim, A., Grunert, O., Putkinen, A., Fritze, H., Bodelier, P.L.E., Ho, A., 2018. Impact of peat mining and restoration on methane

T. Kaupper et al.

Soil Biology and Biochemistry 142 (2020) 107729

- turnover potential and methane-cycling microorganisms in a northern bog. *Applied and Environmental Microbiology* 84 e02218-17.
- Rousk, J., Bååth, E., Brookes, P.C., Lauber, C.L., Lozupone, C., Caporaso, J.G., Knight, R., Fierer, N., 2010. Soil bacterial and fungal communities across a pH gradient in an arable soil. *The ISME Journal* 4, 1340–1351.
- Schnyder, E., Bodelier, P.L.E., Hartmann, M., Henneberger, R., Niklaus, P.A., 2018. Positive diversity-functioning relationships in model communities of methanotrophic bacteria. *Ecology* 99, 714–723.
- Semrau, J.D., DiSpirito, A.A., Gu, W., Yoon, S., 2018. Metals and methanotrophy. *Applied and Environmental Microbiology* 84 e02289-17.
- Semrau, J.D., DiSpirito, A.A., Yoon, S., 2010. Methanotrophs and copper. *FEMS Microbiology Reviews* 34, 496–531.
- Shiau, Y.-J., Cai, Y., Lin, Y.-T., Jia, Z., Chiu, C.-Y., 2018. Community structure of active aerobic methanotrophs in red mangrove (*Kandelia obovate*) soils under different frequency of times. *Microbial Ecology* 75, 761–770.
- Shiau, Y.-J., Cai, Y., Jia, Z., Chen, C.-L., Chiu, C.-Y., 2019. Phylogenetically distinct methanotrophs modulate methane oxidation in rice paddies across Taiwan. *Soil Biology and Biochemistry* 124, 59–69.
- Shrestha, P.M., Kammann, C., Lenhart, K., Dam, B., Liesack, W., 2012. Linking activity, composition and seasonal dynamics of atmospheric methane oxidizers in a meadow soil. *The ISME Journal* 6, 1115–1126.
- Veraart, A.J., Garbeva, P., van Beersum, F., Ho, A., Hordijk, C.A., Meima-Franke, M., Zweers, A.J., Bodelier, P.L.E., 2018. Living apart together – bacterial volatiles influence methanotrophic growth and activity. *The ISME Journal* 12, 1163–1166.
- Veraart, A.J., Steenbergh, A.K., Ho, A., Kim, S.Y., Bodelier, P.L.E., 2015. Beyond nitrogen: the importance of phosphorus for CH<sub>4</sub> oxidation in soils and sediments. *Geoderma* 259–260, 337–346.
- Wen, X., Yang, S., Lieben, S., 2016. Evaluation and update of cutoff values for methanotrophic pmoA gene sequences. *Archives of Microbiology* 198, 629–636.

## **A.8 Supplementary information - Disentangling abiotic and biotic controls of aerobic methane oxidation during re-colonization**

Thomas Kaupper<sup>1#</sup>, Janita Luehrs<sup>1#</sup>, Hyo Jung Lee<sup>2</sup>, Yongliang Mo<sup>3</sup>, Zhongjun Jia<sup>3</sup>, Marcus A. Horn<sup>1\*</sup>, Adrian Ho<sup>1\*</sup>.

<sup>1</sup>Institute for Microbiology, Leibniz Universität Hannover, Herrenhäuser Str. 2, 30419 Hannover, Germany.

<sup>2</sup>Department of Biology, Kunsan National University, Gunsan, Republic of Korea.

<sup>3</sup>Institute of Soil Science, Chinese Academy of Sciences, No. 71 East Beijing Road, Xuan-Wu District, Nanjing City, P.R. China.

#Equal contribution.

\*Correspondence:

Dr. Adrian Ho (Adrian.ho@ifmb.uni-hannover.de).

Included:

- Extended Methods and Materials
- Supporting information figure captions.

## Extended Methods and Materials.

**Soil and soil microcosm setup** A wetland paddy soil and a well-aerated upland agricultural soil was used (Table 6.1). These soils, proven to consume methane, were selected based on their distinct soil characteristics (clay and sandy loam) and the methanotrophic community composition (Table 6.1; Ho et al. (2013b, 2015b)). The paddy soil was collected from a rice field at the CRA Agricultural Research Council, Rice Research Unit (Vercelli, Italy; coordinates 45° 20' N, 8° 25' E) in May 2011. The rice agricultural practices at the sampling field have been described before (Krueger et al., 2001). The upland soil was collected from a potato field post-harvest belonging to the Wageningen University and Research (Vredepeel, the Netherlands; coordinates 51° 32' N, 05° 50' E) in October 2013. The edaphic properties, as well as the methanotrophic community composition in both soils have been characterized before (Ho et al., 2013b, 2015b). In both sites, soils were collected from the plough layer (approximately 10-15 cm from the surface), air-dried at room temperature, crushed, and sieved to 2 mm before storage in sealed plastic containers till incubation setup. A fraction of the same soil was gamma-irradiated (25 kGy; <sup>60</sup>Co).

Each soil microcosm consisted of 9.5 g gamma-irradiated soil and 0.5 g native soil in a Petri dish. The soil was saturated with autoclaved deionized water (0.45 ml g dw soil<sup>-1</sup>), and homogenized. We established three microcosms per time for each treatment: paddy soil + gamma-irradiated paddy soil (designated as 'PP'), paddy soil + gamma-irradiated upland soil ('PU'), upland soil + gamma-irradiated paddy soil ('UP'), and upland soil + gamma-irradiated upland soil ('UU'). The microcosms were incubated in gas tight jars under 10% v/v methane in air in the dark at 27°C as described before (Ho et al., 2011b). Headspace air in the jar was replenish every 2-3 days to ensure that methane was not limiting. At designated intervals (days 8, 12, 19, 26, and 35), individual microcosm was removed from the jar, and placed in a flux chamber to determine the methane uptake rate by linear regression. Additionally, total methane consumed for each treatment during the incubation (35 days) was determined by integrating the area below the curve of methane uptake rates. Methane uptake was measured over 5-6 hours with a minimum of three time points. Negligible or no methane uptake was detected < 8 days in the UP and UU incubation hence, the first methane uptake rate was determined at day 12. After each methane uptake measurement, the soil was homogenized, and destructively sampled. An aliquot of the soil was kept in the 4°C fridge for soil nutrient analysis, while the remaining soil was stored in the -20°C freezer till DNA extraction.

To confirm the sterility of the soil after gamma-irradiation, the soil (9.5 g) was saturated with autoclaved deionized water (0.45 ml g dw soil<sup>-1</sup>) in a 120 ml bottle with an adjusted headspace methane concentration of 1% v/v. The soil was considered free of viable methanotrophs when headspace methane remained unchanged over three weeks (Figure S19).

**Ammonium colorimetric assay and methane measurement** Soil ammonium concentration was determined by a colorimetric method in 2 M KCl extracts (1:5) after filtration (0.2 µm pore size) according to Horn et al. (2005). Headspace methane was mea-

sured using gas chromatography (GC) coupled to a thermal conductivity and pulsed discharge helium ionization detector (7890B, Agilent Technologies, JAS GC systems, Moers, Germany).

**DNA extraction, and *pmoA*-based group-specific qPCR assays** DNA was extracted from soil using the PowerSoil DNA Isolation kit (Qiagen, Hilden, Germany) according to the manufacturer's instructions. The DNA was extracted from each replicate (n=3) per treatment and time, and was stored in the -20°C freezer till further molecular analyses.

The qPCR assays targeting the *pmoA* gene of Type Ia (MBAC assay), Type Ib (MCOC assay), and Type II (TYPEII assay) aerobic proteobacterial methanotrophs were performed as detailed in Kolb et al. (2003), with some minor modifications (Ho et al., 2016c). The primer, and primer concentrations used for these assays are given in Ho et al. (2016c). The qPCR assays were performed using a CFX Connect Real-time PCR system (Biorad, München, Germany) in duplicate for each DNA extract, giving a total of six replicates per time and treatment for each assay. Each qPCR reaction (total volume, 20 µl) comprised of 10 µl 2X SensiFAST SYBR (Bioline GmbH, Luckenwalde, Germany), 3.5 µl of forward and reverse primers each, 1 µl bovine serum albumin (5 mg ml<sup>-1</sup>; Sigma-Aldrich Chemie GmbH, Taufkirchen, Germany), and 2 µl diluted template DNA. Template DNA from microcosms containing gamma-irradiated paddy and upland soil were diluted 100-fold and 50-fold in DNase- and RNase-free water, respectively. In previous qPCR analyses of the same soils, these dilutions resulted in the maximum target yield for the assays (Ho et al., 2011b, 2015b). DNA obtained from clones was used for the calibration curve. The PCR thermal profile consisted of an initial denaturation step at 95°C for 3 mins, followed by 45 cycles of denaturation at 95°C for 10 sec, annealing at 54°C for 10 sec (MBAC assay) / 64°C for 10 sec (MCOC assay) / 60°C for 10 sec (TYPEII assay), and elongation at 72°C for 25 sec. The melt curve for all assays was determined from 70°C to 95°C at 1°C increment. Amplicon specificity was determined from the melt curve, and randomly selected amplicons were additionally checked by 1% gel electrophoresis, showing a single band of the correct size.

***pmoA* gene amplicon sequencing** The *pmoA* gene was amplified using the A189f/mb661r primer combination (6 bp barcoded forward primer) for Illumina MiSeq sequencing. Each PCR reaction (total volume, 50 µl) comprised of 25 µl SYBR Premix Ex TaqTM (Tli RNaseH Plus, TaKaRa, Japan), 1 µl forward/reverse primer each (10 µM), 2 µl template DNA (DNA concentration diluted to 2-8 ng µl<sup>-1</sup>), and 21 µl sterilized distilled water. The PCR thermal profile consisted of an initial denaturation step at 94°C for 2 min, followed by 39 cycles of denaturation at 94°C for 30 s, annealing at 60°C for 30 s, and elongation at 72°C for 45 s (Yun et al., 2013). The final elongation step was at 72°C for 5 mins. After PCR, the *pmoA* gene amplicon was purified using the E.Z.N.A. Cycle-Pure kit (Omega Bio-tek, USA) following 1.2% agarose gel electrophoresis showing a single band of the correct size. The purified amplicons were pooled at equimolar DNA amount (200 ng) for sequencing. The high throughput sequencing was performed using Illumina MiSeq version 3 chemistry (600 cycles). A sequence library was constructed for the *pmoA* gene using the TruSeq Nano DNA LT

---

Sample Prep Kit set A (Illumina, Beijing, China).

***pmoA* gene amplicon sequencing analysis** The *pmoA* gene sequences were analysed as described before (Reumer et al., 2018). Briefly, assembly of paired end reads were performed in Mothur version 1.35.1 (Schloss et al., 2009) using the 'make.contigs' command, before being sorted based on their length, and the quality of the primers ( $\leq 2$  errors) and barcodes ( $\leq 1$  error). Primers and barcodes which do not meet the quality control requirements were removed. Putative chimeric reads were also removed in Mothur version 1.35.1 using the 'chimera.uchime' command with the 'self' option. Illumina MiSeq sequencing generated a total of  $\sim 1.35$  million reads. After filtering,  $\sim 770000$  (on average,  $\sim 14800$  reads per sample) high quality sequences were obtained. These sequences could be affiliated to the *pmoA* gene at the genus level for methanotrophs with cultured representatives. Rarefaction curves were generated to show the coverage of the *pmoA* gene diversity. Classification of the high quality *pmoA* sequence reads were performed using BLAST by comparing to the GenBank nonredundant (nr) database, and the lowest common ancestor algorithm in MEGAN (v 5.11.3), respectively based on curated *pmoA* gene database and MEGAN tree, as detailed in Dumont et al. (2014). The principal component analysis (PCA) was derived from the relative abundance of the classified *pmoA* gene sequences. The PCA was performed in the R statistics software environment (R Core Team, 2014) using the function 'prcomp'. Visualization of the PCA was performed using the 'ggfortify' package. The *pmoA* gene sequences were deposited at the NCBI Sequence Read Archive under the accession number SRR9924748 (NCBI BioProject PRJNA559227).

**Statistical analyses** Significant differences ( $p < 0.01$ ) in the methane uptake and *pmoA* gene abundances (MBAC, MCOC, and TYPEII assays) between treatments over time were determined by analysis of variance (ANOVA) using SigmaPlot version 13.0 (Systat Software Inc., USA).

## Supplementary Figures

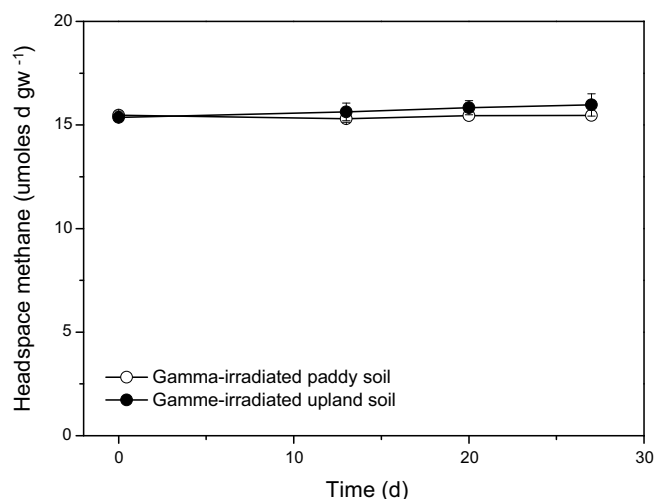


**Figure S19** Headspace methane in the gamma-irradiated rice paddy and upland soils (mean, s.d.,  $n = 2$ ), indicating the absence of viable methanotrophs.

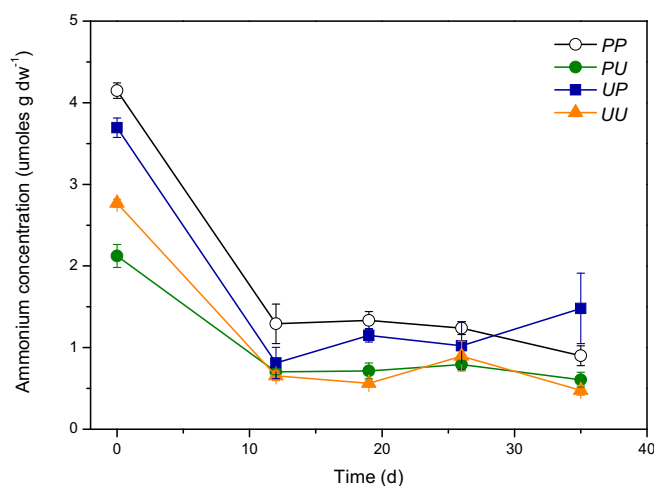


**Figure S20** Changes in ammonium concentrations during incubation (mean, s.d.,  $n = 3$ ). Soil ammonium concentration was determined by a colorimetric method in 2 M KCl extracts (1:5) after filtration ( $0.2 \mu\text{m}$  pore size) according to Horn et al. (2005). Initial (day 0) ammonium concentration in the incubations was higher than in the native soil (Table 6.1), likely contributed by the gamma-irradiated fraction of the soil as a result of mineralization of dead microbial biomass (McNamara et al., 2003).



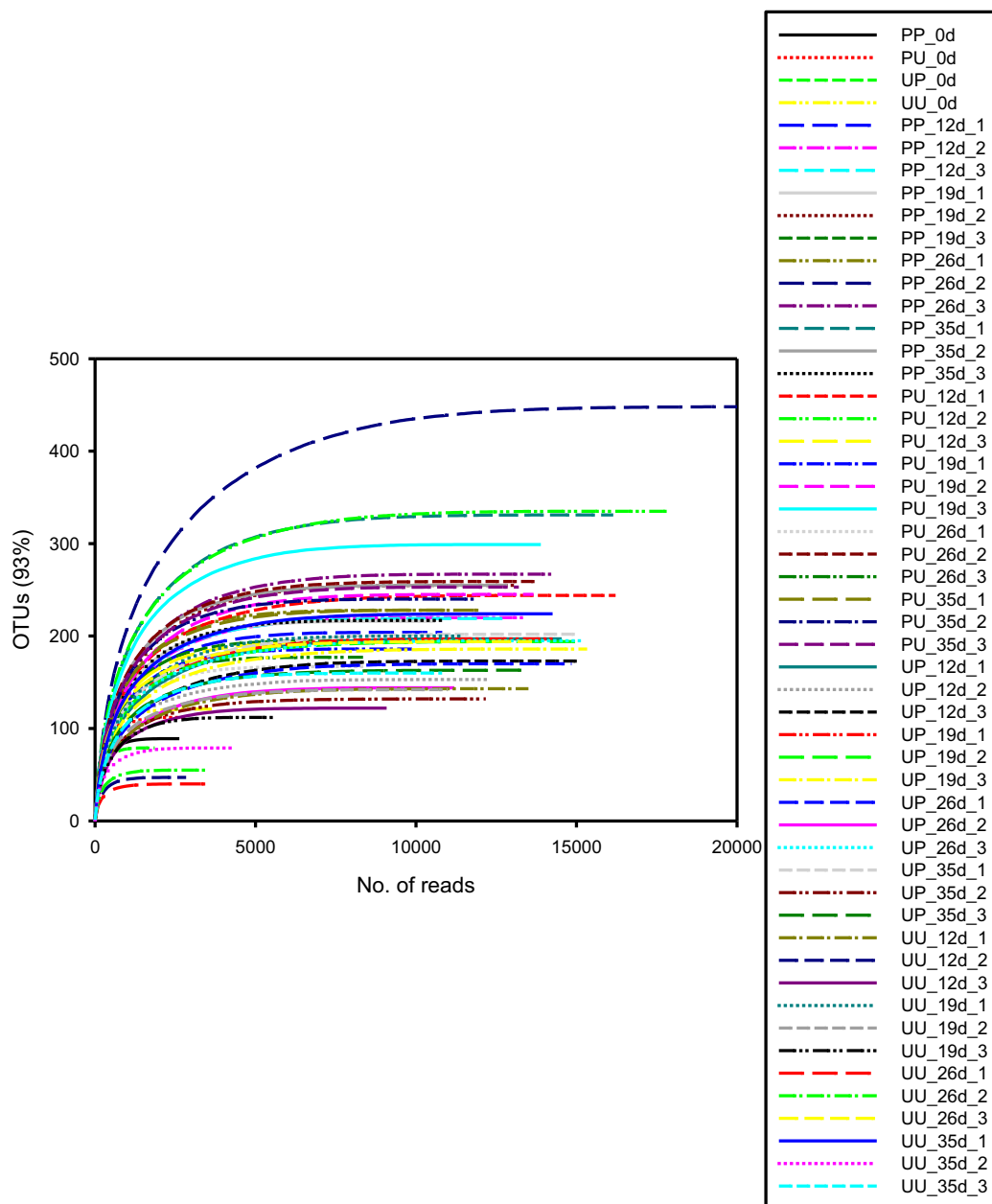


**Figure S21** Rarefaction curve for all samples and replicates approached the asymptote, showing a good coverage of the *pmoA* gene diversity. The samples are labelled denoting the treatment (i.e., PP, PU, UP, or UU; Figure 6.1), days after incubation (i.e., 0d representing starting material; 12d, 19d, 26d, and 35d, represent samples taken on 12, 19, 26, and 35 days after incubation, respectively), and the number of replicate.

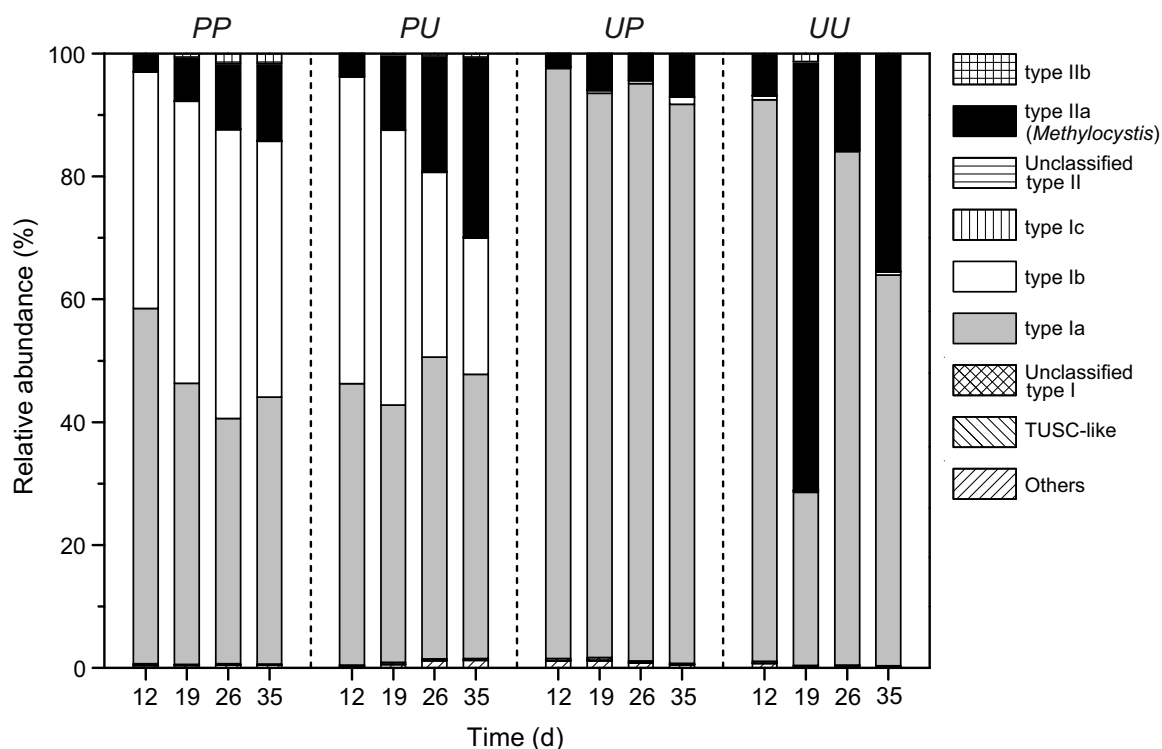


**Figure S22** Mean relative abundance and affiliation of the *pmoA* gene in the PP, PU, UP, and UU incubations ( $n = 3$ ). Type Ia methanotrophs were predominantly comprised of *Methylobacter*, and to a much lesser extent, *Methylosarcina* forming  $< 2\%$  of total reads related to Type Ia methanotrophs. Sequences affiliated to Type Ib and II methanotrophs were predominantly related to rice paddy clusters (RPCs) and *Methylocystis*, respectively. *pmoA* sequences affiliated to RA21-like and M84-P105 clusters, unclassified *pxmA*, and other unclassified methanotrophs are grouped as 'Others'. Collectively, these sequences represented on average 0.6 % (ranging from 0.1 – 1.8 %) of the total number of reads. Abbreviation; TUSC, tropical upland soil cluster.

## **B Further published articles in peer-reviewed journals**

### **Discrepancy in exchangeable and soluble ammonium-induced effects on aerobic methane oxidation: a microcosm study of a paddy soil**

Hester van Dijk<sup>1</sup>, Thomas Kaupper<sup>1</sup>, Clemens Bothe<sup>1</sup>, Hyo Jung Lee<sup>2</sup>, Paul L. E. Bodelier<sup>3</sup>, Marcus A. Horn<sup>1</sup>, Adrian Ho<sup>1,4</sup>

Published in *Biology and Fertility of Soils* (2021) 57, 873 - 880

---

<sup>1</sup>Institute for Microbiology, Leibniz Universität Hannover, Herrenhäuser Str. 2, 30419 Hannover, Germany.

<sup>2</sup>Department of Biology, Kunsan National University, Gunsan, Republic of Korea.

<sup>3</sup>Department of Microbial Ecology, Netherlands Institute of Ecology (NIOO-KNAW), Droevendaalsesteeg 10, 6708 PB Wageningen, the Netherlands

<sup>4</sup>Division of Applied Life Science, Gyeongsang National University, Jinju, South Korea

**The published version of this article can be found online**

## **Response of a methane-driven interaction network to stressor intensification**

Adrian Ho<sup>1</sup>, Lucas W. Mendes<sup>2</sup>, Hyo Jung Lee<sup>3</sup>, Thomas Kaupper<sup>1</sup>, Yongliang Mo<sup>4</sup>, Anja Poehlein<sup>5</sup>, Paul L. E. Bodelier<sup>6</sup>, Zhongjun Jia<sup>4</sup>, Marcus A. Horn<sup>1</sup>

Published in FEMS Microbiology Ecology, Volume 96, Issue 10, October 2020, fiae180

---

<sup>1</sup>Institute for Microbiology, Leibniz Universität Hannover, Herrenhäuser Str. 2, 30419 Hannover, Germany.

<sup>2</sup>Center of Nuclear Energy in Agriculture, University of Sao Paulo (CENA-USP), Avenida Centenario 303, 13416-000, Piracicaba-SP, Brazil

<sup>3</sup> Department of Biology, Kunsan National University, 558 Daehak-ro, Gunsan-si 54150, Republic of Korea

<sup>4</sup> Institute of Soil Science, Chinese Academy of Sciences, No. 71 East Beijing Road, Xuan-Wu District, Nanjing 210008, China

<sup>5</sup>Department of Genomic and Applied Microbiology and Göttingen Genomics Laboratory, Institute of Microbiology and Genetics, Georg-August-Universität Göttingen, Grisebachstr. 8, D-37077 Göttingen, Germany

<sup>6</sup>Department of Microbial Ecology, Netherlands Institute of Ecology (NIOO-KNAW), Droevendaalsesteeg 10, 6708 PB Wageningen, the Netherlands

**The published version of this article can be found online**

**Deforestation for oil palm: impact on microbially mediated methane and nitrous oxide emissions, and soil bacterial communities**

Thomas Kaupper<sup>1</sup>, Stefanie Hetz<sup>1</sup>, Steffen Kolb<sup>2</sup>, Sukhwan Yoon<sup>3</sup>, Marcus A. Horn<sup>1</sup>, Adrian Ho<sup>1</sup>

Published in FEMS Microbiology Ecology, Volume 96, Issue 10, October 2020, fiae180

---

<sup>1</sup>Institute for Microbiology, Leibniz Universität Hannover, Herrenhäuser Str. 2, 30419 Hannover, Germany.

<sup>2</sup>Microbial Biogeochemistry, RA Landscape Functioning, Leibniz Centre for Agricultural Landscape Research (ZALF), Eberswalder Str. 84, 15374 Müncheberg, Germany

<sup>3</sup>Department of Civil and Environmental Engineering, Korea Advanced Institute of Science and Technology, Daejeon 34141, South Korea

**The published version of this article can be found online**

## Chapter 9 Curriculum Vitae

**Thomas Kaupper**

**M.Sc.**

**Work address**

Leibniz University Hannover - Institute of Microbiology  
Herrenhäuser Str. 2  
30419 Hannover, Germany  
E-Mail: thomas.kaupper@ifmb.uni-hannover.de

### Education

**01/2019 - 11/2023**

PhD candidate at the Institute of Microbiology at the Leibniz University of Hannover, Hannover

**Project:** METconnect: Relevance of the methanotroph interactome in modulating methane oxidation activity and microbial community functioning

**10/2016 – 12/2018**

Master of Science in Molecular Microbiology at the Leibniz University of Hannover, Hannover

**Title of master's thesis:** Response of Aerobic Methane Oxidation and the Associated Methanotrophs to Desiccation – Rewetting

**09/2012 – 07/2016**

Bachelor of Science in Bioanalysis at the University of applied sciences and arts Coburg, Coburg

**Title of bachelor's thesis:** The Effect of *Listeria monocytogenes* and Nisin on iceberg lettuce bacterial community: A PCR-DGGE method

## Work experience

### Since 01/2023

Research Associate at the Chair of Ecological Microbiology at the University of Bayreuth, Bayreuth

### 01/2019 - 12/2022

Tutor for Molecular Microbiology masters courses "Environmental Microbiology", "Applied Environmental Microbiology", "Special Methods in Environmental Microbiology" and "Soil microbiology"

### 01/2019 - 12/2022

Tutor for Bachelor and Masters theses in the field of environmental microbiology

### 01/2018 – 02/2018

Research Assistant at the Institute of Microbiology at the Leibniz University of Hannover, Hannover

Tutor for a practical course in microbiology for a B.Sc. course

### 10/2017 – 01/2018

Research Assistant at the Institute of Microbiology at the Leibniz University of Hannover, Hannover

Assistant for a PhD student working with biogas plant samples

Tutor for a practical course in environmental microbiology for a M.Sc. course

### 03/2016 – 07/2016

External bachelor's thesis at the University of Limerick, Limerick, Ireland, under the supervision of Dr. Achim Schmalenberger, funded by a PROMOS grant

**Title of bachelor's thesis:** The Effect of *Listeria monocytogenes* and Nisin on iceberg lettuce bacterial community: A PCR-DGGE method

### 06/2014

Internship at the department Hygienelabor at SYNLAB Medizinisches Versorgungszentrum Weiden GmbH, Weiden in der Obpf.

Analysis of drinking and bath water

Identification of microorganisms via quick tests'

### 02/2014 – 06/2014

Internship at the department PCR-Labor/Zeckenlabor at SYNLAB Medizinisches Versorgungszentrum Weiden GmbH, Weiden in der Obpf.

DNA extractions of clinical samples

PCR direct qualitative detection of Herpes simplex virus (HSV)

Multiplex qPCR

## Contributions to national and international conferences

### ISME18 2022 in Lausanne, Switzerland

**Title:** Site-specificity of methanotrophic interactomes revealed *via* SIP-coupled co-occurrence network analysis

**Contribution:** Poster presentation

### VAAM 2022 (Online conference)

**Title:** The methane - driven interaction network in terrestrial methane hotspots

**Contribution:** Oral presentation (15 minutes)

### World Microbe Forum 2021 (Online conference)

**Title:** Methanotrophic interactomes reflect intensity of a stressor impact

**Contribution:** Oral presentation (8 minutes)

### VAAM 2020 in Leipzig, Germany

**Title:** Response of an active methane-oxidizing community to desiccation-rewetting

**Contribution:** Poster presentation including poster pitch

## Grants

### ISME18 2022 in Lausanne, Switzerland

**Funding:** ISME Travel Grant

### World Microbe Forum 2021 (Online conference)

**Funding:** FEMS Congress Attendance Grant

### VAAM 2020 in Leipzig, Germany

**Funding:** VAAM Travel Grant



## Chapter 10 List of Publications

### A Published articles in peer-reviewed journals

**Mitomycin C-induced effects on aerobic methanotrophs in a landfill cover soil; implications of a viral shunt?**

Heffner, T., Kaupper, T., Heinrichs, M., Lee, H.J., Rueppel, N., Horn, M.A., Ho, A., June 2023, in: FEMS Microbiology Ecology, 99, 6

DOI: 10.1093/femsec/fiad047

**Interkingdom interaction: the soil isopod *Porcellio scaber* stimulates the methane-driven bacterial and fungal interaction**

Heffner, T., Bami, S.A., Mendes, L.W., Kaupper, T., Hannula, E.S., Poehlein, A., Horn, M.A., Ho, A., 2022, in: Environmental Microbiome, 17, 15

DOI: 10.1186/s40793-022-00409-1

**The methane-driven interaction network in terrestrial methane hotspots.**

Kaupper, T., Mendes, L.W., Poehlein, A., Frohloff, D., Rohrbach, S., Horn, M.A., Ho, A., 2022, in: Environmental Microbiome, 17, 15

DOI: 10.1186/s40793-022-00409-1

**Discrepancy in exchangeable and soluble ammonium-induced effects on aerobic methane oxidation: a microcosm study of a paddy soil**

van Dijk, H., Kaupper, T., Bothe, C. H., Lee, H. J., Bodelier, P.L.E., Horn, M. A., Ho, A., June 2021, in: Biology and Fertility of Soils, 57, 873-880

DOI: 10.1007/s00374-021-01579-9

**Recovery of Methanotrophic Activity Is Not Reflected in the Methane-Driven Interaction Network after Peat Mining**

Kaupper, T., Mendes, L. W., Harnisz, M., Krause, S. M. B., Horn, M. A., Ho, A., March 2021, in: Applied and Environmental Microbiology. 87, 5, 13 p.

DOI: 10.1128/AEM.02355-20

**When the going gets tough: Emergence of a complex methane-driven interaction network during recovery from desiccation-rewetting**

Kaupper, T., Mendes, L. W., Lee, H. J., Mo, Y., Poehlein, A., Jia, Z., Horn, M. A., Ho, A., Feb 2021, in: Soil Biology and Biochemistry. 2021, 153, 108109.

DOI: 10.1016/j.soilbio.2020.108109

**Response of a methane-driven interaction network to stressor intensification**

Ho, A., Mendes, L. W., Lee, H. J., Kaupper, T., Mo, Y., Poehlein, A., Bodelier, P. L. E., Jia, Z., Horn, M. A., Okt 2020, in: FEMS microbiology ecology. 96, 10, fiae180.

DOI: 10.1093/femsec/fiae180

**Deforestation for oil palm: impact on microbially mediated methane and nitrous oxide emissions, and soil bacterial communities**

Kaupper, T., Hetz, S., Kolb, S., Yoon, S., Horn, M. A., Ho, A., Apr 2020, in: Biology and fertility of soils. 56, 3, S. 287-298 12 p.

DOI: 10.1007/S00374-019-01421-3

**Disentangling abiotic and biotic controls of aerobic methane oxidation during re-colonization**

Kaupper, T., Luehrs, J., Lee, H. J., Mo, Y., Jia, Z., Horn, M. A., Ho, A., March 2020, in: Soil Biology and Biochemistry. 142, 107729.

DOI: 10.1016/j.soilbio.2020.107729

**Nisin application delays growth of *Listeria monocytogenes* on fresh-cut iceberg lettuce in modified atmosphere packaging, while the bacterial community structure changes within one week of storage**

McManamon, O., Kaupper, T., Scollard, J., Schmalenberger, A., Jan 2019, in: Postharvest biology and technology. 147, S. 185-195 11 p.

DOI: 10.1016/j.postharvbio.2018.10.002

## **B Published abstracts at national and international conferences**

### **VAAM 2020 in Leipzig, Germany**

#### **Response of an active methane-oxidizing community to desiccation-rewetting.**

##### **Contribution: Poster presentation including poster pitch**

Desiccation - re-wetting is a recurring phenomenon in rice paddies exerting an impact on the soil microbial community. Rice paddy soils are drained bi-annually during rice harvest and re-flooded with the start of the new planting season. Since rice paddy soils contribute substantially to global methane emission, it is relevant to determine the methane-oxidizing microbial community (i.e., both the methane-oxidizing bacteria, MOB, as well as other microorganisms associated to the MOB) and their resistance/resilience to desiccation - re-wetting. It is known that methane-oxidizing bacteria form a close network with their interacting partners but it is barely understood how these react/interact in case of a desiccation.

To relate key microorganisms to community functioning, a stable-isotope probing (SIP) experiment was performed using a rice paddy soil to determine the impact of desiccation - re-wetting on the active methane-oxidizing community. Using gas chromatography (GC), methane oxidation was monitored, while the methanotrophic community abundance was followed via group specific qPCR assays targeting the MOB subgroups type Ia, Ib and II. DNA-based SIP was coupled to amplicon MiSeq sequence analysis to determine the change in the active methane-oxidizing community after desiccation - re-wetting.

The disturbance adversely affected methane uptake rate only in the short term. Thereafter the trend in methane uptake was generally comparable in the un-disturbed and disturbed incubations. A dominance of type I over Type II methanotrophs was observed during the incubation, showing community resilience to the disturbance. The abundance of the more oligotrophic type II MOB increased after desiccation in the later stages of incubation, when nutrients became limiting. A shift in the active microbial community composition was detected after desiccation on the overall bacterial community indicated by a change in the abundance of the community members and resulting in a less diverse but more connected network. Altogether, our results showed, that MOB are resilient to single desiccation events given sufficient recovery periods, even though their associated microbial community may change.

## World Microbe Forum 2021 (Online conference)

### Methanotrophic interactomes reflect intensity of a stressor impact

#### Contribution: 8 minute presentation

**Background** The resistance and resilience of a microbial community is often assessed by the response and recovery of the composition, abundance, and activity following disturbances. Rarely has the response of the network of interacting microorganisms been considered, despite accumulating evidence indicating that aerobic methane oxidation is a community functioning, where non-methanotrophs that do not possess the metabolic capability to oxidize methane are also highly relevant, significantly stimulating the methanotrophic activity via interaction-induced effects.

**Objectives and Methods** Here, we determined the response of the methane-driven interaction network, in addition to the recovery in community composition, abundance, and activity > 15 years after peat excavation<sup>1</sup> (i.e., compounded disturbance event) and after desiccation-rewetting<sup>2</sup> (i.e., single disturbance event) using a stable isotope probing approach (<sup>13</sup>C-CH<sub>4</sub>) coupled to a co-occurrence network analysis derived from the <sup>13</sup>C-enriched DNA. By combining SIP-network analysis, we effectively provide direct ecological linkages between the interacting microorganisms, and unambiguously relate the re-structuring of the interaction network after disturbance to methane uptake.

**Results** Despite recovery in community composition, abundance, and methane uptake rates to levels comparable or even higher than in the un-disturbed reference, the interaction network was profoundly altered, becoming less connected with reduced complexity after the compounded disturbance, but the reverse (i.e., increase connectiveness and complexity) was detected after the single disturbance event. Modularity, however, decreased after both disturbances. The altered networks may have consequences in the event of future and/or recurring disturbances, as the network unraveled concomitant to significantly impaired methanotrophic activity upon disturbance intensification<sup>3</sup>. Our work suggests the inclusion of interaction-induced responses, in addition to documenting recovery in community composition/abundances/activity, as a step forward to understand the resilience of microbial communities to disturbances.

<sup>1</sup>Kaupper T, Mendes LW, Harnisz M, Krause SMB, Horn MA, Ho A. (2021) *Appl. Environ. Microbiol* 87: e02355-20.

<sup>2</sup>Kaupper T, Mendes LW, Lee HY, Mo Y, Poehlein A, Jia Z, Horn MA, Ho A. (2021) *Soil Biol Biochem* 153: 108109.

<sup>3</sup>Ho A, Mendes LW, Lee HY, Kaupper T, Mo Y, Poehlein A, Bodelier PLE, Jia Z, Horn MA. (2020) *FEMS Microbiol Ecol* 96: fiae180.

**VAAM 2022 (Online conference)****The methane - driven interaction network in terrestrial methane hotspots.****Contribution: 15 minute presentation**

The composition, activity and diversity of microbial communities is mainly affected by biological interactions. Concerning methanotrophy, aerobic methane oxidation is a community functioning, with emergent community traits arising from the interaction of the methane-oxidizers (methanotrophs) and non-methanotrophs. It is known that methanotrophs thrive better when heterotrophs are present, but little is known of the organization of these interaction networks in naturally-occurring complex communities. We hypothesized that the assembled bacterial community of the interaction network (interactome) in methane hotspots would converge, driven by high substrate availability that favors specific methanotrophs, and consequently influence the recruitment of non-methanotrophs. Such 'hot spots' would also share more co-occurring than site-specific taxa.

To compare the site-specific methanotrophic interactomes, we applied stable isotope probing (SIP) using  $^{13}\text{C}\text{-CH}_4$  coupled to a co-occurrence network analysis to probe trophic interactions in widespread methane-emitting environments. Network analysis revealed predominantly unique co-occurring taxa from different environments, indicating distinctly co-evolved communities more strongly influenced by other parameters than high substrate availability. In the majority of all instances, the networks derived from the  $^{13}\text{C}\text{-CH}_4$  incubation exhibited a less connected and complex topology than the networks derived from the  $^{\text{unlabelled}}\text{C}\text{-CH}_4$  incubations, likely caused by the exclusion of the inactive/non-replicating microbial population and spurious connections; DNA-based networks (without SIP) may thus overestimate the network complexity.

In contrast to our hypothesis, each environment contained distinct interactomes of methanotroph/methanotroph, as well as methanotroph/non-methanotroph. Such data indicate an influence of site specific parameters over substrate availability, which leads to the assumption of different over all community functions.

## ISME18 2022 in Lausanne, Switzerland

### Site-specificity of methanotrophic interactomes revealed *via* SIP-coupled co-occurrence network analysis

#### Contribution: Poster presentation

The composition, activity and diversity of microbial communities is mainly affected by biological interactions. Concerning methanotrophy, aerobic methane oxidation is a community functioning, with emergent community traits arising from the interaction of the methane-oxidizers (methanotrophs) and non-methanotrophs. It is known that methanotrophs thrive better when heterotrophs are present, but little is known of the organization of these interaction networks in naturally-occurring complex communities. We hypothesized that the assembled bacterial community of the interaction network (interactome) in methane hotspots would converge, driven by high substrate availability that favors specific methanotrophs, and consequently influence the recruitment of non-methanotrophs. Such 'hot spots' would also share more co-occurring than site-specific taxa.

To compare the site-specific methanotrophic interactomes, we applied stable isotope probing (SIP) using  $^{13}\text{C}\text{-CH}_4$  coupled to a co-occurrence network analysis to probe trophic interactions in widespread methane-emitting environments. Network analysis revealed predominantly unique co-occurring taxa from different environments, indicating distinctly co-evolved communities more strongly influenced by other parameters than high substrate availability. In the majority of all instances, the networks derived from the  $^{13}\text{C}\text{-CH}_4$  incubation exhibited a less connected and complex topology than the networks derived from the  $^{\text{unlabelled}}\text{C}\text{-CH}_4$  incubations, likely caused by the exclusion of the inactive/non-replicating microbial population and spurious connections; DNA-based networks (without SIP) may thus overestimate the network complexity.

In contrast to our hypothesis, each environment contained distinct interactomes of methanotroph/methanotroph, as well as methanotroph/non-methanotroph. Such data indicate an influence of site specific parameters over substrate availability, which leads to the assumption of different over all community functions.